A parallel computer based study of the automatic control of power generation

Stagg, T. A.

Award date:
1992

Awarding institution:
University of Bath

A PARALLEL COMPUTER BASED STUDY OF THE AUTOMATIC CONTROL OF POWER GENERATION

Submitted by T.A.Stagg, B.Sc.(Hons)
for the degree of
Doctor of Philosophy
of the University of Bath
1992

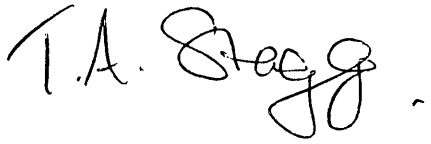

ProQuest LLC
789 East Eisenhower Parkway
P.O. Box 1346
Ann Arbor, MI 48106-1346

Summary

This thesis describes a potential Automatic Generation Control (AGC) scheme for the British power system. The proposal is made to operate the complete grid as two individual control areas, namely, Scotland and England/Wales. It is demonstrated that this would allow not only for centralised frequency control within each area, but also regulation of the power transfer on the tie-lines linking the two areas. It is also shown how a modification to the Area Control Error (ACE) would also allow the automatic control of time error and inadvertent energy interchange between the two areas. Current load-frequency control practice in Britain is described together with general AGC algorithms and some international examples of automatic load-frequency controllers. Research leading to the development of a simulation set up to study the use of AGC on the British system is described, together with details of the models involved. These simulation studies demonstrate the feasibility of this approach and illustrate improvements which are possible.

The simulations were executed on a Transputer based parallel computer using new parallel processing algorithms. As a result of these simulation studies, guidelines are given for setting the various parameters and gains of the control system.

Acknowledgements

The author would like to thank Mr A R Daniels, Project Supervisor, for continued support throughout the course of this work and Prof J F Eastham, Head of School, for the provision of facilities which enabled the work to be carried out. I would also like to thank Dr R W Dunn for technical discussions, Mr V S Gott and Mr B Ross for assistance with the computing facilities, and Mr K W Chan and other colleagues for parallel developments which were helpful to this project.

Thanks are also due to Mr B Murray of the National Grid Company, Industrial Supervisor, for the initial idea for this project and support for it, and Mr C Arkell for technical discussions and supply of information.

The supply of model and controller details from Mr D A Briggs and Dr R Clarke of Nuclear Electric is gratefully acknowledged.

Finally, I would like to thank Dr R W Dunn once again for proof-reading and continued encouragement in this endeavour.

This work was carried out under a SERC[1] CASE[2] award supported by the National Grid Company, Plc.

This document was prepared using LaTeX.

[1]Science and Engineering Research Council
[2]Co-operative Award in Science and Engineering

Contents

Symbols and Abbreviations

ACE	Area Control Error
ACEN	New Area Control Error
AFRC	Area Frequency Response Characteristic
AGC	Automatic Generation Control
ASC	Area Supplementary Control
α	Integral gain in ACEN
BFT	Boiler Follows Turbine
B	Frequency Bias Parameter
β	Area Droop or AFRC
CASO	Computer Assisted System Operation
CED	Constrained Economic Dispatch
CEGB	Central Electricity Generating Board
CRT	Cathode Ray Tube
DMA	Direct Memory Access
DRAM	Dynamic Random Access Memory
EACC	Error Adaptive Control Computer
ED	Economic Dispatch
EDF	Electricité de France
ELD	Economic Load Dispatch
Δf	System frequency error

GOAL	Generator Ordering and Loading
GT	Gas Turbine
I	Integral only Control
IBM	Trademark, International Business Machines, Inc.
II	Inadvertent Interchange
IO	Input/Output
IVO	Imatran Voima Oy, Finland
K_i	Integral Controller Gain
K_p	Proportional Controller Gain
LFC	Load Frequency Control
NAPSIC	North American Power Systems Interconnection Committee
NCC	National Control Centre
OPF	Optimal Power Flow
PC	Personal Computer
PDP	Trademark, Digital Equipment Corporation
PI	Proportional-Integral Control
ΔP_t	Nett tie-line power imbalance
RAM	Random Access Memory
ROM	Read Only Memory
ρ_i	Participation factor of i th generator

SCADA	Supervisory Control and Data Acquisition
SD	Security Dispatch
SED	Secure Economic Dispatch
ss	Steady State
SSEB	South of Scotland Electricity Board
TD	Time Deviation
TFB	Turbine Follows Boiler
VAX	Trademark, Digital Equipment Corporation
VDU	Visual Display Unit
VLSI	Very Large Scale Integration
VSC	Video and System Controller

Symbols relating to primemover model variables and parameters are given in appendices B–E.

List of Figures

Chapter 1

Introduction

> But as it might be supposed that in all the preceding experiments of this section, it was by some peculiar effect taking place during the formation of the magnet, and not by its mere virtual approximation, that the momentary induced current was excited, the following experiment was made. All the similar ends of the compound hollow helix were bound together by copper wire, forming two general terminations, and these were connected with the galvanometer. The soft iron cylinder was removed, and a cylindrical magnet, three-quarters of an inch in diameter and eight inches and a half in length, used instead. One end of this magnet was introduced into the axis of the helix, and then, the galvanometer-needle being stationary, the magnet was suddenly thrust in; immediately the needle was deflected in the same direction as if the magnet had been formed by either of the two preceding processes. Being left in, the needle resumed its first position, and then the magnet being withdrawn the needle was deflected in the opposite direction. These effects were not great; but by introducing and withdrawing the magnet, so that the impulse each time should be added to those previously communicated to the needle, the latter could be made to vibrate through an arc of 180° or more.
>
> *Michael Faraday, Nov, 1831*

1.1 Harnessing Energy

Ever since Man first evolved, his abilities and skills in utilising natural sources of energy have been paramount to his survival and development. Very early on, he learned to use fire to make his lifestyle both safer and more comfortable. Life

was enhanced further by other inventions and discoveries — the bow and arrow to make hunting easier, the use of horses and other beasts of burden for transport and driving machinery, the harnessing of water and wind power enabling easier trade over longer distances and, most recently, the prolific use of fossil fuels which began with the industrial revolution. Now electricity has become one of the most important forms of energy in the modern world. At its point of use it is clean, it is readily transported over large distances, it is easily controllable and it is the only useful way of utilising the potential of some other forms of energy such as radioactivity.

1.2 Birth of the Electricity Supply Industry

With Michael Faraday's discovery of electromagnetic induction in 1831, the scene was set for the development of a world-changing technology. The earlier invention of the steam engine was to provide the mechanical power for this important new energy conversion process. However, it was to be another forty years before the industrial generation of electricity became a practical question with Gramme's production of a dynamo with a ring-wound armature (the "Gramme Ring") [1]. This was followed by a rapid increase in the use of electricity which is still continuing to accelerate today. The earliest supplies were almost exclusively for street lighting, initially by arc lamps and then incandescent lamps, patented by Thomas Edison in 1879. By the end of the century, many other application had developed including electric railways, electric welding, electric smelting and also a number of domestic electrical appliances such as flat irons, fans, immersion heaters and cookers. The induction motor had been invented by Tesla and has formed an increasing share of the electricity demand. Electric washing machines were introduced in the USA in 1907, vacuum cleaners in 1908 and electric refrigerators in

1912. Electric refrigerators were first used in Britain in 1918.

The first public supply of electricity in Great Britain was used to light the streets of Godalming in 1881 using current generated by the waters of the River Wey. The following year, the first steam power stations for public supply were operational. The Holborn Viaduct power station, financed by the Edison Electric Light Co. of London claimed the distinction of being the first public steam power station in the world to cater for the needs of the private consumer as well as for public lighting. The Brighton power station was regarded as the first viable public supply station providing the first permanent public supply in England to all consumers who desired it. These first supplies were direct current but the debate was soon to start over whether direct or alternating current should be used. In 1882 Gaulard and Gibbs obtained British Patents for alternating current distribution by means of transformers operating in series, and in 1884, Dr John Hopkinson showed mathematically that alternators could, in fact, by run in parallel, which was later confirmed by experiments by Prof Grylls Adams. 1884 also saw the construction by Sir Charles Parsons of the world's first turbo-generator, a d.c. unit capable of developing about 75 A at 100 V. In 1888, Parsons supplied the first of four 75 kW single phase turbo-alternators to the Newcastle and District Electric Lighting Co. Ltd. — the earliest use of the steam turbine in a public power station.

The London Electric Supply Corporation's famous Deptford power station — later to be known as Deptford East — started up in 1889. This was designed by Ferranti for the transmission of power at 10,000 V a.c. to transformers placed in the Central London area which reduced the voltage in two steps to 100 V for supplying incandescent lamps. The two 1500 hp, 10,000 V alternators operating at 5000 rpm, or $83\frac{1}{3}$ Hz, were by far the largest in the world at that time. Transmission over the seven miles to Central London was by underground cables designed

and manufactured by Ferranti at the station.

The first overhead transmission lines were erected in Britain in about 1890, and in 1891 the long distance power transmission by three-phase alternating current was foreshadowed by experiments by Oskar van Millar in Germany. The first three-phase public supply in Britain was installed in 1900 from the Neptune Bank power station of the Newcastle-upon-Tyne Electric Supply Co. to local shipyards, works etc. — the first example of bulk supply. Later, in 1903, Parsons supplied this station with a 2 MW three-phase alternator with a rotating field, a radical change which has never been abandoned. This was rated at 2 MW, 6000 V, 40 Hz.

By this time, the so-called Battle of the Systems had effectively been won by the proponents of alternating current. Steady progress had been made towards ever larger machines and higher voltages and this finally dictated the use of a.c. for transmission, though there were pockets of d.c. still operating in the 1950s. By 1910, steam turbines had become the common form of primemover and power stations needed only bled steam, feed water heating, steam reheat and higher initial steam conditions to make them modern [2].

1.3 Automation of Power System Control

With the recent privatisation of the electricity supply industry in Britain and the associated separation of responsibilities for generation and transmission into separate companies, together with a shift of emphasis towards operation under commercial contracts, there has been renewed interest in the automatic control of the power system. The new commercial environment may well provide incentives for automating grid control where contracts would exist with generating stations

for their participation in frequency regulation and load following. Indeed, there is already a move towards centralised setting of generation targets away from the traditional inter-area transfer system where several smaller control areas (within England and Wales) set their own targets for regulation.

The proposal of this thesis is to operate the complete British power system as two individual control areas, namely, Scotland and England/Wales. Automatic Generation Control (AGC) would be applied in each of these areas allowing both system frequency and power transfer between the two areas to be controlled. A simulation has been developed which is suitable for the study of this mode of operation. Results taken from this simulation have allowed suggestions to be made with regard to the setting of various controller parameters and gains.

1.4 About this Thesis

Chapter 2 presents the development of control of the British power system. The current practice is described and the effect of privatisation on future developments is discussed.

General AGC algorithms are presented in chapter 3. This is followed by some international examples of centralised Load-Frequency Control (LFC). Previous experiments of automatic LFC on the British system are discussed together with potential future developments.

Simulations are discussed in chapter 4. Development of power system simulation at the University of Bath is presented and the modifications necessary for the current study are described. Details are given for models of different primemover

types and loads, and generating unit control is discussed.

Chapter 5 gives details of the computing facilities available for this work. Several types of hardware and software were used in both the off-line and on-line aspects of this work. The main engine for the complex simulation work was a Transputer based parallel computer details of which are given in this chapter.

The main results of the simulation work are presented in chapter 6. This describes a series of experiments designed to enable decisions to be made regarding controller parameters and gains. The chapter ends by detailing proposals for the automatic load-frequency control of the British power grid.

Some supplementary results are discussed in chapter 7. These were obtained using a more complex model of the grid network than those of chapter 6 and demonstrate some characteristics arising from the non-uniformity of generator types which exist in a real system.

Conclusions and suggestions for further work are given in chapters 8 and 9 respectively.

Chapter 2

Control of the British National Grid

2.1 Introduction

The electricity supply industry of the early 20th century was made up of a large number of independent power companies and municipal undertakings. In 1926 the Central Electricity Board was set up by the Electricity (Supply) Act to concentrate generation in a number of selected stations and to interconnect these to the existing regional system by a national 'Grid'. By the outbreak of war in 1939, interconnection between the districts was commonplace and the national system was normally operated as one interconnected system with a national control centre in London and six district control centres [3].

Essentially, the purpose of grid control is to meet the demand for electric power as economically as possible subject to the constraints of security of supply and plant availability and performance. The system has always been controlled manually by operators in a hierarchical organisation: national control - area control - plant control, though increasing off-line computer assistance has been available.

The problem is solved in two phases—an off-line one referred to as operational planning, which includes scheduling of generation, and an on-line one called load dispatching. Scheduling defines in advance the generators that will be connected to the system at any time and proposes time for their connection and disconnection, whereas dispatching allocates loads to them in accordance with the criteria of economy and security [4]. Between dispatches instructed by the Grid Control Area control engineers, the balance of generation to demand is maintained by the speed governors of those generators able to respond to system frequency changes.

The main stream developments in grid control over the last thirty years has been the introduction of increasingly powerful computer tools to aid the control engineer. Throughout the 1960s a comprehensive suite of programs was built up [5, 6]. Load flow programs enabled calculations to be made of power flows in each line of a large system and of the resulting flows in the event of circuit outages, fault levels and losses. Demand was predicted using previous demand patterns and allowing for weather. A comprehensive optimisation program fed with data on costs, on plant availability and constraints and on the configuration of the transmission system, calculated the optimum schedule that determined the start-up and shut-down of major units, the required area imports/exports and provided the specified spare. A terminal gave the control engineers access to the computer. In 1970 a new national control centre was commissioned, equipped with comprehensive computer-driven displays and an on-line security assessor [6].

By the early 1980s computational facilities for operational planning work were provided by the CASO (Computer Assisted System Operation) network, which consisted of a network of seven communications processors, five sited at Regional Headquarters or Grid Control Centres, and two at the CEGB's Computing Centre in London. One of these was dedicated to National Control use and the other

provided a general support and standby service for the other six. The processors were connected radially to the Board's Central Computer installation by British Telecom circuits (9.6 kbaud) and also to the Regional main computers as appropriate. Some one hundred VDUs were connected to the system and installed in control rooms and operational planning offices. The system provided facilities for transmission of data between any processors on the system, namely, Regional main-frame processors, the communications processors and the Headquarters Control Centre installation. The original CASO system was later replaced because of obsolescence by a system of colour VDUs using high-definition displays.

1984 saw the introduction into full-time service of the GOAL (Generator Ordering and Loading) program which had been extensively tested and developed operationally since early 1981 [7]. The previous manual system was based on the use of incremental production costs alone and it was recognised that a more rigorous approach was necessary to take account of time dependent factors, principally start-up costs, in the optimisation. Improvements were realised in peak period plant selection, management of plant over low demand periods, scheduling pumped storage in the most economic manner, representing the effects of dual firing and better modelling of the effect of transmission constraints. The GOAL program was also incorporated in the long term planning suite, where it is used to derive annual heat requirements. The associated fuel supply program then derives optimum fuel allocations and associated heat costs.

In addition to the developments in grid control, there have been parallel improvements in the control and performance of the power plants [3, 8, 9, 10, 11, 12, 13, 14]. In the main, these have aimed towards the following, at times contradictory, requirements: increased efficiency, increased flexibility to grid requirements eg.

run-up times and frequency regulation ability, reduced wear and tear, improved environmental impact etc.

2.2 Current Practice

A few statistics describing the size [15] of the British power supply system are as follows:

Net Capability	53 954	MW
Maximum demand met (86/87)	47 925	MW
Annual Energy Sales	228	TWh
Number of Power Stations	74	

Plant mix:	Number	Net Capability		Production	
		MW	%	TWh	%
Coal	36	30 886	57.2	186.4	81.7
Oil	5	8 417	15.6	9.3	4.1
Gas Turbine	11	1 302	2.4	-	-
Coal/Oil	3	4 504	8.3	-	-
Coal/Gas	1	366	0.7	-	-
Nuclear	10	5 069	9.4	32.8	14.4
Pumped Storage	2	2 088	3.9	0.659	0.3
Hydro	6	107	0.2	0.249	0.2
Other (eg Auxiliary GTs)	-	1 215	2.25	0.026	0.01
Total	74	53 954	100.0	228.1	100.0
External (eg. EDF[1], SSEB[2])	-	2 000+		16.524	

The load curve for a typical weekday is shown in figure 2.1.

Under the current manual operation of the system, the National Control Centre directs each of five Area Control Centres to maintain a defined import or export

[1]Electricité de France
[2]South of Scotland Electricity Board

of power until a new instruction is given. This is known as the Inter-Area Transfer system [16]. The power transfers are calculated off-line in advance and updated using the best available information and each unit's costs and constraints and the capability of the transmission system. The targets can be biased by the Area Control Centres in proportion to system frequency error, to reinforce the effect of governor action and the load/frequency controllers operating in some plant. In addition to this form of frequency control, several units at the Dinorwig hydro station may be kept on Low Frequency Relay start such that they will cut in at maximum generation should a serious fall in frequency occur.

Studies into generation and transmission requirements will be carried out by the planning department up to five or ten years ahead. Operational control of the grid system starts about six weeks ahead of the event with the use of DC and AC load flow studies together with predicted demand profiles to produce detailed generation schedules minimising operating costs whilst taking into account the known generation and transmission constraints and allowing sufficient margins for contingencies. As the lead time decreases and more current information becomes available, better estimates can be made of demand, generation and network conditions and the frequency of studies is increased. Estimates of conditions are made daily for the following day, and throughout the day, some eight times a day, for conditions four hours ahead. Extensive use is made of the GOAL program [7] in the production of the generation schedules and loading programme to minimise costs given generation and transmission constraints. State estimation is performed on metered data to ensure consistency before being used by other programs or stored in historical databanks for use in future load prediction studies. Load flow programs are used to ensure that current and proposed operating conditions allow acceptable power flows under normal and outage conditions, and also acceptable fault levels under contingencies.

Control of the grid requires the metering of a large amount of data. The Grid Control Centres acquire data from the power stations and substations, much of which is also transmitted on to National Control, generally via lines hired from British Telecom. The data includes items such as the status (open/closed) of all circuit-breakers and automatic isolators, active and reactive power flows, voltages, frequencies from several points. The frequency of data telemetry ensures that between three and five values for each item are received every minute [17]. These data are asynchronous and are not time-stamped until received by the control centre computers where they are integrated over one and thirty minute periods to reduce measurement noise and to synchronise to a common time.

Post-privatisation, some aspects of grid control are changing. The Inter Area Transfer system is to be superceded by a system whereby total Area Generation Targets are to be sent from national to area control centres instead of area transfers. This move towards centralised dispatching of area targets will be accompanied by the further development of frequency corrections being set nationally instead of by the separate areas as has happened in the past. This centralising of generation dispatching would lead nicely into the form of automatic generation control discussed later in this thesis.

2.3 Summary

This chapter has described the mode of operation of the control of the national grid. Early history, development and current practice have been described together with some operational changes arising from the privatisation of the electricity supply industry. It would appear that current developments are leading towards a more centralised control of system frequency which could well be en-

hanced by the proposals in this thesis. The next chapter describes some aspects of centralised load-frequency control and automatic generation control.

Chapter 3

Automatic Generation Control

3.1 Introduction

There is some discrepancy within the literature as to the exact meaning of the term Automatic Generation Control, or AGC. Some authors consider it to be simply a new name for Load Frequency Control (LFC) [18] although others feel that it covers a wider range of functions [19]. Most recent works have used the term to describe the control function which automatically matches power generation to demand whilst minimising costs. Whether the system is automatic or manual, this is generally done in a two stage manner. An economic optimisation is performed to determine the optimal manner in which the required generation should be shared amongst the generators (Economic Dispatch, ED). At a much faster rate, Load Frequency Control is performed whereby generation is matched to demand by regulating the system frequency and power interchange with neighbouring utilities. The manner in which this regulation is performed will be described in this chapter together with a description of some authors' proposals to improve the basic algorithm whilst taking better account of economy and security.

3.2 The Basic Algorithm

Centralised load-frequency control, LFC, is used extensively in interconnected power systems such as those of continental Europe and the USA. Each area within the system forms its own Area Control Error, ACE, based on the errors in frequency and imported/exported tie-line powers. For many years now, tie-line bias control has been used where,

$$ACE = \Delta P_t + B\Delta f$$

ΔP_t is the imbalance between scheduled and actual tie-line real power, measured positive out of the area, and Δf is the imbalance between scheduled and actual frequency. B is the frequency bias parameter relating frequency to power. Normally, B is set equal to the effective area droop or Area Frequency Response Characteristic, AFRC, as it is often called by American utilities. The AFRC is measured in MW/Hz and in the literature is generally denoted by the symbols K or β. The AFRC can be measured on a given system or area by noting the frequency change for a particular load change [20]. The AFRC, also known as the power/frequency characteristic, depends very much on the prevailing generation and loading conditions. Reference [20] derives an equation for estimating the power/frequency characteristic of the British Grid system of the 1950s from a knowledge of the turbine capacity on the busbars and the system load.

The Area Control Error is used by the controller to calculate a change of generation required to bring the ACE back to zero. In general, European utilities use a proportional-integral, PI, controller, whereas American utilities employ integral, I, only control. In these cases the required change in generation can be calculated from the ACE as:

$$\Delta U = \begin{cases} K_p\, ACE + K_i \int ACE\, dt & \text{for PI control} \\ K_i \int ACE\, dt & \text{for I control} \end{cases}$$

K_p and K_i are controller gains.

The required generation is shared amongst the n participating generators in proportions denoted by their participation factors, ρ_i, where,

$$\sum_{i=1}^{n} \rho_i = 1 \qquad\qquad i = 1,2, \ldots n$$

The participation factors may be calculated off-line, or on-line by the economic dispatch program running at less frequent intervals than load-frequency control. How much of the supplementary generation each generator will be expected to supply will depend on such factors as economy and the speed of response of the generator.

3.3 A History of the Development of AGC

The basic ideas of tie-line bias control were formulated in the 1930s when the earliest European interconnections were made [21]. At this time, the so-called Graner-Darrieus condition of non-intervention was formulated [22, 23] whereby the frequency bias, B, is made equal to the effective droop of the area. With this setting, a load change in one area does not result in a steady state change in the power exported to it by its neighbours.

By the late 1950s, load-frequency control based on these principles was well established in the European system [24]. deQuervain and Frey in [24] outlined a

number of different configurations connecting separate power systems and means of controlling frequency and tie-line powers. They also discussed the design and operation of a digital electronic controller to replace the electro-mechanical types that had previously been in use for many years. They felt that the definite and contractual schedule of power interchange between systems and groups of systems was the very backbone of power economics and that, in this case, load-frequency control, based on system frequency and tie-line power, was essential.

In the mid 1960s, Quazza formalised a general approach to the linear analysis and synthesis of the stiff-interconnection n-area electric power system control [25]. In such a situation, the tie-line power exchanges between each of the n areas was to be controlled together with the system frequency, assumed equal in all areas due to the "stiff" nature of the system. Two approaches to the design of load-frequency controllers were suggested, both of which ensured the basic advantage of splitting the n-dimensional problem into n one-dimensional problems. The first approach required non-interaction between the frequency and tie-line powers controls and the second required that each controlled area took care of its own load variations. The second criterion closely reflected the then current, and subsequent, practice with the sound advantage that each local area controller could be synthesised simply on the basis of its own area transfer function, without any need to know the transfer functions of the other areas. The first criterion required that all control loops had the same transfer functions, which Quazza considered definitely preferable. No real advantage was seen, however, in the non-interaction between frequency and exported power control.

At a similar time, Ross defined the LFC problem as the need to minimize area control error (ACE), inadvertent interchange (II), and time deviation (TD) with a minimum of area supplementary control (ASC) activity [26]. He proposed

an error adaptive control computer, EACC, which, in effect, monitored the error signal and calculated the probability that control action was required. The EACC considered the error signal, ACE, to consist of three components — deterministic, probabilistic and sustained. The first two were assumed to be rapidly varying fluctuations for which no effective control action was possible or desired. Field tests and simulation studies showed a remarkable reduction in control activity with no significant increase in ACE.

A 1970 paper by Elgerd and Fosha [27] questioned the North American Power Systems Interconnection Committee's (NAPSIC) recommendation that each control area set its frequency bias equal to the area frequency response characteristic (AFRC), a practice also followed by European utilities. They presented what they considered to be a set of typical minimum requirements of the controller:

1. The static frequency error following a step-load change must be zero.
2. The transient frequency swings should not exceed $\pm$ 0.02 Hz under normal conditions.
3. The static change in the tie-line power flow following a step-load change in either area must be zero.
4. The time error should not exceed $\pm$ 3 seconds.
5. The individual generators within each area should divide their loads for optimum economy.

The authors presented the development of a ninth-order linear perturbation model of a two-area power system. An analog computer was used to simulate this system and to calculate a cost function based on the integral of the squares

of tie-line power and frequency deviations. These results enabled the authors to propose values for the frequency bias setting and the value of the gain of the typical American integral controller.

Using this model, Fosha and Elgerd went on to develop a full state feedback optimal controller for the two-area power system [28]. In this case, a load-frequency controller was developed for each area which took account of all the model states — ie. even those from the other area. By noting the relatively small size of the gains associated with states from the other area, these states were ignored for the local controller. Consequently, a controller for each area was developed which used only states from its own area. The authors demonstrated the improvement over using the conventional controller possible when more system information was fed back.

This series of two papers, [27, 28], provoked a lot of discussion, much of which was concerned with the lack of detail in the models used, particularly with regard to governor non-linearities and generator rate limits. It was pointed out by several discussers that the simulated results presented were totally unrealistic because of the slow effects that had been ignored. Consequently, the changes to established operating practice recommended could not be taken seriously. However, the application of new control techniques to load-frequency control was welcomed.

Glavitsch and Galiana proposed separating system conditions and disturbances into classes with an appropriate control strategy associated with each class [29]. The proposed classes and strategies were:

I: $\leq 2\%$ in base area — requires maintenance of a smooth control signal. The system should be able to follow trends in the load.

IIA: $< 5\%$ base area — limited control action should be used to keep frequency and tie-line power deviations as small as possible and returned to zero within a reasonable time.

IIB: $< 5\%$ other areas — similar to IIA with the base area being led to support the troubled area.

III: $\geq 5\%$ — spinning reserve must be allocated such that the expected operating cost is a minimum for a given risk of failure.

It was suggested that Kalman filtering techniques should be used to detect the different disturbance classes. The authors developed a simplified linear model which took account of the major dynamics of a power system fed by coal fired plant and the uncertainties associated with modelling some parts of the system — particularly the interconnected areas outside of the base area. The proposed control scheme included a state estimator based upon this model to account for uncertain and unmeasurable quantities. Optimal state-feedback controllers (continuous) were designed off-line for each of the disturbance classes I, IIA and IIB to be applied to the system on detection of the appropriate class. A relatively detailed, non-linear model was used to compare the proposed control scheme with current operating practice. Gains were quoted for conventional LFC of $C_p = 0.1$–1.0 and $T_n = 10$–30 seconds, where,

$$u(t) = C_p\, ACE + \frac{1}{T_n} \int ACE\, dt \tag{3.1}$$

A model addressing many of the shortcomings of that in [27] is that of deMello, Mills and B'Rells presented in [30]. This is a model of one control area tied to a very large interconnected power system. The linear model was able to represent the principal dynamics significant for Automatic Generation Control studies. The

simulation included a number of sub-systems modelling the electro-mechanical plant, the primemover/energy supply system including boiler effects and pressure controls, load reference actuation representing the digital raise/lower pulse logic used to change the turbine load reference, and load disturbance models composed of several components including fairly slow ramps, rapidly changing "noise", and occasional step changes due to, for example, the disconnection of generators.

A companion paper to [30] described techniques for the application of automatic digital generation control and for the evaluation of performance indices which measured the effectiveness of control relative to the control effort [31]. The proposed performance indices included the standard deviation of Area Control Error, the integral of Area Control Error and a measure of the control effort taken as the accumulation of control pulses without regard to sign. In order to prevent unnecessary control action and to not allow the relatively slow generating units to chase high frequency variations in the ACE, the authors proposed non-linear digital filtering in the unit controllers whereby control action would be prevented, or limited, until a sufficient error had been accumulated. Further logic could be included in the AGC to disallow control action if the ACE were already in a direction to reduce the integral of ACE, yet not so large as to warrant immediate control action. Simulation results were presented using the model developed in [30]. The paper addressed some of the significant practical concerns of AGC and the authors reflected that logic and intuitive thinking were invaluable in the design of a control system. However, they also cautioned against the adoption of unnecessarily complex control structures which are relatively easy to implement in software. They further warned against the dangers of using inadequate models with the consequent development of impracticable control strategies.

At the end of the 1970s, the principal concerns of power system operators with

regard to automatic generation control were ones of economy of regulation and quality of regulation — how they might be assessed and how they might be optimised [32]. Criteria for regulation performance in the North American systems were laid down, and constantly reviewed, by NAPSIC. At this time the sort of conditions specified for control performance were quoted as:

A1. The Area Control Error must equal zero at least one time in all ten-minute periods.

A2. The average ACE for all ten-minute periods must be within a specified limit that is determined from the area's rate of change of load characteristic.

B1. For disturbance conditions, the ACE must be returned to zero within ten minutes.

B2. Corrective action must be forthcoming within one minute following a disturbance.

Surveys were carried out amongst member utilities to determine compliance with the criteria.

In 1980 a review paper appeared which presented an overview of current operating practice and also the problems which were emerging as power systems continued to develop [18]. The paper outlined the tried and tested technique of tie-line bias control and quotes typical gains for equation 3.1 of $C_p = 0.1$–0.3 and $T_n =$ 30–100 seconds. Comparing these figures with those given in 1972 [29] (quoted on page 20) reflects the decrease in speed of load-frequency control over this period. There were a number of contributing factors for this, not least of which were the increased proportion of coal-fired regulating plant and the replacement of

analogue controllers with digital ones with associated sampled measurements as systems increased in size and complexity. Glavitsch and Stoffel highlighted the increasing inadequacies of the conventional control algorithm as systems continued to become more heavily interconnected and supplied by ever larger generating units. In a control area connected to other areas with only a few tie-lines, the net interchange power is a reasonable reflection of the generation-load imbalance in the area and the area controller is able to modify it. However, when an area is heavily interconnected with other areas, this is no longer the case as a power transfer across an area does not appear in the net interchange. Consequently, that area cannot control the power flow on the interconnecting lines. Hence, there was an increasing interest in schemes that allowed individual control of lines. It was envisaged that one such scheme might employ optimal power flow techniques whereby the AGC requirements might be dynamically shared amongst generators so as to influence the distribution of power flow.

In the 1980s, studies were aimed at sampled-data automatic generation control using simulations which took account of system non-linearities such as generation rate constraints and governor dead-band effects. The systems being simulated also started to become more complex. Discussions ensued amongst researchers as to the adequacy and validity of some of the models being used.

A 1981 paper by Kothari et al. [33] analysed the effect of generator rate constraints on load-frequency control of a two-area power system. A discrete power system model was developed using the same sampling interval as the proposed controller — 2 seconds. However, the model involved time constants much smaller than this — 0.3 and 0.08 seconds. On modelling a 1% step load perturbation and varying the sampling interval from 0.1 seconds to 1.5 seconds, the results showed increasing instability and loss of higher frequency effects. From this,

the authors concluded that the given controller gain was not suitable for use at higher controller intervals rather than questioning whether the model was still adequate or even valid at the higher modelling interval. Consequently, the results are questionable and the conclusions unproven. This point was taken up by other researchers in this area and a correspondence appeared in IEE proceedings [34].

The same basic model was used by Tripathy et al. in [35] and it is not at all clear that it was not being used in the same invalid way. This paper presented a method of determining optimum gains by minimizing a cost function by the discrete Lyapunov technique, which, unlike as in [33], appeared not to require repeated simulation runs. However, it did use the discrete version of the model with a sampling period given as T. Since the controller gains and states are augmented with the discrete model of the plant, it is not obvious how, if at all, the controller and plant can be modelled with different time intervals. However, the method of using optimal control to choose "best" controller gains was clearly illustrated and the model did attempt to include the very real effects of some system non-linearities.

A further analysis using simulation including representation of governor deadband and minimisation of cost functions to both demonstrate the deteriorating effect of such non-linearities and to present a methodology for choosing controller gains was presented by Basañez and Riera [36]. These authors dismissed the widely accepted model of Elgerd [27] and used a more complete model based on that proposed by Davison [37] into which governor non-linearities had been incorporated. This model represented a rather more complex power system than what was considered to be the rather trivial two equal-area models used extensively in the past. It would appear from [36] that a discrete model had not been considered in this case.

Kumar et al. proposed using a discrete variable structure controller whereby the control action is either integral or proportional depending on the magnitude of the ACE [38]. The authors commenced by taking pains, once again, to stress the importance of adhering to Shannon's sampling theorem when digitising models. However, here a differential, not difference, model was used. The analysis was based on a four-area interconnected system with a mixture of reheat thermal, non-reheat thermal and hydro units. The unit models also incorporated governor deadband models as used in [35], together with generator rate limits.

Another development which came to be more seriously considered in the 1980s for use in Automatic Generation Control was the use of Optimal Power Flow (OPF) techniques [39]. A 1988 paper by Bacher and Van Meeteren described the concept, mathematical formulation and solution of a real-time optimal power flow in an Energy Management System. Traditionally, a full OPF, often referred to as Security Dispatch (SD), uses a State Estimator solution as a base case and reschedules generation whenever a branch overload occurs. An SD execution interval of thirty minutes is typical. New upper or lower unit limits resulting from SD are provided to Economic Dispatch (ED) which shares the total generation optimally (in an economic sense) between units as constrained by these limits. Bacher and Van Meeteren highlighted some disadvantages of this approach:

> "Between two consecutive SD calculations the state of the power system will vary and therefore, the dispatch as provided by ED will not be optimal and secure over this period.
>
> LFC unit mode changes and unit limit changes may result in branch flow violations that cannot be controlled until SD is executed again.
>
> Many unit base points may be set at either their new upper or

lower limit, resulting in a participation factor of zero. This means that fewer units are available to pick up a change in required system generation."

In the proposed approach, Economic Dispatch is replaced by Constrained Economic Dispatch (CED). State Estimator output is used in SD to identify overloaded branches or other violated network flow constraints. Using linear programming techniques, a critical constraint set is then identified by optimising the State Estimator base case subject to network flow constraints. The critical constraint set is used by CED to optimise generation using quadratic programming techniques to determine optimal and secure LFC participation factors. CED would typically run every three minutes, although during periods of rapid load change execution may be initiated every thirty seconds.

M.L.Kothari et al. proposed a new area control error (ACEN) based on tie-power deviation, frequency deviation, time error and inadvertent interchange [40]. A controller using this error always guarantees zero steady state time error and inadvertent interchange, unlike conventional ACE controllers. Based on simulation studies, the authors found that the settling time for tie-power and frequency deviations was more with the new ACE controller. However, conventional ACE controllers require supplementary control whereby offsets are made in scheduled frequency and area net interchange to correct for accumulated errors.

The proposed new Area Control Error is given by:

$$ACEN = \Delta P_{tie} + B\Delta f + a\epsilon + \alpha I$$

where

$\frac{a}{\alpha}$ = $50B$

ϵ = time error

I = inadvertent interchange

a, α = constants

ACEN may alternatively be expressed as:

$$ACEN = (\Delta P_{tie} + B\Delta f) + \alpha \int (\Delta P_{tie} + B\Delta f)\, dt$$

ie.

$$ACEN = ACE + \alpha \int ACE\, dt \tag{3.2}$$

Unfortunately, this analysis was based upon the same model as that previously used in [33] where both the controller and power system were discretised at the controller interval of two seconds. Consequently, the quantitative results are questionable and the use of this model was again questioned in the discussion of [40]. However, the proposal to use a new ACE based upon conventional ACE and integral of conventional ACE appears to be one worth persuing for the additional benefits of automatic correction of time error and inadvertent energy interchange.

Come the end of the 1980s, North American utilities were still very much concerned with the cost of Automatic Generation Control, inadvertent energy interchange and time error [41]. Apart from the initial installation and ongoing maintenance costs, AGC imposes an economic burden on day to day operations. The system operator must consider the startup and running costs of a unit equipped with AGC versus one without. A number of cost factors come into play when AGC is considered, eg., efficiency losses, uneconomic loading of units while trying to satisfy the ACE, wear and tear on units under automatic control and lost

sales due to low frequency operation. If one utility has customers connected to someone else's system, that utility must compare the costs of buying regulation to support that load with the cost of appropriate telemetry to take their load into account in its own AGC. Poor regulation and/or inadequate dispatch of generation lead to further costs through inadvertent energy and time error and the ensuing correction procedures. There is a feeling amongst medium to large American utilities (10,000–25,000 MW) that AGC costs alone are in the millions of dollars per year.

Two very recent papers seem to have fallen into the trap of using very sophisticated control techniques, but inadequate models leading to unrealistic control schemes inappropriate for operational use.

The design of a multivariable self-tuning regulator for a load frequency control system with the inclusion of interaction of voltage on load demand has been presented by Yamashita and Miyagi [42]. The analysis has been performed on a two-area model. The controller inputs are the area frequency deviation and the tie-line power deviation. The controller outputs are commanded changes in speed changer position and excitation voltage. A controller interval of 0.5 seconds was chosen, which is rather faster than the frequently quoted telemetering interval of two seconds for many utilities. The simulation used in the analysis only models non-reheat turbines and consequently does not take account of the slower modern thermal units, neither does it consider plant non-linearities such as generator rate constraints. Having modelled the effect of voltage deviation on load demand, the analysis does not take account of any voltage regulation would would also be attempting to alter the excitation voltage in order to keep the terminal voltage constant.

Aldeen and Marsh have presented a decentralised design method for LFC of a two-area power system in which each area is able to estimate the states of the whole system [43]. The analysis uses the model of Elgerd and Fosha and the authors seem to have totally mistaken the comments given in the discussion of that paper: [27]. Consequently, the final results are unrealistic, being able to return the frequency deviation on a step load change to zero steady state within five seconds. Many modern operational controllers are of the sampled-data type with a control interval of five seconds or more. However, it is very interesting to note that the total state vector of the two-area system is observable from each individual area. The authors state their intention to analyse more complex area interconnections to see if this approach is extendable to more realistic systems.

3.4 Some International Examples of AGC

Further to the examples detailed below, an interesting survey of the application of a standard AGC package to a number of different power systems, varying in both size and structure are to be found in reference [44].

3.4.1 The Hungarian System

The Hungarian power system consists of 750 kV, 400 kV, 220 kV and 120 kV networks with permanent interconnections with neighbouring countries at all levels [45, 46]. The system is mainly thermal based with very little hydro generation, with an average load of 3400 MW, and an area droop of about 350 MW/Hz. More than 20% of energy consumption is imported.

The control objectives for a new AGC in Hungary were set out as follows:

- The area should regulate its own load fluctuations.
- It should contribute to the control of system frequency.
- During the accounting intervals, the exported or imported energy should be of scheduled value.
- The regulator should satisfy the requirement at minimum cost.
- The regulator should reduce the commands sent to the power stations without compromising other control objectives.

Some of these objectives were contradictory, hence an optimal controller was used which implemented a compromise. AGC was realised in two levels: load-frequency control (LFC) and economic load dispatch (ELD). LFC and ELD have been integrated into a single AGC such that LFC is done with regard to generation economics.

In 1979, a load-frequency controller was installed which could adapt to the availability of controllable units [45]. Because the control was performed only by means of slow-acting thermal power plants, it was assumed the dynamic behaviour of the plants could be characterised mainly by their rate of change of generation.

The LFC used a typical Area Control Error:

$$ACE = (P_t - P_o) - B(f - f_o)$$

with the convention that positive ACE required an increase in generation and that P_t was positive for power flow into the area. P_o and f_o are setpoint values.

An adaptive integral controller was designed whereby

$$G_d = C_I \int ACE\, dt$$

such that G_d = desired generation change

$C_I = \frac{M}{ACE}$

M = rate of change of generation

The command sent to each unit was the total desired generation made up of the economical setpoint and some portion of G_d:

$$G_{ci} = G_{bi} + \rho_i G_d$$

where, G_{ci} = command to be sent to the i^{th} plant

G_{bi} = economic setpoint

ρ_i = participation factor

It was found from simulation studies that if there were great differences in the rates of change of generation of the controlled plants, this algorithm did not give the expected optimal results because the participation factors were evaluated on the basis of economics and not on the rates. Consequently, G_{ci} had to be modified to take this into account.

This controller proved to be inconvenient because of the high control effort needed and the requirement to encompass a special half-an-hour accounting system working on the base of the integral of the area control error.

A digital controller was designed which took account of the delay time of the process and output control signals based on predicted load conditions [46]. An autoregressive moving average process was used for modelling the load disturbance. Unneccessary control effort was avoided by limiting the control signal

when the area control error was not too large.

Using filtered values of signals measured every two seconds, the controller operated every minute. Measurements included tie-line powers, system frequency, generation of individual power plants and the number of controllable units within a plant. This was in contrast to the first scheme which operated every two seconds. The second controller was installed in June 1981.

3.4.2 Electricité de France

In recent years Electricité de France, EDF, have been pursuing a major project to replace their grid control system. A new real-time computer system for the national control centre was installed in 1982 and provided: SCADA, LFC, state estimation, security analysis, open-loop secure economic dispatch, power schedule updating, and optimal power flow applications. A longer term project is secure automatic generation control using more powerful computers. The French system is one of the largest in the world to be operated by a single utility — about a quarter as large again as the British National Grid. Major statistics for 1984/85 were [47, 48]:

Total Demand	282	TWh
Total Generation	309	TWh
Peak Generation[1]	60,000	MW
Nuclear	60%	
Fossil	20%	
Hydro	20%	

EDF provides about 90% of this energy, owns and operates the transmission network and most of the distribution network. There are forty nuclear and fossil

[1] January 1985

stations consisting 120 units between 125–1300 MW and 500 hydro plants of which fifty are important. The transmission network is made up of 14,000 km of 400 kV lines, 25,000 km of 225 kV lines, 3000 circuits, 1500 transformers and about thirty links with foreign countries. This is operated through one national and seven regional control centres. The regional centres are mainly concerned with distribution and some 'regional' hydro plants. Currently, only LFC orders are sent directly to the plants by the National Control Centre, all other power changes being carried out through the regional centres.

The National Control Centre directly controls:

- the whole 400 kV network = 70 substations
- 100 225 kV substations
- 40 substations representing foreign networks near borders
- 230 generating units for which active and reactive power is transmitted to NCC. This includes all units connected at 400 kV and the main units at 225 kV.

The network size handled by NCC is 200–300 nodes, whereas taking the whole 225 kV network would lead to a network between 600–700 nodes.

Scheduling is done on two mainframes — an IBM 3033 and a 3081, located at the Research Division with terminals at the control centres. The new real-time computer system of NCC is built around two MITRA 525 mini-computers (0.3 MIPS[2]) with 16-bit words, linked to a data network by two SOLAR 16/40

[2]on a scale where a VAX 11/780 = 1.1 MIPS

front-end computers (0.1 MIPS) operating in a redundant configuration. There are fourteen full graphic four-colour CRTs with a resolution of 2048×2048 pixels with a light pen, track ball and keyboard interface. Two pictures are needed to display the whole of the 400 kV network of seventy substations showing nodes and line flows. An animated mimic board has been kept as a back-up. 2200 telemeasurements and 5500 telesignals are scanned every ten seconds while switch positions are transmitted only on a change or on call.

3.4.2.1 Integral LFC

The current method of Load Frequency Control is very conventional. The ACE (for all of France) is integrated and multiplied by a convenient factor at the national control centre, then sent to all the plants (single control order, the same for all plants). Frequency is measured every second, tie-line powers every two seconds. The controller interval is ten seconds.

3.4.2.2 Secure Automatic Generation Control

An on-going long term development of EDF is secure automatic generation control which will enable Load Frequency Control and Secure Economic Dispatch to be performed together at the current LFC rate of ten seconds [19, 48, 49]. Initial studies were started on the project in 1981 with the agreement to go ahead with it being made in 1985. The latest estimate is for installation in 1995 [19].

The input signals to the closed loop SED control law are the ACE and the binding security constraints. The outputs are the generating unit power setpoints. It

was found necessary to partition the required load changes into two components — a trend component and an oscillatory component. The oscillatory component is range limited and has zero mean. It is shared proportionally amongst all participating generators as for conventional LFC. This has been called 'secondary control' and can be justified because such small amplitude, short duration disturbances have very small consequences with regard to economy and security. The trend component is used by the secure economic dispatch together with the critical constraints to calculate secure and economic generations for all units. This is known as 'tertiary control'. Without this partitioning, the SED would cause the small oscillatory component of the load to be chased by only a few generating units causing undesirable wear and tear. The filter used in the partitioning was made to be adaptive so that for increasing magnitudes of load disturbances, the tertiary control took more responsibility and the secondary less. In this way, large load changes which would have significant consequences on economy and security are reacted to by the tertiary control in a fast manner.

The operating intervals of the various functions making up the secure automatic generation control will be as follows:

- Frequency will be measured every second.
- Tie-line powers will be measured every two seconds (synchronised and time-stamped).
- Every tenth second SCADA will be carried out on the 400 kV/225 kV networks to include about 1000 busses. Critical constraints and AGC outputs are calculated.
- State estimation will be performed every minute as well as AGC supervisory control which checks controller performance and, when necessary, adjusts

the parameters of the control system.

- Global and bus load forecasts will be carried out every fifth minute, producing forecasts for five and twenty minutes ahead and providing an active reduced model to be used by AGC.

- Security analysis will be performed every fifteenth minute, and on call, for a few hours ahead using active/reactive optimal power flows, also producing forecasts for five and twenty minutes ahead.

A number of simulation models have been developed in order to test, improve and validate the new AGC system. Both simple and very detailed models are being used to further develop the controller in an iterative process of design and simulation testing [49]. A first version of a large simulation model with explicit network modelling has now been set up. The simulation consists of three main subsystems modelling the power system, the data transmission system and the central control system. The power system subsystem models the full French 400 kV and 225 kV networks and equivalent networks for Western Europe totalling 1050 nodes. Long term primemover dynamics are represented in detail including control and computer functions at the plants.

3.4.3 The Spanish Peninsular System

The Spanish system is made up off several heavily interconnected utilities [50]. The major statistics at the end of 1983 were:

400 kV lines: 9,140 km
220 kV lines: 15,070 km
total area: 505,000 km^2
4 tie-lines with France

Installed capacity:	36,514 MW
Hydro:	14,003 MW
Conventional Thermal:	17,668 MW
Nuclear:	4,843 MW
Total demand:	98,080 MWh
Peak load:	18,630 MW

A shared regulating system was put into operation in the first quarter of 1983, with seven areas participating. The utilities responsible for load frequency control did not cover the whole power system and consequently, the regulating pool members had to compensate for their non-regulating partners. A hierarchical control scheme was employed whereby the national control centre calculated a total pool regulating requirement based on the net interchange deviation with France and shared this amongst the participating areas. Each area had its own Automatic Generation Control which regulated its own area net interchange deviation as well as system frequency and the total pool regulating requirement.

At the national level, the Pool Regulating Requirement, *PRR*, was calculated as:

$$PRR = G \times FPNID - \sum_{i=0}^{A} NID_i$$

where G is the Pool gain, *FPNID* is the Filtered Pool Net Interchange Deviation, NID_i the regulating area Net Interchange Deviations and A the number of active regulating areas. *PRR* was shared amongst the pool members according to participation factors, PF_i, to produce individual Company Regulating Requirements, CRR_i:

$$CRR_i = PRR \times PF_i \qquad \sum_{i=0}^{A} PF_i = 1$$

The AGC algorithm then used by each area was as follows:

$$ACE_i = NID_i - B_i\Delta f + CRR_i$$

On disconnection from France, each *ACE* took account only of frequency, ie.

$$ACE_i = -B_i\Delta f$$

The Pool Control Function was executed every eight seconds.

3.4.4 Imatran Voima Oy, Finland

Imatran Voima Oy, IVO, is the state owned utility supplying 40–45% of the annual electricity sales in Finland [51, 52]. In 1985 IVO supplied 22.7 TWh of electricity made up of supplies from its own plants, power purchased from other Finnish power companies and imports from the USSR and Sweden. The share of generation in Finland is divided as follows:

40–45%	IVO + other state owned companies
40%	industrial producers
15%	municipal utilities

Total IVO capacity is 4900 MW made up of:

1400 MW	hydro
1200 MW	nuclear
1700 MW	other thermal
600 MW	committed imports

links to Sweden:	2×400 kV + 1×220 kV lines
links to USSR:	1000 MW dc link

In 1984 the total Finnish production was 47.1 TWh plus 4 TWh imported from the USSR.

IVO owns all of the 400 kV grid, most of the 220 kV grid and about a half of the 110 kV grid.

A joint operation agreement exists between Denmark, Finland, Norway and Sweden which deals with, among other things, temporary transactions between partners, generation and voltage control and maintenance of production reserves.

The IVO System Control Centre is regarded as a National Control Centre. A new Control Centre System was commissioned in 1981 in which data received at the National Control Centre from District Centres included about 700 measurements plus 2100 status indications from the power system control and 500 other data items from separated and centralised control system supervisory equipment. This was transmitted via IVO's own radio link and power line carriers. Data transmission for the centralised AGC was carried out by connections separate from the District Centre Systems.

The control system at the National Control Centre consisted of a Front-End computer system made up of three PDP 11/34 computers (two, in a redundant mode, for data transmission and one for telesupervisory and software maintenance use) and a Main computer system. The main computer system consisted of two 16-bit Modcomp Classic mini-computers (in redundant configuration). There were four consoles and monitors in the control centre and remote terminals in the district centres and large power plants. These remote terminals were used to display production plans and for entering manual data that could not be measured, such as generator availability, temporary limitations, control characteristics and fuel

costs.

Load forecasts were performed off-line on VAX 11/785 computers and on-line in the control centre systems. This was done from one hour ahead to one week ahead with hourly mean values corrected for temperature. Temperature is significant in Finland because of the high domestic heating load (10% of the country's consumption). Effects of temporary contracts for selling and purchasing energy were estimated and entered manually.

Dispatched setpoints were sent to control centres and power plant control rooms but were acted on manually, whereas AGC requirements were sent direct to the plant.

The inputs to the Automatic Generation Control were the tie-line power on the links with Sweden and the system frequency. The outputs were the desired outputs from two hydro power plant groups and the dc link with the USSR giving a total of 1200 MW. There were four different operating modes. The normal mode was an hourly energy balance control:

$$ACE = \Delta P + B\,\Delta f$$

$$U = \int_0^{1hr} ACE\,dt$$

In tie-line power control $ACE = \Delta P$, though this is rarely used. When $\Delta f >$ 0.3 Hz, or the interconnection with Sweden is out of service, frequency control mode is employed where $ACE = B\Delta f$. The final mode is manual control where only the turbine governors control frequency.

These algorithms were performed by a digital computer in the Central Control Centre, but there were analogue back-up controllers in two of the district centres. The central controller sent the control signals to the group controllers which in turn shared it between their own power plants, adding the new signal to the current setpoint values and sending the new setpoints to the local controllers. The local controller distributed the signal to the turbine governors, keeping the turbine powers equal.

ΔP was calculated by dedicated equipment in one district centre using load measurements of the tie-lines and the setpoint value. It was then sent to the central controller. Frequency was measured at a 400 kV substation and sent to the central controller which calculated the frequency deviation. The central controller was a PDP 11/34. The AGC application programs were written in-house.

This control centre system was fully operational in 1982. The software was maintained in-house, though it was supplied by an independent supplier. Preliminary studies were started in 1973 and all deliverables were finally accepted in 1983, three years late. This was due mainly to the under-estimation of what was involved and difficulties in preparing completely unambiguous specifications.

3.4.5 Tacoma City Light Division, USA

This is another example of regulating hydro turbines [53]. The company has six hydro generating plants (eighteen generators) with a total capacity of 760 MW in an area whose load is 1100 MW. The area is interconnected to the North West Power Pool via six inter-ties. The communications between the energy control

centre and the generating sites is done via dedicated microwave links. Other remote terminals are connected by microwave or telephone lines. Tie-line real power, line frequency and generator power outputs are each measured at two second intervals.

The AGC algorithm in this case is based upon an Area Control Error calculated from:

$$ACE = \sum_i P_t(i) - P_s + 10B(f - f_s) + TC$$

where

$P_t(i)$ = Power flow in tie-line i, MW

P_s = Net scheduled interchange power, MW

B = Frequency bias setting, MW/0.1Hz

f, f_s = Actual and scheduled frequencies, Hz

TC = time correction, MW, derived from the seconds of time error multiplied by a number, MW/sec

The controller interval in this case is eight seconds. This interval was chosen through operational experience taking into consideration the load and interconnection behaviour, governor action and hydro generator response. ACE is computed every two seconds and the generator control is executed every eight seconds. The controller compares the actual generator outputs with their desired values and sends corrective raise/lower signals to the governors. The basic control loop was analysed and designed using a $\mathcal{Z}$-transform formulation.

Another significant concern of this system was to consider the allocation of water usage among the plants.

3.4.6 The Hellenic System

A Load Frequency Control for the Hellenic power system has been proposed [54] which has three types of LFC: flat frequency, flat tie-line and tie-line bias, and four operating modes which depend on the magnitude of the area control error: steady state, normal, and two emergency modes. An approximate economic dispatch is suggested which uses a predetermined table of the economic loading of units to work within the present computer hardware limitations. The full system is to be implemented on a dual mini-computer system.

The Hellenic power system has been modelled as fourteen power plants — six thermal, eight hydro — and one tie-line to Yugoslavia and hence the West European power pool. The installed capacity is 5566 MW.

The calculation of the Area Control Error is modified according to the type of LFC:

flat frequency: $ACE = B\Delta f$

flat tie-line: $ACE = \Delta P_t$

tie-line bias: $ACE = B\Delta f + \Delta P_t$

The control period is slow — thirty seconds. The authors claim some advantages of slow acting LFC: non-interaction with machine dynamics, relative non-sensitivity to changes in the power system also avoids unnecessary excursions of unit output power due to transient faults. There is no consideration of rate of change of generation in the controller. The authors also claim that the system characteristic (in MW/Hz) is the only necessary information for the design of a slow acting LFC system. They use integral of frequency error feedback to

correct the cumulative frequency error, to filter measurement errors and the statistical load component, and also because the frequency control system responds to transient faults to a far lesser extent.

There are six measurement intervals in every control period, ie. the measurement period is taken as five seconds, each measurement in fact being the average of five one-second measurements. In this way, filtering of the measurements is achieved and transient values will not be acted upon by the controller. The control period is thirty seconds. The comparatively long control interval has been dictated by the slow communications speeds available on the Hellenic system.

The required change in generation required is calculated from:

$$\Delta G = p\, ACE_n + (1-p) \sum_{j=1}^{n} \frac{1}{n} ACE_j$$

where n is the measuring intervals per control interval. Simulation studies have found that $p = .25$ is adequate to filter out possible measurement errors without deteriorating the speed of response.

A computational algorithm has been developed to evaluate the approximate participation factors of all the generating units participating in the frequency control scheme from a matrix containing generator loading information under various system loading levels. The algorithm is implemented every fifteen minutes.

3.5 Application to the British System

3.5.1 Introduction

Since the formation of the National Grid, the British power system has been operated as an isolated system by a single utility. It has not had the contractual obligations to neighbouring utilities as happens on the continent and in America, for instance, which requires a tight control of tie-line power flows and system frequency. Consequently, there has been little progress made towards automating the dispatch/loading function and providing centralised frequency control. However, it may be beneficial to have some form of automatic generation control even in an isolated system in that it may allow, for example, for a system-wide rather than a local optimisation to handle short term variations from predictions and for economic benefits arising from more frequent optimisation [16]. Indeed, there are a number of isolated power systems in the world which have chosen to use standard AGC software as part of their modernised control systems [55, 56, 57].

3.5.2 Previous Experiments

Some of the earliest interest in providing automatic generation control for the CEGB system was provoked by the examination of the possibility of establishing an a.c. link between the French and British systems in the early 1950s. This need disappeared with the decision to use a d.c. cable for technical and economic reasons. However, some experimental work continued to investigate the feasibility and requirements of automatic frequency control for the isolated British system [20, 58].

Two quite major experiments have since been carried out by the CEGB into automatic and centralised control of the grid. The first of these took place in the mid 1960s and was concerned with the automatic control of a number of generators in the South West region [59, 60, 61, 62, 63, 64, 65, 66, 67]. The second was a study of centralised dispatch in the early to mid 1980s [4, 16, 17].

3.5.2.1 The South West Region AGC Experiment

A 1960 paper by Casson, Moran and Taylor [68] foreshadowed the requirement for the automatic loading of the generating plant on the CEGB system. A few years later a limited experimental scheme was set up on part of the CEGB system in order to clarify the technical and economic issues involved [66, 67]. The field trials were preceded by a laboratory experiment which was effectively an exercise in automatic control using a digital computer and a model of a power system [69].

Three major procedures were included in the automatic system:

1. Prediction of future demand [62].
2. Preparation and periodic revision of a schedule of plant outputs, giving the minimum operating costs.
3. Instructions of plant outputs in accordance with the schedule.

A total of 1820 MW of installed capacity from thirty-one generators in six generating stations were directly controlled. The control system produced two sets of target outputs for each generator, the first (at T minute intervals, T being within

the range two to ten minutes) for actual loading and the second (thirty minute target) for warning (under normal conditions) and loading (under reversion conditions, following any control-system faults leading to the loss of the T minute targets).

Some of the major problems encountered arose from the extra demands imposed on the stations. One particular difficulty was that most of the stations were range stations, with a common steam supply to several generating units, whereas, initially, the load scheduler treated each unit as independent. It was also found that the unit outputs were changed far more frequently under automatic control compared with manual control as the system continuously attempted to minimise running costs and keep to a fixed level of spinning spare capacity. At times this led to generators dropping load for only a short period before picking up again, increasing hidden costs in terms of wear and tear which had not been taken into account in the optimisation. The scheme also provided valuable experience in the use of computer displays as an operator interface for the monitoring and control of a large system and an insight into the amount of computing power and storage required for such a task.

3.5.2.2 The Centralised Dispatch Project

By the 1980s significant changes in the way in which the system was controlled were foreseen [4]. The likely driving force was seen to be the continuing increase in the cost of energy in real terms combined with the evolving technical characteristics of the system including a much increased pumped storage capacity. It was felt that a contribution to this might be achieved by dispatching targets in one form or another to individual generators, rather than transfers to Areas. By

the mid 1980s the situation had changed from that in the 1960s when each of the Areas had contained between 100 and 200 generators, mainly connected to the low-voltage networks and weakly interconnected at 132 kV. The formulation of the problem at that time was formidable and the computers potentially available for its solution were rudimentary. The situation had come in the eighties to one where, with the closing down of old stations, the system would in future comprise largely of a relatively few big stations directly coupled to a strong 400/275 kV system designed for bulk transfers. In view of the developments in computer power, the problem now appeared feasible. It had also been argued [70] that with the commissioning of Dinorwig and the resulting substantial increase in pumped storage capacity that it would be uneconomic for much of the time to hold reserve on steam plant, provided that adequate provision was made for emergency reserve and regulatory action. The conclusions favoured some form of nationally optimised generation dispatch rather than the traditional method of inter-Area transfer control. Consequently an investigatory project was set up which provided a facility for centralised computer-aided manual dispatch [16].

A series of experiments was performed between February and May 1985, in which the system was controlled centrally for periods of up to one week. The dispatch algorithm performed on-line economic allocation of generator outputs as part of a larger control system. Of particular importance to dispatch was the demand prediction, reported by Laing and Brewer [17]. A mainframe computer provided the schedule of thermal generator startup and shutdown events calculated by the GOAL program [7]. The dispatch calculation was performed every five minutes to ensure that it was always sufficiently up to date. However, the implementation of the results was by manual means on an "as necessary" basis, typically every fifteen to thirty minutes. Automatic implementation would be required to sustain a five minute or faster cycle in order to realise the full economic benefit suggested

by Farmer [70]. Frequency control was not part of the dispatch formulation, since the five minute cycle was not suitable for such control.

The project succeeded in demonstrating the feasibility of centralised dispatch, although considerable difficulty was encountered in making economic comparisons. It was concluded that to meet operational standards, the hardware would need to be made more reliable by duplication, and the software would require further validation and development to make it more "user-friendly". There was also felt to be scope for improving performance through further algorithmic developments.

3.5.3 Proposal for the Automatic Generation Control of the British National Grid

It is proposed that the British National Grid be considered as two control areas, namely, Scotland and England/Wales. By applying the algorithms of section 3.2, this would enable not only the control of system frequency in each area, but also the automatic regulation of the power transfer on the tie-lines between Scotland and England which is not available in the current control method. This thesis investigates the implementation of such a controller with the aid of simulation studies. However, the question of economic optimisation has not been addressed at this stage.

3.6 Summary

This chapter has addressed three major topics — general AGC algorithms, some international examples of centralised LFC, and the automatic load-frequency con-

trol of the British National Grid. The proposal was made to operate the British Grid as two control areas, Scotland and England/Wales, and apply typical AGC algorithms to this system. The next chapter discusses the need for simulations in the study of these proposals and describes the simulator developed for this work.

Chapter 4

Power System Simulation

4.1 The Requirement for Simulations

Simulations allow for the study of the behaviour of systems which would be impossible to perform in the real environment due to constraints such as time, cost, safety and accessibility. Nowadays, digital computers are almost invariably used for such studies because of their cheapness, compactness and flexibility. Powerful modern processors, particularly when working in parallel, allow quite complex systems to be modelled in, or even faster than, real time. In addition to the convenience of being able to compare behaviour under different system conditions and the results of different control strategies as quickly as possible, real time operation allows the realistic interaction necessary for operator training and operational controller testing. Faster than real time operation enables model reference control and fault anticipation when the simulation is run in parallel with the real system.

The structure and complexity of a simulation will depend upon its ultimate use and will generally be a compromise between speed, cost and accuracy. Fairly low

order, linear models are generally used in model-reference control applications in order to achieve faster than real time operation at an acceptable price [29]. Models used for the evaluation of energy management systems might have time scales of several hours, with system states calculated at intervals of one second or more [71, 72]. For transient stability studies concerned with the detailed system response following severe disturbances such as network faults, system states are evaluated at intervals of 10–100ms over time scales of about ten seconds [73, 74, 75, 76]. To achieve the real time speed necessary for operator training, either more powerful computers, or lower order models are required [77].

4.2 Simulation of the British National Grid

A number of simulations of the British grid system have been developed over the years [61, 69, 73, 74, 75, 76, 78, 79, 80]. Applications range from a test-bed for an automatic grid control system [61, 69] or investigations into the system frequency response [78, 80] to system transient stability studies [73, 74, 75, 76].

For the current study into the automatic control of the British power system and its effects on and requirements from the power plants, a simulation is required which covers time scales of a few seconds to many minutes.

4.3 Real Time Power System Simulation at the University of Bath

4.3.1 Introduction

The interest in real-time power system simulation at the University of Bath began in the late 1970's when the increased availability of relatively inexpensive microprocessors changed the approach researchers were able to take with regard to simulating complex dynamic systems [81, 82]. Hardware, software and algorithms were developed that allowed dedicated microprocessors to be used for the real-time or faster than real-time simulation of power systems.

Following these initial investigations, a real-time multiple processor simulator was developed to enable studies of short-term multi-machine power system transient behaviour [74, 75, 76, 83]. The structure of this model is shown in figure 4.1.

The first multi-processor system, developed by Dale [74], was written in the BCPL programming language [84] and ran on six MC68000 microprocessors [85, 86] under the Tripos operating system [87, 88, 89]. This enabled a simulation of a power system consisting of four generators and six busbars to be run in real time (as defined in [74]).

The system used by Berry [75] was made up of one MC68000 acting as an IO/host processor together with up to twelve MC68020/MC68881 processing nodes [90, 91] also running BCPL under Tripos. In conjunction with an enhanced network solution technique this allowed real-time parallel simulation of twenty generators and sixty busbars.

The simulation has since been translated to the C high level language [92] and transported to the Helios operating system [93] running on INMOS T800 transputers [94, 95] for reasons of standardisation and improved portability. Chan [76] has developed the basic simulation further to the stage where it is able model an eighty machine, 811 busbar system in real time. This has been achieved through improved sparse matrix solution techniques and the use of a parallel processing computer made up of sixteen INMOS T800 Transputers hosted by a PC computer with a further two transputer plug-in boards (see section 5.2.1).

Work has also been done to provide an enhanced user interface to the simulator based on windowing graphics techniques [96].

Serial versions of the simulator have also been ported to run on other hardware such as directly on PCs, SUN and APOLLO workstations and an Intel i860 processor plug-in board hosted by a PC [97].

4.3.2 Developments Required for Automatic Generation Control Studies

A suitable simulation of the British power system was required against which to evaluate various automatic control/dispatch algorithms. There was also a need to further develop the existing simulator, with an aim to have a common user interface to a simulation offering the opportunity to perform studies on a power system at various time-scales from transient stability studies spanning a second or two to load-frequency control spanning minutes to hours. It was felt that such a simulation should also be of great benefit in operator training and educational use. Consequently, it was decided to develop the existing simulation so that it could be used for load frequency control studies. As noted by other authors,

[30], this required an emphasis on the detail of representation of the primemover systems.

To study system behaviour on the longer time scales a number of enhancements were made to the existing simulator, namely:

Development of detailed primemover models. The existing simulation included a linear turbine model which assumed a constant head of steam at the inlet to the governor valve for thermal plants, or constant head of water for pumped storage plants. Only the mechanical speed governors were included as a straight gain on speed error. Studies of load control and frequency regulation need to be concerned with the nonlinear characteristics of the governor valve, rate limits and deadband in the speeder motor, the time constants involved in raising steam in the boiler, and the type of controllers applied to fossil-fired units which affects the way in which they behave with respect to setpoint changes and transients in load and frequency.

The existing pumped storage unit model was extremely simple comprising only two lags without concern for starting/running up characteristics. To study the effects of pumped storage plant on system frequency, such considerations needed to be taken into account, together with the logic for starting up a unit on low frequency.

To study system behaviour under serious low frequency transients, or at peak loads, gas turbine units would also need to be modelled. The current research did not consider scenarios as extreme as this, but it would be anticipated that the detail of such models need not be as great as those of fossil plants as they are usually either off or at full load with very fast run up times and are not used for normal frequency regulation and under steady load conditions because of their high costs.

British nuclear units are not used for frequency regulation or load following because of their lack of flexibility, so they too did not need to be modelled in quite the same detail as the fossil-fired units. However, the non-linear governor characteristics did have to be taken into account as this affects what regulation is achievable with a given governor droop gain. This requirement was met in a simple manner by using the fossil model to simulate nuclear units but with a high droop and no frequency regulation.

Development of Load Models. Frequency and voltage sensitive loads needed to be modelled in the simulation as they modify the system response to frequency transients and variations in demand.

Variable simulation step length. Modifications were needed to allow slower plant, eg. boilers, to be simulated with longer time-steps than the faster electrical plant in order to save unnecessary processing time.

Power system control function. Code to simulate the power system control function was written. This emulated the telemetering of system data available to the grid control centres and the control signals sent from control centres to plants together with the automatic generation control algorithms.

Miscellaneous. Other, less major, modifications were also made to allow, for instance, logging over much longer time periods, the real-time display of new model variables and more flexible plotting of all model variables.

4.4 Primemover Models

Two basic models have been implemented — a ninth order model (excluding controllers) of a fossil-fired unit and a twentieth order model of a hydro unit (including governor control). The fossil-fired model is based on a model of a

500 MW fossil-fired unit passed to the author by Mr D Briggs, at that time of the Central Electricity Generating Board [98]. The hydro model is based on a model of the Dinorwig pumped storage scheme, also obtained from Mr D Briggs [99]. The models have been incorporated with the existing power system simulator [74, 75, 76]. The fossil-fired model can be characterised to provide simulations of oil and coal-fired stations of different MW output by altering the fixed parameter data stored in an initialising 'study file'. The hydro model can be used to simulate plants of different sizes in a similar way. As mentioned in the preceeding section, the fossil-fired model is also used to model nuclear units which are characterised by having high droop characteristics and not controlled to regulate frequency.

4.4.1 The Existing Primemover Models

The existing primemover model consisted of a linear turbine model with simple speed control as a direct gain on to governor valve position. A constant head of steam was assumed at the inlet to the valve. This is shown in figure 4.2. The hydro model was similar with different gains and an assumed constant head of water.

4.4.2 New Fossil-Fired Boiler Model

This model had been used and developed by various departments within the CEGB for boiler control and grid control studies [78].

A schematic diagram of the boiler model is shown in figure 4.3.

The model variables are listed in Appendix B. The model equations are listed in

Appendix C.

Initially, routines simulating the fossil-fired boiler were integrated into the existing power system simulator running on a single MC68000 Tripos system. The power system simulation with the detailed boiler model incorporated was then transferred to an IBM PC hosted T800 transputer running the Helios operating system. At the same time as this, other work was being done to integrate the basic simulator more fully with the Helios parallel transputer environment [76], and finally, the modifications necessary for detailed primemover simulation were incorporated into this parallel system.

The basic 500 MW oil-fired model was modified to obtain models of 500 MW coal-fired units and 660 MW oil- and coal-fired units as outlined in appendix J.

4.4.3 New Hydro Model

This model was developed within the CEGB to study the governor requirements of the, at that time, soon to be commissioned pumped storage scheme at Dinorwig [99].

A schematic diagram of the hydro model is shown in figure 4.4.

The model variables are listed in Appendix D. The model equations are listed in Appendix E.

The detailed hydro model was incorporated into the power system simulator which ran under the Helios operating system on parallel transputers.

4.4.4 Simulation of the Models

The algorithm used to simulate the fossil-fired model was of a predictor-corrector type as detailed below, where $\underline{y}_k$ and $\underline{u}_k$ are vectors of the integrable and non-integrable states at simulation step k:

1. Knowing $\underline{y}_k$, calculate $\underline{u}_k$.
2. Use $\underline{y}_k$ and $\underline{u}_k$ to give $\mathcal{F}(\underline{y}_k)$. Where $\mathcal{F}(\underline{y}_k) = \frac{d}{dt}(\underline{y}_k)$.
3. Use $\underline{y}_k$ and $\mathcal{F}(\underline{y}_k)$ to give a prediction, $\underline{y}'_{k+1}$, by the explicit Euler algorithm:

$$\underline{y}'_{k+1} = \underline{y}_k + h\mathcal{F}(\underline{y}_k)$$

   where h is the simulation step length.

4. Use $\underline{y}'_{k+1}$ to calculate $\underline{u}'_{k+1}$.
5. Use $\underline{y}'_{k+1}$ and $\underline{u}'_{k+1}$ to give $\mathcal{F}(\underline{y}'_{k+1})$.
6. Use $\underline{y}'_{k+1}$, $\mathcal{F}(\underline{y}'_{k+1})$ and $\mathcal{F}(\underline{y}_k)$ to give $\underline{y}''_{k+1}$ by the implicit trapezoidal algorithm:

$$\underline{y}''_{k+1} = \underline{y}_k + \frac{h}{2}\left(\mathcal{F}(\underline{y}_k) + \mathcal{F}(\underline{y}'_{k+1})\right)$$

7. Compare $\underline{y}'_{k+1}$ and $\underline{y}''_{k+1}$. Repeat from step 4 until the solution converges.

Conceptually, this was the simplest integration technique that could be used, though not necessarily the fastest. However, it did allow software routines to be written which quite literally listed the relationships for the non-integrable and state variables as illustrated in appendix A and this was considered to be a great advantage in implementing the simulation. Using this algorithm, the fossil-fired boiler model could be simulated with a time step of 0.2 seconds, ie. five times

slower than the 40ms time-step required to adequately model the power system equations.

It was found, however, that the hydro model could not be solved at the 0.2 second time step using the algorithm above. The equations to be modelled involved time constants comparable to those of the electrical system (as shown in appendix D) due to the nature of the model and the use to which it had originally been put. Consequently, it was decided to use a more sophisticated integration algorithm, and after some investigation, it was found that a fourth order Runge-Kutta algorithm with a step length of 20ms was successful. This resulted in the full simulation being solved at the common time step of 20ms.

The widely used fourth-order Runge-Kutta algorithm is as follows, where the equation being modelled is $\frac{dy}{dx} = \mathcal{F}(x, y)$, and h is the integration step length [100].

$$\begin{aligned} y_{n+1} &= y_n + \tfrac{1}{6}(k_1 + 2k_2 + 2k_3 + k_4), \\ k_1 &= h\mathcal{F}(x_n, y_n), \\ k_2 &= h\mathcal{F}(x_n + \tfrac{1}{2}h, y_n + \tfrac{1}{2}k_1), \\ k_3 &= h\mathcal{F}(x_n + \tfrac{1}{2}h, y_n + \tfrac{1}{2}k_2), \\ k_4 &= h\mathcal{F}(x_n + h, y_n + k_3). \end{aligned}$$

This algorithm was used to simulate the model equations listed in appendix E in the following way, where $\underline{y}_k$ and $\underline{u}_k$ are vectors of the integrable and non-integrable states at simulation step k, and h is the integration step length:

1. Use current $\underline{y}_k$ and h to calculate $\underline{u}_k$.
2. Use $\underline{y}_k$, $\underline{u}_k$ and h to give $\mathcal{F}(\underline{y}_k)$. Where $\mathcal{F}(\underline{y}_k) = \frac{d}{dt}(\underline{y}_k)$.

3. Calculate k_1 as above.

4. In a similar manner, use $\underline{y}_k$ and $\frac{h}{2}$ to calculate another $\underline{u}_k$ and $\mathcal{F}(\underline{y}_k)$.

5. Calculate k_2 as above.

6. Similarly calculate k_3 and k_4.

7. Use k_1–k_4 to calculate new states, $\underline{y}_{k+1}$, as above.

8. Recalculate $\underline{u}_k$ using whole step length, h, to hold up-to-date values for non-integrable variables to be displayed and logged.

4.4.5 Load Models

Changes in system voltage and frequency away from the nominal alters the effective load of the system. This effect was modelled in an algebraic manner by introducing 'load groups' at each busbar which altered the current injection at the busbars according to variations in voltage and frequency seen at that busbar [101, 102]. Consequently, the real and imaginary powers were changed from their nominal or 'reference' values using the following algebraic equations:

$$P = P_{ref}(P_{vk} + P_{vi}V_m + P_{vy}V_m^2)(P_{f_0} + P_{f_1}\frac{\omega + \omega_s}{\omega_s}) \quad (4.1)$$

$$Q = Q_{ref}(Q_{vk} + Q_{vi}V_m + Q_{vy}V_m^2)(Q_{f_0} + Q_{f_1}\frac{\omega + \omega_s}{\omega_s}) \quad (4.2)$$

where V_m is the magnitude of the busbar voltage,

ω is the derivative of busbar voltage angle, and

P_x, Q_x are weighting factors, $\sum P_{vx} = 1$ etc.

Speed (ω) is calculated as $\frac{s}{1+sT}\times$angle to filter discontinuities, where s is the Laplace operator.

According to Weedy [103] a typical composition of a substation load is:

Induction Motors	50–70%
Lighting and Heating	20–25%
Synchronous Motors	10%
(Transmission losses	10–12%)

Heating maintains constant resistance with voltage and hence the power varies with (voltage)^2. The power consumed in *Lighting* load does not vary as the (voltage)^2, but approximately as (voltage)$^{1.6}$. However, no further breakdown on load proportions was to be found, and it was decided to model a combined lighting and heating load with real power proportional to V_m^2 and zero reactive power.

The power consumed by *Synchronous motors* is approximately constant. Using the data in figure 3.46 of [103] and a second order least squares fit [100] the following expression for Q in terms of V was found:

V (pu)	Q (pu)
0.882	1.103
0.803	1.152
0.705	1.177
0.7	1.167
1.0	1.0

$$Q = -0.069 + 3.478V - 2.438V^2$$

Similarly, figure 3.48 of [103] was used to find the following expression for the Q-V characteristics of an *Induction motor* operating at constant shaft torque. Real power, P, was taken to be constant with respect to V.

Induction motor at full load:

V (pu)	Q (pu)
1.069	1.076
1.0	1.0
0.931	0.938
0.862	0.931
0.793	0.893
0.724	0.938
0.655	1.117

$$Q = 3.045 - 4.751V + 2.646V^2$$

Induction motor at 75% load:

V (pu)	Q (pu)
1.069	1.103
1.0	1.0
0.931	0.903
0.862	0.834
0.793	0.779
0.724	0.755
0.655	0.766

$$Q = 1.895 - 3.310V + 2.408V^2$$

Induction motor at 50% load:

V (pu)	Q (pu)
1.069	1.124
1.0	1.0
0.931	0.879
0.862	0.779
0.793	0.690
0.724	0.624
0.655	0.576

$$Q = 0.883 - 1.58V + 1.693V^2$$

It has been observed by National Grid Company staff that the sensitivity of demand to changes in system frequency is approximately 2%/Hz [104]. Consequently, the frequency sensitivity weights of all loads were set to reflect this overall effect.

The simulation of the network works on per unit values to a base of 100 MVA. This requires that the weights describing the characteristics of the loads which

are listed in the setup data sum to one hundred, rather than unity as they do within the internal calculations. This led to the definitions of the different loads in the study data as shown in table 4.1, other weights being zero or calculated when used, knowing that the sum is unity.

Type	Pv0	Pv1	Qv0	Qv1	Pf1	Qf1
Default					100	
Lighting/Heating	-100				100	
Synchronous Motor			-6.9	347.8	100	
Induction Motor 100%			304.5	-475.1	100	
Induction Motor 75%			189.5	-331.0	100	
Induction Motor 50%			88.3	-158.0	100	

Table 4.1: Load Parameter Settings

It was decided to use a mixture of loads in the approximate proportions shown in table 4.2.

70%	Induction Motors —	50%	full load
		30%	75% load
		20%	50% load
20%	Lighting and Heating		
10%	Synchronous Motors		

Table 4.2: Load Composition

Two study setups were used throughout the project — one a four generator, six busbar equivalent model of the British National Grid, the other a more detailed twenty-five generator, sixty busbar equivalent model. The load distribution for the sixty busbar version, as detailed in the study file, is shown in section G.7.

4.4.6 Running the Simulator

As mentioned previously, the situation to be simulated is set up in a study file, or set of study files. These files describe such things as the number of generating groups, the structure of the network and the powers consumed or generated at

the different busbars. Parameter settings for individual model units such as generating sets, and primemover types are also given. For the investigations reported here, two studies were used. The full supergrid system to be modelled is shown in figure 4.5(a). The first study modelled this system as an equivalent four generators, with a network of six busbars as shown in figure 4.5(b). The CEGB group models the equivalent of 21 identical generators, DINORWIG six, NWALES one and SCOTLAND five. Appendix F lists the study files describing this equivalent system. The second study modelled the grid as an equivalent twenty-five generators and sixty-six busbars. This study is based upon that used by Berry [75], with modifications to allow frequency and voltage sensitive loads as described in section 4.4.5 and to model the Dinorwig pumped storage scheme in North Wales as six independant generating groups rather than one common group. The network diagram of this system is shown in figure 4.5(c). Appendix G lists the study files describing this system.

On first running the simulator, the master study file is read and the data copied to the simulator's internal database, with conversions to per unit values as appropriate. Using the network interconnection data and the data for generated and consumed powers, a total network admittance matrix is constructed. The simulation then proceeds to solve the generator and load equations in parallel to produce current injections at the network nodes. This stage is followed by the calculation of the network equations to solve for the network voltages. The network calculation may also be performed in parallel if appropriate hardware is available (see section 5.2.1 for the different hardware setups available to run the simulator) and the network is complex enough to justify a parallel solution [76]. A check for convergence of the network solution is made, and these two stages re-iterated until the solution converges. The simulator then progresses on to the next model time step.

Under steady state model conditions, each step requires only one iteration. However, when the model states are changing rapidly, several iterations may be required. Real-time operation can be achieved if the time taken for each model time step is the same as the true 'clock' time that that step represents, ie. 20ms in the particular studies reported here. When model states change and more than one iteration per step is required, the simulation may slow down. As long as the solution for one iteration takes less than the time alloted, once the model states settle down, the simulator can run fast for a while until it has caught up the lost time. This is known as 'soft' real-time operation, as the simulator falls behind 'clock' time while it is busy, and catches up again during steady state operation, meaning that over an extended period it follows 'clock' time.

How quickly a model step can be calculated depends on the complexity of the problem, ie. the size of the network and the detail of the generator and load models, and the processing power available. The most powerful computing facility available to the author was the sixteen transputer rig described in section 5.2.1 and by Chan [76]. The four machine study of appendix F could be run in real-time using one Transputer. However, the twenty-five machine study including frequency and voltage sensitive loads was rather slower than real-time when run on all the processors available.

For the extent of investigations covered by this report, real-time is not of importance, other than meaning less time to wait for results to be acquired. However, in any future work to test operational controller software prior to installation on a live system, a real-time simulation would be invaluable.

4.4.7 Controllers

4.4.7.1 Boiler Control

It was necessary to add a closed loop boiler control system to the fossil-fired primemover model. Within a power station boiler a number of variables need to be controlled, such as steam temperature and the pressure within the furnace. However, as far as the characteristics presented to the grid are concerned, it is the load control system which is the most important. Hence, the simplifying assumption was made that all other controls held their outputs constant and were not modelled in detail.

The control of load output of a power station unit is part of a two-input, two-output system. The inputs are the fuel flow into the furnace and the positions of the governing valves (modelled as one main governor valve in this simulation). The outputs are the load of the unit, the MW, and the steam pressure at the output of the secondary superheater.

There are a number of controller structures which can be used with this multi-variable system. The most traditional system, known as boiler-follows-turbine (BFT), uses the position of the governor valve to control load, L, and the fuel input to control the changes in pressure, Ps, inflicted by the movement of the valve. This is shown in figure 4.6. A second structure is known as turbine-follows-boiler (TFB) and is shown in figure 4.7. In this case, the governor valve is used to control the steam pressure, and changes in load are affected by altering the fuel input to the boiler. This method has an advantage in terms of wear and tear on the boiler as it does not allow such severe transients in pressure as the BFT

method. However, it requires modifications in order to be responsive enough to load changes required for the regulation of grid frequency. The two figures also illustrate the means by which the unit control is modified in order to help regulate the system frequency, f.

The initial control system implemented in the simulation was of a multi-variable type based on one installed at a British power station [105]. This was chosen for ease of access to the algorithms. Later, a BFT system based upon the model parameters was designed as described in section 4.4.7.2. This was to enable the characterisation of controllers for different size of units, since the multi-variable controller was designed specifically for that station and was found not to be so successful on models of other sized units.

4.4.7.2 Design of a Boiler-Follows-Turbine Unit Control System

A block diagram of the fossil-fired boiler model is shown in figure 4.8. The variables and parameters relate to the definitions given in appendix B. Two control loops need to be designed for the unit control system — a loop controlling superheater outlet pressure by varying the fuel input, and a loop controlling load output by varying the governor valve position. Because of the wide difference in the time constants dominating the plant of these two loops, they can be designed quite separately. Since the plant is non-linear, a linearised reduction of each loop was made at several different operating points. In general, the variation in pressure to allow operation at different unit power outputs is quite small compared to the range of the load output, ie. the relative operational variation in MW is rather larger than the corresponding variation in pressure. Consequently, it was decided to form a reduced model of each loop at varying loads, ie. MW, but

constant superheater outlet pressure.

Appendix H details the derivation of the linearised models used in the design of the pressure control loop, whilst appendix I details the corresponding derivation for the load loop. The figures used in these illustrations are for the 500 MW oil-fired boiler model.

Pressure Loop Neglecting d.c. gain, the following fourth order equivalent transfer functions were derived for the plant in the pressure loop at different load levels.

$$G(s)|_{170\,MW} = \frac{1}{s^4 + 0.57906s^3 + 0.0966963s^2 + 0.00418037s + 7.4823.10^{-7}} \tag{4.3}$$

$$G(s)|_{250\,MW} = \frac{1}{s^4 + 0.498633s^3 + 0.0757525s^2 + 0.00324256s + 7.4828.10^{-6}} \tag{4.4}$$

$$G(s)|_{390\,MW} = \frac{1}{s^4 + 0.43117s^3 + 0.0579801s^2 + 0.00240117s + 1.03934.10^{-5}} \tag{4.5}$$

$$G(s)|_{490\,MW} = \frac{1}{s^4 + 0.408192s^3 + 0.0521148s^2 + 0.00216454s + 1.38646.10^{-5}} \tag{4.6}$$

A proportional plus integral, PI, controller was chosen to control this system and appropriate gains acquired through the design process outlined in appendix H. Subsequently, it was found that the following gains adequately controlled the superheater outlet pressure of the non-linear 500 MW oil-fired boiler model throughout the load range:

$$K_p = 0.6366 \tag{4.7}$$

$$K_i = 0.006366 \tag{4.8}$$

where K_p and K_i are the controller's proportional and integral gains respectively. This leads to a controller of the form shown in figure 4.9.

Load Loop Using a similar block diagram reduction technique the following transfer functions were obtained for the plant in the load loop, as outlined in appendix I.

$$G(s)|_{170\,MW} = \frac{47322.3(s^2 + 4.42745s + 0.522409)}{s^3 + 5.89927s^2 + 6.81264s + 0.0230386} \tag{4.9}$$

$$G(s)|_{250\,MW} = \frac{19371.1(s^2 + 3.29252s + 0.370477)}{s^3 + 4.76775s^2 + 5.07439s + 0.151419} \tag{4.10}$$

$$G(s)|_{390\,MW} = \frac{20294.1(s^2 + 2.30094s + 0.243892)}{s^3 + 3.78077s^2 + 3.55595s + 0.388158} \tag{4.11}$$

$$G(s)|_{490\,MW} = \frac{19101.4(s^2 + 1.94571s + 0.197154)}{s^3 + 3.42798s^2 + 3.012003s + 0.678126} \tag{4.12}$$

To achieve zero steady state step error and reasonable speed, integral, I, control is all that is required to control a system of this form as shown in figure 4.10. Subsequently, it was found that the following gain adequately controlled the load

output of the non-linear 500 MW oil-fired boiler model throughout the load range, as detailed in appendix I.

$$K_i = 0.00025 \tag{4.13}$$

Controller Implementation The model of the boiler assumed the unit was controlled by a digital rather than analogue controller, as is the case in modern power station practice. Therefore, to implement the controllers within the simulator software they needed to be digitised. This digitisation is shown in appendix K for both PI and I controllers.

A similar design to that explained above, and outlined in appendices H and I was performed for a 500 MW coal-fired boiler, leading to the use of the controller gains listed in table 4.3 and as specified in the simulation study files.

Boiler Type	Pressure Loop		Load Loop
	K_p	K_i	K_p
Coal 500 MW	0.6295	0.003777	0.00025
Oil 500 MW	0.6566	0.006566	0.00025

Table 4.3: Boiler-Follows-Turbine Controller Gains

By simulation, it was found that these gains were also adequate to control the 660 MW boiler models, whose dynamics were not very much different to the 500 MW units.

4.5 Summary

This chapter has presented details of the simulation used for the study of automatic load-frequency control on the British grid system. The need for simulations in such work has been discussed together with examples of other simulations.

The development of power system simulation at the University of Bath has been described and further developments necessary for the current study have been presented. Detailed models have been given for different primemover types and for loads sensitive to frequency and voltage variations. Finally, load control of the generating units has been described.

Chapter 5

Computing Facilities

A variety of computing facilities was used during the course of this work for both the off-line development and analysis, as well as the on-line simulation studies. This chapter describes some of the hardware and software used.

5.1 Off-Line Facilities

A good deal of the off-line work, including linearisation of the fossil unit models and the corresponding design of unit controllers, was performed on a Motorola MC68000 based multi-user, multi-processor machine under the Tripos operating system [87, 88, 89]. This hardware was based on the single board computer units described by Dale [74]. The original Tripos was a single-user, multi-tasking operating system for small computers initially developed at the University of Cambridge and modified at the University of Bath to also support a multi-user, multi-processor environment. Tripos itself is written in the BCPL high level language and also supports FORTRAN, LISP, PASCAL and ANSI C. A number of facilities were available on this system, such as the symbolic mathematics program REDUCE [106], a root locus generating program and a graph plotter. The

first C version of the Bath University Power System Simulator was also available on this system having been translated from the original BCPL version [92]. Consequently, this was a convenient environment for the initial development of generating unit models and off-line analyses. However, this system did not offer sufficient computing power to run the full power system simulator at a reasonable speed.

5.2 On-Line Facilities

5.2.1 Hardware

In order to use the standard power system simulator to simulate yet more complex systems in real-time, more powerful computing facilities were needed. At this time, the simulator programs were written in BCPL and ran on a Motorola MC68020 based parallel computer under the Tripos operating system as described by Berry [75]. Decisions were taken with regard to the best way forward to improve the performance of the power system simulator. Other simulation work on diesel engines within the department also required the use of more processing power and this led to the development of a new parallel computer based on the Inmos Transputer [107]. The other options available at the time were to redesign the existing MC68020 based computer using new high speed components or to use an upgraded version of the same family of processors, for example, the MC68030, or to use the then new Intel 80386 processor in a new computer design. However, it was found that the transputer based option promised the best improvement in performance still at a reasonable cost.

The standard means of inter-processor communication in a transputer system

is via transputer links. However, this did not provide sufficient communication bandwidth for the diesel engine simulation which had a high communication burden in relation to the calculation burden on the processors. Hence, a shared memory architecture was designed together with a new fast multiprocessor backplane bus [108] as well as the transputer link bus. Building an in-house parallel computer based on the T800 transputer [94] was found to be less costly than buying a commercial system with all of these facilities.

It was felt that the new transputer based parallel computer would also offer significant improvements in the performance of the power system simulator and allow more complex systems to be modelled in real time. Initially, it was estimated that the communication burden of the power system simulation would match the calculation burden when the transputer links were used as the communication mechanism. Using the shared memory for communication would lead to a saving approaching 50% of the total processor burden by significantly reducing the communications burden. However, in practice, it was found that the T800 transputer did not improve the calculation performance as well as the initial data suggested it might. Consequently, the calculation burden was still significantly higher than the communication burden rather than being comparable. In this situation, the saving to be gained by using shared memory as the communication mechanism represented only about 15% of total processor burden. In order to use the shared memory instead of the standard transputer links for communication, it was necessary to provide special software primitives for accessing the shared memory. This meant that non-standard and non-portable software would have to be used if advantage was to be taken of the shared memory communication mechanism. In the case of the power system simulator, it was decided that the realisable 15% saving was not sufficient to warrant losing portability of the software and consequently this facility was not used.

A block diagram of the T800 based parallel computer is shown in figure 5.1. The machine is housed in several 19-inch racks and has sixteen processing nodes per rack. Each processing node consists of an Inmos T800 transputer, 1 MByte of dynamic RAM (DRAM), a multiprocessor bus interface, local and multiprocessor bus arbiter logic and high speed line drivers to connect the transputer links to other boards via the backplane. A block diagram of the T800 processing node is shown in figure 5.3.

A transputer is a single VLSI micro-processor with on-chip memory, a central processing unit and communication links for direct connections to other transputers. The T800 transputer used in the parallel computer has a 32 bit bus, 4 KBytes of on-chip memory, a 64 bit floating point co-processor and four direct memory access (DMA) controlled serial links [94]. Figure 5.2 shows a block diagram of the T800 transputer.

The T800 exploits fast on-chip memory by having only a small number of registers and simple instructions. It uses multiplexed address and data signals in its 32 bit memory bus. A built-in memory controller provides DRAM control and refresh timing. The internal processor speed is link selectable and is generated by a 5 MHz external clock. The transputer can be booted either from a communication link or from a ROM (Read Only Memory). All the processing nodes in the parallel computer are booted via links.

The input/output (IO) system for the transputer based parallel computer was developed by Hafeez and is based on the Philips SCC68070 micro-processor [109]. Figure 5.4 shows a block diagram of the IO board. The SCC68070 has an on-chip memory management unit, a two channel DMA controller, a serial interface, and inter-integrated circuit (I^2C) bus interface and a timer. The IO system built

around it exploits these features to connect to external devices such as disk drives, printer and a console. Floppy disks, a hard disk drive and a tape streamer are available. In order to connect the IO board to the other T800 based boards in the system, a bi-directional, two wire transputer link is provided via an IMSC012 link adapter.

A graphics board is also provided which consists of a T800 transputer, a Philips SCN66470 Video and System Controller (VSC), a Philips 68070 micro-processor, keyboard and mouse interfaces, a colour palette and two banks of memory. A block diagram of the board is shown in figure 5.5. The 4 MBytes of local memory is available to the operating system and is refreshed by the T800. The other 1 MByte bank is used for video and display data and is controlled by the VSC.

The hardware just described forms a complete computing system. However, in these studies, an alternative arrangement was used. It was convenient to use extra space on the graphics card just described for other circuitry. In this arrangement, differential line driving circuitry was employed to provide an interface between the sixteen transputer rack and a remote computer. The parallel computer is connected to a commercial transputer card [110] plugged into a personal computer (PC) [111] in an adjacent room. The physical arrangement of the hardware is such that one transputer link on the plug-in card is used for PC-transputer communications while the remaining three links connect into the parallel computer via the differential lines. Further circuitry, also situated on the graphics board, provides hard-wired links to connect together the sixteen transputers of the parallel computer, the transputer on the graphics card and the transputer plugged into the PC to form a network as shown in figure 5.6. Peripheral devices such as monitor, graphics monitor, keyboard and disks are available via the PC. Hosting the transputer network via a PC in this way was not only a convenient

interface to the parallel computer but also provided flexibility and allowed the use of readily available PC software for off-line work. For the smaller simulations it was adequate to use just the single transputer plugged into the PC which allowed other users to take advantage of the computing power of the multi-processor computer. When it was required to use the parallel computer, it was necessary to connect the differential line between the transputer rack and the PC and to run the appropriate operating system for the network.

5.2.2 Software

The operating system chosen to run on this hardware was Helios [93]. Helios is a multi-user, multi-processor distributed operating system designed to run on a wide range of multi-processor architectures and originally targetted at transputer based networks. Much of Helios is written in C and C was chosen as the high level language in which to implement the newest version of the power system simulator. Helios is intended to provide a Unix compatible programming interface.

The natural choice of operating system for a transputer based computer might have seemed to be the Transputer Development System (TDS) supported by the manufacturers, Inmos. This would have encouraged the use of OCCAM as the high level progamming language, the transputer having been developed to exploit the OCCAM model of parallel programming. However, OCCAM had a number of disadvantages. It did not support dynamic memory allocation making it unsuitable for use in complex programs. It was a specialist language with little prospect of being ported to a large number of other processors. This meant that if future versions of the simulator were to be run on other processors, the software would have to be rewritten in yet another new language. Finally, this

option would not have allowed useful programs and tools to be readily ported from other systems such as Unix based machines.

The Helios/C solution did not suffer from these disadvantages. C was a language which was becoming increasingly popular and supported on a wide range of processors. This would mean little or no re-writing of code to port the simulator to other hardware. It would also mean that other applications written in C could easily be ported to the Helios environment. Helios provides a Unix like user interface which would make the simulator more readily accessible to users already familiar with Unix or similar environments. It was also hoped that Helios would be developed to run on other new processors as technology progressed. However, in the event, the use of C has proved to be the most useful factor in allowing serial versions of the simulator to be run on a variety of different computers without the Helios operating system, including SUN and APOLLO workstations and IBM PCs [76]. To take full advantage of the processing power available from the transputer based parallel computer to run the more complex simulations in real-time, Chan took advantage of Helios' explicit message passing protocols and produced a parallel version of the simulator based on the typical Helios client-server model [76]. It was to this version of the simulator that the more detailed models of this study were added.

5.2.2.1 Helios

Helios controls all the resources available within a transputer network, and provides a consistent mechanism for accessing these resources, hiding the distributed nature of the architecture from the user. A standard server program for the host machine acts as an interface to the transputer network and allows the user to

access all the standard features of the host environment. The main components of Helios are the nucleus, servers, the posix library and the user interface.

The user interface is provided by a task called Shell that acts as a command line interface to the operating system and enables the user to create and control jobs interactively, both in the background and the foreground. Shell includes various shorthand techniques to save typing and personalisation methods to enable users to define their own commands. Several shells may be run simultaneously.

The nucleus is the minimum system that must be present on every processor in the network. Its prime purpose is to control the resources of a single processor and to integrate it into the global system. The nucleus consists of six parts: Kernel, System Library, Server Library, Utility Library, Processor Manager and Loader. The Kernel is responsible for the processor hardware and provides low-level calls such as message passing, semaphore synchronisation, and creating and destroying processes. The System Library provides the basic interface between clients and servers containing library routines such as `Open()` and `Read()`. The Server Library exists to assist in writing Helios servers and the Utility Library provides a number of further library routines. The Loader is a Helios server which takes care of pieces of code loaded into its processor, and which ensures that code is shared between programs where possible. The Processor Manager is also a server which allows clients to run programs or tasks on that processor. It takes care of signals sent to a particular task and ensures that any resources used by a program are freed when a program exits.

Helios is based on the client-server model of computing in which a client program wanting some service sends a message to a server program which performs the operation and returns a reply message. For example, to read data from a file it is

necessary to interact with a file server. A general server protocol (GSP) defining the structure of these messages is supported by all Helios servers. Each server consists of a single task within which a single dispatcher process is dedicated to receiving the requests and queuing them for attention by a second process. This second process may be either a static process, a dynamically created process or a pool of worker processes to handle each request as it arrives.

The posix library is provided in Helios to make it compatible with Unix. This facility aids portability of existing programs and tools from the Unix environment to Helios.

5.3 Summary

This chapter has described the hardware facilities and programming environments available for the development of the power system simulator as well as for off-line analyses. The on-line simulation work was performed on a Transputer based parallel computer hosted by a PC and running the Helios operating system. The simulation software was written in C. Several environments were available for off-line work including the Helios machine, the PC running the MSDOS operating system and another in-house multi-user computer based on Motorola MC68000 processors running the Tripos operating system and using a variety of programming languages.

Chapter 6

Four Machine Studies

6.1 Validation of Fossil Model

6.1.1 Stored Energy Tests

The fossil unit model was validated by comparing its response to stored energy tests with those of the model on which it was based which had itself been validated against stored energy tests performed at Ratcliffe Power Station in October 1969 [98]. The tests were performed by forcing a step change in governor valve position from a part load condition to fully open. The resulting transients in load and pressure characterise the plant. Results of the tests performed on the model are shown in figures 6.1, 6.2 and 6.3. These compare with the base results as shown in table 6.1.

The current model results can be seen to compare quite well with those of the earlier model. The discrepancies with the plant test results are mostly due to effects which have not been modelled such as the fact that superheater spray flow is not actually constant as is modelled and that steam temperature is also

Test	Ratcliffe 450 MW/MAX	Base Model 450 MW/MAX	Simulation 450 MW/MAX
Initial load change	457–502 MW	450–487.9 MW	450.602–479.812 MW
Time to load peak	54 sec	30 sec	22.9 sec
Δ load	45 MW	37.9 MW	29.21 MW
Test	Ratcliffe 400 MW/MAX	Base Model 400 MW/MAX	Simulation 400 MW/MAX
Initial load change	400–486 MW	400–474.82 MW	399.998–473.015 MW
Time to load peak	50 sec	30 sec	25.4 sec
Δ load	86 MW	74.82 MW	73.017 MW
Test	Ratcliffe 350 MW/MAX	Base Model 350 MW/MAX	Simulation 350 MW/MAX
Initial load change	348–462 MW	350–462.46 MW	350.11–466.027 MW
Time to load peak	36 sec	30 sec	22.9 sec
Δ load	114 MW	112.46 MW	115.917 MW

Table 6.1: Results of stored energy tests

not held absolutely constant as the steam flow changes. It was also found from simulation tests that the actual operating condition of the plant, particularly the value of superheater outlet pressure made a significant difference to the absolute results of stored energy tests.

6.1.2 Generating Unit Load/Pressure Control Tests

As described in section 4.4.7.1, two principal control loops in a fossil-fired unit are those regulating superheater outlet pressure, and controlling turbine output power. Tests were performed to investigate the behaviour of the two types of controller, ie. Boiler-Follows-Turbine (BFT) control and a multi-variable controller currently in operational use in a British power station. Changes in both power setpoint, often called load setpoint, and pressure setpoint were used.

6.1.2.1 Load Setpoint Changes

Figures 6.4 and 6.5 show the results of a load setpoint increase in the one NWALES unit (figure 6.4 for the BFT, and figure 6.5 for the multi-variable controllers). In order to maintain the overall load/generation balance, this has been accompanied by a decrease in load setpoint in the twenty-one CEGB units. In order to reduce the effect of load changes on the pressure control, the setpoint, L_{sp}, is rate limited and ramps towards the new desired value, L_{dv}. From the NWALES generation traces it can be seen that both controllers enable the generation, P_{mw}, to closely follow the ramping setpoint, L_{sp}. The multi-variable control is a little tighter but also has slightly more overshoot. Because the twenty-one CEGB units can complete their small load change faster than the single NWALES unit can complete its rather larger change (since each individual unit has the same rate limit on L_{sp}), during the load change there is a load/generation imbalance which results in an error in frequency. For this test, there is no frequency error term in the $L_{sp}s$ so that they simply follow L_{dv}. However, the speed control onto the governor valves forces an offset proportional to frequency error in the valve position Z_{gv} away from its nominal position set by the speeder motor, Z_{gvc}. This effect prevents the CEGB units from following the L_{sp} ramp but rather to lag it to reduce the frequency error. This mismatch of Z_{gv} and Z_{gvc} can clearly be seen in both CEGB governor graphs (figures 6.4(b) and 6.5(b)). The most obvious differences in the behaviour of the two types of unit controller may be seen in the pressure and fuel flow graphs. In the BFT case, two separate control loops operate, one altering speeder motor position in order to control load and the other varying fuel flow to regulate pressure. In figure 6.4(b), the pressure variations, P_2, caused by the changes in governor valve position can be seen together with the changes in fuel flow, M_{fu}, required to correct them. The multi-variable controller does not treat the system as two independent loops, but rather calcu-

lates changes in both Z_{gvc} and M_{fu} required to control both P_2 and P_{mw}. This controller achieves a tighter pressure control than the BFT controller, as shown in figure 6.5(b), by varying the fuel flow more rapidly. This comes about because the BFT controller requires the pressure to have changed before it has an error to correct which it reacts to fairly slowly, whereas the multi-variable controller is able to, in effect, anticipate the changes required in fuel flow immediately to support the change in load.

6.1.2.2 Pressure Setpoint Changes

Figures 6.6 and 6.7 show the results of a pressure setpoint decrease in the single NWALES unit. In this case, the load controllers are operating in a sustained mode whereby L_{sp} contains a component proportional to frequency error as can be seen in all the generation graphs where L_{sp} is slightly offset from L_{dv} because of the small error in frequency.

As in the case of the load setpoint change, the pressure setpoint, P_{sp}, is rate limited and ramps towards the desired value, P_{dv}, rather than following it directly. However, it may be seen from the NWALES pressure graphs that the dynamics of this particular unit are rather too slow to follow this ramp very closely.

Considering the BFT case (figure 6.6(b)), it can clearly be seen how the fuel flow, M_{fu}, reduces at the start of the downward ramp of the setpoint. Gradually, the pressure, P_2, starts to decrease. The decrease in pressure has an effect on the load loop since it leads to a decrease in steam flow. Thus, in order to maintain the power output, the load loop increases the governor valve position to compensate for the decrease in pressure. The load loop has rather faster dynamics than the

pressure loop and easily copes with the speed of the pressure change. This results in only a small fluctuation in the power, P_{mw}, away from its setpoint, L_{sp}, as the pressure changes (see figure 6.6(a)). Because the NWALES generation fluctuates only very slightly, there is no noticeable effect on the other generators.

In the case of the multi-variable controller, figure 6.7(b) illustrates how both inputs, Z_{gvc} and M_{fu}, are varied rather more rapidly to effect the change in pressure. However, it would appear from the P_2 trace that this controller is not really appropriate to the very slow dynamics of this loop, and, in particular, M_{fu} appears to be changed too quickly. There is interaction apparent in P_{mw} which is sufficient to effect slightly the other generators. The structure and gains for this controller were taken from an operational load controller which had been specifically designed for that particular plant using a discrete "black-box modelling" approach. Consequently, it was not possible to "tune" this loop simply since the physical meaning of the gains in this type of controller are not evident as they are in the PI type of controllers used in the BFT design. Hence, the BFT design was used throughout the following results since it was more flexible.

6.2 Validation of Hydro Model

The hydro model used for these studies was based upon the model of Dinorwig power station described in [99]. The current simulation of Dinorwig was validated with reference to this original model.

6.2.1 Lookup Tables for Non-Linear Characteristics

Certain model non-linearities such as the torque/speed and discharge/speed characteristics were implemented within the simulation by means of a lookup table. To validate the operation of this code, it was used to reproduce graphs of these characteristics which were then compared to the original characteristics given in [99], figures 2.2 and 2.3. The reproduced graphs are shown in figure 6.8 and compare well with those of [99].

6.2.2 Response to Manual Ramping of Guide Vane Position

A similar validation test to that used in [99] was performed whereby the guide vanes were ramped open at their maximum rate. The results of this test are shown in figure 6.9. The initial conditions were such that the DINORWIG group representing all six units was spinning in water, synchronised to the grid, but delivering no power. The results compare quite closely with those given in figures 3.1 and 3.2 of [99]. The small discrepancies in absolute level of some variables are due to the difficulties of matching the operating conditions exactly. However, the dynamic responses match closely.

6.2.3 Response to Power Setpoint Change

In [99] the model was used to perform a series of tests to investigate the governor characteristics of Dinorwig, some of which were responses to power setpoint changes. One of these was repeated with the current simulation to further validate the matching of the two models. These results are shown in figure 6.10.

The conditions of this test were similar to those in figure 6.18 of [99], where the input was a 0.2 pu. power setpoint change. There is fairly good matching of the dynamics as seen before. However, there is some discrepancy in the levels of some variables. This is due to the different operating points at which the simulations were performed and differences in the simulations outside of the dynamics of just the hydro system, ie. in the modelling of the rest of the power system to which the hydro model was connected.

6.3 System Split Studies

It has been proposed (see section 3.5.3) to operate the system as two separate control areas such that the frequency in each area may be controlled together with the power flow on the tie-lines linking the two areas. The system characteristics required for the design of the controller can be determined from system split tests [20]. The following discusses a series of results of system split tests on the four machine simulation which were used to determine the system power-frequency characteristics of the two areas. In these tests, all tie-lines between the two areas were opened whilst the power being carried by them was approximately 565 MW. The accompanying figures illustrate the resulting frequency and generation changes.

6.3.1 System with Dinorwig Generating and Insensitive Loads

6.3.1.1 Sustained Unit Controllers with 5% MCR/min Setpoint Rate Limits

Figure 6.11(a) shows the response of the frequencies in the two areas following the disconnection of the inter-ties and the resultant changes in generation, while figure 6.11(b) shows the corresponding mechanical torque changes and the movements of the speeder motor position (Z_{gvc}) and the governor valve (Z_{gv}).

SCOTLAND Generation in figure 6.11(a) illustrates clearly in P_{mw} the immediate decrease in electrical load on the Scottish machines when the tie-lines are opened. There are five machines each with a decrease in load of about 113 MW, ie. a total of 565 MW, corresponding to the power being exported by the tie-lines prior to the split. This decrease in electrical load causes an imbalance between the electrical load and the mechanical power into the generator (as illustrated by SCOTLAND Mechanical Torque, T_m, in figure 6.11(b)). This causes the machine to increase in speed (as illustrated by f_{sco} in figure 6.11(a)). The increase in speed causes the governor speed controller to close the governor valve (Z_{gv} in SCOTLAND Governor, figure 6.11(b)) which, in turn, causes a reduction in mechanical torque produced (SCOTLAND T_m). During this time, the unit load controller is attempting to match generation, P_{mw}, with the setpoint, L_{sp}. In response to the rise in frequency, L_{sp} is reduced by the controller to help correct that rise. However, the rate limit on L_{sp} prevents it from falling very quickly and there is a substantial error between L_{sp} and P_{mw}. This error causes the load controller to increase the speeder motor position Z_{gvc}. This does not, however, cause an increase in the governor valve position since the speed controller is

forcing an offset between Z_{gvc} and Z_{gv} proportional to the frequency error. Once Z_{gvc} reaches its upper limit, Z_{gv} is able to remain at a level which matches the mechanical torque, T_m, with the electrical load, P_{mw}, so that the frequency remains constant. A much longer run reveals that once L_{sp} has reduced to the level of P_{mw}, the governor motor comes off its limit and allows the offset between Z_{gvc} and Z_{gv} to reduce T_m so that the frequency falls back towards 50 Hz. This long term trend is further discussed in section 6.3.3.

The response of the machines in England and Wales is a little different because of the regulating action of DINORWIG. When the system splits, the electrical load on the machines immediately increases. DINORWIG is in a mode whereby it is responding only to errors in frequency and is not also trying to maintain its generation at any particular setpoint. This means that after the initial increase in generation, DINORWIG continues to rise taking increasingly more of the share of the extra load. This allows the CEGB and NWALES machines to reduce their generation back towards their setpoints. Because of the rate limit on the CEGB and NWALES setpoints, L_{sp}, the response is rather slow and oscillatory until all the England and Wales machines settle out with a proportionate share of the extra load.

The situation of a slow oscillatory response due to rate limits reflects what can happen in practice. However, it is difficult to determine what is the frequency change due to the sudden load/generation imbalance. It would be impractical to wait for the system to reach a steady state condition as other disturbances would be likely to occur before that happened. Consequently, the simulation was repeated with no rate limit on the $L_{sp}s$ of the fossil units.

6.3.1.2 Sustained Unit Controllers without Setpoint Rate Limits

Figure 6.12(a) shows that the frequencies in both subsystems settle out much sooner than in the systems with setpoint rate limits. From the graphs of generation in figure 6.12(a) it can be seen that the generation setpoints come very much more quickly to the level required to balance mechanical torque with electrical load allowing a more rapid recovery of frequency. This is particularly evident in the results for SCOTLAND. These results allow the difference in frequency before and after the split to be readily obtained from a fairly short simulation run.

6.3.1.3 Non-Sustained Unit Controllers

The results of this test are shown in figures 6.13(a)&(b). When non-sustained load controllers are used for the fossil units, the generation setpoints, L_{sp}, are not augmented with a term based on frequency error and hence remain constant when the frequency changes due to the system split.

In the England/Wales subsystem, the speed controllers directly onto the governor valves still ensure that the valves open when the frequency falls thus increasing mechanical torque to help support the increase in electrical load. However, as the power output from DINORWIG slowly increases because of its regulating action, the fossil unit load controllers reduce the speeder motor position, Z_{gvc}, so that their power output returns to the setpoint.

The SCOTLAND machines are not supported by other regulating units. The governor valve, Z_{gv}, is closed in response to the increase in frequency. However,

the speeder motor position, Z_{gvc}, increases in an attempt to return the generation to its setpoint. When the speeder motor hits its upper limit, the speed controller is able to position the governor valve in order to arrest the rise in frequency.

6.3.1.4 No Fossil Unit Load Control

In the set of results shown in figures 6.14(a)&(b), only the speed control directly onto the governor valve is active in the fossil units and hence they show that part of the more complex responses previously discussed which is due only to the speed loop. Because there is no unit load control, the speeder motor positions, Z_{gvc}, remain constant. The speed controller moves the governor valves, away from the nominal position set by the speeder motor, in response to frequency error and thus ensures that the mechanical torque matches the electrical load. Again, in the England/Wales subsystem, DINORWIG generation is still responsive to frequency error and, on a slower timescale, DINORWIG gradually takes on a share of the correction of the frequency error, allowing the extra generation of the CEGB and NWALES machines to decrease a little.

6.3.2 System with Dinorwig Pumping and Insensitive Loads

In order to investigate the regulating abilities solely of the fossil units without the assistance of DINORWIG, the system characteristics whilst DINORWIG is pumping were investigated. The previous four runs were repeated for a system where DINORWIG was pumping instead of generating.

6.3.2.1 Sustained Unit Controller with 5% MCR/min Setpoint Rate Limits

Figures 6.15(a)&(b) correspond to similar conditions to figures 6.11(a)&(b) (discussed in section 6.3.1.1). The response of the Scottish system is the same since the changed status of DINORWIG does not affect the Scottish subsystem. The CEGB and NWALES machines do not reduce output as previously happened since the DINORWIG generation is not there to take a share of the increased load. The frequency in the England/Wales subsystem continues to fall as it is not arrested by the increased generation from DINORWIG as before. The slow ramp of the CEGB generation setpoint, L_{sp}, prolongs the time for which there is an error in the unit load controller. This causes the stepper motor position, Z_{gvc}, to continue to decrease. The governor speed controller ensures that the governor valve position, Z_{gv}, is kept high. However, until Z_{gvc} stops falling, ie. when the L_{sp} ramp meets the generation P_{mw}, the offset of Z_{gv} from Z_{gvc} produced by the speed controller will not be sufficient to arrest the fall in frequency.

6.3.2.2 Sustained Unit Controller without Setpoint Rate Limits

The results of figures 6.16(a)&(b) compare with those in figures 6.12(a)&(b). Again, the response of the SCOTLAND subsystem is essentially the same as before. The difference in the setpoint trace, L_{sp}, is due to the fact that the frequency fall occurs at a slightly different point within the three-second digital unit load controller interval. This results in a slight difference in the timing of the speeder motor movement, Z_{gvc}. As has been seen before, the difference between Z_{gvc} and the governor valve position, Z_{gv}, reflects the frequency variations.

The response of the CEGB and NWALES unit load controllers are such as to ensure that the speeder motor position, Z_{gvc}, does not decrease unnecessarily as in the test of section 6.3.2.1.

Comparing the results of this test with those of the similar setup with DINORWIG generating, section 6.3.1.2, figure 6.12, it can be seen that the CEGB and NWALES units take on more of the required generation increase now that DINORWIG is not contributing.

6.3.2.3 Non-Sustained Unit Controllers

The conditions in figures 6.17(a)&(b) compare with those in figures 6.13(a)&(b) (discussed in section 6.3.1.3). Again, the response of the Scottish machines is the same. As for the responses of the CEGB and NWALES machines, and the continuing fall in frequency, similar comments to those in section 6.3.2.1 may be made. The governor speed control ensures that the generation is kept above its setpoint due to the falling frequency. Because of the non-sustained unit controllers, the generation setpoints, L_{sp}, have no frequency term and so remain constant. The error between L_{sp} and P_{mw} causes the unit load controller to decrease Z_{gvc}. As discussed before in section 6.3.2.1, the offset of Z_{gv} above Z_{gvc} cannot arrest the fall of frequency until Z_{gvc} stops decreasing. The conditions of this test produce a more severe decrease in frequency since Z_{gvc} will continue to ramp down until its bottom limit.

6.3.2.4 No Fossil Unit Load Control

The controllers used for the results of figures 6.18(a)&(b) were the same as those for figures 6.14(a)&(b). As before, the SCOTLAND response is the same. In the case of the CEGB and NWALES units, the governor valves open in response to the fall in frequency, but the speeder motor position does not change because there is no unit load control and the frequency fall is arrested. Whereas in the test of section 6.3.1.4, DINORWIG took a share of the increased load, here the CEGB and NWALES units remain at the higher output powers to take all the increase themselves. Because their mechanical torque has to rise higher than before and takes a short time to achieve this the overall frequency fall is a little further than that for section 6.3.1.4.

6.3.3 Longer Timescale Responses

It was noted previously (section 6.3.1.1) that when the unit load controller employed has a rate limited setpoint, in the case of the Scottish subsystem, this resulted in the speeder motor position being limited at its upper position. Even without limiting, as happens in the England/Wales subsystem, the fact that the speeder motor position moves contrary to that of the governor valve in the controller's attempt to redress the load error, results in a slow oscillatory recovery of the system to a steady state condition. It has been assumed (section 6.3.1.1) that this final steady state condition matches that more quickly achieved when the unit load controllers have no setpoint rate limit.

The runs of sections 6.3.2.1 and 6.3.2.2 were repeated over a longer timescale. The results are shown in figures 6.19(a)&(b) (setpoint rate limit of 5% MCR/min)

and 6.20(a)&(b) (no rate limits). The oscillatory response due to the rate limit can clearly be seen in figure 6.19. Comparing the final steady state conditions of the two sets of results confirms that they are indeed the same. Hence it is justifiable to use the results of the unlimited case to calculate the system power/frequency characteristics of the more realistic limited case. Consequently, the power/frequency characteristics of the two areas were calculated from the results of sections 6.3.1.2 and 6.3.2.2 for the cases of DINORWIG generating and pumping respectively.

6.3.4 Systems with Frequency and Voltage Dependent Loads

The system model was enhanced with the addition of frequency and voltage dependent loads as described in section 4.4.5 so that the effect of this could be assessed. Results were taken for the two systems considered most appropriate (as just described in section 6.3.3) where the unit load controllers have no setpoint rate limits and the two conditions correspond to DINORWIG generating and pumping. The results of these test are shown in figures 6.21(a)&(b) and 6.22(a)&(b) respectively. These correspond to the results of figures 6.12 and 6.16 where the loads were insensitive.

The differences in response with and without variable loads is not large in this test. However, it is best illustrated in the comparison of the CEGB mechanical torques. When the load is sensitive to frequency, a slightly smaller increase in mechanical torque is required to redress the torque/load imbalance as the frequency has fallen. The effect is more obvious in the calculation of the power/frequency characteristics which follow.

6.3.5 Power/Frequency Characteristics Calculations

The power/frequency characteristic of a control area, or Area Frequency Response Characteristic, AFRC, relates the size of the frequency change (Δf) resulting from a given load change to the size of the load change (ΔP) and is defined as

$$K = \frac{\Delta P}{\Delta f}$$

These quantities were determined for the four cases highlighted previously, namely,

(a) DINORWIG generating, constant loads.

(b) DINORWIG pumping, constant loads.

(c) DINORWIG generating, frequency & voltage dependent loads.

(d) DINORWIG pumping, frequency & voltage dependent loads.

In each case, the frequency/power characteristics, K, were determined for the Scotland and the England/Wales control areas as shown in table 6.2.

condition	$\lvert\Delta P\rvert$	$\lvert\Delta f_{Sco}\rvert$	$\lvert\Delta f_{Eng}\rvert$	K_{Sco}	K_{Eng}
(a)	564.5	0.413667	0.0638333	1365	8843
(b)	557.3	0.408000	0.0781667	1366	7130
(c)	566.2	0.407333	0.0615000	1390	9207
(d)	556.9	0.400333	0.0743333	1391	7492

Table 6.2: Power/Frequency Characteristics for Four-Machine System

In the case of the Scottish control area, it can be seen that a difference in the operating mode of DINORWIG makes a minimal difference to the power/frequency characteristic since DINORWIG is not within this area. What slight difference

there is could be accounted for by the fact that the overall system operating conditions are slightly different when DINORWIG is pumping rather than generating as is illustrated in the different ΔP figures which represent a difference in power being exported from Scotland to England prior to the split.

The figures for the England/Wales area show a reduction in the power/frequency characteristic when DINORWIG is pumping. This reflects the fact that there is less regulation available in the system when DINORWIG cannot contribute to the frequency control.

The figures for both areas show an increase in the power/frequency characteristic when loads are frequency dependent. The load dependency is such that a reduction in frequency causes a reduction in load. Consequently, in this case, the load change caused in each area because of the split does not have as large an effect as before and the generators are better able to cope with it.

6.4 Step Load Change Studies

A not too uncommon incident which any system frequency control must cope with is the sudden loss of a generating unit. This results in an immediate step increase in the load applied to the remaining generators. The response to this type of incident was used to assess the relative performance of different system frequency controllers. It was difficult to simulate the complete loss of a generator due to the structure of the simulator. Consequently, these incidents were emulated by a step increase in load at one of the system busbars.

6.4.1 Tests with Distributed Frequency Regulation

6.4.1.1 Sustained Fossil Unit Load Controllers with Rate Limited Setpoints (5% MCR/min). Dinorwig Generating. Insensitive Loads.

Figures 6.23(a)&(b) show the response of the system when a step load change of 500 MW (approx. 4% of total system load) was applied to busbar CEGB4. Immediately, there is an imbalance between mechanical torque and electrical load which results in the machines slowing down and a drop in frequency. The frequency fall causes the turbine speed controllers of the fossil fired plant to open their governor valves giving a surge in mechanical torque which initially arrests the fall in frequency. Meanwhile, the unit load controllers start to reduce the speeder motor position, Z_{gvc}, since the generation is now higher than the setpoint. The action of the sustained load controller is to increase the setpoint to compensate for the decrease in frequency. The speeder motor position then increases again until setpoint and generation settle out at a level to correct the frequency fall. During this run, DINORWIG was freely regulating and its output increased accordingly to take a share of the higher load. The power on the tie-lines between Scotland and England reflects the increased generation of the SCOTLAND machines as this increase is being transferred to support the extra load in England. The system frequency finally settles out with a steady-state error of about 0.04 Hz.

6.4.1.2 Sustained Fossil Unit Load Controllers with Rate Limited Setpoints (5% MCR/min). Dinorwig Pumping. Insensitive Loads.

The results of figures 6.24(a)&(b) show the response to the same test as in section 6.4.1.1 (results in figure 6.23) when DINORWIG is not contributing to the regulation. On comparison with figure 6.23, it is immediately apparent that the control of frequency is not so good in a number of points: the size of the frequency fall, the time taken to reach steady state and the steady state error. As before, on the very initial fall in frequency, the governor valves of the fossil-fired units open rapidly. However, in this test, this is not supported by extra generation from DINORWIG and the frequency continues to fall faster than in the previous test. The governor valves do not re-close as quickly as before and there is less of a fall-off in mechanical torque and generated power. The system finally settles with each fossil unit taking a larger share of the extra generation to make up for the fact that there is no contribution from DINORWIG. It can also be seen that the larger movements of the governor valves result in larger pressure deviations and consequently larger changes in fuel input to correct these.

6.4.1.3 Sustained Fossil Unit Load Controllers with no Setpoint Rate Limits. Dinorwig Pumping. Insensitive Loads.

The test of section 6.4.1.2 was repeated with no setpoint rate limits in the fossil unit load controllers. The results are shown in figures 6.25(a)&(b). Here it can be seen that the frequency fall is arrested almost immediately by the initial opening of the governor valves when the frequency drops. Because there is no rate limit on the setpoint, L_{sp}, it quickly increases to correct the fall in frequency. This

means there is little error between the setpoint, L_{sp}, and the generation, P_{mw}, so the stepper motor, Z_{gvc}, is not moved in the opposite direction to the governor as happened in the previous test. Thus the mechanical torque is not held back from matching the electrical load and the system recovers very much more quickly.

6.4.1.4 No Fossil Unit Load Controllers. Dinorwig Pumping. Insensitive Loads.

This test was performed to investigate the effect of the speed governor alone. The results are shown in figures 6.26(a)&(b). These show that it is indeed the speed controller opening the governor in response to the initial drop in frequency that causes the initial abrupt arrest of the fall. However, the longer term control of frequency is not so tight as when the load controller also changes the speeder motor position to compensate for frequency error (compare with figures 6.24 and 6.25).

6.4.1.5 The Effect of Using Oil-Fired Plant instead of Coal-Fired Plant.

The results of section 6.4.1.2 were taken on a system where all of the fossil units were coal-fired. This test was repeated using oil-fired units, all other conditions being the same. The results are shown in figure 6.27. A comparison of figures 6.27 and 6.24 shows that the overall response of the two systems is very similar. The only significant difference is in the effectiveness of the pressure control. The fuel system of the oil-fired plant is more responsive than that of the coal-fired plant. Consequently, a tighter control can be kept on superheater outlet pressure, P_2, by

varying the fuel flow, M_{fu}. This of itself does not improve the output performance in respect of frequency regulation. However, it has already been seen that a major limitation on the performance in respect of frequency regulation is the rate limit of the generation setpoint, L_{sp}. (Compare the results of sections 6.4.1.2 and 6.4.1.3.) The reason for imposing a rate limit on the setpoint, L_{sp}, is to minimise the pressure excursions on changing load. It can be concluded that with the tighter pressure control obtainable with oil-fired plant, a higher setpoint rate limit could be tolerated before the size of the pressure excursions on load changes were unreasonable.

6.4.1.6 The Effect of Setpoint Rate Limits

It could be noted from the results so far in this section that the setpoint rate limit has very little effect on the quality of pressure control (compare P_2 in figures 6.24(b) and 6.25(b)). Based on these results it might be argued that there is no need for a setpoint rate limit at all. To investigate the effect of setpoint rate limits further, tests were carried out to simulate scheduled load changes rather than those forced by frequency regulation.

Figures 6.28(a)&(b) and 6.29(a)&(b) are the results of applying a change in load demand to the CEGB and SCOTLAND machines when they are operating in a sustained load control mode. Figure 6.28 shows the results when the setpoints, L_{sp}, are rate limited by 5% MCR/min and 6.29 shows the results with no setpoint rate limits.

The setpoint rate limit can be clearly seen in L_{sp} in figure 6.28(a). To maintain the load/generation balance, an increase of 500 MW by the twenty-one CEGB ma-

chines has been offset by a decrease of 500 MW in the five SCOTLAND machines. Each individual machine has its setpoint, L_{sp}, rate limited to 5% MCR/min. Consequently, each CEGB machine requires an increase of about 22 MW whereas each SCOTLAND machine needs to decrease its output by 100 MW. At the same ramp rate, the SCOTLAND machines will take longer for the setpoint, L_{sp}, to reach the desired value, L_{dv}.

Initially, both the CEGB and SCOTLAND machines start to follow a setpoint ramping at its rate limit towards the desired value. Because there are more CEGB machines than SCOTLAND machines, their combined effect is to increase total CEGB generation faster than the SCOTLAND generation is decreasing and so the system frequency rises. The NWALES machine is also regulating, though not changing its generation desired value, and its setpoint, L_{sp}, decreases to help offset the increase in frequency. The ramping up of the CEGB setpoint reverses to also offset the increase in frequency. Having arrested the rise in frequency, the rate limit on the fall of power from SCOTLAND, through the effect on frequency, forces the CEGB machines to ramp to their final output at a slower rate. The NWALES machine is also able to increase its output back to its desired value. The effect of these power changes on the superheater output pressures can clearly be seen in P_2.

In figure 6.29(a), the load setpoints, L_{sp}, are not rate limited when they follow the change in L_{dv}. In this case, there is only a slight imbalance between the CEGB increase in power and the SCOTLAND decrease. Consequently, there is a much smaller change in frequency. In this case, frequency tends to fall and then recover, rather than rise as in the previous situation. The limiting factor on the rate of change of generation is now the dynamics of the generating units which will be slightly different because of the different operating points of the CEGB

and SCOTLAND machines. As before, the NWALES generation also changes in response to the frequency deviation. However, a comparison of the resulting pressure deviations, P_2, demonstrates how much more seriously this control is affected by the actions of the load control when no setpoint rate limit is used. Hence the use of a rate limit on the load setpoint, L_{sp}.

6.4.1.7 The Effect of Frequency and Voltage Dependent Loads

The test of section 6.4.1.1 (with results shown in figure 6.23) was repeated on a system with loads sensitive to frequency and voltage. These results are shown in figures 6.30(a)&(b). The load dependency is such that the overall effect of a reduction in system frequency is to also reduce the total system load (a rule-of-thumb figure is often quoted as 2% of total load per Hertz). Hence, on the sudden increase in load, the resulting fall in frequency actually reduces the effective load and consequently the frequency does not fall as far as it would have done if the load were insensitive to frequency. This effect can clearly be seen in a comparison of the frequencies in figures 6.23(a) and 6.30(a). The resulting transient changes in torque and generation are also slightly reduced since the frequency deviation is smaller. However, the final values of generation are the same as before since the frequency has returned to near its original value and so the same total increase in generation needs to be provided to match the imposed increase in load.

An equivalent Area Control Error has been included with the results of this last test so that it may be compared with those that follow. This ACE did not occur in practice since Automatic Generation Control was not running, but was calculated from the frequency and tie-line power data as if the standard AGC were running as described in the next section.

6.4.2 Tests with Centralised Automatic Generation Controllers

Automatic Generation Control (AGC) was applied to the simulation as described in section 3.5.3. Initially, a flat-frequency control mode was applied to compare the results with those of the distributed controllers and then frequency-bias mode was implemented to also control the tie-line power. The Area Frequency Response Characteristics, or power/frequency characteristics, used were those calculated in section 6.3.5. The AGC gains, T_n and C_p in equation 3.1, were initially selected as 65 and 0.2 respectively, these being the average of values specified by Glavitsch and Stoffel in [18] (see discussion on page 22).

6.4.2.1 Flat Frequency Mode AGC. Dinorwig Generating. Frequency and Voltage Sensitive Loads.

The results of this test are shown in figures 6.31(a)&(b). The conditions of the test were similar to those of section 6.4.1.7 (with results in figure 6.30), except that, rather than frequency regulation being performed by the sustained fossil unit load controllers, in this case, frequency regulation was performed for each control area by the AGC algorithm. The fossil unit load controllers then acted in a non-sustained mode to follow the desired values set by the AGC.

It can be seen from figure 6.31(a) that frequency takes longer to come to a steady state since the frequency transient has continued to rise to completely correct the error. The very initial torque and generation transients are similar to the non-AGC case which is because this part of the response is due to the turbine speed governors as discussed in section 6.4.1.4. The medium term response of the fossil units is still dictated somewhat by the rate limit on the setpoints. However,

the AGC algorithm shares the total extra required generation between all of the fossil units and their final levels of generation are sufficient to make up the whole increase in load. In this case, DINORWIG is not part of the AGC algorithm. Consequently, having reacted to the initial frequency error through governor action, its generation gradually returns to its original level as the frequency returns to its setpoint. The power being transferred on the tie-lines illustrates the increased contribution that the Scottish machines are making, now that DINORWIG has no steady state increase in its generation.

6.4.2.2 Tie-Line Bias Mode AGC. Dinorwig Generating. Frequency and Voltage Sensitive Loads.

Figures 6.32(a)&(b) and 6.33(a)&(b) illustrate the response of the system when the AGC is in tie-line bias mode. In this mode, the tie-line power is also regulated. By comparing these results with those of the previous section (shown in figure 6.31) it can be seen that the frequency response is very similar, but the tie-line power now returns to its initial value. By controlling the tie-line power, the AGC ensures that the load increase is matched by an increase in generation only from the area in which it occurred. The generation results show how the SCOTLAND generation is returned to its previous value while the CEGB and NWALES machines pick up all of the extra load between themselves.

6.4.3 The Effect of the AGC Frequency Bias Parameter B

Ordinarily, AGC is implemented with the frequency bias, B, (relating frequency to power in forming the Area Control Error, equation 3.2) set equal to the Area

Frequency Response Characteristic. It has been suggested [27] that it might be preferable to operate with B set to half the value of the AFRC. Several simulation runs were performed to investigate the effect of the parameter B.

Figures 6.34(a)&(b) show the results of the same test as before but with half the value of B for the England/Wales area. Figures 6.35(a)&(b) show the results when B is twice the value of the AFRC. Comparing these with the results for B equal to the AFRC (figures 6.32 and 6.33), the effect on the CEGB Area Control Error can clearly be seen where it incorporates a lesser and a greater contribution from the frequency error. However, the result of this on the frequency and tie-line power responses is not nearly so marked. From the frequency graphs in figures 6.33(a), 6.34(a) and 6.35(a), a slight increase in speed with increasing value of B can be observed. However, the differences are not large and it would appear that the rate limit on the fossil unit setpoints prevents an increase in the speed of response of the generation as the Area Control Error gets larger with increasing B. In order to investigate just the effect of the controller, the tests were repeated with no setpoint rate limits and with DINORWIG pumping so that it had no effect on the regulation.

The unlimited results are shown in figures 6.36(a)&(b), 6.37(a)&(b) and 6.38(a)&(b) for B of the CEGB control area equal to AFRC, half AFRC and twice AFRC, respectively. The effect of changing B is now very obvious. As the value of B increases, the time taken for the Area Control Error to come to zero decreases. With both the high and low values of B, there is more overshoot in the frequency response than when B is set to the value of the AFRC. The faster control available from using a higher value of B results in less disturbance to the superheater pressure control in the other area and, conversely, a low value of B results in a greater disturbance. This may be explained by observing that with a lower value

of B, the local area controller is less reactive to frequency deviations and does not try so hard to correct them. The persisting errors cause the other area controller to demand more regulation from its generators. Consequently, a low value of B in just one area causes the other area to perform more regulation even when the disturbance is not in the other area.

The results were also repeated with the B values in both area controllers set to half of their respective AFRCs. These are shown in figures 6.39(a)&(b). Here the response is slow as before. However, the effect on the pressure control of both areas is similar illustrating how they are taking a similar share of the regulation when compared to the case when both Bs are set equal to the AFRCs. Hence, the practice of setting all area controllers to have B equal to that area's AFRC ensures some level of "fairness" in the regulating duties of the different areas, even though the ultimate correction of ACE to zero is assured for whatever value of B.

None of these effects is very obvious when the speed of response of the generating units is dominated by the load setpoint rate limits. Consequently, the relatively small differences in AFRC calculated in section 6.3.5 for different system operating conditions were not taken into account in the results of this chapter and all AGC controllers used the same parameter values. This insensitivity in the presence of rate limits may suggest that in an area dominated by slow, rate limited units the value of B may not need to be changed with different operating conditions, resulting in a simpler controller. However, the effect of system loading must also be considered (see later in section 6.4.7.2).

6.4.4 The Effect of AGC Controller Gains T_n and C_p

A sequence of runs was performed varying the AGC controller gains T_n and C_p. In all instances, the controllers for the two areas, Scotland and England/Wales, were the same. The base case was taken as that described in section 6.4.2.2 where, for both areas, $T_n = 65$ seconds and $C_p = 0.2$.

6.4.4.1 The Effect of T_n

Figures 6.40(a)&(b) show the results with T_n increased to 100 seconds, while figures 6.41(a)&(b) were obtained with $T_n = 30$ seconds. These may be compared with the nominal case of $T_n = 65$ seconds shown to the same scale in figures 6.33(a)&(b). The frequencies in figure 6.41(a) show an obviously underdamped response for the shorter T_n, corresponding to a higher gain for the integral term of the controller. The frequencies in figure 6.40(a) for $T_n = 100$ seconds are the most damped as would be expected. However, the response in this case has been slowed down slightly by the increased damping. This is best seen in the Z_{gv}/Z_{gvc} trace where it can be surmised that the frequency error is zero when Z_{gvc} meets Z_{gv}. For the results, this time can be seen to be shortest for the middling value of $T_n = 65$ seconds (figure 6.33).

6.4.4.2 The Effect of C_p

Figures 6.42(a)&(b) and 6.43(a)&(b) show the results with $C_p = 0.1$ and $C_p = 0.3$ respectively. Again, these may be compared with the nominal case shown in figure 6.33 where $C_p = 0.2$. A comparison of these three figures would suggest

that a low value of C_p produces a slower, less well damped response as is seen in figure 6.42(a). The results of figure 6.43(a) would suggest that a higher value of C_p would be most desirable to produce the fastest and best damped response. However, the comparison may be clouded a little because of the contribution from DINORWIG. The time taken for the DINORWIG generation to finally return to its initial value is very similar in all three cases. However, with the higher values of C_p, DINORWIG generation is on average higher during its transient increase from its steady state level. In other words, the integral of DINORWIG P_{mw} is higher for higher C_p. This relates to energy and consequently water usage and so the final choice of C_p may be based on making a compromise between the damping of the frequency transient and the use of hydro plant in helping the regulation.

6.4.4.3 Choice of Optimal Values for T_n and C_p

The results of this section would suggest that the most appropriate values for T_n and C_p lie well within the range of those in use for other systems [18]. A common approach to this type of problem is to minimise some cost function with respect to the controller gains. The simulation may be used to perform a series of tests with T_n and C_p taking different values within the range already identified as being appropriate. The choice of the "best" values for the gains will be based on a comparison of several factors such as speed of response, control effort, contribution from hydro units and damping of response. These factors may be used to formulate a cost function for each set of T_n/C_p values. Among the simplest cost functions which may be used are $\int ACE$ and $\int ACE^2$ though these may not take into account all of the significant factors. Plotting the cost function against T_n and C_p at several different values would enable the gains

which minimise the cost function to be estimated.

6.4.5 A New Area Control Error

The new Area Control Error (ACE) proposed by M.L.Kothari et al. in [40], given in equation 3.2, was implemented in the AGC code. A controller using this error always guarantees zero steady state time error and inadvertent energy interchange, unlike conventional ACE controllers (see discussion on page 26). This was initially implemented with a gain on $\int ACE$ of $\alpha = 0.01$ as suggested in [40].

The previous step load change test was repeated with the new ACE. The results are given in figures 6.44(a)&(b). Comparing these with the results of the similar controller using a conventional ACE given in figure 6.33, it can be seen that it takes longer for both the frequency and the tie-line power to settle. However, the integral of frequency error is brought to zero by the end of the transient by forcing the frequency to remain high for a while after the initial fall. This ensures that the time error introduced by the initial error in frequency is reduced to zero. Similar comments can be made with regard to the tie-line power. The integral of tie-line power error which is inadvertent energy interchange, is also reduced to zero by the time the system comes back to steady state.

6.4.5.1 The Effect of the Integral Gain α

Two further runs were carried out with $\alpha = 0.02$ and $\alpha = 0.005$, the results of which are shown in figures 6.45(a)&(b) and 6.46(a)&(b) respectively. These may

be compared with the results of the previous run with $\alpha = 0.01$ as shown in figure 6.44. In figure 6.45 the controller tries to correct the integral error more severely by, for example, allowing the frequency to rise higher to correct the integral error from the initial fall more quickly. However, this leads to a rather oscillatory response with rather large overswings. This also has a larger effect on the excursions of superheater pressures. Making the gain α smaller as shown in figure 6.46 produces a rather more gentle control action which nonetheless finally reduces the integral of frequency and tie-line power error to zero. The final choice of α would have to be a compromise between speed of response and severity of control action. However, it would appear that α need not be very large.

6.4.6 The Effect of Controller Interval

The implementation of the AGC controller used in these studies was of a discrete kind with an associated control interval time. In all the runs so far discussed, this interval was five seconds. Five seconds had been chosen since this was generally the shortest interval considered for real controllers in the literature (see section 3.4). Many theoretical papers use a control interval of two seconds (see section 3.3), however, the results here would suggest that five seconds is perfectly adequate. A longer interval still may be more desirable from the point of view of practical implementation, hence the effect on the quality of control of using longer control intervals was investigated. The major disadvantage of a long control interval is that if an event occurs on the system immediately after one control action, this will not be acted upon by the controller until another whole control interval has elapsed. In the case of a sudden fall in frequency due to, say, the loss of a generator, in the case of a long control interval the frequency will have fallen further before corrective action is taken than in the case of a shorter con-

trol interval. Even if there is no delay in noticing the frequency fall, performance deteriorates with increasing control interval, a feature which is worsened with the use of rate limited setpoints. These points are illustrated in the following results.

The results of figure 6.44 may be taken as the base case. Here, the controller interval was 5 seconds and the fall in frequency was noticed immediately. Figures 6.47(a)&(b) show the corresponding case when the AGC controller does not react until a whole control interval, ie. five seconds, after the initial frequency drop. In the second case where there is a delay in the controller response, the frequency falls very slightly further and its fall is arrested very slightly later. However, the overall responses and recovery times are very similar.

Figures 6.48(a)&(b) and 6.49(a)&(b) show the responses when the control interval is ten seconds, figure 6.48 with no delay, figure 6.49 with a delay of one control interval, ie. ten seconds. On comparing one with the other, the effect of the delay with this interval is more obvious. With the delay, the frequency falls further before being arrested. This then results in a slightly larger overshoot on recovery as the controller attempts to correct for time error, ie. integral of frequency error. The delay is obvious in the CEGB $P_{mw}/L_{dv}/L_{sp}$ trace. In the first case, L_{dv} changes and L_{sp} starts to change at the same time as the governor speed controller opens the governor valve and causes the initial surge in power. In the second case, the setpoints do not start to change until after the speed governor action. Consequently, considering the England/Wales subsystem, the load controllers decrease the speeder motor positions, Z_{gvc}, further than in the previous case since the lagging change in setpoints means there is a larger load error ($L_{sp} - P_{mw}$). All in all, this results in a delay in recovering the frequency error.

On comparing the ten-second results with the five-second results, with no delays, ie. figures 6.48 and 6.44, it can be seen that the longer control interval results in a slightly more oscillatory frequency response and a larger tie-line power error with consequently larger corrections to bring the integral of tie-line power error, ie. inadvertent energy interchange, to zero.

Figures 6.50(a)&(b) and 6.51(a)&(b) show the responses when the control interval is fifteen seconds, again with no delay (figure 6.50) and with delay (figure 6.51). With the longer control interval, the response is now obviously more oscillatory. Again, the frequency fall is larger when there is a delay before the controller reacts causing larger overshoots and a slightly longer settling time.

Increasing the control interval too far results in limit cycling, or even an unstable response, as shown in figures 6.52(a)&(b) and 6.53(a)&(b) where the control interval is twenty seconds.

As has been noted previously, the rate limit imposed on the fossil unit load controllers setpoints, L_{sp}, has a detrimental effect on the quality of load-frequency control. This effect exacerbates the worsening response that is obtained as the controller interval is lengthened. To demonstrate this, the fifteen-second controller responses (shown in figures 6.50 and 6.51) were repeated without setpoint rate limits. These results are shown in figures 6.54(a)&(b) and 6.55(a)&(b) (immediate reaction to frequency fall and delayed reaction respectively). Without the rate limits, the response is very much less oscillatory and the differences in speed with which the frequency fall is arrested is more obvious. Figures 6.56(a)&(b) show the base case (ie. five-second controller) when there are no rate limits. As would be expected, this shows a tighter control than the corresponding rate limited case (shown in figure 6.44). Comparing the five-second and fifteen-second

controllers without rate limits (figures 6.56 and 6.54 respectively) it can be seen that there is still some reduction in quality of control with the longer interval in that there is a slightly more oscillatory response with larger overshoots. As seen before in the rate limited case, the effect of a delay in noticing the frequency fall produces an obviously worse result as shown in figure 6.55.

6.4.7 Effects of System Operating Conditions

6.4.7.1 The Effect of Machine Loading

The standard step load change test was applied to a system in which the individual generators were more heavily loaded than in previous runs. The standard AGC was used as in section 6.4.5 (with results in figure 6.44). This was achieved by using twenty instead of twenty-one generators in the CEGB group, and four instead of five in the SCOTLAND group. The results of this test are shown in figures 6.57(a)&(b).

A comparison of the frequency traces in figures 6.44(a) and 6.57(a) shows that the frequency falls further before being arrested in the case of the more heavily loaded machines. The initial "blip" in the frequency trace due to the first abrupt opening of the governor valves is also lower. There are differences, too, in the tie-line power traces. With heavily loaded units there is not such a high surge in tie-line power resulting from the initial fall in frequency. This reflects the changes in generation of the SCOTLAND units. The reason for these differences is the deteriorating responsiveness of the generating units as they are operated with the governor valves further open. This is due to the non-linear characteristic of the governor valves relating steam flow to valve opening. The reduced regulation of

the fossil units is also reflected in the DINORWIG generation where, in the case of more heavily loaded fossil units, DINORWIG takes on a larger share of the regulation.

The non-linear effect of the valves may be illustrated by considering the governor valve movements of figures 6.44(b) and 6.57(b). The size of the initial opening of both the CEGB and SCOTLAND units is larger in the case of more heavily loaded machines (figure 6.57) as would be expected from the larger fall in frequency. However, under these operating conditions, this does not result in a larger increase in power in the SCOTLAND machines. Rather, because of the valve non-linearity, a smaller power change results even from this larger movement of the valve. In the case of the CEGB units, a larger movement of the governor valves results in a similar power increase compared to the less heavily loaded condition. In fact, the difference in operating points between the two sets of results is greater for the SCOTLAND group than for the CEGB group.

6.4.7.2 The Effect of Network Loading

The standard step load change test was also applied to a system with twice the load of the previous runs. The numbers of generators in each group was doubled in order that each individual generator should be operating under the same conditions as before. The results of this test are shown in figures 6.58(a)&(b).

From a comparison of figures 6.58 and 6.44 it can be seen that the 500 MW step load change results in a lower fall of frequency in the more heavily loaded network. This is to be expected since, in this case, the load change relative to the total load is only half that of the previous case. So, in this respect, a generation loss

of a given size will be less severe in a system which has a larger total load.

There is another significant difference between the results in figures 6.58 and 6.44. The response of the more heavily loaded case is rather slower and more oscillatory. On inspection of the generation curves of the fossil units in figure 6.58(a), it can be seen that the setpoints are not rate limited for all but the first few seconds of the response. This, then, reflects a condition similar to that shown in figure 6.38 and discussed in section 6.4.3 where the value of the ACE parameter B was only half the value of the AFRC. In changing the conditions of the system such that there are now twice as many generators regulating than previously, it might be reasonable to assume that the AFRC is also doubled. From figure 6.58(a) it can be seen that in this particular case the response is no longer dominated by the setpoint rate limits. In order to improve the response, a better value of B would need to be used in the calculation of the Area Control Errors. This would suggest that in a system where AGC is required to operate over a fairly wide range of loading conditions, a constant value of B may not be appropriate unless it is such that the response is actually dominated by the setpoint rate limits over the full load range.

6.5 Summary

A large number of results have been presented in this chapter and this section has been included in order to clarify the outcome of this work.

In summary, then, the following proposals are made with regard to the control of the British power system:

1. Operate the complete system as two distinct control areas, England/Wales and Scotland, so that the power on the tie-lines between the two may be regulated and each area will make up for its own losses in generation whilst maintaining frequency at the setpoint.

2. Within each control area, implement a centralised form of load-frequency control to give zero steady state frequency errors and to enable the tie-line power to be taken into account.

3. Use a form of area control error (ACE) which incorporates the integrals of frequency and tie-line power as well as the frequency and tie-line power themselves, in order to be able to automatically reduce time error and inadvertent energy interchange to zero.

4. Set the ACE frequency bias parameter, B, to the Area Frequency Response Characteristic (AFRC) in both areas to ensure fairness of regulating duties between the two areas. The value of B has some effect on the speed of response of the controller. However, fairness will only be ensured if the Bs of both areas are set according to the same criteria.

5. Use middling values of the controller gains, $T_n = 65$ and $C_p = 0.2$, which would appear to be adequate in the first instance. However, further simulation and analysis could be performed to choose more optimal values.

6. With regard to the gain on the integrals of frequency and tie-line power, use the value of $\alpha = 0.01$ recommended in the literature. It would appear that the value of α is not very critical and may be quite small. The final choice would depend on the timescale over which it is intended that time error and inadvertent energy interchange be corrected.

7. Use a controller interval of five seconds. There is little point in operating very much faster than this because of the typical value of intervals used

by generating unit load controllers. A slower rate may be desirable from an implementation point of view. However, long intervals may lead to instability and these initial results suggest an interval no slower than once every ten seconds should be used.

The following chapter presents results from the more complex 25-machine study in order to illustrate a few points that could not be demonstrated in the 4-machine study. However, this adds little to the proposals listed above, but does point to some further issues which would need to be taken into account in an operational system.

Chapter 7

Twenty-Five Machine Studies

Although most of the significant properties of centralised load/frequency control were illustrated by the four-machine studies discussed in chapter 6, it was necessary to model a more complex system in order to demonstrate certain other characteristics. This model consisted of a total of twenty-five generating groups, six of which modelled each Dinorwig unit independently, and sixty load groups. This level of complexity allowed a more realistic mix of plant to be modelled, for example, by allowing the six Dinorwig units to act independently. It also allowed for the regulation to be performed by a smaller proportion of the generators than could be implemented on the fairly crude four machine system.

7.1 System Split Test

As with the four machine system, the initial test to be performed was a system split disconnecting Scotland and England. The resultant trends are shown in figures 7.1(a)–(e). For this test, all hydro units, including the six units at Dinorwig, were pumping.

Considering first the generators in Scotland (results are shown for LONGANNET, HUNTERSTN and PETERHEAD), immediately the tie-lines are broken, the electrical load on each of these machines falls abruptly by around 100 MW. This relates to the total load lost of approximately 609 MW shared between the six thermal units and the hydro units at FOYERS and CRUACHAN (not shown). The load control on the thermal units is such that LONGANNET (Coal-fired) is operating in a sustained load control mode whereby its load setpoint, L_{sp}, varies from the desired value, L_{dv}, in order to help correct frequency errors. The other units, HUNTERSTN and PETERHEAD, are nuclear and as such do not regulate with respect to frequency except through their speed governors. For all but severe frequency errors, the governor droop, or gain between frequency error and offset of Z_{gv}, the governor valve position, from Z_{gvc}, its nominal position set by the speeder motor, is such as to be less sensitive in nuclear units than in fossil units. This can be illustrated by considering the Governor graphs for LONGANNET and HUNTERSTN given in figure 7.1(d). For the initial rise in Scotland frequency, f_{sco}, of about 0.9 Hz, the LONGANNET governor valve closes by about 0.45 pu. whereas the HUNTERSTN governor moves only about 0.1 pu. Because of the non-sustained response of the nuclear units, the load setpoints, L_{sp}, remain constant. Consequently, the speeder motor position, Z_{gvc}, is increased in an attempt to bring the generation, P_{mw}, back to meet the setpoint, L_{sp}. At the same time, the LONGANNET setpoint is decreasing in response to the high frequency and the LONGANNET generation remains low. In fact, the LONGANNET generation continues to decrease which allows the generation in the nuclear units to increase again to their setpoints. The Scotland system finally settles with all the decrease in load being taken by the LONGANNET units, and the frequency constant at about 50.8 Hz.

The situation in the England/Wales subsystem is the opposite to that in Scotland.

When the tie-lines are split, the load on the machines is abruptly increased and the frequency falls. There is again a mixture of fossil, nuclear and hydro units in this area. The governor valves of all thermal units open quickly in response to the fall in frequency, those of the fossil units (results are shown for DRAX.B, COTTAM, RATCLIFFE, EGGBORO. and RUGELEY) moving further than those of the nuclear units (results are given for HINKLEY and HEYSHAM). In fact, in two of these fossil units the governor valve positions become limited since they are fully open (DRAX.B and RUGELEY in figure 7.1(d)). As in the Scottish area, the fossil units are operating in a sustained load control mode whereas the nuclear units are not. In the case of the fossil units, the load setpoints, L_{sp}, rise to take account of the decrease in frequency, whereas, in the nuclear units, they remain constant. Consequently, the nuclear units' generation falls back again to its original level while the generation of the fossil units rises yet further to take on the total increase in load. Again, the difference in droop between the nuclear and fossil units is clearly illustrated by a comparison of the COTTAM or RATCLIFFE Governor graphs with the HINKLEY graph in figure 7.1(d).

The results of this run were used to obtain the Area Frequency Response Characteristics of the Scotland and England/Wales area, calculated as explained in section 6.3.5. These are shown in table 7.1.

Area	$\|\Delta P\|$	$\|\Delta f\|$	K
England/Wales	609.4	0.1448	4208
Scotland	609.4	0.8148	748

Table 7.1: Power/Frequency Characteristics for Twenty-five Machine System

From table 7.1 it can be seen that the AFRCs for the two areas are rather lower than those obtained for the four machine study (given in table 6.2). This reflects how the operating conditions of the twenty-five machine study allow for less reg-

ulation than under the conditions of the four machine study. There are a number of reasons for this. The operating conditions of the twenty-five machines study were set up to model a summer night time loading condition. In this situation, the load on the network is low and there is also a relatively high proportion of unresponsive generation such as the nuclear units whose generation is not reduced during the night. As small a number of fossil units as possible will be run with consequently a number of these generating near their maximum. Finally, pumped-storage units will be pumping rather than generating during the night and so will not be contributing to frequency regulation. Consequently, this is a scenario which represents a worst case situation for load/frequency control.

7.2 Step Load Change Studies

Similar step load change tests to those of chapter 6 were performed on the twenty-five machine system. These consisted of a step load change of 500 MW at busbar EGGB4J while an AGC controller was running in tie-line bias mode with the controller parameters T_n and C_p set to 65 and 0.2 respectively in both areas. The controllers used the Area Control Error investigated in section 6.4.5. Initially, all hydro units were pumping and all fossil unit setpoints were rate limited to 5% MCR/min.

The results of the first test are shown in figures 7.2(a)-(e). The response is poor, allowing the frequency to fall by nearly 0.5 Hz and resulting in a very underdamped recovery. This is as a result of the small amount of regulation available as explained in section 7.1. There is only a small assistance to frequency regulation from the nuclear units, HUNTERSTN, HINKLEY, PETERHEAD and HEYSHAM, whose governor valves do not move far from their nominal positions

because of their high droop. The response to the load change is also hindered by the fact that several fossil units do not make as much of a contribution as they might because they are limited at or near maximum output: DRAX.B, EGGBORO. and RUGELEY. In addition to this, there is the slugging of the response due to the rate limits on the power setpoints compounded by the fact that those units near their maximum limits are unable to follow the setpoint changes. The response is also degraded by the fact that there is no contribution from the hydro units. In fact, this response is rather unrealistic since such a large fall in frequency as seen here would, in reality, cause automatic cutting in of some hydro units. This action is investigated later in section 7.2.3.

7.2.1 More Effective Regulation

The previous test was repeated with two Dinorwig units generating, and regulating, instead of pumping. To counterbalance this extra generation, the generation levels of some other units were reduced. The results of this test are shown in figures 7.3(a)–(e).

With the two Dinorwig units helping with the regulation, the response to the step change in load is altogether more stable. The frequency does not fall as far before being arrested and there are no oscillations on recovery. It can be seen from the generation traces that while the faster hydro units arrest the fall in frequency, the slower fossil units in England and Wales follow their rate limited setpoints to eventually take up all of the change in load. The Scottish generation (LONGANNET) increases initially to help offset the fall in frequency, but, as frequency recovers, it is reduced to bring the tie-line power back to zero. Indeed, the Scottish generation is low for a while in order to reduce the integral

of the ACE and hence the time error and inadvertent energy interchange on the tie-lines to zero as illustrated in figure 7.3(e). A clear distinction can also be seen between the regulating fossil units and the non-regulating nuclear units in figure 7.3(b). In fact, now that the control of frequency is improved, there is very much less disturbance to the nuclear generators as compared to the previous situation (compare figure 7.3(b) with figure 7.2(b)). The dominance of the setpoint rate limits in the fossil units is also clearly illustrated in figures 7.2(a) & (b).

7.2.2 The Effect of Different Setpoint Rate Limits

The step load change test was again repeated. In this instance, several of the England/Wales units had their setpoint rate limits increased from 5% MCR/min to 10% MCR/min. The results of this test are shown in figures 7.4(a)–(e). Again, there is an improvement in the regulation of the frequency and tie-line power when compared with the previous test. The excursions of frequency and tie-line power are not so large and the errors are reduced to zero more quickly. This is due to the greater regulation now being performed by the faster fossil-fired units. The difference in response between slow and fast units can be seen from a comparison of the COTTAM and RATCLIFFE or EGGBORO. and RUGELEY Generations in figure 7.4(b). Because the units with the faster setpoint ramps (COTTAM and EGGBORO.) increase their generation more quickly they finally take up a larger share of the increased load than do the slower units (RATCLIFFE and RUGELEY). Although this increase in responsiveness of some fossil units has reduced the regulating requirements of the DINORWIG units (compare figures 7.4(a) and 7.3(a)), and the impact of the disturbance on the nuclear units, there is now, in fact, a level of "unfairness" between the regulating duties of the slow and fast fossil units. It may be acceptable to allow the faster units to take

on a greater share of the regulation. Then again, from an economic viewpoint, it might be more desirable that in the longer term, the slower units finally take on a greater share of the load thus allowing the faster units to reduce generation again back towards their economic levels. This requires a more sophisticated AGC algorithm which splits the generation setpoints into two components for economic operation and load/frequency regulation. This important aspect of AGC is not considered here but would be a significant further development to these studies.

7.2.3 The Use of Low Frequency Relays on Hydro Plant

As previously mentioned, it is common practice for hydro units such as those at Dinorwig to operate in a mode whereby on an excessively low frequency their output is rapidly increased to maximum. Such a mode of operation was incorporated into the model of the Dinorwig units. The step load change test was repeated with DINORWIG1 having a Low Frequency Relay (LFR) setting of 49.85 Hz and a dead time of 2.75 seconds. This meant that the relay would operate if the frequency had been below 49.85 Hz for more than 2.75 seconds. It would then take a Dinorwig unit about ten seconds to change from full pumping to maximum generation. The simulation results of this situation are given in figures 7.5(a)–(e).

The rapid rise in the DINORWIG1 generation is clearly shown in figure 7.5(a). Initially, DINORWIG1 generation starts to rise through normal governor action as before but then, once the LFR has responded, the generation quickly rises to its maximum. The effect of this is to arrest the fall in frequency rather sooner than in the previous tests. The recovery of frequency and tie-line power to their original values is faster. The reaction from other regulating units is smaller than in the previous case since DINORWIG1 has taken a significant portion of the

increase in load (about 200 MW of the 500 MW change). With the frequency fall having been arrested by the rise in generation from DINORWIG1, on a longer timescale, the AGC varies the generations of the other units to bring the steady state values of Area Control Error and its integral to zero.

Chapter 8

Conclusions

A computer simulation has been set up which is suitable for the study of Automatic Generation Control on the British power grid. This has entailed the incorporation of more detailed model units into a pre-existing electro-mechanical power system simulator at the University of Bath. This simulation has been used in a preliminary study of centralised load/frequency control which could be used to replace the current distributed type of control and amalgamated with economic dispatch calculations to provide Automatic Generation Control.

Models of the order of ten to twenty states of fossil-fired generation units and hydro units have been implemented and incorporated into the existing power system simulator. Nuclear units were modelled as unresponsive, high droop, fossil units. The hydro model also included the response of low frequency relays. These models were validated by comparison with results from the original models from which they were taken and, to an extent, with real plant data where this was available. Models were also implemented of loads sensitive to frequency and voltage variation.

The implementation of the fossil-fired unit models also required the development

of controllers to control the power generation and the steam pressure of the boiler. This was designed as a traditional Boiler-Follows-Turbine (BFT) control whereby two independent controllers were implemented, one controlling power output by varying the nominal position of the governor valve set by the speeder motor position and the other regulating steam pressure by varying fuel flow into the boiler. The structure and gains of an operational controller were available and this was also implemented. This was a multi-variable controller which had been designed for one particular plant via a discrete "black-box modelling" approach to plant identification and controller design. Although this controlled the boiler model very well under some conditions it was found not to be robust for the range of plants that were required to be modelled. Consequently, it was found more successful to use the cruder, but more flexible and more readily tunable BFT design.

In order to design for the BFT control, it was necessary to produce a linear model of the plant from the non-linear model used for the simulation. This was performed with the assistance of a symbolic mathematics program to produce simplified third order linear models for the two sections of plant to be controlled. This then enabled simple Proportional-Integral and Integral controllers to be designed for the pressure and load loops.

The simulation was used to investigate the operation of load/frequency control on the British grid system. Two set-ups were implemented. The first modelled the system as four generating groups each representing a number of identical generating units. The second modelled the system as twenty-five groups and allowed each of the six units at Dinorwig to be modelled independently.

A centralised load/frequency controller has been developed which would allow for

the automatic control of system frequency together with the power flow on the tie-lines linking England and Scotland. In addition, modifications to this controller have been implemented which would also allow for the automatic regulation of the integrals of these quantities leading to zero steady state time error and zero inadvertent energy interchange.

The effects of a variety of parameters on the quality of load/frequency control have been discussed. Studies were performed to investigate the response to a step change in system load. With distributed frequency regulation, it was found that there was a small steady state frequency error after the recovery of the initial fall caused by the step load change. It was also found that the speed of recovery was significantly affected by the rate of change limit on the individual fossil unit generation setpoints.

The use of rate limited generation setpoints in the fossil units was illustrated in the case of scheduled generation changes. The reduction of interaction with the superheater pressure control when rate limits were applied was clearly shown by the results.

When Automatic Generation Control (AGC) was applied to the system, to control the frequency (flat frequency mode), it was shown how this results in zero steady state frequency error. By modification of the Area Control Error (ACE) to also include the tie-line power imbalance (tie-line bias mode), it was shown how the AGC could force both the frequency and the tie-line power error to zero. In tie-line bias mode, the results illustrated how the load increase was matched by an increase in generation only from within the area in which the load increase occurred.

Tests were performed in which the AGC parameter B, relating frequency deviation to power, took values of half the Area Frequency Response Characteristic (AFRC), AFRC and twice AFRC in one area while keeping B of the other area equal to the AFRC. It was found that a high value of B produced a faster but more oscillatory response, whereas, a low value of B produced a slower response and forced the other area to perform more regulation. It was concluded that the Bs of all areas should be set by the same criterion so as to ensure fairness between the regulating duties of all areas. It was also found that these effects were obscured in the presence of rate limited setpoints. This prompted the conclusion that the value of B has little effect if the response is dominated by the setpoint rate limits. However, given the variety of operating conditions that can occur and, particularly the fact the the maximum load on the British system can easily be twice the minimum, it would seem unlikely that this domination would hold under all conditions. Consequently, B would need to be changed with operating conditions.

The effects of the AGC controller gains, T_n, the integral time, and C_p, the proportional gain, were investigated. It was found that, for the system studied here, choosing moderate values of $T_n = 65$ seconds and $C_p = 0.2$ as reported in the literature, produced a perfectly adequate response.

A further modification was made to the Area Control Error to include a term proportional to the integral of the standard ACE, as proposed in the literature. It was demonstrated that this modification successfully enabled the controller to bring the time error and inadvertent energy interchange to zero as well as the frequency and tie-line power. It was concluded that the gain on this integral term need not be very large at all in order to act as a slow trim to ensure zero time error and inadvertent energy interchange over a period of time. The use of such

a controller would prevent the need within the current practice to change the frequency and tie-line power setpoints from time to time in order to manually correct accumulated errors in time and energy interchange.

An important aspect of any discrete controller is the time interval between control actions. The base case for these studies was taken to have a control interval of five seconds based upon examples found in the literature. From an operational point of view with regard to sending new setpoints to the generating plants, it may be desirable to have a longer interval than this. The effect of increasing the interval to ten, fifteen and twenty seconds was investigated. It was found that the response to a step load change got progressively less damped as the interval was increased, an effect that was made even worse in the presence of rate limited setpoints. The most serious problem associated with a long time interval for any discrete controller is the fact that any sudden change in conditions, such as the step change in load and its effect on frequency, may not be noticed and acted upon for a whole control period if the change occurs immediately after the previous control action. With a control interval of five seconds, it was found that such a delay caused only a very slight degradation in the response to correct the frequency error. However, at twenty seconds the response was at the limit of stability, and even at fifteen seconds the oscillatory response may be considered unacceptable. At the other end of the scale, there is seen to be little point in running the control at very much less than five second intervals, particularly when it is considered that a typical load controller on fossil fired plant which is controlling to the setpoints sent by the AGC might be running at about three second intervals.

The more detailed model was used to investigate the effect of different setpoint rate limits on different generating units. As would be expected, speeding up

the response of some of the generators improved the overall response to a fall in frequency. It was found that the faster units took on a larger share of the extra load than the slower units. In practice, it would be expected that the faster units would do more regulating in the short term to correct the frequency error, but would then drop back while the slower units increased their generation until the extra load was equally shared amongst all of them. The fact that the studies here do not illustrate this effect is due to the fact that the generation setpoints do not include an economic component but are changed only with respect to ACE.

Throughout the studies it was apparent how significant was the effect of the setpoints rate limits. The rate limits are effected within the unit load controllers to prevent rapid load changes which would affect superheater pressure control. Because of this it was found necessary to take account of these rate limits within the AGC so that the required load change could be correctly distributed amongst slow and fast units. However, from investigating the effects with and without setpoint rate limits, it would appear that only the economic component needs to be rate limited and not the regulation component of the setpoints sent to the generating plants. If this were the case, it would be important that no further limiting took place within the unit load controllers as happens at the moment or significant amounts of regulation would be "lost" as units did not change generation as expected by the central controller. Alternatively, the two components would have to be sent to the units separately and the rate limit applied to only one of them.

Finally, the simulation was used to illustrate the further improvement in regulation possible when fast hydro units are able to cut in on low frequency and quickly increase generation to maximum. This action can greatly improve the speed with which a frequency fall can be arrested. However, it is only used as an

emergency measure since increased generation from a hydro unit uses up more water reserves and the size of the increase in generation is uncontrolled being simply the difference between the original level of generation and maximum generation, which may be more than necessary if such action is taken on frequency falls which are too small.

Chapter 9

Further Work

There are a number of directions in which this work can be progressed and developed. Should the approach described here be used in earnest to develop a real operational AGC, more confidence will be required in the models used. In this study, nuclear units have only been modelled as high droop fossil units. Gas turbine units, which have a significant role in the control of frequency under emergency conditions, have not been included at all. In order to draw any quantitative conclusions, the simulation and each of its components need to be matched closely to the real system. This would require more thorough validation of the generating unit models against real plant data.

A very significant aspect of full AGC that has not been considered here is economic dispatch. In reality, the generation setpoints sent to each generator from a centralised controller will be made up of two components: an economic base loading plus an offset for frequency/tie-line power regulation. Investigations could be performed into the characteristics and interactions of these two components. For instance, whether it is necessary to rate limit the combined setpoint or only the economic component.

The simulation itself could be used as a test bed for evaluating economic dispatch methods. However, further enhancements to the models may need to be made such as incorporating coal-mills in the coal-fired unit model to produce more realistic characteristics on load changing. A more complex power system model may be required so that the current control areas may be adequately represented.

The power system models used in the current work are a little weak in their representation of the system in Scotland. Should quantitative results be required about the behaviour of the Scottish plant, more detailed representation of this area will be needed. A large proportion of the generating plant in Scotland is hydro. In order to implement a successful centralised frequency controller in this area, it may be very necessary to incorporate the hydro units into the AGC. Investigations could then be performed into the relative amounts of regulation required of, and obtainable from, the different types of generator.

The load on a real power system is never really constant and even if not changing significantly, varies randomly as individual consumers vary their demand. The quality of frequency regulation under these conditions should also be investigated.

Any further investigations would be facilitated by having a faster simulation. In particular, in order to test operational controllers, a real-time simulation would be required. Other than using the latest more powerful micro-processors such as the Intel i860, further work could be done on the modelling itself to make it more efficient. The load models, especially, although not very complex, take up a significant proportion of the computing time since they are so numerous in a complex grid system. Another significant burden is the calculation of the hydro model which uses the more complex Runge-Kutta algorithm and requires a small integration time step to be stable. Investigations could be made into a more

efficient hydro model.

Further enhancement of the simulator is also possible by implementing functions available to the standard University of Bath power system simulator which were not necessary to the work of this project and so not included in the version used for these studies. Such functions include the `seq` and `help` facilities described in [76].

Appendix A

Fossil-Fired Boiler Model Routine Listings

```
void non_integrable(float *y, float *u, grp_ptr *grp)
{
/* Calculates non-integrable variables at step k */

   machine *mat = mat_vec;
   float *Tm = &(mat->uvec->row[s_tm]);
   float w = ((mat->xvec->row[s_w])+w0);
   float ratio1, fun1, ratio2, ratio3, f;

   hs    = Cs + Ds * Pd;
   Ms1   = K1 * (float)sqrt( Pd - P1 );
   Ms2   = K2 * (float)sqrt( P1 - P2 );
   Ms3   = K3 * (float)sqrt( P2 - Ph1);
                                          /* DDC governor - part  */
                                          /* of digital procedure */
   Zgvce = (Zgvci - Zgvc) * Ksm;          /* Rate limited speeder */
   Zgvce = limit(Zgvce_llim,Zgvce_ulim,Zgvce); /*  motor          */
   f     = w*wtof;
   Zgv   = Zgvc + Kgov * (f0-f);          /* Add in mechanical    */
                                          /* governor contribution*/
   Zgv   = limit(Vpmin,Vpmax,Zgv);        /* arithmetic limits */
   Agv   = Zgv;                           /* assume linear governor */
                                          /* ie pu area = pu lift   */
   ratio1= Ph2/Ph1;
   fun1  = (float)pow(ratio1,gam2) - (float)pow(ratio1,gam1);
                                          /* gam1 = (gamma+1)/gamma */
                                          /* gam2 = 2/gamma         */
   Ms4   = Kgv * Agv * Ph1 * (float)sqrt(fun1/Th1);
   Ms5   = K5 * (float)sqrt( Ph2*Ph2 - P5*P5 );
   Ms6   = K6 * (float)sqrt( P5 - P6 );
   Ms7   = K7 * P6;                       /* assumes 'P7' is vacuum */
   ratio2= Ph2/Ph1;
   Th2   = (float)pow(ratio2,gam3) * Th1;       /* gam3 = (gamma-1)/gamma */
   ratio3= P5/Ph2;
```

```
   DelHhp= gam4 * R * Th2 * ( (float)pow(ratio3,gam1) - 1 ) / 2;
                                                /* gam1 = (gamma+1)/gamma */
                                                /* gam4 = gamma/(1-gamma) */
   *Tm   = ( Ms5 * DelHhp  +  Ms7 * DelHlp ) * w * kWtoTm;
                                   /* Tm to be used in generator equations */
}



void rate_of_change(float *y, float *u, float *dydt, grp_ptr *grp)
{
/* Calculates rate of change of integrable variables at step k */

   ddt_lamb = ( Mfu - lamb) / Tf2;
   ddt_Q    = ( Kfur * lamb - Q ) / Tf1;
   ddt_Pd   = ( Q + Ms1 * (hfd - hs) ) / Tb;
   ddt_P1   = Kv1 * ( Ms1 - Ms2 * (1-Msppu) );
   ddt_P2   = Kv2 * ( Ms2 - Ms3 );
   ddt_Ph1  = Kh1 * ( Ms3 - Ms4 );
   ddt_Ph2  = Kh2 * ( Ms4 - Ms5 );
   ddt_P5   = Kv5 * ( Ms5*(1 - Msbpu) - Ms6 );
   ddt_P6   = Kv6 * ( Ms6 - Ms7 );
   ddt_Zgvc = Zgvce;
}
```

Appendix B

Fossil-Fired Boiler Model Variables

Name	Description	Units
λ	Intermediate fuel variable	kg/s
Q	Heat input to boiler	kJ
P_d	Drum Pressure	bars
P_1	Primary superheater outlet pressure	bars
P_2	Secondary superheater outlet pressure	bars
P_{h1}	Pressure before governor valve	bars
P_{h2}	Pressure after governor valve	bars
P_5	Pressure after Turbine HP stage	bars
P_6	Pressure after reheater	bars
Z_{gvc}	Governor valve controller position	p.u.
ω	Frequency/speed in initial study simulation	Hz

Table B.1: Fossil-Fired Boiler Model State Variables

Name	Description	Units
h_s	Enthalpy of steam leaving drum	kJ/kg
M_{s1}	Steam flow in primary superheater	kg/s
M_{s2}	Steam flow in secondary superheater	kg/s
M_{s3}	Steam flow in steam leads	kg/s
M_{s4}	Steam flow through governor valve	kg/s
M_{s5}	Steam flow in turbine HP stage	kg/s
M_{s6}	Steam flow in reheater	kg/s
M_{s7}	Steam flow in turbine LP stage	kg/s
A_{gv}	Governor valve area	p.u.
T_{h2}	Temperature of steam after governor valve	°C
Z_{gv}	Governor valve lift	p.u.
ΔH_{hp}	Enthalpy drop in turbine HP stage	kJ/kg
Z_{gvce}	Governor valve stepper motor positiir error	p.u.
M_{fu}	Fuel flow into boiler	kg/s
Z_{gvci}	Input to governor valve speeder motor	p.u.
L_d	Turbine power in initial study simulation	MW
L_l	Turbine load in initial study simulation	MW

Table B.2: Fossil-Fired Boiler Model Non-Integrable Variables

Name	Description	Units
T_{f1}	Fuel to Heat input time constant	s
T_{f2}	Fuel time constant	s
K_{fur}	Furnace gain - λ to Q	kJ/kg
ψ	Boiler 'time constant'	kJ/bar
K_{v1}	Gain - steam flow to pressure P_1	bar/kg
K_{v2}	Gain - steam flow to pressure P_2	bar/kg
K_{h1}	Gain - steam flow to pressure P_{h1}	bar/kg
K_{h2}	Gain - steam flow to pressure P_{h2}	bar/kg
K_{v5}	Gain - steam flow to pressure P_5	bar/kg
K_{v6}	Gain - steam flow to pressure P_6	bar/kg
K_1	Gain - pressure drop to steam flow M_{s1}	kg/s/bar
K_2	Gain - pressure drop to steam flow M_{s2}	kg/s/bar
K_3	Gain - pressure drop to steam flow M_{s3}	kg/s/bar
K_{gv}	Governor valve gain	
K_5	Gain - pressure drop to steam flow M_{s5}	kg/s/bar
K_6	Gain - pressure drop to steam flow M_{s6}	kg/s/bar
K_7	Gain - pressure drop to steam flow M_{s7}	kg/s/bar
$Z_{gvce_{llim}}$	Lower limit to limit speeder motor rate	p.u.
$Z_{gvce_{ulim}}$	Upper limit to limit speeder motor rate	p.u.
$V_{p_{min}}$	Lower limit on governor valve position	p.u.
$V_{p_{max}}$	Upper limit on governor valve position	p.u.
$\dot{V}_{p_{min}}$	Negative rate limit on governor position	p.u.
$\dot{V}_{p_{max}}$	Positive rate limit on governor position	p.u.
M_{sp}	Fixed attemperator spray flow	kg/s
M_{sb}	Fixed bled steam flow from turbine	kg/s
T_{h1}	Fixed superheater outlet steam temperature	°C
h_{fd}	Fixed feed water enthalpy	kJ/kg
ΔH_{lp}	Fixed turbine LP stage enthalpy drop	kJ/kg
η	Turbine efficiency in initial study simulation	
K_ω	Power to acceleration gain in initial simulation	Hz/s/MW

Table B.3: Fossil-Fired Boiler Model Constants

Name	Description	Value
C_s	fit of enthalpy to saturation line	3126.710937
D_s	of steam tables	-3.416025
γ	ratio of specific heats for superheated steam	1.3
R	gas constant for superheated steam	0.4619

Table B.4: Fossil-Fired Boiler Model Physical Constants

Appendix C

Fossil-Fired Boiler Model Equations

The model equations are as follows:

Fuel

$$\frac{d\lambda}{dt} = \frac{M_{fu}}{T_{f2}} - \frac{\lambda}{T_{f2}} \tag{C.1}$$

Boiler

$$\frac{dQ}{dt} = \frac{K_{fur}\lambda}{T_{f1}} - \frac{Q}{T_{f1}} \tag{C.2}$$

Drum Pressure

$$\frac{dP_d}{dt} = \frac{1}{\psi}[Q + M_{s1}\,[h_{fd} - h_s]] \tag{C.3}$$

Steam Enthalpy

$$h_s = C_s + D_s P_d \tag{C.4}$$

Steam Flow - primary superheater

$$M_{s1} = K_1\sqrt{P_d - P_1} \tag{C.5}$$

Steam Flow - secondary superheater

$$M_{s2} = K_2\sqrt{P_1 - P_2} \tag{C.6}$$

Steam Flow - steam leads

$$M_{s3} = K_3\sqrt{P_2 - P_{h1}} \tag{C.7}$$

Steam Flow - valve nozzle

$$M_{s4} = \frac{K_{gv}A_{gv}P_{h1}}{\sqrt{T_{h1}}}\sqrt{\left(\frac{P_{h2}}{P_{h1}}\right)^{\frac{2}{\gamma}} - \left(\frac{P_{h2}}{P_{h1}}\right)^{\frac{\gamma+1}{\gamma}}} \tag{C.8}$$

Steam Flow - HP turbine

$$M_{s5} = K_5\sqrt{P_{h2}^2 - P_5^2} \tag{C.9}$$

Steam Flow - Reheater

$$M_{s6} = K_6\sqrt{P_5 - P_6} \tag{C.10}$$

Steam Flow - LP Turbine

$$M_{s7} = K_7P_6 \tag{C.11}$$

Pressure - Primary/secondary superheater interface

$$\frac{dP_1}{dt} = K_{v1}\left(M_{s1} + M_{sp} - M_{s2}\right) \tag{C.12}$$

Pressure - Secondary superheater/steam leads interface

$$\frac{dP_2}{dt} = K_{v2}\left(M_{s2} - M_{s3}\right) \tag{C.13}$$

Pressure before valve nozzle

$$\frac{dP_{h1}}{dt} = K_{h1}\left(M_{s3} - M_{s4}\right) \tag{C.14}$$

Pressure after valve nozzle

$$\frac{dP_{h2}}{dt} = K_{h2}\left(M_{s4} - M_{s5}\right) \tag{C.15}$$

Pressure after HP Turbine

$$\frac{dP_5}{dt} = K_{v5}\left(M_{s5} - M_{sb} - M_{s6}\right) \tag{C.16}$$

Pressure after reheater

$$\frac{dP_6}{dt} = K_{v6}\left(M_{s6} - M_{s7}\right) \tag{C.17}$$

Enthalpy Drop across HP turbine

$$\Delta H_{hp} = \frac{\gamma}{1-\gamma}\frac{RT_{h2}}{2}\left[\left(\frac{P_5}{P_{h2}}\right)^{\frac{\gamma+1}{\gamma}} - 1\right] \tag{C.18}$$

Temperature after HP turbine

$$T_{h2} = \left(\frac{P_{h2}}{P_{h1}}\right)^{\frac{\gamma-1}{\gamma}} T_{h1} \tag{C.19}$$

Turbine Speed

$$\frac{d\omega}{dt} = K_{\omega}\left(L_d - L_l\right) \tag{C.20}$$

Turbine Power

$$L_d = \eta\left(M_{s5}\Delta H_{hp} + M_{s7}\Delta H_{lp}\right) \tag{C.21}$$

Appendix D

Pumped-Storage Model Variables

Name	Description	Units
U_{pu}	penstock upper region water velocity	m/s
H_{pm}	static head at mid-penstock	m
U_{pl}	penstock lower region water velocity	m/s
H_{ti}	static head at spiral inlet	m
H_t	static head at draft tube	m
U_{t1}	tail tunnel 1st region water velocity	m/s
H_{tm}	static head at mid tail-tunnel	m
U_{t2}	tail tunnel 2nd region water velocity	m/s
Q_t	single turbine water flow	m^3/s
L_{ta}	single turbine power output	MW
F_{ta}	frequency/speed of turbine	pu
C_{ftf}	filtered frequency error	pu
C_{ltrl}	rate limited power setpoint	pu
L_{taf}	filtered power measurement	pu
C_{f1}	filtered derivative of frequency error	pu
C_{f2}	filtered derivative of frequency error	pu
C_{e2}	filtered frequency and power error	pu
C_{e4}	Integral term of governor	pu
C_{s6}	filtered governor output signal	pu
C_{sa1}	1st stage actuator output	pu
C_{sa2}	2nd stage actuator output	pu

Table D.1: Pumped-Storage Model State Variables

Name	Description	Units
U_{pt}	velocity of water in penstock at turbine	m/s
U_{tt}	velocity of water in tail tunnel at turbine	m/s
H_{tit}	Full head (static + dynamic) at turbine inlet (spiral)	m
H_{tot}	Full head at turbine outlet (draft tube)	m
H_{tdif}	Full head (static + dynamic) across turbine	m
H_{tsqrt}	square root of Htdif	
N_{ta}	speed of turbine in rpm	RPM
N_{11}	unit speed of turbine	pu
X_{gv}	guide vane angle	degrees
Q_{11}	unit discharge of turbine	pu
U_{tro}	velocity of water at runner outlet	m/s
T_{11}	unit torque of turbine	pu
L_{dps}	total power generated by station	MW
X_{Load}	Grid total load	pu
X_{Ltot}	Grid total generation	pu
F_{tae}	frequency error	pu
C_{fte}	filtered frequency error	pu
C_{ltr}	governor load setpoint input	pu
C_{ru}	rate limit for power setpoint change	pu/s
C_{lt}	power setpoint feed forward signal	pu
C_{lte}	power error signal	pu
C_{ft3}	derivative term of governor	pu
C_{e1}	frequency and power error	pu
C_{e3}	proportional term of governor	pu
C_{iul}	integral term upper limit	pu
C_{s5}	governor output signal	pu
C_{s7}	position limited governor output signal	pu

Table D.2: Pumped-Storage Model Non-Integrable Variables

Name	Description	Units
L_{gen}	Grid size	MW
L_{oad}	size of load	MW
L_{gde}	size of load disturbance	MW
F_t	Frequency of grid	Hz
F_{tar}	Frequency setpoint	pu
L_{tar}	manual load setpoint	pu
L_{rlr}	rapid loading setpoint	pu
C_{ltr}	governor load setpoint input	pu
C_{rll}	rate limit for power setpoint change	pu/s
B_{gd}	ASEA governor derivative gain	s
B_{gp}	ASEA governor proportional gain	pu/pu
B_{gi}	ASEA governor integral gain	1/s
E_p	ASEA governor droop gain	pu/pu
C_{ftr}	manual run up speed setpoint	pu
$C_{act_{ul}}$	actuator position upper limit	pu
C_{iul}	integral term upper limit	pu
C_{lt}	power setpoint feed forward signal	pu
L_{int}	power integral	MJ
T_{int}	time integral	s
R_{amp}	value of ramp criterion	MJ
R_{delay}	ramp delay	s

Table D.3: Pumped-Storage Model Constants

Appendix E

Pumped-Storage Model Equations

The model equations are as follows:

Penstock upper region velocity

$$\frac{dU_{pu}}{dt} = g\left[\sin(op) - \frac{F_{pw}}{Z_{pe}}U_{pu}^2 + \frac{H_{ur} - H_{pm}}{Z_{pe}}\right] \tag{E.1}$$

Mid-penstock static head

$$\frac{dH_{pm}}{dt} = \frac{H_{ur} - H_{pm}}{Z_{pe}}U_{pu} + \frac{U_{pu} - U_{pl}}{Z_{pe}}\frac{1}{W_{pq}W_{pw}} \tag{E.2}$$

Penstock lower region velocity

$$\frac{dU_{pl}}{dt} = g\left[\sin(op) - \frac{F_{pw}}{Z_{pe}}U_{pl}^2 + \frac{H_{pm} - H_{ti}}{Z_{pe}}\right] \tag{E.3}$$

Velocity in penstock at turbine

$$U_{pt} = \frac{N_{sets}Q_t}{A_{pen}} \tag{E.4}$$

Static head at spiral inlet

$$\frac{dH_{ti}}{dt} = \frac{H_{pm} - H_{ti}}{Z_{pe}}U_{pl} + \frac{U_{pl} - U_{pt}}{Z_{pe}}\frac{1}{W_{pq}W_{pw}} \tag{E.5}$$

Velocity in tail tunnel at turbine

$$U_{tt} = \frac{N_{sets} Q_t}{A_{tail}} \tag{E.6}$$

Static head in draft tube

$$\frac{dH_t}{dt} = \frac{U_{tt} - U_{t1}}{Z_{te}} \frac{1}{W_{tq} W_{tw}} \tag{E.7}$$

Velocity in tail tunnel 1st region

$$\frac{dU_{t1}}{dt} = g \left[\sin(ot) - \frac{F_{tw}}{Z_{te}} U_{t1}^2 + \frac{H_{to} - H_{tm}}{Z_{te}} \right] \tag{E.8}$$

Static head at mid-tail tunnel

$$\frac{dH_{tm}}{dt} = \frac{H_{to} - H_{tm}}{Z_{te}} U_{t1} + \frac{U_{t1} - U_{t2}}{Z_{te}} \frac{1}{W_{tq} W_{tw}} \tag{E.9}$$

Velocity in tail tunnel 2nd region

$$\frac{dU_{t2}}{dt} = g \left[\sin(ot) - \frac{F_{tw}}{Z_{te}} U_{t2}^2 + \frac{H_{tm} - H_{lr}}{Z_{te}} \right] \tag{E.10}$$

Full head at turbine inlet (spiral)

$$H_{tit} = H_{ti} + \frac{Q_t^2}{2gA_{ti}^2} \tag{E.11}$$

Full head at turbine outlet (draft tube)

$$H_{tot} = H_{to} + \frac{Q_t^2}{2gA_{to}^2} \tag{E.12}$$

Total head across turbine

$$H_{tdif} = H_{tit} - H_{tot} \tag{E.13}$$

$$H_{tsqrt} = \sqrt{H_{tdif}} \tag{E.14}$$

Turbine speed

$$N_{ta} = 500 F_{ta} \tag{E.15}$$

Unit turbine speed

$$N_{11} = \frac{D_{dt} N_{ta}}{H_{tsqrt}} \tag{E.16}$$

Guide vane angle

$$X_{gv} = 31C_{sa2} + 3 \tag{E.17}$$

Turbine unit discharge

$$Q_{11} = \mathcal{F}(X_{gv}, N_{11}) \tag{E.18}$$

Turbine water flow

$$\frac{dQ_t}{dt} = \frac{Q_{11}D_{dt2}H_{tsqrt} - Q_t}{Y_q} \tag{E.19}$$

Runner outlet velocity

$$Y_{tro} = \frac{Q_t}{A_{tro}} \tag{E.20}$$

Torque

$$T_{11} = \mathcal{G}(X_{gv}, N_{11}) \tag{E.21}$$

Power

$$\frac{dL_{ta}}{dt} = \frac{T_{11}D_{dt3}H_{tdif}gK_{nt}F_{ta} - L_{ta}}{Y_L} \tag{E.22}$$

pu power

$$L_{dps} = N_{sets}L_{ta} \tag{E.23}$$

Load

$$L_{oad} = (L_{tar} + L_{gde})\, N_{sets}300 \tag{E.24}$$

Grid Load

$$X_{Load} = \frac{1 + K_C\,(1 - F_{ta})\,(L_{gen} + L_{oad})}{300N_{sets} + L_{gen}} \tag{E.25}$$

Grid generation

$$X_{Ltot} = \frac{L_{dps} + L_{gen}}{300N_{sets} + L_{gen}} \tag{E.26}$$

pu speed

$$\frac{dF_{ta}}{dt} = \frac{X_{Ltot} - X_{Load}}{2F_{ta}H} \tag{E.27}$$

Low frequency trip - sets C_{slr} and A_{uto}

$$F_{ta} \leq 0.994 \tag{E.28}$$

Frequency error

$$F_{tae} = F_{tar} - F_{ta} \tag{E.29}$$

Filtered frequency error

$$\frac{dC_{ftf}}{dt} = \frac{F_{tae} - C_{ftf}}{C_{yf2}} \tag{E.30}$$

$$C_{fte} = C_{ftf} \tag{E.31}$$

Load pu setpoint

$$C_{ltr} = C_{slc}\left(1 - C_{slr}\right) L_{tar} + C_{slr} L_{rlr} \tag{E.32}$$

Rate limit

$$C_{rll} = \left(1 - C_{slr}\right) C_{rl1} + C_{slr} C_{rl2} \tag{E.33}$$

Rate limited setpoint

$$\frac{dC_{ltrl}}{dt} = C_{rll}\left(C_{ltr} - C_{ltrl}\right) \tag{E.34}$$

$$-C_{rll} < \frac{dC_{ltrl}}{dt} < C_{rll} \tag{E.35}$$

Power setpoint feed forward

$$C_{lt} = C_{ltrl}\frac{(31 - 8)}{(34 - 3)} \tag{E.36}$$

Filtered power

$$\frac{dL_{taf}}{dt} = \frac{\frac{L_{ta}}{300} - L_{taf}}{C_{yf1}} \tag{E.37}$$

pu power error

$$C_{lte} = C_{ltrl} - L_{taf} \tag{E.38}$$

Filtered derivative of frequency error

$$\frac{dC_{f1}}{dt} = \frac{C_{fte} - C_{f1}}{C_{yf}} \tag{E.39}$$

$$\frac{dC_{f2}}{dt} = \frac{C_{f1} - C_{f2}}{C_{yf}} \tag{E.40}$$

Governor derivative term

$$C_{ft3} = B_{gd}\frac{dC_{f2}}{dt} \tag{E.41}$$

Frequency and power error

$$C_{e1} = C_{lte}E_p + (1 - C_{slc})C_{ftr} + C_{fte} \tag{E.42}$$

Filter frequency and power error

$$\frac{dC_{e2}}{dt} = \frac{C_{e1} - C_{e2}}{C_{yf}} \tag{E.43}$$

Governor proportional term

$$C_{e3} = B_{gp}C_{e2} \tag{E.44}$$

Integral upper limit

$$C_{iul} = C_{act_{ul}} - C_{lt} \tag{E.45}$$

Governor integral term

$$\frac{dC_{e4}}{dt} = \begin{cases} B_{gi}C_{e2} \\ B_{gi}\left(C_{e2} + (1 - A_{uto})\,K_{track}\left(C_{sa1} - C_{s6}\right)\right) \\ 5\left(C_{iul} - C_{e4}\right) \\ 5\left(-C_{lt} - C_{e4}\right) \end{cases} \tag{E.46}$$

Governor output

$$C_{s5} = C_{ft3} + C_{e3} + C_{e4} + C_{lt} \tag{E.47}$$

Filtered output

$$\frac{dC_{s6}}{dt} = \frac{C_{s5} - C_{s6}}{C_{yf}} \tag{E.48}$$

Position limited governor output

$$C_{s7} = C_{s6} \tag{E.49}$$

$$0 < C_{s7} < C_{act_{ul}} \tag{E.50}$$

Actuator output 1st stage

$$\frac{dC_{sa1}}{dt} = \frac{(C_{s7} - C_{sa1})A_{uto}}{C_{y1}} \tag{E.51}$$

$$\frac{-C_{sal}}{2} < \frac{dC_{sa1}}{dt} < C_{sal} \tag{E.52}$$

Actuator output 2nd stage

$$\frac{dC_{sa2}}{dt} = \frac{C_{sa1} - C_{sa2}}{C_{y1}} \tag{E.53}$$

Appendix F

Four Equivalent Machine Study Files

F.1 Master File

```
* Four machine study with Dinorwig generating
*
NETWORK proc 16 tstep .02
PROCESSORS 16

* default governor
GOV simple G000 reg 0.04 ta 0.3 tb 0.5 tc 10. k1 1.   vpmax 1.1 vpmin \
                          -1.1 pvpmax 0.2 pvpmin -5. constant power

* Busbar data :-
GET "study/m4/b6gen.std"
GET "study/govs"
GET "study/m4/m4tan"

GET "study/m4/p6"

*  GROUP Specifications :-

GROUP DINORWIG  bbar DIN04 set DIN001 avr A001 gov dinogov no 6 \
            vt 1.00346 mw 1000.0 mvar -223.652 area 1
GROUP CEGB      bbar CEGB4 set CEGB01 avr A001 gov pembgovsus no 20\
            vt 0.996656 mw 9677.88  mvar -3.10936 area 1
GROUP NWALES    bbar NWAL4 set NWAL01 avr A001 gov pembgovsus no 1 \
            vt 0.997527 mw 339.116  mvar -66.0287 area 1
GROUP SCOTLAND  bbar SCOT4 set SCOT01 avr A001 gov pembgovsus no 4 \
            vt 1.00511  mw 1810.95  mvar 18.0024 area 2
```

```
* Load data

* LOAD L001 pv0 100 qv0 100
LOAD L001 pf1 100 qf1 100
LOADGROUP LDEES4 bbar DEES4 load L001 mw -2500 mvar 0.0
LOADGROUP LPENT4 bbar PENT4 load L001 mw -200 mvar 0.0
LOADGROUP LCEGB4 bbar CEGB4 load L001 mw -8200 mvar 0.0
LOADGROUP LNWAL4 bbar NWAL4 load L001 mw -100 mvar 0.0
LOADGROUP LSCOT4 bbar SCOT4 load L001 mw -1200 mvar 0.0

* Picture definition file for four machine study

DIAGRAM "pic.fourmach" info freq

PICTURE single overview
groups  white DINORWIG green NWALES yellow CEGB blue SCOTLAND

PICTURE single overview
busbars white DEES4 green PENT4 yellow DIN04 blue CEGB4 magenta \
                                                NWAL4 cyan SCOT4

DISPLAY all

END
```

F.2 Busbar and Line Data

```
*  Busbar data :-

BBAR DEES4 pg 0.00     qg 0.00     pl 2803.68  ql -521.26  \
           vmag 1.01819  vang -98.1135
BBAR PENT4 pg 0.00     qg 0.00     pl 247.147  ql -113.237 \
           vmag 1.01894  vang -93.6863
BBAR DIN04 pg 1000.0   qg -223.653 pl 0.00     ql 0.00     \
           vmag 1.01932  vang -93.0448
BBAR CEGB4 pg 9677.88  qg -3.10669 pl 8403.54  ql 189.12   \
           vmag 0.996656 vang -93.5999
BBAR NWAL4 pg 339.117  qg -66.0301 pl 113.684  ql 68.4929  \
           vmag 0.997527 vang -92.5236
BBAR SCOT4 pg 1810.95  qg 17.9993  pl 1243.42  ql -23.1189 \
           vmag 1.00511  vang -82.7423

*  Line data :-

LINE name L1 bbar1 DEES4  bbar2 PENT4  r 0.095    x 1.264    b 52.38
LINE name L2 bbar1 DEES4  bbar2 PENT4  r 0.095    x 1.264    b 52.38
```

```
LINE          bbar1 PENT4  b -200
LINE name L1 bbar1 DIN04  bbar2 PENT4  r 0.0073   x 0.121    b 220
LINE name L2 bbar1 DIN04  bbar2 PENT4  r 0.0094   x 0.1385   b 124.06
LINE name L3 bbar1 DEES4  bbar2 PENT4  r 0.2034   x 2.0261
LINE          bbar1 DEES4  bbar2 CEGB4  r -0.0272  x 0.6801
LINE          bbar1 DEES4  bbar2 NWAL4  r 0.3008   x 8.3052
LINE          bbar1 DEES4  bbar2 SCOT4  r 1.0308   x 17.6785  Tie S-N
LINE          bbar1 PENT4  bbar2 CEGB4  r -2.4097  x 19.573
LINE          bbar1 PENT4  bbar2 NWAL4  r 0.0348   x 1.9251
LINE          bbar1 PENT4  bbar2 SCOT4  r -24.5471 x 1899.61  Tie S-N
LINE          bbar1 CEGB4  bbar2 NWAL4  r -14.9109 x 79.0945
LINE          bbar1 CEGB4  bbar2 SCOT4  r 0.2317   x 4.5942   Tie S-N
LINE          bbar1 NWAL4  bbar2 SCOT4  r -594.561 x 7730.81  Tie S-N
```

F.3 Primemover Data

```
GOV simple dinogovsimp \
      reg      0.0        ta       1.         tb       100    \
      tc       100        k1       1.         vpmax    1.1    \
      vpmin   -1.1        pvpmax   5.         pvpmin  -5.
GOV hydro  dinogov \
      Apen     78.5398    Atail    160.368    Ati      4.15476 \
      Ato      11.0447    Ddt      2.03       Knt      0.0000523599 \
      Yq       0.01       Kgv1     31.0       Kgv2     3.0      \
      Atro     3.2647     Fta_ul   0.994      Crl1     0.125    \
      Crl2     0.125      Kff1     31.0       Kff2     8.0      \
      Kff3     34.0       Kff4     3.0        Cy1      0.1      \
      Cy2      0.2        Ckll     100.0                        \
      Cyf      0.03       Cyf1     4.0        Cyf2     0.02     \
      Csal     0.166667   sinop    0.488333   Fpw      0.124616 \
      Zpe      600.0      sinot   -0.129083   Ftw      0.0885605 \
      Zte      300.0      Hur      0.0        Hlr      0.0      \
      Wpq      5.0e-10    Wpw      9810.0     Wtq      5.0e-10  \
      Wtw      9810.0     Bgd      0.0        Bgp      10.0     \
      Bgi      1.0        Ep       0.01       Cftr     0.0      \
      Cactul   0.903226   Ciul     0.903226   Ktrack   10.0     \
      Yl       0.1        pmint    0.01       Csa2inc  0.05
GOV simple pembgovsimp \
      reg      .04        ta       .3         tb       .5       \
      tc       10         k1       1.         vpmax    1.1      \
      vpmin    0.         pvpmax   0.2        pvpmin  -5.
GOV fossil pembgovsus  \
      reg      0.04       Tf1      15.        Tf2      5.       \
      Kfur     15840.513  Tb       434078.    Kv1      0.0088438 \
      Kv2      0.0088438  Kh1      0.0576422  Kh2      0.462517 \
      Kv5      0.0128247  Kv6      0.0286832  K1       120.127  \
```

```
      K2        216.267    K3        211.294    Kgv       397.153  \
      K5        3.0228     K6        158.027    K7        9.362    \
      Zgvcemin  -0.025     Zgvcemax  0.025      vpmax     1.1      \
      vpmin     -1.1       pvpmax    5.         pvpmin    -5.      \
      Ksm       0.4        Msppu     0.0303     Msbpu     0.1854   \
      Th1       813.       hfd       1284.      DelHlp    599.23   \
      pmint     0.1        MfuGain   1.0        ZgvGain   1.0      \
      Kcpp      0.6566     Kcpi      0.006566   Kcli      0.00025  \
      sustained
GOV fossil pembgovnonsus  \
      reg       0.04       Tf1       15.        Tf2       5.       \
      Kfur      15840.513  Tb        434078.    Kv1       0.0088438 \
      Kv2       0.0088438  Kh1       0.0576422  Kh2       0.462517 \
      Kv5       0.0128247  Kv6       0.0286832  K1        120.127  \
      K2        216.267    K3        211.294    Kgv       397.153  \
      K5        3.0228     K6        158.027    K7        9.362    \
      Zgvcemin  -0.025     Zgvcemax  0.025      vpmax     1.1      \
      vpmin     -1.1       pvpmax    5.         pvpmin    -5.      \
      Ksm       0.4        Msppu     0.0303     Msbpu     0.1854   \
      Th1       813.       hfd       1284.      DelHlp    599.23   \
      pmint     0.1        MfuGain   1.0        ZgvGain   1.0      \
      Kcpp      0.6566     Kcpi      0.006566   Kcli      0.00025  \
      nonsustained
```

F.4 Generator and AVR Data

```
* Set data :-

SET DIN001 pf .95 h 4.5 ra .117 xdd 21.6 xd 115.20 xddd 14.3 \
    xq 64.3 xa 10. tdd 2.6 tddd .04 tl .02 pmax .97 rt .07 xt 4.7 \
    mva 330. 50.00 60.35 70.75 82.00 94.34 109.43 129.24 166.98

SET CEGB01 pf .85 h 4.46 ra .31 xdd 30.5 xd 277. xddd 22.8 \
    xq 263. xa 17. tdd .78 tddd .021 tl .02 pmax .88 rt 0.0 xt 0. \
    mva 588. 50.0 60.0 70.0 81.6 95.4 111.0 135.0 178.0

SET NWAL01 pf .85 h 4.46 ra .31 xdd 30.5 xd 277. xddd 22.8 \
    xq 263. xa 17. tdd .78 tddd .021 tl .02 pmax .88 rt 0.0 xt 0. \
    mva 588. 50.0 60.0 70.0 81.6 95.4 111.0 135.0 178.0

SET SCOT01 pf .85 h 4.46 ra .31 xdd 30.5 xd 277. xddd 22.8 \
    xq 263. xa 17. tdd .78 tddd .021 tl .02 pmax .88 rt 0.0 xt 0. \
    mva 588. 50.0 60.0 70.0 81.6 95.4 111.0 135.0 178.0

*  AVR data :-
```

```
AVR pembavr kg 200 tg .5 ks 0.05 ts .5 vfmax 2.0 vfmin 0.0 \
    pvfmax 100 pvfmin -100
AVR A001 kg 30 ag 0.3 vfmax 2.0 vfmin 0.0 pvfmax 3.0 pvfmin -2.0
```

F.5 Admittance Matrix Ordering Data

```
* Reordering information :-

REORDER DEES4     row    1
REORDER PENT4     row    2
REORDER DIN04     row    0
REORDER CEGB4     row    3
REORDER NWAL4     row    4
REORDER SCOT4     row    5

* Type 0 , elements 1 , processors 1 - Time 3536
* Total number of data transfers 24  = 4% Bus bandwidth
* Network Factoring information :-

PART part.L  r1   0 r2   5        size 15 start  0 end  1 task  1
PART part.U  r1   0 r2   5        size 21 start  1 end  2 task  1
```

Appendix G

Twenty-Five Equivalent Machine Study Files

G.1 Master File

```
NETWORK proc 16 tstep .02

* default governor
GOV simple G000 reg 0.04 ta 0.3 tb 0.5 tc 10. k1 1. vpmax 1.1 \
    vpmin -1.1  pvpmax 0.2 pvpmin -5. constant power

GET "study/govs"
GET "study/m20/machines"
* set avr and gov data

GET "study/m20/b60din"
* bbar and line data

GET "study/m20/m20din"
* group data

GET "study/m20/r60din"
* reorder data

GET "study/m20/l60din"
* load data
```

G.2 Primemover Data

```
GOV fossil Coal500 \
      reg       0.04        Tf1       40.         Tf2       20.       \
      Kfur      15840.513   Tb        434078.     Kv1       0.0088438 \
      Kv2       0.0088438   Kh1       0.0576422   Kh2       0.462517  \
      Kv5       0.0128247   Kv6       0.0286832   K1        120.127   \
      K2        216.267     K3        211.294     Kgv       356.04    \
      K5        3.0228      K6        158.027     K7        9.362     \
      Zgvcemin  -0.025      Zgvcemax  0.025       vpmax     1.1       \
      vpmin     -1.1        pvpmax    5.          pvpmin    -5.       \
      Ksm       0.4         Msppu     0.0303      Msbpu     0.1854    \
      Th1       813.        hfd       1284.       DelHlp    599.23    \
      pmint     0.1         MfuGain   0.5         ZgvGain   1.0       \
      Kcpp      0.6295      Kcpi      0.003777    Kcli      0.00025   \
      nonsustained
GOV fossil Oil500 \
      reg       0.04        Tf1       15.         Tf2       5.        \
      Kfur      15840.513   Tb        434078.     Kv1       0.0088438 \
      Kv2       0.0088438   Kh1       0.0576422   Kh2       0.462517  \
      Kv5       0.0128247   Kv6       0.0286832   K1        120.127   \
      K2        216.267     K3        211.294     Kgv       356.04    \
      K5        3.0228      K6        158.027     K7        9.362     \
      Zgvcemin  -0.025      Zgvcemax  0.025       vpmax     1.1       \
      vpmin     -1.1        pvpmax    5.          pvpmin    -5.       \
      Ksm       0.4         Msppu     0.0303      Msbpu     0.1854    \
      Th1       813.        hfd       1284.       DelHlp    599.23    \
      pmint     0.1         MfuGain   1.0         ZgvGain   1.0       \
      Kcpp      0.6566      Kcpi      0.006566    Kcli      0.00025   \
      nonsustained
GOV fossil Coal600 \
      reg       0.04        Tf1       40.         Tf2       20.       \
      Kfur      15840.288   Tb        513992.     Kv1       0.00749   \
      Kv2       0.00749     Kh1       0.048816    Kh2       0.391698  \
      Kv5       0.010861    Kv6       0.024291    K1        158.663   \
      K2        285.65      K3        279.078     Kgv       470.265   \
      K5        3.992       K6        208.72      K7        12.365    \
      Zgvcemin  -0.025      Zgvcemax  0.025       vpmax     1.1       \
      vpmin     -1.1        pvpmax    5.          pvpmin    -5.       \
      Ksm       0.4         Msppu     0.0303      Msbpu     0.1854    \
      Th1       813.        hfd       1284.       DelHlp    613.356   \
      pmint     0.1         MfuGain   0.422       ZgvGain   0.845     \
      Kcpp      0.6295      Kcpi      0.003777    Kcli      0.00025   \
      nonsustained
GOV fossil Oil600 \
      reg       0.04        Tf1       15.         Tf2       5.        \
      Kfur      15840.288   Tb        513992.     Kv1       0.00749   \
      Kv2       0.00749     Kh1       0.048816    Kh2       0.391698  \
```

```
      Kv5       0.010861   Kv6       0.024291   K1        158.663  \
      K2        285.65     K3        279.078    Kgv       470.265  \
      K5        3.992      K6        208.72     K7        12.365   \
      Zgvcemin  -0.025     Zgvcemax  0.025      vpmax     1.1      \
      vpmin     -1.1       pvpmax    5.         pvpmin    -5.      \
      Ksm       0.4        Msppu     0.0303     Msbpu     0.1854   \
      Th1       813.       hfd       1284.      DelHlp    613.356  \
      pmint     0.1        MfuGain   0.845      ZgvGain   0.845    \
      Kcpp      0.6566     Kcpi      0.006566   Kcli      0.00025  \
      nonsustained
GOV hydro Hydro \
      Apen      78.5398    Atail     160.368    Ati       4.15476  \
      Ato       11.0447    Ddt       2.03       Knt       0.0000523599 \
      Yq        0.01       Kgv1      31.0       Kgv2      3.0      \
      Atro      3.2647     Fta_ul    0.994      Crl1      0.125    \
      Crl2      0.125      Kff1      31.0       Kff2      8.0      \
      Kff3      34.0       Kff4      3.0        Cy1       0.1      \
      Cy2       0.2        Ckll      100.0                         \
      Cyf       0.03       Cyf1      4.0        Cyf2      0.02     \
      Csal      0.166667   sinop     0.488333   Fpw       0.124616 \
      Zpe       600.0      sinot     -0.129083  Ftw       0.0885605 \
      Zte       300.0      Hur       0.0        Hlr       0.0      \
      Wpq       5.0e-10    Wpw       9810.0     Wtq       5.0e-10  \
      Wtw       9810.0     Bgd       0.0        Bgp       10.0     \
      Bgi       1.0        Ep        0.01       Cftr      0.0      \
      Cactul    0.903226   Ciul      0.903226   Ktrack    10.0     \
      Yl        0          pmint     0.01       Csa2inc   0.05
GOV fossil AGR \
      reg       0.19       Tf1       15.        Tf2       5.       \
      Kfur      15840.288  Tb        513992.    Kv1       0.00749  \
      Kv2       0.00749    Kh1       0.048816   Kh2       0.391698 \
      Kv5       0.010861   Kv6       0.024291   K1        158.663  \
      K2        285.65     K3        279.078    Kgv       470.265  \
      K5        3.992      K6        208.72     K7        12.365   \
      Zgvcemin  -0.025     Zgvcemax  0.025      vpmax     1.1      \
      vpmin     -1.1       pvpmax    5.         pvpmin    -5.      \
      Ksm       0.4        Msppu     0.0303     Msbpu     0.1854   \
      Th1       813.       hfd       1284.      DelHlp    663.18   \
      pmint     0.1        MfuGain   0.845      ZgvGain   0.845    \
      Kcpp      0.6295     Kcpi      0.003777   Kcli      0.00025  \
      nonsustained
GOV fossil Mag147 \
      reg       0.19       Tf1       15.        Tf2       5.       \
      Kfur      15841      Tb        257487.    Kv1       0.014724 \
      Kv2       0.014724   Kh1       0.095966   Kh2       0.77003  \
      Kv5       0.030379   Kv6       0.047754   K1        35.133   \
      K2        62.953     K3        61.505     Kgv       103.36   \
      K5        0.87989    K6        46.0       K7        2.7252   \
      Zgvcemin  -0.025     Zgvcemax  0.025      vpmax     1.1      \
```

```
      vpmin    -1.1       pvpmax   5.         pvpmin  -5.       \
      Ksm      0.4        Msppu    0.0303     Msbpu    0.1854   \
      Th1      813.       hfd      1284.      DelHlp   613.37   \
      pmint    0.1        MfuGain  1.686      ZgvGain  1.686    \
      Kcpp     0.6295     Kcpi     0.003777   Kcli     0.00025  \
      nonsustained
GOV fossil Mag339 \
      reg      0.19       Tf1      15.        Tf2      5.       \
      Kfur     15840      Tb       352195     Kv1      0.010853 \
      Kv2      0.010853   Kh1      0.070741   Kh2      0.56762  \
      Kv5      0.015739   Kv6      0.035138   K1       80.638   \
      K2       145.18     K3       141.84     Kgv      239.01   \
      K5       2.0291     K6       106.08     K7       6.2846   \
      Zgvcemin -0.025     Zgvcemax 0.025      vpmax    1.1      \
      vpmin    -1.1       pvpmax   5.         pvpmin  -5.       \
      Ksm      0.4        Msppu    0.0303     Msbpu    0.1854   \
      Th1      813.       hfd      1284.      DelHlp   613.37   \
      pmint    0.1        MfuGain  1.232      ZgvGain  1.232    \
      Kcpp     0.6295     Kcpi     0.003777   Kcli     0.00025  \
      nonsustained
```

G.3 Generator Data

```
* SET data

SET COTT   pf 0.85 h 3.5  ra 0.23 xdd 30.  xd 245. xddd 21.1 \
    xq 233. xa 15. tdd 0.46 tddd 0.01 tl 0.02 pmax 0.88 rt 0.03 \
    xt 2.86 mva 588.  50. 60.  71.4  84.   98.1  114.  139.  180.
SET CRU1X2 pf 0.9  h 5.2  ra 0.26 xdd 22.  xd 123. xddd 15.  \
    xq 76.  xa 12.5 tdd 1.25 tddd 0.027 tl 0.02 pmax 0.93 rt 0.24 \
    xt 9.91 mva 111.  50. 60.  70.   80.   90.   104.  121.  150.
SET DINO   pf 0.95 h 4.5  ra 0.11 xdd 30.  xd 115. xddd 14.  \
    xq 64.  xa 10. tdd 2.6  tddd 0.04 tl 0.02 pmax 0.97 rt 0.07 \
    xt 4.7  mva 330.  50. 60.  70.   82.   94.   109.  129.  165.
SET DRAX   pf 0.85 h 3.79 ra 0.24 xdd 29.4 xd 213. xddd 20.3 \
    xq 202. xa 15. tdd 1.01 tddd 0.03 tl 0.02 pmax 0.88 rt 0.024 \
    xt 1.98 mva 776.  50. 60.  72.1  85.6  101.  123.  155.  203.
SET DUNG-B pf 0.85 h 3.16 ra 0.24 xdd 28.7 xd 215. xddd 22.3 \
    xq 205. xa 15. tdd 0.88 tddd 0.02 tl 0.02 pmax 0.88 rt 0.021 \
    xt 2.05 mva 776.  50. 60.  70.   81.6  95.4  111.  135.  178.
SET EGGB   pf 0.85 h 4.12 ra 0.25 xdd 28.1 xd 266. xddd 22.1 \
    xq 253. xa 17. tdd 0.55 tddd 0.0115 tl 0.02 pmax 0.88 rt 0.055 \
    xt 2.68 mva 588.  50. 60.  70.   80.8  94.5  113.  139.  181.
SET FERR-C pf 0.85 h 4.46 ra 0.31 xdd 30.5 xd 277. xddd 22.8 \
    xq 263. xa 17. tdd 0.78 tddd 0.021 tl 0.02 pmax 0.88 rt 0.059 \
    xt 2.68 mva 588.  50. 60.  70.   81.6  95.4  111.  135.  178.
```

```
SET FFESX2 pf 0.95 h 3.23 ra 0.36 xdd 26.5 xd 152. xddd 16.8 \
    xq 78.5 xa 11.4 tdd 0.82 tddd 0.03 tl 0.02 pmax 0.98 rt 0.54 \
    xt 19.54 mva 95.  50. 61.1  73.3  87.6  104.  123.  148.  184.
SET FIDF   pf 0.85 h 3.5  ra 0.23 xdd 30.  xd 245. xddd 21.1 \
    xq 233. xa 15. tdd 0.46 tddd 0.01 tl 0.02 pmax 0.88 rt 0.031 \
    xt 2.93 mva 588.  50. 60.   71.4  84.   98.1  114.  139.  180.
SET FOYEX2 pf 0.85 h 3.5  ra 0.39 xdd 25.0 xd  88. xddd 13.0 \
    xq  55. xa 10.0 tdd 2.3  tddd 0.06 tl 0.02 pmax 0.87 rt 0.13 \
    xt 8.53 mva 353.  50. 60.   70.   80.   91.9  106.  123.  145.
SET HATL   pf 0.85 h 3.15 ra 0.22 xdd 35.2 xd 227. xddd 29.2 \
    xq 215. xa 17. tdd 1.   tddd 0.02 tl 0.02 pmax 0.88 rt 0.036 \
    xt 2.2  mva 776.  51. 62.   74.   86.5  102.  120.  144.  186.
SET HEYS   pf 0.85 h 3.15 ra 0.22 xdd 35.2 xd 227. xddd 29.2 \
    xq 215. xa 17. tdd 1.   tddd 0.02 tl 0.02 pmax 0.88 rt 0.023 \
    xt 1.97 mva 776.  51. 62.   74.   86.5  102.  120.  144.  186.
SET HINP-B pf 0.85 h 3.15 ra 0.22 xdd 35.2 xd 227. xddd 29.2 \
    xq 215. xa 17. tdd 1.   tddd 0.02 tl 0.02 pmax 0.88 rt 0.023 \
    xt 2.11 mva 776.  51. 62.   74.   86.5  102.  120.  144.  186.
SET HUER-B pf 0.85 h 3.84 ra 0.24 xdd 26.6 xd 212. xddd 19.  \
    xq 201. xa 14.2 tdd 0.88 tddd 0.04 tl 0.02 pmax 0.88 rt 0.021 \
    xt 2.06 mva 776.  50. 60.   70.   82.9  96.6  115.  146.  204.
SET LOA2XA   pf 0.85 h 3.79 ra 0.24 xdd 29.4 xd 213. xddd 20.3 \
    xq 202. xa 15. tdd 1.01 tddd 0.03 tl 0.02 pmax 0.88 rt 0.024 \
    xt 1.98 mva 776.  50. 60.   72.1  85.6  101.  123.  155.  203.
SET PEHE   pf 0.85 h 3.18 ra 0.19 xdd 33.7 xd 217. xddd 28.  \
    xq 206. xa 21. tdd 1.   tddd 0.02 tl 0.02 pmax 0.88 rt 0.029 \
    xt 1.93 mva 776.  50. 61.8  72.9  86.1  101.  122.  151.  194.
SET RATS   pf 0.85 h 4.46 ra 0.31 xdd 30.5 xd 277. xddd 22.8 \
    xq 263. xa 17. tdd 0.78 tddd 0.021 tl 0.02 pmax 0.88 rt 0.056 \
    xt 2.45 mva 588.  50. 60.   70.   81.6  95.4  111.  135.  178.
SET RUGE-B pf 0.85 h 4.46 ra 0.31 xdd 30.5 xd 277. xddd 22.8 \
    xq 263. xa 17. tdd 0.78 tddd 0.021 tl 0.02 pmax 0.88 rt 0.04 \
    xt 2.28 mva 588.  50. 60.   70.   81.6  95.4  111.  135.  178.
SET TRAW   pf 0.85 h 7.1  ra 0.18 xdd 29.4 xd 261. xddd 22.5 \
    xq 248. xa 16.9 tdd 0.74 tddd 0.023 tl 0.02 pmax 0.88 rt 0.28 \
    xt 9.72 mva 170.6 50. 60.   70.5  82.3  94.5  110.  128.  151.
SET WYLF   pf 0.9  h 5.37 ra 0.24 xdd 30.8 xd 233. xddd 19.7 \
    xq 221. xa 14. tdd 0.6  tddd 0.022 tl 0.02 pmax 0.93 rt 0.097 \
    xt 4.67 mva 372.2998  50. 60. 70.7  82.4  95.4  111.  134.  172.

* AVR data

AVR A001 Kg 30. Ag 0.3 Vfmax 2.  Vfmin 0.  PVfmax 3.  Pvfmin -2.
AVR A002 Kg 30. Ag 0.3 Vfmax 1.3 Vfmin 0.  PVfmax 1.  Pvfmin -1.

* DIRECTORY data

CONTROL  set COTT    avr A001  gov Coal500
CONTROL  set CRU1X2  avr A001  gov Hydro
```

```
CONTROL  set DINO    avr A001  gov Hydro
CONTROL  set DRAX    avr A001  gov Coal600
CONTROL  set DUNG-B  avr A001  gov AGR
CONTROL  set EGGB    avr A001  gov Coal500
CONTROL  set FERR-C  avr A001  gov Coal500
CONTROL  set FFESX2  avr A001  gov Hydro
CONTROL  set FIDF    avr A001  gov Coal500
CONTROL  set FOYEX2  avr A001  gov Hydro
CONTROL  set HATL    avr A001  gov AGR
CONTROL  set HEYS    avr A001  gov AGR
CONTROL  set HINP-B  avr A001  gov AGR
CONTROL  set HUER-B  avr A001  gov AGR
CONTROL  set LOA2XA  avr A001  gov Coal600
CONTROL  set PEHE    avr A001  gov AGR
CONTROL  set RATS    avr A001  gov Coal500
CONTROL  set RUGE-B  avr A001  gov Coal500
*CONTROL  set TRAW    avr A002  gov Mag147
*CONTROL  set WYLF    avr A002  gov Mag339
CONTROL  set TRAW    avr A002  gov AGR
CONTROL  set WYLF    avr A002  gov AGR
                             * Although actually Magnox, model all
                             * nuclears as the same for now - ie
                             * unresponsive fossil stations
```

G.4 Generator Group Data

```
* Group data for 25 machine study - 6 separate Dinorwig groups

* Use when DIN1 and DIN2 pumping
GROUP HARTLEPL.    bbar HATL2  set HATL   no 1       mw 653.2     \
      mvar -113.7  vt 1.       area 0     splim 0.05
* Use when DIN1 and DIN2 generating
*GROUP HARTLEPL.    bbar HATL2  set HATL   no 1       mw 453.2     \
*      mvar -113.7  vt 1.       area 0     splim 0.05
GROUP TRAWS.       bbar TRAW2  set TRAW   no 2       mw 194.7     \
      mvar -37.    vt 1.       area 0     splim 0.05
GROUP COTTAM       bbar COTT4  set COTT   no 3       mw 969.0999  \
      mvar -7.5    vt 1.       area 1     splim 0.05
GROUP RATCLIFFE    bbar RATS4J set RATS   no 3       mw 998.5999  \
      mvar -17.6   vt 1.       area 1     splim 0.05
GROUP FERRYBR.     bbar FERR2J set FERR-C no 3       mw 998.7     \
      mvar 52.3    vt 1.       area 1     splim 0.05
GROUP DRAX.B       bbar DRAX4J set DRAX   no 4       mw 2636.7998 \
      mvar -201.1  vt 1.       area 1     splim 0.05
GROUP WYLFA        bbar WYLF4  set WYLF   no 2       mw 419.5     \
      mvar -28.9   vt 1.       area 0     splim 0.05
```

```
* Treat Dinorwig as 6 separate groups so can set individual low
* frequency relay levels
GROUP DINORWIG1    bbar DIN041 set DINO   no 1       mw -299.6333 \
      mvar -4.0667 vt 1.       area 0     lfr 40     lflogic 2.75
GROUP DINORWIG2    bbar DIN042 set DINO   no 1       mw -299.6333 \
      mvar -4.0667 vt 1.       area 0     lfr 40     lflogic 2.75
*GROUP DINORWIG1    bbar DIN041 set DINO   no 1       mw 100.0    \
*      mvar -4.0667 vt 1.       area 0     lfr 49.85  lflogic 2.75
*GROUP DINORWIG2    bbar DIN042 set DINO   no 1       mw 100.0    \
*      mvar -4.0667 vt 1.       area 0     lfr 40     lflogic 2.75
GROUP DINORWIG3    bbar DIN043 set DINO   no 1       mw -299.6333 \
      mvar -4.0667 vt 1.       area 0     lfr 40     lflogic 2.75
GROUP DINORWIG4    bbar DIN044 set DINO   no 1       mw -299.6333 \
      mvar -4.0667 vt 1.       area 0     lfr 40     lflogic 2.75
GROUP DINORWIG5    bbar DIN045 set DINO   no 1       mw -299.6333 \
      mvar -4.0667 vt 1.       area 0     lfr 40     lflogic 2.75
GROUP DINORWIG6    bbar DIN046 set DINO   no 1       mw -299.6333 \
      mvar -4.0667 vt 1.       area 0     lfr 40     lflogic 2.75
*GROUP FOYERS       bbar FOYE2  set FOYEX2 no 2       mw -299.5999 \
*      mvar 59.2    vt 1.       area 0     splim 0.05
* Change no from 2 to 1 so sets are pumping flat out as they should
* be. T.Stagg 19/4/91
GROUP FOYERS       bbar FOYE2  set FOYEX2 no 1       mw -299.5999 \
      mvar 59.2    vt 1.       area 0     splim 0.05
* Use when DIN1 and DIN2 generating
*GROUP PETERHEAD    bbar PEHE2  set PEHE   no 1       mw 410.2    \
*      mvar -31.8   vt 1.       area 0     splim 0.05
* Use when DIN1 and DIN2 pumping
GROUP PETERHEAD    bbar PEHE2  set PEHE   no 1       mw 610.2    \
      mvar -31.8   vt 1.       area 0     splim 0.05
*GROUP FFESTIN.     bbar FFES2  set FFESX2 no 4       mw -279.5999 \
*      mvar -6.6    vt 0.95     area 0     splim 0.05
* Change no from 4 to 3 so sets are pumping flat out as they should
* be. T.Stagg 19/4/91
GROUP FFESTIN.     bbar FFES2  set FFESX2 no 3       mw -279.5999 \
      mvar -6.6    vt 0.95     area 0     splim 0.05
GROUP CRUACHAN     bbar CRUA2Q set CRU1X2 no 4       mw -399.3999 \
      mvar -32.8   vt 1.       area 0     splim 0.05
GROUP FIDDLERS     bbar FIDF2J set FIDF   no 3       mw 972.7998  \
      mvar -37.4   vt 1.       area 1     splim 0.05
GROUP HUNTERSTN    bbar HUER4  set HUER-B no 2       mw 690.2998  \
      mvar -150.4  vt 1.       area 0     splim 0.05
* Use when DIN1 and DIN2 generating
*GROUP DUNGENESS    bbar DUNG4  set DUNG-B no 2       mw 504.0999 \
*      mvar -44.2   vt 1.       area 0     splim 0.05
* Use when DIN1 and DIN2 pumping
GROUP DUNGENESS    bbar DUNG4  set DUNG-B no 2       mw 704.0999  \
      mvar -44.2   vt 1.       area 0     splim 0.05
*GROUP LONGANNET   bbar LOAN2  set LOA2XA no 4       mw 1198.5    \
```

```
*      mvar -235.3 vt 1.       area 2     splim 0.05
* Using Drax 660MW machines for Longannet, having been told by NGC
* (Clive Arkell, Steve Brown, NC) that this is a station with large
* sets, not little ones. - T.Stagg 19/4/91
GROUP LONGANNET    bbar LOAN2  set LOA2XA no 2       mw 1198.5    \
      mvar -235.3  vt 1.       area 2     splim 0.05
* Use when DIN1 and DIN2 generating
*GROUP HINKLEY      bbar HINP4  set HINP-B no 2       mw 624.      \
*      mvar 18.3    vt 1.       area 0     splim 0.05
* Use when DIN1 and DIN2 pumping
GROUP HINKLEY      bbar HINP4  set HINP-B no 2       mw 824.      \
      mvar 18.3    vt 1.       area 0     splim 0.05
GROUP RUGELEY      bbar RUGE4  set RUGE-B no 1       mw 484.3999  \
      mvar 4.6     vt 1.       area 1     splim 0.05
GROUP HEYSHAM      bbar HEYS4  set HEYS   no 1       mw 653.2     \
      mvar -64.    vt 1.       area 0     splim 0.05
GROUP EGGBORO.     bbar EGGB4J set EGGB   no 2       mw 892.8999  \
      mvar -30.5   vt 1.       area 1     splim 0.05
```

G.5 Busbar and Line Data

```
* Extra detail to treat DINORWIG as 6 separate groups

* Load Flow data

* TWENTY MACHINE , SIXTY BUSBAR REDUCTION
* DINORWIG STABILISER & LINE SWITCHING STUDIES
* CEGB 1984 SUMMER NIGHT MIN 22%(10GW) ACS DEMAND
* DINORWIG IN PUMP MODE. 500MW TRANSFER FROM SSEB
* ORIGINAL STUDY H.LU R4G3539,R4G3540

* Busbar data

BBAR LOVE4  vmag 0.99978 vang -36.09 pl 423.11  ql -227.17
BBAR BRFO4  vmag 1.01338 vang -33.20 pl 143.72  ql -213.40
BBAR PELH4  vmag 1.00106 vang -33.38 pl 545.08  ql -11.97
BBAR DUNG4  vmag 1.00000 vang -32.83 pl -270.30 ql 26.90
BBAR SUND4  vmag 0.99433 vang -32.38 pl 409.37  ql 39.24
BBAR ECLA4  vmag 0.99550 vang -33.25 pl 381.81  ql -32.49
BBAR BRLE4  vmag 0.99900 vang -35.75 pl 399.76  ql -71.36
BBAR COWL4  vmag 0.99645 vang -34.63 pl 75.93   ql -153.31
BBAR EXET4  vmag 1.00324 vang -35.03 pl 282.10  ql -38.24
BBAR HINP4  vmag 1.00497 vang -33.70 pl -711.24 ql -52.25
BBAR MELK4  vmag 0.99234 vang -35.13 pl 103.17  ql 2.40
BBAR WALH4  vmag 0.99662 vang -35.06 pl -10.49  ql 84.67
BBAR ABTH2J vmag 0.97360 vang -38.78 pl 443.76  ql 92.01
BBAR CILF4  vmag 0.98216 vang -37.29 pl 170.80  ql 14.33
BBAR PEMB4  vmag 0.99111 vang -37.55 pl 129.81  ql 53.61
BBAR WALP4  vmag 1.00159 vang -30.24 pl 171.71  ql -9.74
BBAR COTT4  vmag 0.99997 vang -22.75 pl -892.89 ql -108.09
BBAR HIGM4  vmag 0.99964 vang -23.80 pl 170.51  ql -37.86
BBAR RATS4J vmag 0.99995 vang -26.70 pl -863.85 ql -57.70
BBAR WBUR4  vmag 0.99863 vang -23.18 pl 97.06   ql -101.96
BBAR CELL4  vmag 0.99785 vang -29.05 pl 107.66  ql 35.94
BBAR DRAK4  vmag 0.99717 vang -29.42 pl 285.92  ql 67.71
BBAR FECK4  vmag 0.99657 vang -32.78 pl 180.32  ql 43.04
BBAR IRON4  vmag 0.99925 vang -32.10 pl 229.79  ql -6.42
BBAR RUGE4  vmag 0.99992 vang -29.36 pl -459.43 ql -4.62
BBAR WILL4  vmag 0.99692 vang -27.92 pl 196.30  ql 53.39
BBAR DEES4  vmag 0.99918 vang -32.61 pl 324.13  ql -5.35
BBAR LEGA4  vmag 0.99821 vang -32.85 pl 58.71   ql 106.37
BBAR PENT4  vmag 0.99969 vang -36.96 pl 31.46   ql -9.79
BBAR TRAW2  vmag 0.99922 vang -35.44 pl -183.44 ql 13.73
BBAR TRAW4  vmag 1.00074 vang -34.98 pl 0.0     ql 0.0
```

```
BBAR WYLF4  vmag 0.99783 vang -36.60 pl -220.47 ql 105.15
BBAR DINO41  vmag 0.99983 vang -37.63 pl 0.0 ql 0.0
BBAR DINO42  vmag 0.99983 vang -37.63 pl 0.0 ql 0.0
BBAR DINO43  vmag 0.99983 vang -37.63 pl 0.0 ql 0.0
BBAR DINO44  vmag 0.99983 vang -37.63 pl 0.0 ql 0.0
BBAR DINO45  vmag 0.99983 vang -37.63 pl 0.0 ql 0.0
BBAR DINO46  vmag 0.99983 vang -37.63 pl 0.0 ql 0.0
BBAR DINO4  vmag 0.99983 vang -37.63 pl 1979.80 ql 24.43
BBAR FFES2  vmag 0.99796 vang -35.67 pl 279.57  ql 6.60
BBAR FIDF2J vmag 0.99990 vang -28.34 pl -230.33 ql -17.29
BBAR DAIN4  vmag 1.00003 vang -28.94 pl 352.28  ql -7.83
BBAR HEYS4  vmag 1.00995 vang -23.07 pl -465.39 ql -44.04
BBAR PEWO4  vmag 1.00726 vang -24.27 pl 60.25   ql -64.88
BBAR FERR2J vmag 1.00000 vang -16.60 pl -528.65 ql 3.73
BBAR CREB4  vmag 1.00138 vang -19.74 pl 129.86  ql 29.10
BBAR DRAX4J vmag 0.99998 vang -17.45 pl -2464.19 ql 258.95
BBAR EGGB4J vmag 0.99998 vang -18.11 pl -859.01 ql 20.17
BBAR HAWP4R vmag 1.01572 vang -16.70 pl 26.84   ql -48.44
BBAR KEAR4Q vmag 0.99315 vang -22.73 pl 179.33  ql 8.83
BBAR NORT4Q vmag 1.01370 vang -18.08 pl 48.90   ql -5.54
BBAR OSBA4Q vmag 1.00486 vang -17.30 pl 28.82   ql -32.72
BBAR STAL4Q vmag 0.99446 vang -22.98 pl 118.60  ql 33.35
BBAR THOM4  vmag 0.99499 vang -20.42 pl 353.86  ql -78.66
BBAR BLYT2J vmag 1.01868 vang -16.49 pl -90.72  ql 41.69
BBAR HATL2  vmag 1.01498 vang -14.94 pl -426.25 ql 72.87
BBAR STEW2J vmag 1.02011 vang -16.55 pl 217.27  ql -85.34
BBAR HARK2  vmag 1.01196 vang -18.99 pl 148.40  ql -108.12
BBAR FOYE2  vmag 0.99999 vang -16.34 pl 338.40  ql -52.05
BBAR KINT2  vmag 1.01631 vang -9.57  pl 138.11  ql -52.19
BBAR PEHE2  vmag 1.01998 vang -7.81  pl -550.52 ql 4.78
BBAR CRUA2Q vmag 1.00501 vang -17.77 pl 427.49  ql -9.20
BBAR HUER4  vmag 1.02418 vang -10.94 pl -460.14 ql -44.20
BBAR KINC2  vmag 1.02009 vang -11.10 pl 176.28  ql -33.84
BBAR LOAN2  vmag 1.01498 vang -9.47  pl -946.52 ql 169.58
BBAR STHA2  vmag 1.02416 vang -12.87 pl 281.20  ql -134.91


* Line data

LINE name L1 bbar1 LOVE4  bbar2 BRFO4  r -25.8094  x 342.6487
LINE name L1 bbar1 LOVE4  bbar2 PELH4  r -45.5669  x 354.5898
LINE name L1 bbar1 LOVE4  bbar2 DUNG4  r 0.1574    x 2.5810
LINE name L1 bbar1 LOVE4  bbar2 SUND4  r -186.6696 x 1319.3962
LINE name L1 bbar1 LOVE4  bbar2 ECLA4  r -73.2008  x 619.8848
LINE name L1 bbar1 LOVE4  bbar2 BRLE4  r 0.0670    x 0.6524
LINE name L1 bbar1 LOVE4  bbar2 EXET4  r 0.1145    x 1.6635
LINE name S1 bbar1 LOVE4                                    \
```

```
     b -200.0000
LINE name L1 bbar1 BRFO4  bbar2 PELH4  r -0.0994   x 14.9289
LINE name L1 bbar1 BRFO4  bbar2 DUNG4  r 0.4820    x 5.4116
LINE name L1 bbar1 BRFO4  bbar2 SUND4  r 0.5919    x 26.8656
LINE name L1 bbar1 BRFO4  bbar2 ECLA4  r 0.4491    x 18.9649
LINE name L1 bbar1 BRFO4  bbar2 BRLE4  r 0.0777    x 29.2029
LINE name L1 bbar1 BRFO4  bbar2 WALP4  r 0.3038    x 2.7027
LINE name L2 bbar1 BRFO4  bbar2 PELH4  r 0.0831    x 1.1086  \
     b 45.9393
LINE name L1 bbar1 PELH4  bbar2 DUNG4  r 0.2033    x 8.2666
LINE name L1 bbar1 PELH4  bbar2 SUND4  r 0.3266    x 1.0651
LINE name L1 bbar1 PELH4  bbar2 ECLA4  r -0.4487   x 12.4916
LINE name L1 bbar1 PELH4  bbar2 BRLE4  r -1.1483   x 20.6784
LINE name L1 bbar1 PELH4  bbar2 WALP4  r 0.1080    x 1.4632
LINE name L1 bbar1 PELH4  bbar2 COTT4  r 35.5218   x 136.5681
LINE name L1 bbar1 DUNG4  bbar2 SUND4  r 0.7113    x 24.3294
LINE name L1 bbar1 DUNG4  bbar2 ECLA4  r 0.5477    x 12.8785
LINE name L1 bbar1 DUNG4  bbar2 BRLE4  r 0.3169    x 18.6089
LINE name L1 bbar1 SUND4  bbar2 ECLA4  r 0.2252    x 5.8471
LINE name L1 bbar1 SUND4  bbar2 BRLE4  r 0.5620    x 10.5452
LINE name L1 bbar1 SUND4  bbar2 COTT4  r 0.2386    x 3.4606
LINE name L1 bbar1 SUND4  bbar2 WBUR4  r 0.3731    x 3.2971
LINE name L1 bbar1 ECLA4  bbar2 BRLE4  r 0.2414    x 6.3296
LINE name L1 bbar1 ECLA4  bbar2 RATS4J r 0.2402    x 2.2025
LINE name L2 bbar1 ECLA4  bbar2 SUND4  r 0.0347    x 0.4631  \
     b 19.1900
LINE name L1 bbar1 BRLE4  bbar2 COWL4  r 0.0591    x 0.8002
LINE name L1 bbar1 BRLE4  bbar2 MELK4  r 0.1964    x 1.5546  \
     b 48.1900
LINE name L1 bbar1 COWL4  bbar2 MELK4  r 0.2298    x 2.2791
LINE name L1 bbar1 COWL4  bbar2 WALH4  r 3.0580    x 57.3653
LINE name S1 bbar1 COWL4                                     \
     b -200.0000
LINE name L1 bbar1 COWL4  bbar2 ECLA4  r 0.0437    x 0.5822  \
     b 24.1266
LINE name L2 bbar1 COWL4  bbar2 WALH4  r 0.1320    x 1.5196  \
     b 93.7054
LINE name L1 bbar1 EXET4  bbar2 HINP4  r 0.0729    x 0.5871
LINE name L1 bbar1 MELK4  bbar2 WALH4  r 1.4294    x 16.2805
LINE name L1 bbar1 MELK4  bbar2 ABTH2J r 0.6887    x 3.6260
LINE name L1 bbar1 MELK4  bbar2 CILF4  r 0.1140    x 1.7669
LINE name L1 bbar1 MELK4  bbar2 PEMB4  r 26.2089   x 207.9795
LINE name S1 bbar1 MELK4                                     \
     b -200.0000
LINE name L1 bbar1 MELK4  bbar2 HINP4  r 0.2083    x 1.6494  \
     b 50.0014
```

```
LINE name L2 bbar1 MELK4  bbar2 HINP4  r 0.2083    x 1.6494  \
     b 50.0014
LINE name L1 bbar1 ABTH2J bbar2 CILF4  r 0.0663    x 1.0250
LINE name L1 bbar1 ABTH2J bbar2 PEMB4  r 0.4419    x 8.9373
LINE name L1 bbar1 CILF4  bbar2 PEMB4  r 0.1836    x 2.7436
LINE name S1 bbar1 CILF4                                     \
     b -200.0000
LINE name L2 bbar1 CILF4  bbar2 PEMB4  r 0.1725    x 2.3005  \
     b 97.9100
LINE name L1 bbar1 CILF4  bbar2 WALH4  r 0.1213    x 1.6282  \
     b 109.6999
LINE name L1 bbar1 PEMB4  bbar2 WALH4  r 0.2637    x 3.5265  \
     b 190.4900
LINE name L1 bbar1 COTT4  bbar2 WBUR4  r 0.1169    x 1.7705
LINE name L1 bbar1 COTT4  bbar2 CREB4  r 0.1852    x 1.8166
LINE name L1 bbar1 COTT4  bbar2 DRAX4J r 0.1682    x 2.0260
LINE name L1 bbar1 COTT4  bbar2 RATS4J r 0.1697    x 1.3433  \
     b 40.7232
LINE name L2 bbar1 COTT4  bbar2 WBUR4  r 0.0096    x 0.1280  \
     b 5.3040
LINE name L1 bbar1 HIGM4  bbar2 THOM4  r 0.0857    x 3.5369
LINE name L1 bbar1 HIGM4  bbar2 RATS4J r 0.1549    x 1.2287  \
     b 42.3955
LINE name L1 bbar1 HIGM4  bbar2 WBUR4  r 0.0273    x 0.2580  \
     b 9.1930
LINE name L1 bbar1 RATS4J bbar2 WILL4  r 0.0525    x 0.4159  \
     b 12.6086
LINE name L1 bbar1 WBUR4  bbar2 CREB4  r 0.1399    x 1.3459
LINE name L1 bbar1 WBUR4  bbar2 DRAX4J r 0.1277    x 1.5011
LINE name S1 bbar1 WBUR4                                     \
     b -200.0000
LINE name L1 bbar1 WBUR4  bbar2 WALP4  r 0.1245    x 1.6594  \
     b 70.6300
LINE name L1 bbar1 CELL4  bbar2 DRAK4  r 0.1080    x 0.8546  \
     b 25.9085
LINE name L1 bbar1 CELL4  bbar2 WILL4  r 0.1492    x 1.1810  \
     b 35.8041
LINE name L1 bbar1 DRAK4  bbar2 FECK4  r 0.1250    x 1.1740
LINE name L1 bbar1 DRAK4  bbar2 IRON4  r 0.1833    x 4.4715
LINE name L1 bbar1 DRAK4  bbar2 WILL4  r 0.1036    x 8.2848
LINE name L1 bbar1 DRAK4  bbar2 RATS4J r 0.0793    x 0.6288  \
     b 30.0000
LINE name L1 bbar1 DRAK4  bbar2 RUGE4  r 0.0521    x 0.3963  \
     b 12.0154
LINE name L1 bbar1 FECK4  bbar2 IRON4  r 0.2257    x 7.7258
LINE name L1 bbar1 FECK4  bbar2 WILL4  r 0.0889    x 10.3370
```

```
LINE name L2 bbar1 FECK4  bbar2 IRON4  r 0.1561    x 1.2359  \
     b 37.4688
LINE name L1 bbar1 FECK4  bbar2 MELK4  r 0.2572    x 2.0364  \
     b 63.1290
LINE name L1 bbar1 FECK4  bbar2 WALH4  r 0.1365    x 1.2945  \
     b 40.1285
LINE name L1 bbar1 IRON4  bbar2 WILL4  r 1.2734    x 20.6581
LINE name L1 bbar1 RUGE4  bbar2 IRON4  r 0.1406    x 1.1134  \
     b 33.7536
LINE name L1 bbar1 DEES4  bbar2 LEGA4  r 1.9592    x 18.3865
LINE name L1 bbar1 DEES4  bbar2 FIDF2J r 0.0274    x 1.0798
LINE name L1 bbar1 DEES4  bbar2 HEYS4  r 1.1580    x 27.7890
LINE name L1 bbar1 DEES4  bbar2 PEWO4  r 0.0887    x 37.1891
LINE name L1 bbar1 DEES4  bbar2 DAIN4  r 0.1508    x 1.1459  \
     b 34.7386
LINE name L2 bbar1 DEES4  bbar2 DAIN4  r 0.1508    x 1.1459  \
     b 34.7386
LINE name L2 bbar1 DEES4  bbar2 LEGA4  r 0.0661    x 0.5170  \
     b 14.8832
LINE name L1 bbar1 DEES4  bbar2 PENT4  r 0.0950    x 1.2640  \
     b 52.3770
LINE name L2 bbar1 DEES4  bbar2 PENT4  r 0.0950    x 1.2640  \
     b 52.3770
LINE name L1 bbar1 DEES4  bbar2 TRAW4  r 0.1884    x 1.4913  \
     b 45.2091
LINE name L1 bbar1 LEGA4  bbar2 IRON4  r 0.1513    x 1.1979  \
     b 37.1400
LINE name L2 bbar1 LEGA4  bbar2 IRON4  r 0.1464    x 1.1590  \
     b 35.1360
LINE name L1 bbar1 LEGA4  bbar2 TRAW4  r 0.1906    x 1.4607  \
     b 43.6105
LINE name L1 bbar1 PENT4  bbar2 TRAW2  r 29.9219   x 111.9125
LINE name L1 bbar1 PENT4  bbar2 WYLF4  r 16.8170   x 62.8052
LINE name S1 bbar1 PENT4                                     \
     b -200.0000
LINE name L1 bbar1 PENT4  bbar2 TRAW4  r 0.0603    x 0.8215  \
     b 136.9016
LINE name L2 bbar1 PENT4  bbar2 WYLF4  r 0.0423    x 0.5634  \
     b 23.3455
LINE name L3 bbar1 PENT4  bbar2 WYLF4  r 0.0423    x 0.5634  \
     b 23.3455
LINE name L1 bbar1 TRAW2  bbar2 WYLF4  r 226.2408  x 406.8196
LINE name L1 bbar1 TRAW2  bbar2 FFES2  r 0.0842    x 0.2952  \
     b 1.9296
LINE name L2 bbar1 TRAW2  bbar2 FFES2  r 0.0842    x 0.2952  \
     b 1.9296
```

```
LINE name L1 bbar1 TRAW4  bbar2 TRAW2  r 0.0200    x 1.6000  \
     b -0.5740
LINE name L2 bbar1 TRAW4  bbar2 TRAW2  r 0.0200    x 1.6000  \
     b -0.5740
* Extra lines to treat Dinorwig as 6 separate groups
LINE name L1 bbar1 DINO41 bbar2 DINO4  r 0.02      x 1.6     \
     b -0.574
LINE name L1 bbar1 DINO42 bbar2 DINO4  r 0.02      x 1.6     \
     b -0.574
LINE name L1 bbar1 DINO43 bbar2 DINO4  r 0.02      x 1.6     \
     b -0.574
LINE name L1 bbar1 DINO44 bbar2 DINO4  r 0.02      x 1.6     \
     b -0.574
LINE name L1 bbar1 DINO45 bbar2 DINO4  r 0.02      x 1.6     \
     b -0.574
LINE name L1 bbar1 DINO46 bbar2 DINO4  r 0.02      x 1.6     \
     b -0.574

LINE name L1 bbar1 DINO4  bbar2 PENT4  r 0.0094    x 0.1385  \
     b 124.0600
LINE name L2 bbar1 DINO4  bbar2 PENT4  r 0.0073    x 0.1210  \
     b 220.0000
LINE name L1 bbar1 FIDF2J bbar2 HEYS4  r 0.2667    x 3.1693
LINE name L1 bbar1 FIDF2J bbar2 PEWO4  r 0.1896    x 4.3138
LINE name L1 bbar1 DAIN4  bbar2 FERR2J r 0.5441    x 14.0039
LINE name L1 bbar1 DAIN4  bbar2 KEAR4Q r 0.0011    x 3.5267
LINE name L1 bbar1 DAIN4  bbar2 OSBA4Q r 38.9901   x 507.3882
LINE name L1 bbar1 DAIN4  bbar2 STAL4Q r 0.0640    x 3.8385
LINE name L1 bbar1 DAIN4  bbar2 CELL4  r 0.1355    x 1.0300  \
     b 31.2249
LINE name L1 bbar1 HEYS4  bbar2 PEWO4  r -0.0297   x 4.7691
LINE name L1 bbar1 HEYS4  bbar2 HARK2  r 0.3175    x 3.5973
LINE name L2 bbar1 HEYS4  bbar2 PEWO4  r 0.0997    x 0.8019  \
     b 24.2281
LINE name L1 bbar1 PEWO4  bbar2 HARK2  r 0.3709    x 4.0129
LINE name L1 bbar1 PEWO4  bbar2 DAIN4  r 0.1375    x 1.0886  \
     b 33.0008
LINE name L1 bbar1 FERR2J bbar2 EGGB4J r 0.0245    x 1.0165
LINE name L1 bbar1 FERR2J bbar2 KEAR4Q r -0.3095   x 17.6632
LINE name L1 bbar1 FERR2J bbar2 OSBA4Q r 0.3128    x 2.9619
LINE name L1 bbar1 FERR2J bbar2 STAL4Q r 4.9395    x 68.5685
LINE name L1 bbar1 CREB4  bbar2 DRAX4J r 0.1864    x 1.5391
LINE name L2 bbar1 CREB4  bbar2 DRAX4J r 0.0643    x 0.8570  \
     b 35.5103
LINE name L1 bbar1 CREB4  bbar2 NORT4Q r 0.1500    x 2.0000  \
     b 83.0000
```

```
LINE name L1 bbar1 DRAX4J bbar2 EGGB4J r 0.0126    x 0.1674  \
     b 7.1300
LINE name L1 bbar1 DRAX4J bbar2 OSBA4Q r 0.0970    x 0.6266  \
     b 26.6700
LINE name L1 bbar1 EGGB4J bbar2 PEWO4  r 0.1874    x 2.2208  \
     b 89.8230
LINE name L1 bbar1 EGGB4J bbar2 THOM4  r 0.0388    x 0.4500  \
     b 25.2000
LINE name L1 bbar1 HAWP4R bbar2 NORT4Q r -2.9415   x 23.2616
LINE name L1 bbar1 HAWP4R bbar2 OSBA4Q r 0.1675    x 2.2264
LINE name L1 bbar1 HAWP4R bbar2 BLYT2J r 0.2675    x 7.0335
LINE name L1 bbar1 HAWP4R bbar2 HATL2  r 0.1640    x 3.9136
LINE name L1 bbar1 HAWP4R bbar2 STEW2J r 0.7376    x 18.5964
LINE name L1 bbar1 KEAR4Q bbar2 OSBA4Q r 13.0471   x 641.3445
LINE name L1 bbar1 KEAR4Q bbar2 STAL4Q r 0.5776    x 17.2903
LINE name L1 bbar1 KEAR4Q bbar2 EGGB4J r 0.2140    x 1.8667  \
     b 66.7337
LINE name L1 bbar1 NORT4Q bbar2 BLYT2J r -0.2006   x 21.8337
LINE name L1 bbar1 NORT4Q bbar2 HATL2  r 0.2260    x 4.4241
LINE name L1 bbar1 NORT4Q bbar2 STEW2J r 0.3236    x 5.7698
LINE name L1 bbar1 OSBA4Q bbar2 STAL4Q r 273.4753  x 2481.2468
LINE name L1 bbar1 STAL4Q bbar2 THOM4  r 0.0917    x 1.1885  \
     b 127.2291
LINE name S1 bbar1 THOM4                                     \
     b -200.0000
LINE name L1 bbar1 BLYT2J bbar2 HATL2  r 0.2757    x 1.9263
LINE name L1 bbar1 BLYT2J bbar2 STEW2J r 2.6969    x 17.1202
LINE name L1 bbar1 BLYT2J bbar2 HARK2  r 1.0719    x 4.3264  \
     b 31.0660
LINE name L2 bbar1 BLYT2J bbar2 HARK2  r 1.2936    x 4.4652  \
     b 32.8780
LINE name L2 bbar1 BLYT2J bbar2 STEW2J r 0.3124    x 1.0947  \
     b 7.1556
LINE name L3 bbar1 BLYT2J bbar2 STEW2J r 0.2087    x 1.3827  \
     b 15.4300
LINE name L1 bbar1 HATL2  bbar2 STEW2J r 0.7552    x 3.4342
LINE name L1 bbar1 STEW2J bbar2 HARK2  r 13.2056   x 90.0208
LINE name L1 bbar1 STEW2J bbar2 HUER4  r 328.2522  x 805.8992  \
     tie S-N
LINE name L1 bbar1 STEW2J bbar2 KINC2  r 0.8067    x 7.5937    \
     tie S-N
LINE name L1 bbar1 STEW2J bbar2 LOAN2  r 433.6880  x 2959.3398 \
     tie S-N
LINE name L1 bbar1 STEW2J bbar2 STHA2  r 1.3335    x 12.3274   \
     tie S-N
LINE name L1 bbar1 HARK2  bbar2 CRUA2Q r 1623.9790 x 3523.8098 \
```

```
     tie S-N
LINE name L1 bbar1 HARK2  bbar2 HUER4  r 48.7814   x 176.9920  \
     tie S-N
LINE name L1 bbar1 HARK2  bbar2 KINC2  r 17.0829   x 97.1360   \
     tie S-N
LINE name L1 bbar1 HARK2  bbar2 LOAN2  r 767.3965  x 2147.3860 \
     tie S-N
LINE name L1 bbar1 HARK2  bbar2 STHA2  r 0.6514    x 2.9655    \
     tie S-N
LINE name S1 bbar1 HARK2                                      \
     b -55.0000
LINE name L1 bbar1 FOYE2  bbar2 KINT2  r 1.4392    x 5.1141
LINE name L1 bbar1 FOYE2  bbar2 PEHE2  r 1.6031    x 12.8385
LINE name L1 bbar1 KINT2  bbar2 PEHE2  r 0.2555    x 1.9819
LINE name L1 bbar1 KINT2  bbar2 KINC2  r 1.4266    x 9.2284
LINE name L1 bbar1 KINT2  bbar2 LOAN2  r 1.1685    x 7.5587
LINE name S1 bbar1 KINT2                                      \
     b -120.0000
LINE name L2 bbar1 KINT2  bbar2 KINC2  r 0.9000    x 7.3800  \
     b 52.0000
LINE name L2 bbar1 KINT2  bbar2 PEHE2  r 0.3000    x 2.5600  \
     b 25.0000
LINE name L3 bbar1 KINT2  bbar2 PEHE2  r 0.2500    x 2.1900  \
     b 13.0000
LINE name L1 bbar1 CRUA2Q bbar2 HUER4  r 0.3261    x 4.8861
LINE name L1 bbar1 CRUA2Q bbar2 KINC2  r 12.4490   x 132.3524
LINE name L1 bbar1 CRUA2Q bbar2 LOAN2  r 1.1974    x 9.7261
LINE name L1 bbar1 CRUA2Q bbar2 STHA2  r 2.5726    x 47.4988
LINE name L1 bbar1 HUER4  bbar2 KINC2  r 6.4401    x 94.9287
LINE name L1 bbar1 HUER4  bbar2 LOAN2  r 0.3067    x 5.5502
LINE name L1 bbar1 HUER4  bbar2 STHA2  r 0.1035    x 1.4395
LINE name L1 bbar1 KINC2  bbar2 LOAN2  r 0.4313    x 7.1606
LINE name L1 bbar1 KINC2  bbar2 STHA2  r 0.6681    x 5.8200
LINE name L2 bbar1 KINC2  bbar2 LOAN2  r 0.0271    x 2.1153  \
     b 4.6748
LINE name L3 bbar1 KINC2  bbar2 LOAN2  r 0.0271    x 2.1153  \
     b 4.6748
LINE name L1 bbar1 LOAN2  bbar2 STHA2  r 0.1202    x 1.4220
```

G.6 Admittance Matrix Reordering Data

```
* Reordering information :-

REORDER LOVE4     row   46
```

```
REORDER BRFO4     row   48
REORDER PELH4     row   49
REORDER DUNG4     row   45
REORDER SUND4     row   50
REORDER ECLA4     row   51
REORDER BRLE4     row   47
REORDER COWL4     row   22
REORDER EXET4     row    2
REORDER HINP4     row    3
REORDER MELK4     row   23
REORDER WALH4     row   16
REORDER ABTH2J    row   13
REORDER CILF4     row   14
REORDER PEMB4     row   15
REORDER WALP4     row   17
REORDER COTT4     row   52
REORDER HIGM4     row   18
REORDER RATS4J    row   53
REORDER WBUR4     row   54
REORDER CELL4     row   19
REORDER DRAK4     row   31
REORDER FECK4     row   55
REORDER IRON4     row   24
REORDER RUGE4     row    4
REORDER WILL4     row   32
REORDER DEES4     row   33
REORDER LEGA4     row    9
REORDER PENT4     row    7
REORDER TRAW2     row    6
REORDER TRAW4     row    8
REORDER WYLF4     row    5
REORDER DINO4     row    0
REORDER FFES2     row    1
REORDER FIDF2J    row   20
REORDER DAIN4     row   56
REORDER HEYS4     row   21
REORDER PEWO4     row   25
REORDER FERR2J    row   34
REORDER CREB4     row   26
REORDER DRAX4J    row   36
REORDER EGGB4J    row   57
REORDER HAWP4R    row   29
REORDER KEAR4Q    row   35
REORDER NORT4Q    row   44
REORDER OSBA4Q    row   58
REORDER STAL4Q    row   37
```

```
REORDER THOM4     row   27
REORDER BLYT2J    row   30
REORDER HATL2     row   28
REORDER STEW2J    row   43
REORDER HARK2     row   59
REORDER FOYE2     row   10
REORDER KINT2     row   12
REORDER PEHE2     row   11
REORDER CRUA2Q    row   38
REORDER HUER4     row   39
REORDER KINC2     row   40
REORDER LOAN2     row   41
REORDER STHA2     row   42
REORDER DINO41    row   60
REORDER DINO42    row   61
REORDER DINO43    row   62
REORDER DINO44    row   63
REORDER DINO45    row   64
REORDER DINO46    row   65
```

G.7 Load Data

```
* Load Group data for 60 busbar system plus 6 Dinorwig groups
*
* Load data
*
* L001 = Lighting & heating, P proportional to V^2, Q=0.
* L002 = Synchronous motor, P approx constant,
*        Q = 0.069 + 3.478*V - 2.438*V^2.
* L003 = Induction motor @ 100% full load, constant torque,
*        P approx constant
*       Q = 3.045 - 4.751*V + 2.646*V^2.
* L004 = Induction motor @ 75% full load, constant torque,
*        P approx constant
*       Q = 1.895 - 3.310*V + 2.408*V^2.
* L005 = Induction motor @ 50% full load, constant torque,
*        P approx constant
*       Q = 0.883 - 1.58*V + 1.693*V^2.
*
* All loads include pf1=100 to reflect observed variation of
* 2% MW/Hz.
*
* Approx load share:
*      70%      Induction motors
```

```
*       20%       Lighting and Heating
*       10%       Synchronous motors
*
LOAD L000 pf1 100
LOAD L001 pv0 -100 pf1 100
LOAD L002 qv0 -6.9 qv1 347.8 pf1 100
LOAD L003 qv0 304.5 qv1 -475.1 pf1 100
LOAD L004 qv0 189.5 qv1 -331.0 pf1 100
LOAD L005 qv0 88.3 qv1 -158.0 pf1 100

LOADGROUP LOAD_LOVE4  bbar LOVE4  load L003 mw -423 mvar 227
LOADGROUP LOAD_BRFO4  bbar BRFO4  load L001 mw -143 mvar 0.0
LOADGROUP LOAD_PELH4  bbar PELH4  load L003 mw -545 mvar 11
LOADGROUP LOAD_SUND4  bbar SUND4  load L003 mw -490 mvar -39
LOADGROUP LOAD_ECLA4  bbar ECLA4  load L004 mw -381 mvar 32
LOADGROUP LOAD_BRLE4  bbar BRLE4  load L003 mw -399 mvar 71
LOADGROUP LOAD_COWL4  bbar COWL4  load L002 mw -75 mvar 153
LOADGROUP LOAD_EXET4  bbar EXET4  load L005 mw -282 mvar 38
LOADGROUP LOAD_MELK4  bbar MELK4  load L002 mw -103 mvar -2
LOADGROUP LOAD_ABTH2J bbar ABTH2J load L003 mw -443 mvar -92
LOADGROUP LOAD_CILF4  bbar CILF4  load L001 mw -170 mvar 0.0
LOADGROUP LOAD_PEMB4  bbar PEMB4  load L002 mw -129 mvar -53
LOADGROUP LOAD_WALP4  bbar WALP4  load L001 mw -171 mvar 0.0
LOADGROUP LOAD_HIGM4  bbar HIGM4  load L001 mw -170 mvar 0.0
LOADGROUP LOAD_WBUR4  bbar WBUR4  load L002 mw -97 mvar 101
LOADGROUP LOAD_CELL4  bbar CELL4  load L002 mw -107 mvar -35
LOADGROUP LOAD_DRAK4  bbar DRAK4  load L004 mw -285 mvar -67
LOADGROUP LOAD_FECK4  bbar FECK4  load L001 mw -180 mvar 0.0
LOADGROUP LOAD_IRON4  bbar IRON4  load L005 mw -229 mvar 6
LOADGROUP LOAD_WILL4  bbar WILL4  load L001 mw -196 mvar 0.0
LOADGROUP LOAD_DEES4  bbar DEES4  load L004 mw -324 mvar 5
LOADGROUP LOAD_LEGA4  bbar LEGA4  load L005 mw -58 mvar -106
LOADGROUP LOAD_PENT4  bbar PENT4  load L001 mw -31 mvar 0.0
LOADGROUP LOAD_FFES2  bbar FFES2  load L005 mw -279 mvar -6
LOADGROUP LOAD_DAIN4  bbar DAIN4  load L004 mw -352 mvar 7
LOADGROUP LOAD_PEWO4  bbar PEWO4  load L002 mw -60 mvar 64
LOADGROUP LOAD_CREB4  bbar CREB4  load L002 mw -129 mvar -29
LOADGROUP LOAD_HAWP4R bbar HAWP4R load L002 mw -26 mvar 48
LOADGROUP LOAD_KEAR4Q bbar KEAR4Q load L001 mw -179 mvar 0.0
LOADGROUP LOAD_NORT4Q bbar NORT4Q load L001 mw -48 mvar 0.0
LOADGROUP LOAD_OSBA4Q bbar OSBA4Q load L002 mw -28 mvar 32
LOADGROUP LOAD_STAL4Q bbar STAL4Q load L002 mw -118 mvar -33
LOADGROUP LOAD_THOM4  bbar THOM4  load L004 mw -353 mvar 78
LOADGROUP LOAD_STEW2J bbar STEW2J load L005 mw -217 mvar 85
LOADGROUP LOAD_HARK2  bbar HARK2  load L001 mw -148 mvar 0.0
LOADGROUP LOAD_FOYE2  bbar FOYE2  load L004 mw -338 mvar 52
```

```
LOADGROUP LOAD_KINT2  bbar KINT2  load L001 mw -138 mvar 0.0
LOADGROUP LOAD_CRUA2Q bbar CRUA2Q load L003 mw -427 mvar 9
LOADGROUP LOAD_KINC2  bbar KINC2  load L001 mw -176 mvar 0.0
LOADGROUP LOAD_STHA2  bbar STHA2  load L005 mw -281 mvar 134
```

Appendix H

BFT Pressure Loop Controller Design

A block diagram of the plant for this controller is given in figure H.1, where the signal names correspond to those given in appendix B and the following block names apply:

$$A(s) = \frac{1}{1+sT_{f2}} \qquad I = K_2$$

$$B(s) = \frac{K_{fur}}{1+sT_{f1}} \qquad J = 1 - M_{sp_{pu}}$$

$$C(s) = \frac{1}{\psi s} \qquad K(s) = \frac{K_{v2}}{s}$$

$$D = D_s \qquad L = \sqrt{P_2 - P_{h1}}$$

$$E = \sqrt{P_d - P_1} \qquad M = K_3$$

$$F = K_1 \qquad N(s) = \frac{K_{h1}}{s}$$

$$G(s) = \frac{K_{v1}}{s} \qquad O = \mathcal{F}(P_{h1}, A_{gv}, P_{h2})$$

$$H = \sqrt{P_1 - P_2} \qquad = \frac{K_{gv}A_{gv}P_{h1}}{\sqrt{T_{h1}}}\sqrt{(\frac{P_{h2}}{P_{h1}})^{\frac{2}{\gamma}} - (\frac{P_{h2}}{P_{h1}})^{\frac{\gamma+1}{\gamma}}}$$

The block diagram can be manipulated to give an overall transfer function for a plant with M_{fu} as its input and P_2 as its output. The sequence of transformations

is shown in figures H.2(a)–(c). The resulting output function, Z_{out}, was expanded to an expression in terms of the block names A–O using the symbolic mathematics program REDUCE [106].

The non-linear blocks, E, H, L and O, were linearised at the different load operating points at which the controller was to be designed by finding the small signal gain through differentiation.

Hence, for blocks of the form

$$f(x) = \sqrt{x}$$

the linearised block was taken to be

$$f'(x)|_{x=x_{ss}} = \frac{1}{2\sqrt{x}}$$

where $f'(x) = \frac{df}{dx}$.

The linearisation of block O was found with the aid of the REDUCE program and is given by,

$$\left.\frac{dO}{dP_{h1}}\right|_{\substack{P_{h2}=ss \\ A_{gv}=ss}} = \frac{A_{gv}K_{gv}(\gamma-1)}{2\gamma\sqrt{T_{h1}}P_{h1}^{\frac{5\gamma+8}{2\gamma}}} \frac{\left(2\left(\frac{P_{h2}}{P_{h1}}\right)^{\frac{2}{\gamma}} - \left(\frac{P_{h2}}{P_{h1}}\right)^{\frac{\gamma+1}{\gamma}}\right)}{\sqrt{\left(\frac{P_{h2}}{P_{h1}}\right)^{\frac{2}{\gamma}} - \left(\frac{P_{h2}}{P_{h1}}\right)^{\frac{\gamma+1}{\gamma}}}}$$

The four equivalent machine simulation was run using the default multi-variable controller to obtain steady state variable values at varying loads. These are shown in table H.1.

Table H.2 shows the relevant model constants necessary to form blocks A–O above.

Using the data in tables H.1 and H.2 linear blocks can be obtained at each

	170 MW	250 MW	390 MW	490 MW
P_{mw}	169.66	247.05	391.18	487.12
L_{dv}	169.56	250.00	400.00	500.00
L_{sp}	169.63	247.02	391.13	487.09
P_{dv}	170.89	170.89	170.89	170.89
P_d	173.45	175.67	181.42	186.27
P_1	171.93	172.82	175.13	177.07
P_2	171.44	171.88	173.06	174.05
P_{h1}	170.91	170.90	170.90	170.89
P_{h2}	52.323	71.927	106.95	129.55
h_s	2534.2	2526.6	2507.0	2490.4
M_{s1}	147.85	203.02	301.23	364.38
M_{s4}	152.49	209.38	310.67	375.77
A_{gv}	0.32566	0.40226	0.58454	0.78507

Table H.1: Model States at Different Steady-State Loads

T_{f2}	5	$M_{sp_{pu}}$	0.0303
K_{fur}	15840.513	K_{v2}	0.0088438
T_{f1}	15	K_3	211.294
ψ	434078	K_{h1}	0.0576422
D_s	-3.416025	K_{gv}	356.04
K_1	120.127	T_{h1}	813
K_{v1}	0.0088438	γ	1.3
K_2	216.267		

Table H.2: Model Constants for BFT Pressure Loop

operating point as shown in table H.3.

	170 MW	250 MW	390 MW	490 MW
A	$\frac{1}{1+5s}$	$\frac{1}{1+5s}$	$\frac{1}{1+5s}$	$\frac{1}{1+5s}$
B	$\frac{15840.513}{1+15s}$	$\frac{15840.513}{1+15s}$	$\frac{15840.513}{1+15s}$	$\frac{15840.513}{1+15s}$
C	$\frac{1}{434078s}$	$\frac{1}{434078s}$	$\frac{1}{434078s}$	$\frac{1}{434078s}$
D	-3.416025	-3.416025	-3.416025	-3.416025
E	0.40555	0.29566	0.199363	0.156556
F	120.127	120.127	120.127	120.127
G	$\frac{0.0088438}{s}$	$\frac{0.0088438}{s}$	$\frac{0.0088438}{s}$	$\frac{0.0088438}{s}$
H	0.71429	0.515711	0.347524	0.287242
I	216.267	216.267	216.267	216.267
J	0.9697	0.9697	0.9697	0.9697
K	$\frac{0.0088438}{s}$	$\frac{0.0088438}{s}$	$\frac{0.0088438}{s}$	$\frac{0.0088438}{s}$
L	0.686803	0.505076	0.340207	0.281718
M	211.294	211.294	211.294	211.294
N	$\frac{0.0576422}{s}$	$\frac{0.0576422}{s}$	$\frac{0.0576422}{s}$	$\frac{0.0576422}{s}$
O	0.478387	0.922218	2.25564	4.35156

Table H.3: Model Blocks for BFT Pressure Loop

Substitution of these values into the expanded form for the plant transfer function Z_{out} using REDUCE, produces the following results.

$$Z_{out}|_{170\,MW} = \frac{2.86394.10^{-4}(s+8.31782)}{s^6+13.1168s^5+33.9745s^4+16.6273s^3+2.62553s^2 + 0.111244s+1.99095.10^{-5}} \quad \text{(H.1)}$$

with open loop poles at $s =$ -0.000179733, -0.0666674, -0.200016,
-0.312197, -2.70797, -9.82988
and open loop zero at $s =$ -8.31782

$$Z_{out}|_{250\,MW} = \frac{1.50747.10^{-7}(s+6.20472)}{s^6+9.77539s^5+19.0512s^4+7.8608s^3+1.117s^2 + 0.0465932s+1.07362.10^{-4}} \quad \text{(H.2)}$$

with open loop poles at $s =$ -0.00244512, -0.0666665, -0.200015,
-0.229506, -1.96174, -7.31507
and open loop zero at $s =$ -6.20472

$$Z_{out}|_{390\,MW} = \frac{6.8498.10^{-5}(s+4.27355)}{s^6+6.76681s^5+9.44955s^4+3.24117s^3+0.401339s^2 + 0.016056s+6.92132.10^{-5}} \quad \text{(H.3)}$$

with open loop poles at $s =$ -0.00488374, -0.0666614, -0.159628,
-0.199997, -1.33066, -5.005
and open loop zero at $s =$ -4.27355

$$Z_{out}|_{490\,MW} = \frac{4.44596.10^{-6}(s+3.68201)}{s^6+5.77869s^5+6.96360s^4+2.20837s^3+0.257563s^2 + 0.0102876s+6.54172.10^{-5}} \quad \text{(H.4)}$$

with open loop poles at $s =$ -0.00777324, -0.0666852, -0.133739,
-0.199995, -1.10689, -4.26362
and open loop zero at $s =$ -3.68201

It can be seen from these transfer functions, that all four cases show the expected open loop poles at $s = -0.0666667$ and $s = -0.2$ from the linear fuel blocks A and B. In all four cases again, it can be seen that the two fastest poles were much

more than five times faster than the next making their effect negligible. This effect is reinforced by the presence of the fast zero. Therefore, it was decided to ignore these fast poles and zero and design for the fourth order systems shown below, where the d.c. gain has been neglected for the moment and the characteristic equations are formed simply from the product of the four slowest open loop poles.

$$G(s)|_{170\,MW} = \frac{1}{s^4 + 0.57906s^3 + 0.0966963s^2 + 0.00418037s + 7.4823.10^{-7}}$$

$$G(s)|_{250\,MW} = \frac{1}{s^4 + 0.498633s^3 + 0.0757525s^2 + 0.00324256s + 7.4828.10^{-6}}$$

$$G(s)|_{390\,MW} = \frac{1}{s^4 + 0.43117s^3 + 0.0579801s^2 + 0.00240117s + 1.03934.10^{-5}}$$

$$G(s)|_{490\,MW} = \frac{1}{s^4 + 0.0.408192s^3 + 0.0521148s^2 + 0.00216454s + 1.38646.10^{-5}}$$

First of all, proportional control of these systems was investigated as shown in block diagram form in figure H.3. As the proportional gain, K, is varied the root loci for these systems are of the form shown in figure H.4. From this it can be determined that these systems will quickly go unstable with increasing K as the locus quickly passes into the unstable right-hand region, and also have a non-zero steady-state step error shown by there being no open loop pole at the origin.

It was decided, therefore, to use proportional plus integral, PI, control as shown in figure H.5, choosing the position of the resulting zero appropriately to provide adequate damping. The system under consideration here is of the form,

$$G(s) = \frac{1}{g(s)}$$

where $g(s)$ is a fourth order polynomial in s.

The PI controller is of the form,

$$\begin{aligned} C(s) &= K_P + \frac{K_I}{s} \\ &= \frac{K_P\left(s + \frac{K_I}{K_P}\right)}{s} \\ &= \frac{K_P(s+z)}{s} \end{aligned} \tag{H.5}$$

$s = -z$ being the position of the open loop zero introduced by this form of controller.

Root loci can be plotted as K_P varies. By analysis of the form of the root loci it was determined that the zero needed to be between the two slowest open loop poles—if it were nearer the origin than the slowest pole, ie. between that pole and the pole introduced at the origin, the system would be dominated by a slow first order response. However, the system would again quickly go unstable if the zero were too distant from the origin. Consequently, the design required a compromise between the loci illustrated in figures H.6 and H.7.

Using a computer program that was able to plot root loci given corresponding transfer functions, it was found, by experiment, that placing the zero at $s = -0.01$ was adequate for all cases, resulting in a root locus of the form shown in figure H.8. It was desirable to place the closed loop poles in such positions that the damping of the resulting system would be fairly insensitive to changes in system gain.

From equation H.5 it can be seen that in order to have the open loop zero at $s = -0.01$ then $K_I = 0.01K_P$. The forward path transfer function of the controlled system is then:

$$C(s)G(s) = \frac{K_P\,(s+z)}{sg(s)}$$

where $z = 0.01$ for this design.

The closed loop system transfer function is obtained from

$$T(s) = \frac{C(s)G(s)}{1 + C(s)G(s)}$$

Hence,

$$T(s) = \frac{K_P(s+z)}{sg(s) + K_P(s+z)}$$

The closed loop poles of the system are the roots of

$$\begin{aligned} t(s) &= sg(s) + K_P(s+z) \\ &= sg(s) + K_Ps + K_Pz \\ &= sg(s) + K_Ps + 0.01K_P \end{aligned}$$

so, given a desired value for s at the closed loop poles, K_P can be found from,

$$0 = sg(s) + K_P(s + 0.01)$$

or,

$$K_P = \left.\frac{sg(s)}{s + 0.01}\right|_{s=p} \tag{H.6}$$

where p is a desired closed loop pole.

Using the root locus plotting program, a value for p was obtained at an appropriate point on the root locus, and then K_P calculated from equation H.6. This is illustrated below for the system at the operating point of 390 MW, chosen for being around the middle of the normal operating range.

$$g(s)|_{390\,MW} = s^4 + 0.43117s^3 + 0.0579801s^2 + 0.00240117s + 1.03934.10^{-5}$$

with $z = 0.01$, then,

$$\begin{aligned} t(s)|_{390\,MW} &= s^5 + 0.43117s^4 + 0.0579801s^3 + 0.00240117s^2 \\ &\quad + \left(1.03934.10^{-5} + K_P\right) s + 0.01K_P \end{aligned}$$

As previously described, choose closed loop pole to be at

$$s = -0.01108 \pm \jmath 0.01033$$

Using equation H.6, this gives,

$$K_P = 2.79817.10^{-5} \mp \jmath 1.8068.10^{-7}$$

so that,

$$|K_P| = 2.79823.10^{-5}$$

thus, K_P was considered to be adequately 'real' to be an acceptable solution.

In fact, the controller design is only concerned with obtaining a reasonable estimate for K_P, not an exact value, so it was decided to use

$$K_P|_{390\,MW} = 2.798.10^{-5}$$

in the closed loop characteristic equation, $t(s)$.

This results in closed loop poles at,

$$\begin{aligned} s &= -0.0341812, \\ &\quad -0.0111238 \pm \jmath 0.0102305, \\ &\quad -0.187368 \pm \jmath 0.0271412 \end{aligned}$$

Plotting these solutions on the root locus shows that they are quite adequate, as seen in figure H.9.

The above value for K_P was also used with the systems at the other operating points being considered and it was found that in the 170 MW case this produced dominant closed loop poles with rather low damping at

$$s = -0.0029 \pm j0.009$$

The design exercise was repeated with the 170 MW system to improve the damping resulting in,

$$K_P|_{170\,MW} = 8.7.10^{-5}$$

with closed loop poles at,

$$\begin{aligned} s \;=\; & -0.024788, \\ & -0.30022, \\ & -0.22675, \\ & -0.013559 \pm j0.018746 \end{aligned}$$

which illustrates the improvement in damping of the dominant closed loop poles.

So far, the design process has only considered a system of the form,

$$G(s) = \frac{1}{s^4 + b_3 s^3 + b_2 s^2 + b_1 s + b_0}$$

and produced a controller of the form,

$$C(s) = \frac{K_P\left(s + \frac{K_I}{K_P}\right)}{s}$$

The full system, shown by equations H.1–H.4, is of the form,

$$G'(s) = \frac{K_s\,(s + c_0)}{(s^2 + a_1 s + a_0)\,(s^4 + b_3 s^3 + b_2 s^2 + b_1 s + b_0)}$$

and this requires a full system controller,

$$C'(s) = \frac{K'_P\left(s + \frac{K'_I}{K'_P}\right)}{s}$$

The d.c. gains of the two systems must be matched.

The full system d.c. gain is,

$$K' = \frac{K'_P K_s c_0}{a_0 b_0}$$

and the reduced system d.c. gain is,

$$K = \frac{K_P}{b_0}$$

Matching the two enables K'_P to be found from,

$$K'_P = \frac{K_P a_0}{K_s c_0} \qquad \text{(H.7)}$$

At 390 MW, equation H.7 gives,

$$\begin{aligned} K'_P|_{390\,MW} &= \frac{2.798.10^{-5} \times 1.33066 \times 5.005}{6.8498.10^{-5} \times 4.27355} \\ &= 0.6366 \end{aligned}$$

$$\Rightarrow K'_I = 0.006366$$

At 170 MW, equation H.7 gives,

$$\begin{aligned} K'_P|_{170\,MW} &= \frac{8.7.10^{-5} \times 2.70797 \times 9.82988}{2.86394.10^{-4} \times 8.31782} \\ &= 0.9722 \end{aligned}$$

It can be seen from these calculations that, because of other non-linear gains in the plant, $K'_P|_{170\,MW}$ is not as far from $K'_P|_{390\,MW}$ as $K_P|_{170\,MW}$ is from $K_P|_{390\,MW}$. In fact, simulation (non-linear) of the full system showed quite adequate control for a fixed value of K_P (0.6366) at different loads. Simulation also demonstrated that a fixed K_P was adequate at different pressures. Scheduling this gain had been considered. However, the simulation results suggested that this was unnecessary.

Appendix I

BFT Load Loop Controller Design

A block diagram of the plant for this controller is given in figure I.1, where the signal names correspond to those given in appendix B and the following block names apply:

$$A : M_{s4} = \frac{K_{gv} A_{gv} P_{h1}}{\sqrt{T_{h1}}} \sqrt{\left(\frac{P_{h2}}{P_{h1}}\right)^{\frac{2}{\gamma}} - \left(\frac{P_{h2}}{P_{h1}}\right)^{\frac{\gamma+1}{\gamma}}}$$

$$B(s) = \frac{K_{h2}}{s} \qquad J = K_6$$

$$C : P_{h2}^2 \qquad K(s) = \frac{K_{v6}}{s}$$

$$D : \sqrt{P_{h2}^2 - P_5^2} \qquad L = K_7$$

$$E = K_5 \qquad M = \Delta H_{lp}$$

$$F = 1 - M_{sb_{pu}} \qquad N : \Delta H_{hp} = \frac{\gamma}{1-\gamma} \frac{R T_{h2}}{2} \left[\left(\frac{P_5}{P_{h2}}\right)^{\frac{\gamma+1}{\gamma}} - 1\right]$$

$$G(s) = \frac{K_{v5}}{s} \qquad O : T_{h2} = \left(\frac{P_{h2}}{P_{h1}}\right)^{\frac{\gamma-1}{\gamma}} T_{h1}$$

$$H : P_5^2 \qquad X : \Delta H_{hp} M_{s5}$$

$$I : \sqrt{P_5 = P_6} \qquad W = \frac{1}{1000}$$

The block diagram can be manipulated to give an overall transfer function for a plant with A_{gv} as its input and L as its output. The sequence of transformations is shown in figures I.2(a)–(d). The resulting output function, Z_{out}, was expanded to an expression in terms of the block names A–W using the symbolic mathematics program REDUCE [106].

The non-linear blocks, A, C, D, H, I, O and N, were linearised at the different load operating points at which the controller was to be designed by finding the small signal gain through differentiation, producing the following linear blocks:

$$
\begin{aligned}
A_1 &= \left.\frac{\delta M_{s1}}{\delta A_{gv}}\right|_{P_{h2}=ss} \\
&= \frac{K_{gv}P_{h1}}{\sqrt{T_{h1}}}\sqrt{\left(\frac{P_{h2}}{P_{h1}}\right)^{\frac{2}{\gamma}} - \left(\frac{P_{h2}}{P_{h1}}\right)^{\frac{\gamma+1}{\gamma}}}
\end{aligned}
$$

$$
\begin{aligned}
A_2 &= \left.\frac{\delta M_{s1}}{\delta P_{h2}}\right|_{A_{gv}=ss} \\
&= \frac{A_{gv}K_{gv}P_{h1}\left[2\left(\frac{P_{h2}}{P_{h1}}\right)^{\frac{2}{\gamma}} - (1+\gamma)\left(\frac{P_{h2}}{P_{h1}}\right)^{\frac{\gamma+1}{\gamma}}\right]}{2\sqrt{T_{h1}}P_{h2}\gamma\sqrt{\left(\frac{P_{h2}}{P_{h1}}\right)^{\frac{2}{\gamma}} - \left(\frac{P_{h2}}{P_{h1}}\right)^{\frac{\gamma+1}{\gamma}}}}
\end{aligned}
$$

$$
\begin{aligned}
C &= \left.\frac{d\left(x^2\right)}{dx}\right|_{x=P_{h2}} \\
&= 2P_{h2}
\end{aligned}
$$

$$
\begin{aligned}
D &= \left.\frac{d\left(\sqrt{x}\right)}{dx}\right|_{x=P_{h2}^2-P_5^2} \\
&= \frac{1}{2\sqrt{P_{h2}^2-P_5^2}}
\end{aligned}
$$

$$
\begin{aligned}
H &= \left.\frac{d\left(x^2\right)}{dx}\right|_{x=P_5} \\
&= 2P_5
\end{aligned}
$$

$$
\begin{aligned}
I &= \left.\frac{d\left(\sqrt{x}\right)}{dx}\right|_{x=P_5-P_6} \\
&= \frac{1}{2\sqrt{P_5-P_6}}
\end{aligned}
$$

$$
\begin{aligned}
O &= \frac{dT_{h2}}{dP_{h2}} \\
&= \left(\frac{P_{h1}}{P_{h2}}\right)^{\frac{1}{\gamma}} \frac{T_{h1}}{P_{h1}} \frac{(\gamma-1)}{\gamma}
\end{aligned}
$$

$$
\begin{aligned}
N_1 &= \left.\frac{\delta \Delta H_{hp}}{\delta T_{h2}}\right|_{\substack{P_5 = ss \\ P_{h2} = ss}} \\
&= \frac{\gamma}{(1-\gamma)}\frac{R}{2}\left[\left(\frac{P_5}{P_{h2}}\right)^{\frac{\gamma+1}{\gamma}} - 1\right]
\end{aligned}
$$

$$
\begin{aligned}
N_2 &= \left.\frac{\delta \Delta H_{hp}}{\delta P_5}\right|_{\substack{T_{h2} = ss \\ P_{h2} = ss}} \\
&= \frac{(\gamma+1)}{(1-\gamma)}\frac{RT_{h2}}{2}\left(\frac{P_5}{P_{h2}}\right)^{\frac{1}{\gamma}}\frac{1}{P_{h2}}
\end{aligned}
$$

$$
\begin{aligned}
N_3 &= \left.\frac{\delta \Delta H_{hp}}{\delta P_{h2}}\right|_{\substack{T_{h2} = ss \\ P_5 = ss}} \\
&= \frac{\left(\gamma^2-1\right)}{(\gamma^2-2\gamma+1)}\frac{RT_{h2}}{2}\left(\frac{P_5}{P_{h2}}\right)^{\frac{\gamma+1}{\gamma}}\frac{1}{P_{h2}}
\end{aligned}
$$

The four equivalent machine simulation was run using the default multi-variable controller to obtain steady state variable values at varying loads. These are shown in table I.1.

	170 MW	250 MW	390 MW	490 MW
P_{mw}	169.66	247.05	391.18	487.12
L_{dv}	169.56	250.00	400.00	500.00
L_{sp}	169.63	247.02	391.13	487.09
P_{dv}	170.89	170.89	170.89	170.89
P_{h1}	170.91	170.90	170.90	170.89
P_{h2}	52.323	71.927	106.95	129.55
P_5	13.886	19.383	29.595	36.449
P_6	13.268	18.218	27.031	32.697
M_{s5}	152.49	209.38	310.66	375.77
T_{h2}	618.66	665.82	729.64	762.66
ΔH_{hp}	559.92	600.85	655.00	682.29
A_{gv}	0.32566	0.40226	0.58454	0.78507

Table I.1: Model States at Different Steady-State Loads

Table I.2 shows the relevant model constants necessary to form blocks *A–W* above.

K_{gv}	356.04	T_{h1}	813
γ	1.3	K_{h2}	0.462517
K_5	3.0228	$M_{sb_{pu}}$	0.1854
K_{v5}	0.0128247	K_6	158.027
K_{v6}	0.0286832	K_7	9.362
ΔH_{lp}	599.23	R	0.4619

Table I.2: Model Constants for BFT Load Loop

Using the data in tables I.1 and I.2 linear blocks can be obtained at each operating point as shown in table I.3.

Substitution of these values into the expanded form for the plant transfer function Z_{out} using REDUCE, produces the following results.

$$Z_{out}|_{170\,MW} = \frac{15229.8(s^2 + 4.42754s + 0.522409)}{s^3 + 5.89927s^2 + 6.81264s + 0.0230386} \qquad \text{(I.1)}$$

with open loop poles at $s =$ -0.0033917, -1.57037, -4.32551
and open loop zeroes at $s =$ -0.125061, -4.30015

$$Z_{out}|_{250\,MW} = \frac{19371.1(s^2 + 3.29252s + 0.370477)}{s^3 + 4.76775s^2 + 5.07439s + 0.151419} \qquad \text{(I.2)}$$

with open loop poles at $s =$ -0.0307209, -1.54329, -3.19374
and open loop zeroes at $s =$ -0.116654, -3.17587

$$Z_{out}|_{390\,MW} = \frac{20294.1(s^2 + 2.30094s + 0.243892)}{s^3 + 3.78077s^2 + 3.55595s + 0.388158} \qquad \text{(I.3)}$$

	170 MW	250 MW	390 MW	490 MW
A_1	419.764	520.5	531.466	478.626
A_2	1.17125	0.719746	−0.699633	−2.8397
B	$\frac{0.462517}{s}$	$\frac{0.462517}{s}$	$\frac{0.462517}{s}$	$\frac{0.462517}{s}$
C	104.646	143.854	213.9	259.1
D	$9.9114.10^{-3}$	$7.21875.10^{-3}$	$4.86506.10^{-3}$	$4.02198.10^{-3}$
E	3.0228	3.0228	3.0228	3.0228
F	0.8146	0.8146	0.8146	0.8146
G	$\frac{0.0128247}{s}$	$\frac{0.0128247}{s}$	$\frac{0.0128247}{s}$	$\frac{0.0128247}{s}$
H	27.772	38.766	59.19	73.394
I	0.636027	0.46324	0.31226	0.25813
J	158.027	158.027	158.027	158.027
K	$\frac{0.0286832}{s}$	$\frac{0.0286832}{s}$	$\frac{0.0286832}{s}$	$\frac{0.0286832}{s}$
L	9.362	9.362	9.362	9.362
M	599.23	599.23	599.23	599.23
N_1	0.271478	0.270706	0.269301	0.268382
N_2	−7.54602	−5.97771	−4.49625	−3.92973
N_3	2.00264	1.61088	1.24419	1.10563
O	2.72862	2.60841	1.75423	1.44821
$\Delta h_{hp_{ss}}$	559.49	600.85	655.0	682.29
$M_{s5_{ss}}$	152.49	209.38	310.66	375.77

Table I.3: Model Blocks for BFT Pressure Loop

with open loop poles at $s =$ -0.125296, -1.33511, -2.32037
and open loop zeroes at $s =$ -0.111389, -2.18955

$$Z_{out}|_{490\,MW} = \frac{19101.4(s^2 + 1.94571s + 0.197154)}{s^3 + 3.42798s^2 + 3.012003s + 0.678126} \tag{I.4}$$

with open loop poles at $s =$ -0.351, -0.878973, -2.19801
and open loop zeroes at $s =$ -0.107238, -1.83847

Neglecting the d.c. gain to start with, the design was carried out for systems of the form:

$$\begin{aligned} G(s) &= \frac{s^2 + a_1 s + a_0}{s^3 + b_2 s^2 + b_1 s + b_0} \\ &= \frac{g_n(s)}{g_d(s)} \end{aligned} \tag{I.5}$$

First of all, proportional control of these systems was investigated as shown already in block diagram form in figure H.3. As the proportional gain, K, is varied the root loci for these systems are of the form shown in figures I.3–I.6. From this it can be determined that these systems are stable and quite fast, but have a non-zero steady state error to a step input.

In order to achieve zero steady state step error, an integral control is required as shown in figure I.7. Since there is already a system zero close to the origin, no further improvements will be gained from using PI control and introducing another zero. The I controller is of the form,

$$C(s) = \frac{K_I}{s} \tag{I.6}$$

Root loci for these systems with Integral control as K_I varies are shown in figures I.8–I.11. To obtain similar dominant closed loop poles in all cases, it was

decided to use make the gain K_I high enough to place the closed loop pole near the system zero under all conditions.

Using a computer program that was able to plot root loci given corresponding transfer functions, it was found, by experiment, that using $K_I = 5$ was quite sufficient to place the dominant closed loop poles near the slowest system zero as required in all cases, resulting in a root locus of the form shown in figure I.12.

From equations I.5 and I.6, the forward path transfer function of the controlled system can be formed as:

$$C(s)G(s) = \frac{K_I g_n(s)}{s g_d(s)}$$

The closed loop system transfer function is obtained from

$$T(s) = \frac{C(s)G(s)}{1 + C(s)G(s)}$$

Hence,

$$T(s) = \frac{K_I g_n(s)}{s g_d(s) + K_I g_n(s)}$$

The closed loop poles of the system are the roots of the characteristic equation,

$$t(s) = s g_d(s) + K_I g_n(s)$$

The characteristic equations of the closed loop system at the different operating points under consideration with integral only control are:

$$\begin{aligned} t(s)|_{170MW} &= s^4 + 5.89927 s^3 + (K_I + 6.81264)\, s^2 \\ &\quad + (4.42521 K_I + 0.0230386)\, s + 0.53778 K_I \\ t(s)|_{250MW} &= s^4 + 4.76775 s^3 + (K_I + 5.07439)\, s^2 \\ &\quad + (3.29252 K_I + 0.151419)\, s + 0.370477 K_I \end{aligned}$$

$$
\begin{aligned}
t(s)|_{390\,MW} &= s^4 + 3.78077s^3 + (K_I + 3.55595)\,s^2 \\
&\quad + (2.30094K_I + 0.388158)\,s + 0.243892K_I \\
t(s)|_{490\,MW} &= s^4 + 3.42798s^3 + (K_I + 3.012003)\,s^2 \\
&\quad + (1.94571K_I + 0.678126)\,s + 0.197154K_I
\end{aligned}
$$

With $K_I = 5.0$, the closed loop poles from these characteristic equations are:

@170 MW	-0.129818,	-4.31815,	$-0.725429 \pm j2.06684$
@250 MW	-0.119704,	-3.18515,	$-0.721613 \pm j2.0793$
@390 MW	-0.110975,	-2.22655,	$-0.721613 \pm j2.10108$
@490 MW	-0.102464,	-1.93221,	$-0.695874 \pm j2.12031$

So far, the design process has only considered a system of the form,

$$G(s) = \frac{s^2 + a_1 s + a_0}{s^3 + b_2 s^2 + b_1 s + b_0}$$

and produced a controller of the form,

$$C(s) = \frac{K_I}{s}$$

The full system, is of the form,

$$G(s) = K_s \frac{s^2 + a_1 s + a_0}{s^3 + b_2 s^2 + b_1 s + b_0}$$

and this requires a full system controller,

$$C'(s) = \frac{K_I'}{s}$$

The d.c. gains of the two systems must be matched, enabling K_I' to be found from,

$$K_I' K_s = K_I$$

hence,

$$K_I' = \frac{K_I}{K_s}$$

This leads to the following controller gains required at each operating point,

@170 MW: $K_I' =$	0.000328	@390 MW: $K_I' =$	0.000246
@250 MW: $K_I' =$	0.000258	@490 MW: $K_I' =$	0.000261

From root locus analysis, it was found that the positions of the dominant closed loop poles were not very sensitive to the value of K_I, or K_I', at the design point. Hence, it was considered that any value of K_I' around the values calculated above would do. Thus K_I' was chosen as,

$$K_I' = 0.00025$$

Appendix J

Conversion of Fossil Model for Coal and for 660 MW Units

J.1 Creation of Coal-Fired Model

Coal-fired and oil-fired boilers are very similar in all aspects except for the fuel system. Consequently, the only modification necessary to convert the original oil-fired boiler model to coal-fired was to increase the time constants of the fuel system, T_{f1} and T_{f2} to 40 and 20 seconds respectively instead of 15 and 5.

J.2 Creation of 660 MW Unit Model

The original boiler model was for a 505 MW unit and a model was needed for a 667 MW unit. Certain assumptions were made in order to convert the 505 MW model to a 667 MW model. The conversion is outlined below. Both model parameters and initial conditions of variables needed to be converted.

Firstly, it is assumed that the pressure conditions in the two sizes of unit will be

similar. Hence,

$$P_{d_{667}} = P_{d_{505}} = 174 \text{ bar}$$

$$P_{1_{667}} = P_{1_{505}} = 167.6 \text{ bar}$$

$$P_{2_{667}} = P_{2_{505}} = 165.5 \text{ bar}$$

$$P_{h1_{667}} = P_{h1_{505}} = 163.3 \text{ bar}$$

$$P_{h2_{667}} = P_{h2_{505}} = 107.9 \text{ bar}$$

$$P_{5_{667}} = P_{5_{505}} = 29.88 \text{ bar}$$

$$P_{6_{667}} = P_{6_{505}} = 27.27 \text{ bar}$$

Secondly, it is assumed that the time constants of the fuel supply systems are similar. Hence, for a coal-fired boiler,

$$T_{f1_{667}} = T_{f1_{505}} = 40 \text{ sec}$$

$$T_{f2_{667}} = T_{f2_{505}} = 20 \text{ sec}$$

Thirdly, it is assumed that fuel flow and steam flows are proportional to the unit

output power. Hence,

$$
\begin{aligned}
M_{fu_{667}} &= M_{fu_{505}} \times \tfrac{667}{505} = 23.949 \times \tfrac{667}{505} = 31.632 \ \text{m}^3/\text{sec} \\
\lambda_{667} &= \lambda_{505} \times \tfrac{667}{505} = 23.949 \times \tfrac{667}{505} = 31.632 \ \text{m}^3/\text{sec} \\
M_{s1_{667}} &= M_{s1_{505}} \times \tfrac{667}{505} = 303.9 \times \tfrac{667}{505} = 401.39 \ \text{m}^3/\text{sec} \\
M_{sp_{667}} &= M_{sp_{505}} \times \tfrac{667}{505} = 9.5 \times \tfrac{667}{505} = 12.548 \ \text{m}^3/\text{sec} \\
M_{s2_{667}} &= M_{s2_{505}} \times \tfrac{667}{505} = 313.4 \times \tfrac{667}{505} = 413.94 \ \text{m}^3/\text{sec} \\
M_{s3_{667}} &= M_{3_{505}} \times \tfrac{667}{505} = 313.4 \times \tfrac{667}{505} = 413.94 \ \text{m}^3/\text{sec} \\
M_{s4_{667}} &= M_{s4_{505}} \times \tfrac{667}{505} = 313.4 \times \tfrac{667}{505} = 413.94 \ \text{m}^3/\text{sec} \\
M_{s5_{667}} &= M_{s5_{505}} \times \tfrac{667}{505} = 313.4 \times \tfrac{667}{505} = 413.94 \ \text{m}^3/\text{sec} \\
M_{sb_{667}} &= M_{sb_{505}} \times \tfrac{667}{505} = 58.1 \times \tfrac{667}{505} = 76.738 \ \text{m}^3/\text{sec} \\
M_{s6_{667}} &= M_{s6_{505}} \times \tfrac{667}{505} = 255.3 \times \tfrac{667}{505} = 337.2 \ \text{m}^3/\text{sec} \\
M_{s7_{667}} &= M_{s7_{505}} \times \tfrac{667}{505} = 255.3 \times \tfrac{667}{505} = 337.2 \ \text{m}^3/\text{sec}
\end{aligned}
$$

Assuming the same economiser outlet conditions and steam drum outlet conditions, means that,

$$
\begin{aligned}
h_{fd_{667}} &= h_{fd_{505}} = 1284.00 \ \text{kJ/kg} \\
h_{s_{667}} &= h_{s_{505}} = 2532.32 \ \text{kJ/kg}
\end{aligned}
$$

An initial condition for boiler heat input can be found from

$$Q_{667} = M_{s1_{667}} \left(h_{fd_{667}} - h_{s_{667}}\right) = 501060 \ \text{kJ/sec}$$

Now,

$$\frac{dP_d}{dt} = \frac{1}{\psi}\left[Q + M_{s1}\left(h_{fd} - h_s\right)\right]$$

Smaller units will respond more quickly to heat input changes, hence

$$\psi_{505} < \psi_{667}$$

Boiler time constants are in the approximate range of 250 sec–450 sec for boilers ranging from 200 MW–660 MW. ψ will be assumed to vary in a similar proportion even though it is not strictly the same thing. Hence, assuming a linear relationship between boiler time constant and unit size and using T_B to denote boiler time constant,

$$T_{B_{667}} = 250 + (T_{B_{505}} - 200) \times \frac{200}{460}$$

This leads to,

$$\begin{aligned} \psi_{667} &= \psi_{505} \times \frac{T_{B_{667}}}{T_{B_{505}}} \\ &= 434078 \times 1.1841 \\ &= 513992 \end{aligned}$$

Also,

$$\begin{aligned} K_{fur_{667}} &= \frac{Q_{667}}{\lambda_{667}} \\ &= \frac{501060}{31.632} \\ &= 15840.288 \end{aligned}$$

Using the basic model equations C.5, C.6 and C.7, other gains may now be found as,

$$K_{1_{667}} = \frac{M_{s1_{667}}}{\sqrt{P_{d_{667}} - P_{1_{667}}}} = 158.663$$

$$K_{2_{667}} = \frac{M_{s2_{667}}}{\sqrt{P_{1_{667}} - P_{2_{667}}}} = 285.65$$

$$K_{3_{667}} = \frac{M_{s3_{667}}}{\sqrt{P_{2_{667}} - P_{h1_{667}}}} = 279.078$$

Using equation C.8, K_{gv} may be found from,

$$K_{gv} = \frac{M_{s4}\sqrt{T_{h1}}}{A_{gv}P_{h1}} \frac{1}{\sqrt{\left(\frac{P_{h2}}{P_{h1}}\right)^{\frac{2}{\gamma}} - \left(\frac{P_{h2}}{P_{h1}}\right)^{\frac{\gamma+1}{\gamma}}}}$$

Assuming the same physical conditions as before, ie. $T_{h1} = 813$, $\gamma = 1.3$ and $A_{gv} = 0.7$, then,

$$\begin{aligned} K_{gv_{667}} &= \frac{413.94 \times \sqrt{813}}{0.7 \times 163.3} \times \frac{1}{\sqrt{\left(\frac{107.9}{163.3}\right)^{\frac{2}{1.3}} - \left(\frac{107.9}{163.3}\right)^{\frac{2.3}{1.3}}}} \\ &= 470.265 \end{aligned}$$

Further gains may be found from equations C.9, C.10 and C.11, thus,

$$K_{5_{667}} = \frac{M_{s5_{667}}}{\sqrt{P^2_{h2_{667}} - P^2_{5_{667}}}} = 3.992$$

$$K_{6_{667}} = \frac{M_{s6_{667}}}{\sqrt{P_{5_{667}} - P_{6_{667}}}} = 208.72$$

$$K_{7_{667}} = \frac{M_{s7_{667}}}{P_{6_{667}}} = 12.365$$

Reheat time constants range from approximately 9–16 seconds for unit sizes ranging from 200–660 MW. This implies a reheat time constant of 13.641 seconds for a 505 MW unit and 16.107 seconds for a 667 MW unit. The gains relating steam flow to pressure drop need to be smaller with increasing MW in the same ratio as the reheat time constant. Hence,

$$\begin{aligned} \frac{1}{K_{667}} &= \frac{1}{K_{505}} \times \frac{T_{R_{667}}}{T_{R_{505}}} \\ &= \frac{1}{K_{505}} \times 1.1808 \\ \Rightarrow K_{667} &= \frac{K_{505}}{1.1808} \end{aligned}$$

This leads to the following gains for the 667 MW model,

$$
\begin{aligned}
K_{v1_{667}} &= K_{v1_{505}} 1.1808 = 0.00749 \\
K_{v2_{667}} &= K_{v2_{505}} 1.1808 = 0.00749 \\
K_{h1_{667}} &= K_{h1_{505}} 1.1808 = 0.048816 \\
K_{h2_{667}} &= K_{h2_{505}} 1.1808 = 0.391698 \\
K_{v5_{667}} &= K_{v5_{505}} 1.1808 = 0.010861 \\
K_{v6_{667}} &= K_{v6_{505}} 1.1808 = 0.024291
\end{aligned}
$$

Also assume,

$$T_{h2_{667}} = T_{h2_{505}} = 738.86$$

and so,

$$
\begin{aligned}
\Delta H_{hp_{667}} &= \frac{\gamma}{1-\gamma} \frac{RT_{h2}}{2} \left[\left(\frac{P_5}{P_{h2}} \right)^{\frac{\gamma+1}{\gamma}} - 1 \right] \\
&= \Delta H_{hp_{505}} \\
&= 663.18 \text{ kJ/kg}
\end{aligned}
$$

Using,

$$L_d = \eta \left(M_{s5} \Delta H_{hp} + M_{s7} \Delta H_{lp} \right) \div 1000$$

Then,

$$
\begin{aligned}
\Delta H_{lp_{667}} &= \left(\frac{1000 \times L_d}{\eta} - M_{s5_{667}} \Delta H_{hp} \right) \frac{1}{M_{s7_{667}}} \\
&= \left(\frac{1000 \times 0.7}{0.97} - 413.94 \times 663.18 \right) \frac{1}{337.2} \\
&= 613.356 \text{ kJ/kg}
\end{aligned}
$$

Appendix K

Digitisation of Controllers

K.1 Symbols

$C(s)$	Controller Transfer Function
$u(s)$	Laplace Transform of Controller Output
$e(s)$	Laplace Transform of System Error
K_P	Proportional Gain
K_I	Integral Gain
s	Laplace Operator
T	Digital Controller Time Interval
u_k	Controller Output at sample k
e_k	System Error at sample k

K.2 Integral Controller

The transfer function of the I controller is

$$C(s) = \frac{K_I}{s}$$

The controller output is

$$\begin{aligned} u(s) &= C(s)e(s) \\ &= \frac{K_I}{s}e(s) \end{aligned}$$

Hence,

$$su(s) = K_I T e(s)$$

Digitising at a sample interval of T and using first difference approximations to differentiations leads to,

$$\frac{u_k - u_{k-1}}{T} = K_I T e_k$$

Hence,

$$u_k = u_{k-1} + K_I T e_k \qquad \text{(K.1)}$$

Equation K.1 is used for the digital I controller.

K.3 Proportional-Integral Controller

The transfer function of the PI controller is

$$C(s) = K_P + \frac{K_I}{s}$$

The controller output is

$$\begin{aligned} u(s) &= C(s)e(s) \\ &= \frac{K_P\left(s + \frac{K_I}{K_P}\right)}{s} e(s) \end{aligned}$$

Hence,

$$su(s) = K_P s e(s) + K_I e(s)$$

Digitising at a sample interval of T and using first difference approximations to differentiations leads to,

$$\frac{u_k - u_{k-1}}{T} = K_P \frac{e_k - e_{k-1}}{T} + K_I e_k$$

Hence,

$$\begin{aligned} u_k &= u_{k-1} + K_P e_k - K_P e_{k-1} + K_I T e_k \\ &= u_{k-1} + (K_P + TK_I)\, e_k - K_P e_{k-1} \end{aligned} \qquad \text{(K.2)}$$

Equation K.2 is used for the digital PI controller.

Appendix L

Details of Four Machine Simulation Runs

Run	Study	AGC mode	Length	Figure
1	4 m'c Scotland-England Split Dinorwig: Generating Fossil: Coal, BFT sustained L_{sp} rate limit 5%MCR/min Loads: insensitive	none	50 sec	6.11
2	4 m'c Scotland-England Split Dinorwig: Generating Fossil: Coal, BFT sustained no L_{sp} rate limit Loads: insensitive	none	50 sec	6.12
2l	4 m'c Scotland-England Split Dinorwig: Generating Fossil: Coal, BFT sustained no L_{sp} rate limit Loads: variable	none	50 sec	6.21
3	4 m'c Scotland-England Split Dinorwig: Generating Fossil: Coal, BFT non-sustained L_{sp} rate limit 5%MCR/min Loads: insensitive	none	50 sec	6.13
4	4 m'c Scotland-England Split Dinorwig: Generating Fossil: Coal, no load control Loads: insensitive	none	50 sec	6.14
5	4 m'c Scotland-England Split Dinorwig: Pumping Fossil: Coal, BFT sustained L_{sp} rate limit 5%MCR/min Loads: insensitive	none	50 sec	6.15
5a	4 m'c Scotland-England Split Dinorwig: Pumping Fossil: Coal, BFT sustained L_{sp} rate limit 5%MCR/min Loads: insensitive	none	1000 sec	6.19
6	4 m'c Scotland-England Split Dinorwig: Pumping Fossil: Coal, BFT sustained no L_{sp} rate limit Loads: insensitive	none	50 sec	6.16

Run	Study	AGC mode	Length	Figure
6a	4 m'c Scotland-England Split Dinorwig: Pumping Fossil: Coal, BFT sustained no L_{sp} rate limit Loads: insensitive	none	1000 sec	6.20
6l	4 m'c Scotland-England Split Dinorwig: Pumping Fossil: Coal, BFT sustained no L_{sp} rate limit Loads: variable	none	50 sec	6.22
7	4 m'c Scotland-England Split Dinorwig: Pumping Fossil: Coal, BFT non-sustained L_{sp} rate limit 5%MCR/min Loads: insensitive	none	50 sec	6.17
8	4 m'c Scotland-England Split Dinorwig: Pumping Fossil: Coal, no load control Loads: insensitive	none	50 sec	6.18
9	4 m'c Step Load Increase busbar CEGB4 Dinorwig: Generating Fossil: Coal, BFT sustained L_{sp} rate limit 5%MCR/min Loads: insensitive	none	700 sec	6.23
10	4 m'c Step Load Increase busbar CEGB4 Dinorwig: Pumping Fossil: Coal, BFT sustained L_{sp} rate limit 5%MCR/min Loads: insensitive	none	700 sec	6.24
11	4 m'c Step Load Increase busbar CEGB4 Dinorwig: Pumping Fossil: Coal BFT sustained no L_{sp} rate limit Loads: insensitive	none	700 sec	6.25
12	4 m'c Step Load Increase busbar CEGB4 Dinorwig: Pumping Fossil: Coal, no load control Loads: insensitive	none	700 sec	6.26
13	4 m'c Step Load Increase busbar CEGB4 Dinorwig: Pumping Fossil: Oil, BFT sustained L_{sp} rate limit 5%MCR/min Loads: insensitive	none	700 sec	6.27
14	4 m'c SCOTLAND Ldv + 500 MW CEGB -500 MW Dinorwig: Pumping Fossil: Oil, BFT sustained L_{sp} rate limit 5%MCR/min Loads: insensitive	none	700 sec	6.28
15	4 m'c SCOTLAND Ldv + 500 MW CEGB -500 MW Dinorwig: Pumping Fossil: Oil, BFT sustained no L_{sp} rate limit Loads: insensitive	none	700 sec	6.29
16	4 m'c Step Load Increase busbar CEGB4 Dinorwig: Generating Fossil: Coal, BFT sustained L_{sp} rate limit 5%MCR/min Loads: variable	none	700 sec	6.30

Run	Study	AGC mode	Length	Figure
18	4 m'c Step Load Increase busbar CEGB4 Dinorwig: Generating Fossil: Coal, BFT non-sustained L_{sp} rate limit 5%MCR/min Loads: variable	flat frequency immediate notice interval: 5 P_{line} SP: 565 B_1: 8843 B_2: 1365 C_{p_1}: 65 C_{p_2}: 65 T_{n_1}: 0.2 T_{n_2}: 0.2 α_1: α_2:	700 sec	6.31
19	4 m'c Step Load Increase busbar CEGB4 Dinorwig: Generating Fossil: Coal, BFT non-sustained L_{sp} rate limit 5%MCR/min Loads: variable	frequency bias immediate notice interval: 5 P_{line} SP: 565 B_1: 8843 B_2: 1365 C_{p_1}: 65 C_{p_2}: 65 T_{n_1}: 0.2 T_{n_2}: 0.2 α_1: α_2:	700 sec	6.32 6.33
20	4 m'c Step Load Increase busbar CEGB4 Dinorwig: Generating Fossil: Coal, BFT non-sustained L_{sp} rate limit 5%MCR/min Loads: variable	frequency bias immediate notice interval: 5 P_{line} SP: 565 B_1: 4422 B_2: 1365 C_{p_1}: 65 C_{p_2}: 65 T_{n_1}: 0.2 T_{n_2}: 0.2 α_1: α_2:	700 sec	6.34
21	4 m'c Step Load Increase busbar CEGB4 Dinorwig: Generating Fossil: Coal, BFT non-sustained L_{sp} rate limit 5%MCR/min Loads: variable	frequency bias immediate notice interval: 5 P_{line} SP: 565 B_1: 17686 B_2: 1365 C_{p_1}: 65 C_{p_2}: 65 T_{n_1}: 0.2 T_{n_2}: 0.2 α_1: α_2:	700 sec	6.35
19b	4 m'c Step Load Increase busbar CEGB4 Dinorwig: Pumping Fossil: Coal, BFT non-sustained no L_{sp} rate limit Loads: variable	frequency bias immediate notice interval: 5 P_{line} SP: 565 B_1: 8843 B_2: 1365 C_{p_1}: 65 C_{p_2}: 65 T_{n_1}: 0.2 T_{n_2}: 0.2 α_1: α_2:	700 sec	6.36

Run	Study	AGC mode	Length	Figure
20b	4 m'c Step Load Increase busbar CEGB4 Dinorwig: Pumping Fossil: Coal, BFT non-sustained no L_{sp} rate limit Loads: variable	frequency bias immediate notice interval: 5 P_{line} SP: 565 B_1: 4422 B_2: 1365 C_{p_1}: 65 C_{p_2}: 65 T_{n_1}: 0.2 T_{n_2}: 0.2 α_1: α_2:	700 sec	6.37
21b	4 m'c Step Load Increase busbar CEGB4 Dinorwig: Pumping Fossil: Coal, BFT non-sustained no L_{sp} rate limit Loads: variable	frequency bias immediate notice interval: 5 P_{line} SP: 565 B_1: 17686 B_2: 1365 C_{p_1}: 65 C_{p_2}: 65 T_{n_1}: 0.2 T_{n_2}: 0.2 α_1: α_2:	700 sec	6.38
22b	4 m'c Step Load Increase busbar CEGB4 Dinorwig: Pumping Fossil: Coal, BFT non-sustained no L_{sp} rate limit Loads: variable	frequency bias immediate notice interval: 5 P_{line} SP: 565 B_1: 4422 B_2: 683 C_{p_1}: 65 C_{p_2}: 65 T_{n_1}: 0.2 T_{n_2}: 0.2 α_1: α_2:	700 sec	6.39
23	4 m'c Step Load Increase busbar CEGB4 Dinorwig: Generating Fossil: Coal, BFT non-sustained L_{sp} rate limit 5%MCR/min Loads: variable	frequency bias immediate notice interval: 5 P_{line} SP: 565 B_1: 8843 B_2: 1365 C_{p_1}: 100 C_{p_2}: 100 T_{n_1}: 0.2 T_{n_2}: 0.2 α_1: α_2:	700 sec	6.40
24	4 m'c Step Load Increase busbar CEGB4 Dinorwig: Generating Fossil: Coal, BFT non-sustained L_{sp} rate limit 5%MCR/min Loads: variable	frequency bias immediate notice interval: 5 P_{line} SP: 565 B_1: 8843 B_2: 1365 C_{p_1}: 30 C_{p_2}: 30 T_{n_1}: 0.2 T_{n_2}: 0.2 α_1: α_2:	700 sec	6.41

Run	Study	AGC mode	Length	Figure
25	4 m'c Step Load Increase busbar CEGB4 Dinorwig: Generating Fossil: Coal, BFT non-sustained L_{sp} rate limit 5%MCR/min Loads: variable	frequency bias immediate notice interval: 5 P_{line} SP: 565 B_1: 8843 B_2: 1365 C_{p_1}: 65 C_{p_2}: 65 T_{n_1}: 0.1 T_{n_2}: 0.1 α_1: α_2:	700 sec	6.42
26	4 m'c Step Load Increase busbar CEGB4 Dinorwig: Generating Fossil: Coal, BFT non-sustained L_{sp} rate limit 5%MCR/min Loads: variable	frequency bias immediate notice interval: 5 P_{line} SP: 565 B_1: 8843 B_2: 1365 C_{p_1}: 65 C_{p_2}: 65 T_{n_1}: 0.3 T_{n_2}: 0.3 α_1: α_2:	700 sec	6.43
27	4 m'c Step Load Increase busbar CEGB4 Dinorwig: Generating Fossil: Coal, BFT non-sustained L_{sp} rate limit 5%MCR/min Loads: variable	frequency bias immediate notice interval: 5 P_{line} SP: 565 B_1: 8843 B_2: 1365 C_{p_1}: 65 C_{p_2}: 65 T_{n_1}: 0.2 T_{n_2}: 0.2 α_1: 0.01 α_2: 0.01	700 sec	6.44
27b	4 m'c Step Load Increase busbar CEGB4 Dinorwig: Generating Fossil: Coal, BFT non-sustained no L_{sp} rate limit Loads: variable	frequency bias immediate notice interval: 5 P_{line} SP: 565 B_1: 8843 B_2: 1365 C_{p_1}: 65 C_{p_2}: 65 T_{n_1}: 0.2 T_{n_2}: 0.2 α_1: 0.01 α_2: 0.01	700 sec	6.56
28	4 m'c Step Load Increase busbar CEGB4 Dinorwig: Generating Fossil: Coal, BFT non-sustained L_{sp} rate limit 5%MCR/min Loads: variable	frequency bias immediate notice interval: 5 P_{line} SP: 565 B_1: 8843 B_2: 1365 C_{p_1}: 65 C_{p_2}: 65 T_{n_1}: 0.2 T_{n_2}: 0.2 α_1: 0.02 α_2: 0.02	700 sec	6.45

Run	Study	AGC mode	Length	Figure
29	4 m'c Step Load Increase busbar CEGB4 Dinorwig: Generating Fossil: Coal, BFT non-sustained L_{sp} rate limit 5%MCR/min Loads: variable	frequency bias immediate notice interval: 5 P_{line} SP: 565 B_1: 8843 B_2: 1365 C_{p_1}: 65 C_{p_2}: 65 T_{n_1}: 0.2 T_{n_2}: 0.2 α_1: 0.005 α_2: 0.005	700 sec	6.46
30	4 m'c Step Load Increase busbar CEGB4 Dinorwig: Generating Fossil: Coal, BFT non-sustained L_{sp} rate limit 5%MCR/min Loads: variable	frequency bias delayed notice interval: 5 P_{line} SP: 565 B_1: 8843 B_2: 1365 C_{p_1}: 65 C_{p_2}: 65 T_{n_1}: 0.2 T_{n_2}: 0.2 α_1: 0.01 α_2: 0.01	700 sec	6.47
31	4 m'c Step Load Increase busbar CEGB4 Dinorwig: Generating Fossil: Coal, BFT non-sustained L_{sp} rate limit 5%MCR/min Loads: variable	frequency bias delayed notice interval: 10 P_{line} SP: 565 B_1: 8843 B_2: 1365 C_{p_1}: 65 C_{p_2}: 65 T_{n_1}: 0.2 T_{n_2}: 0.2 α_1: 0.01 α_2: 0.01	700 sec	6.49
32	4 m'c Step Load Increase busbar CEGB4 Dinorwig: Generating Fossil: Coal, BFT non-sustained L_{sp} rate limit 5%MCR/min Loads: variable	frequency bias immediate notice interval: 10 P_{line} SP: 565 B_1: 8843 B_2: 1365 C_{p_1}: 65 C_{p_2}: 65 T_{n_1}: 0.2 T_{n_2}: 0.2 α_1: 0.01 α_2: 0.01	700 sec	6.48
33	4 m'c Step Load Increase busbar CEGB4 Dinorwig: Generating Fossil: Coal, BFT non-sustained L_{sp} rate limit 5%MCR/min Loads: variable	frequency bias immediate notice interval: 20 P_{line} SP: 565 B_1: 8843 B_2: 1365 C_{p_1}: 65 C_{p_2}: 65 T_{n_1}: 0.2 T_{n_2}: 0.2 α_1: 0.01 α_2: 0.01	700 sec	6.52

Run	Study	AGC mode	Length	Figure
34	4 m'c Step Load Increase busbar CEGB4 Dinorwig: Generating Fossil: Coal, BFT non-sustained L_{sp} rate limit 5%MCR/min Loads: variable	frequency bias delayed notice interval: 20 P_{line} SP: 565 B_1: 8843 B_2: 1365 C_{p_1}: 65 C_{p_2}: 65 T_{n_1}: 0.2 T_{n_2}: 0.2 α_1: 0.01 α_2: 0.01	700 sec	6.53
35a	4 m'c Step Load Increase busbar CEGB4 Dinorwig: Generating Fossil: Coal, BFT non-sustained L_{sp} rate limit 5%MCR/min Loads: variable	frequency bias delayed notice interval: 15 P_{line} SP: 565 B_1: 8843 B_2: 1365 C_{p_1}: 65 C_{p_2}: 65 T_{n_1}: 0.2 T_{n_2}: 0.2 α_1: 0.01 α_2: 0.01	700 sec	6.51
35b	4 m'c Step Load Increase busbar CEGB4 Dinorwig: Generating Fossil: Coal, BFT non-sustained no L_{sp} rate limit Loads: variable	frequency bias delayed notice interval: 15 P_{line} SP: 565 B_1: 8843 B_2: 1365 C_{p_1}: 65 C_{p_2}: 65 T_{n_1}: 0.2 T_{n_2}: 0.2 α_1: 0.01 α_2: 0.01	700 sec	6.55
36a	4 m'c Step Load Increase busbar CEGB4 Dinorwig: Generating Fossil: Coal, BFT non-sustained L_{sp} rate limit 5%MCR/min Loads: variable	frequency bias immediate notice interval: 5 P_{line} SP: 565 B_1: 8843 B_2: 1365 C_{p_1}: 65 C_{p_2}: 65 T_{n_1}: 0.2 T_{n_2}: 0.2 α_1: 0.01 α_2: 0.01	700 sec	6.50
36b	4 m'c Step Load Increase busbar CEGB4 Dinorwig: Generating Fossil: Coal, BFT non-sustained no L_{sp} rate limit Loads: variable	frequency bias immediate notice interval: 5 P_{line} SP: 565 B_1: 8843 B_2: 1365 C_{p_1}: 65 C_{p_2}: 65 T_{n_1}: 0.2 T_{n_2}: 0.2 α_1: 0.01 α_2: 0.01	700 sec	6.54

Run	Study	AGC mode	Length	Figure
40	4 m'c Step Load Increase busbar CEGB4, heavily loaded network Dinorwig: Generating Fossil: Coal, BFT non-sustained L_{sp} rate limit 5%MCR/min Loads: variable	frequency bias immediate notice interval: 5 P_{line} SP: 1130 B_1: 8843 B_2: 1365 C_{p_1}: 65 C_{p_2}: 65 T_{n_1}: 0.2 T_{n_2}: 0.2 α_1: 0.01 α_2: 0.01	700 sec	6.58
41	4 m'c Step Load Increase busbar CEGB4, heavily loaded machines Dinorwig: Generating Fossil: Coal, BFT non-sustained L_{sp} rate limit 5%MCR/min Loads: variable	frequency bias immediate notice interval: 5 P_{line} SP: 565 B_1: 8843 B_2: 1365 C_{p_1}: 65 C_{p_2}: 65 T_{n_1}: 0.2 T_{n_2}: 0.2 α_1: 0.01 α_2: 0.01	700 sec	6.57
42	4 m'c NWALES Pressure Setpoint change Dinorwig: Generating Fossil: Oil, BFT sustained L_{sp} rate limit 5%MCR/min Loads: variable	none	800 sec	6.6
43	4 m'c NWALES & CEGB Load Setpoint changes Dinorwig: Generating Fossil: Oil, BFT non-sustained L_{sp} rate limit 5%MCR/min Loads: variable	none	800 sec	6.4
44	4 m'c NWALES Pressure Setpoint change Dinorwig: Generating Fossil: Oil, Multi-variable sustained, L_{sp} rate limit 5%MCR/min Loads: variable	none	800 sec	6.7
45	4 m'c NWALES & CEGB Load Setpoint changes Dinorwig: Generating Fossil: Oil, Multi-variable non-sustained, L_{sp} rate limit 5%MCR/min Loads: variable	none	800 sec	6.5
47c	4 m'c NWALES Stored Energy Test @350 MW Dinorwig: Generating Fossil: Coal, BFT sustained L_{sp} rate limit 5%MCR/min Loads: variable	none	500 sec	6.1
48c	4 m'c NWALES Stored Energy Test @400 MW Dinorwig: Generating Fossil: Coal, BFT sustained L_{sp} rate limit 5%MCR/min Loads: variable	none	500 sec	6.2
49c	4 m'c NWALES Stored Energy Test @450 MW Dinorwig: Generating Fossil: Coal, BFT sustained L_{sp} rate limit 5%MCR/min Loads: variable	none	500 sec	6.3

Run	Study	AGC mode	Length	Figure
51	4 m'c DINORWIG Manual Guide Vane Ramp, no frequency regulation Dinorwig: Generating Fossil: Coal, BFT sustained L_{sp} rate limit 5%MCR/min Loads: variable	none	20 sec	6.9
52	4 m'c DINORWIG Response to Power Setpoint Increase Dinorwig: Generating Fossil: Coal, BFT sustained L_{sp} rate limit 5%MCR/min Loads: variable	none	100 sec	6.10

Appendix M

Details of Twenty-Five Machine Simulation Runs

Run	Study	AGC mode	Length	Figure
1	25 m'c Scotland-England Split Dinorwig: Generating Fossil: Coal, BFT sustained L_{sp} rate limit 5%MCR/min Loads: variable	none	100 sec	7.1
10	25 m'c Step Load Increase busbar EGGB4J Dinorwig: 1–6: Pumping, LFR 40.00 Hz, 2.75 secs Fossil: Coal, BFT sustained L_{sp} rate limit 5%MCR/min Loads: variable	frequency bias immediate notice interval: 5 P_{line} SP: 609 B_1: 4208 B_2: 748 C_{p_1}: 65 C_{p_2}: 65 T_{n_1}: 0.2 T_{n_2}: 0.2 α_1: 0.01 α_2: 0.01	700 sec	7.2
9	25 m'c Step Load Increase busbar EGGB4J Dinorwig: 1–2: Generating, LFR 40.00 Hz 2.75 secs 3–6: Pumping, LFR 40.00 Hz 2.75 secs Fossil: Coal, BFT sustained L_{sp} rate limit 5%MCR/min Loads: variable	frequency bias immediate notice interval: 5 P_{line} SP: 609 B_1: 4208 B_2: 748 C_{p_1}: 65 C_{p_2}: 65 T_{n_1}: 0.2 T_{n_2}: 0.2 α_1: 0.01 α_2: 0.01	700 sec	7.3
8	25 m'c Step Load Increase busbar EGGB4J Dinorwig: 1–2: Generating, LFR 40.00 Hz 2.75 secs 3–6: Pumping, LFR 40.00 Hz 2.75 secs Fossil: Coal, some BFT sustained L_{sp} rate limit 5%MCR/min some BFT sustained L_{sp} rate limit 2%MCR/min Loads: variable	frequency bias immediate notice interval: 5 P_{line} SP: 609 B_1: 4208 B_2: 748 C_{p_1}: 65 C_{p_2}: 65 T_{n_1}: 0.2 T_{n_2}: 0.2 α_1: 0.01 α_2: 0.01	700 sec	7.4

Run	Study	AGC mode	Length	Figure
7	25 m'c Step Load Increase busbar EGGB4J Dinorwig: 1: Generating, LFR 49.85 Hz 2.75 secs 2: Generating, LFR 40.00 Hz 2.75 secs 3–6: Pumping, LFR 40.00 Hz 2.75 secs Fossil: Coal, some BFT sustained L_{sp} rate limit 5%MCR/min some BFT sustained L_{sp} rate limit 2%MCR/min Loads: variable	frequency bias immediate notice interval: 5 P_{line} SP: 609 B_1: 4208 B_2: 748 C_{p_1}: 65 C_{p_2}: 65 T_{n_1}: 0.2 T_{n_2}: 0.2 α_1: 0.01 α_2: 0.01	700 sec	7.5

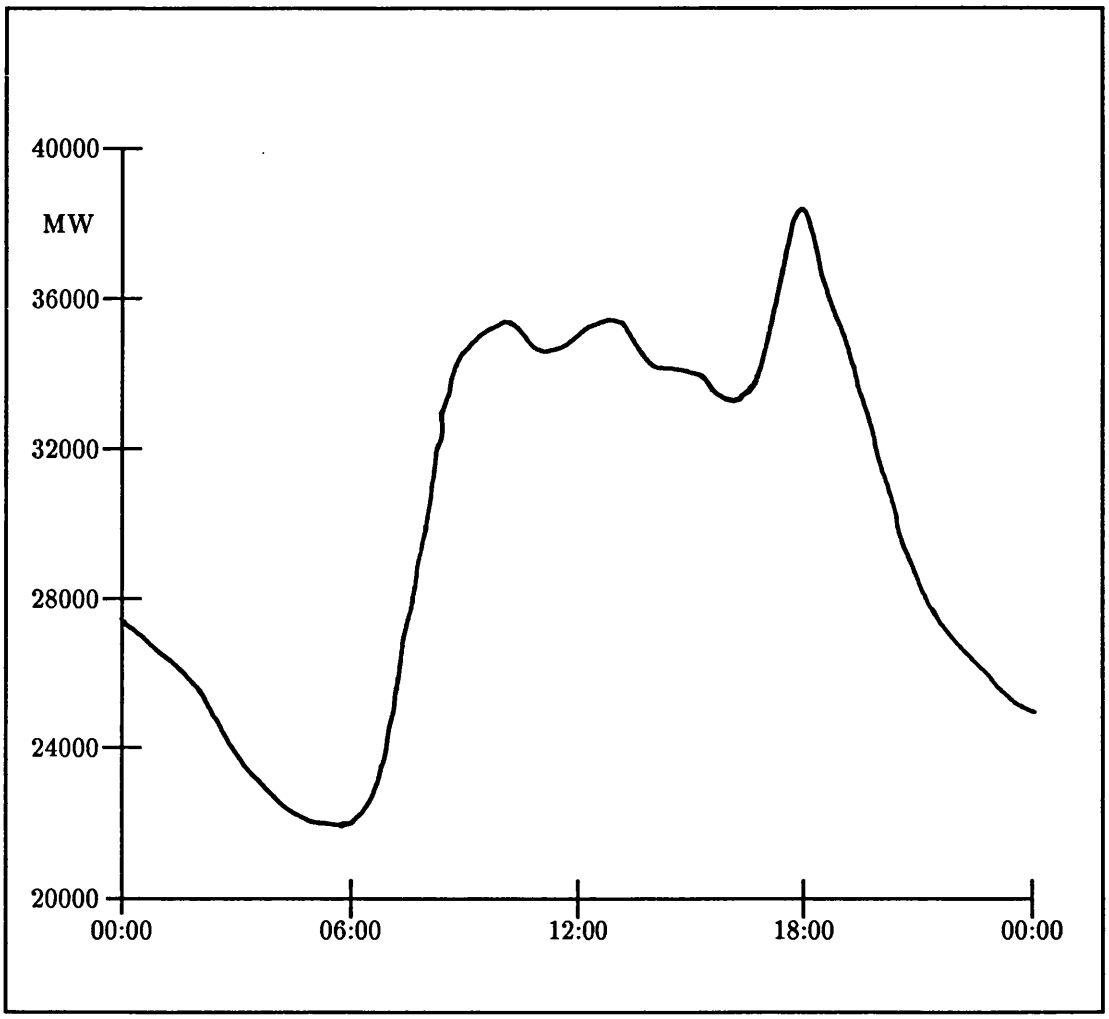

Figure 2.1: Typical Daily Load Curve

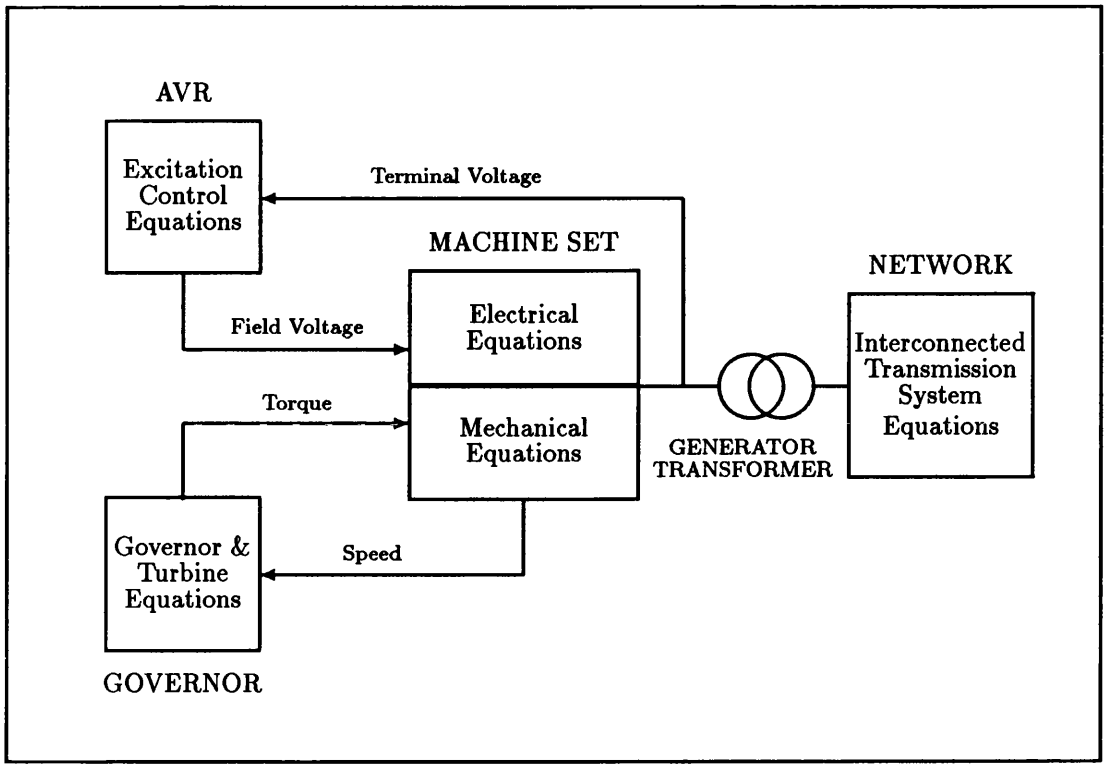

Figure 4.1: Schematic of Simulator Model Structure

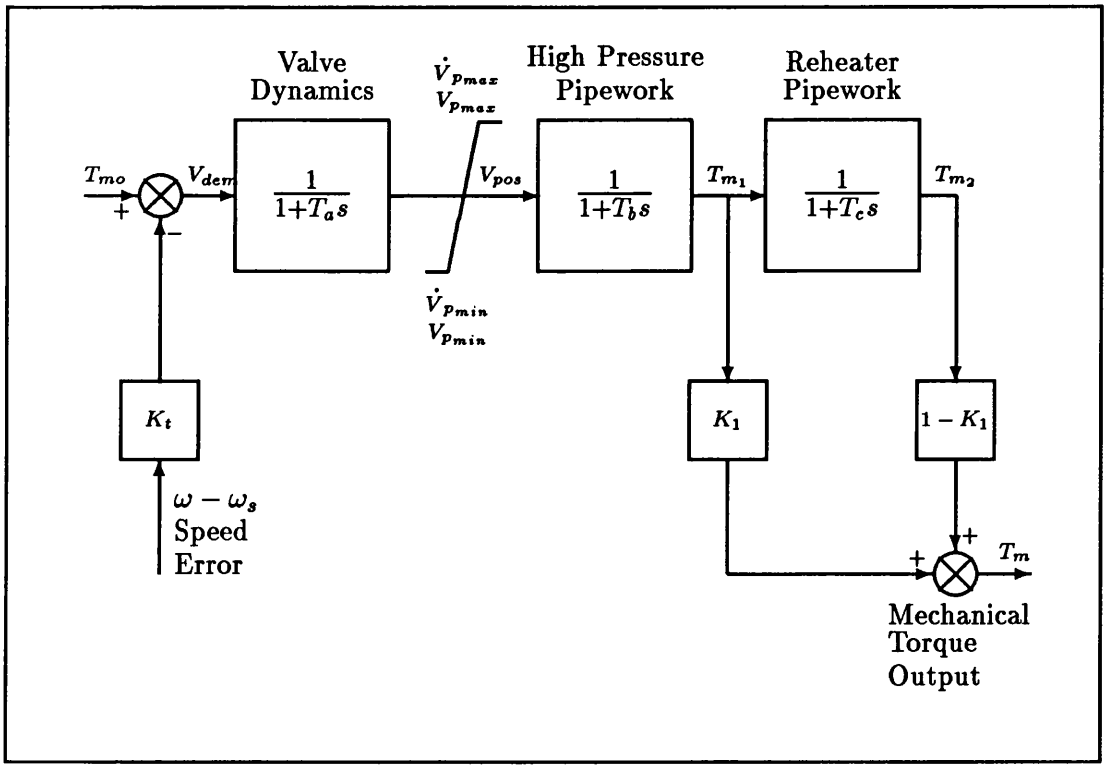

Figure 4.2: Schematic of Original General Governor Model

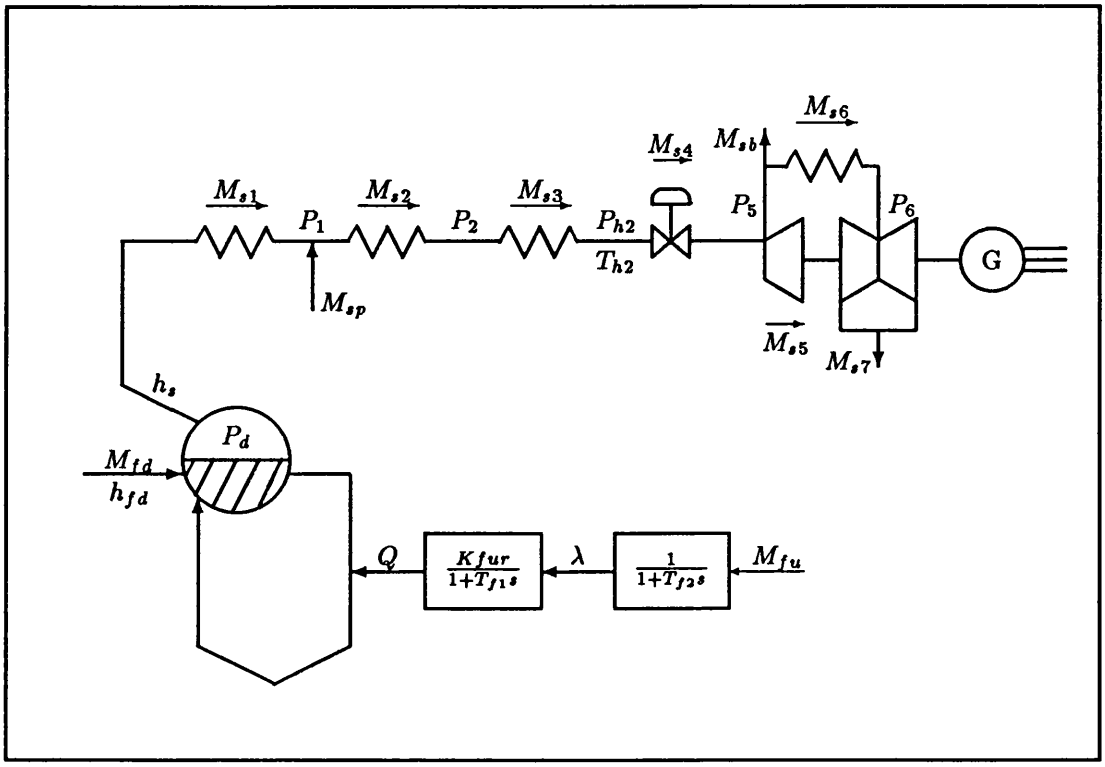

Figure 4.3: Fossil-Fired boiler schematic

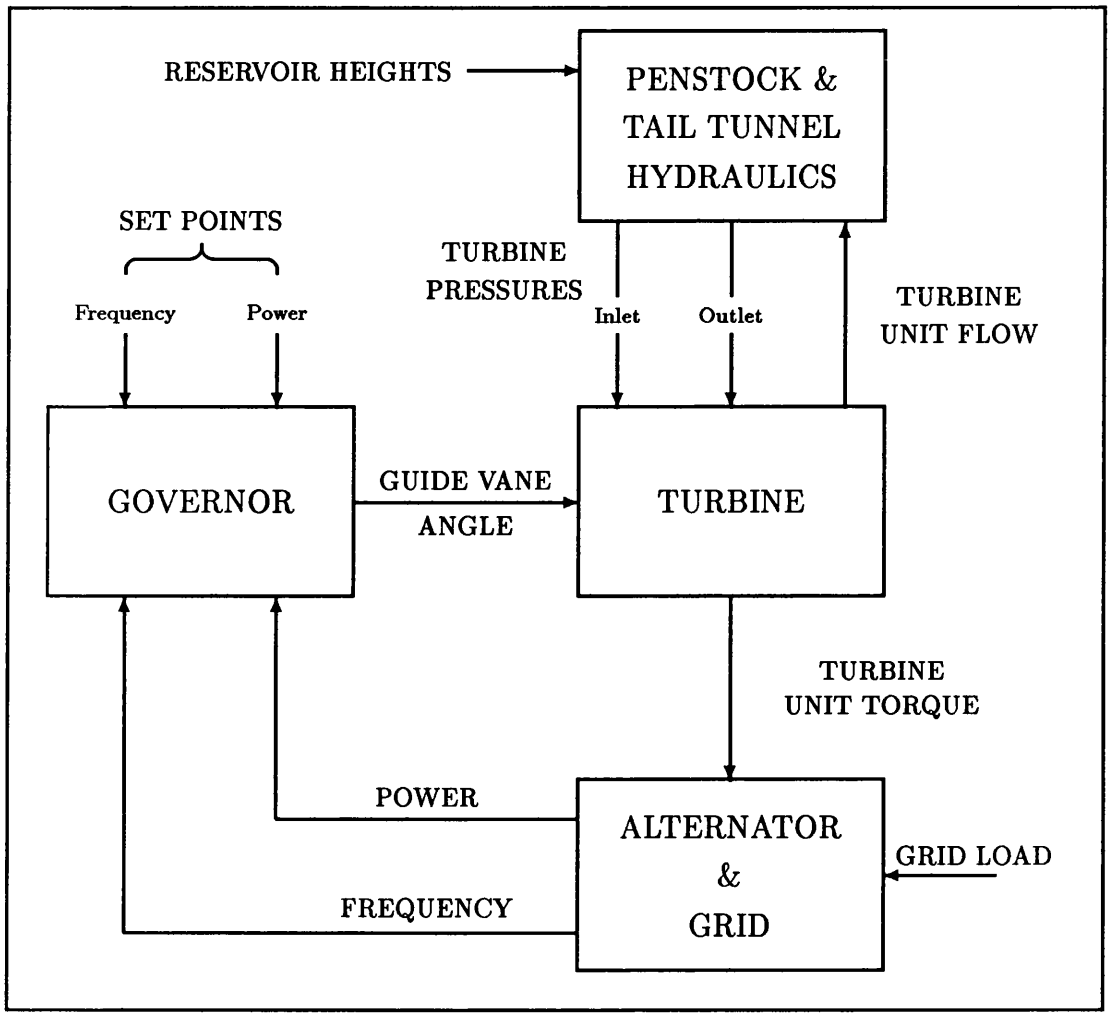

Figure 4.4: Schematic of Dinorwig Pumped Storage Scheme

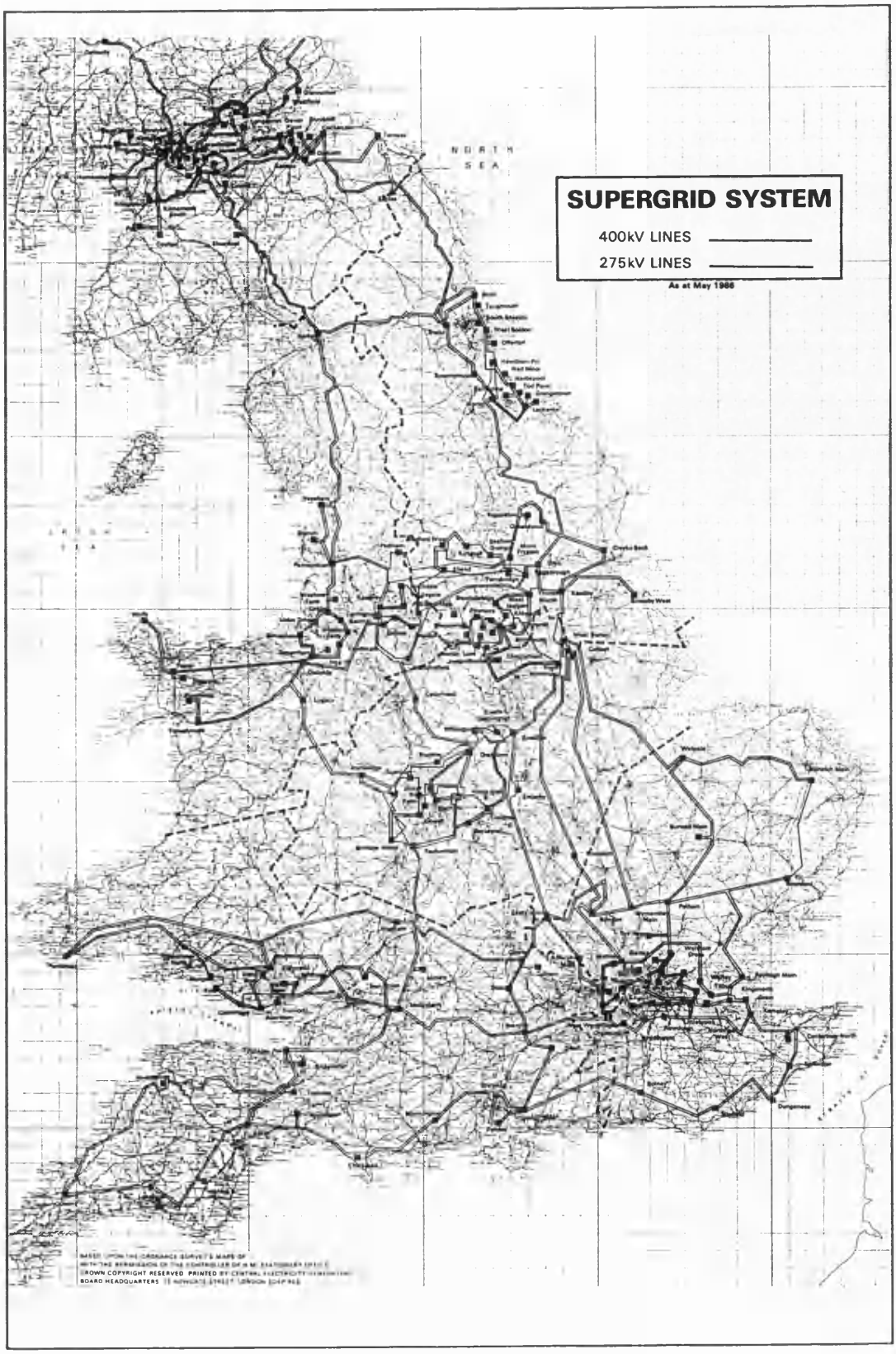

Figure 4.5a: The British SuperGrid System [112]

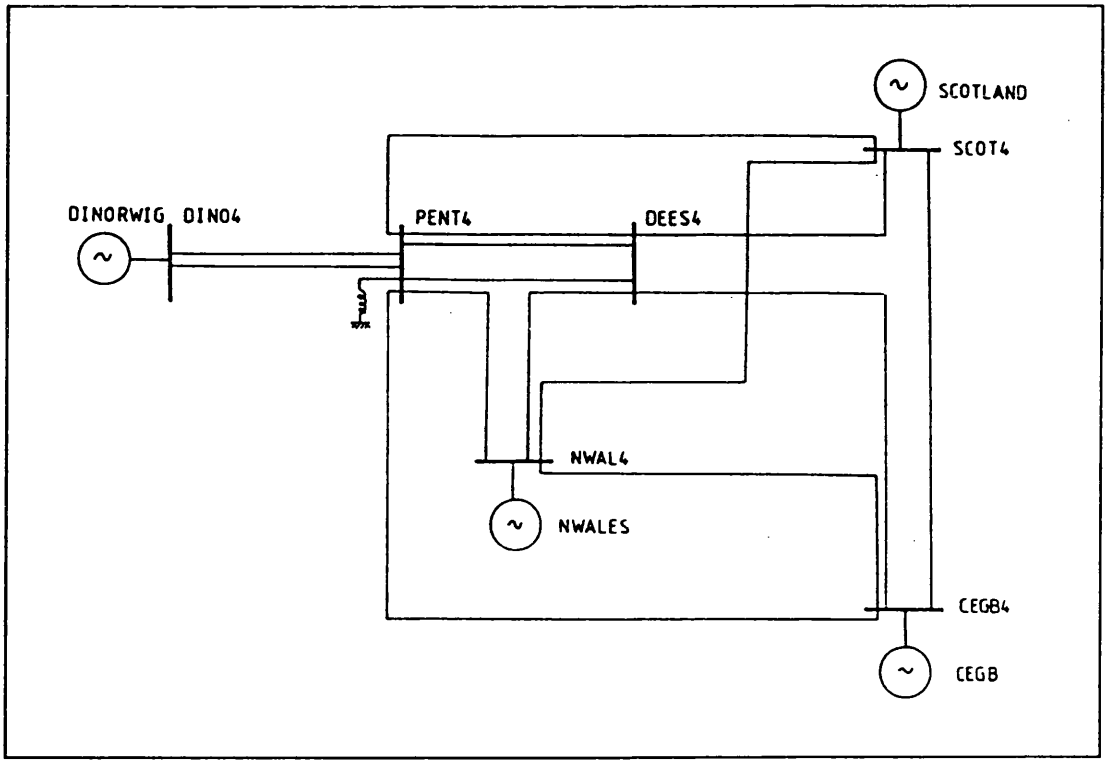

Figure 4.5b: Equivalent Four Machine Network

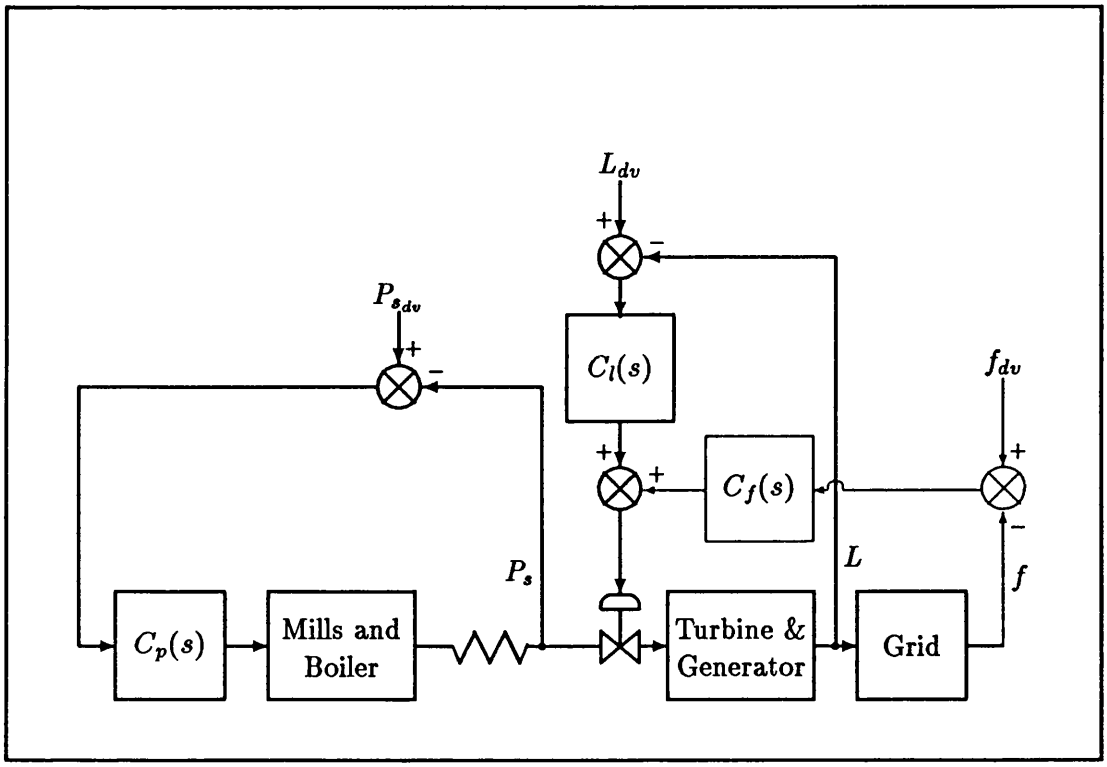

Figure 4.6: Typical Boiler Follows Turbine structure

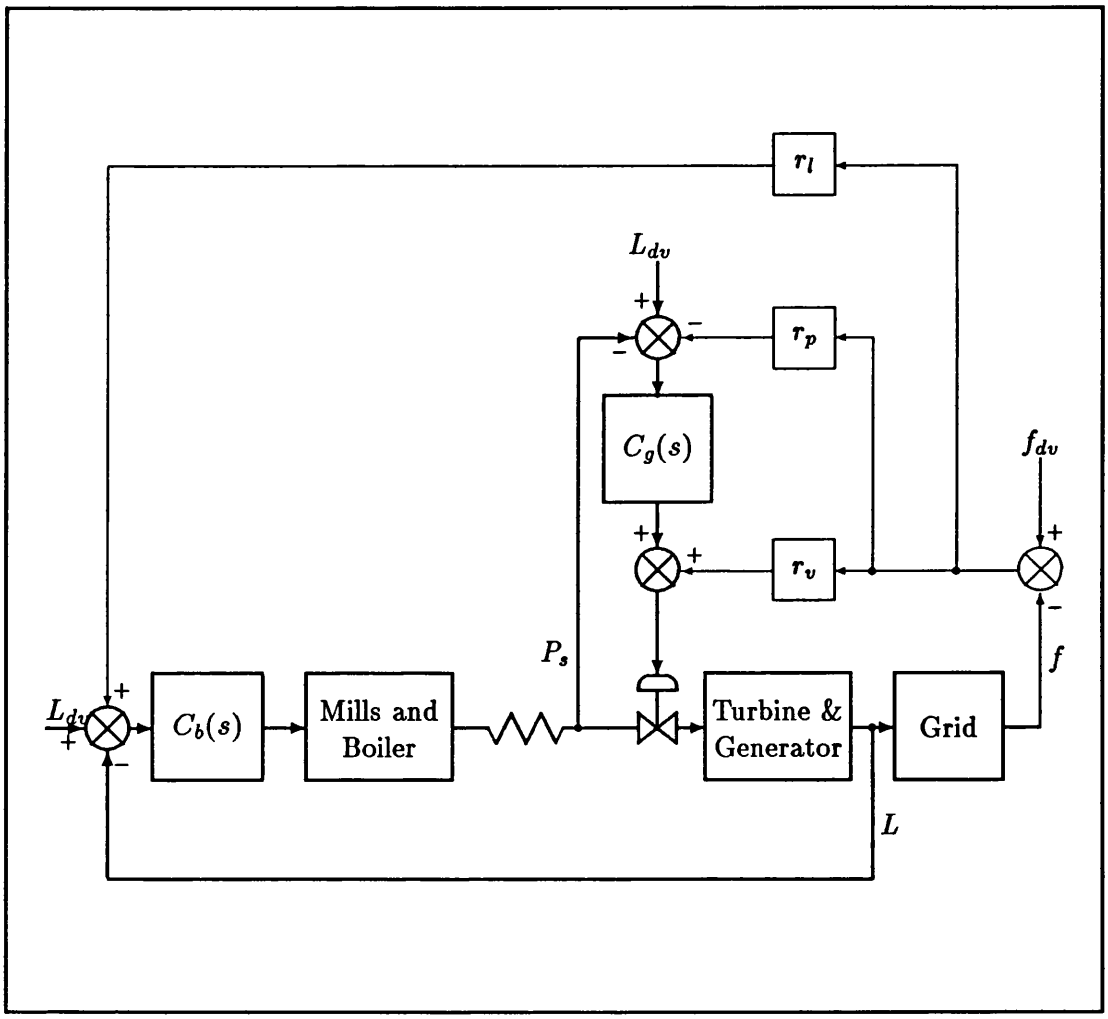

Figure 4.7: Typical Turbine Follows Boiler structure

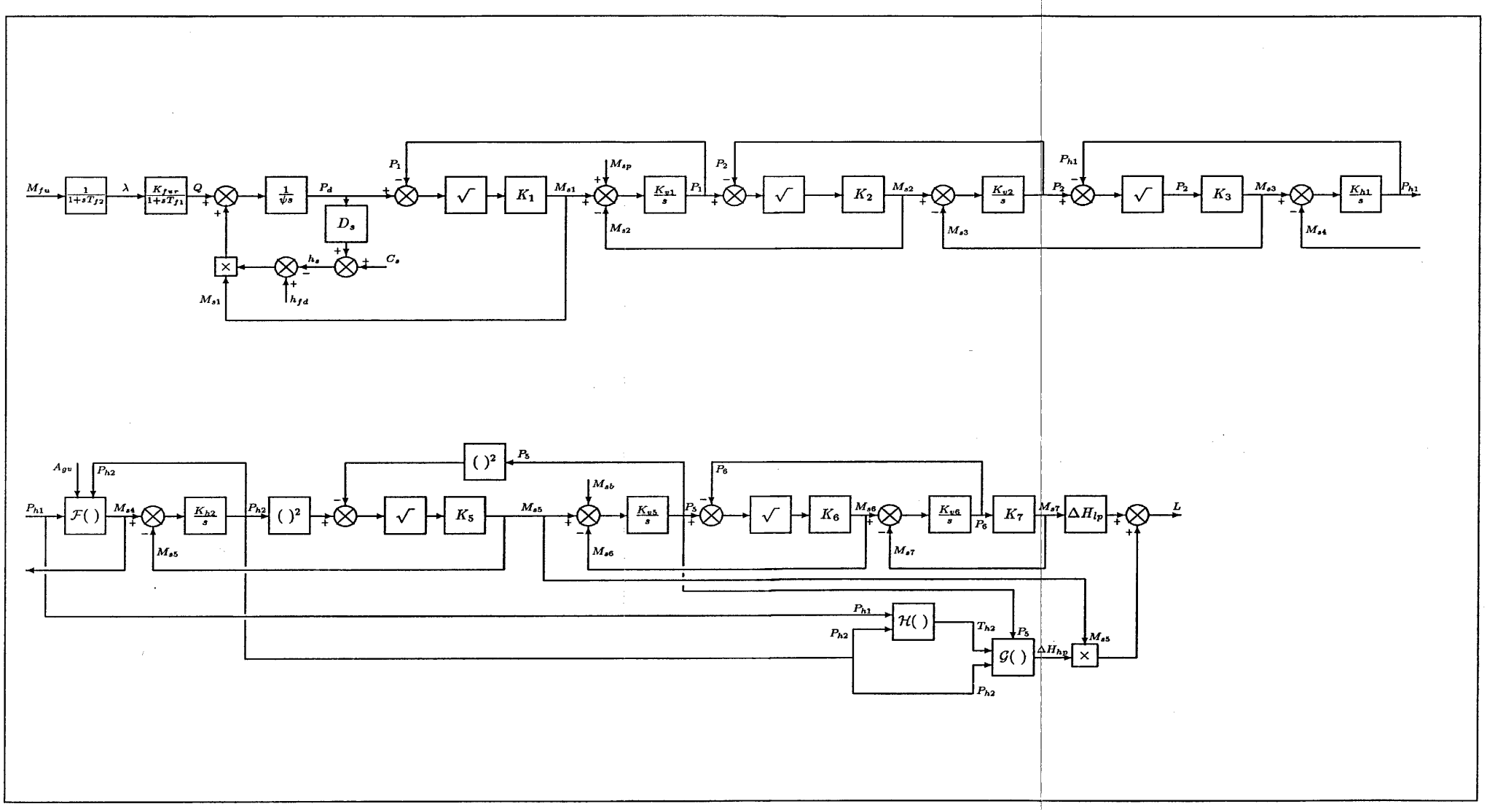

Figure 4.8: Block Diagram of Fossil-Fired Boiler Model

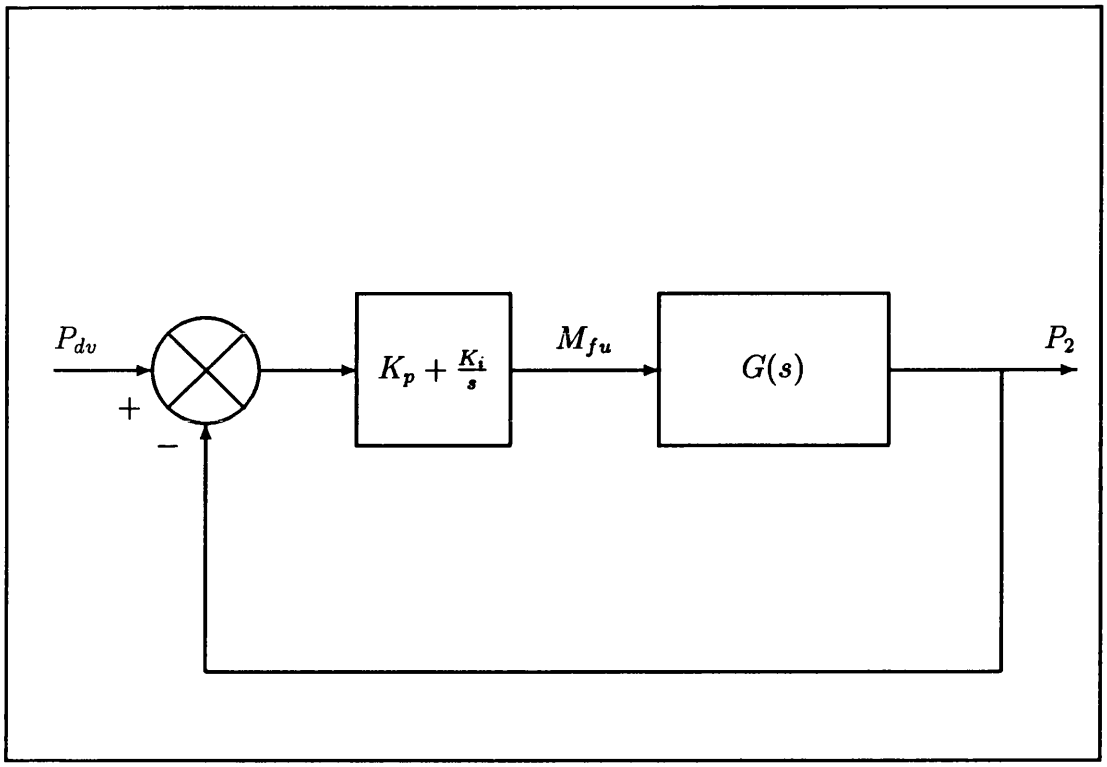

Figure 4.9: Block Diagram of BFT Pressure Loop PI Control

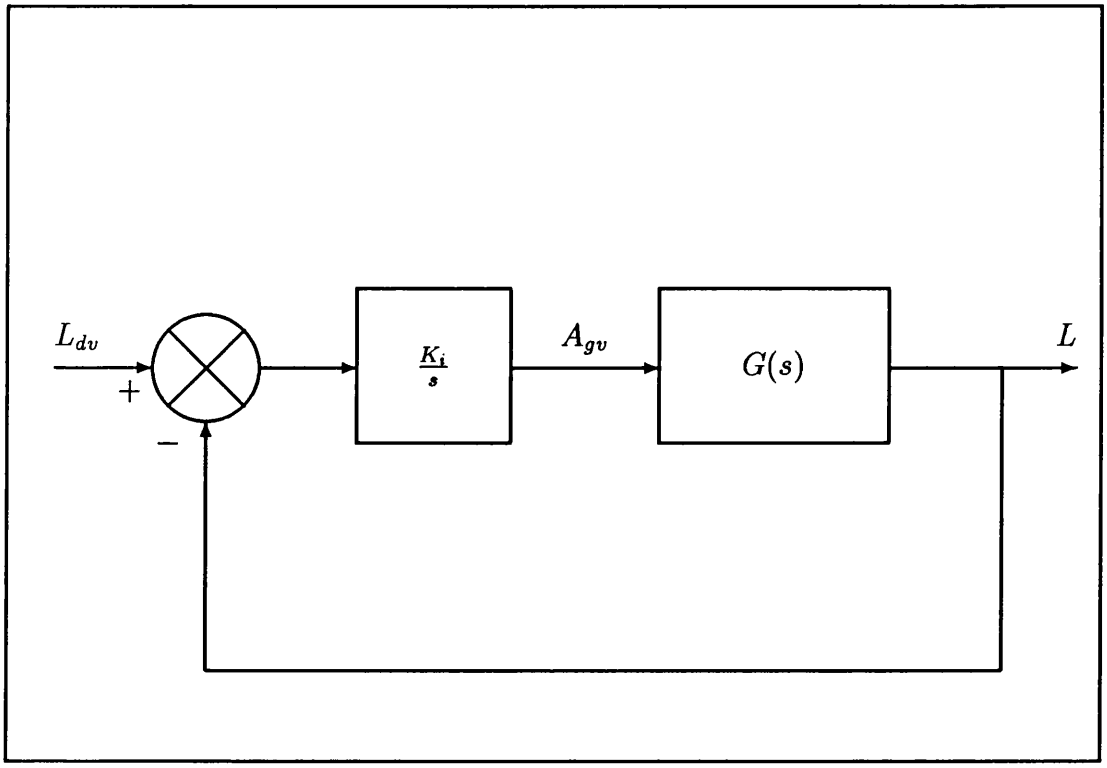

Figure 4.10: Block Diagram of BFT Load Loop I Control

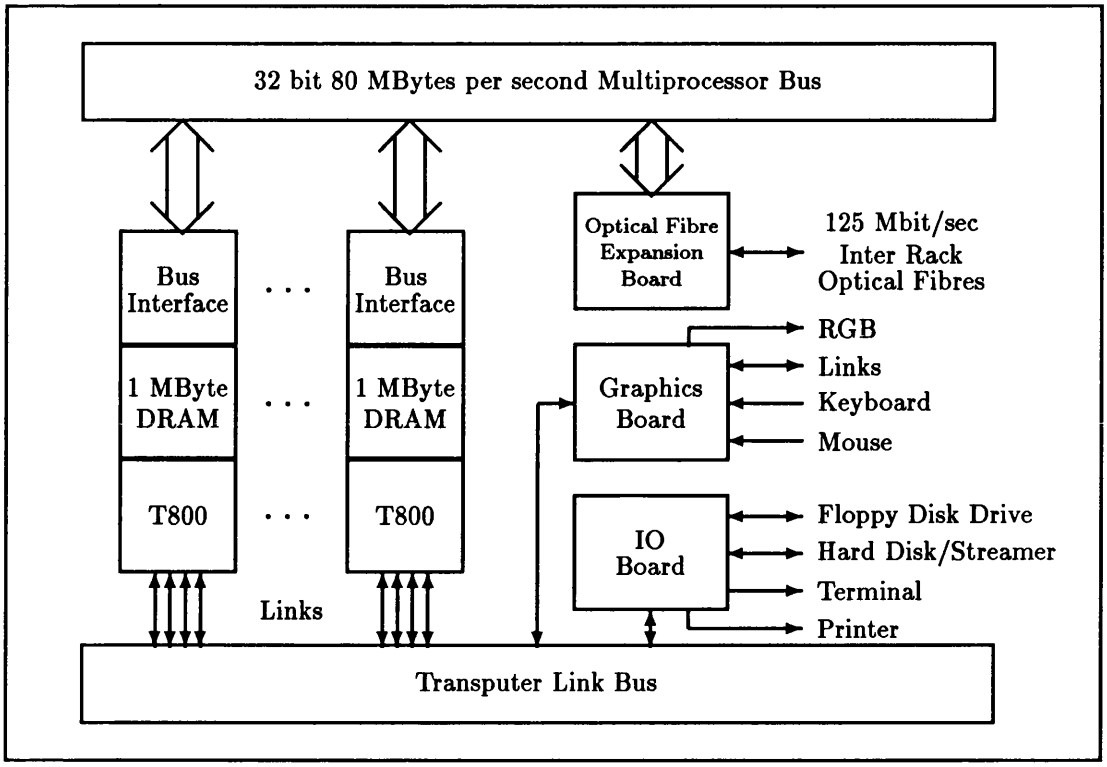

Figure 5.1: Block Diagram of the Parallel Transputer Computer

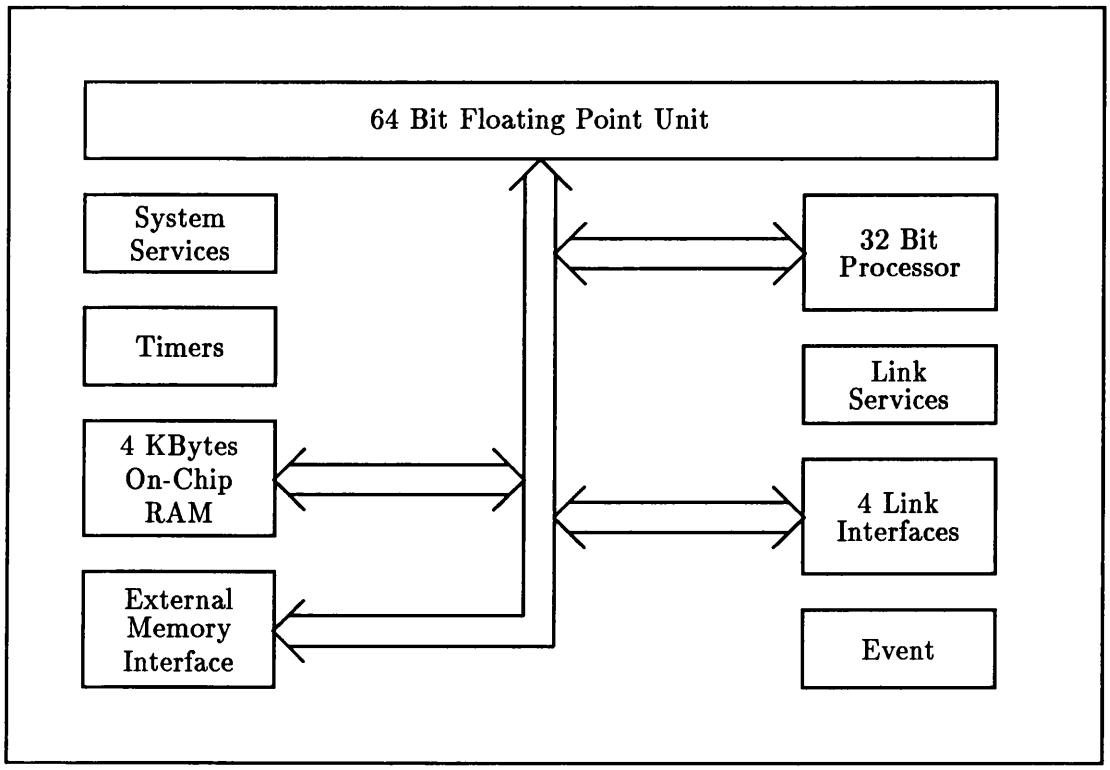

Figure 5.2: Block Diagram of the Inmos T800 Transputer

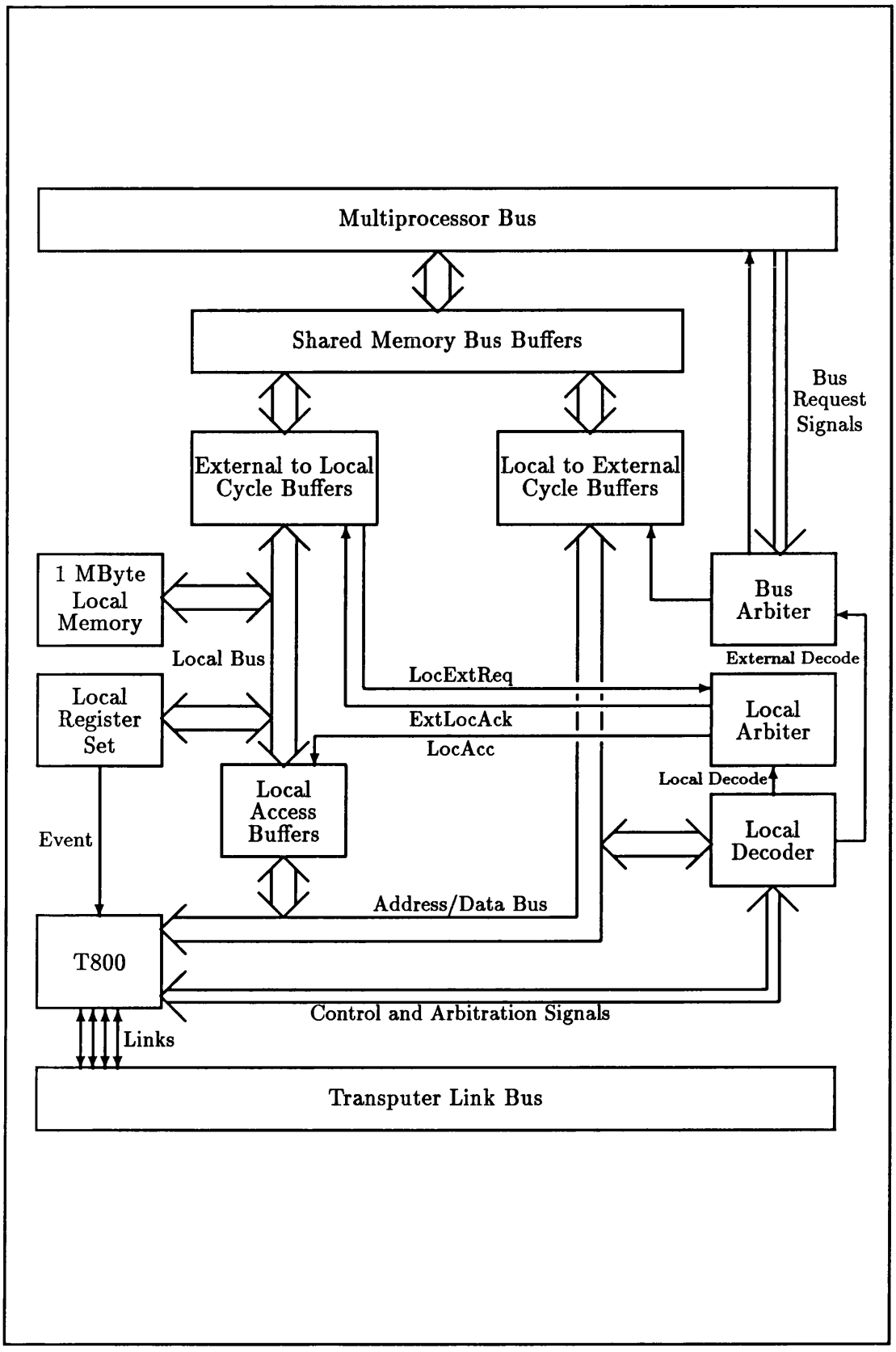

Figure 5.3: Block Diagram of the T800 Processing Node

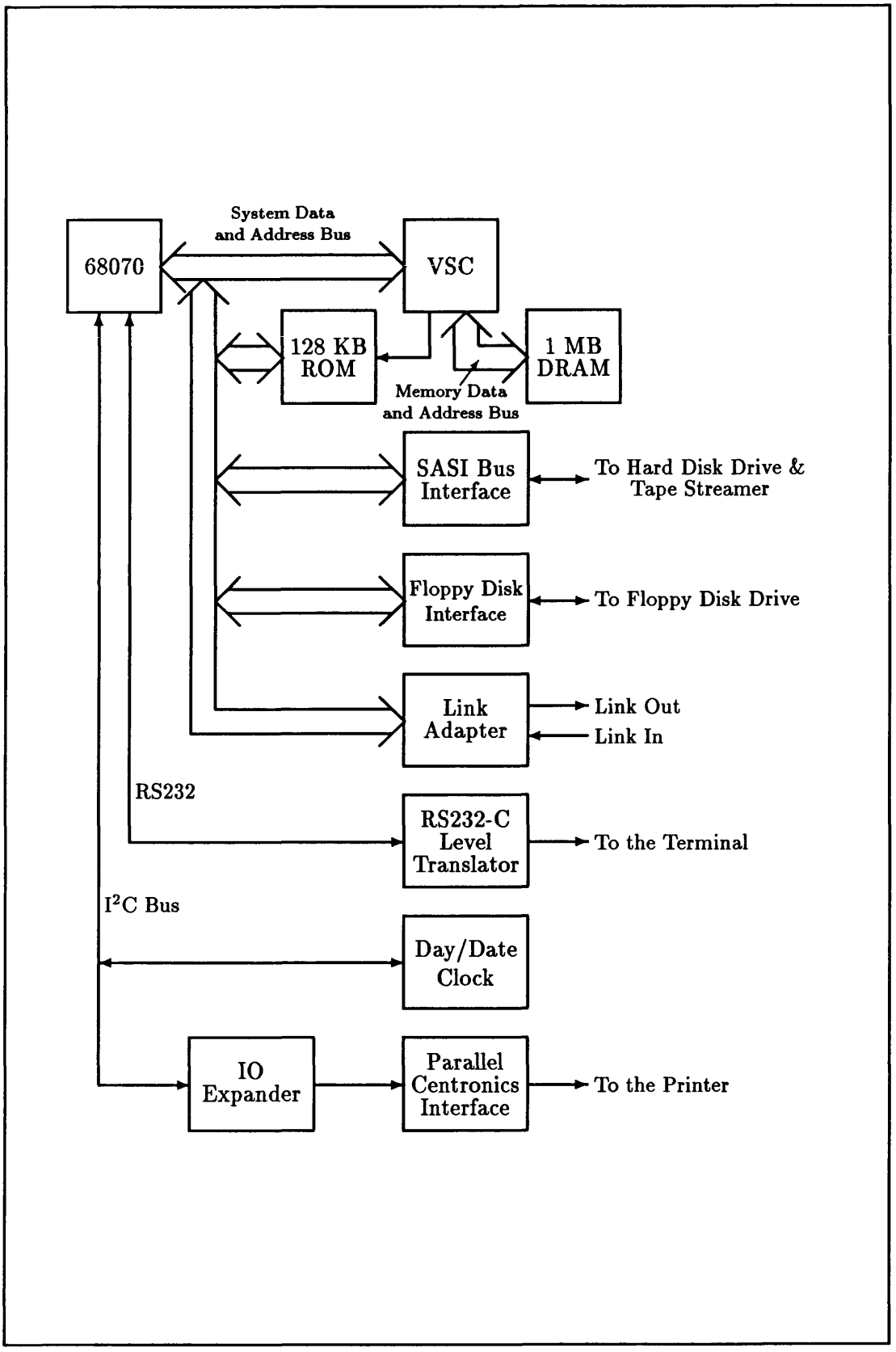

Figure 5.4: Block Diagram of the IO Board

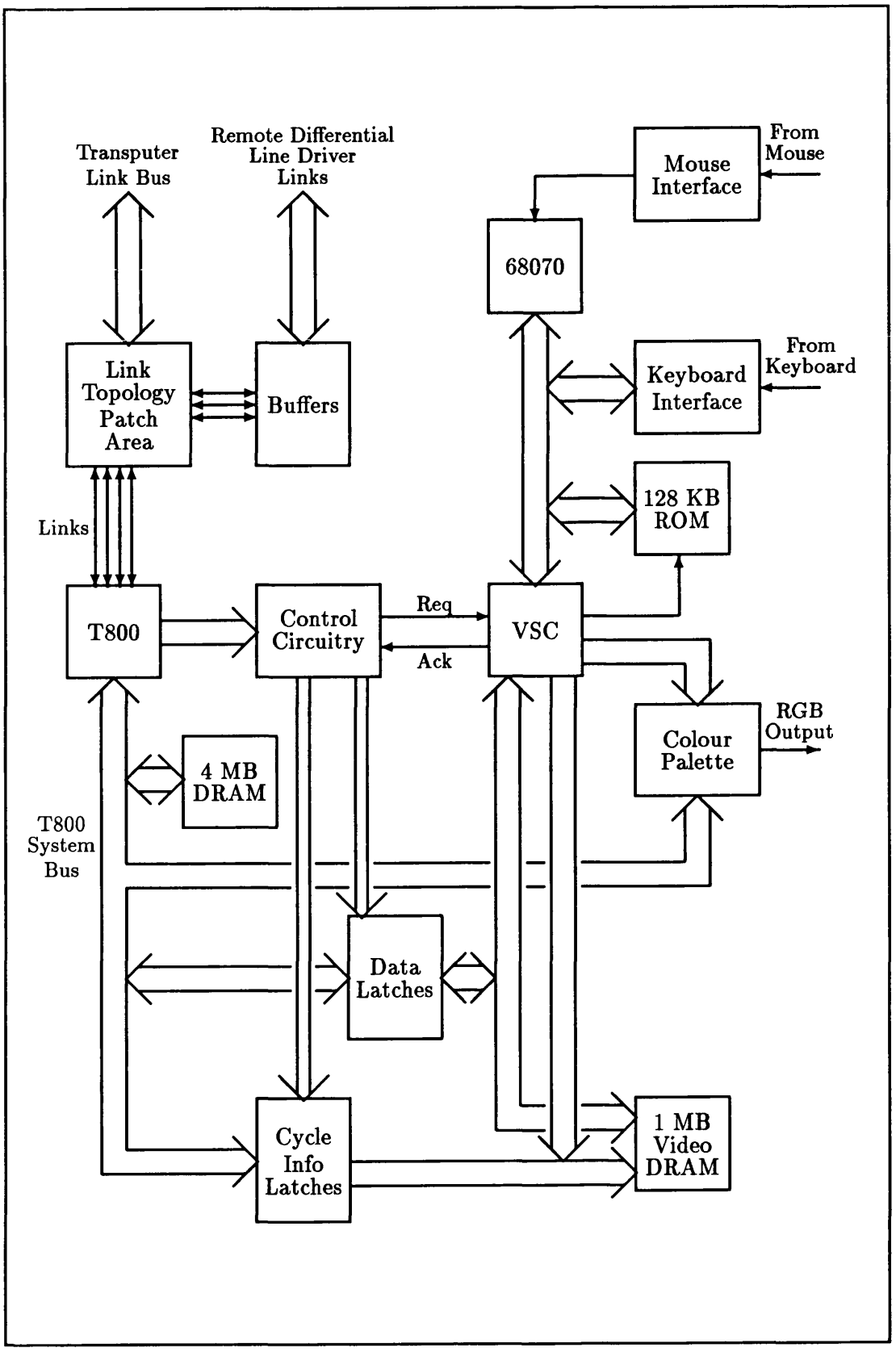

Figure 5.5: Block Diagram of the Graphics Board

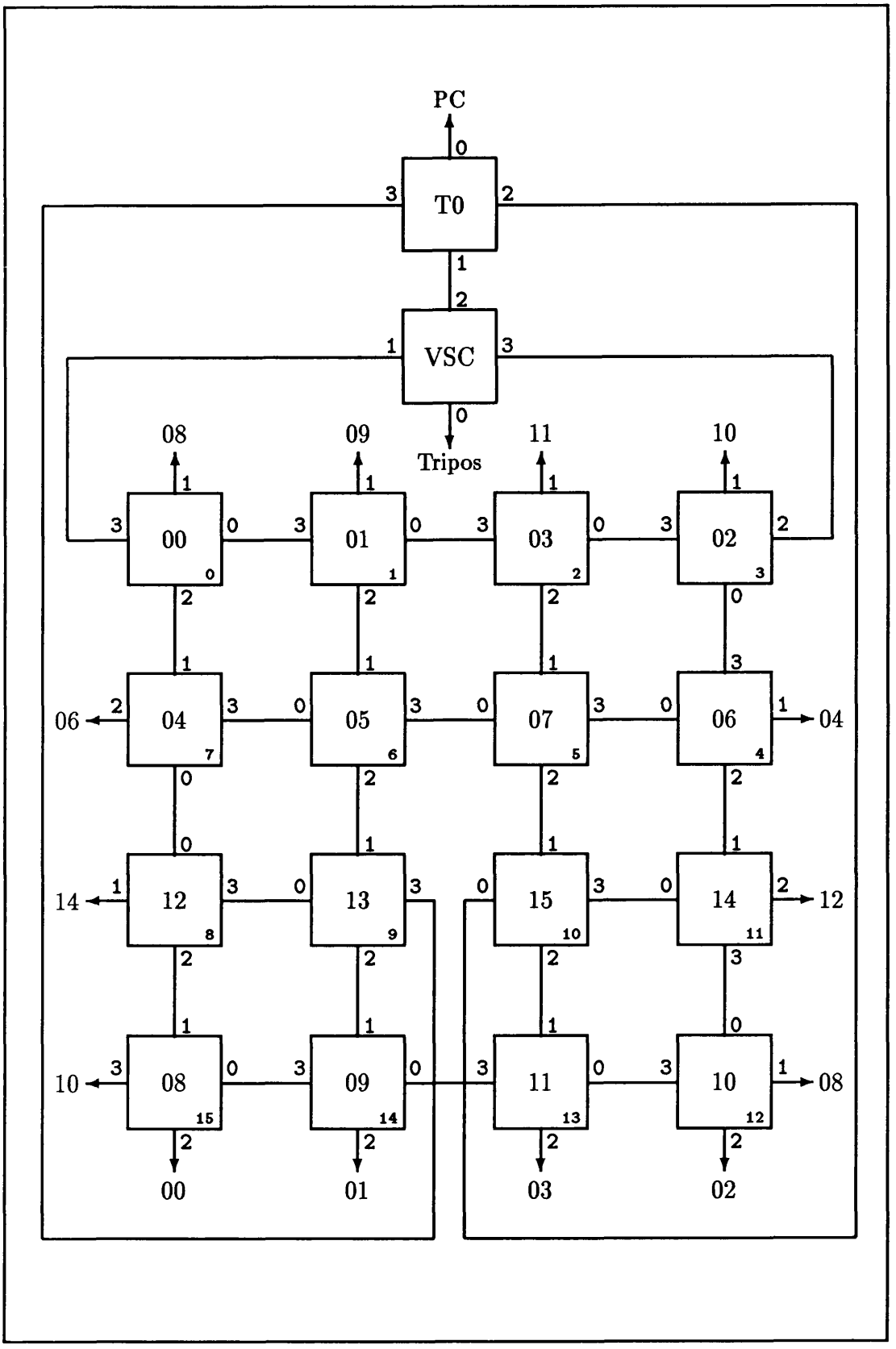

Figure 5.6: Block Diagram of Transputer Network Configuration

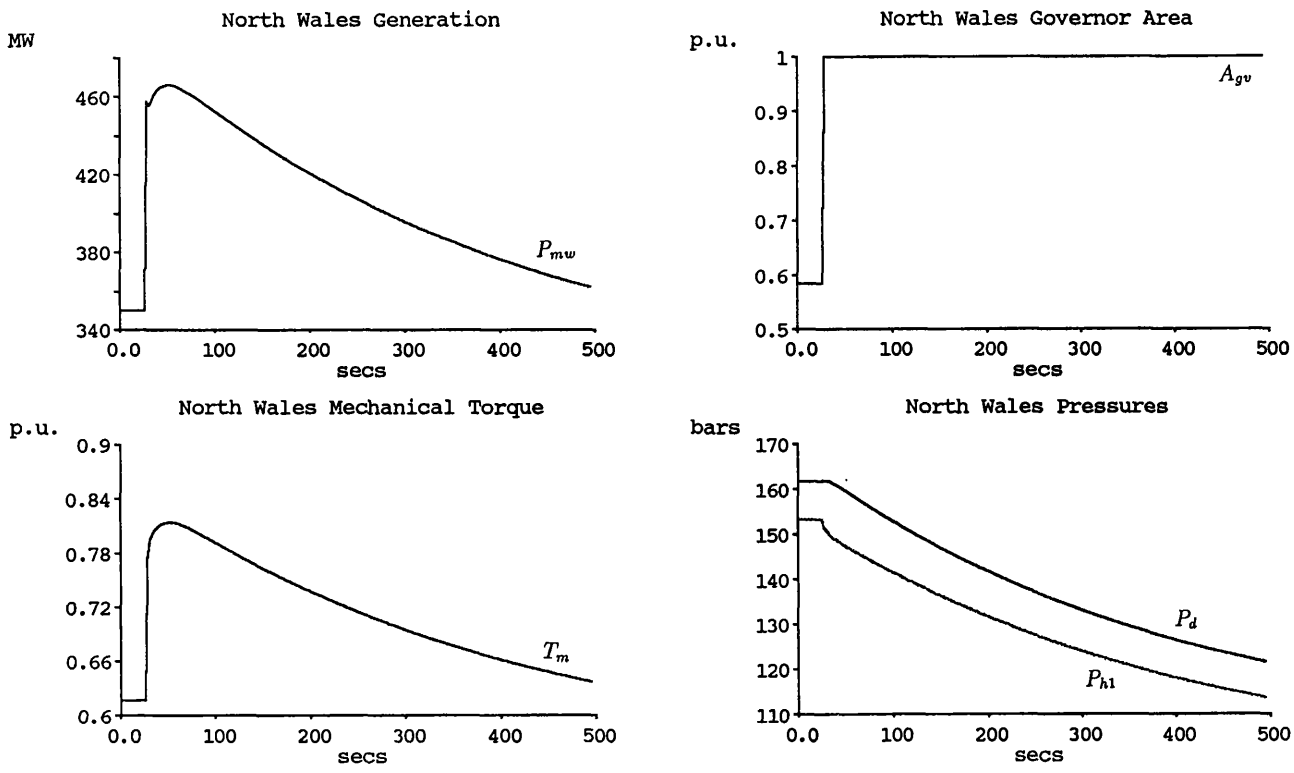

Figure 6.1: 4 m'c NWALES Stored Energy Test 400 MW (Run 47c)

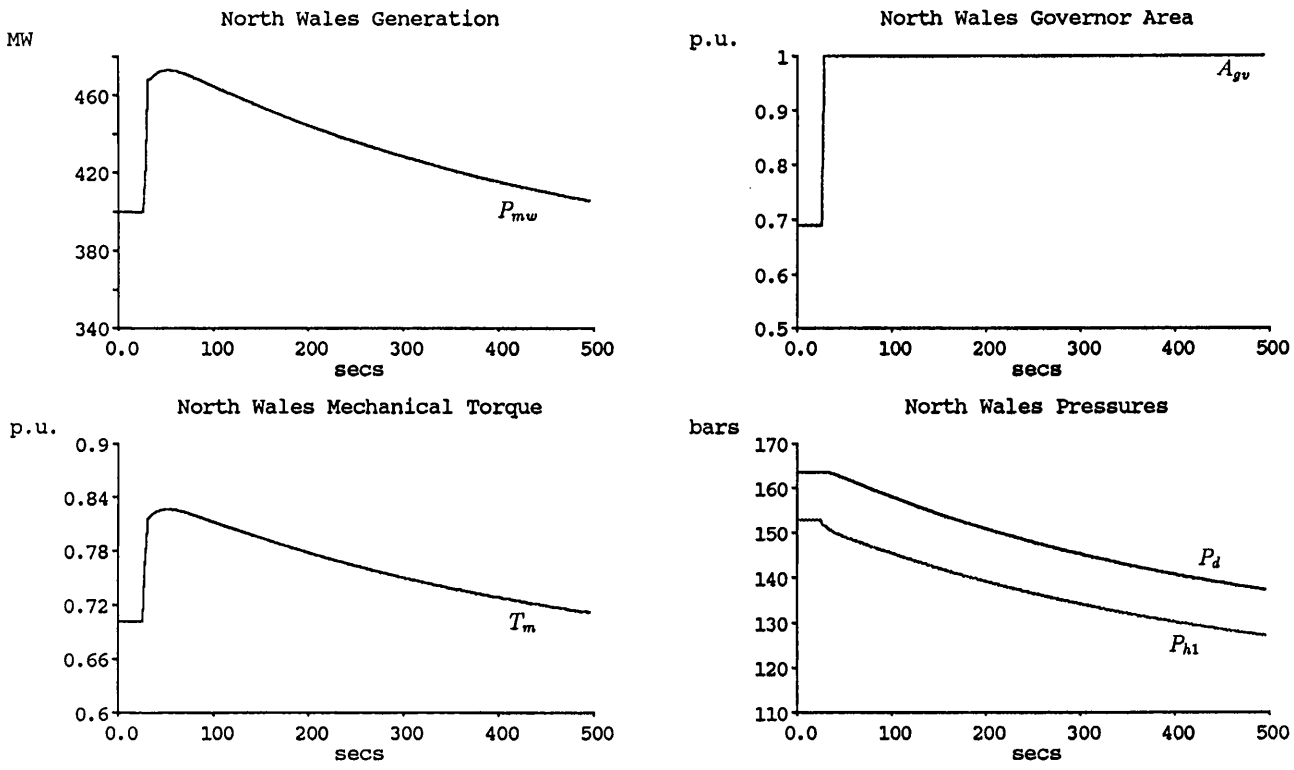

Figure 6.2: 4 m'c NWALES Stored Energy Test 400 MW (Run 48c)

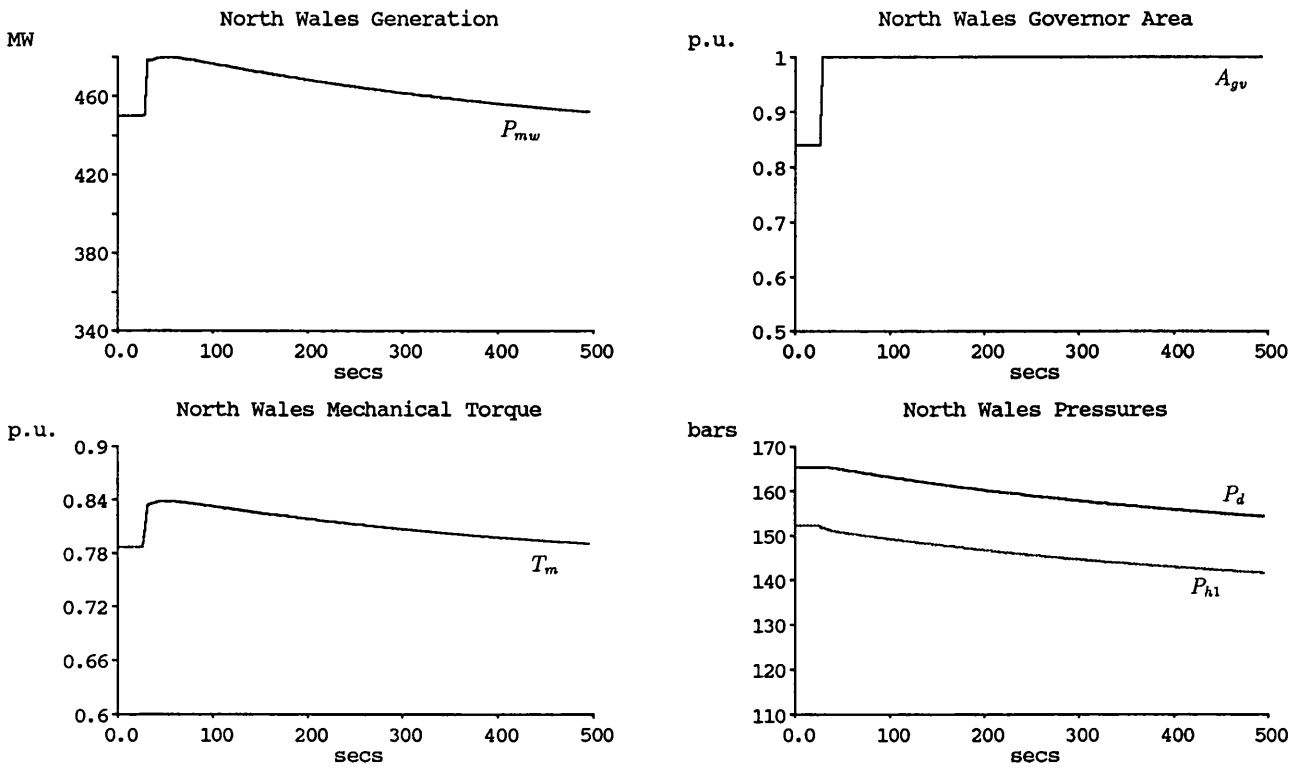

Figure 6.3: 4 m'c NWALES Stored Energy Test 400 MW (Run 49c)

49c fig 6.3

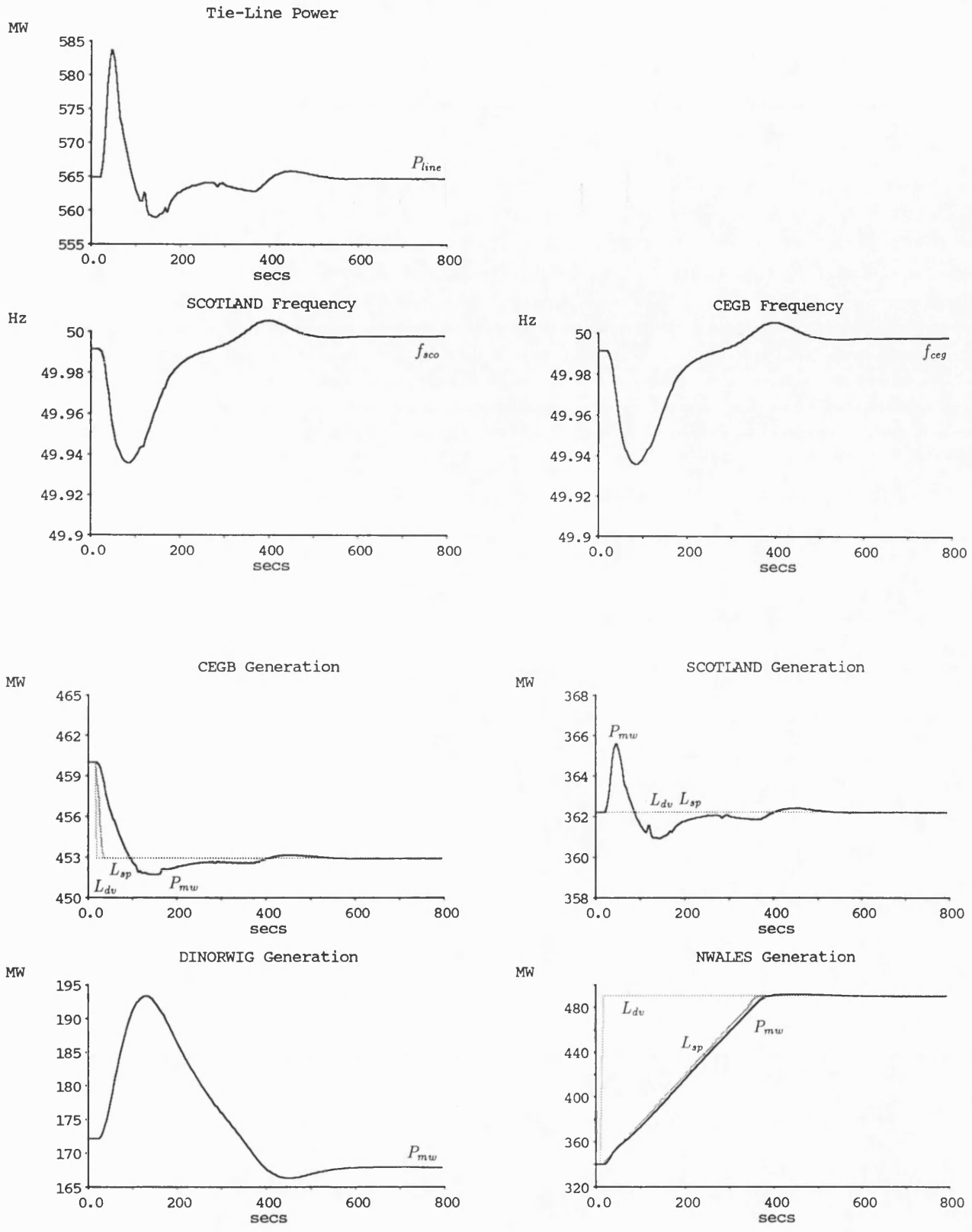

Figure 6.4: (a) 4 m'c NWALES and CEGB Load Setpoint Changes (Run 43)

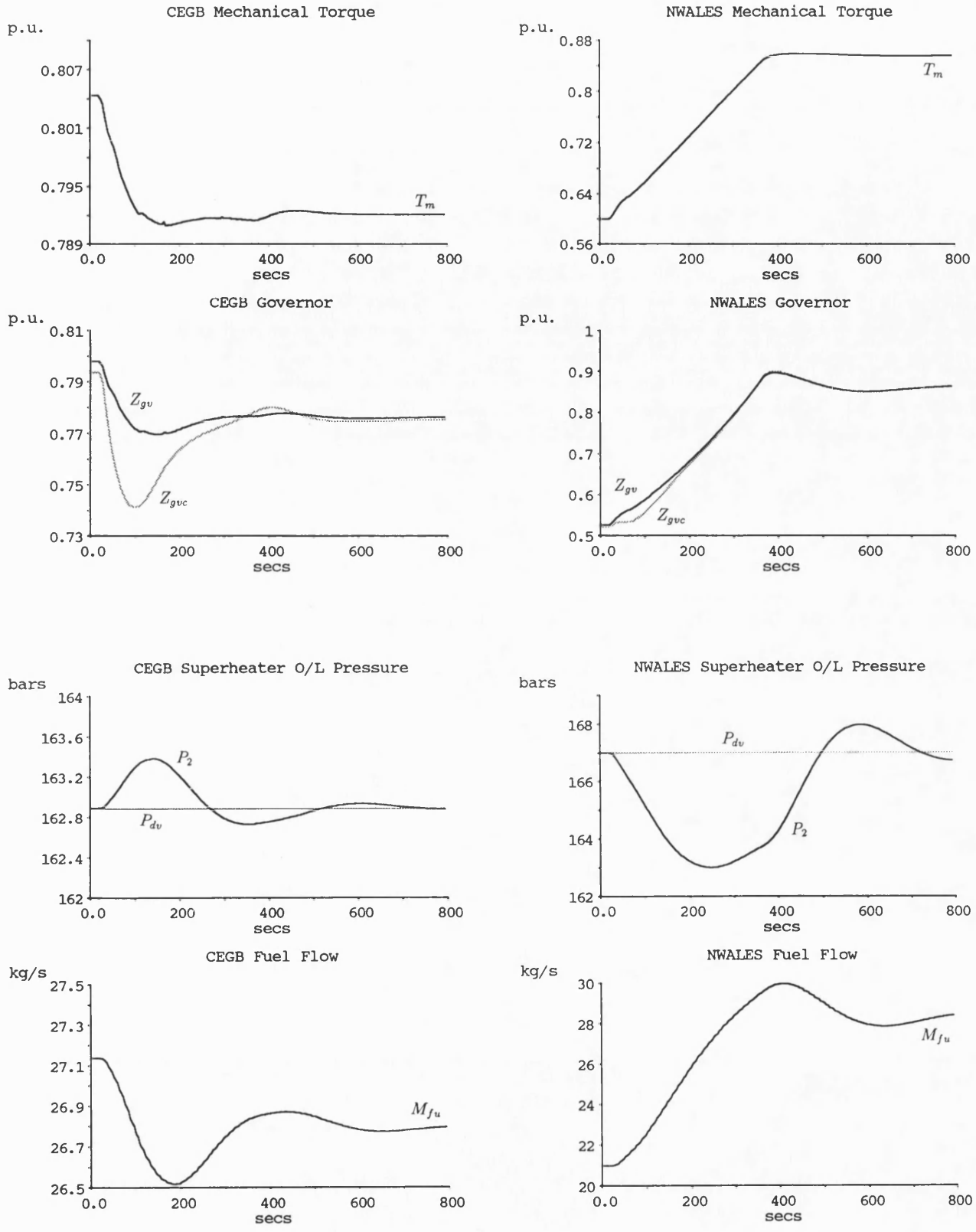

Figure 6.4: (b) 4 m'c NWALES and CEGB Load Setpoint Changes (Run 43)

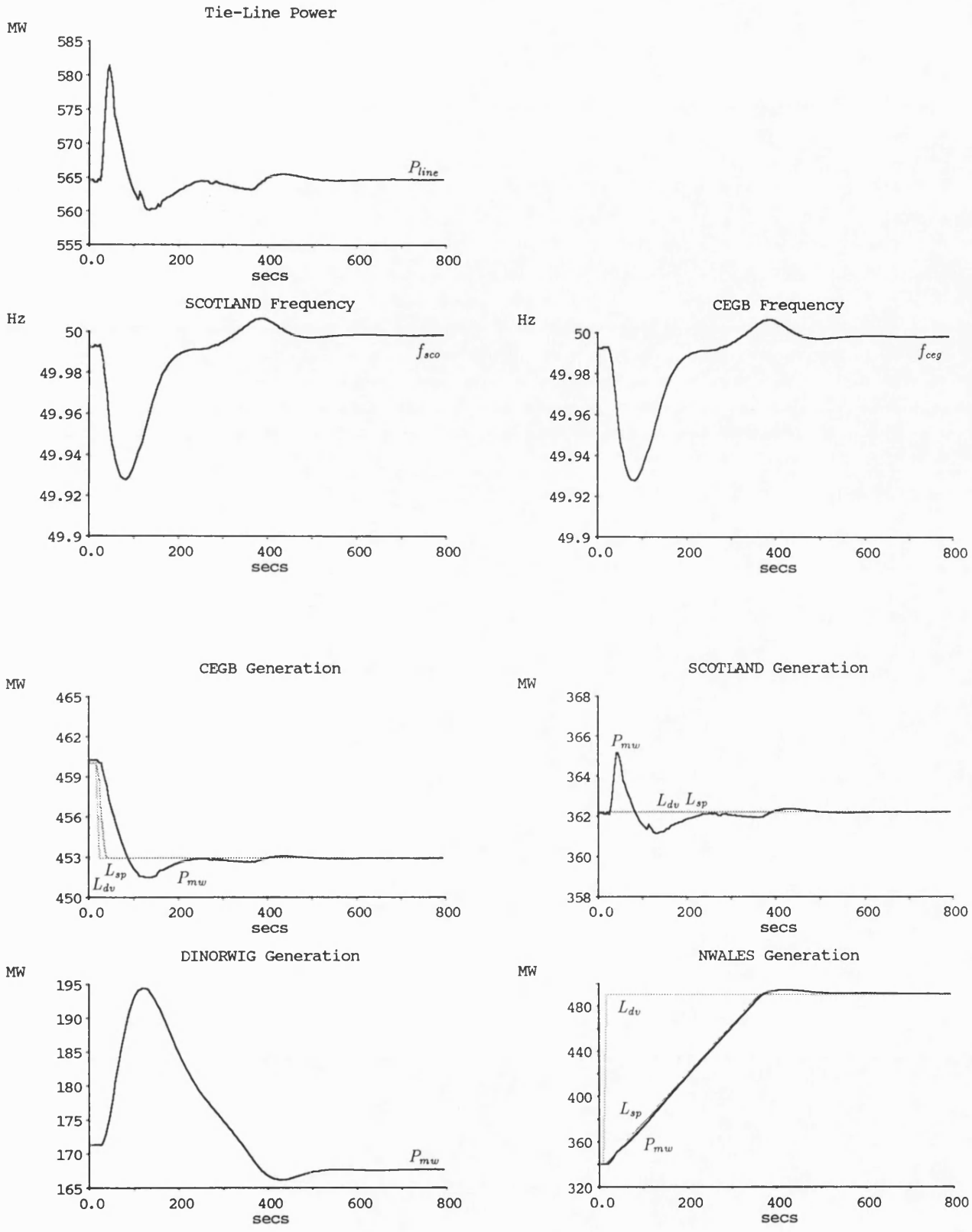

Figure 6.5: (a) 4 m'c NWALES and CEGB Load Setpoint Changes (Run 45)

45 fig 6.5 (a)

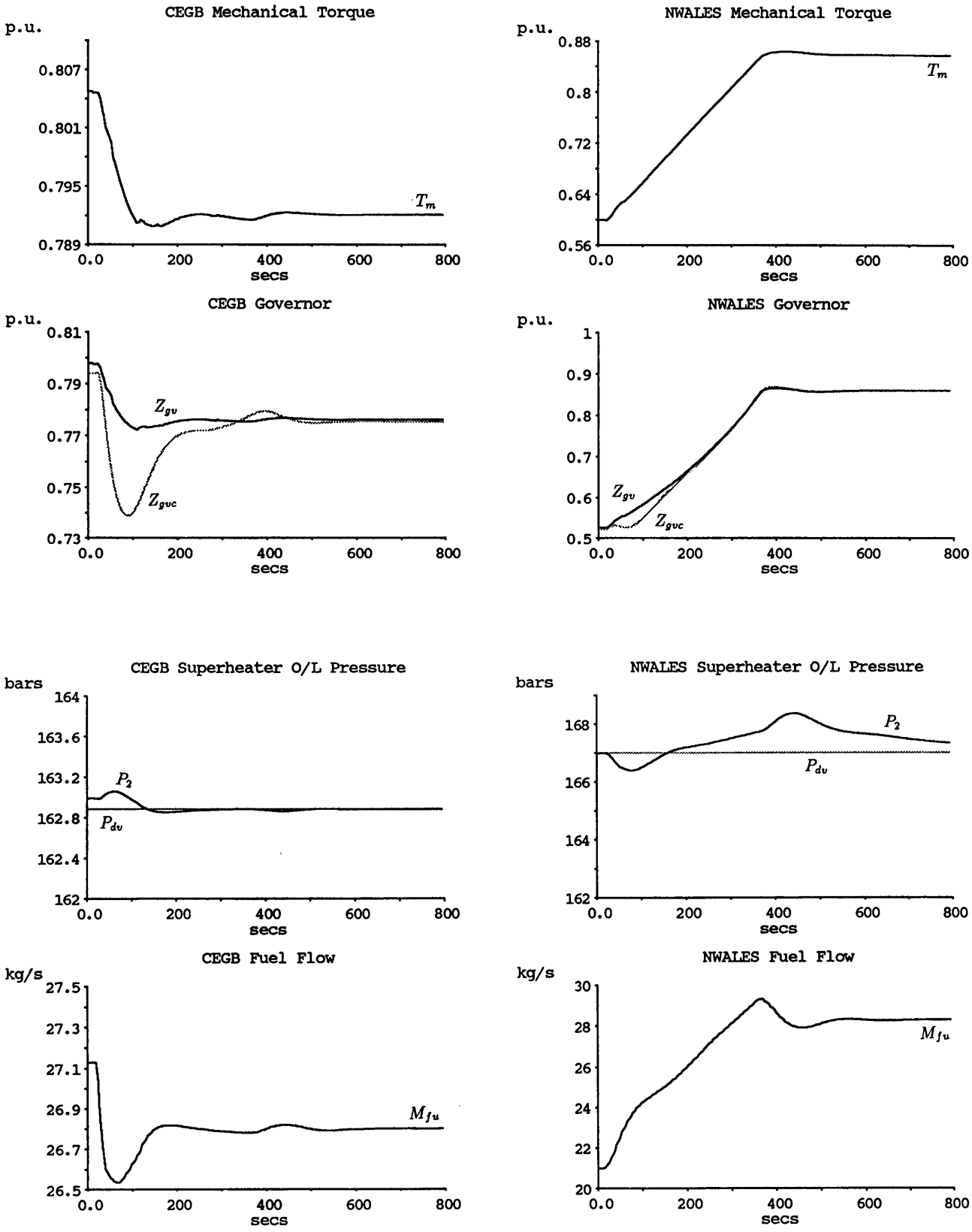

Figure 6.5: (b) 4 m'c NWALES and CEGB Load Setpoint Changes (Run 45)

45 Fig 6.5(b)

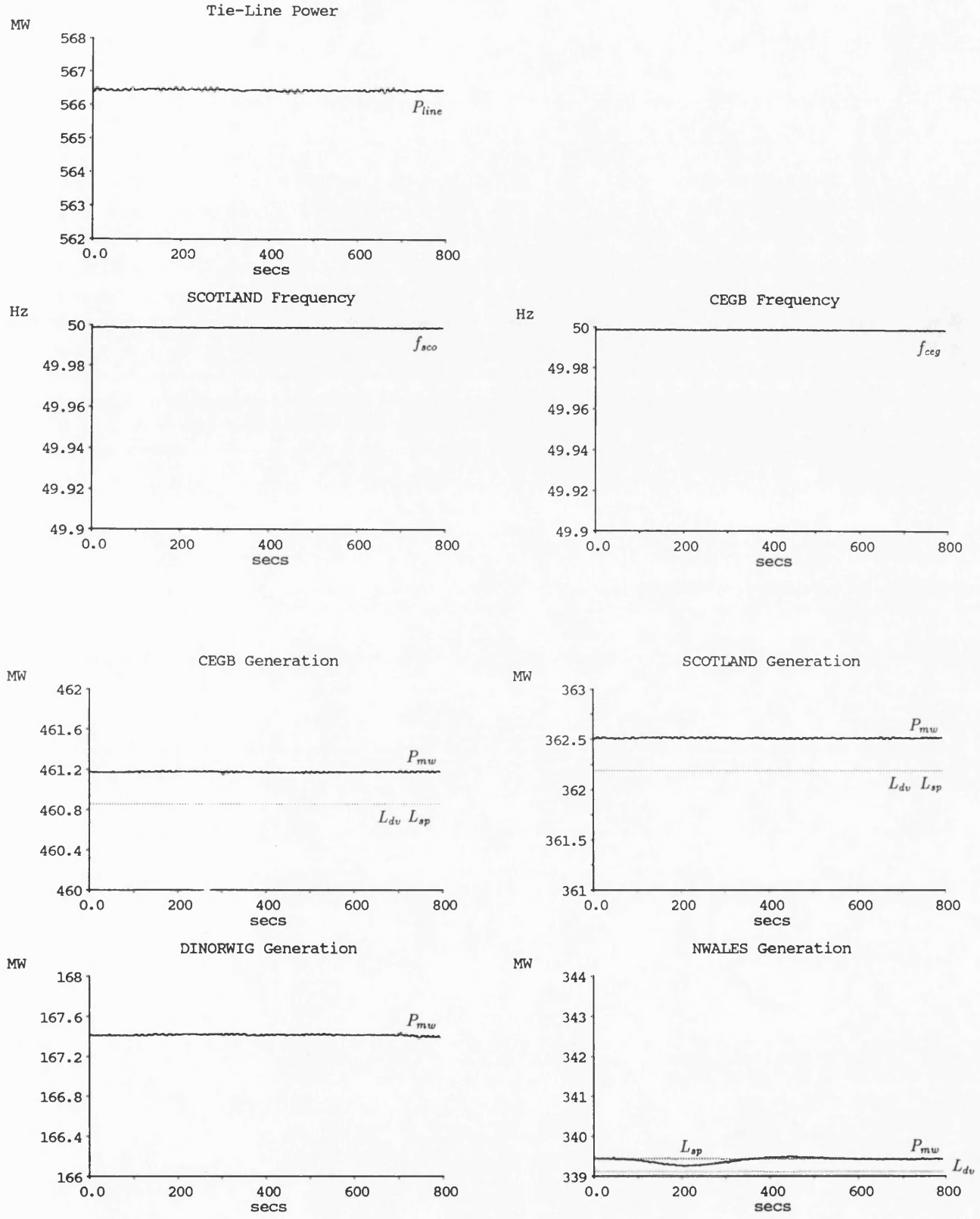

Figure 6.6: (a) 4 m'c NWALES Pressure Setpoint Change (Run 42)

42 fig. 6.6 (a)

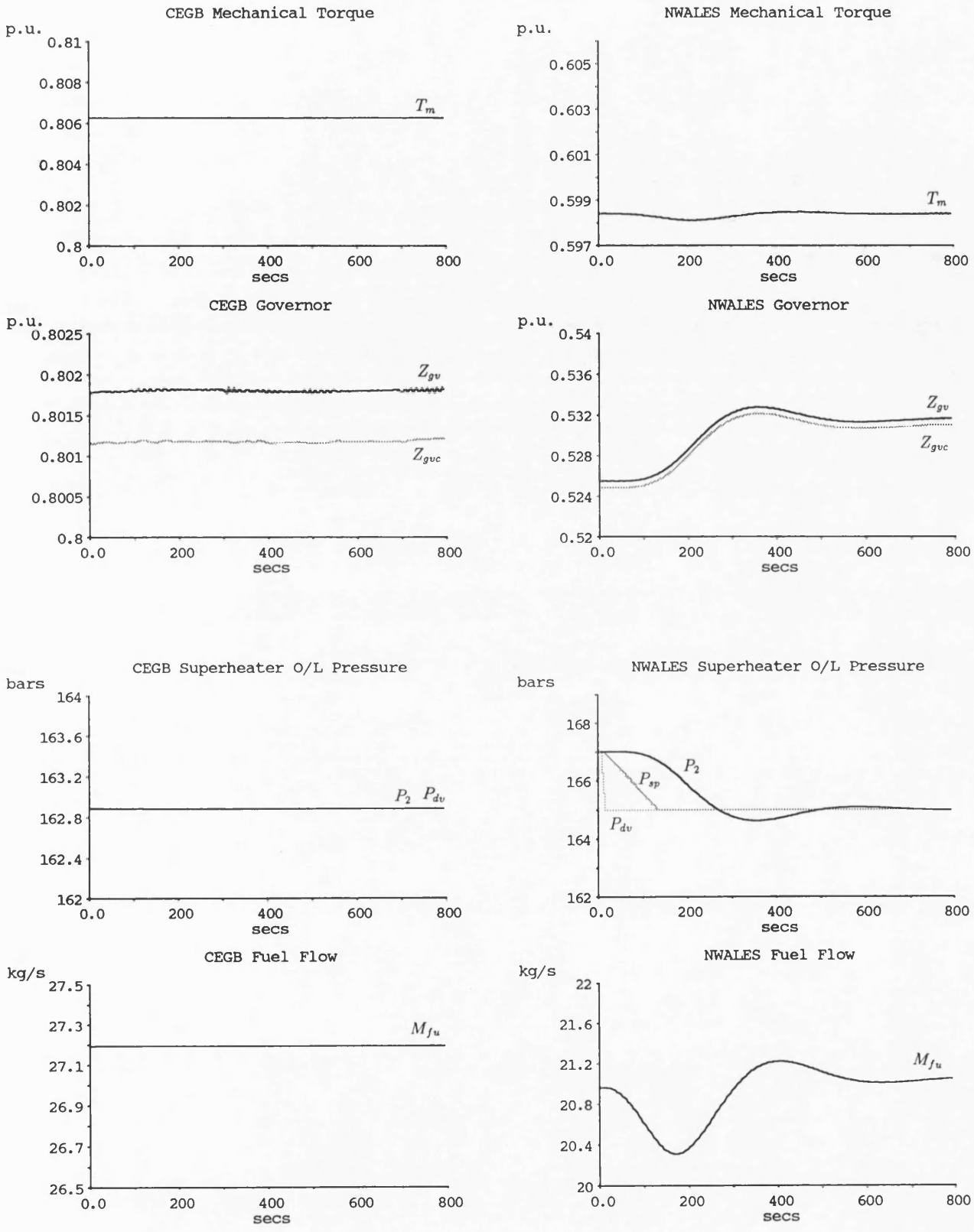

Figure 6.6: (b) 4 m'c NWALES Pressure Setpoint Change (Run 42)

42 Fig 6.6 (b)

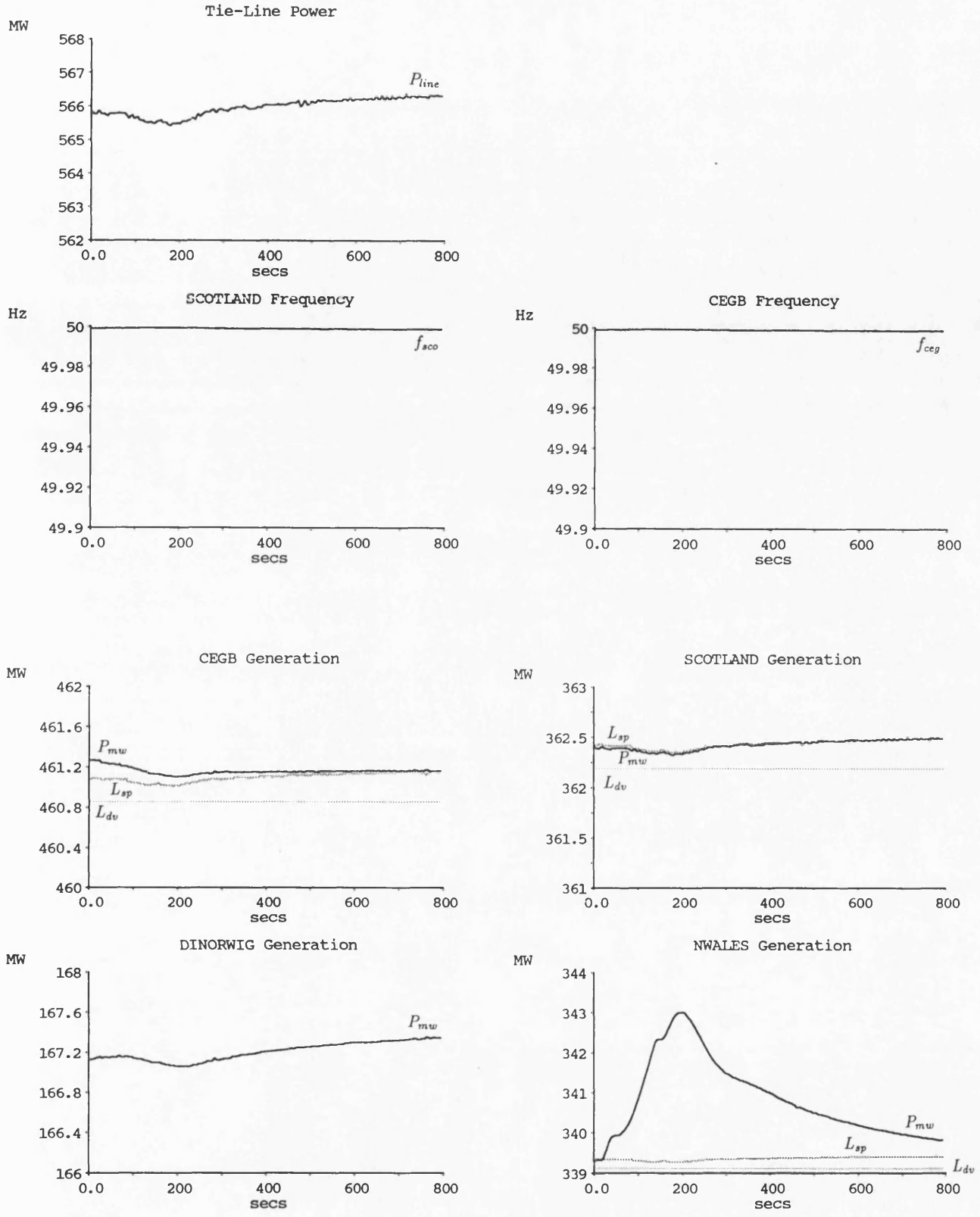

Figure 6.7: (a) 4 m'c NWALES Pressure Setpoint Change (Run 44)

44 fig 6.7 (a)

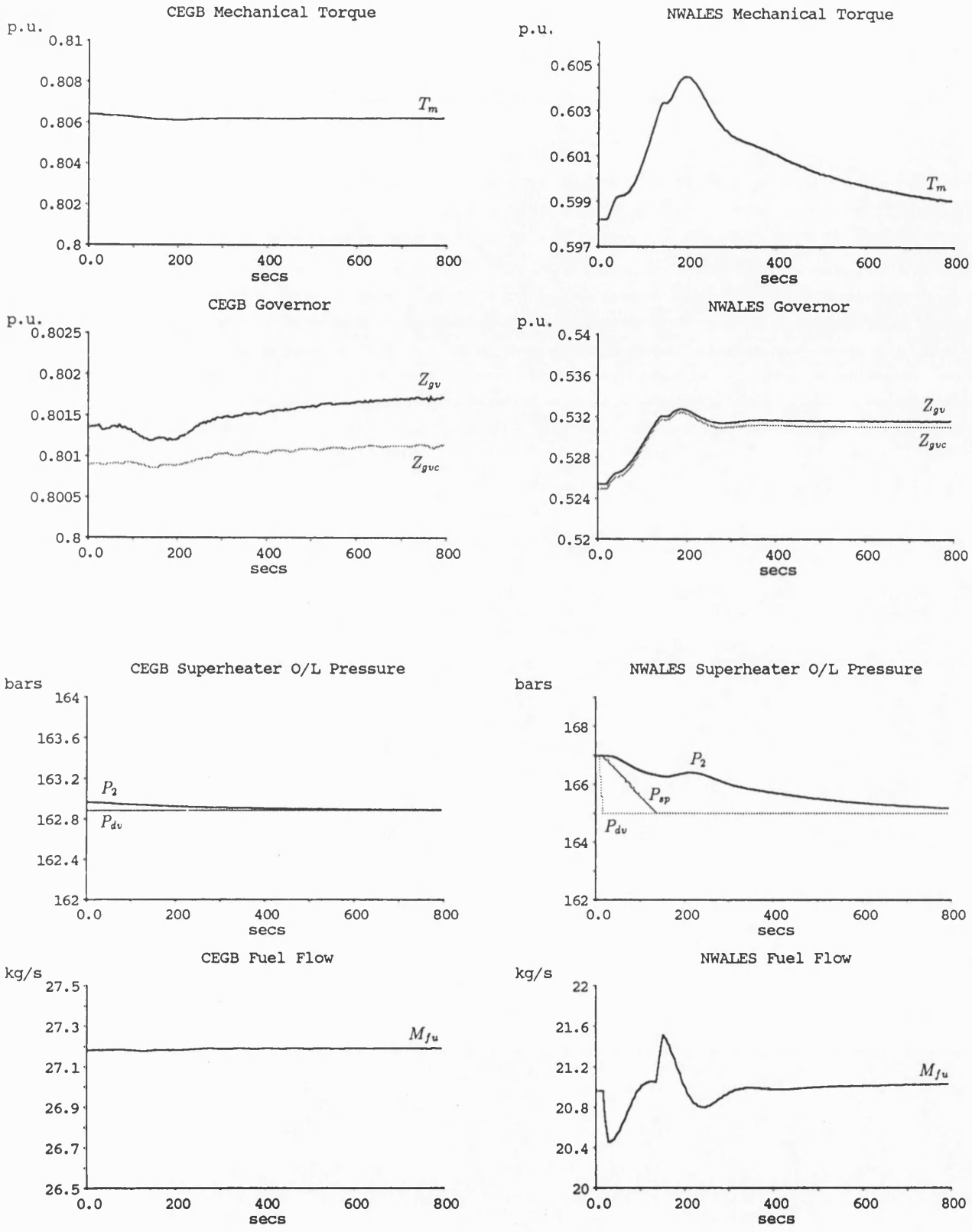

Figure 6.7: (b) 4 m'c NWALES Pressure Setpoint Change (Run 44)

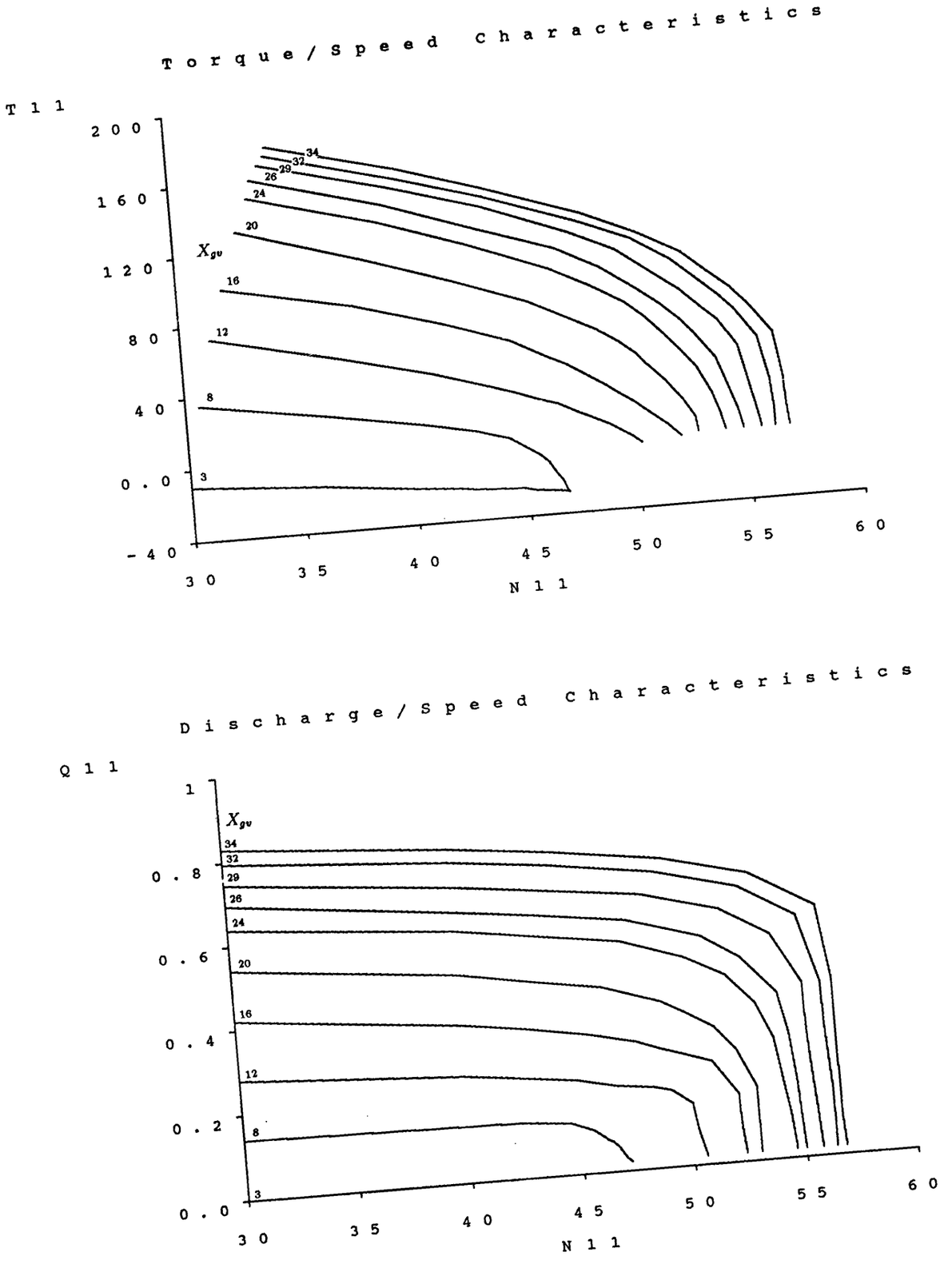

Figure 6.8: DINORWIG Non-Linear Characteristics

fig 6.8

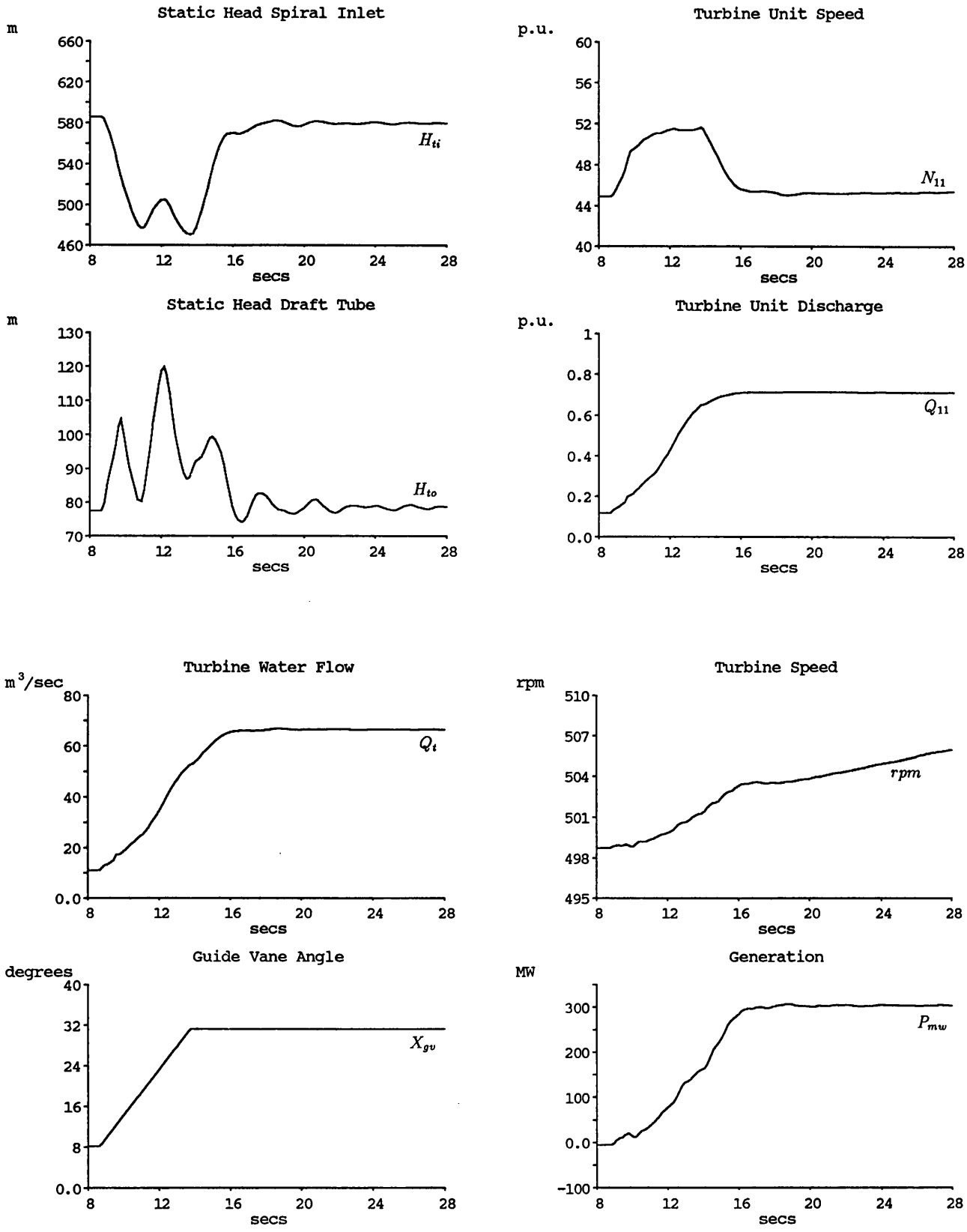

Figure 6.9: 4 m'c DINORWIG Manual Guide Vane Ramp (Run 51)

51 Fig. 6.9

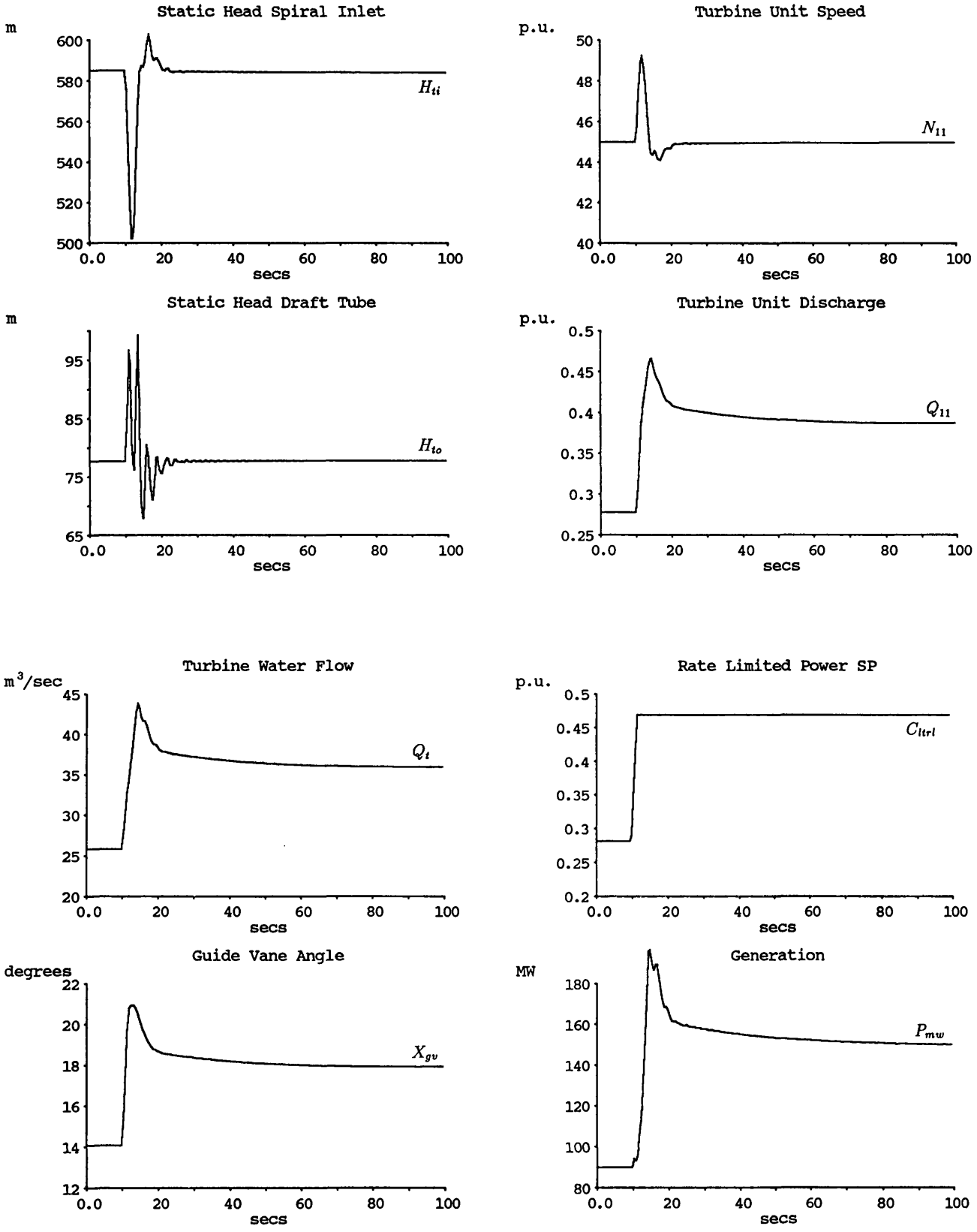

Figure 6.10: 4 m'c DINORWIG Response to Step Load Increase (Run 52)

52 Fig 6.10

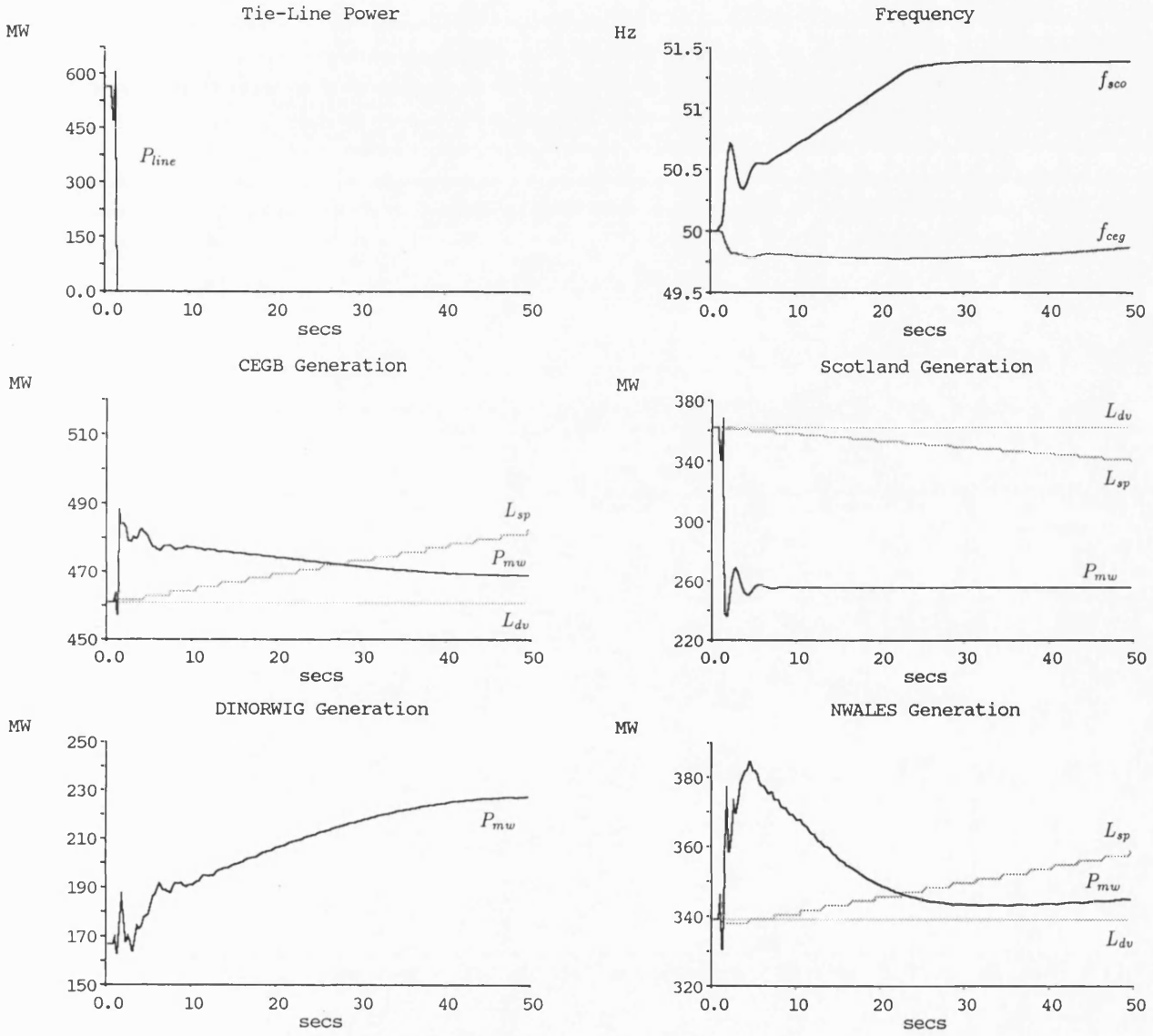

Figure 6.11: (a) 4 m'c Scotland-England Split (Run 1)

Fig. 11(a)

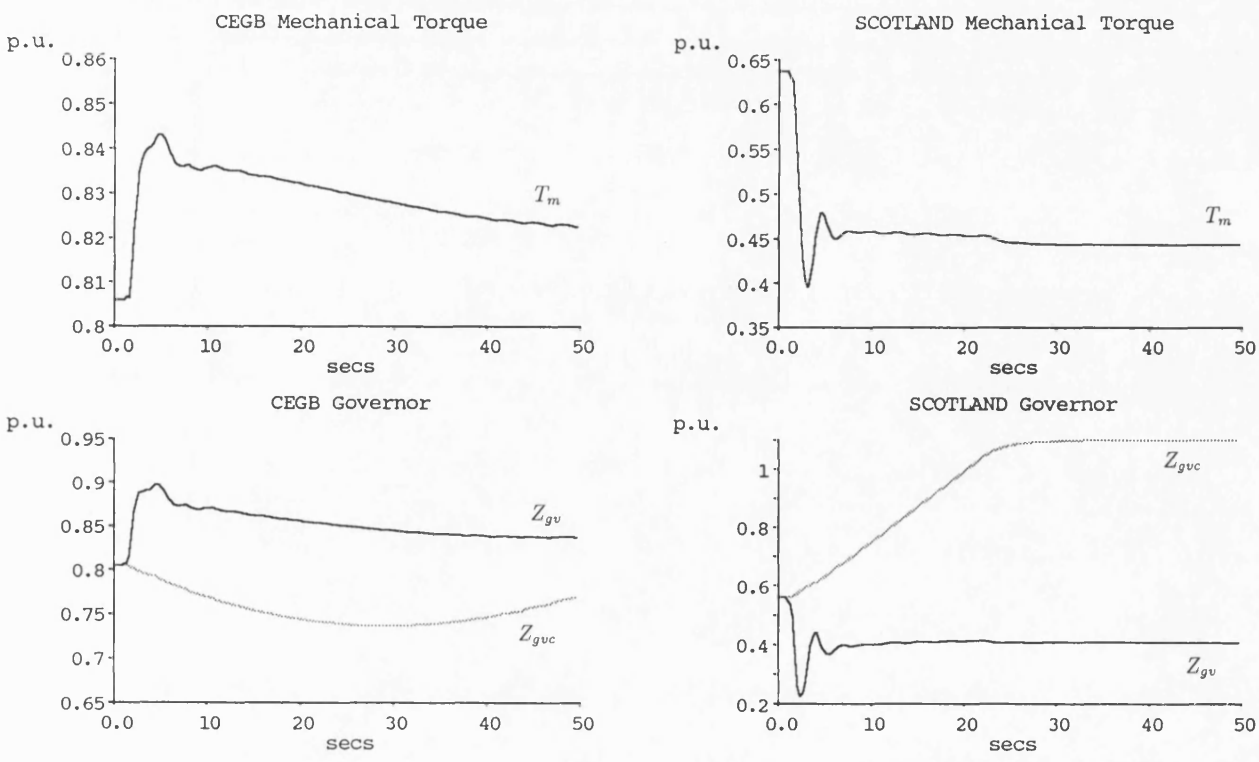

Figure 6.11: (b) 4 m'c Scotland-England Split (Run 1)

Fig. 6.11(b)

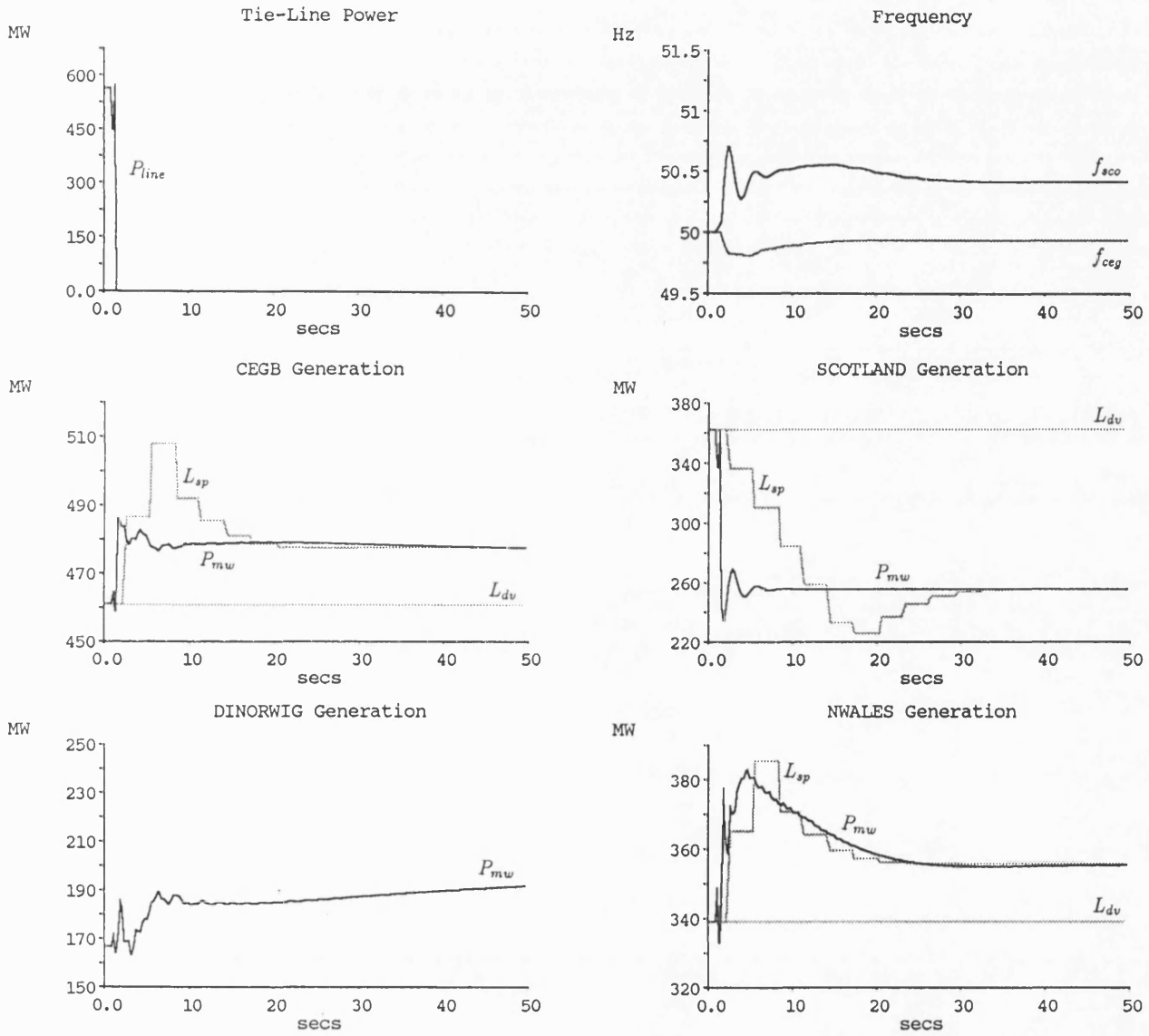

Figure 6.12: (a) 4 m'c Scotland-England Split (Run 2)

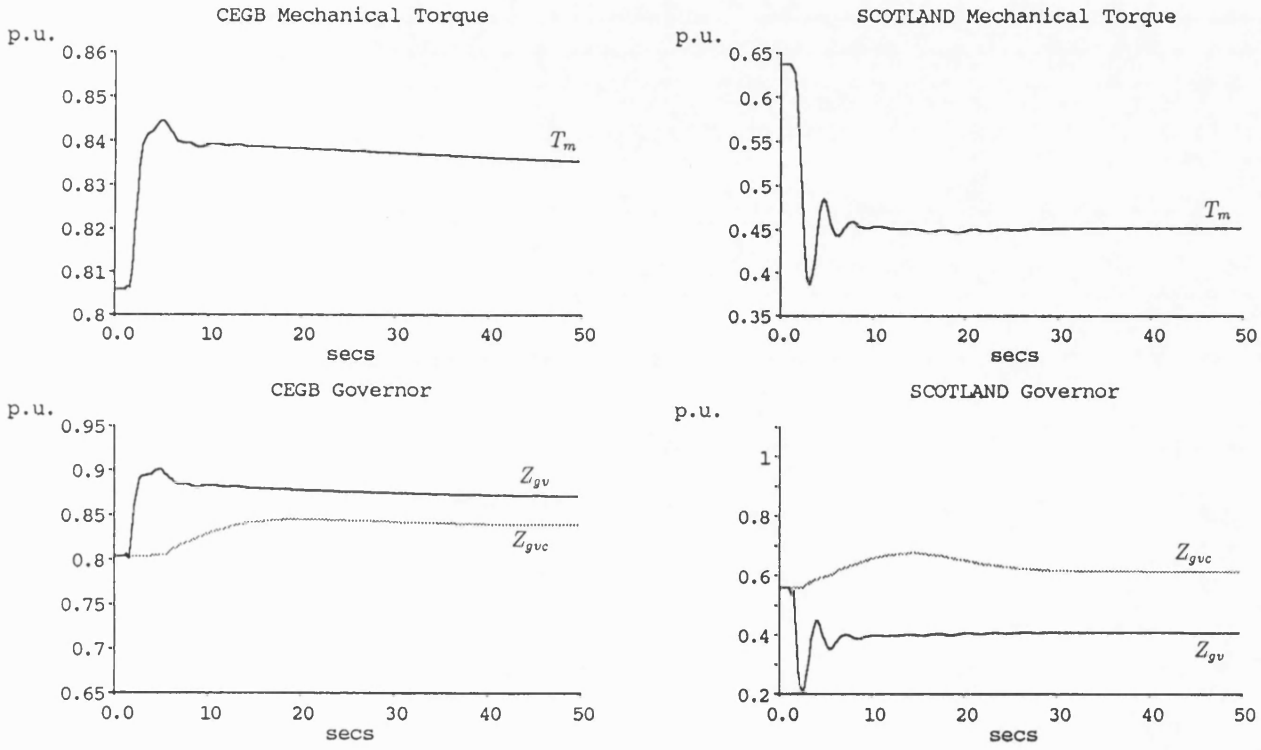

Figure 6.12: (b) 4 m'c Scotland-England Split (Run 2)

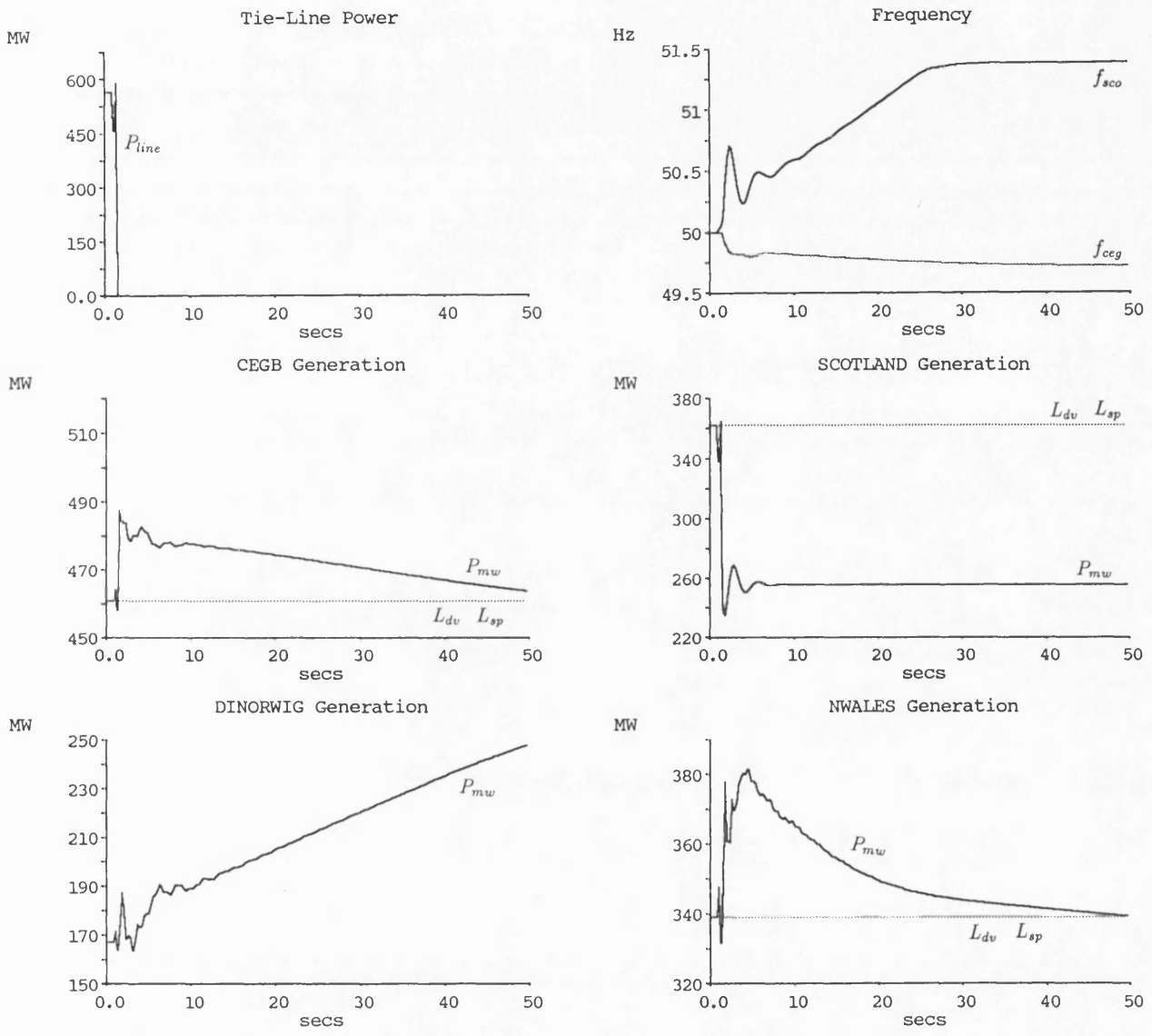

Figure 6.13: (a) 4 m'c Scotland-England Split (Run 3)

> fg6.12(b)

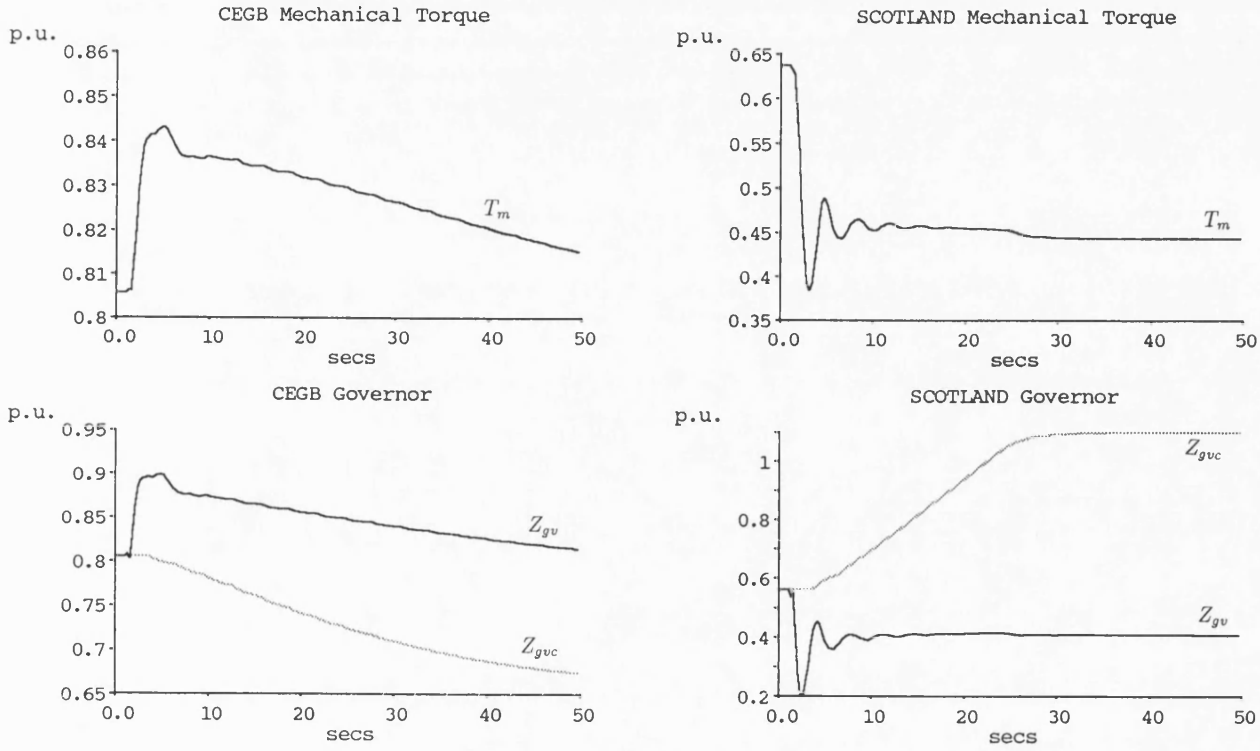

Figure 6.13: (b) 4 m'c Scotland-England Split (Run 3)

3 Fig 6.13(a)

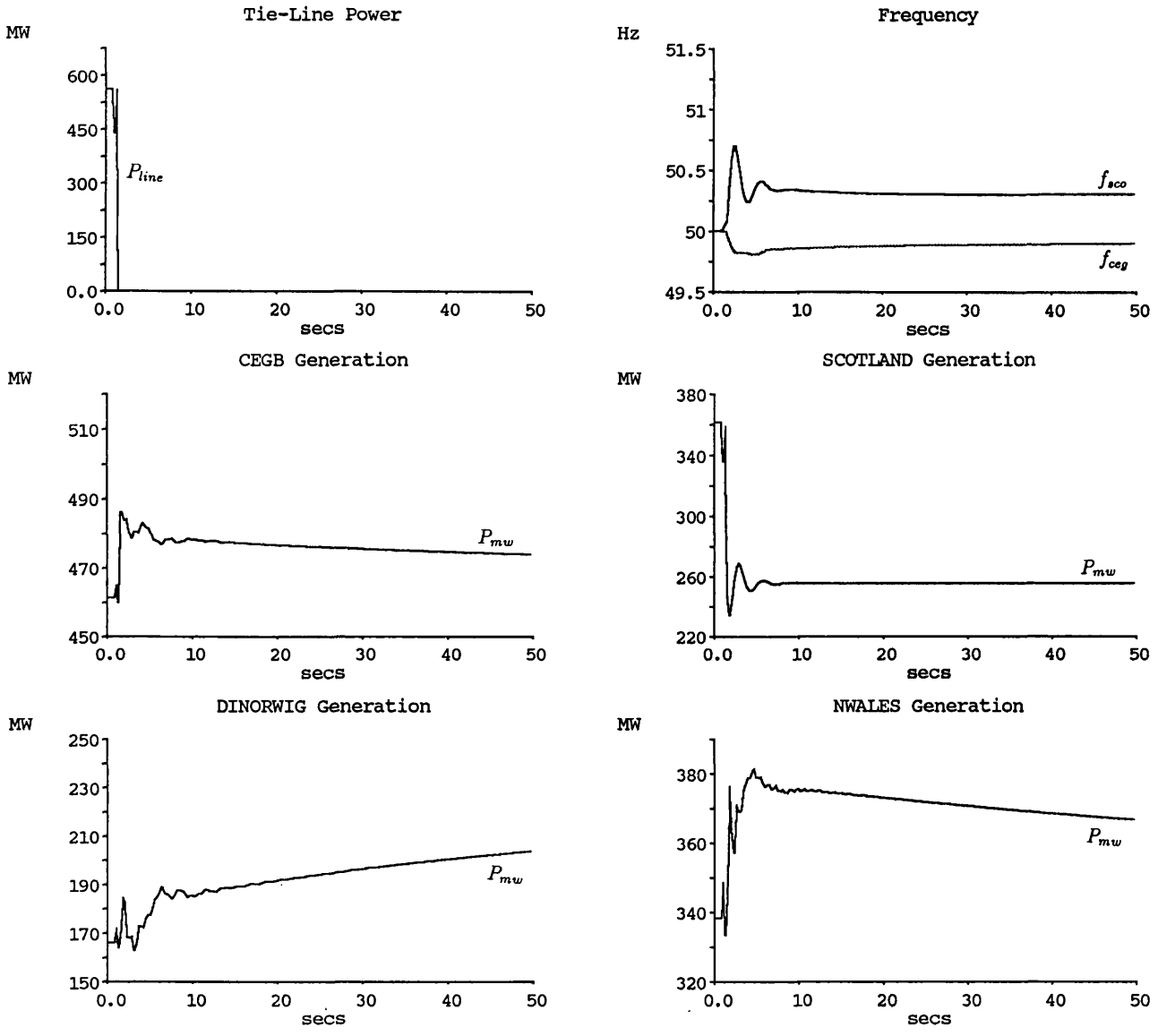

Figure 6.14: (a) 4 m'c Scotland-England Split (Run 4)

Fig. 14(b)

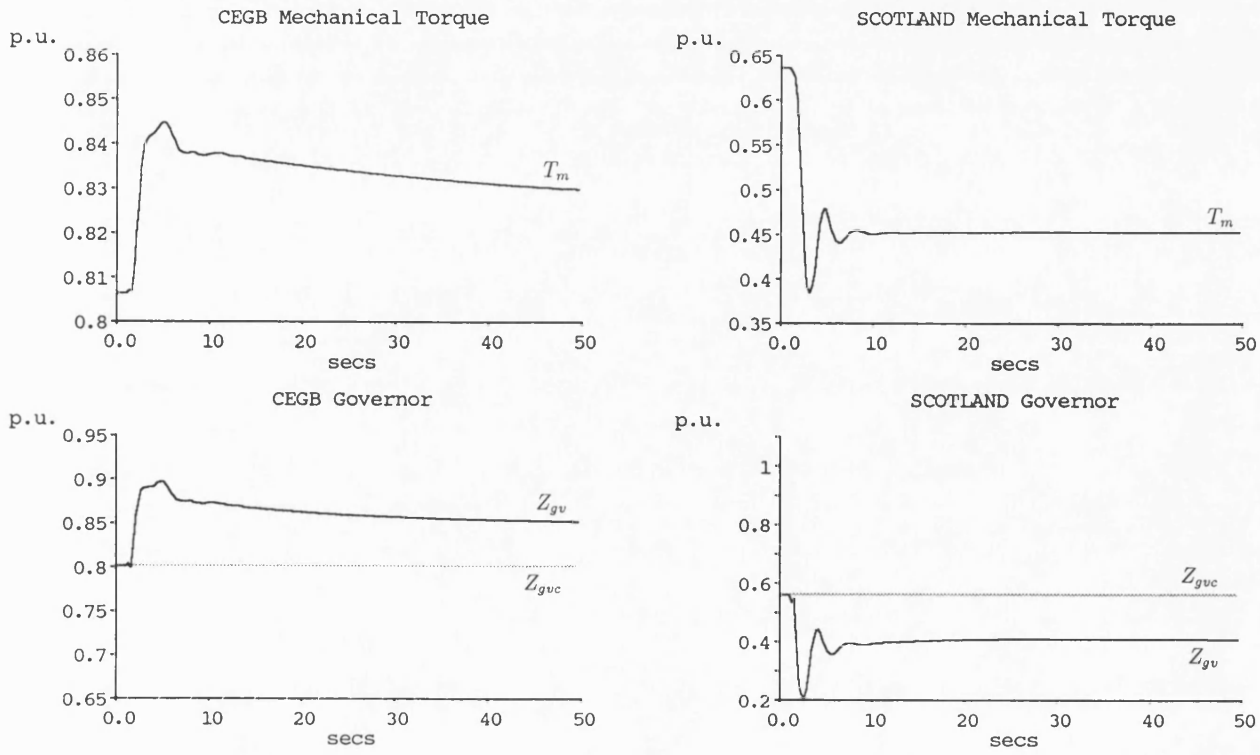

Figure 6.14: (b) 4 m'c Scotland-England Split (Run 4)

4 Kgb.14.(a)

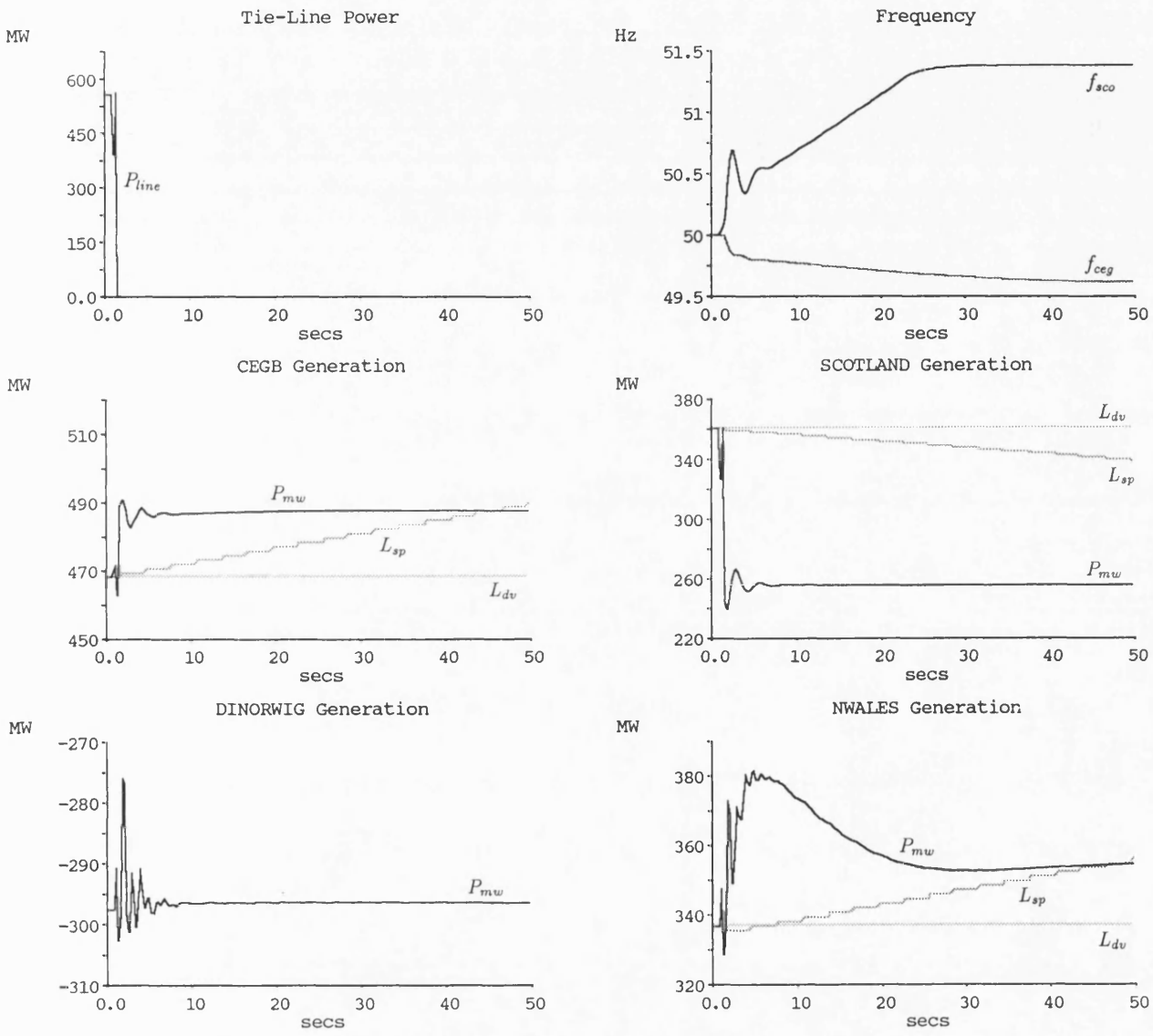

Figure 6.15: (a) 4 m'c Scotland-England Split (Run 5)

Fig. 15(b)

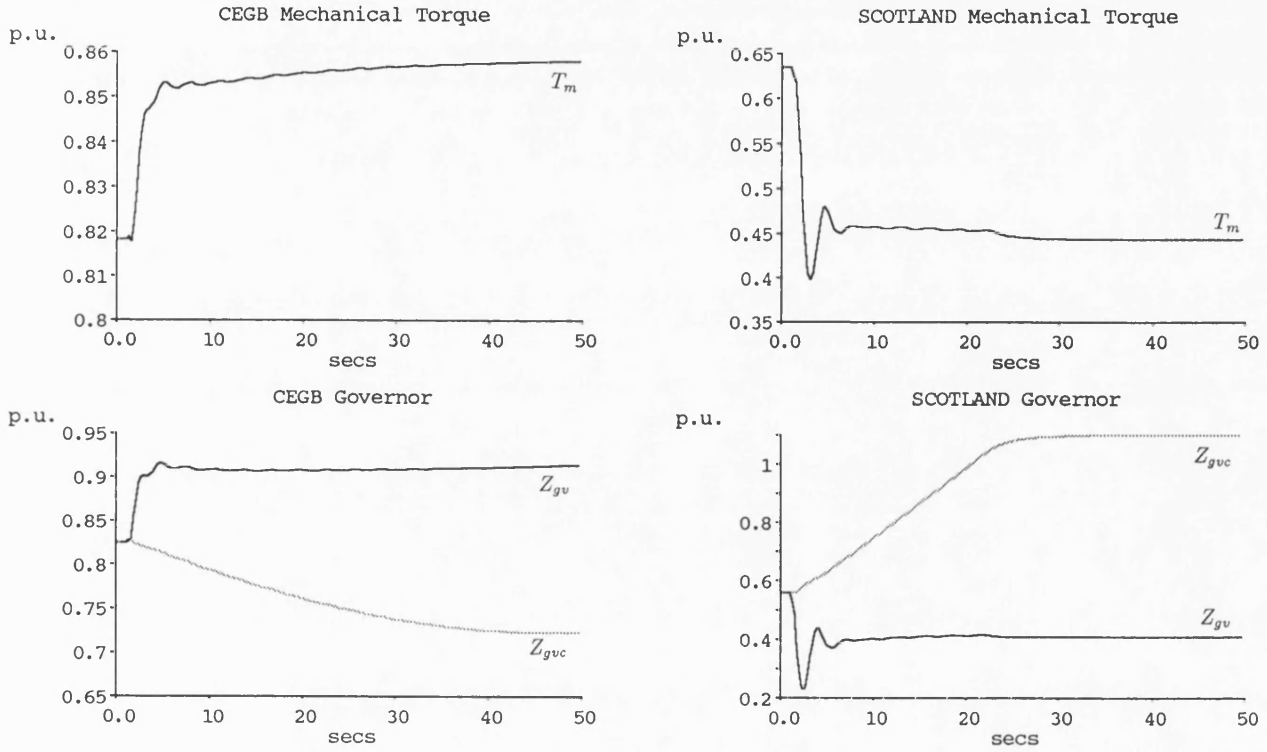

Figure 6.15: (b) 4 m'c Scotland-England Split (Run 5)

Fig. 15(a)

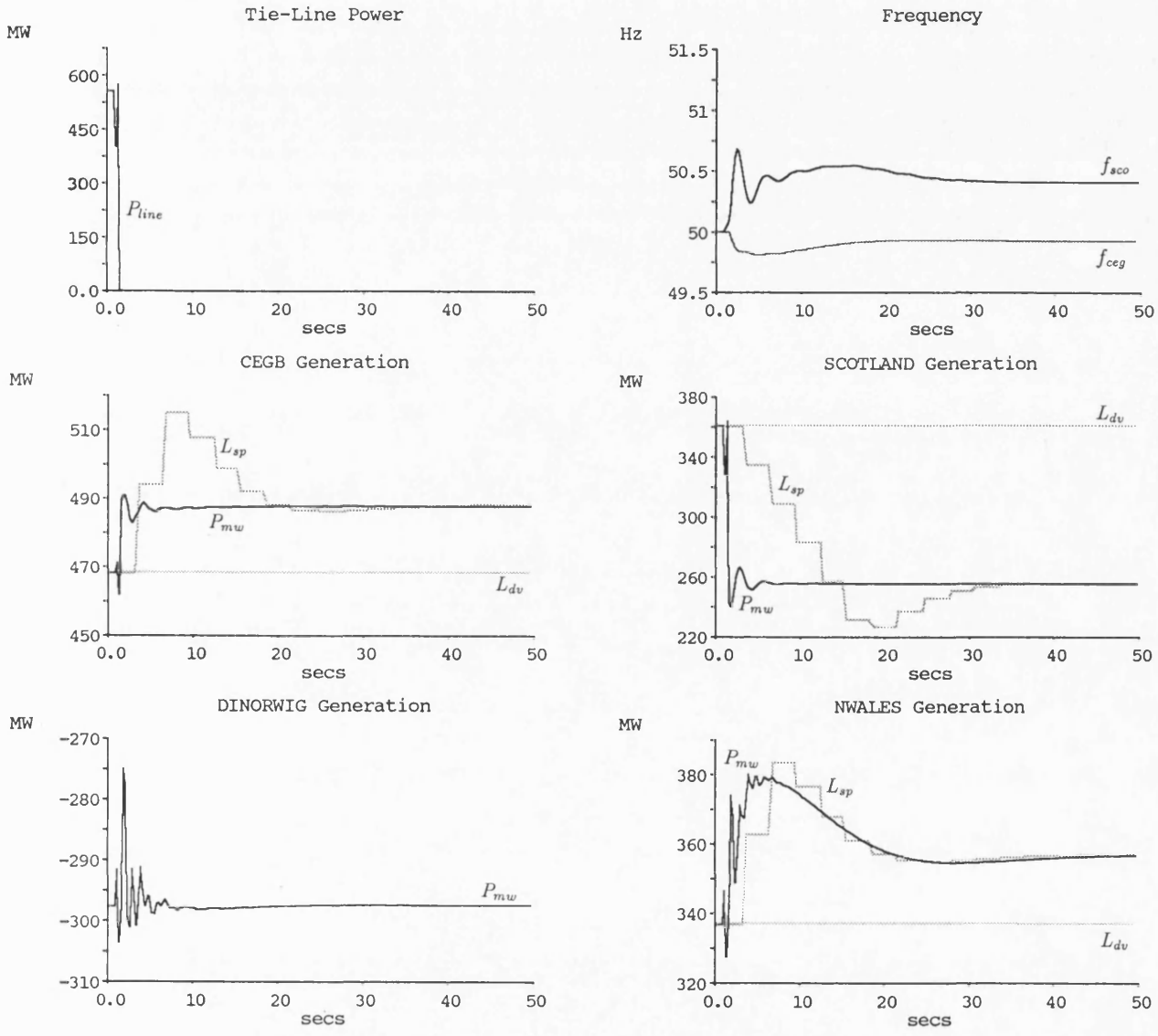

Figure 6.16: (a) 4 m'c Scotland-England Split (Run 6)

Fig 6.16(b)

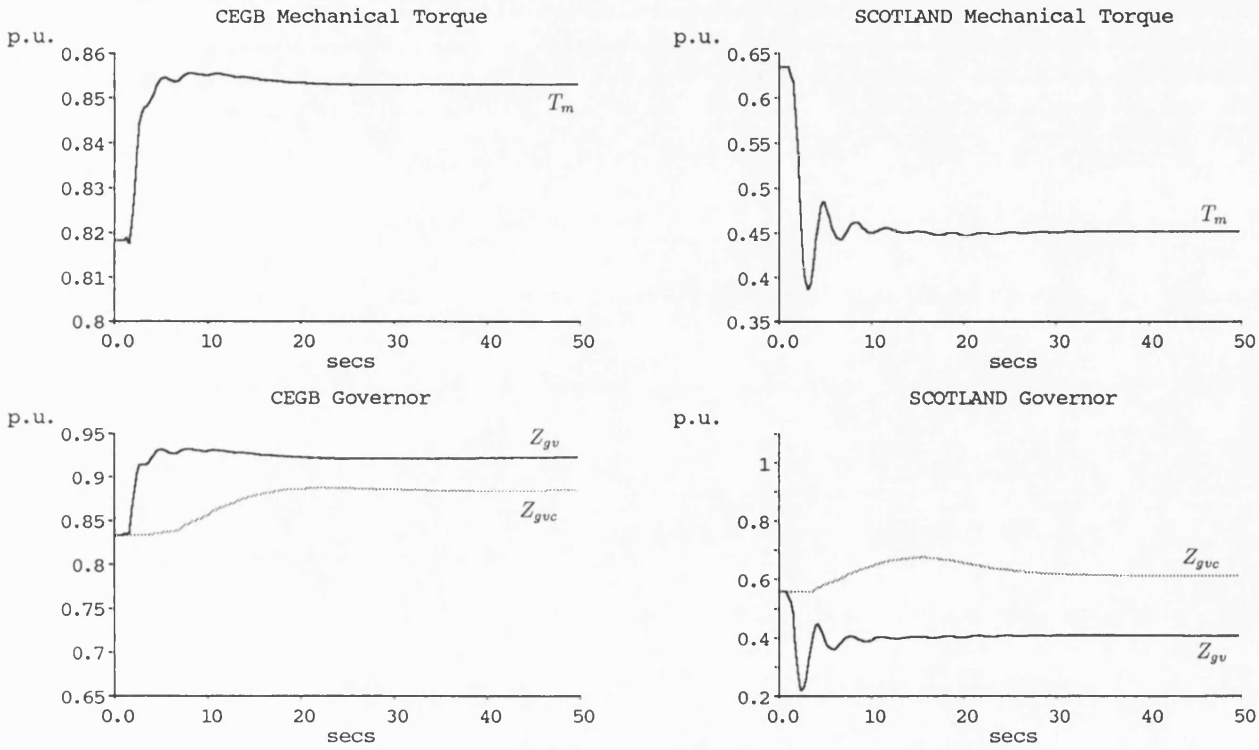

Figure 6.16: (b) 4 m'c Scotland-England Split (Run 6)

Fig 6.16(a)

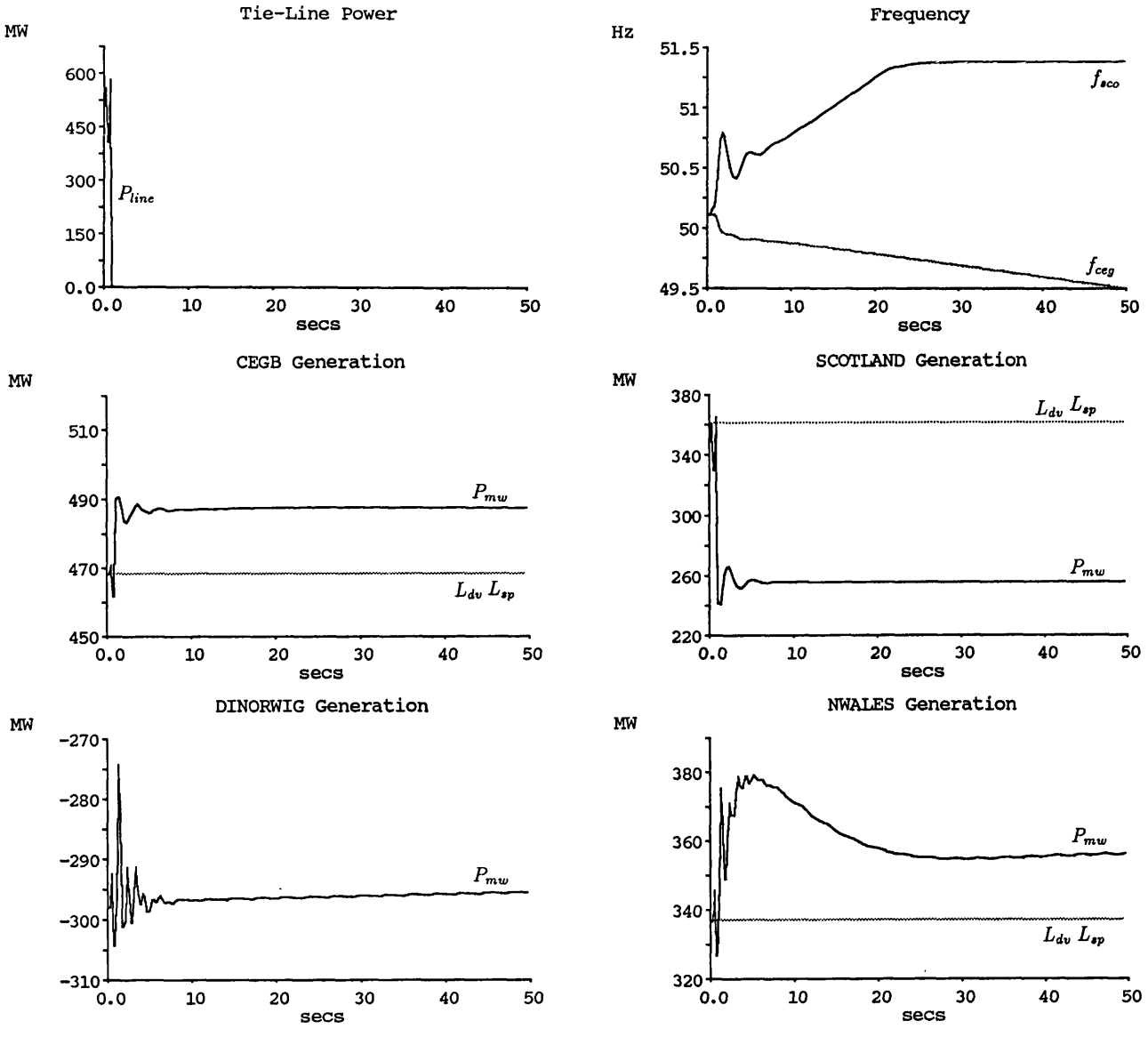

Figure 6.17: (a) 4 m'c Scotland-England Split (Run 7)

fig 6.17(b)

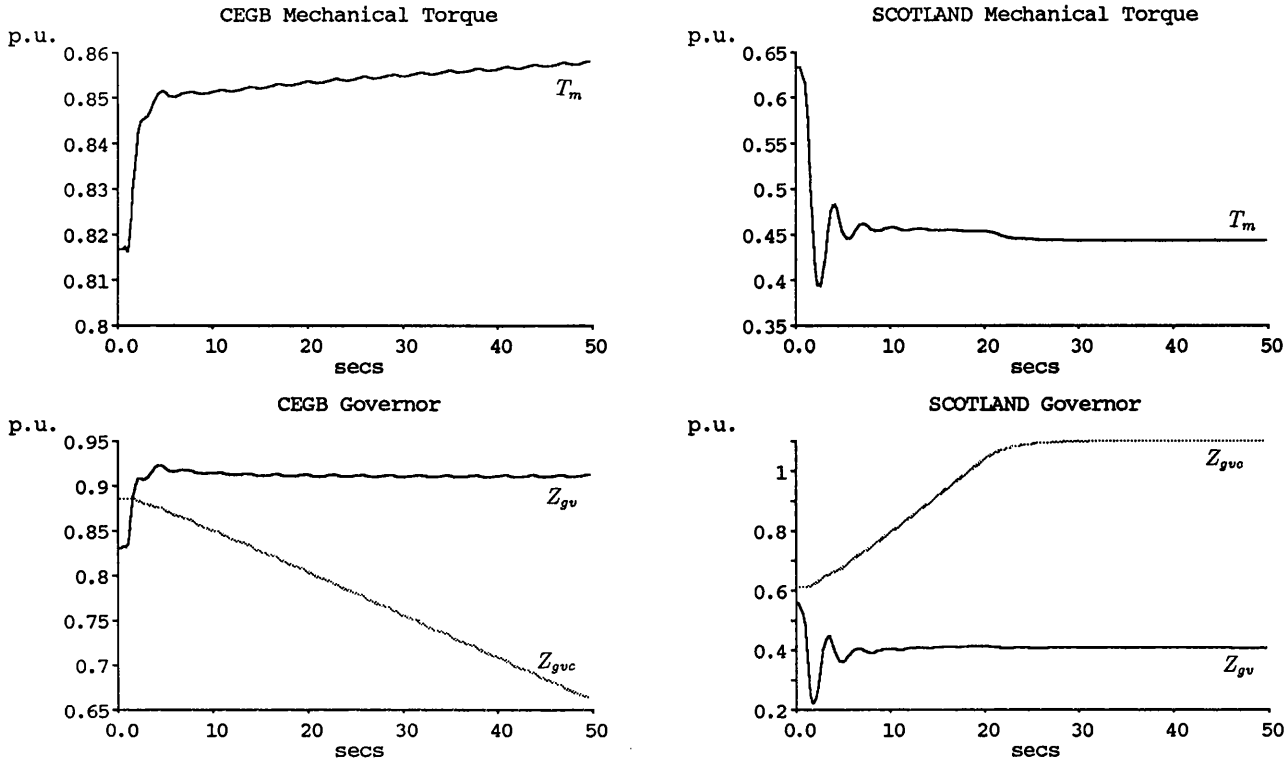

Figure 6.17: (b) 4 m'c Scotland-England Split (Run 7)

Fig. 17(a)

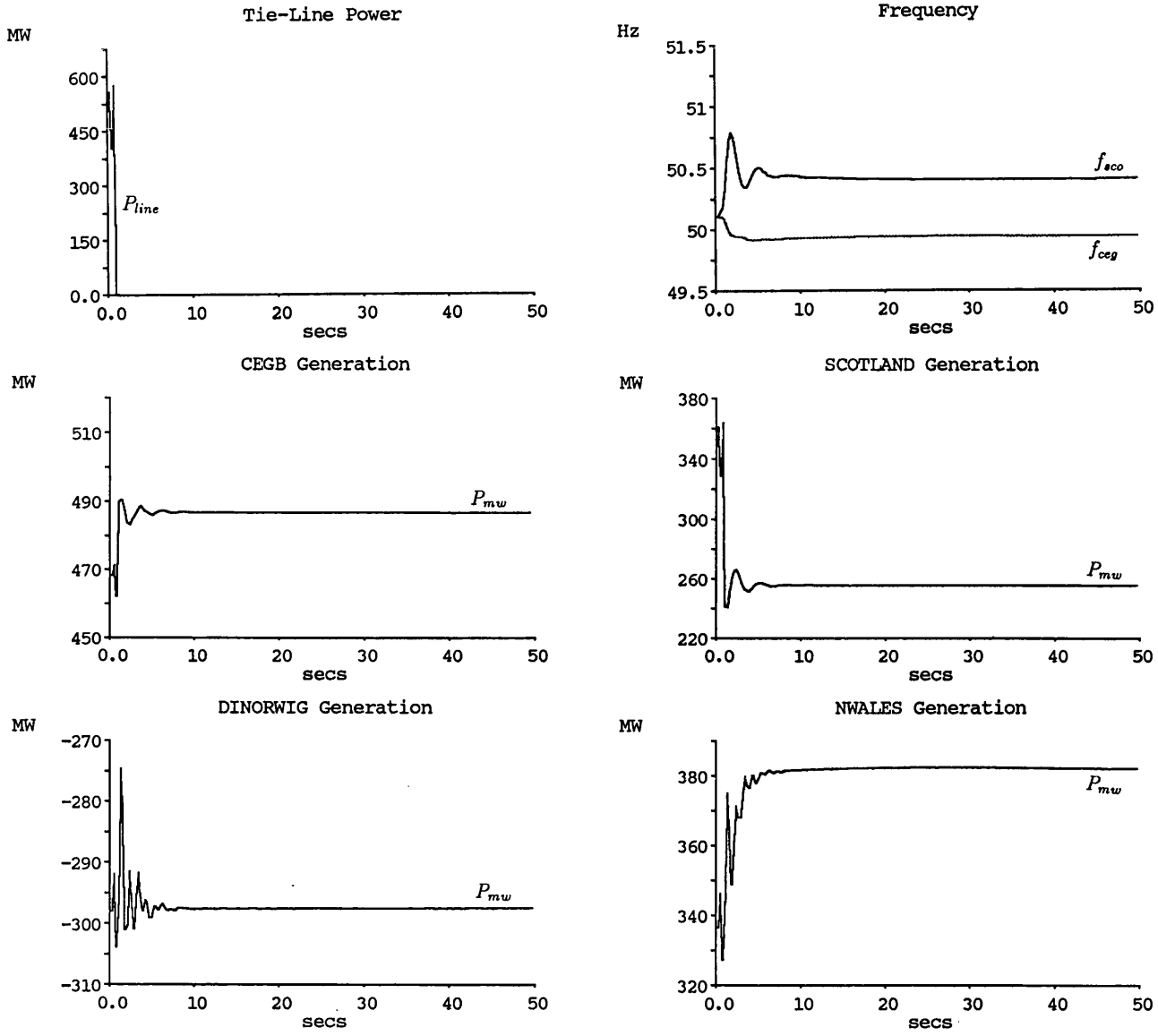

Figure 6.18: (a) 4 m'c Scotland-England Split (Run 8)

8 Fig 6.18(b)

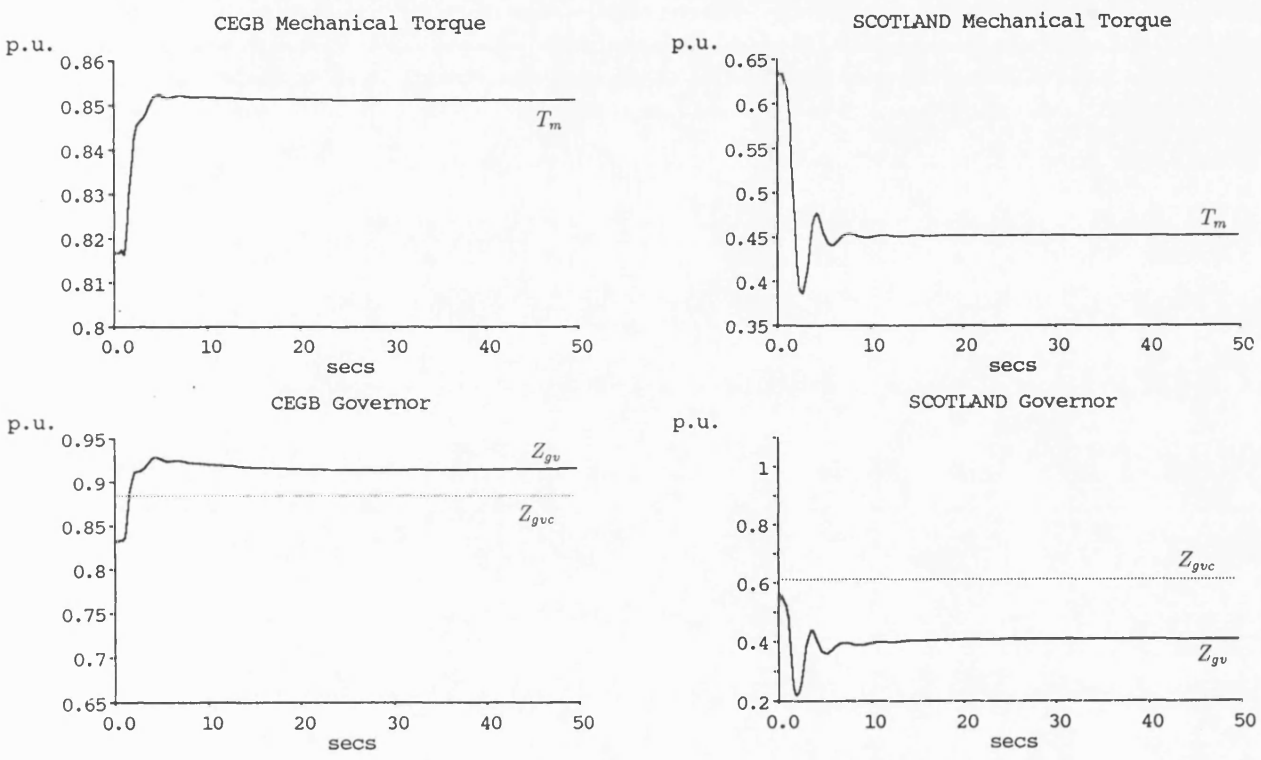

Figure 6.18: (b) 4 m'c Scotland-England Split (Run 8)

Fig. 12(a)

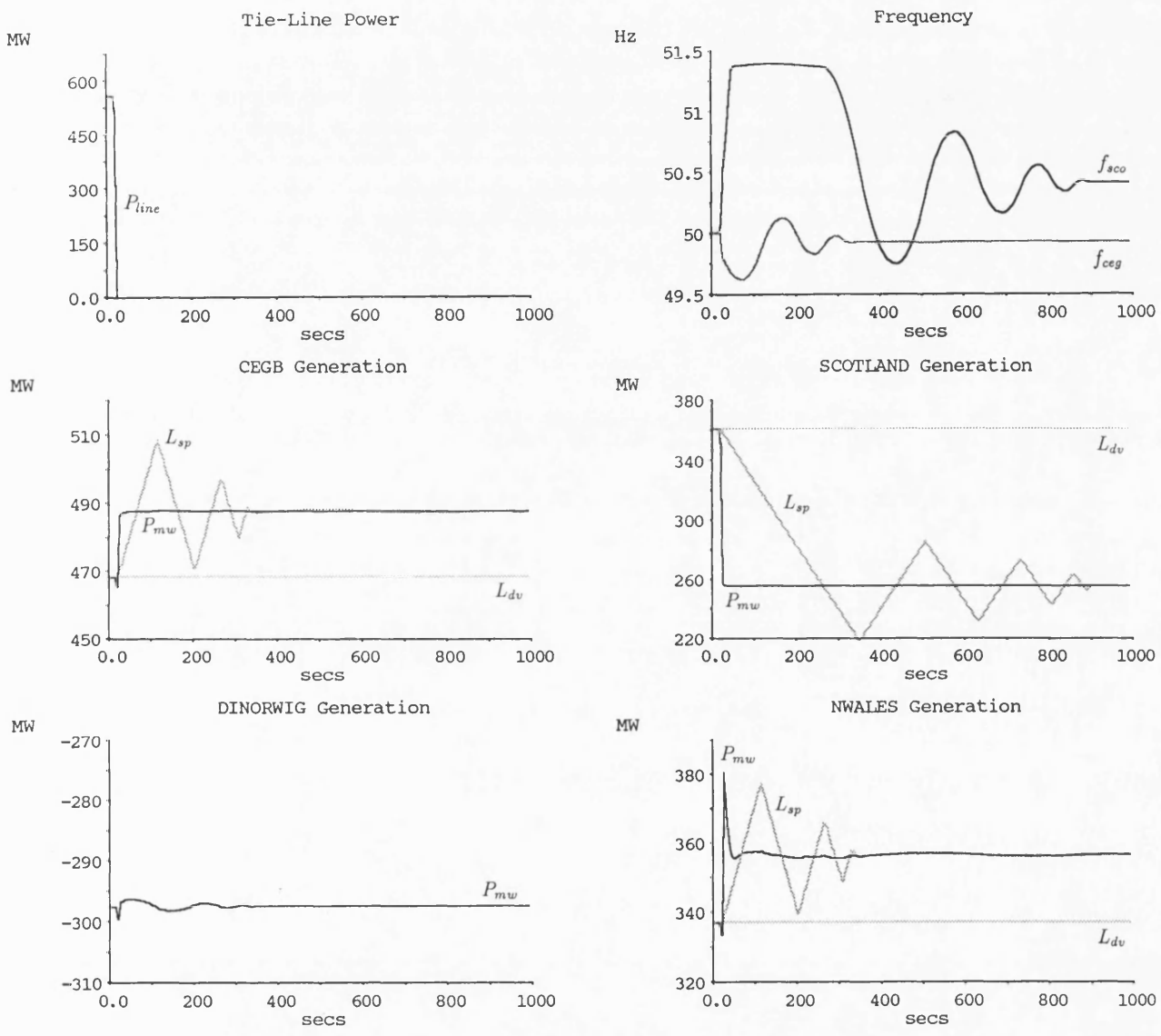

Figure 6.19: (a) 4 m'c Scotland-England Split (Run 5a)

Safig6.19(b)

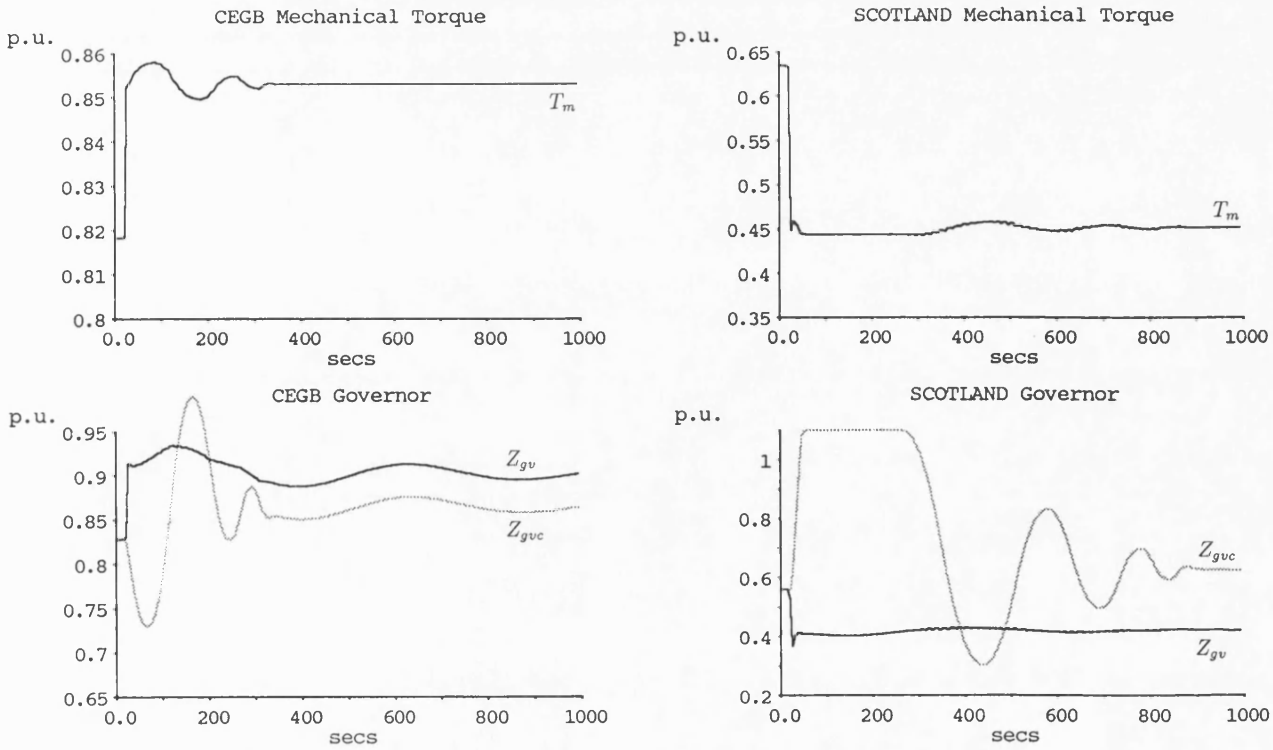

Figure 6.19: (b) 4 m'c Scotland-England Split (Run 5a)

5a Fig 6. 19(a)

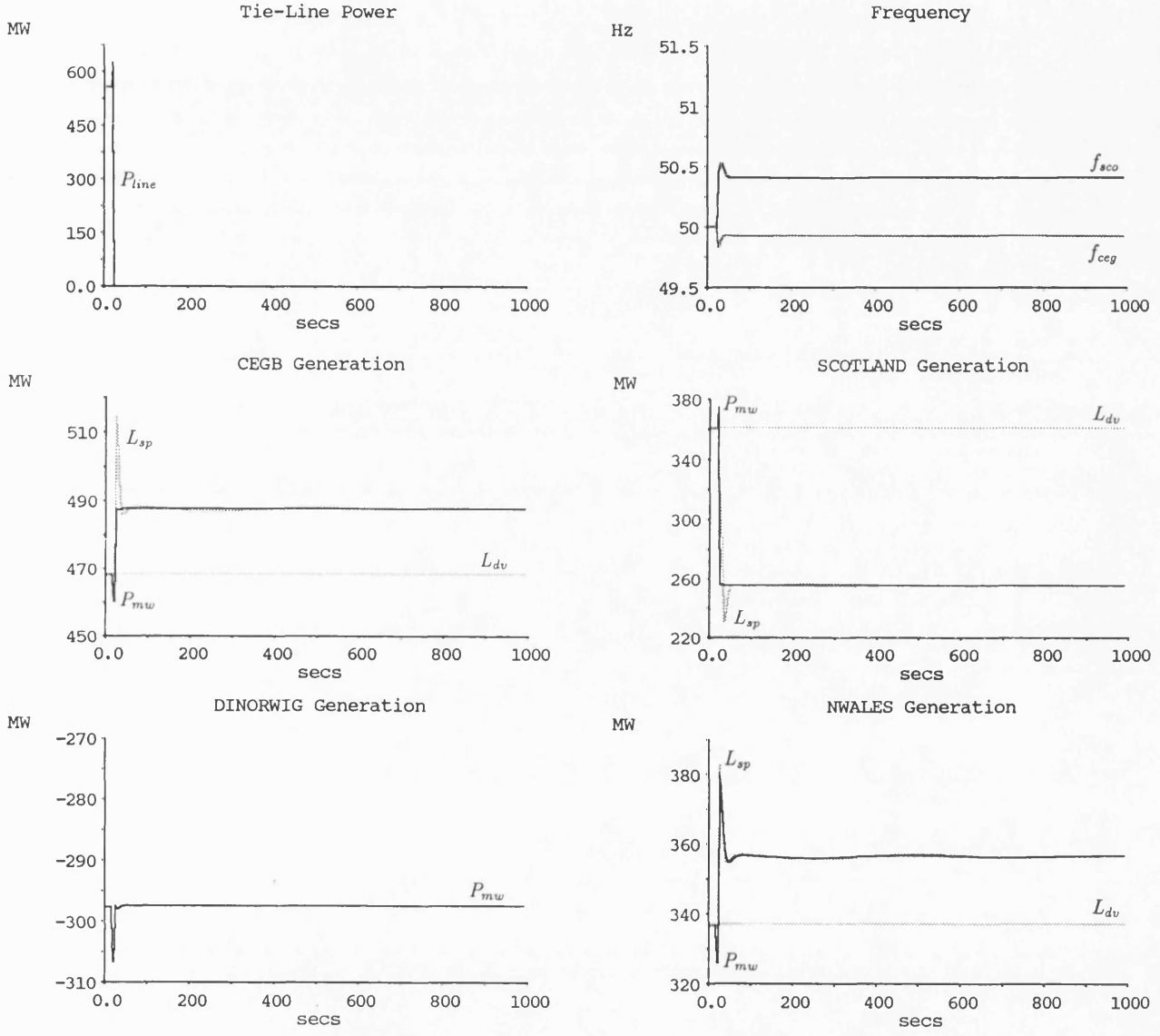

Figure 6.20: (a) 4 m'c Scotland-England Split (Run 6a)

6a fig 6.20(b)

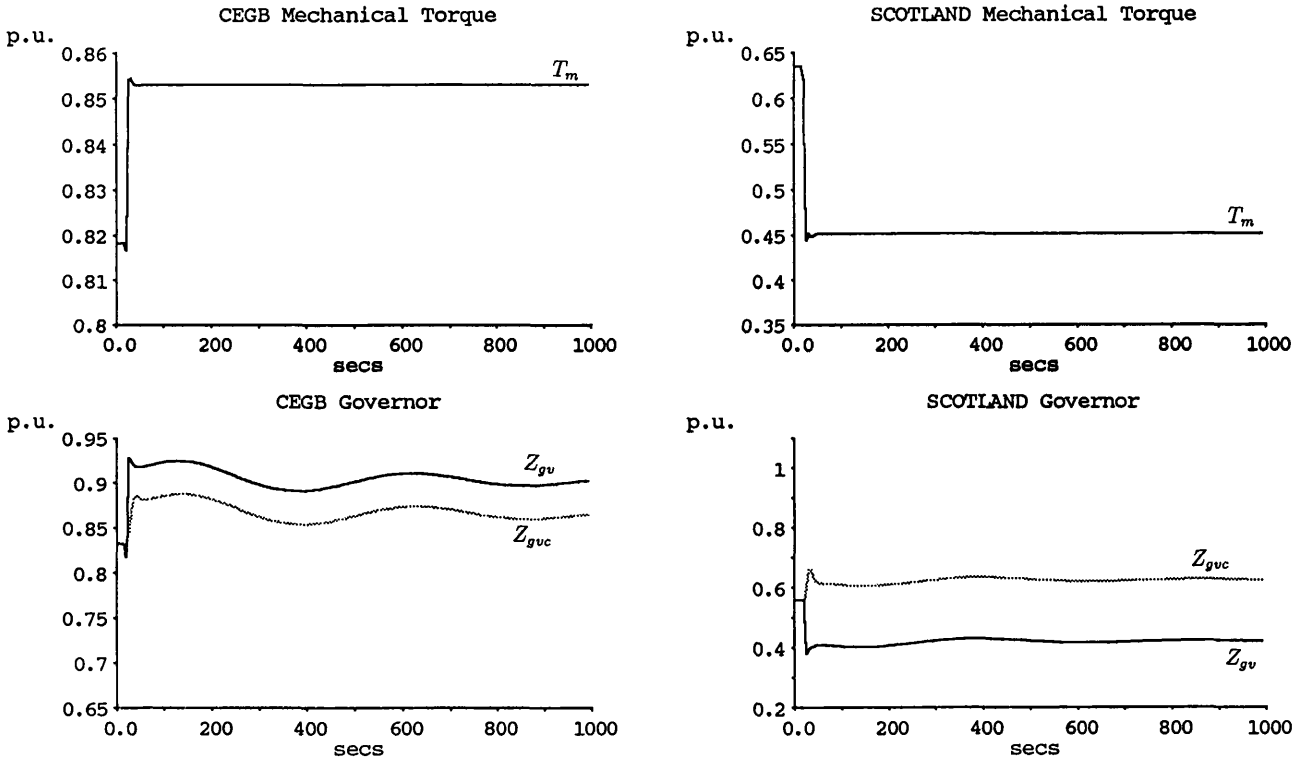

Figure 6.20: (b) 4 m'c Scotland-England Split (Run 6a)

Eg 6.20(a)

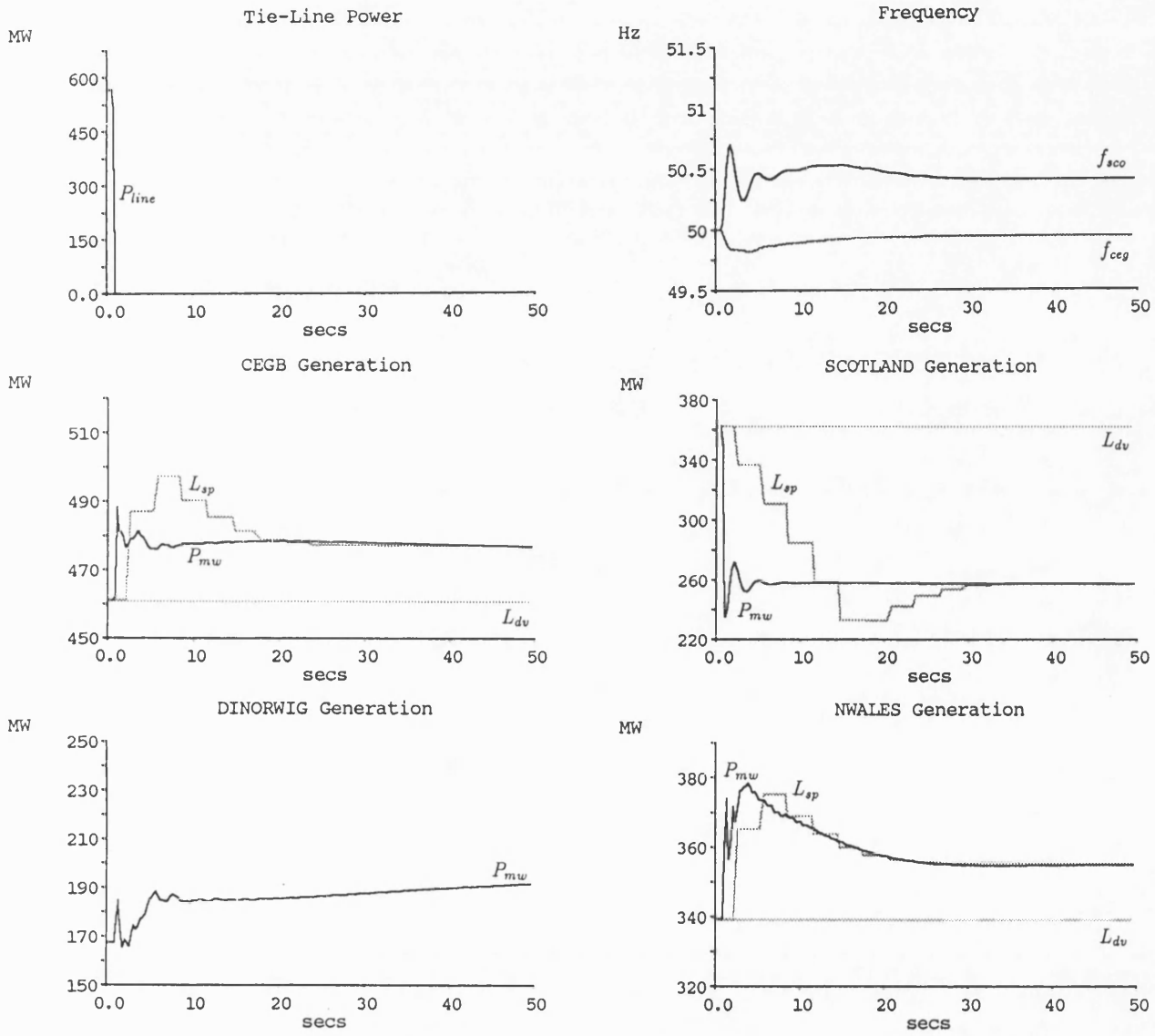

Figure 6.21: (a) 4 m'c Scotland-England Split (Run 2l)

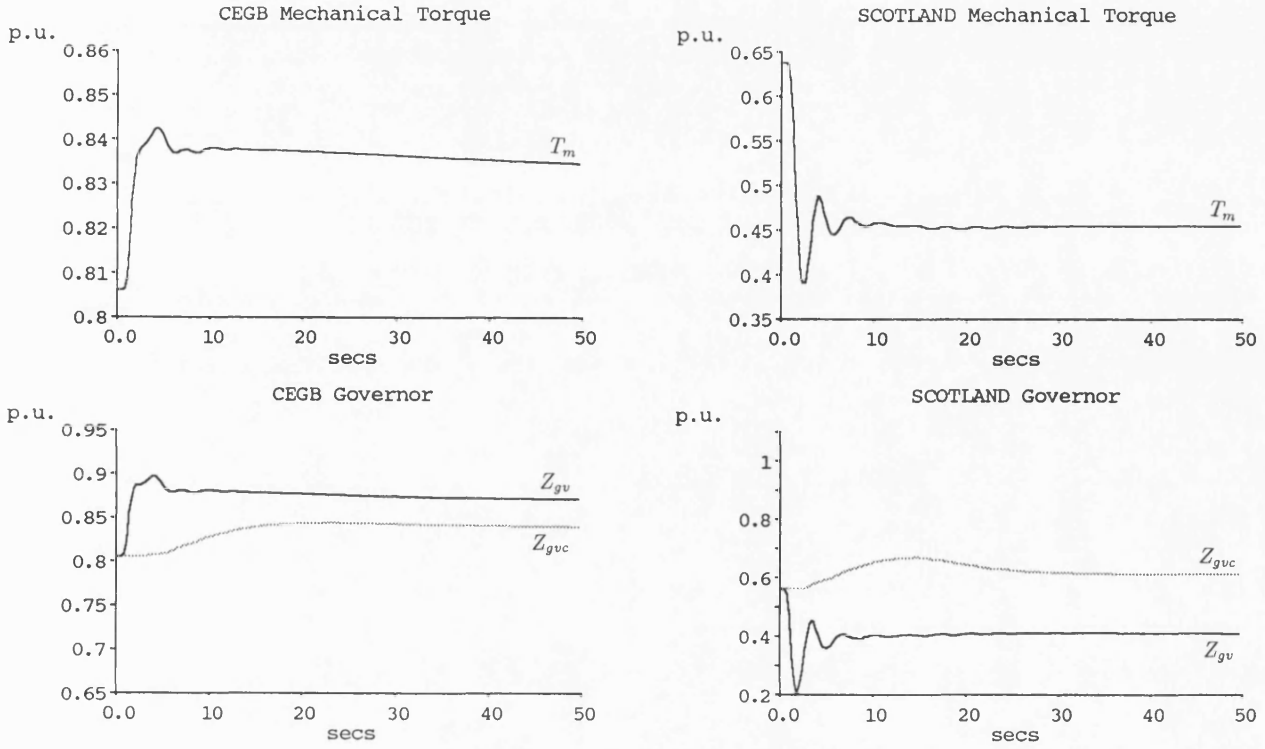

Figure 6.21: (b) 4 m'c Scotland-England Split (Run 2l)

24 Fig 6.21(a)

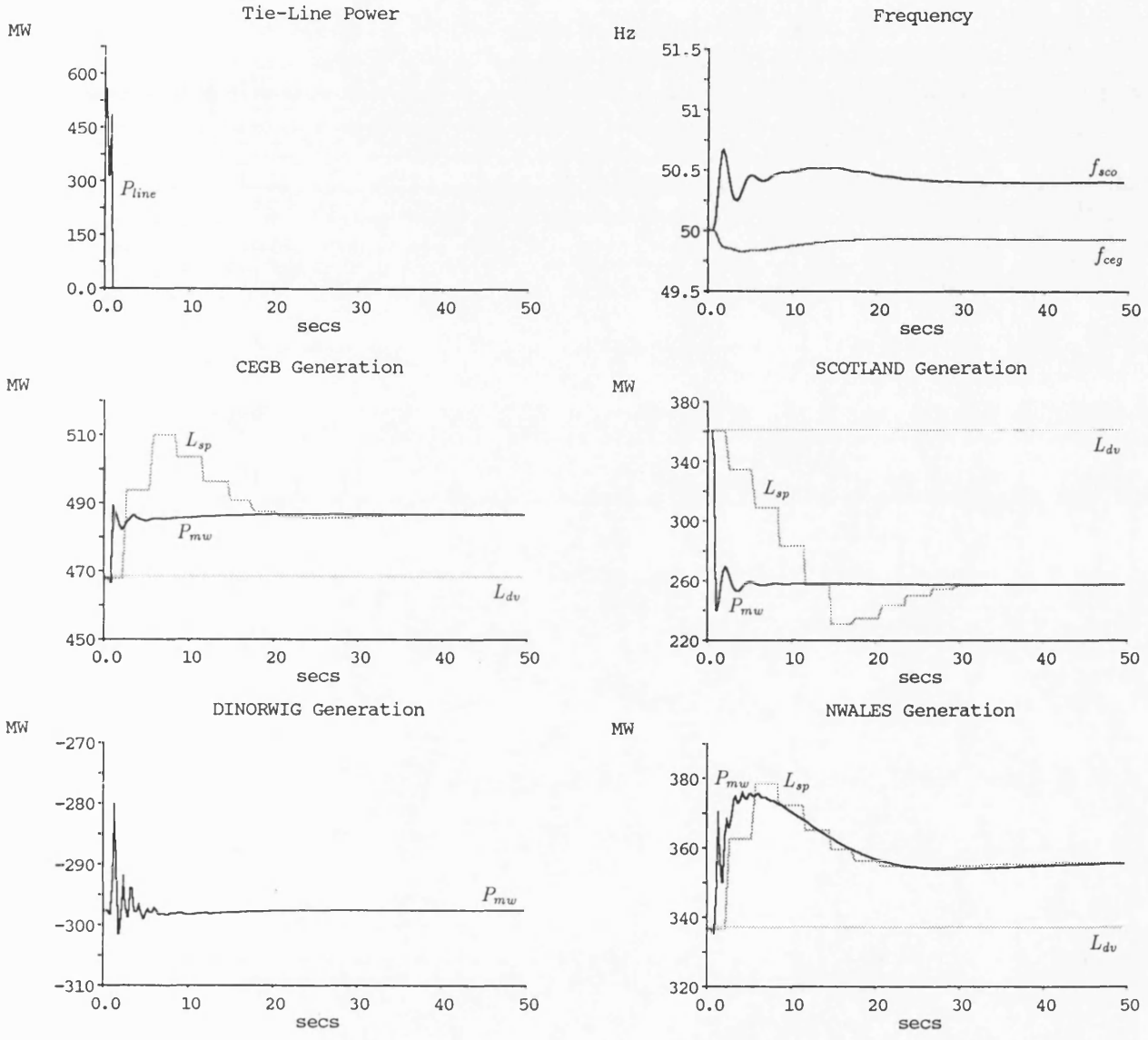

Figure 6.22: (a) 4 m'c Scotland-England Split (Run 6l)

6c Pg 6.22(a)

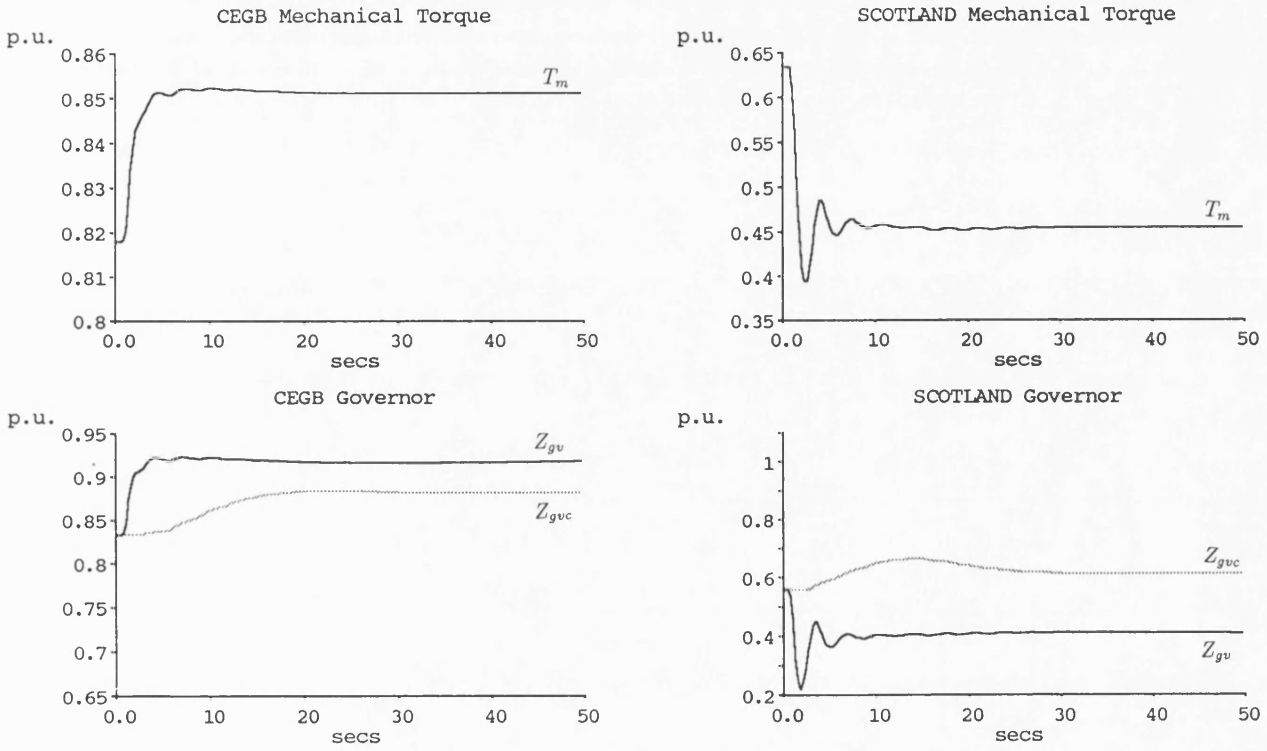

Figure 6.22: (b) 4 m'c Scotland-England Split (Run 6l)

Fig 6.22(a)

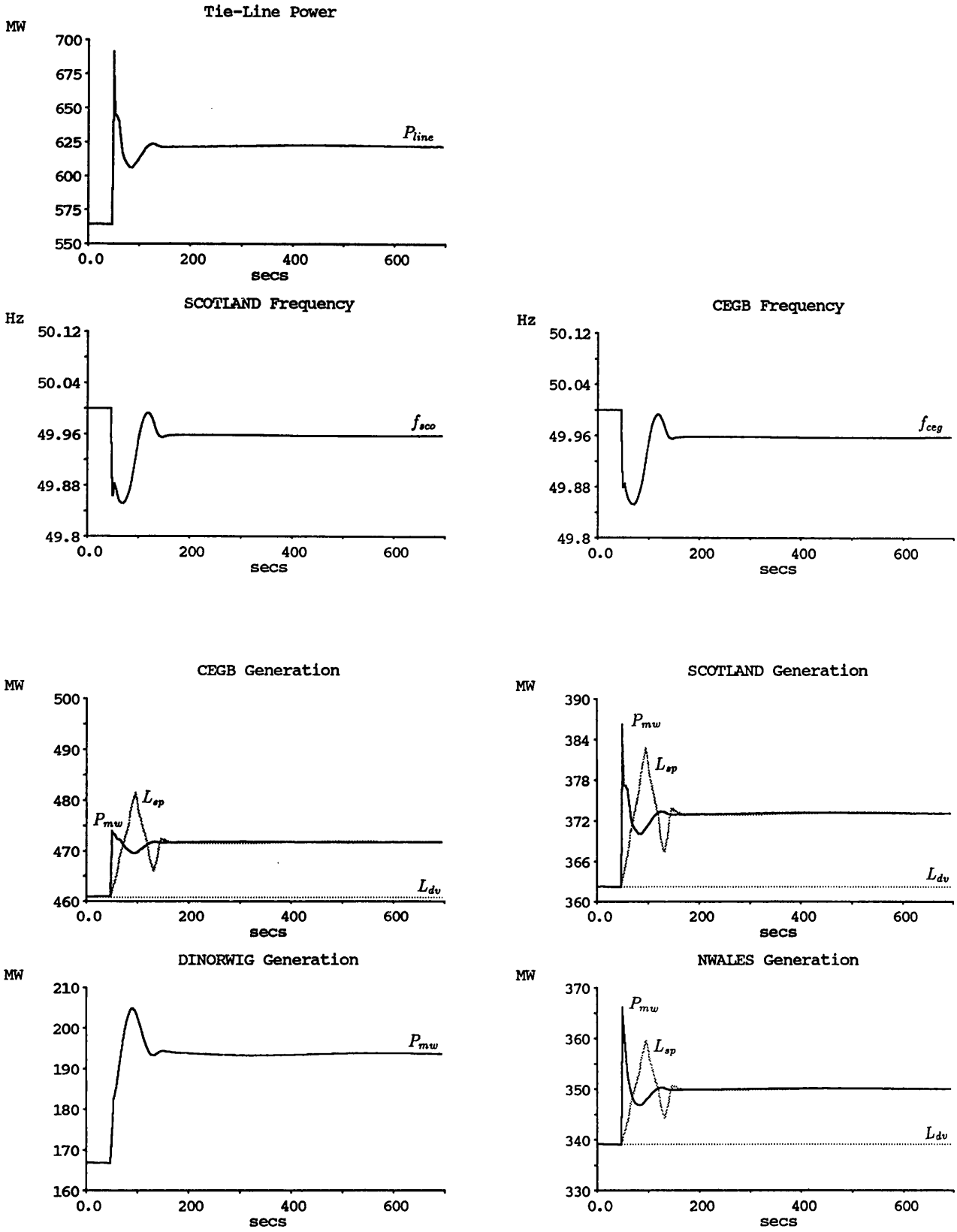

Figure 6.23: (a) 4 m'c Step Load Increase busbar CEGB4 (Run 9)

9 Fig 6.23(a)

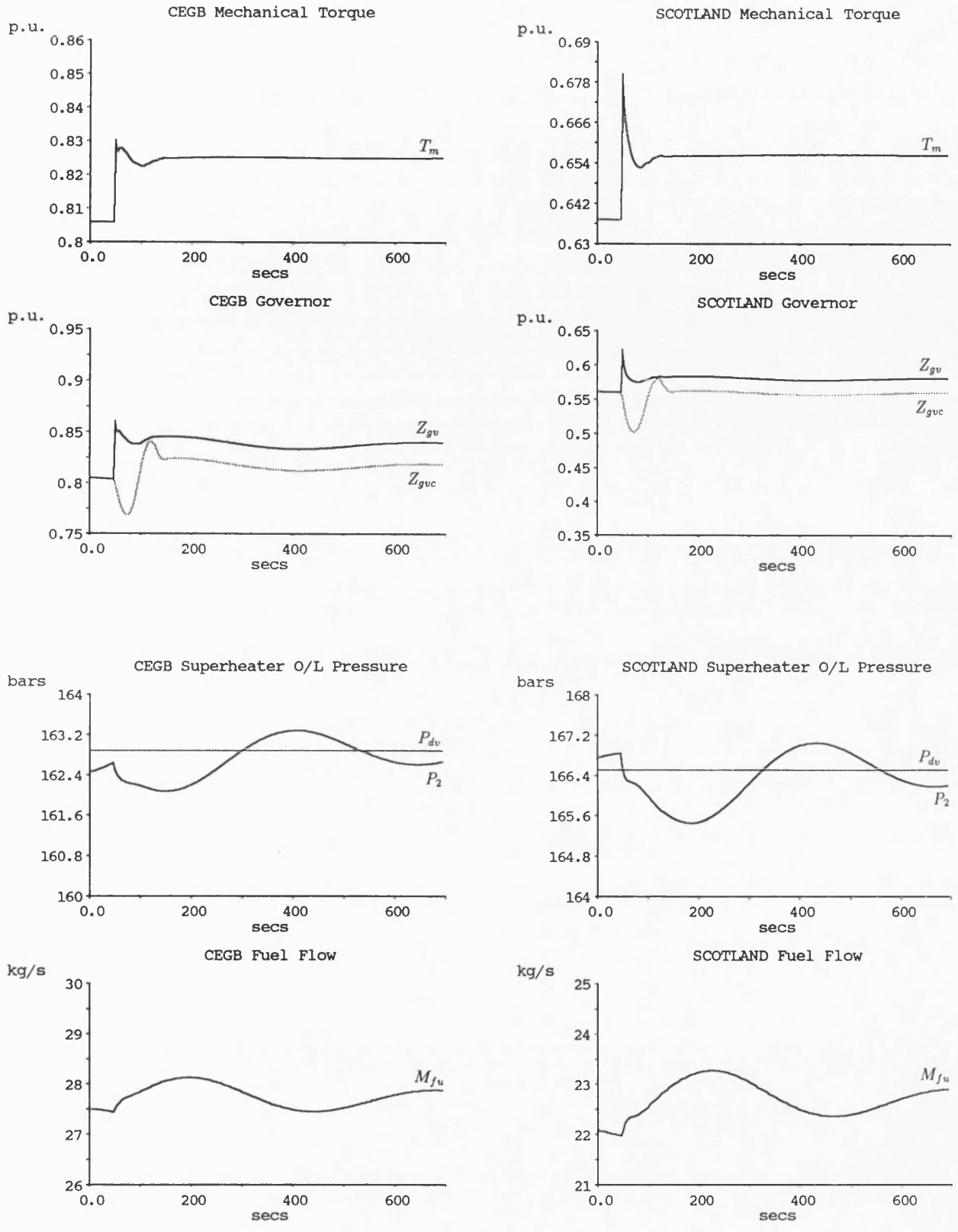

Figure 6.23: (b) 4 m'c Step Load Increase busbar CEGB4 (Run 9)

Fig 6.23(b)

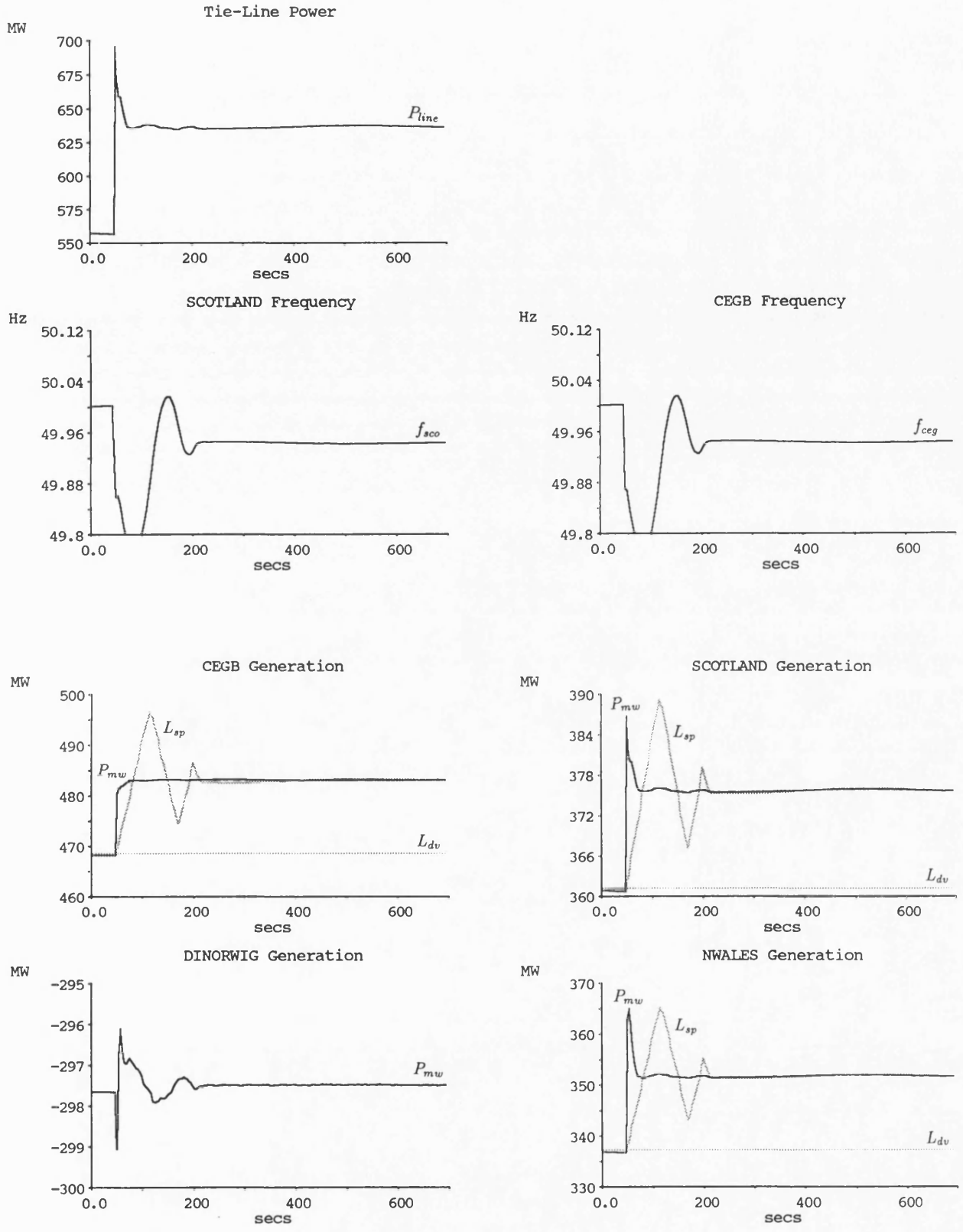

Figure 6.24: (a) 4 m'c Step Load Increase busbar CEGB4 (Run 10)

(0 fig 6.24(a)

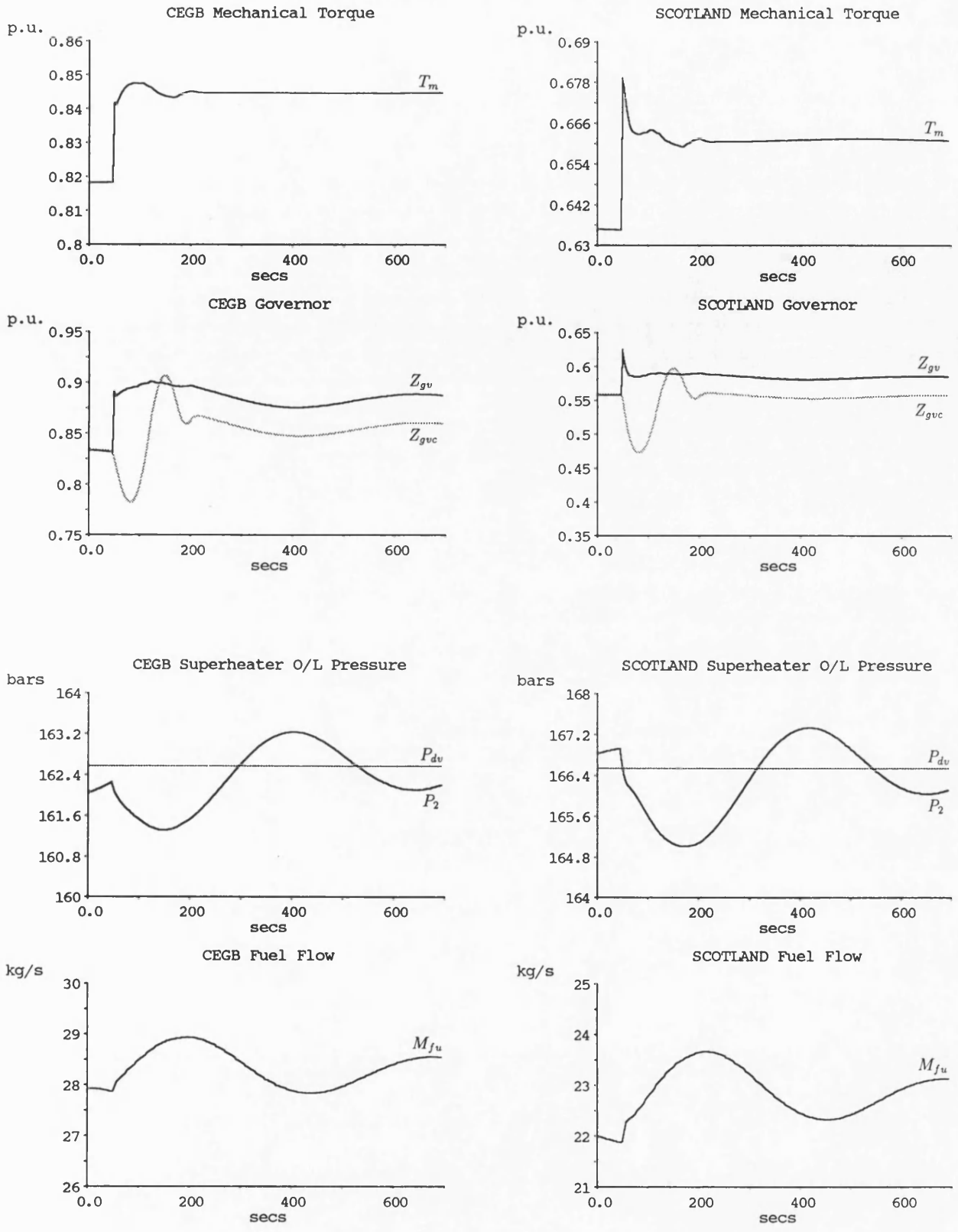

Figure 6.24: (b) 4 m'c Step Load Increase busbar CEGB4 (Run 10)

10 fig 6.24(b)

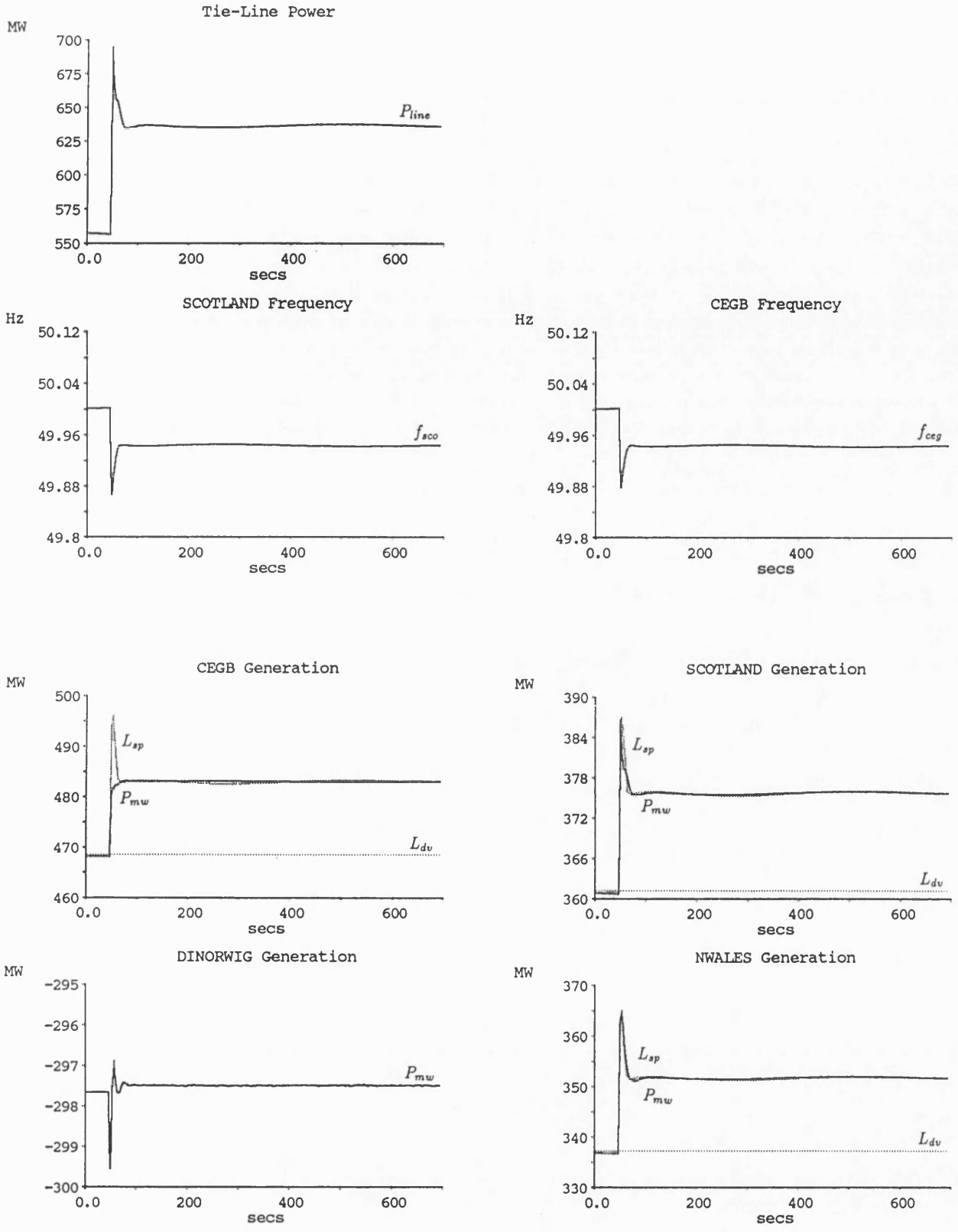

Figure 6.25: (a) 4 m'c Step Load Increase busbar CEGB4 (Run 11)

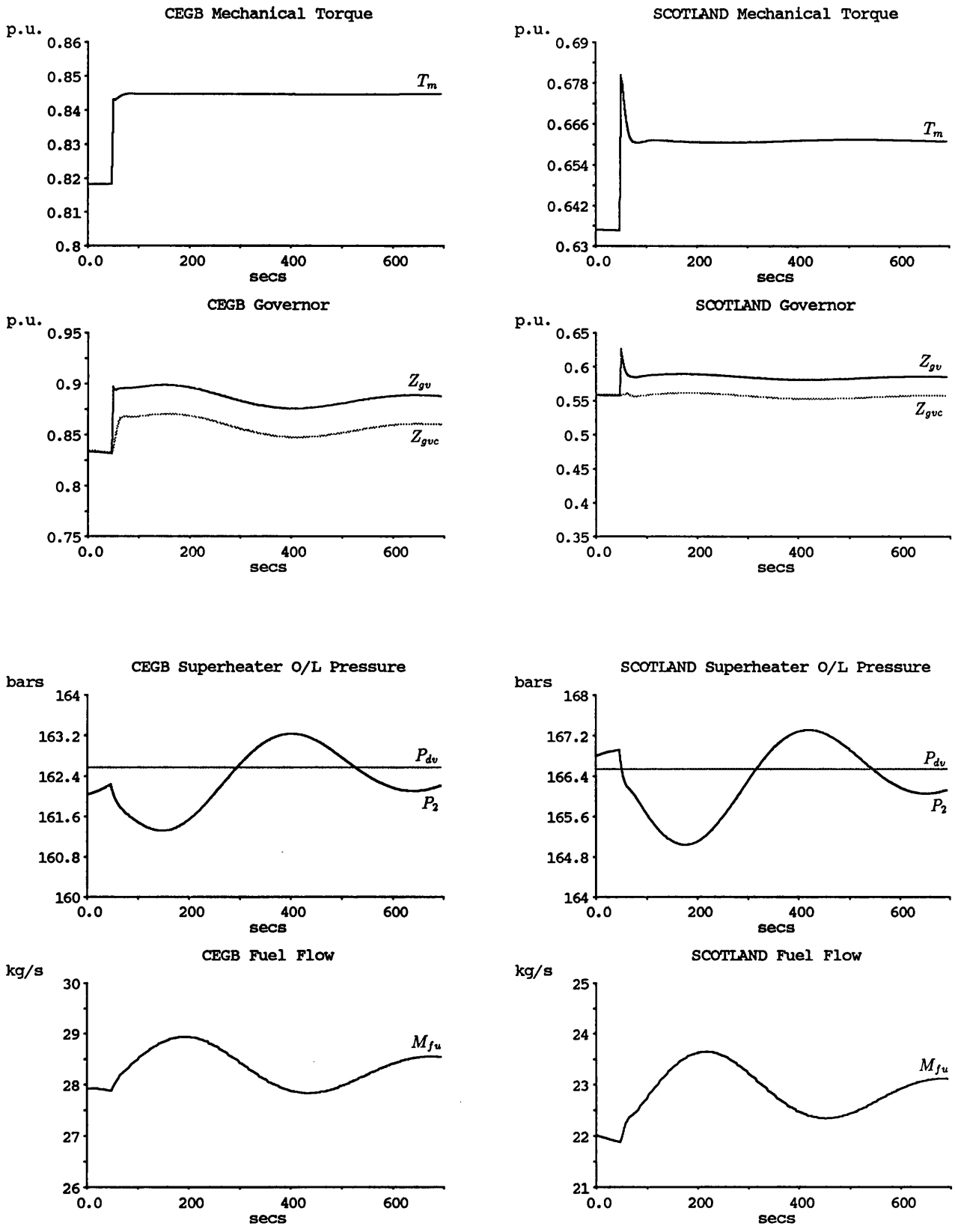

Figure 6.25: (b) 4 m'c Step Load Increase busbar CEGB4 (Run 11)

11 Fig 6.25(b)

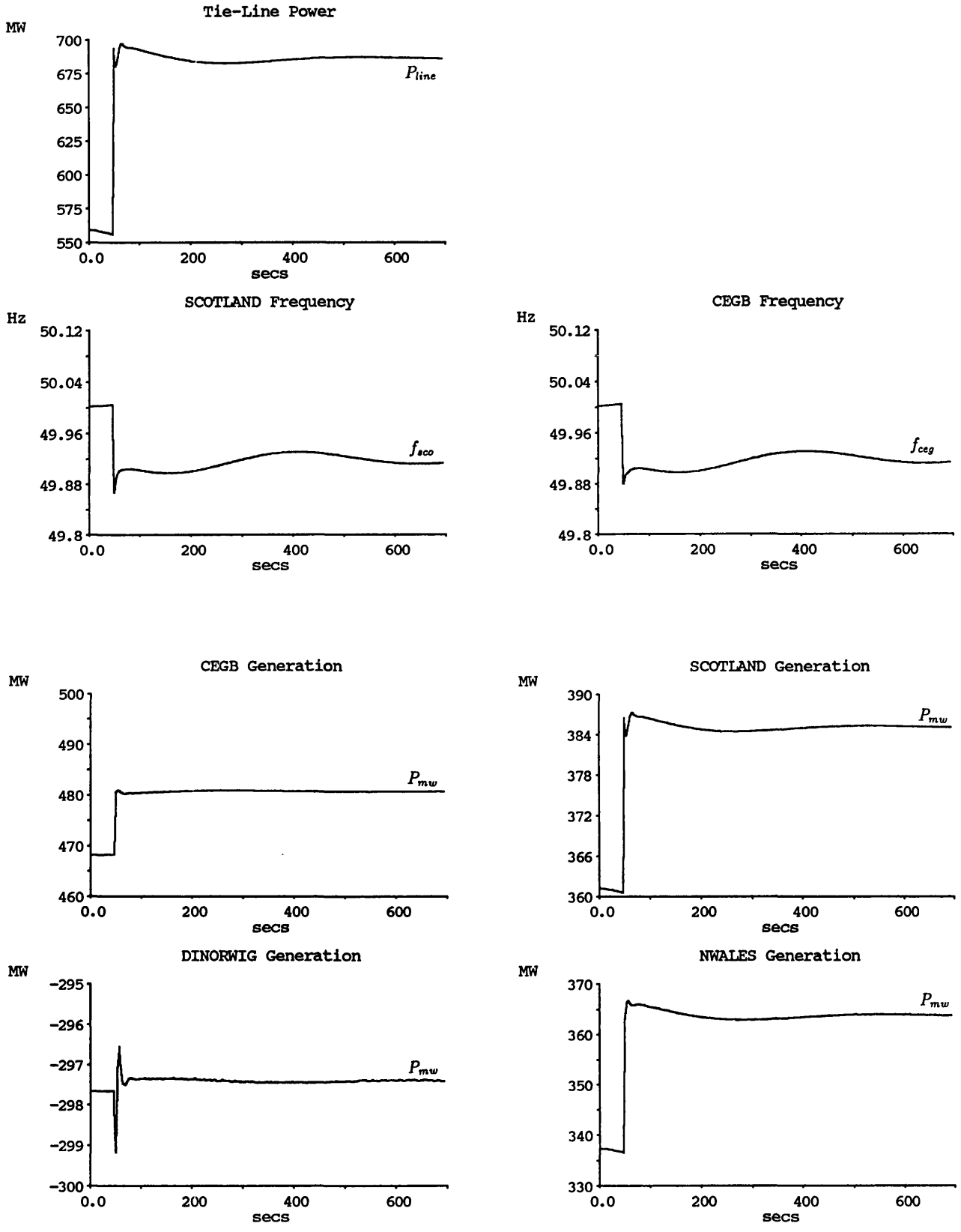

Figure 6.26: (a) 4 m'c Step Load Increase busbar CEGB4 (Run 12)

12 Fig. 2.4(a)

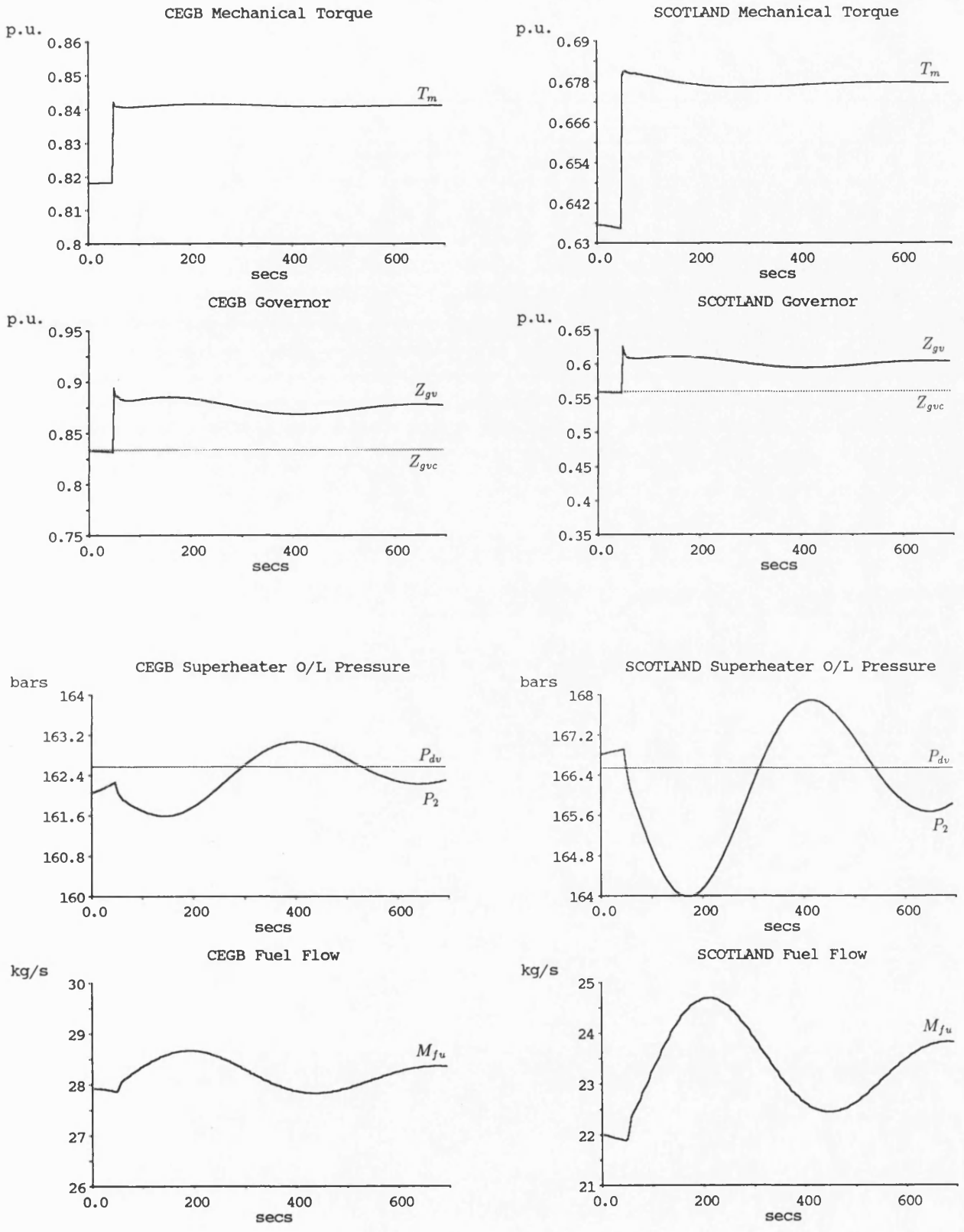

Figure 6.26: (b) 4 m'c Step Load Increase busbar CEGB4 (Run 12)

Fig 6.26(b)

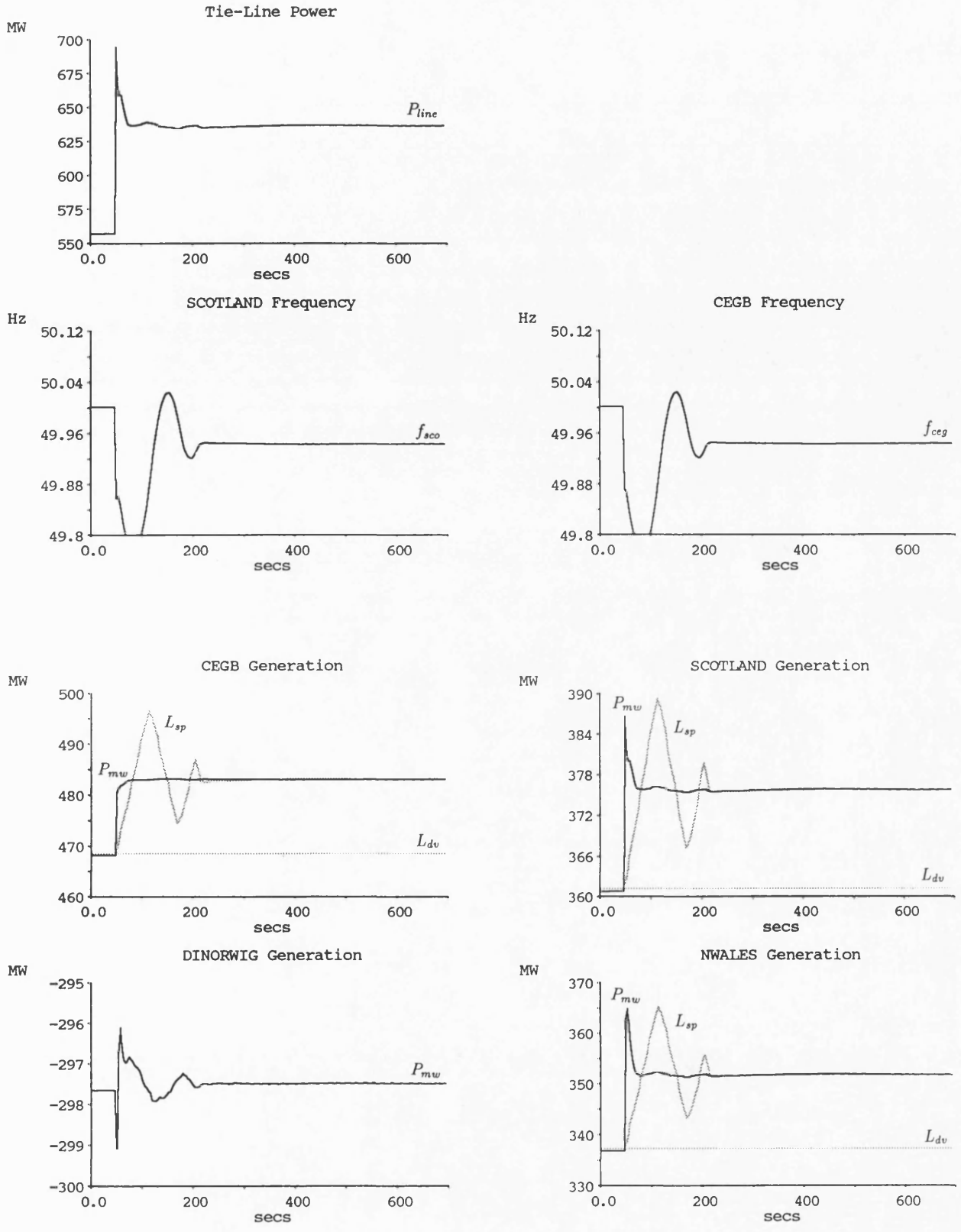

Figure 6.27: (a) 4 m'c Step Load Increase busbar CEGB4 (Run 13)

13 Fig 6.27(a)

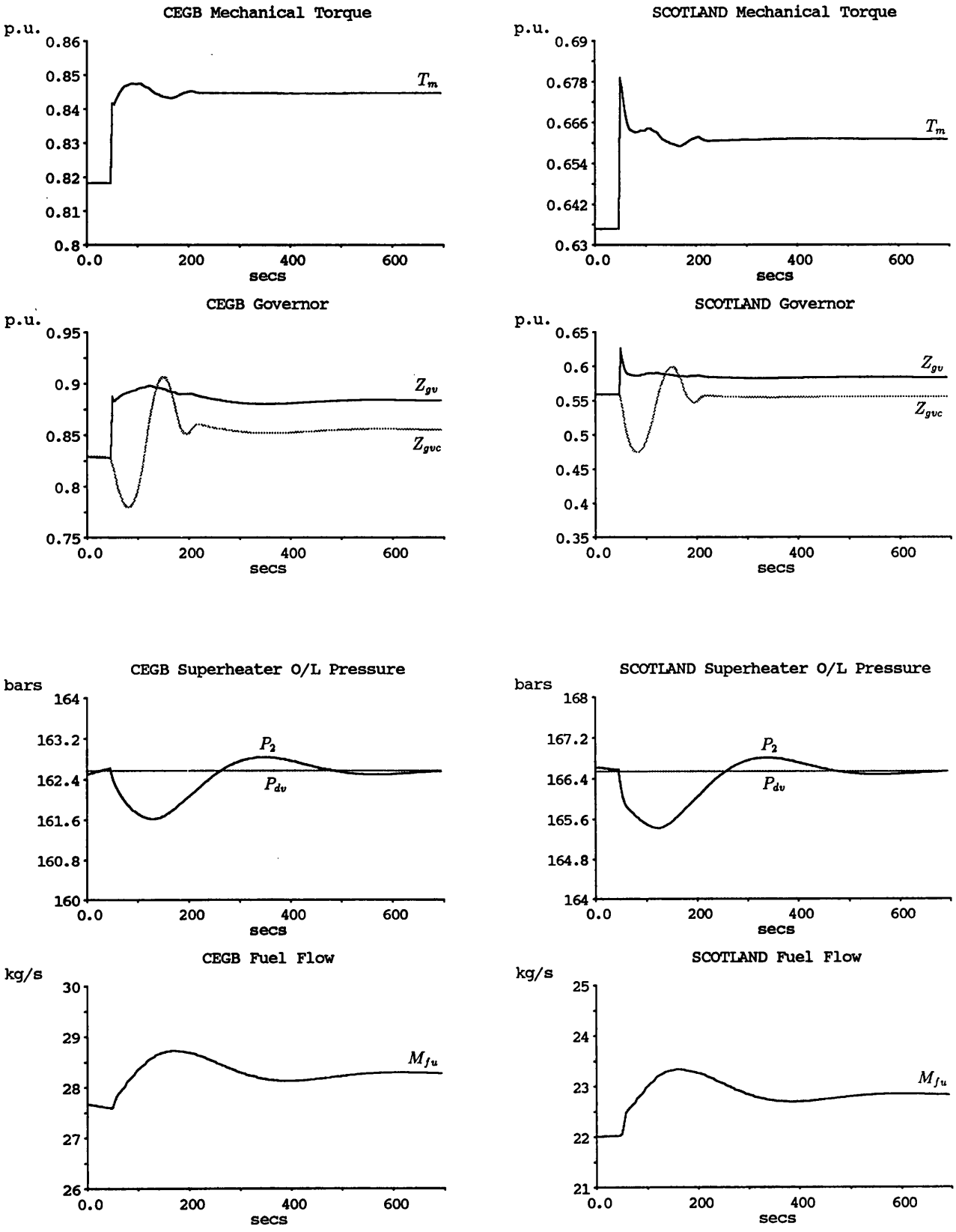

Figure 6.27: (b) 4 m'c Step Load Increase busbar CEGB4 (Run 13)

13 fig 6.27(b)

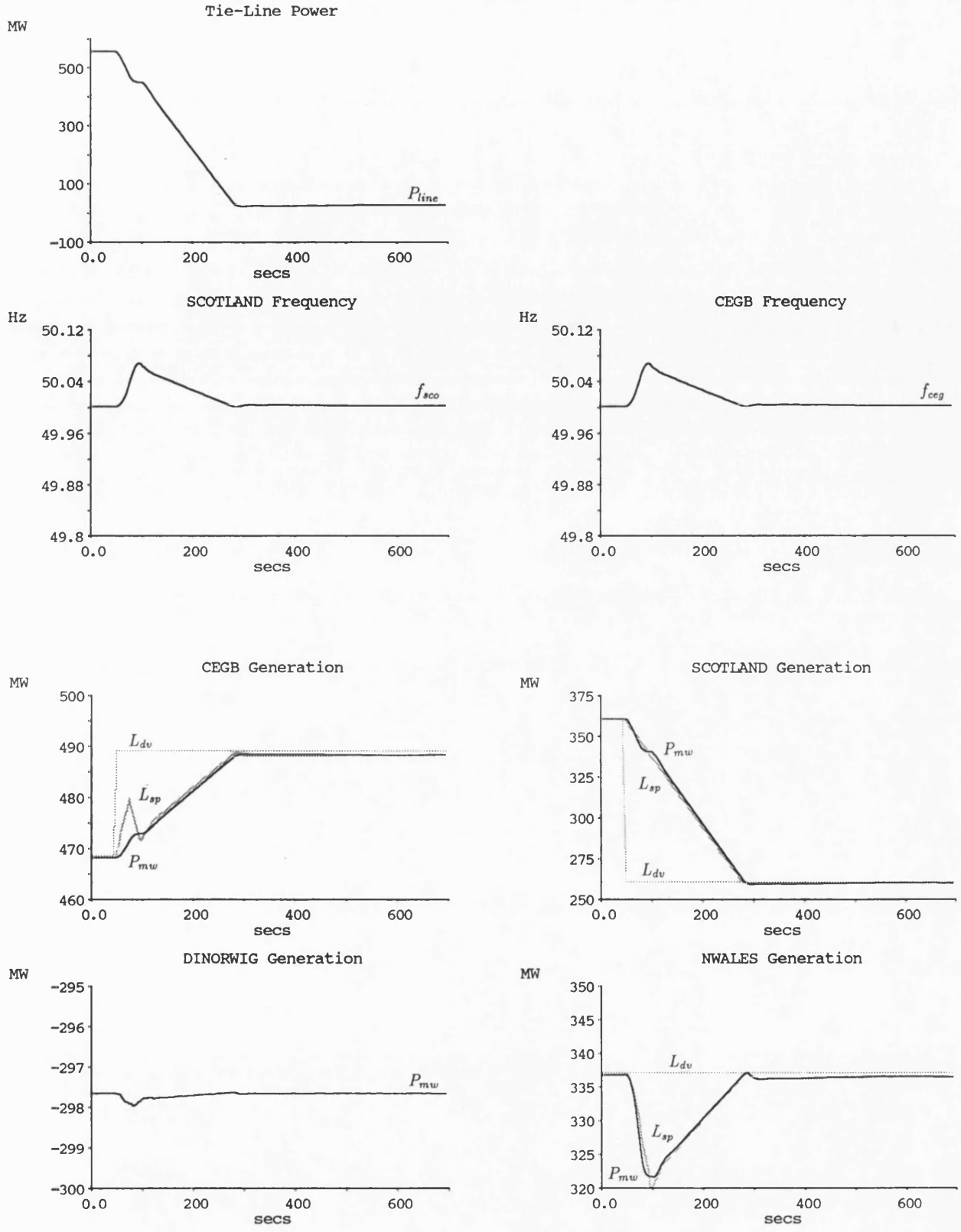

Figure 6.28: (a) 4 m'c SCOTLAND $Ldv + 500\,\text{MW}$ CEGB $-500\,\text{MW}$ (Run 14)

14 Fig 6.28(a)

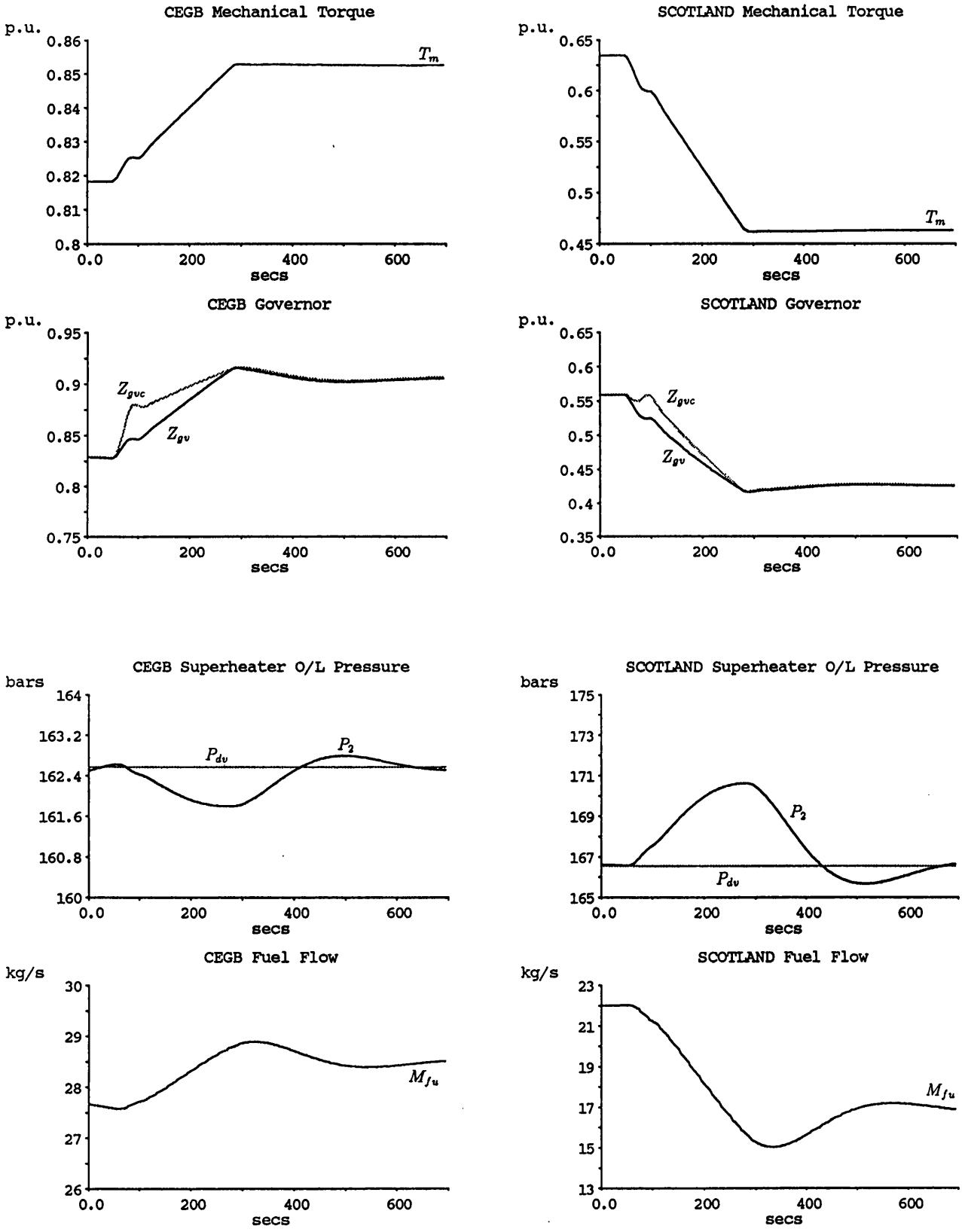

Figure 6.28: (b) 4 m'c SCOTLAND $Ldv + 500\,\text{MW}$ CEGB $-500\,\text{MW}$ (Run 14)

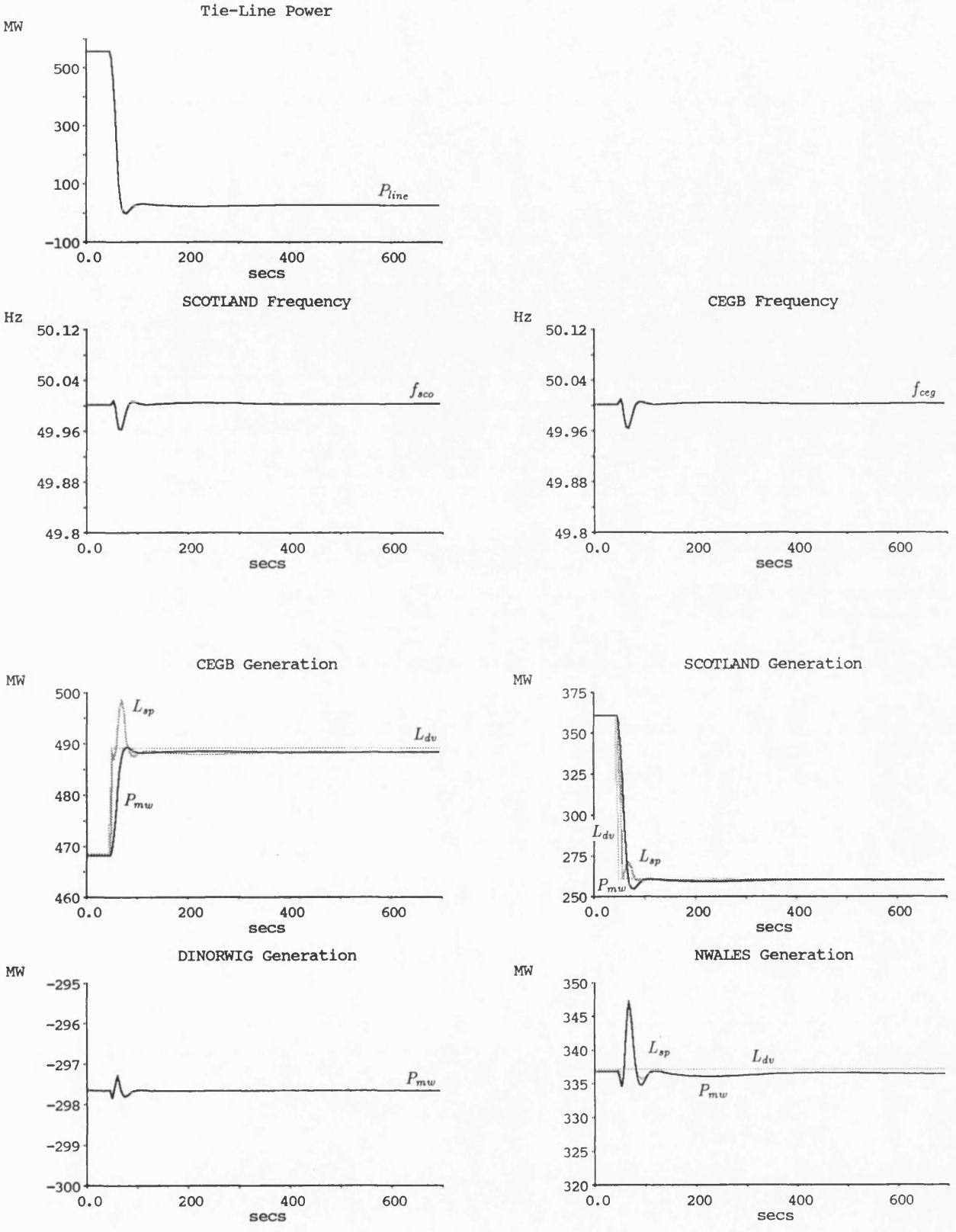

Figure 6.29: (a) 4 m'c SCOTLAND $Ldv + 500\,\mathrm{MW}$ CEGB $-500\,\mathrm{MW}$ (Run 15)

5 Fig 6.29(a)

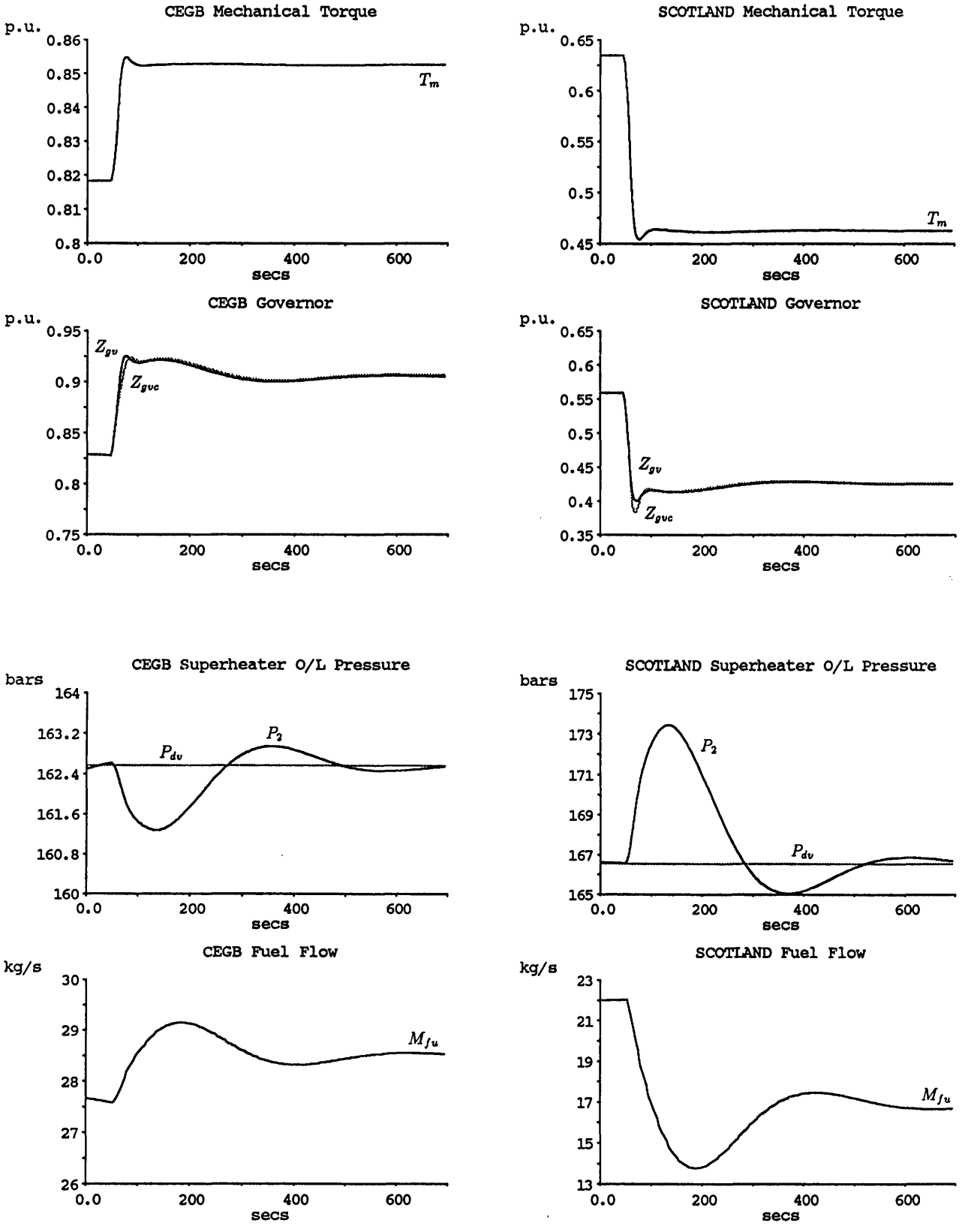

Figure 6.29: (b) 4 m'c SCOTLAND $Ldv + 500\,\text{MW}$ CEGB $-500\,\text{MW}$ (Run 15)

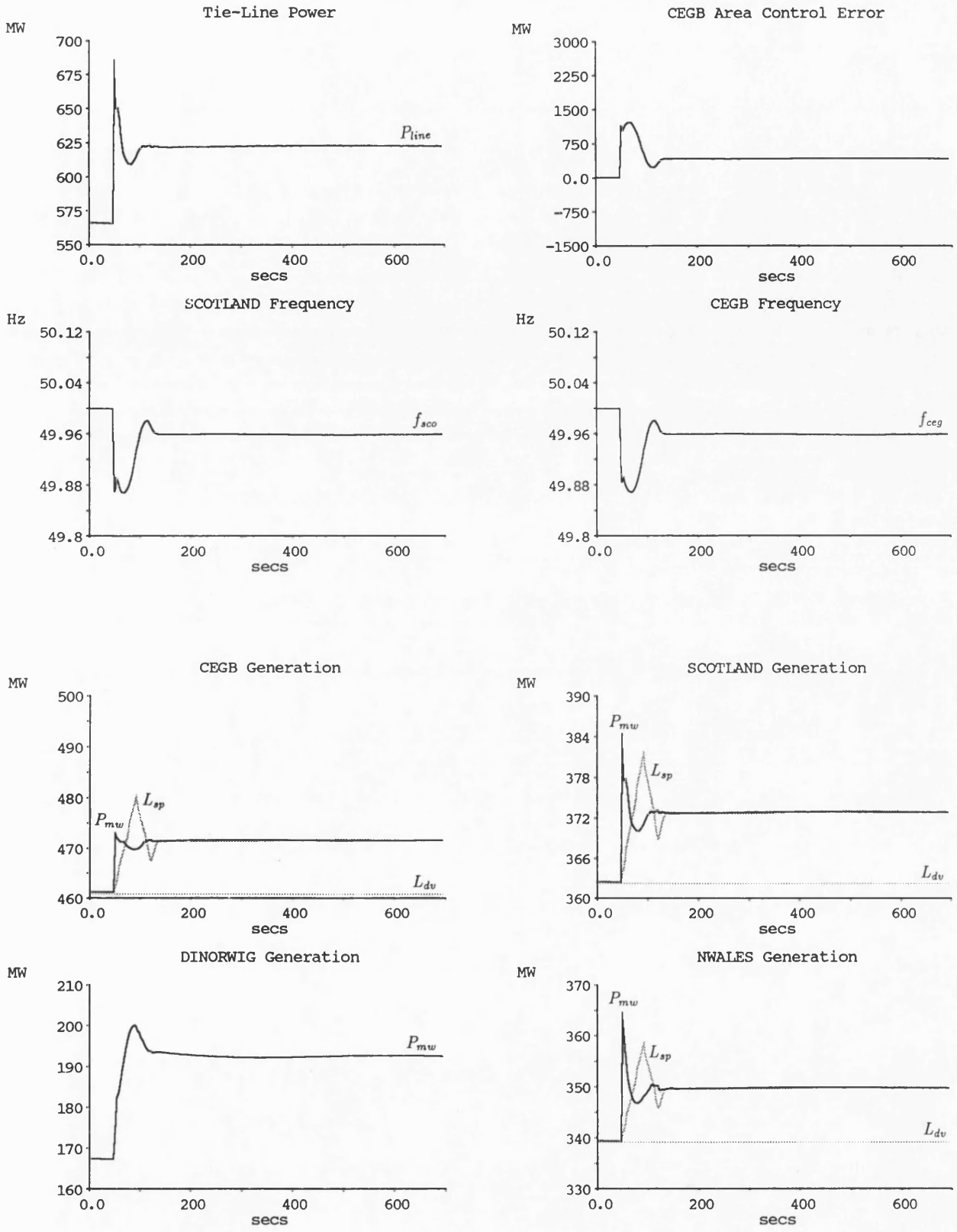

Figure 6.30: (a) 4 m'c Step Load Increase busbar CEGB4 (Run 16)

16 Fig. 30(a)

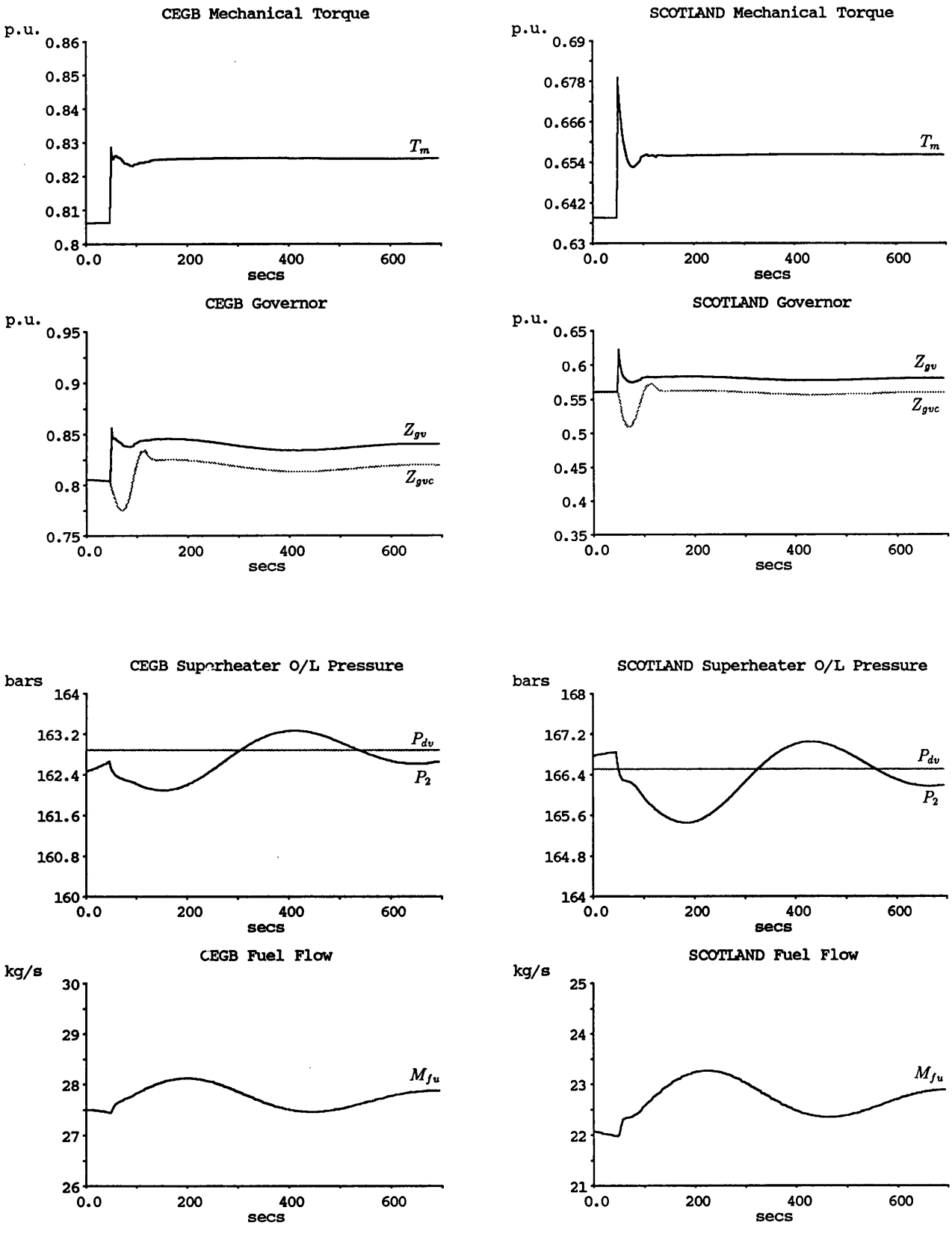

Figure 6.30: (b) 4 m'c Step Load Increase busbar CEGB4 (Run 16)

16 Eg 6.30(b)

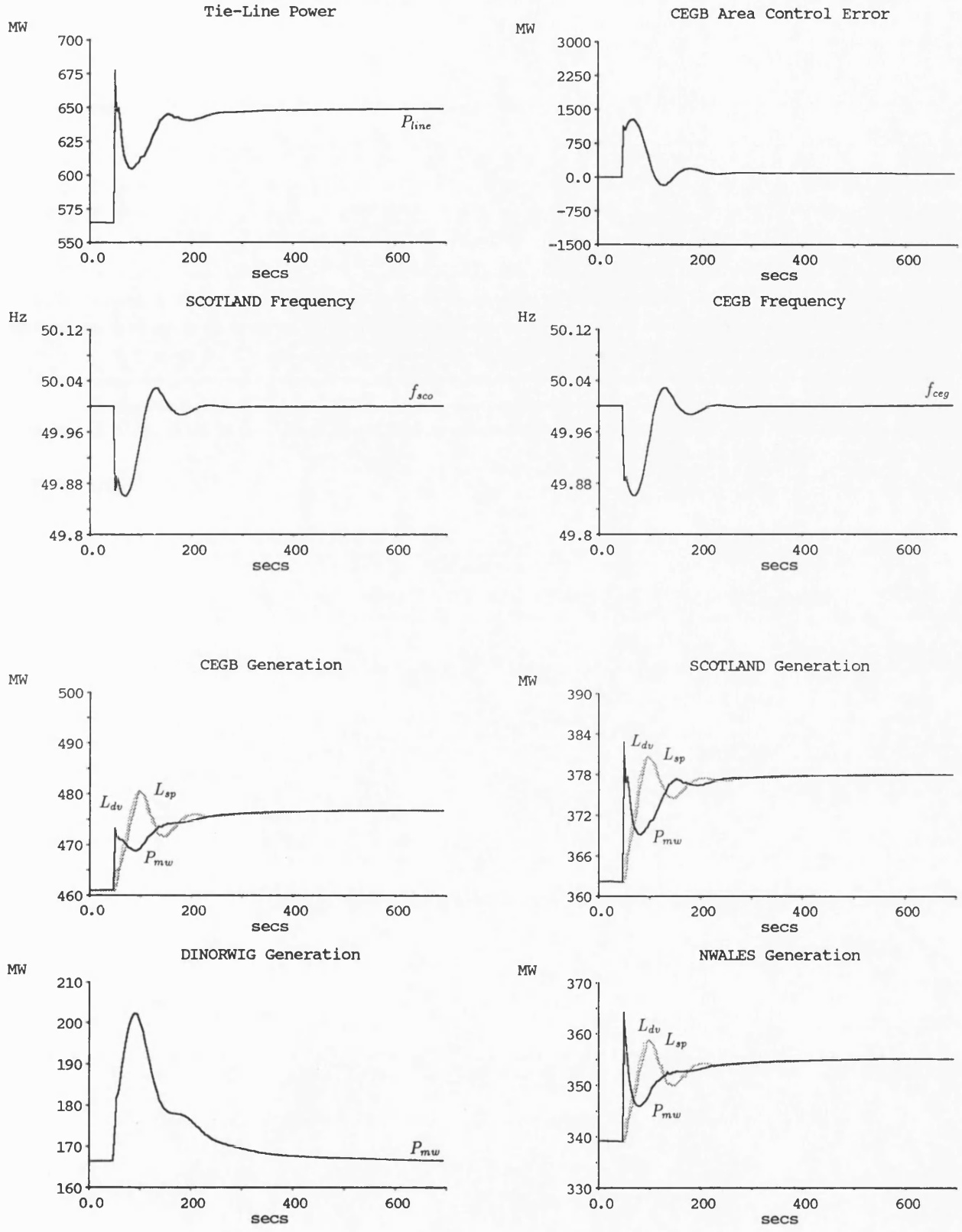

Figure 6.31: (a) 4 m'c Step Load Increase busbar CEGB4 (Run 18)

8 fig 5.31(a)

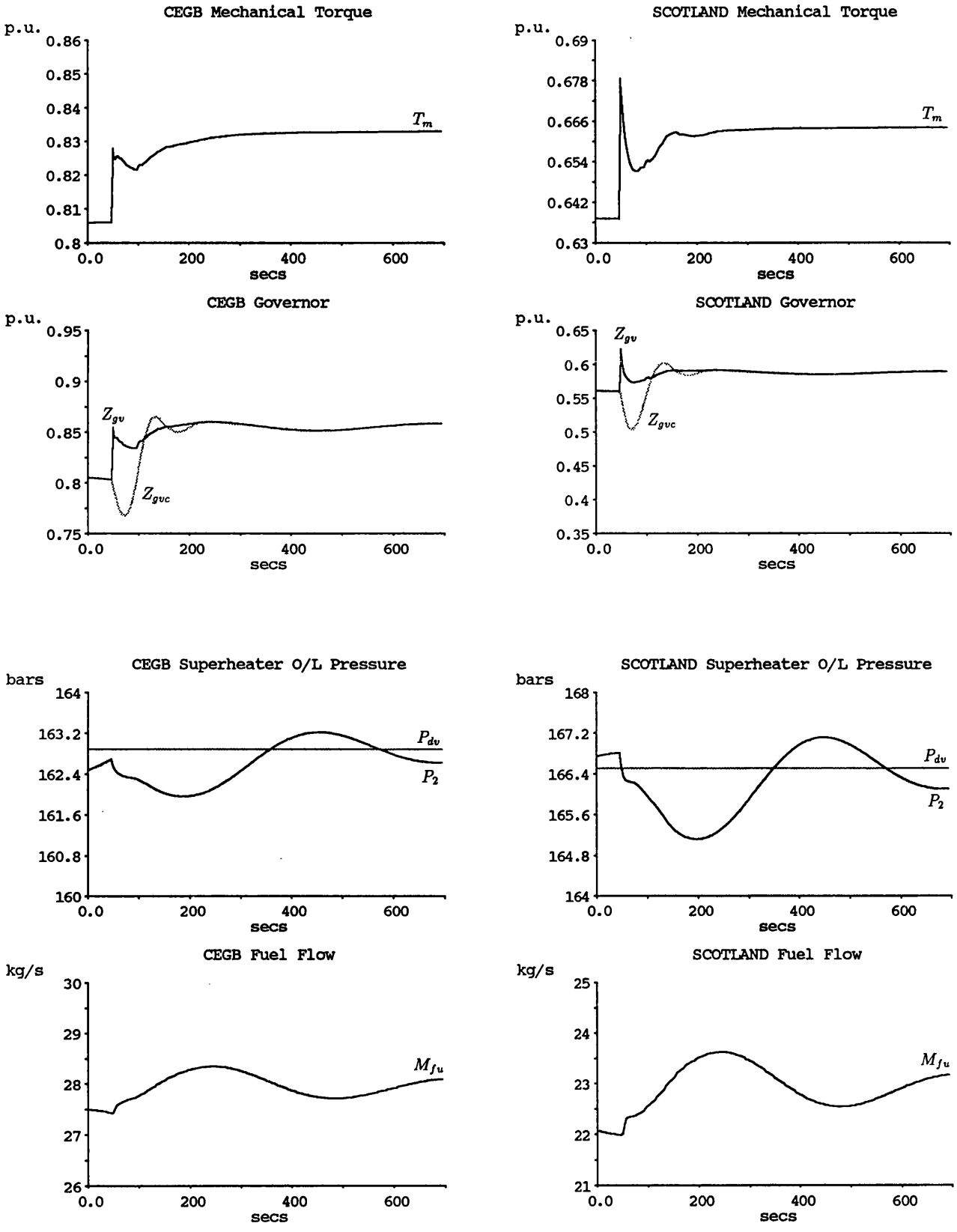

Figure 6.31: (b) 4 m'c Step Load Increase busbar CEGB4 (Run 18)

8 Fig 6.31(b)

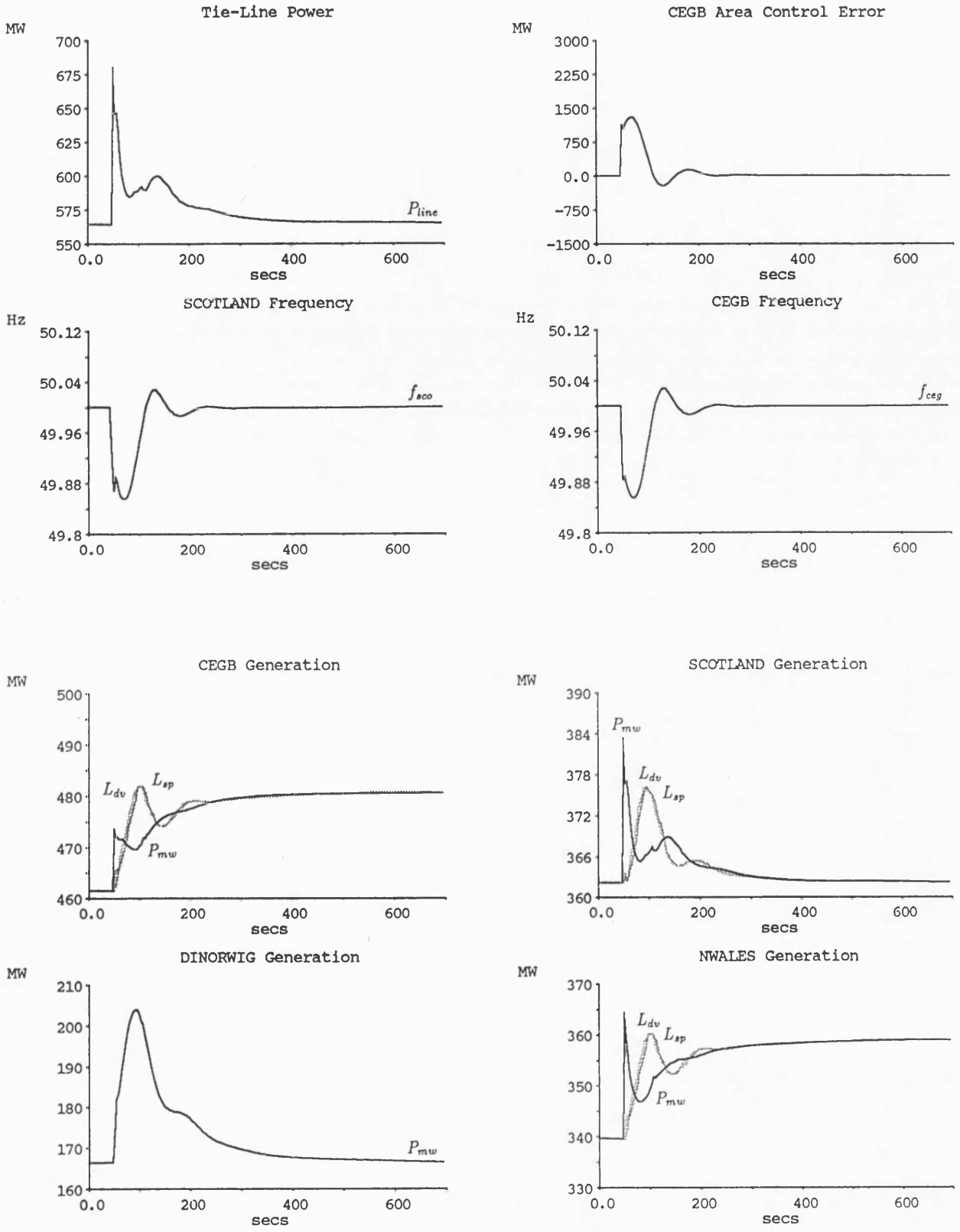

Figure 6.32: (a) 4 m'c Step Load Increase busbar CEGB4 (Run 19)

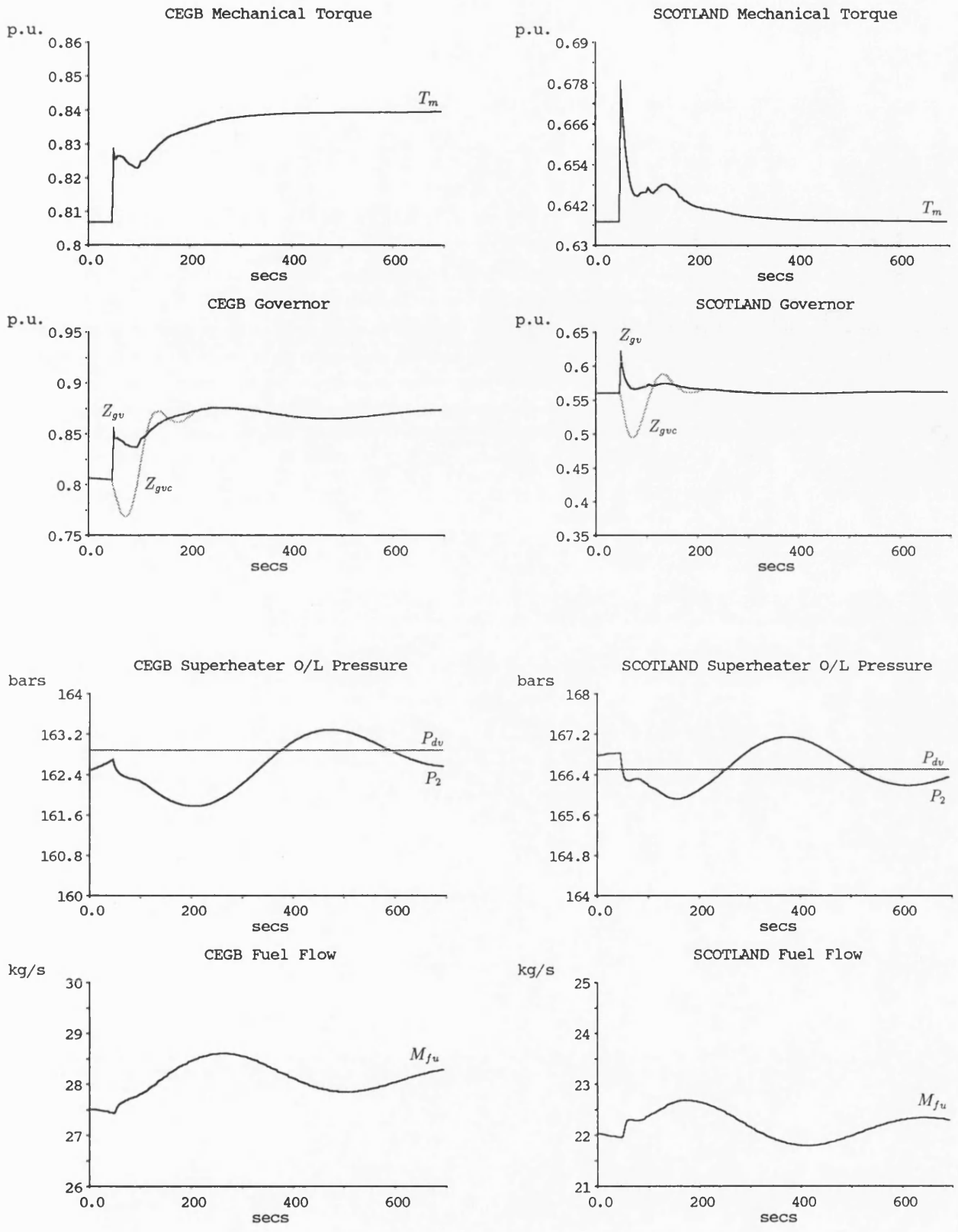

Figure 6.32: (b) 4 m'c Step Load Increase busbar CEGB4 (Run 19)

9 Fig 6.32(b)

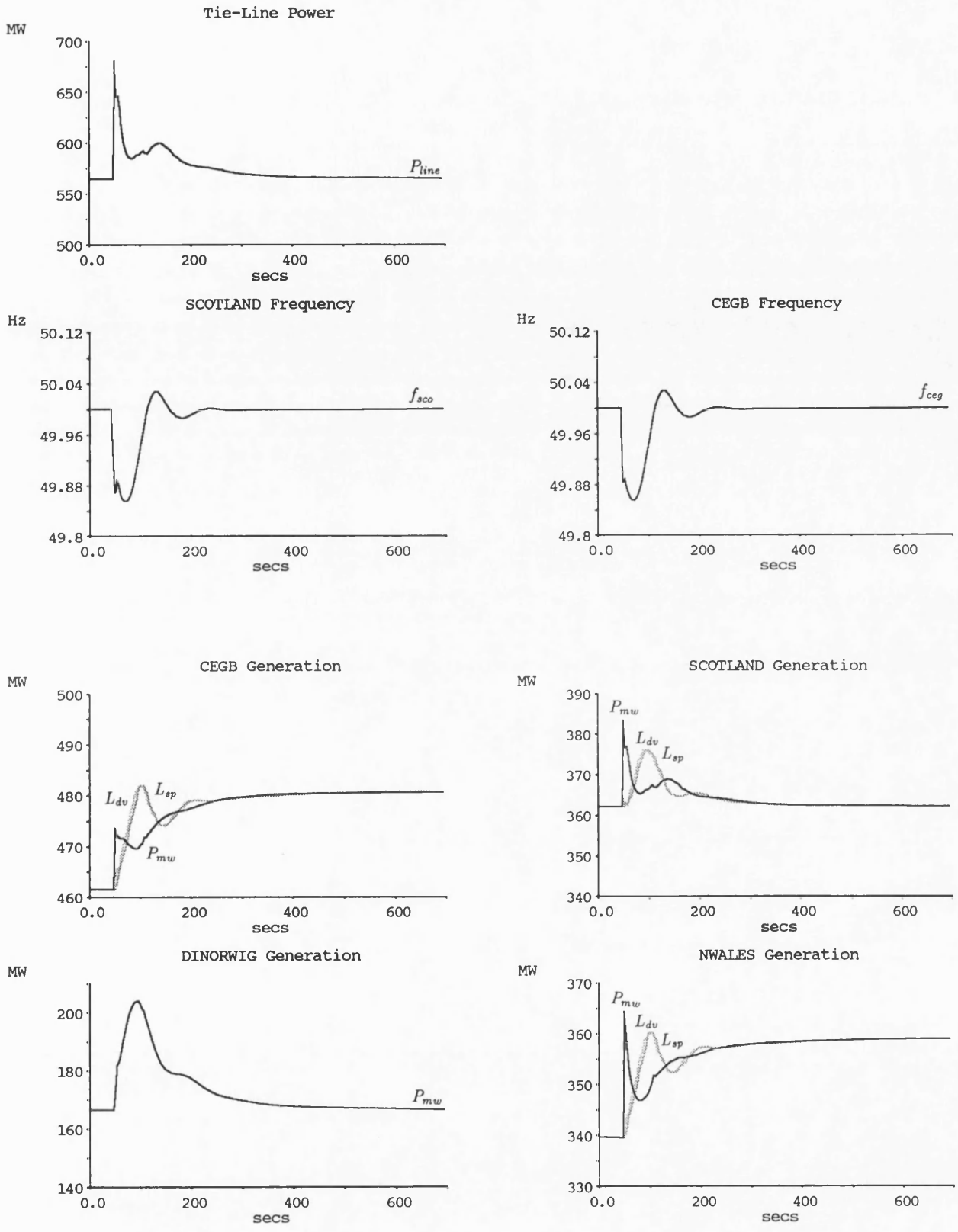

Figure 6.33: (a) 4 m'c Step Load Increase busbar CEGB4 (Run 19)

(9 Fig 6.33 (a)

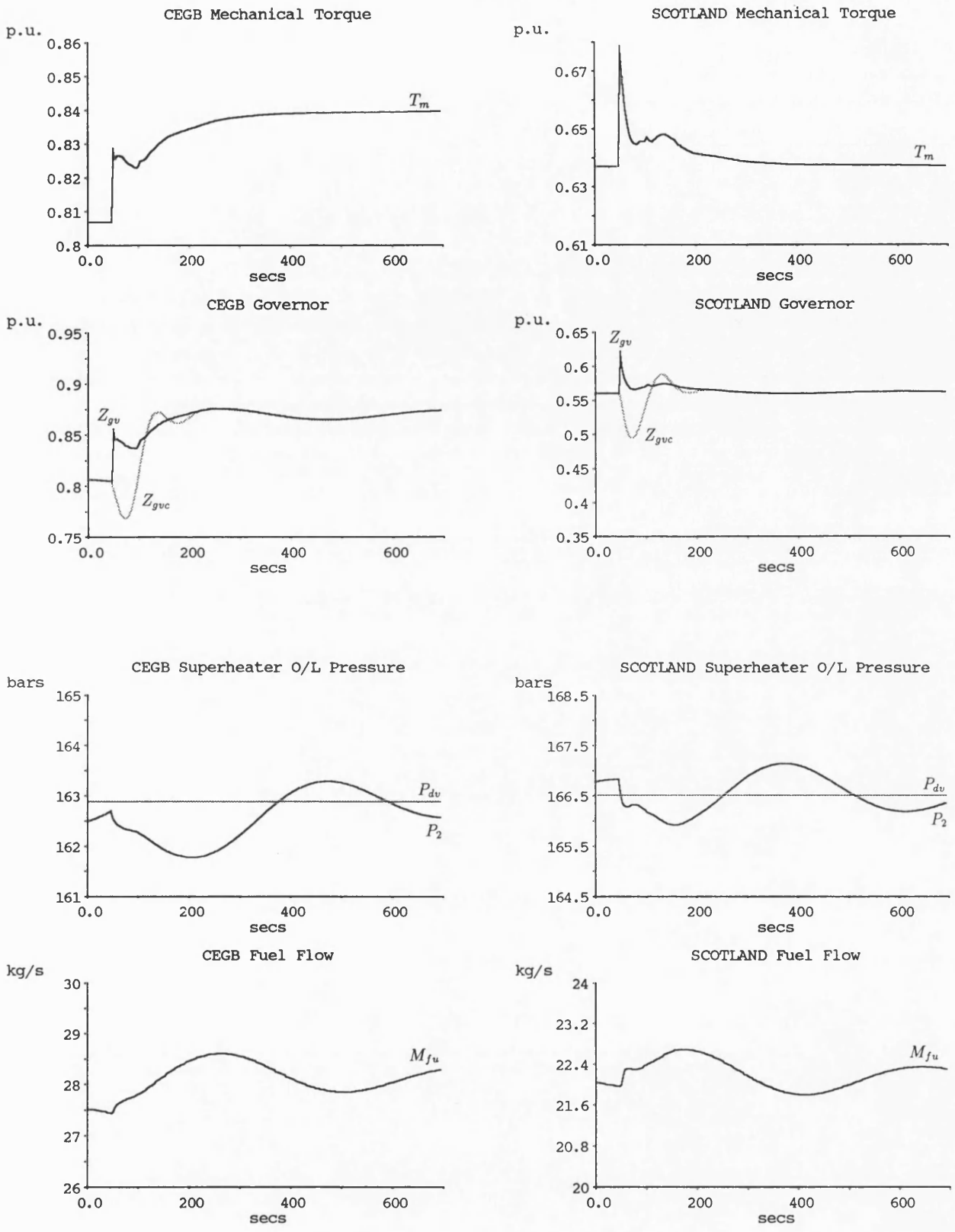

Figure 6.33: (b) 4 m'c Step Load Increase busbar CEGB4 (Run 19)

Kg 6.33(b)

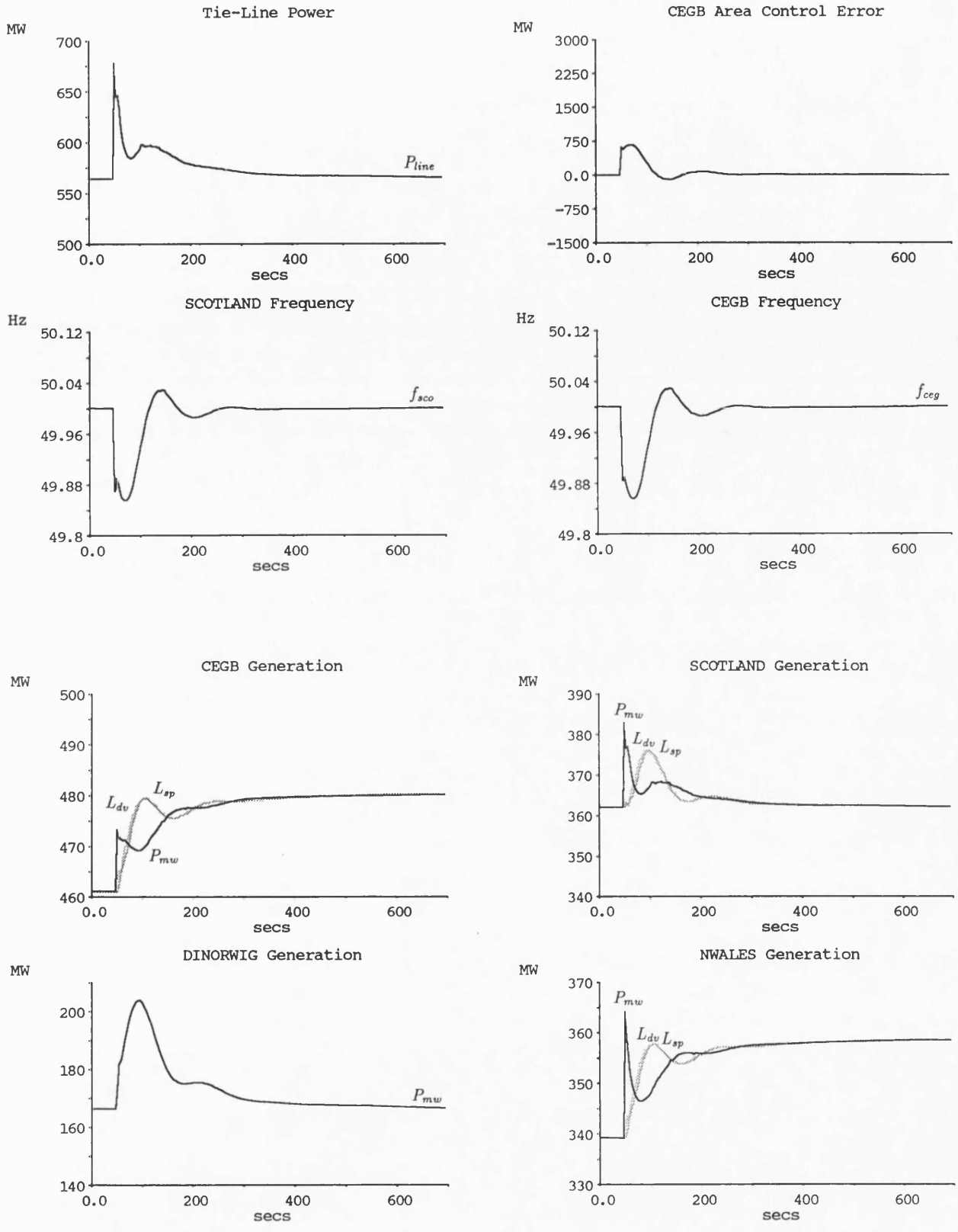

Figure 6.34: (a) 4 m'c Step Load Increase busbar CEGB4 (Run 20)

10 Fig 6.34(a)

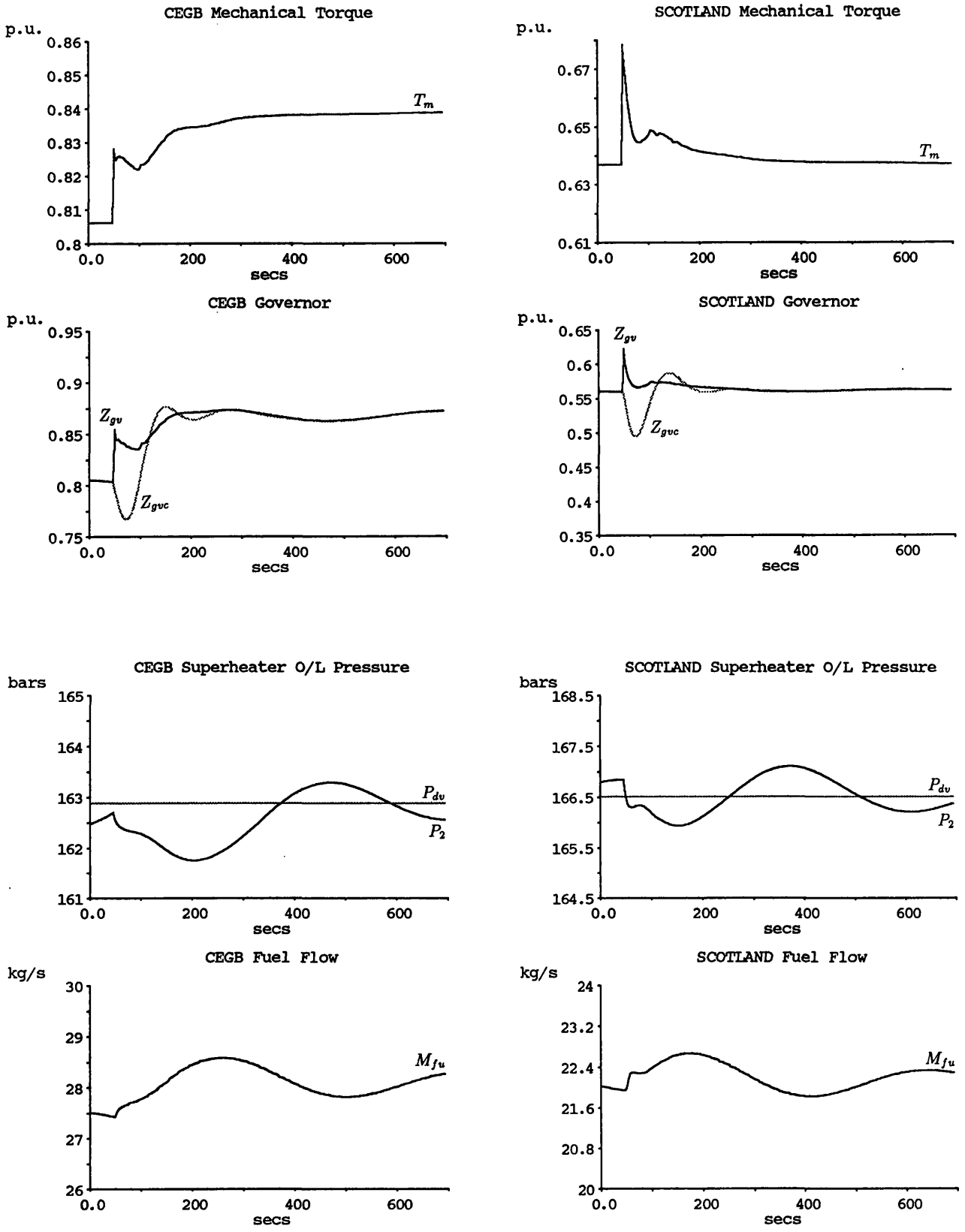

Figure 6.34: (b) 4 m'c Step Load Increase busbar CEGB4 (Run 20)

10 Fig 6.34(b)

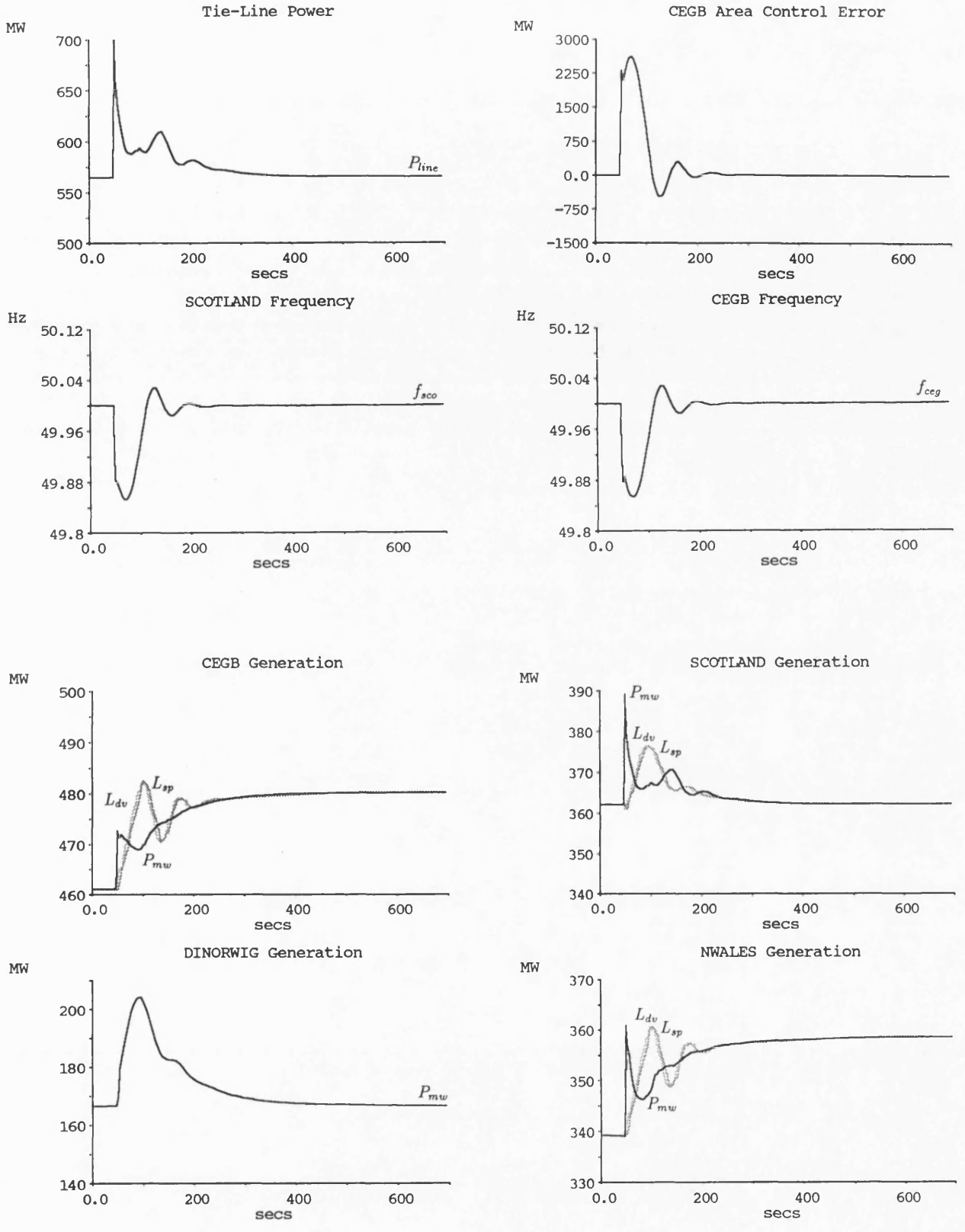

Figure 6.35: (a) 4 m'c Step Load Increase busbar CEGB4 (Run 21)

21 Fig 6.35(a)

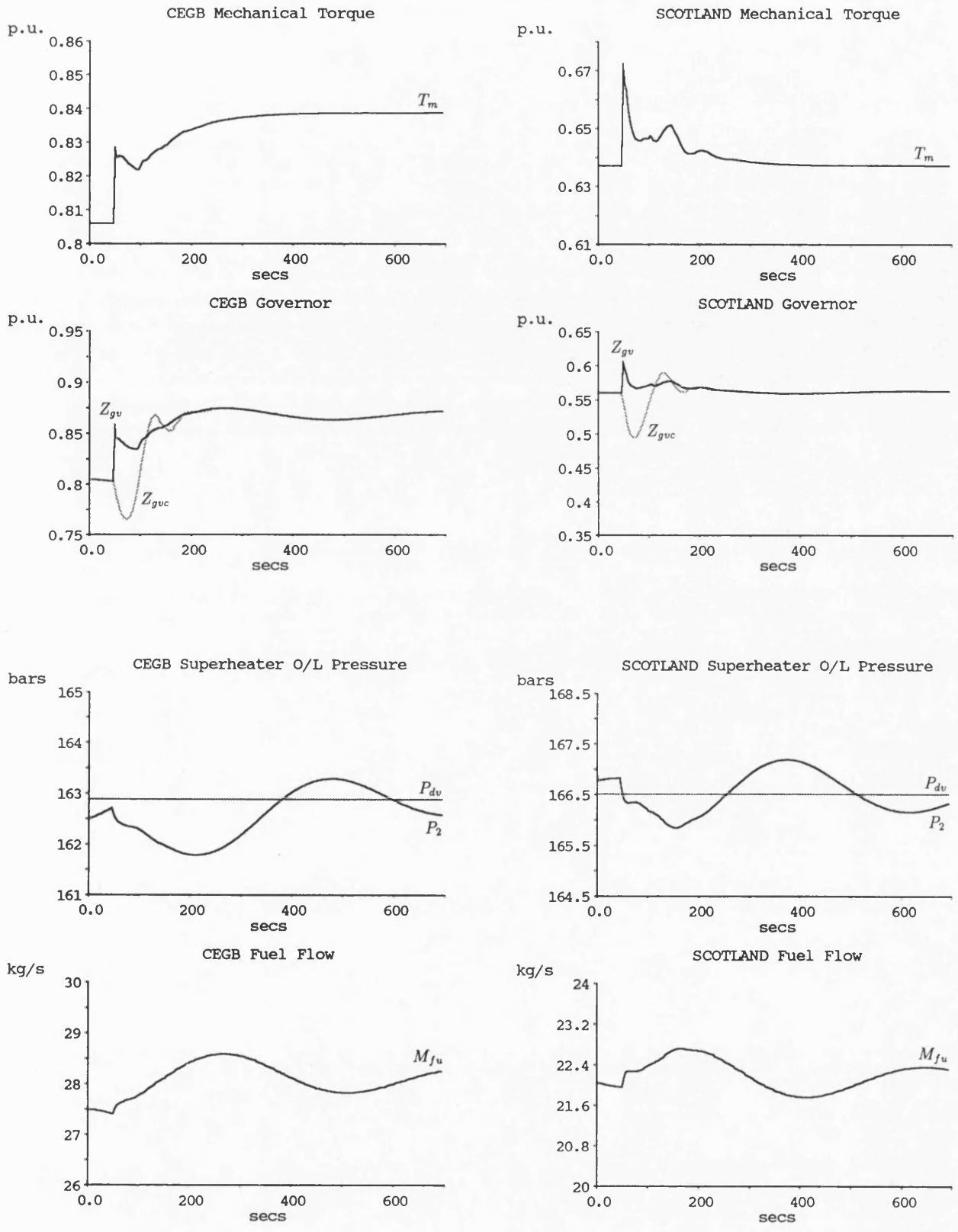

Figure 6.35: (b) 4 m'c Step Load Increase busbar CEGB4 (Run 21)

21 Fig. 35(b)

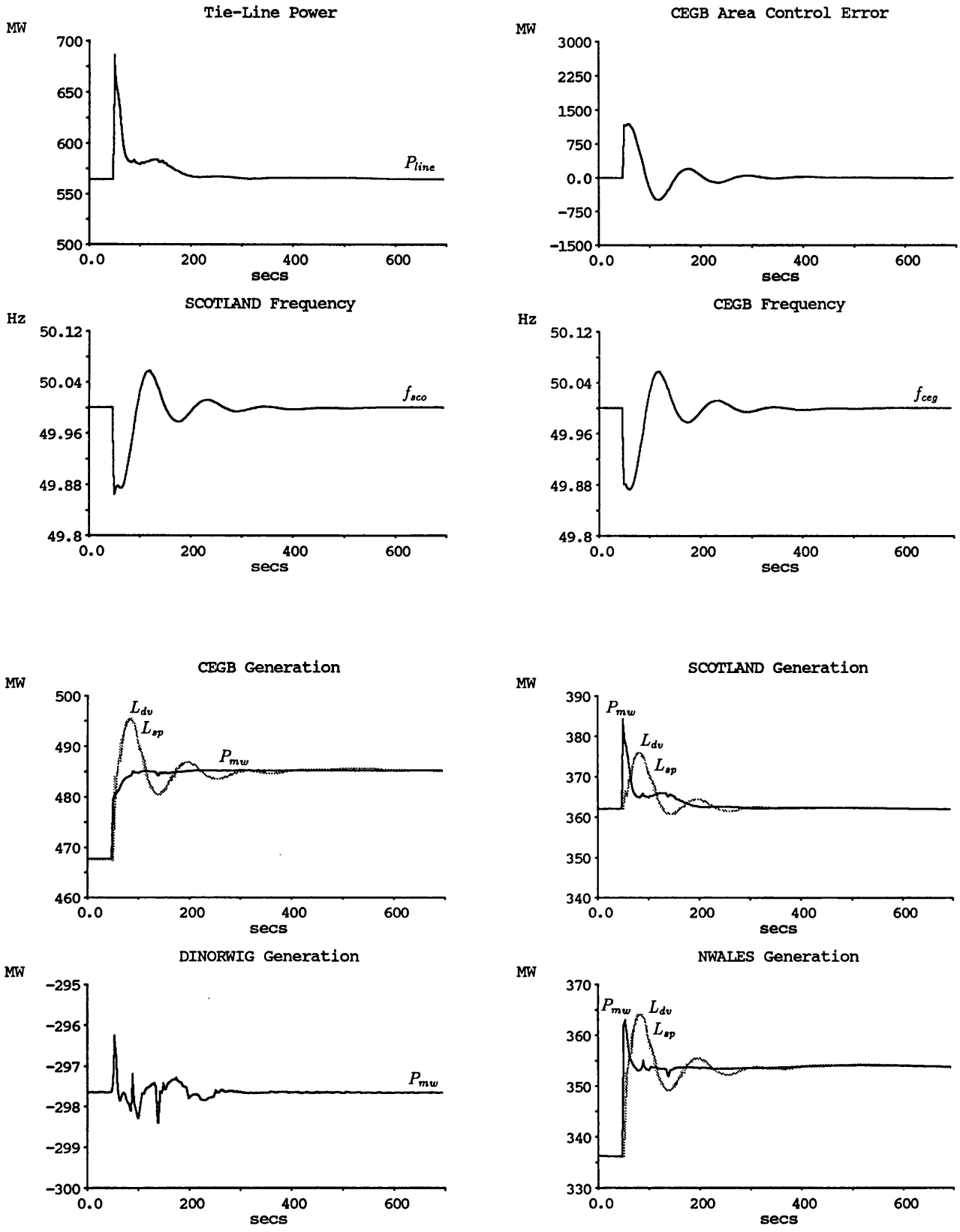

Figure 6.36: (a) 4 m'c Step Load Increase busbar CEGB4 (Run 19b)

ib Fig 6.36(a)

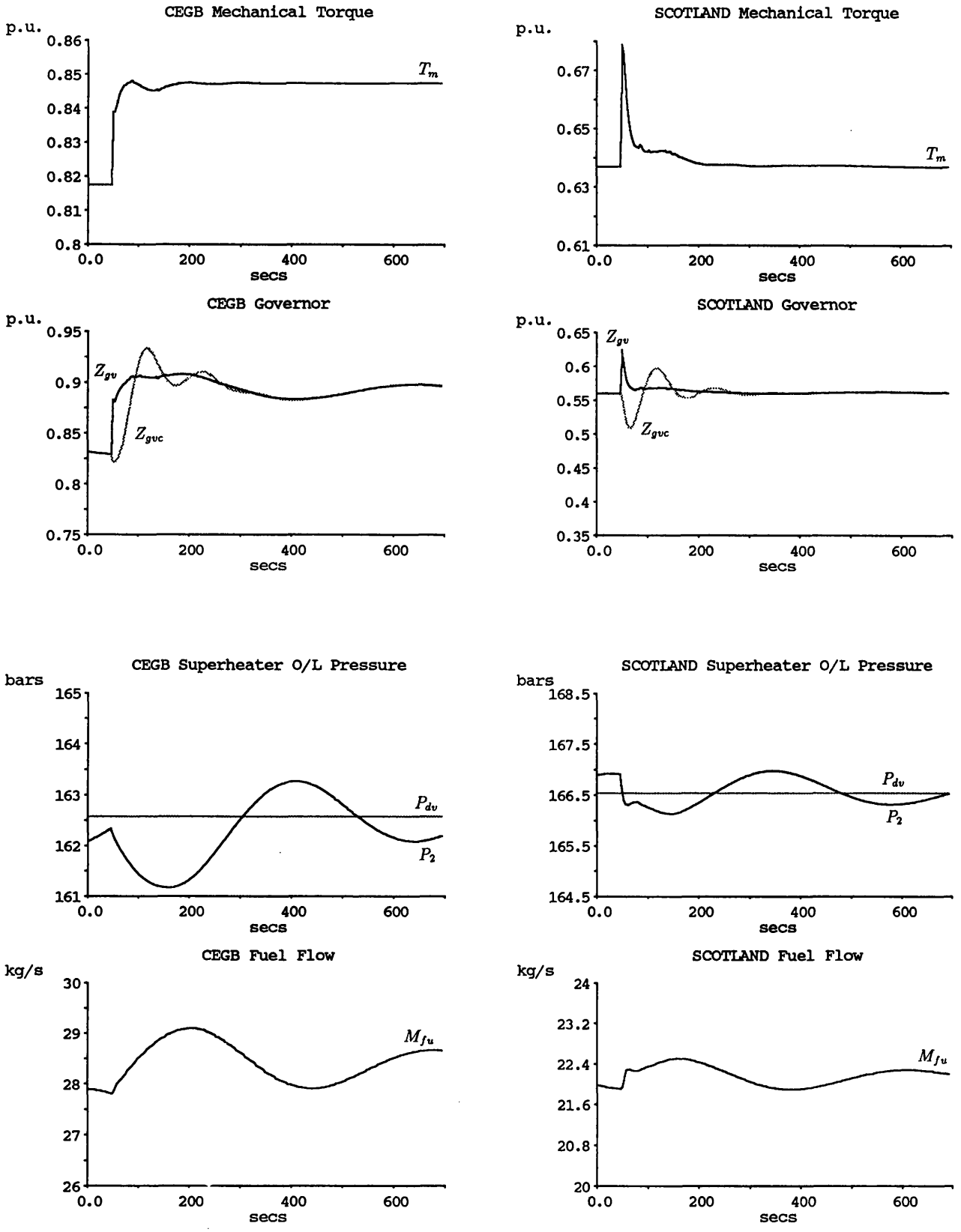

Figure 6.36: (b) 4 m'c Step Load Increase busbar CEGB4 (Run 19b)

76 Fig 6.36(b)

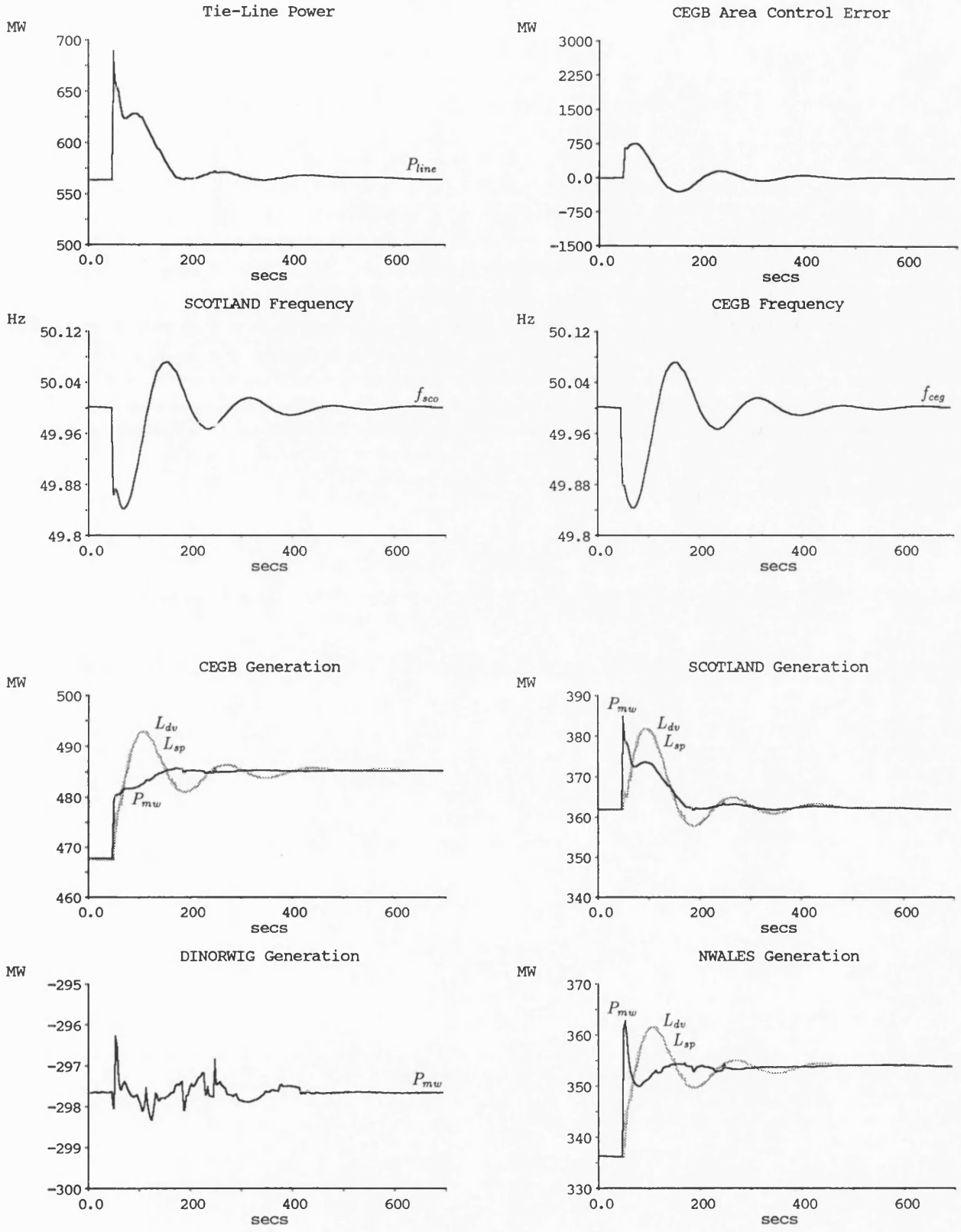

Figure 6.37: (a) 4 m'c Step Load Increase busbar CEGB4 (Run 20b)

Fig 6.37(a)

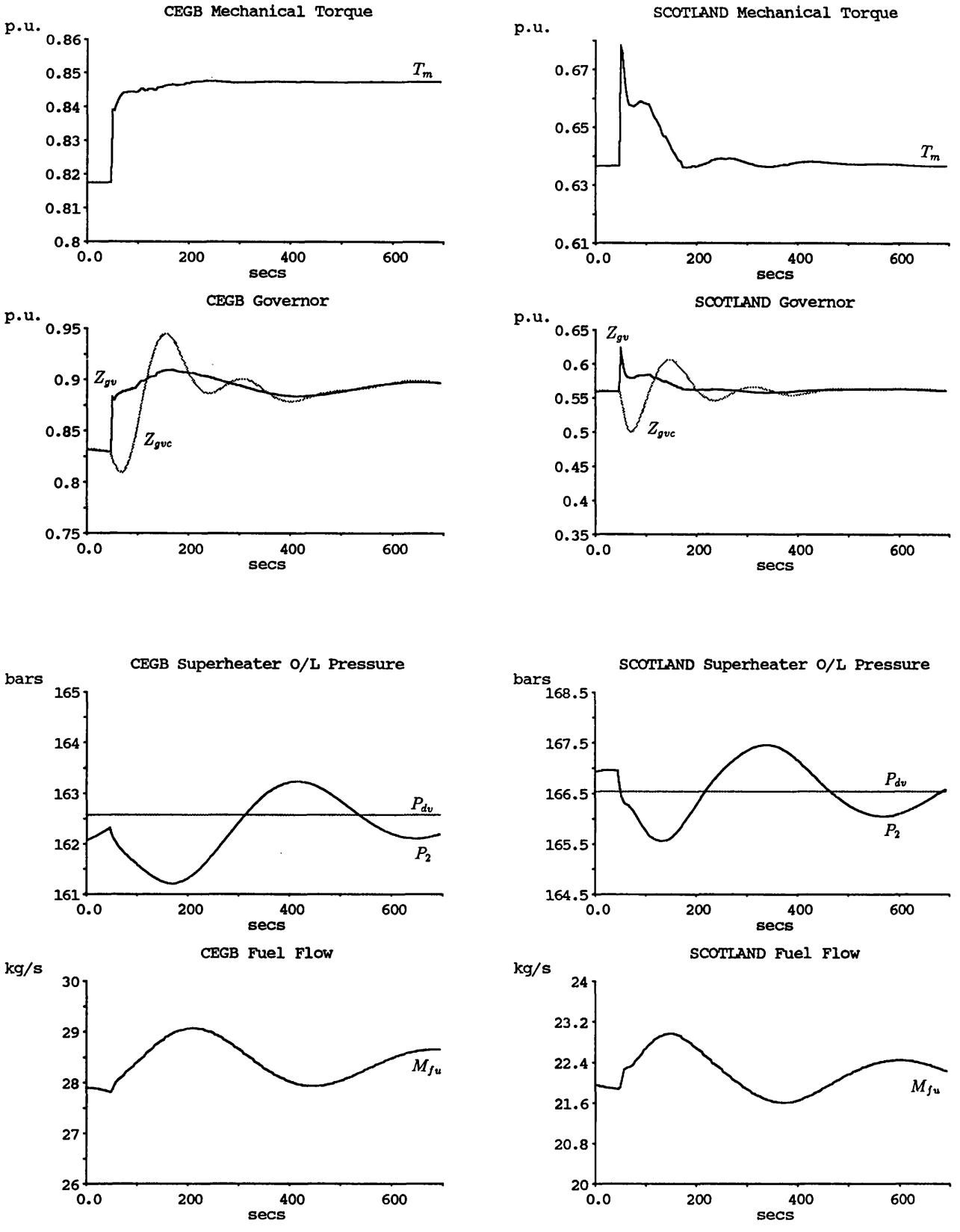

Figure 6.37: (b) 4 m'c Step Load Increase busbar CEGB4 (Run 20b)

Fig 6.37(b)

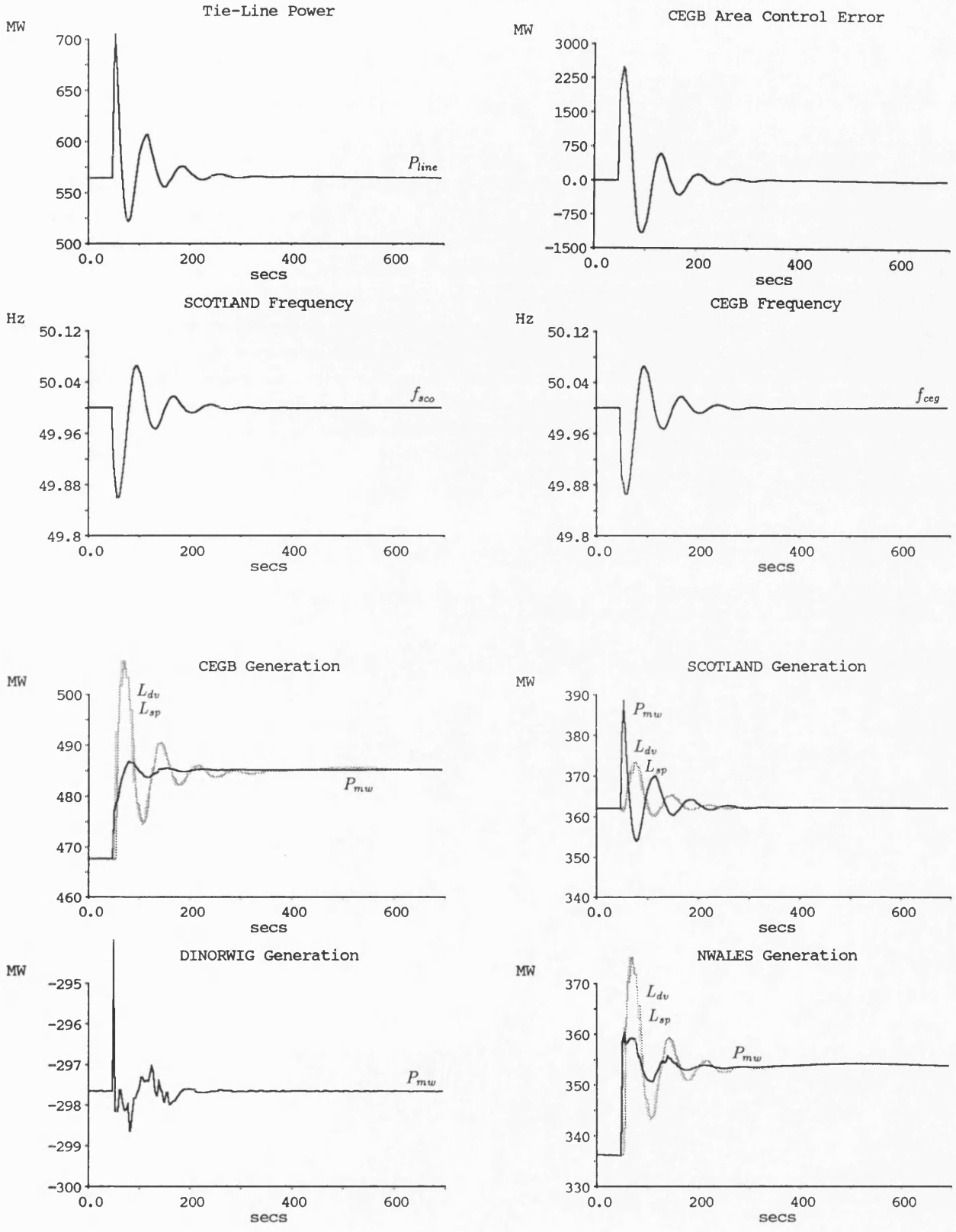

Figure 6.38: (a) 4 m'c Step Load Increase busbar CEGB4 (Run 21b)

Fig 6.38(a)

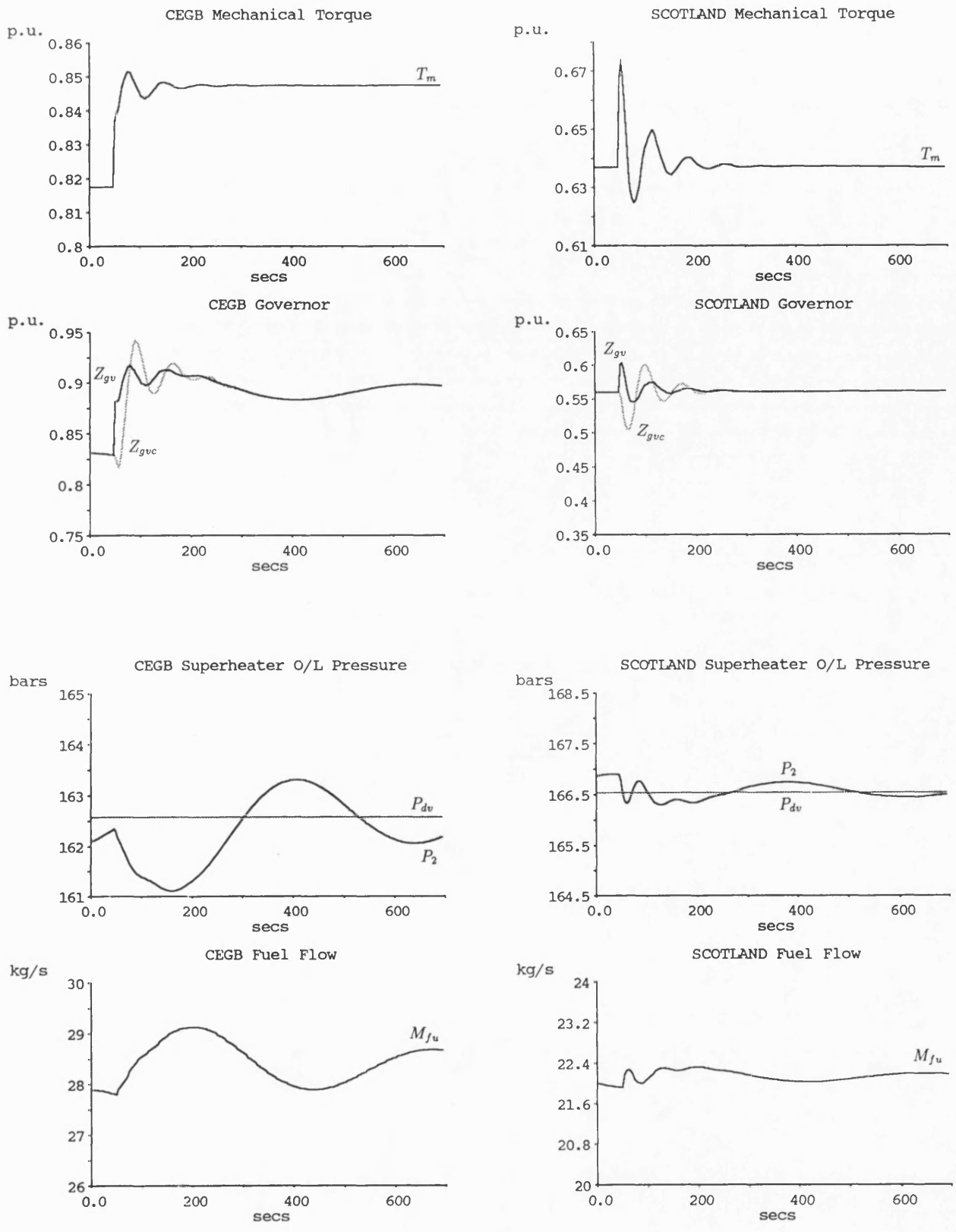

Figure 6.38: (b) 4 m'c Step Load Increase busbar CEGB4 (Run 21b)

(b) fig 6.38(b)

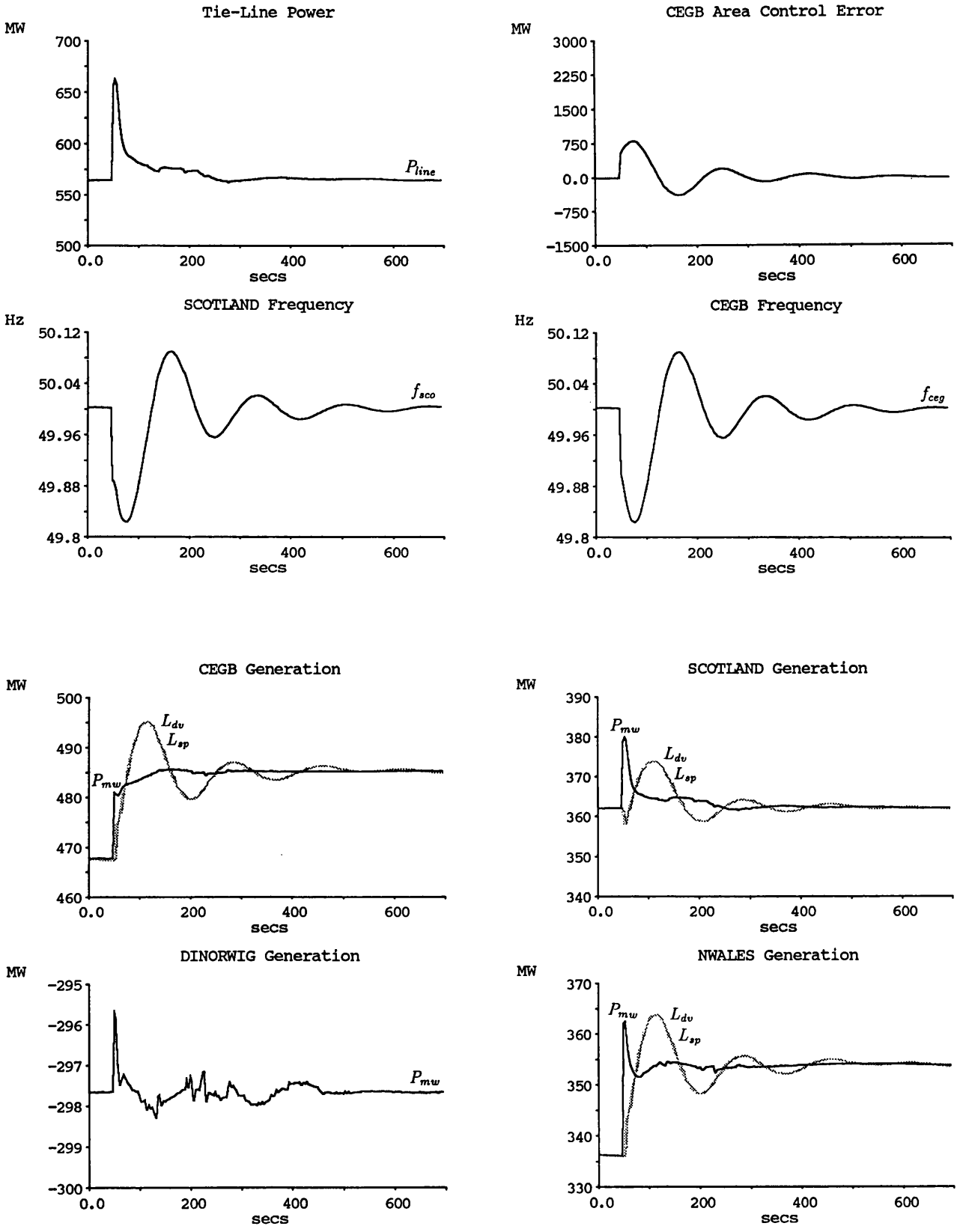

Figure 6.39: (a) 4 m'c Step Load Increase busbar CEGB4 (Run 22b)

Eg 6.39(a)

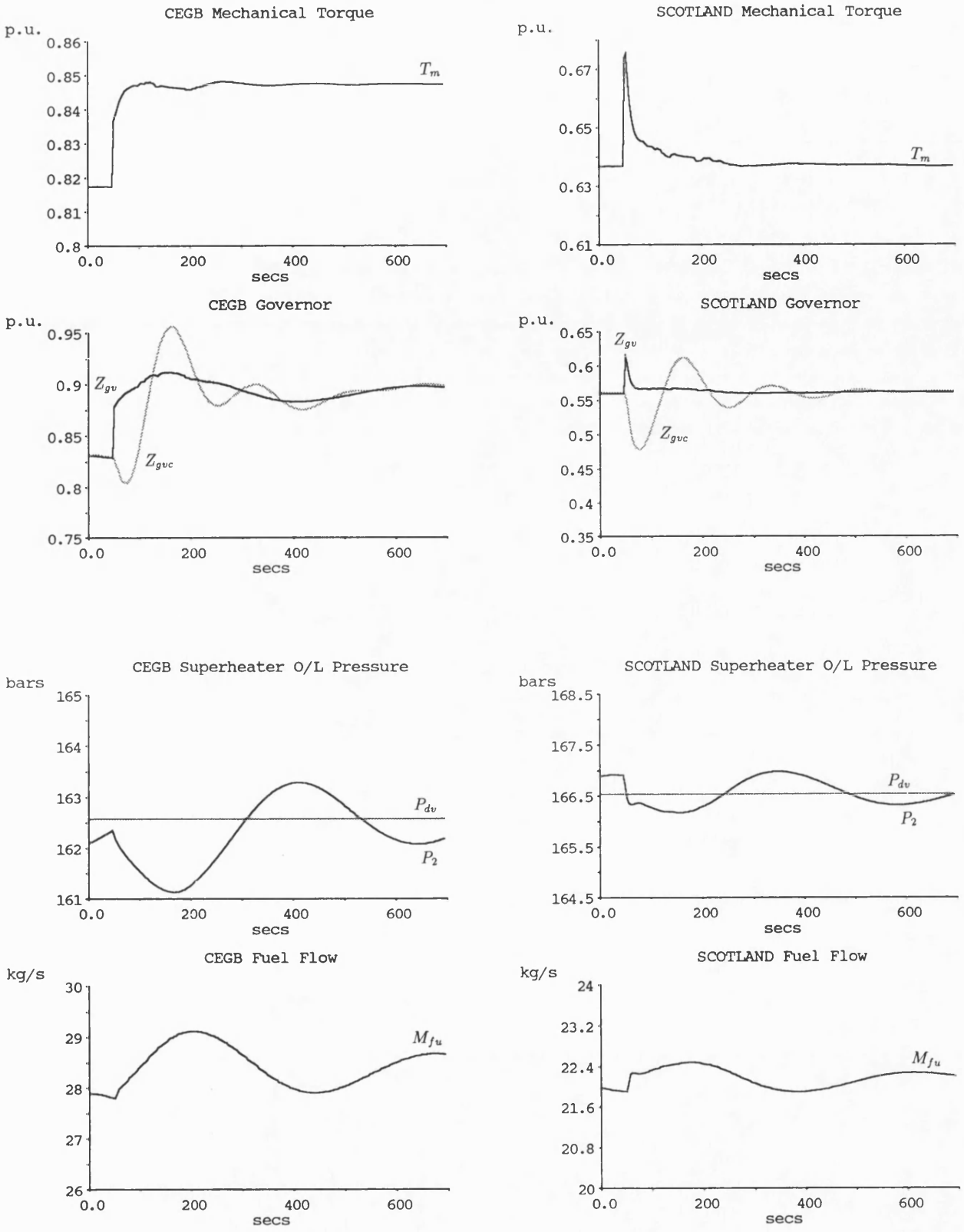

Figure 6.39: (b) 4 m'c Step Load Increase busbar CEGB4 (Run 22b)

2b Eg 6.39(b)

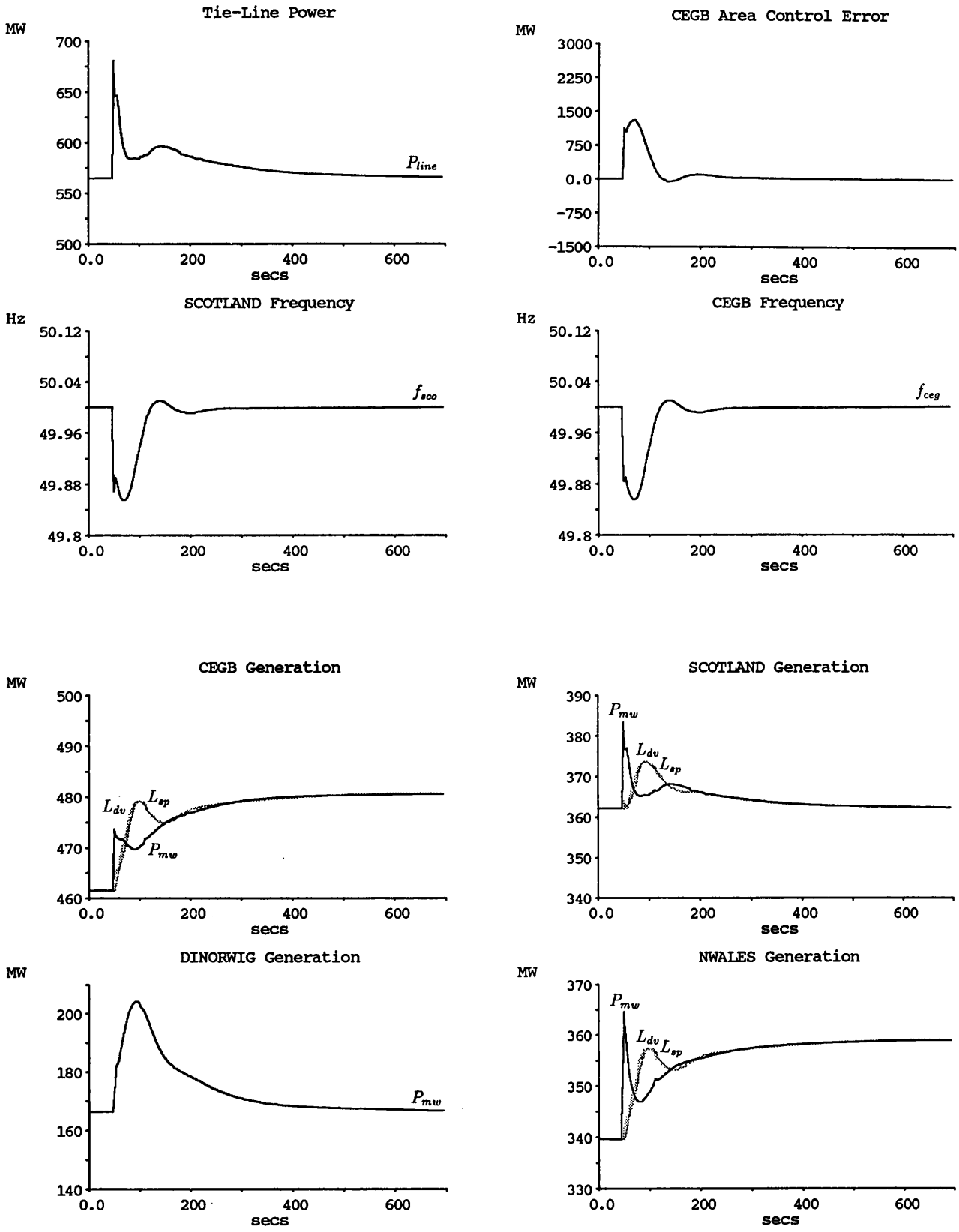

Figure 6.40: (a) 4 m'c Step Load Increase busbar CEGB4 (Run 23)

23 Fig 6.40(a)

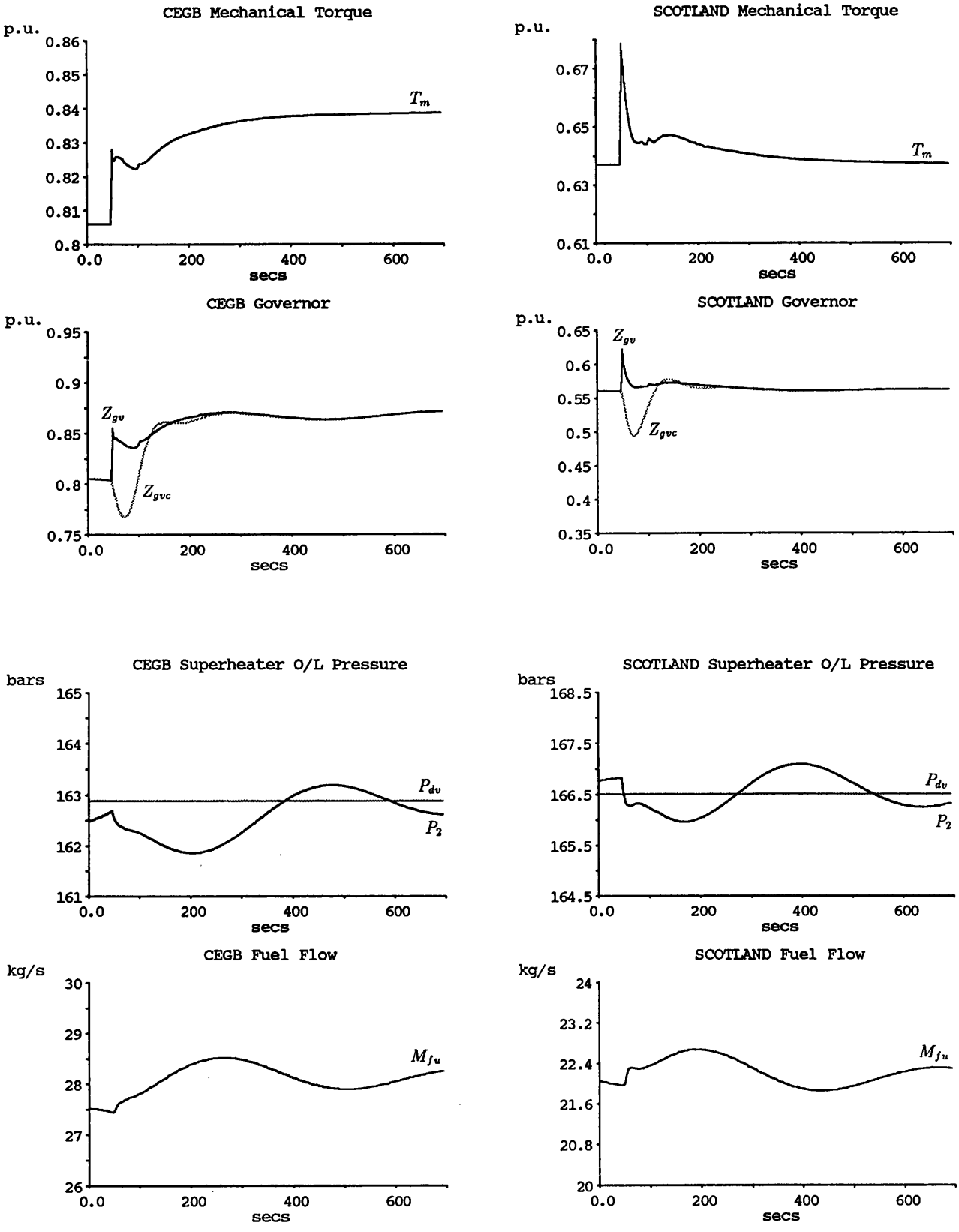

Figure 6.40: (b) 4 m'c Step Load Increase busbar CEGB4 (Run 23)

13 Fig 6.40(b)

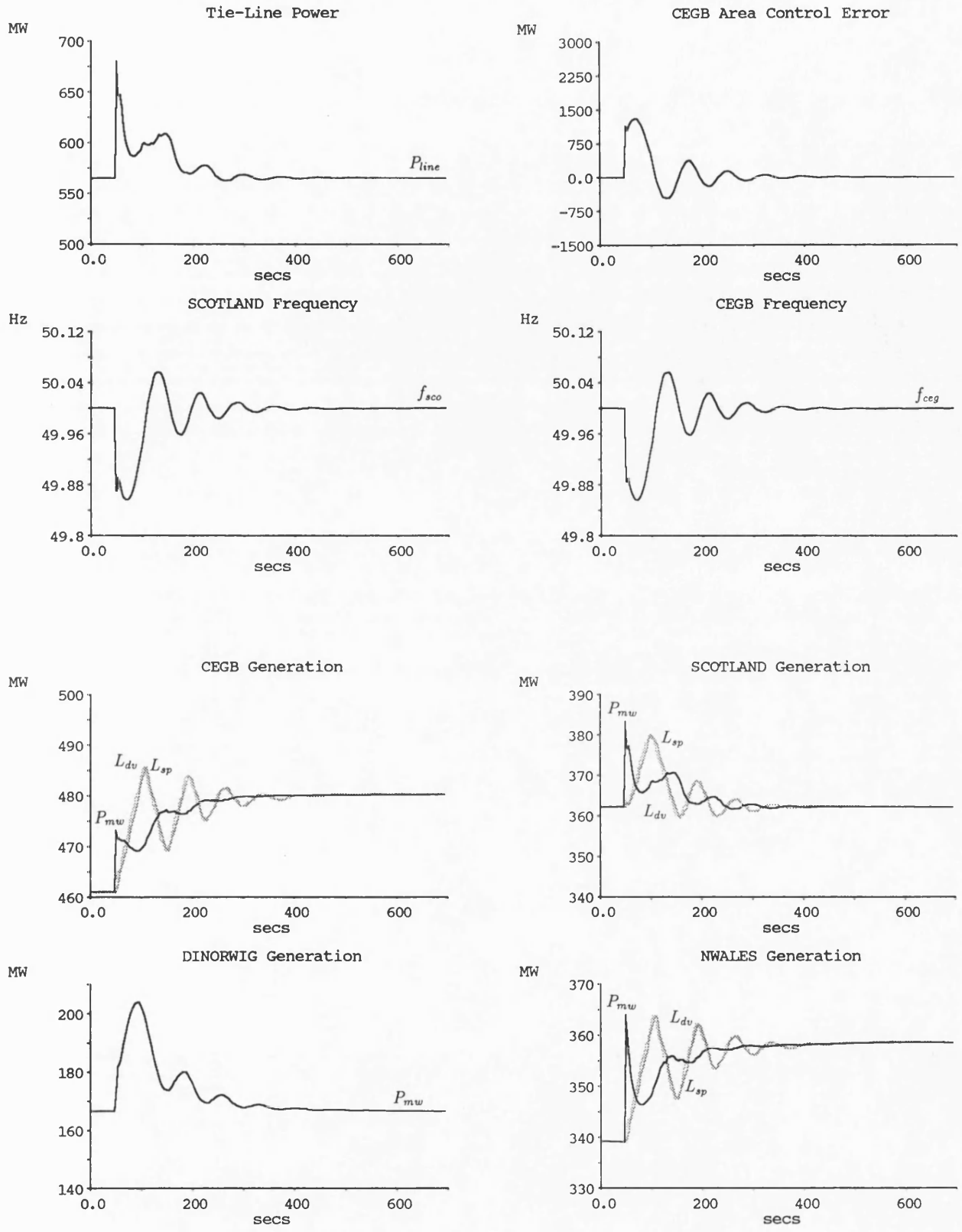

Figure 6.41: (a) 4 m'c Step Load Increase busbar CEGB4 (Run 24)

24 Fig 6.41(a)

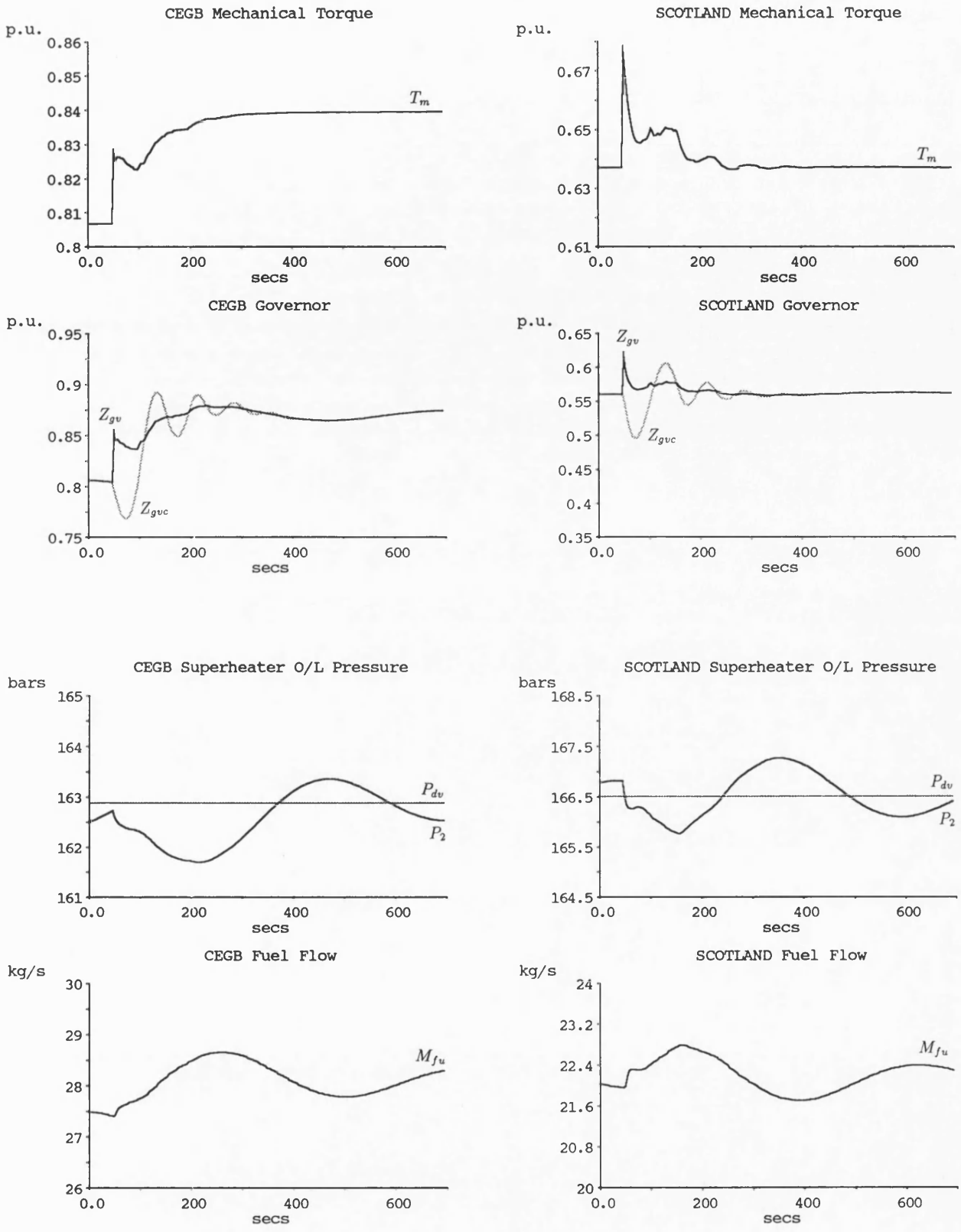

Figure 6.41: (b) 4 m'c Step Load Increase busbar CEGB4 (Run 24)

Ref. Fig 6:41(b)

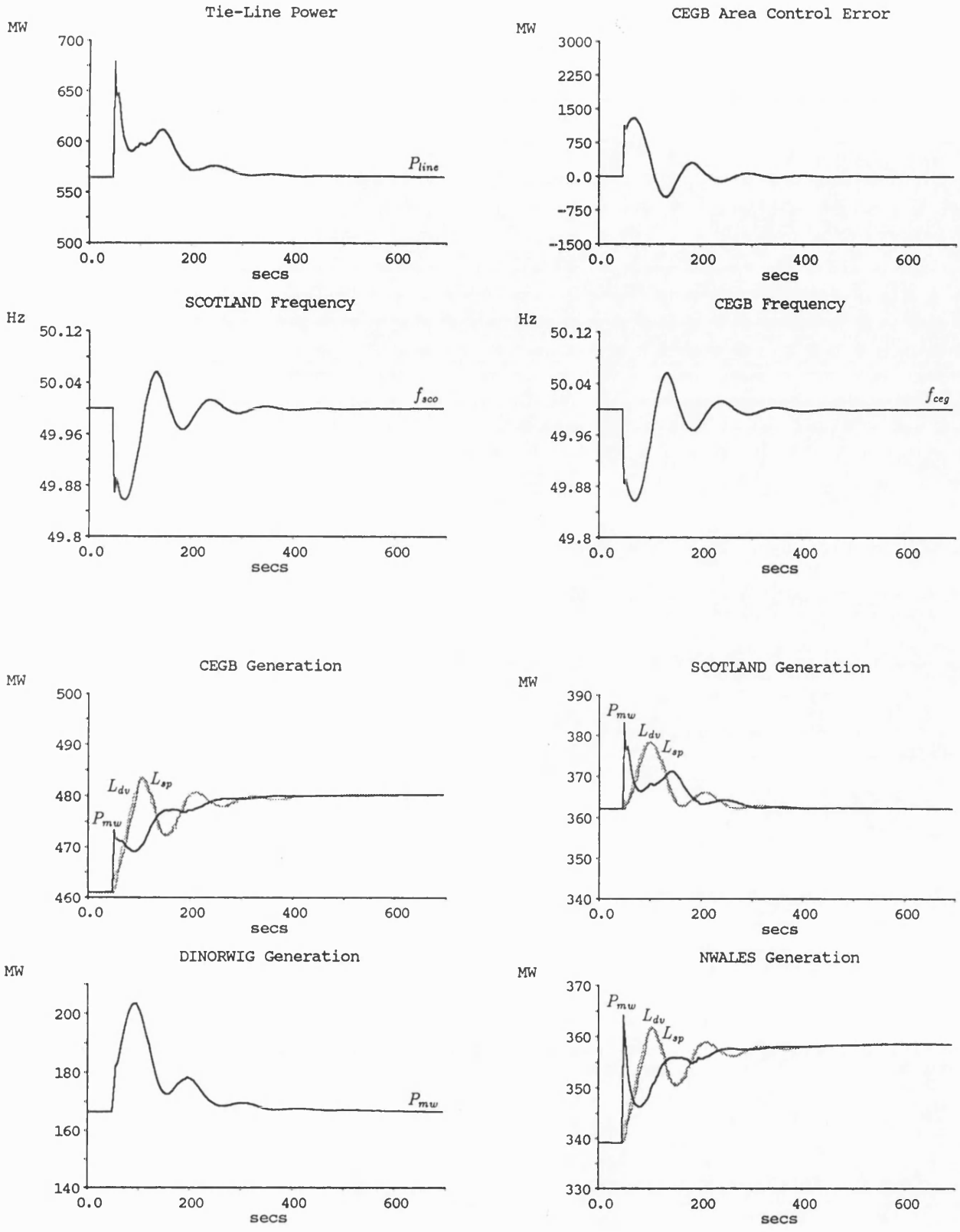

Figure 6.42: (a) 4 m'c Step Load Increase busbar CEGB4 (Run 25)

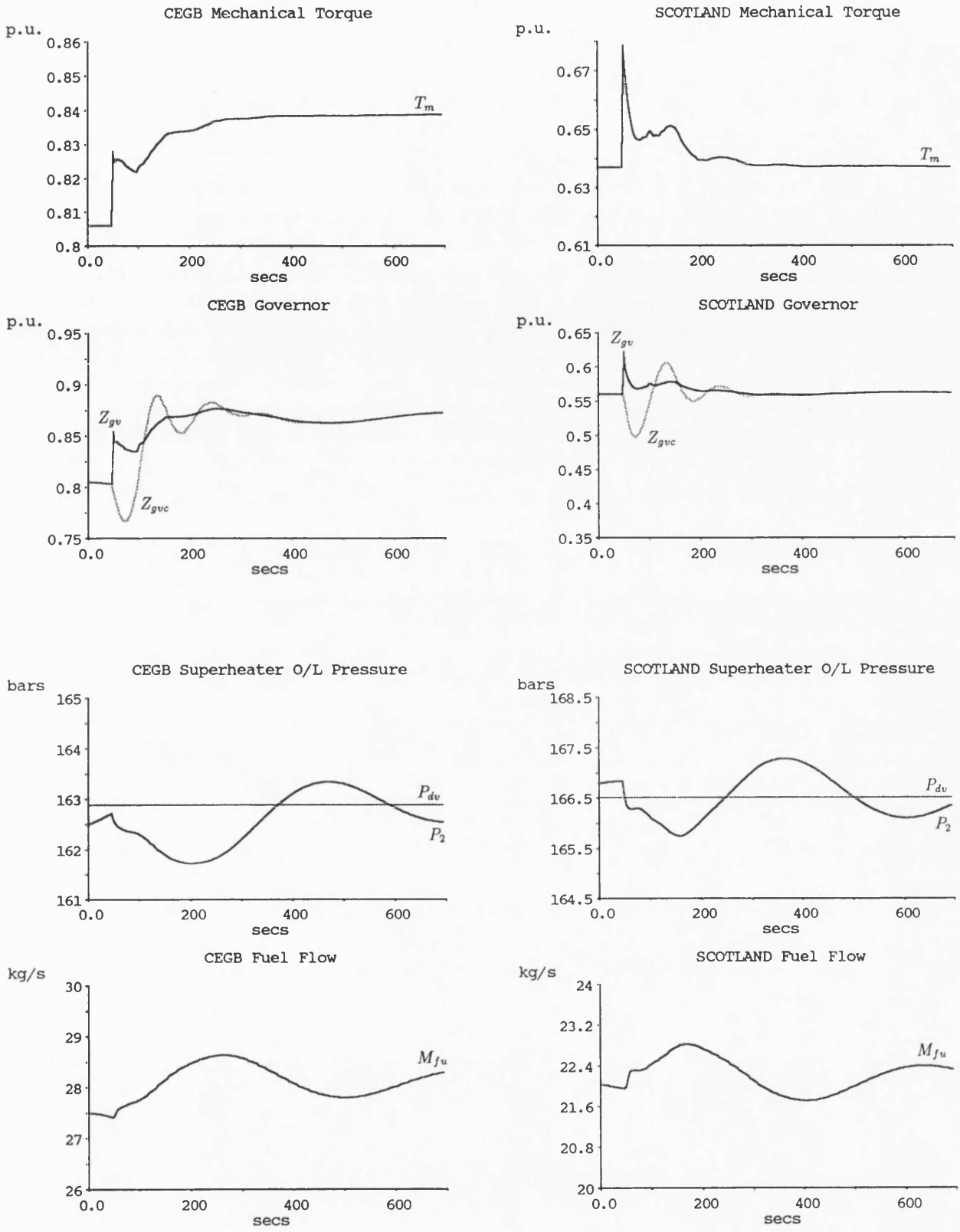

Figure 6.42: (b) 4 m'c Step Load Increase busbar CEGB4 (Run 25)

5 Fig 6:42(b)

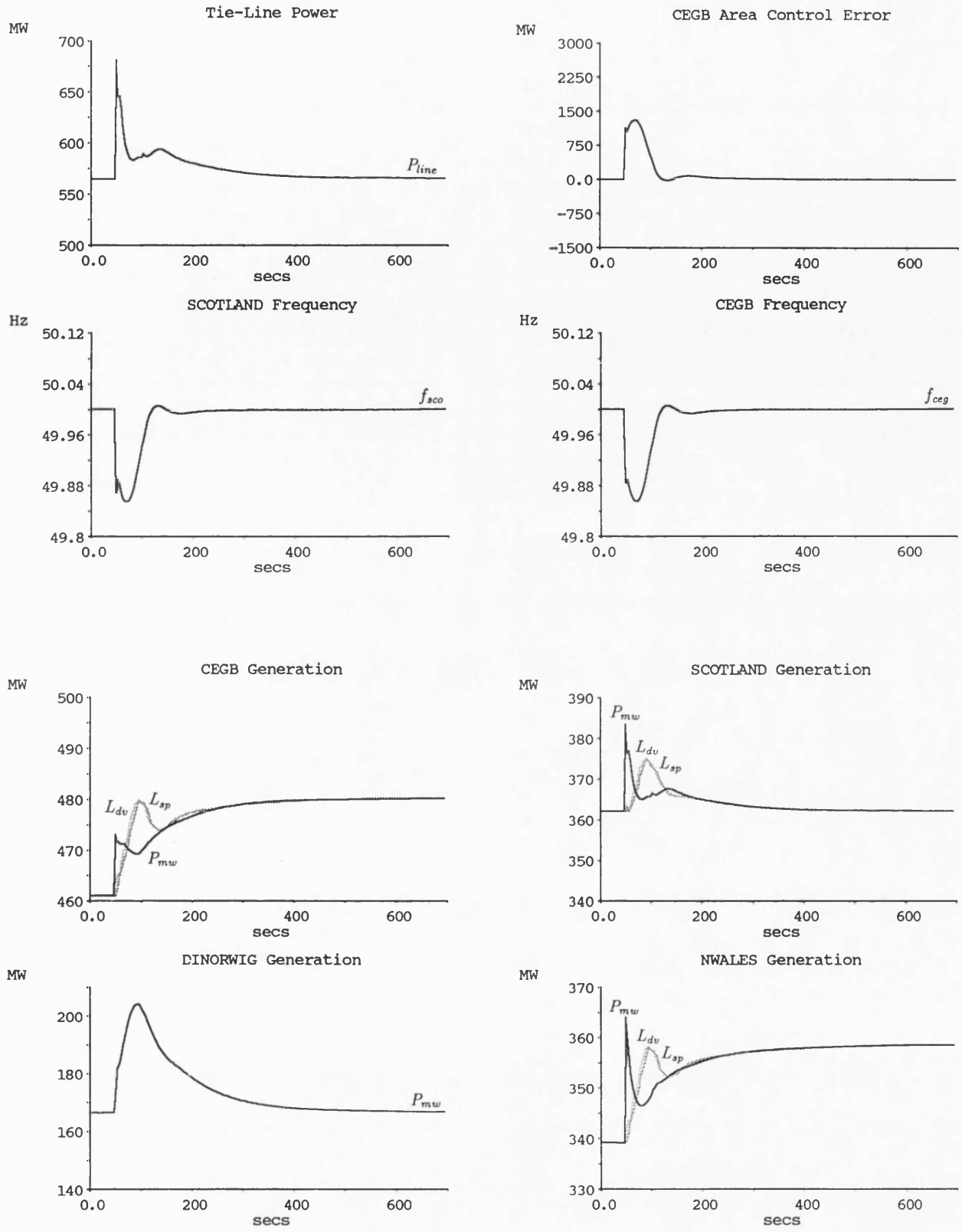

Figure 6.43: (a) 4 m'c Step Load Increase busbar CEGB4 (Run 26)

26 Fig 6.43(a)

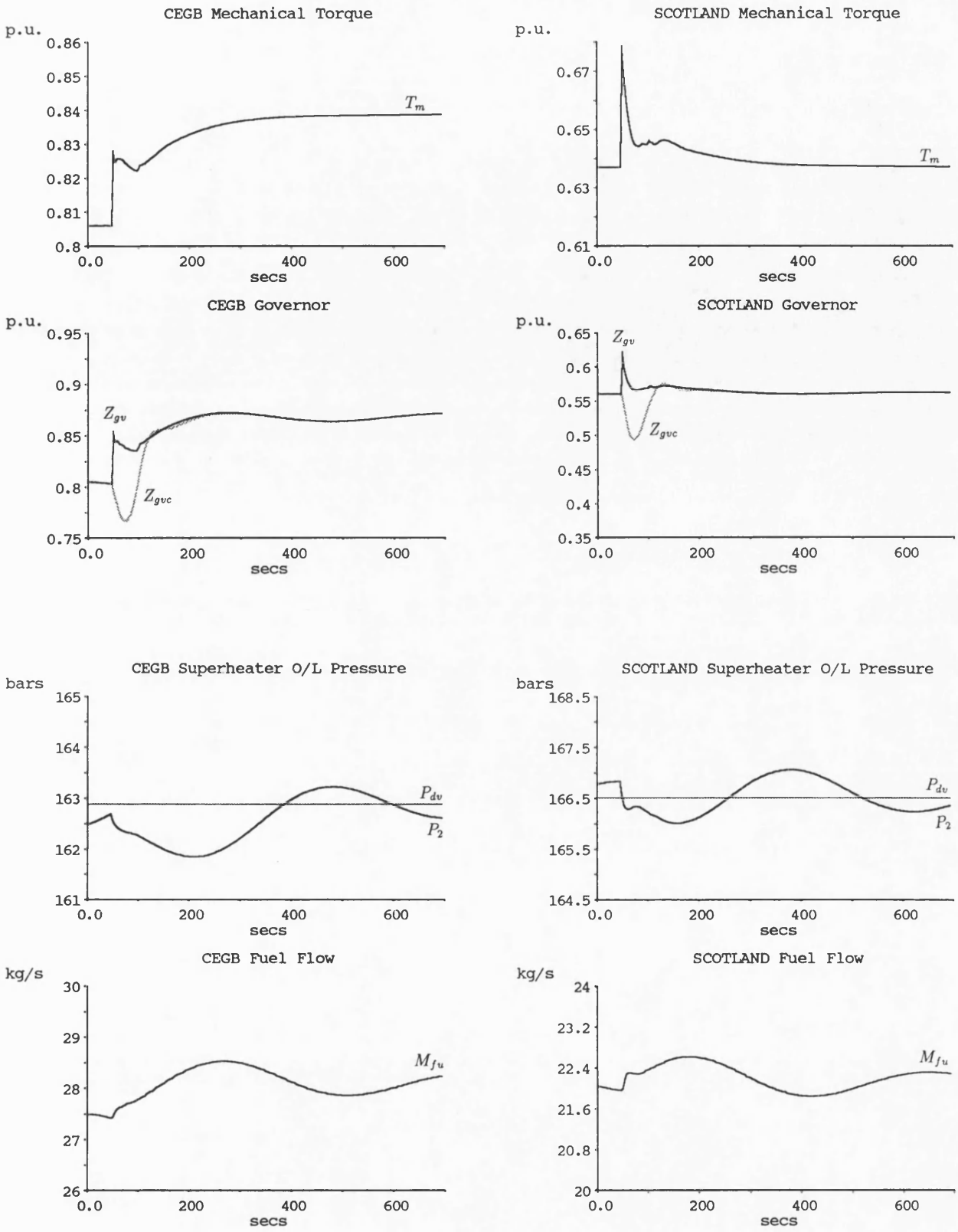

Figure 6.43: (b) 4 m'c Step Load Increase busbar CEGB4 (Run 26)

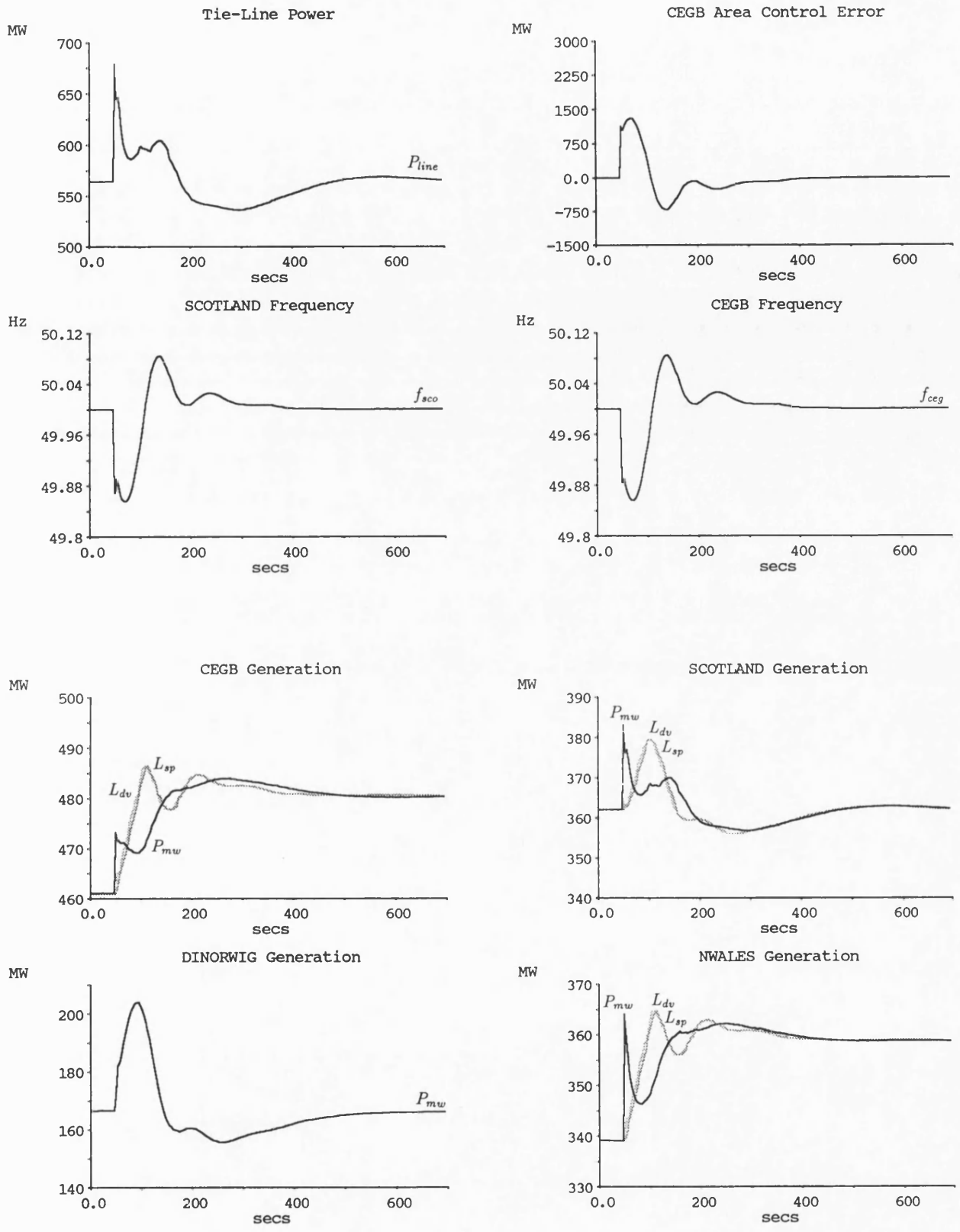

Figure 6.44: (a) 4 m'c Step Load Increase busbar CEGB4 (Run 27)

27 Fig 6.44(a)

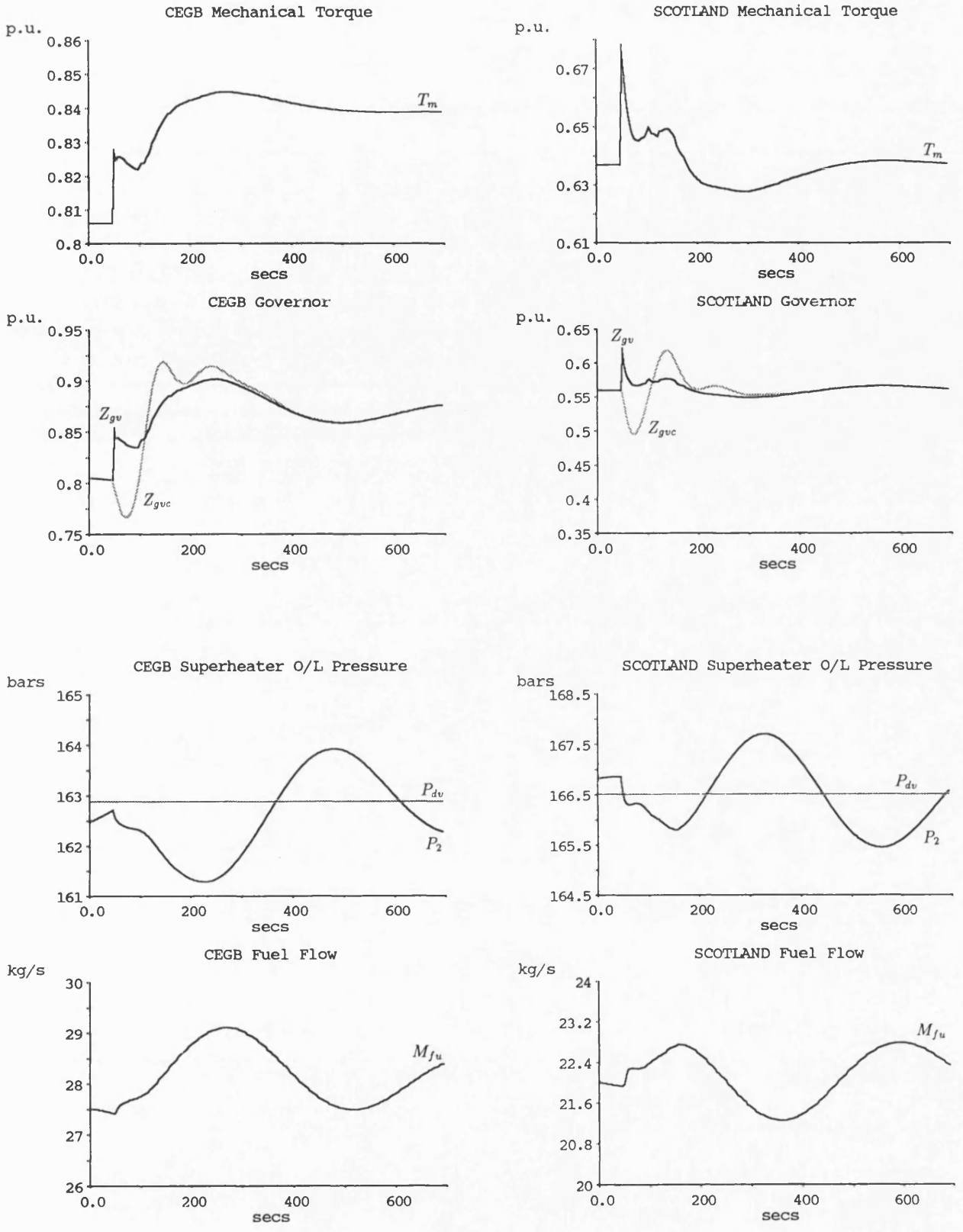

Figure 6.44: (b) 4 m'c Step Load Increase busbar CEGB4 (Run 27)

Eg 6.44(b)

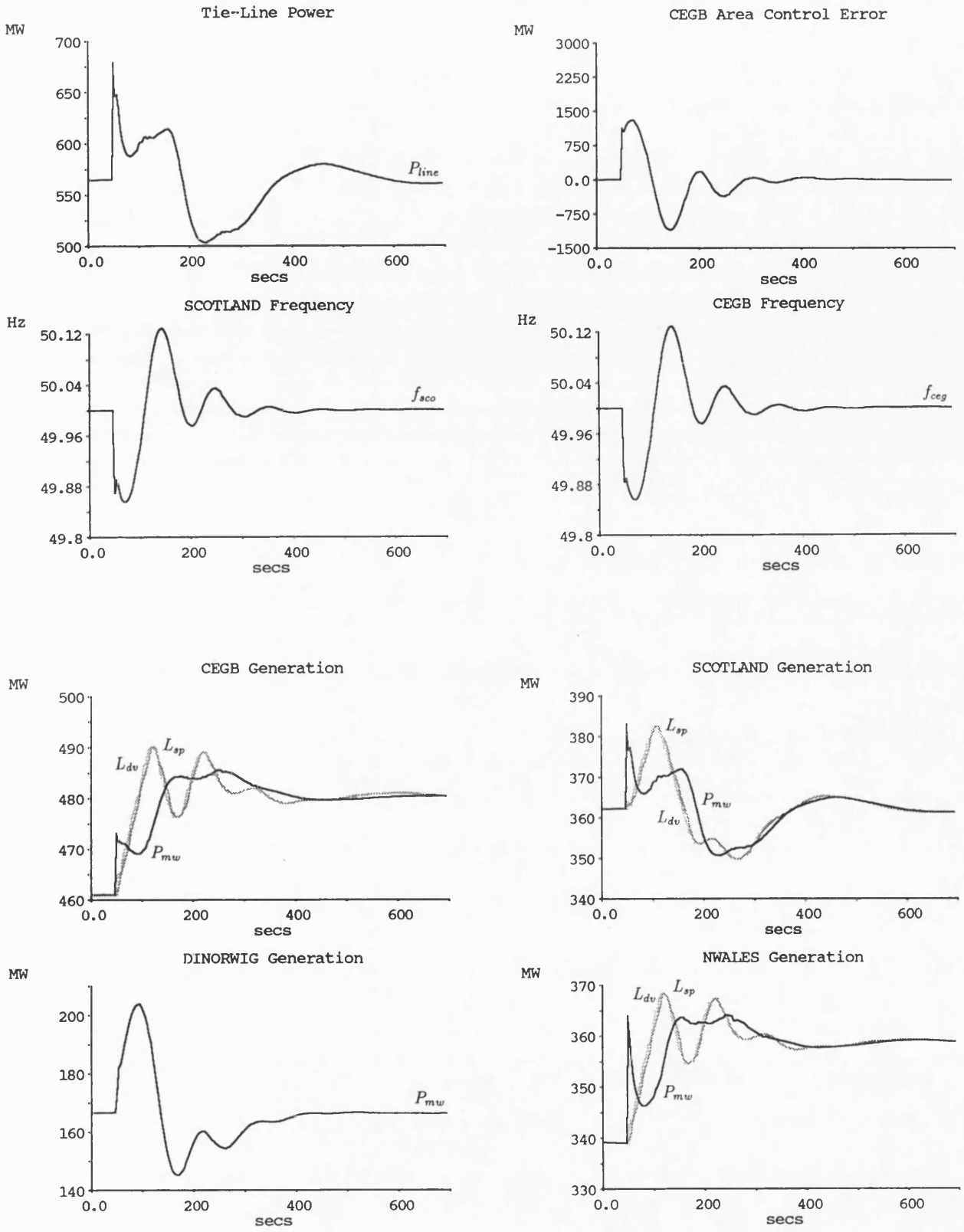

Figure 6.45: (a) 4 m'c Step Load Increase busbar CEGB4 (Run 28)

28 fig 6.45(a)

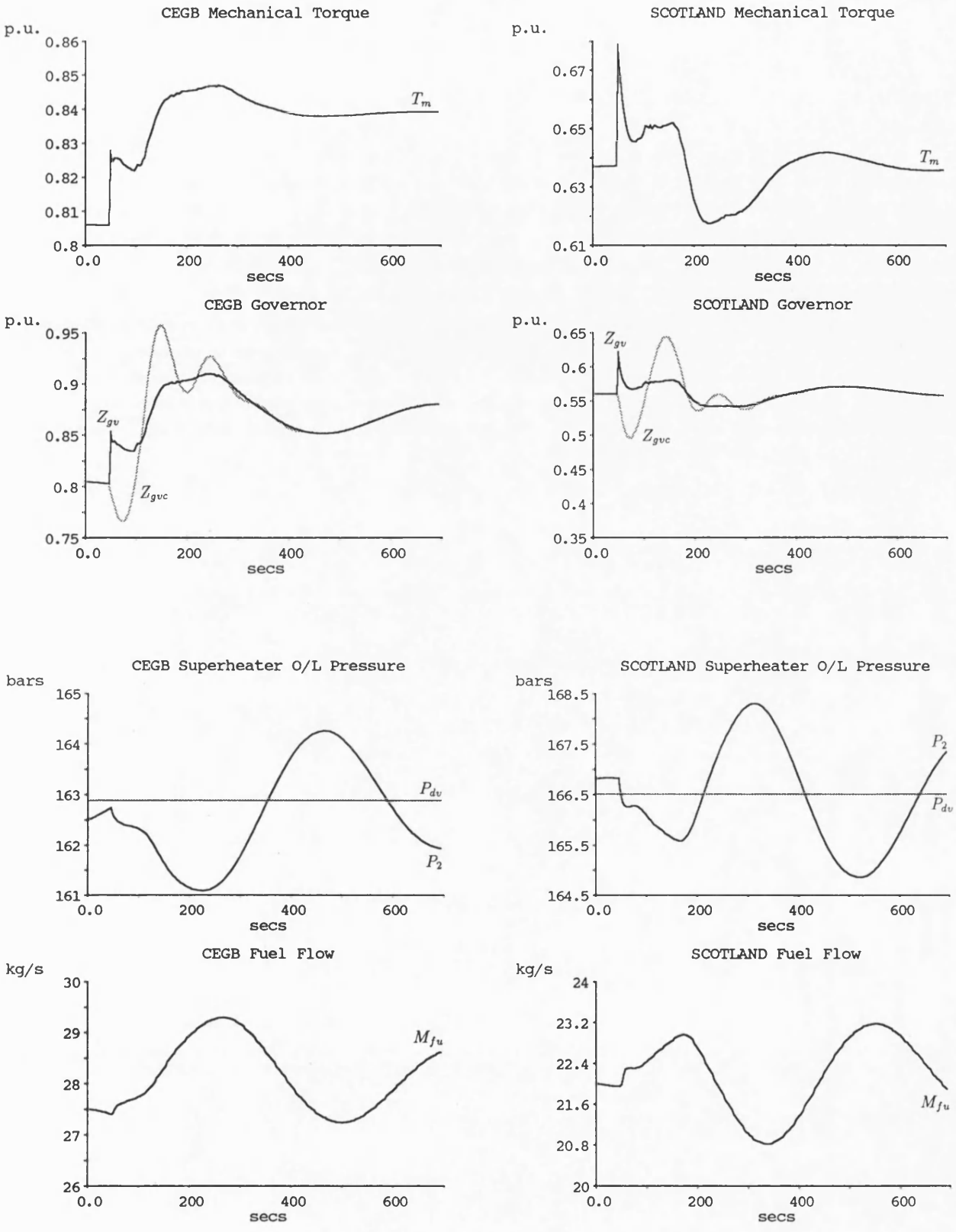

Figure 6.45: (b) 4 m'c Step Load Increase busbar CEGB4 (Run 28)

28 fig 6.45(b)

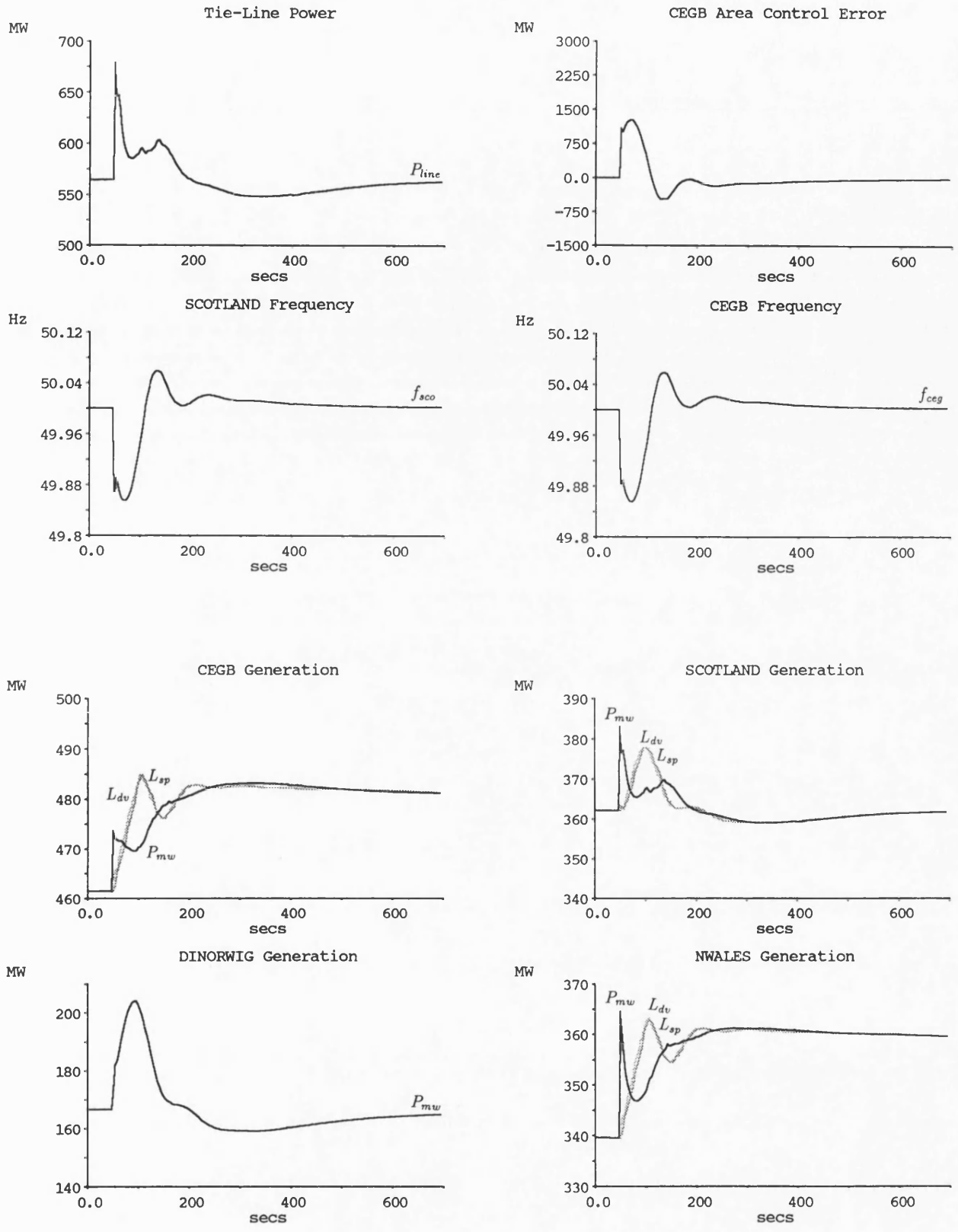

Figure 6.46: (a) 4 m'c Step Load Increase busbar CEGB4 (Run 29)

29 Rgb.46(a)

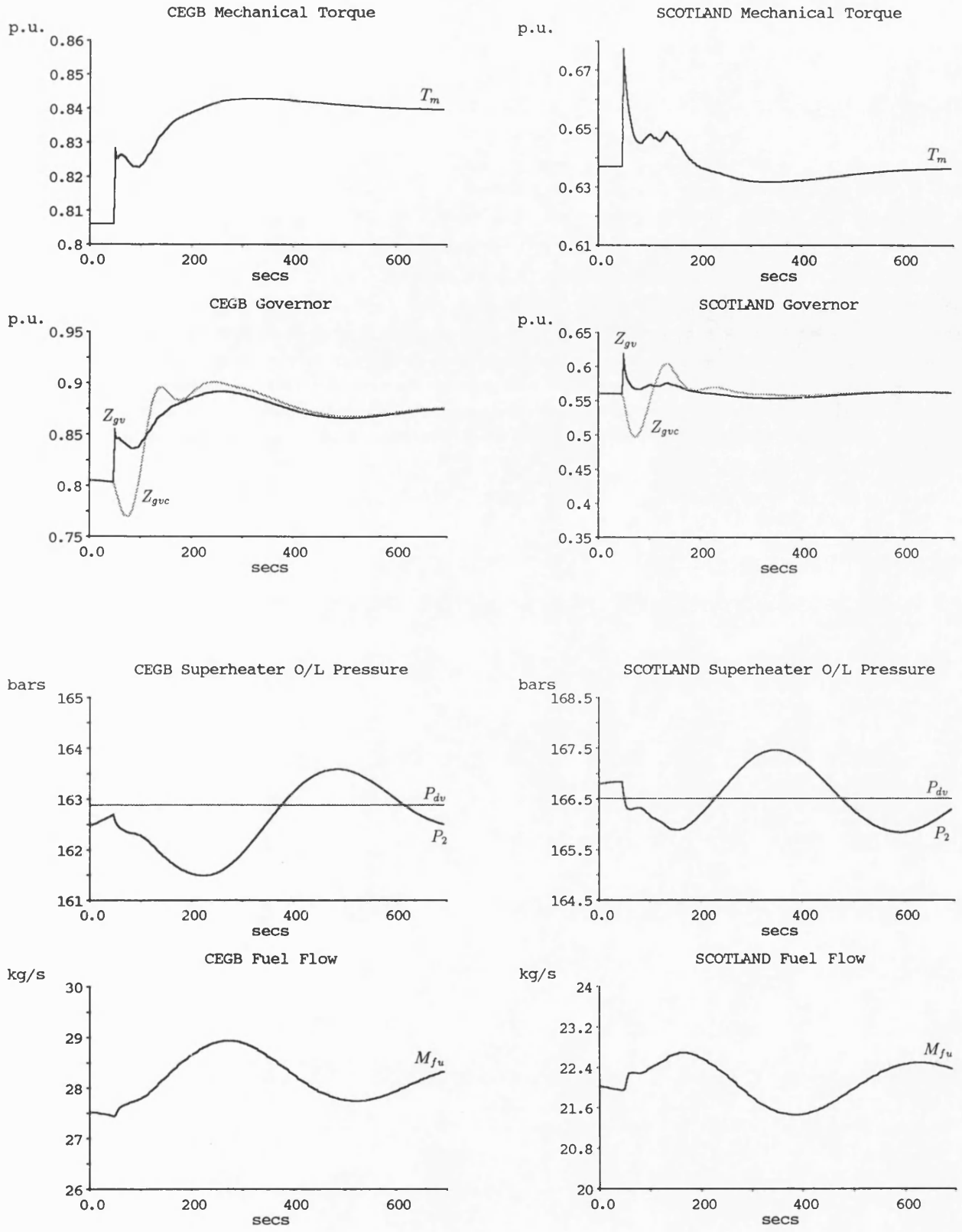

Figure 6.46: (b) 4 m'c Step Load Increase busbar CEGB4 (Run 29)

Eg 6.46(b)

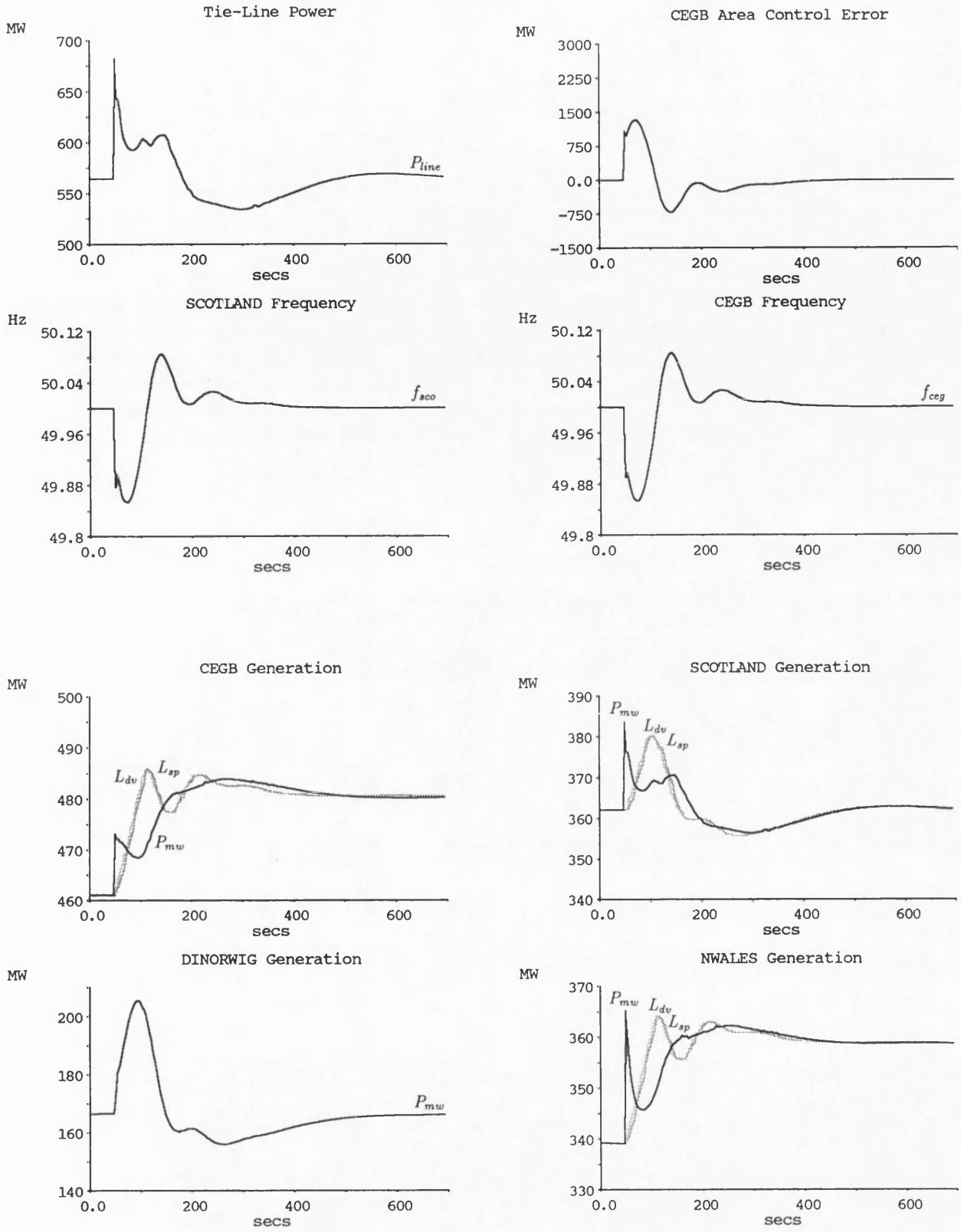

Figure 6.47: (a) 4 m'c Step Load Increase busbar CEGB4 (Run 30)

50 Fig 6.47(a)

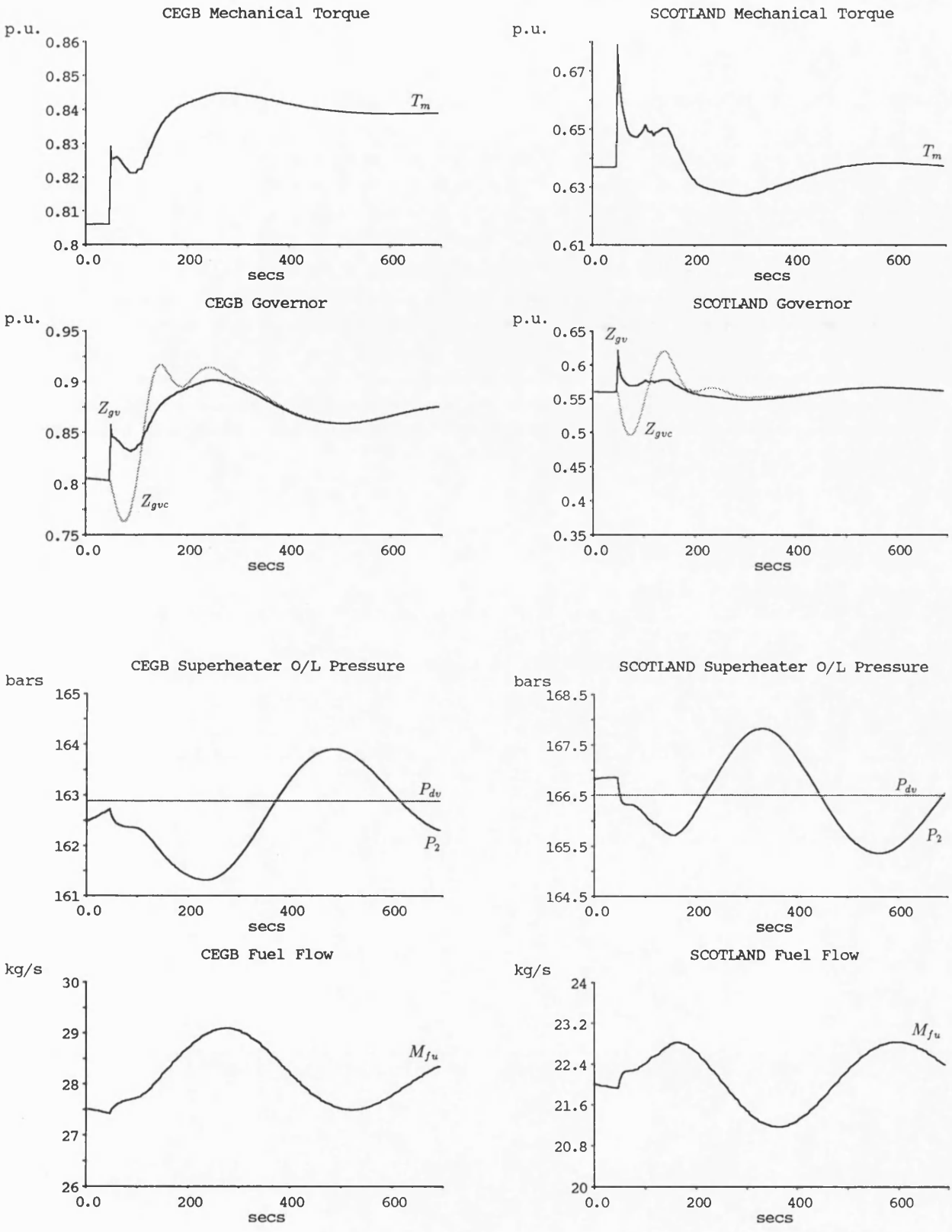

Figure 6.47: (b) 4 m'c Step Load Increase busbar CEGB4 (Run 30)

30 fig 6.47(b)

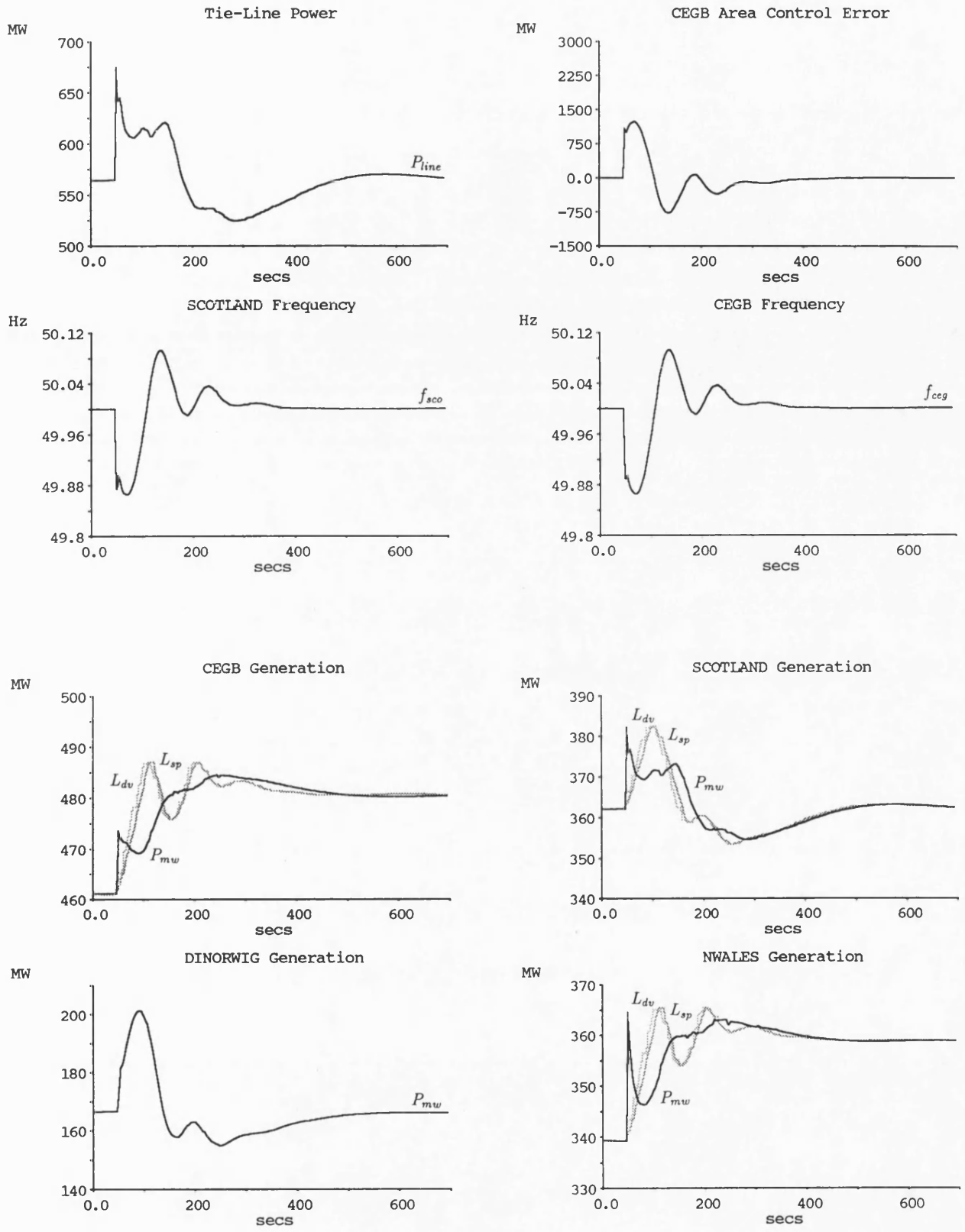

Figure 6.48: (a) 4 m'c Step Load Increase busbar CEGB4 (Run 32)

32 fig 6.48(a)

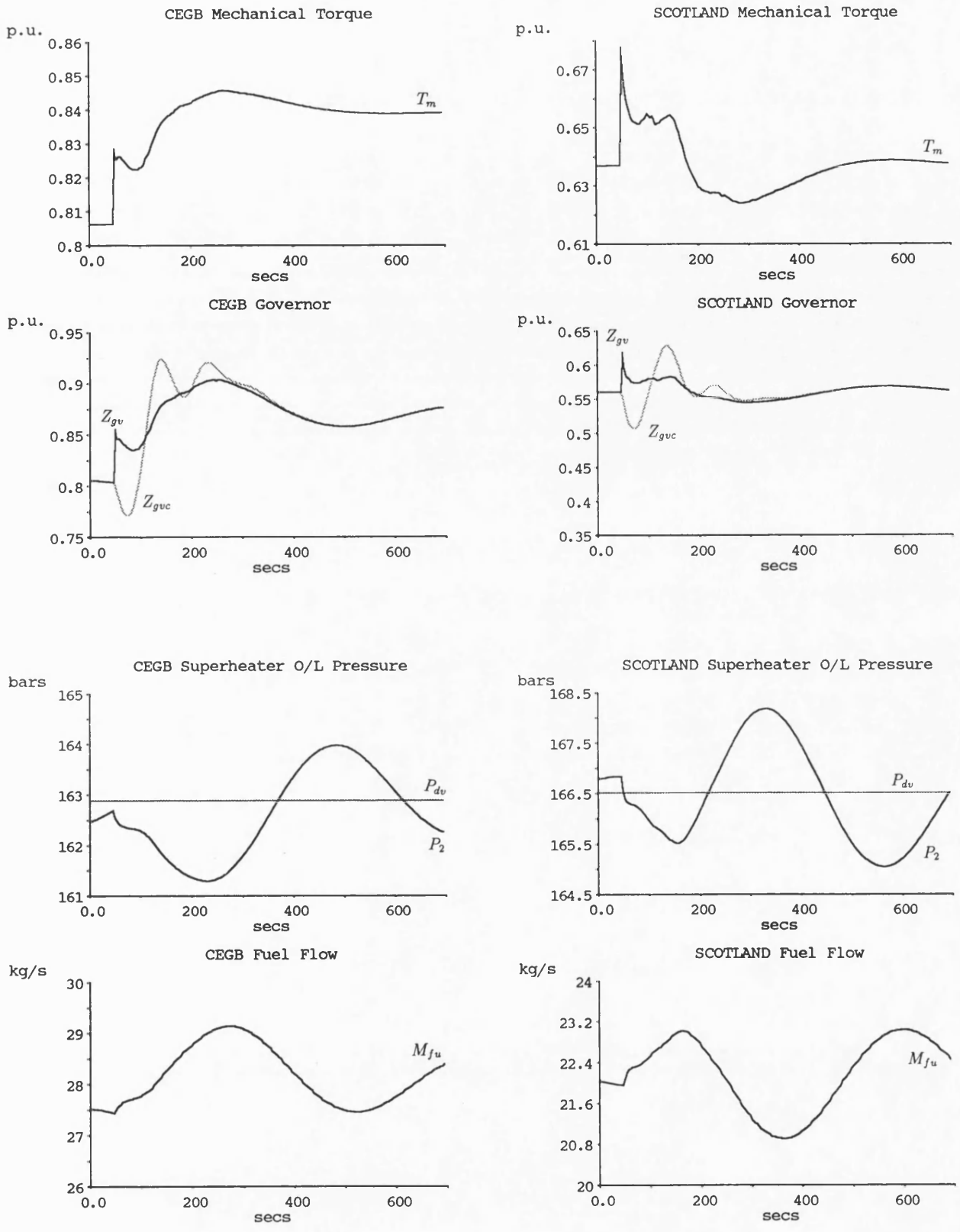

Figure 6.48: (b) 4 m'c Step Load Increase busbar CEGB4 (Run 32)

.2 fig 6.48(b)

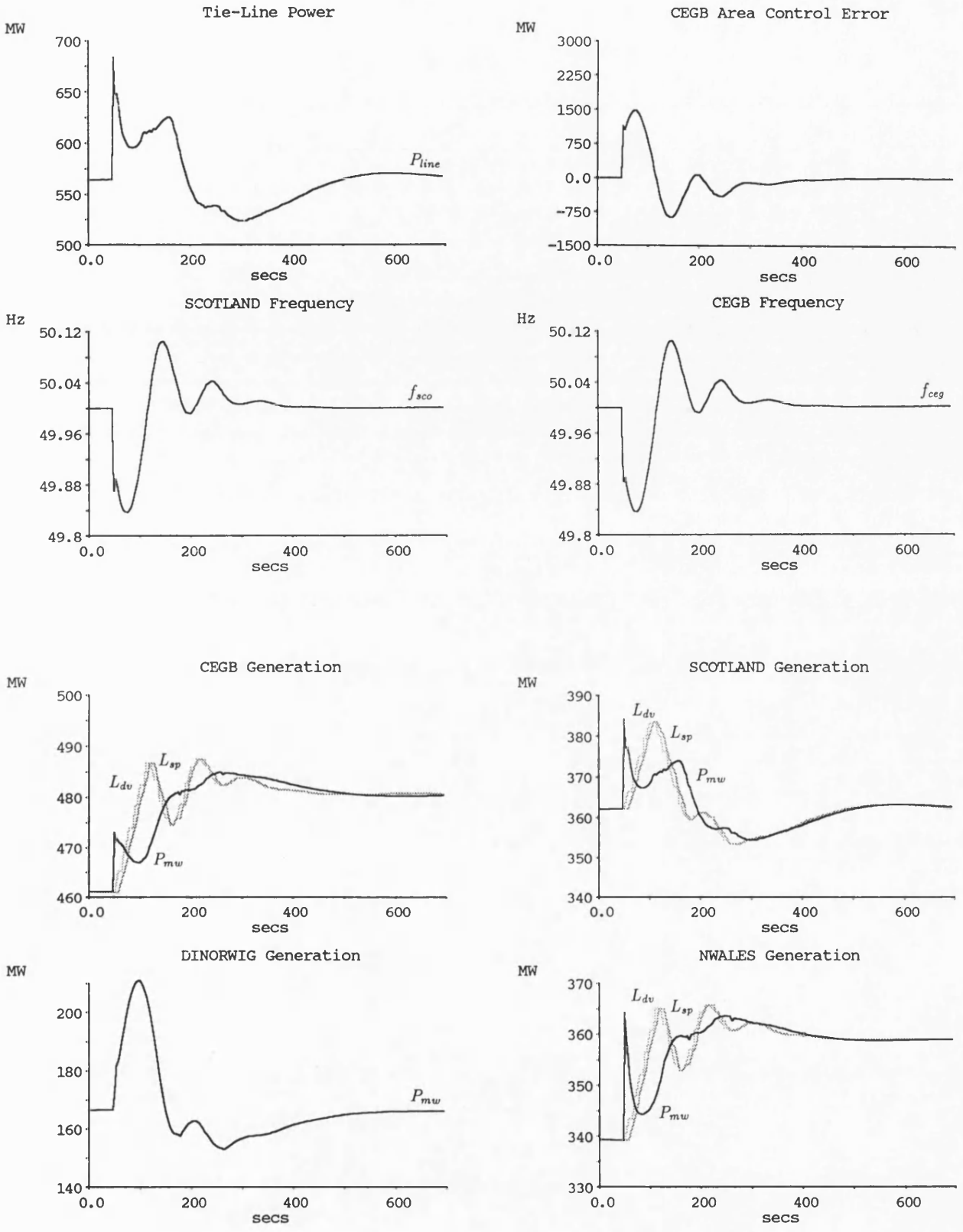

Figure 6.49: (a) 4 m'c Step Load Increase busbar CEGB4 (Run 31)

31 Fig 6.4 9(a)

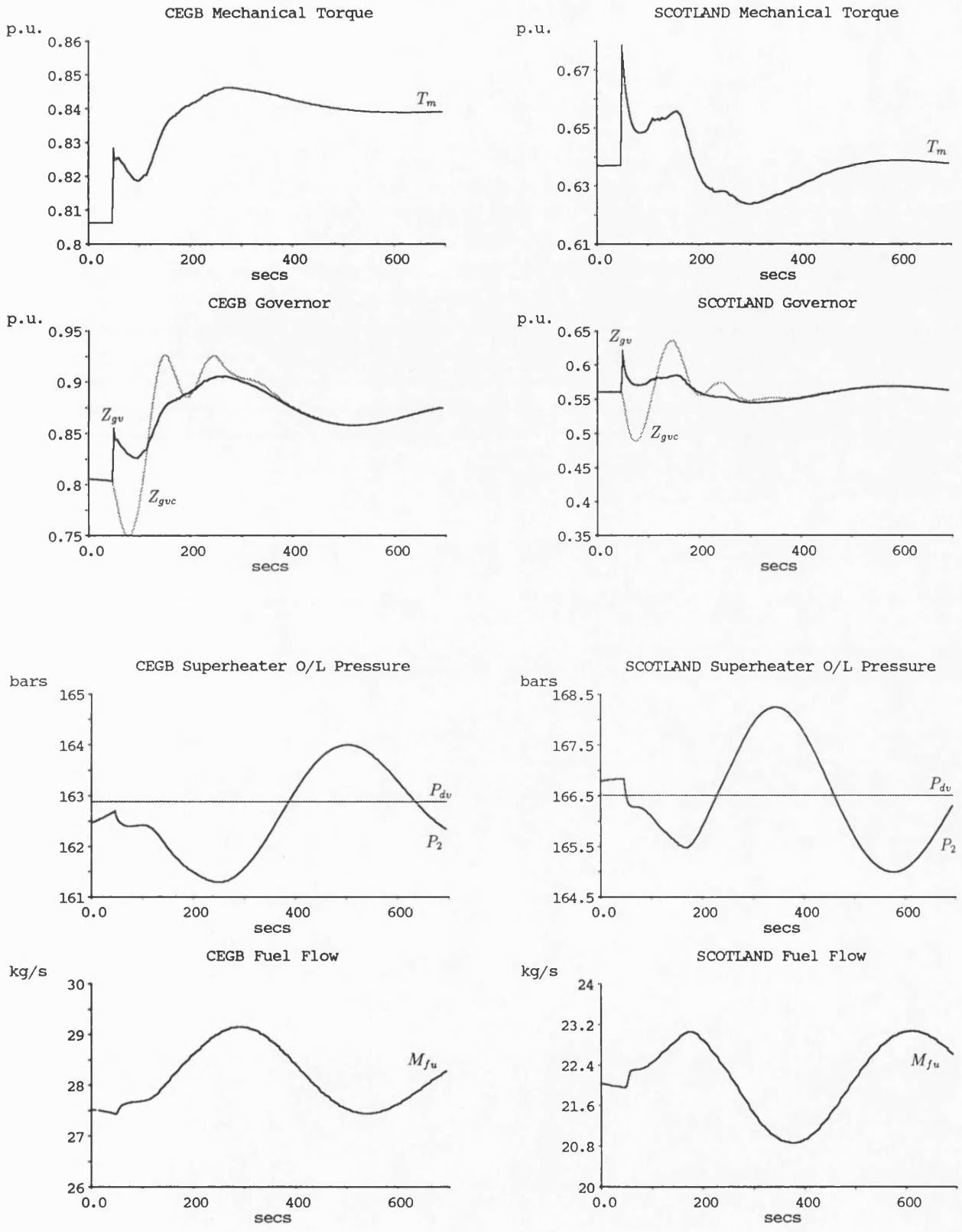

Figure 6.49: (b) 4 m'c Step Load Increase busbar CEGB4 (Run 31)

31 Fig 6.49(b)

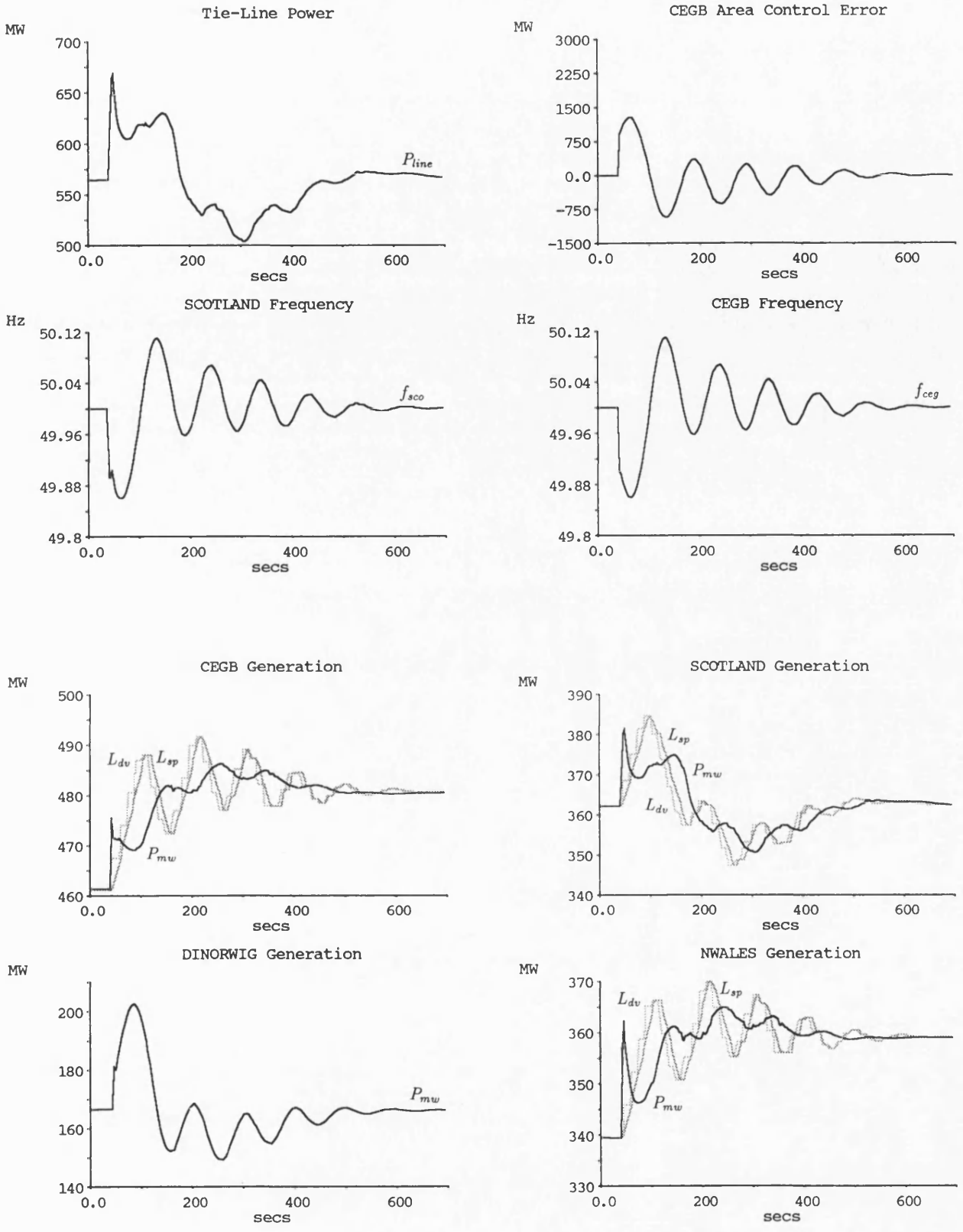

Figure 6.50: (a) 4 m'c Step Load Increase busbar CEGB4 (Run 36a)

36a Fig 6.50(a)

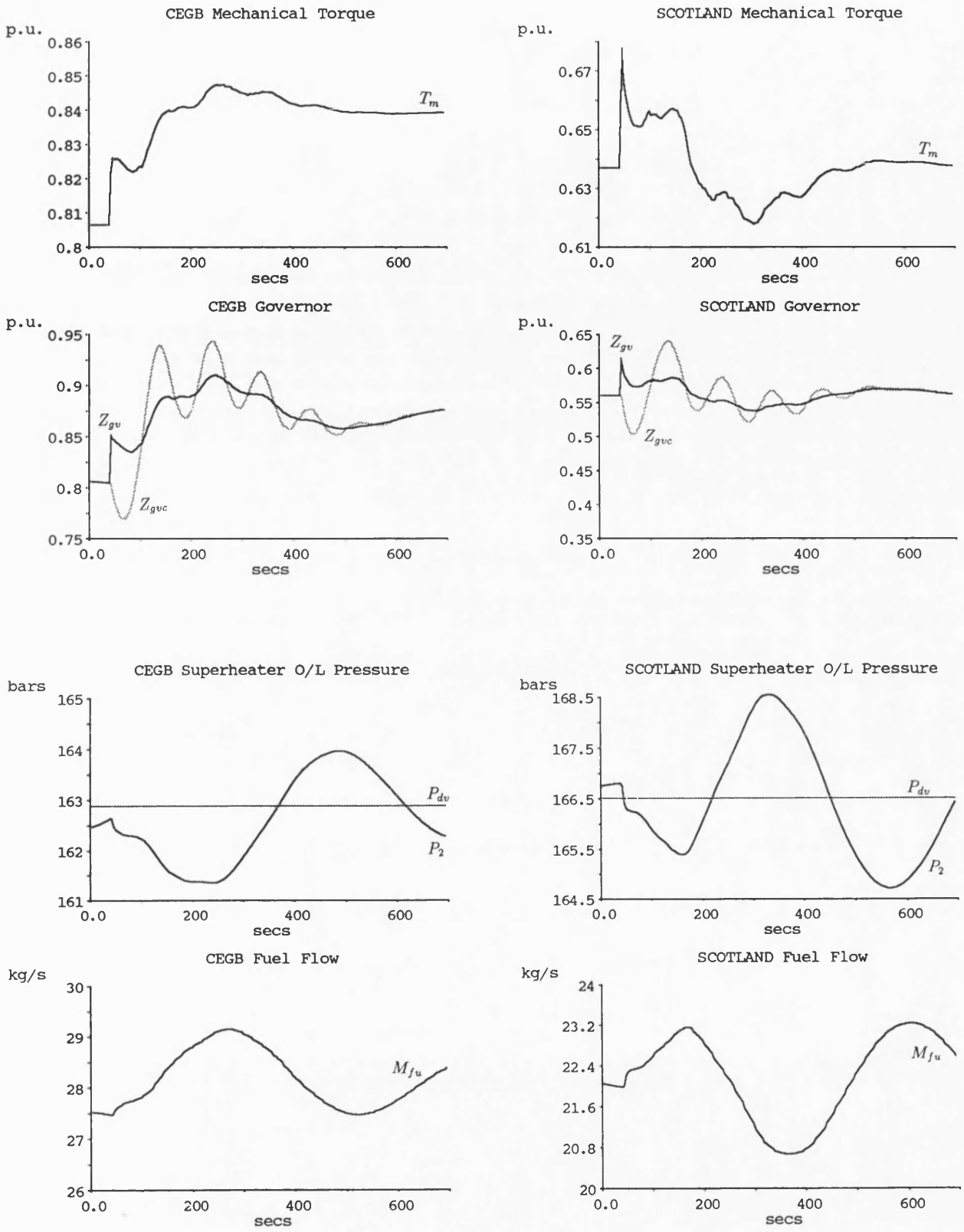

Figure 6.50: (b) 4 m'c Step Load Increase busbar CEGB4 (Run 36a)

36a Fig 6.50(b)

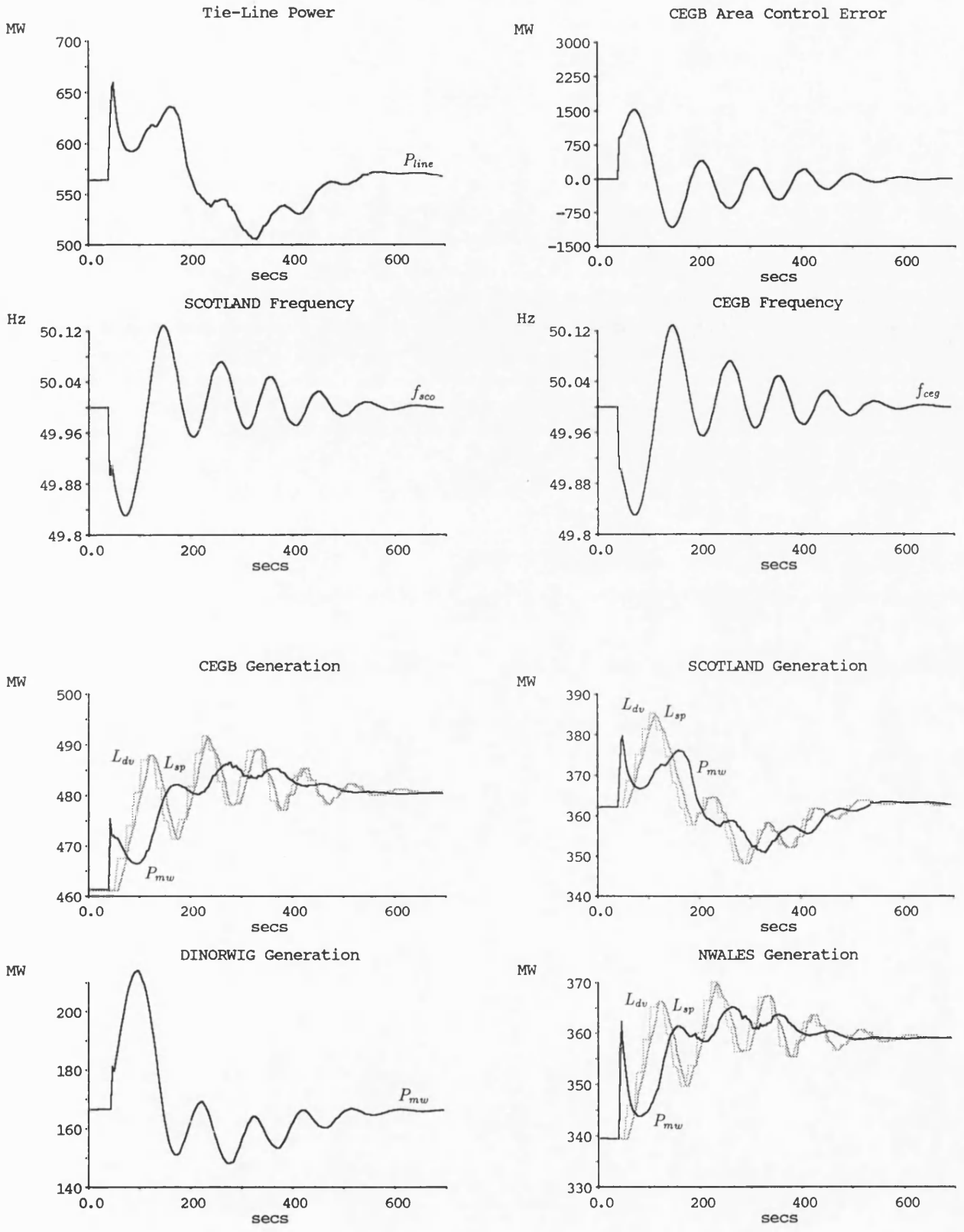

Figure 6.51: (a) 4 m'c Step Load Increase busbar CEGB4 (Run 35a)

35a Fig 6.51(a)

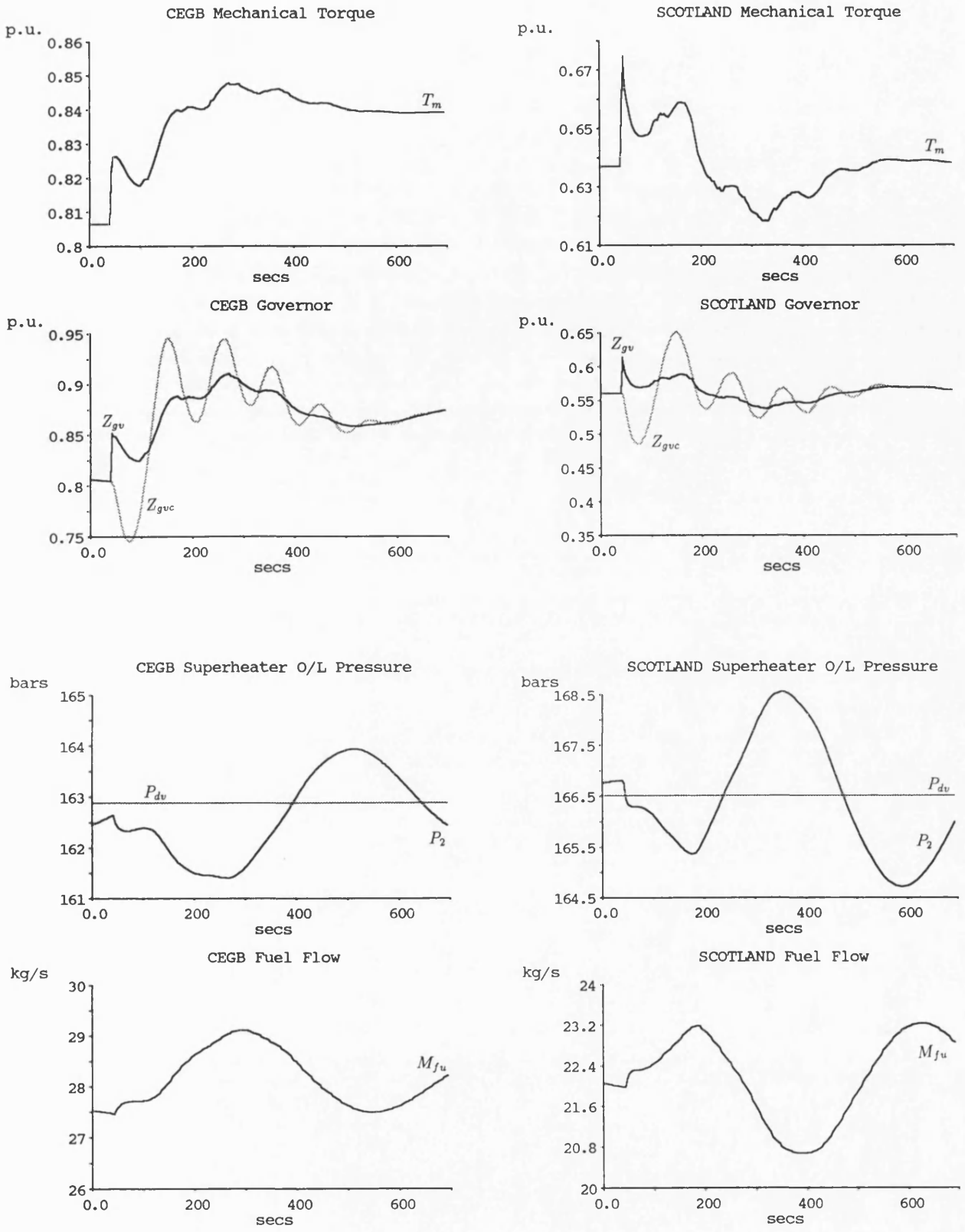

Figure 6.51: (b) 4 m'c Step Load Increase busbar CEGB4 (Run 35a)

35a Fig 6.51(b)

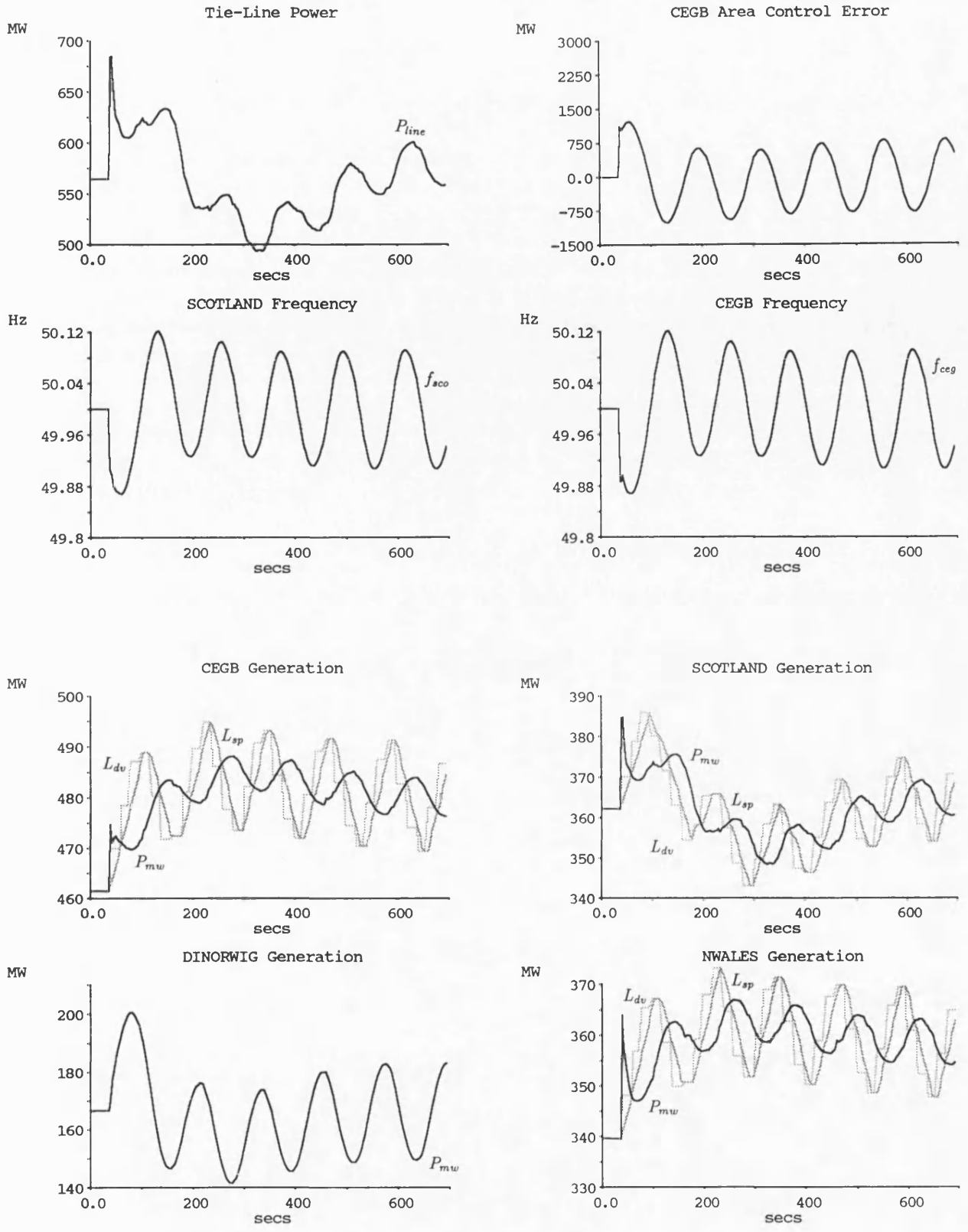

Figure 6.52: (a) 4 m'c Step Load Increase busbar CEGB4 (Run 33)

33 fg 6.52(a)

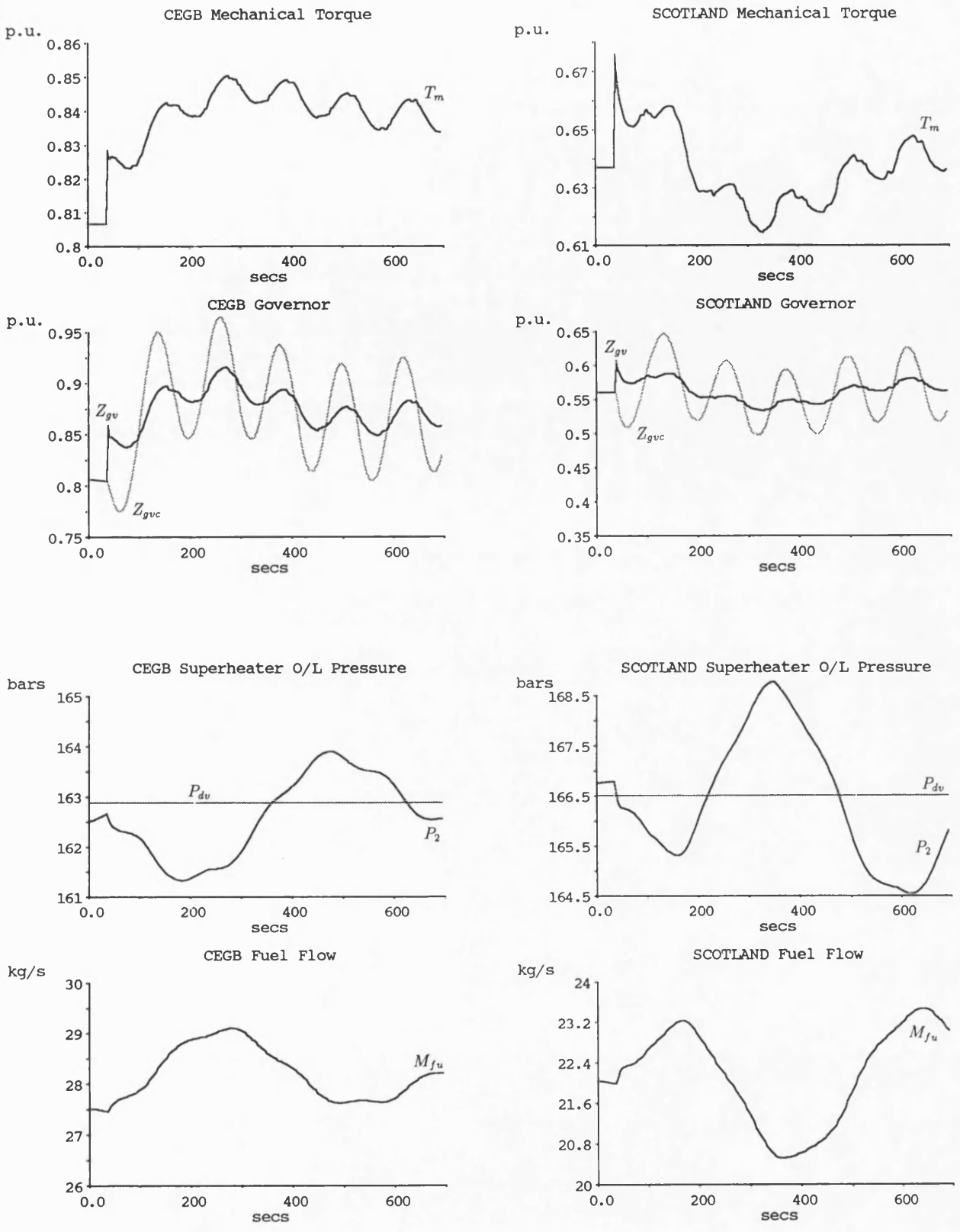

Figure 6.52: (b) 4 m'c Step Load Increase busbar CEGB4 (Run 33)

33 Fig 6.52(b)

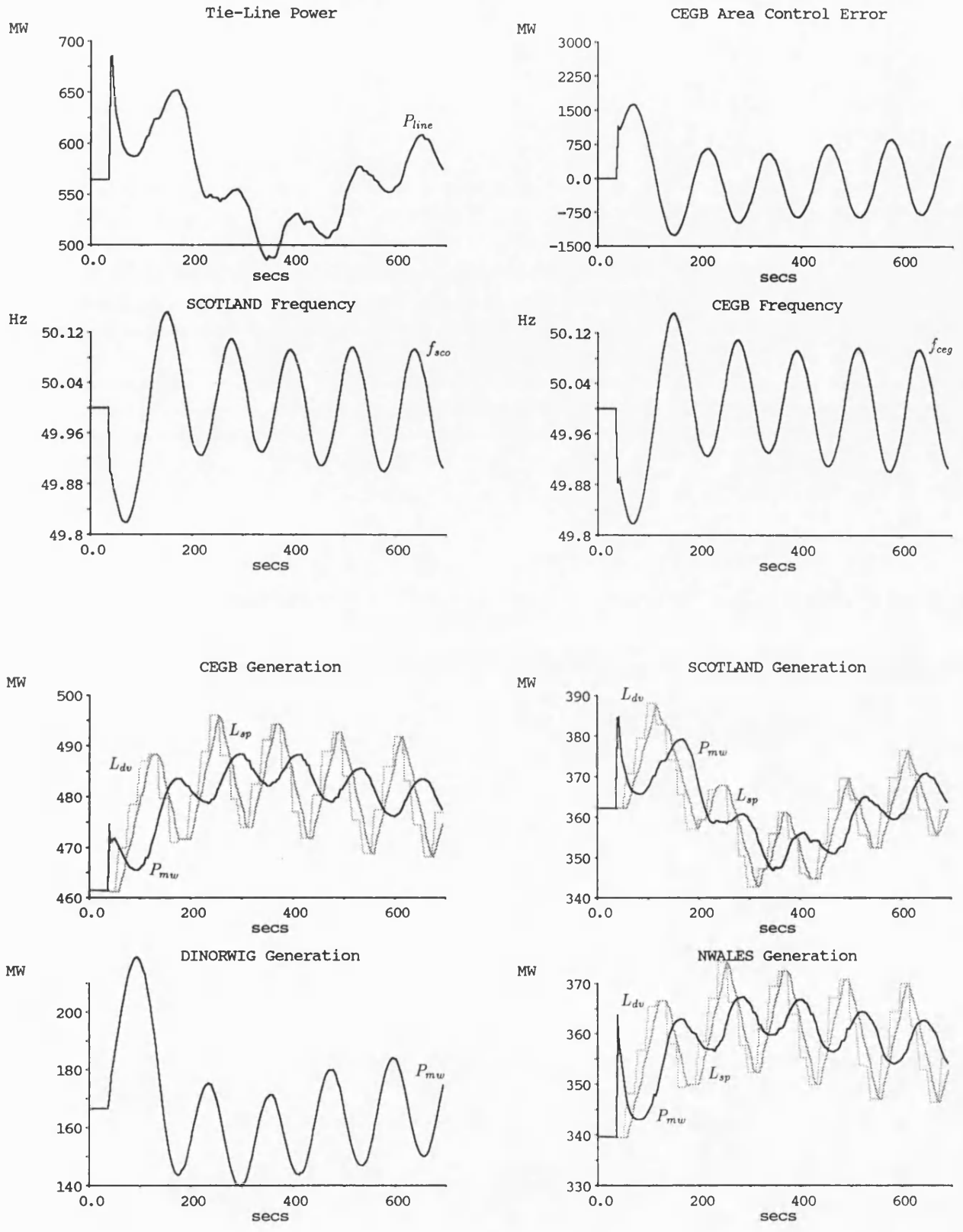

Figure 6.53: (a) 4 m'c Step Load Increase busbar CEGB4 (Run 34)

34 fg 6.53(a)

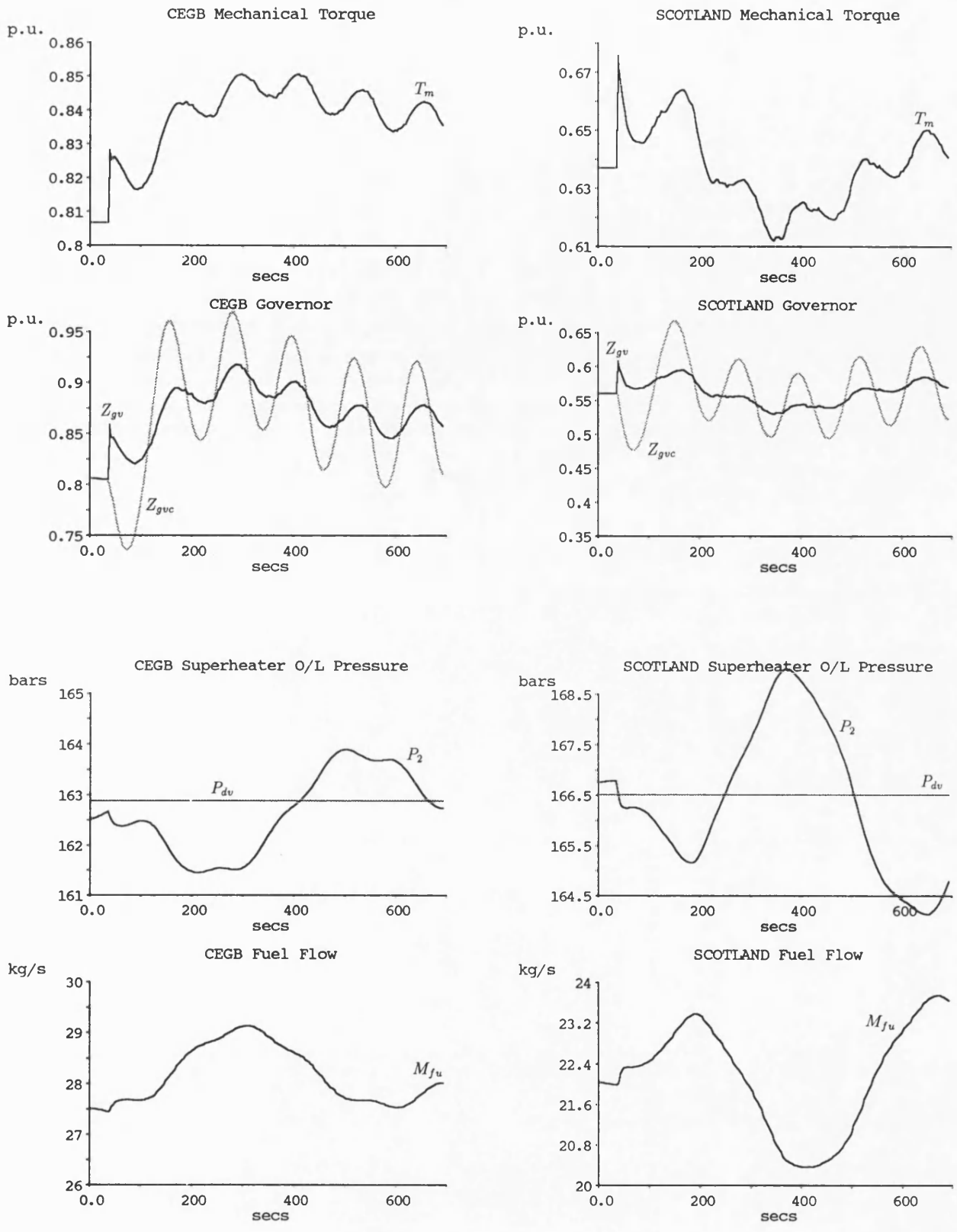

Figure 6.53: (b) 4 m'c Step Load Increase busbar CEGB4 (Run 34)

4 Fig 6.53(b)

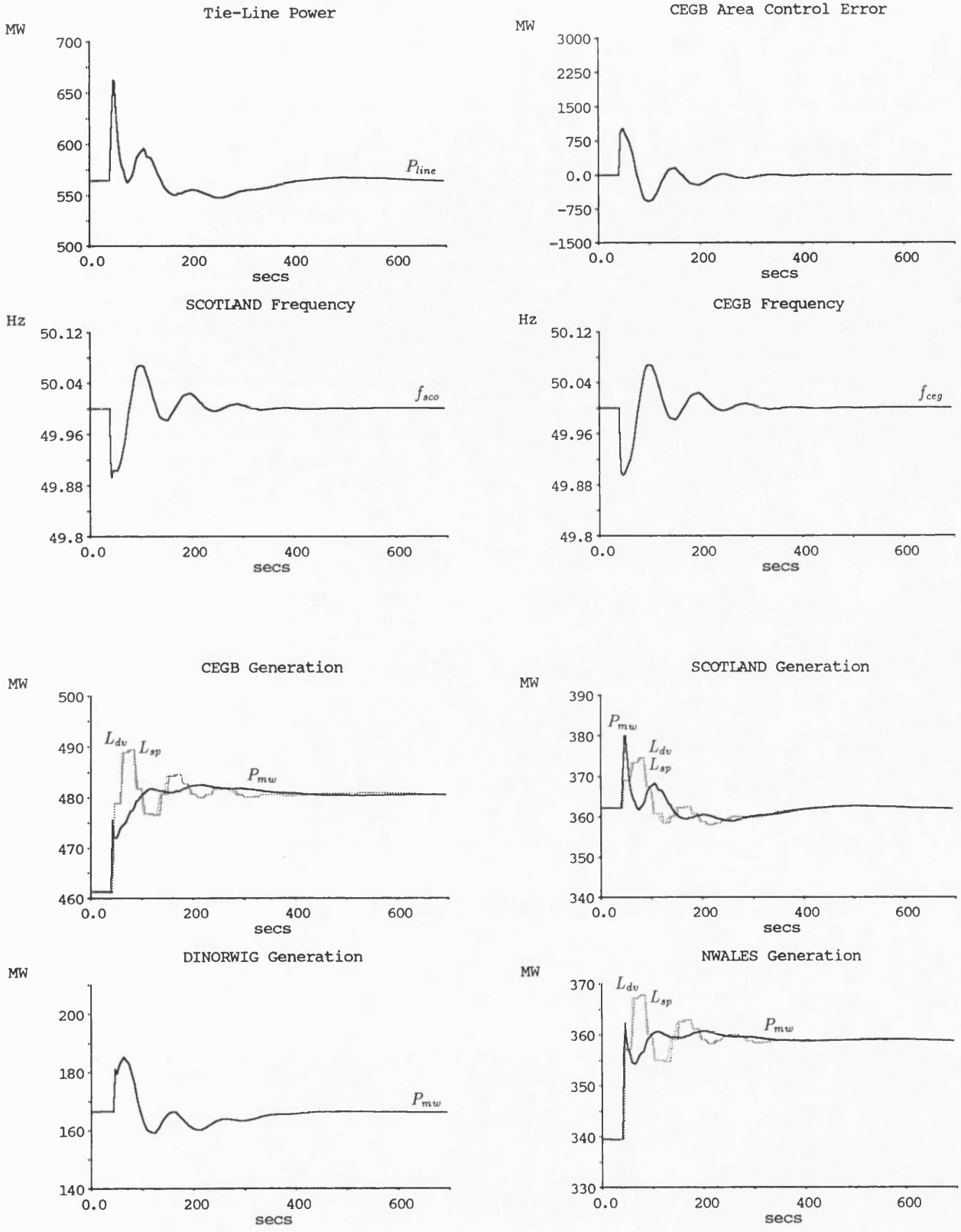

Figure 6.54: (a) 4 m'c Step Load Increase busbar CEGB4 (Run 36b)

366 Fig 6.54(a)

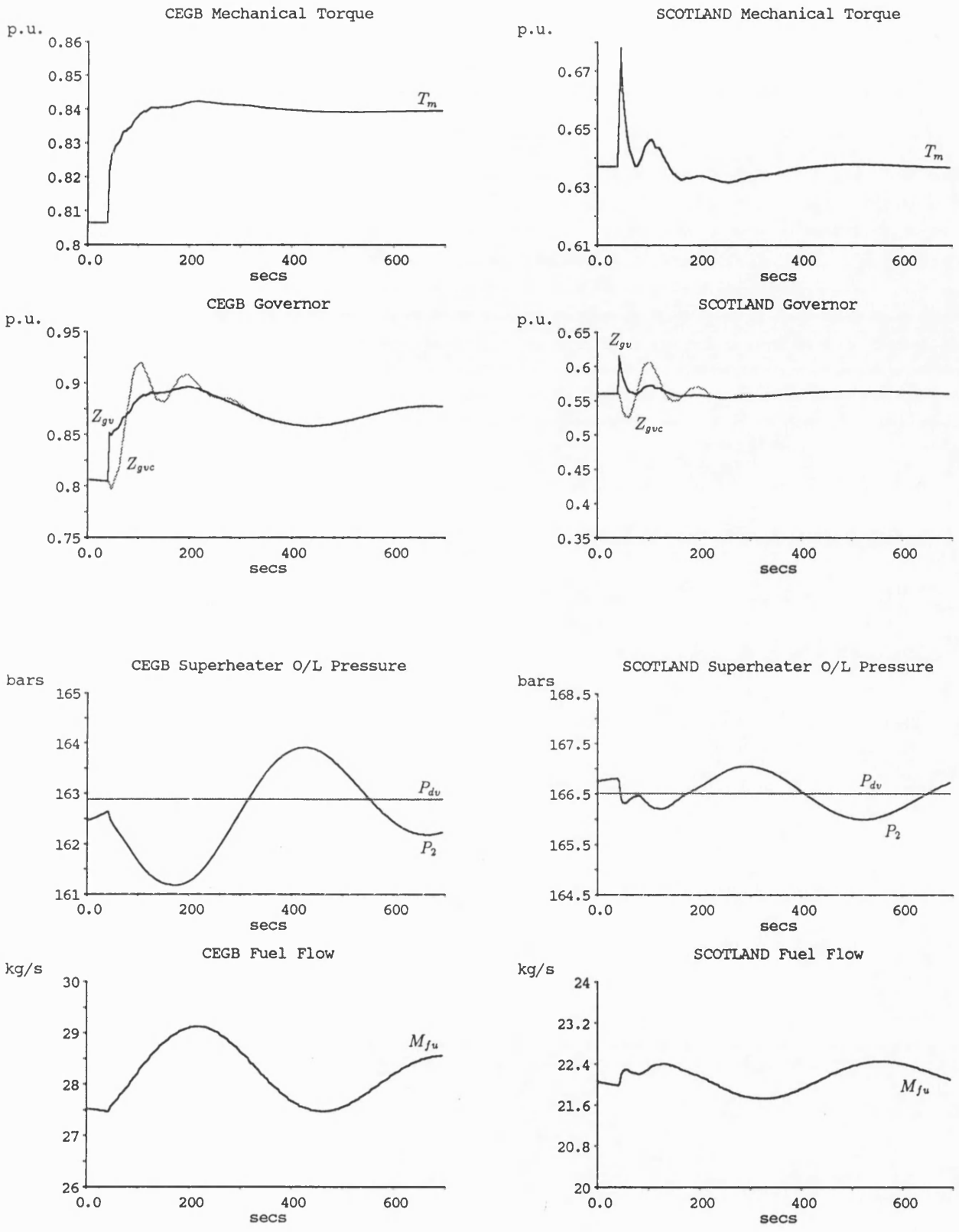

Figure 6.54: (b) 4 m'c Step Load Increase busbar CEGB4 (Run 36b)

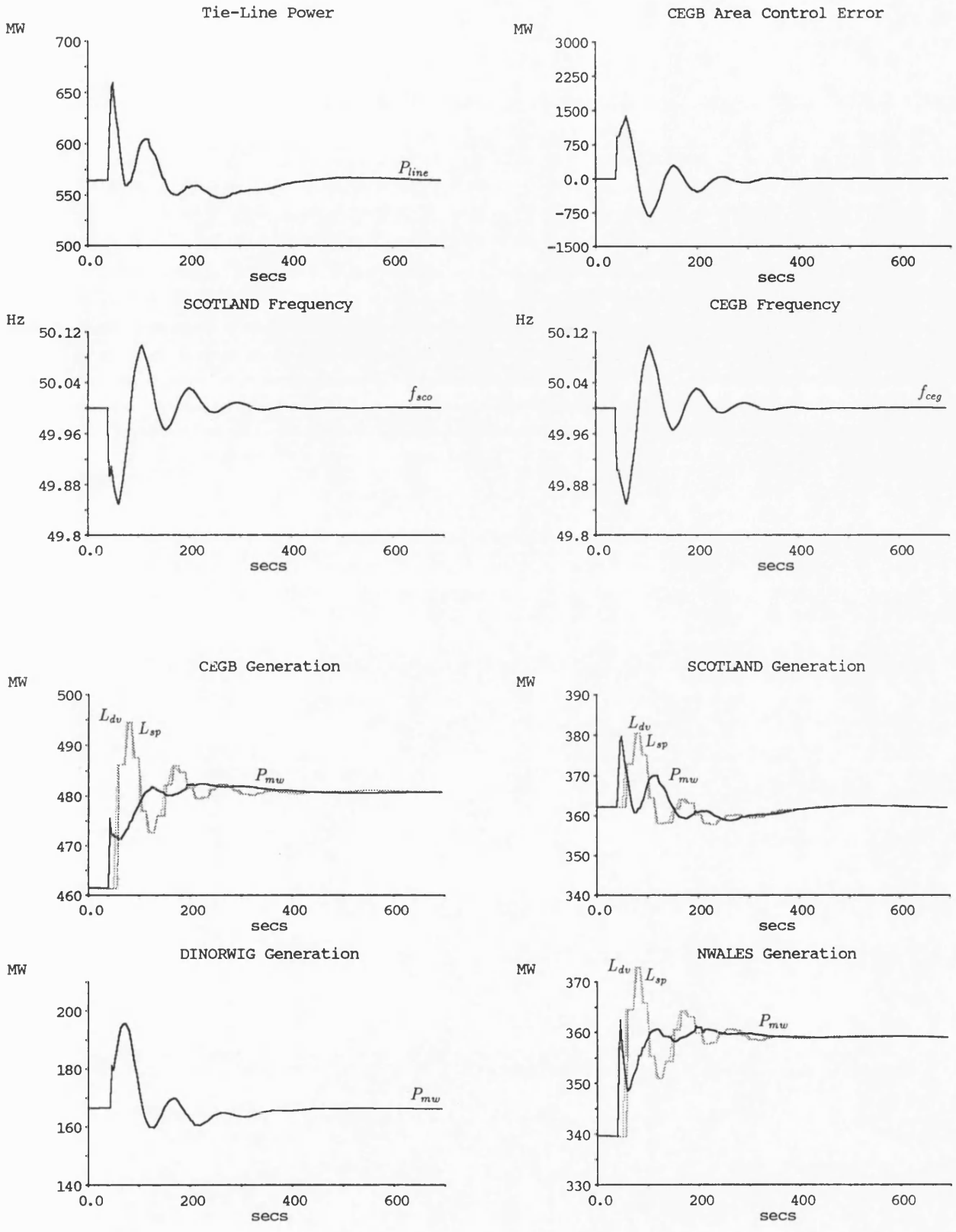

Figure 6.55: (a) 4 m'c Step Load Increase busbar CEGB4 (Run 35b)

fig 6.55(a)

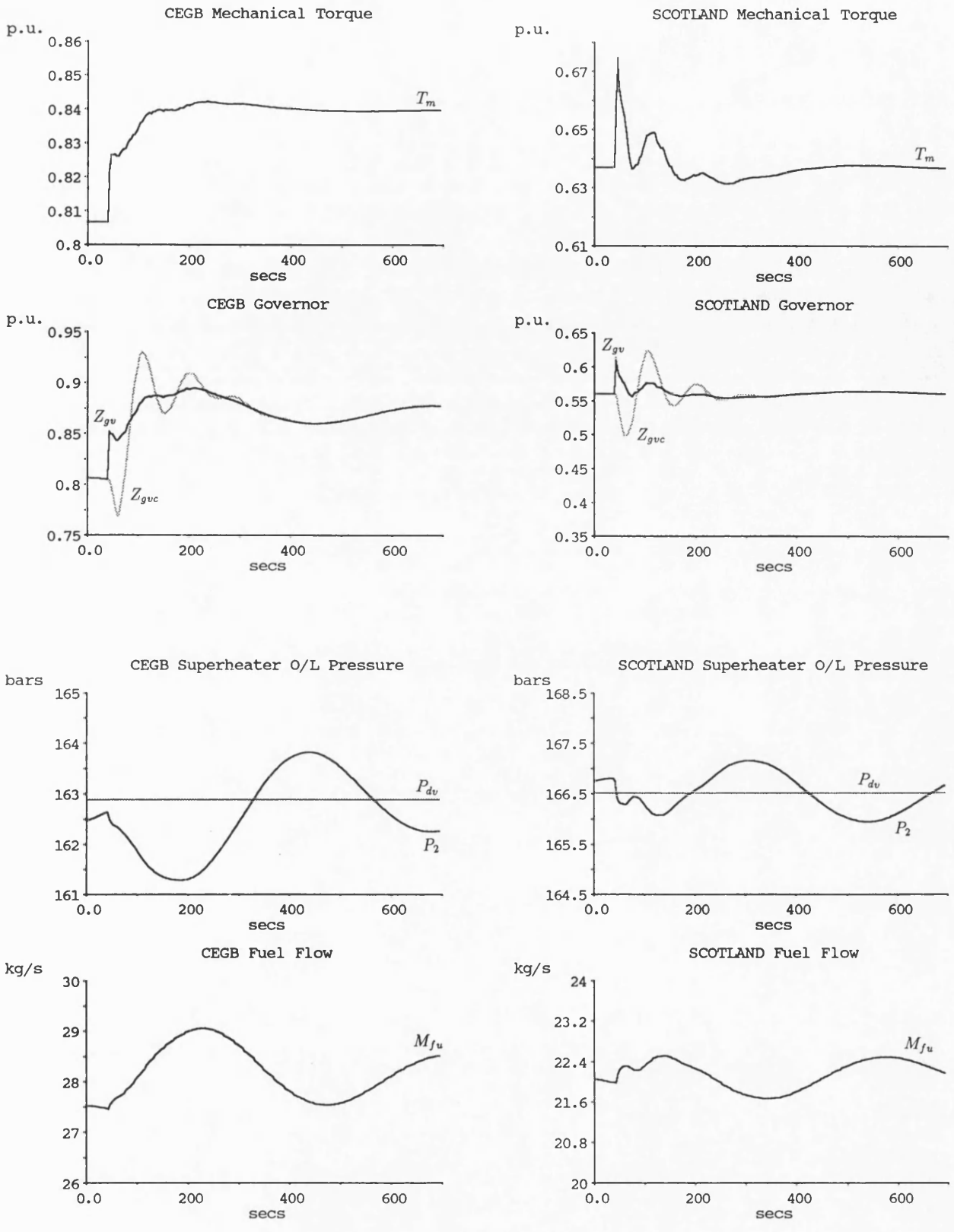

Figure 6.55: (b) 4 m'c Step Load Increase busbar CEGB4 (Run 35b)

356 Fig 6.55(b)

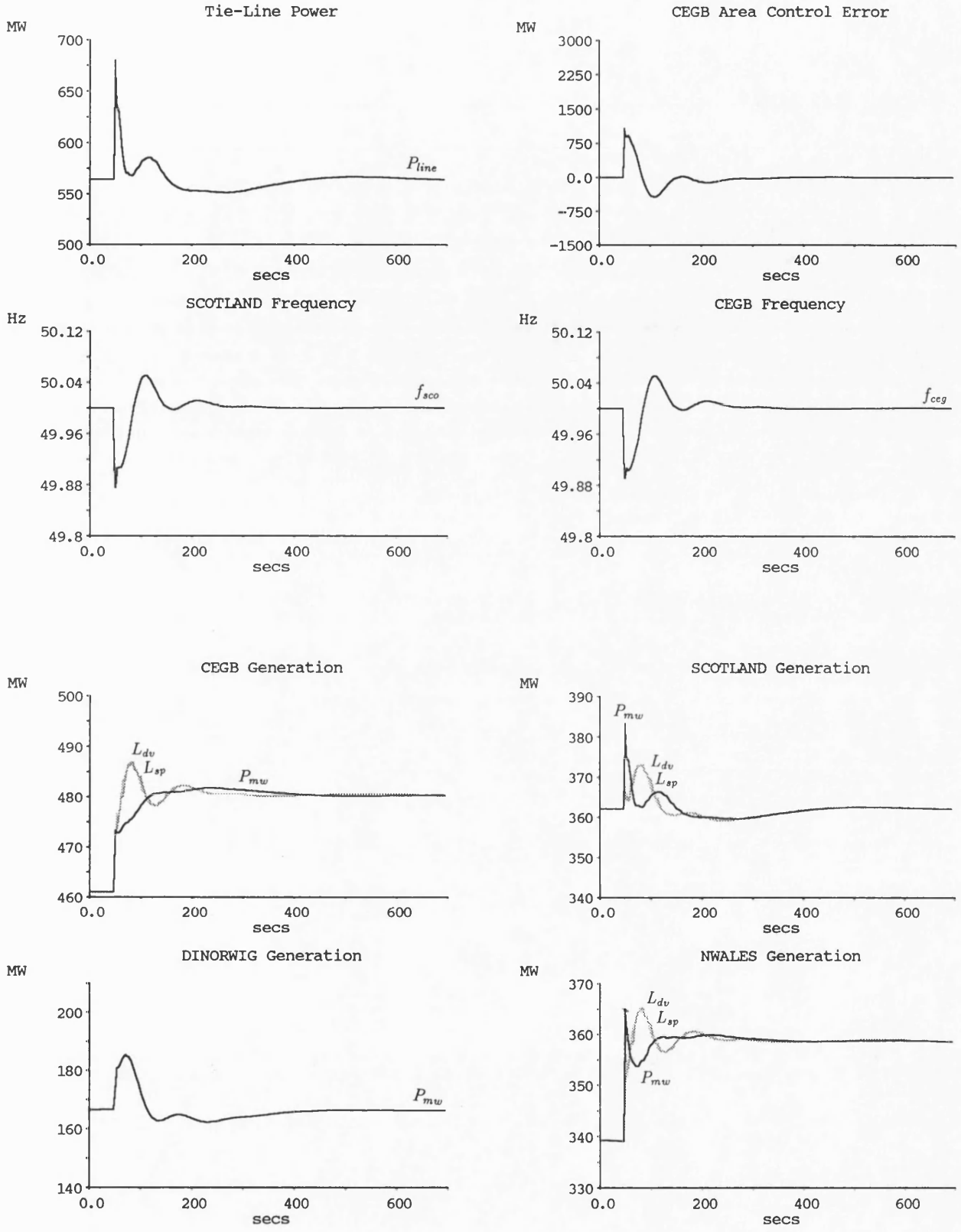

Figure 6.56: (a) 4 m'c Step Load Increase busbar CEGB4 (Run 27b)

Fig 6.56(a)

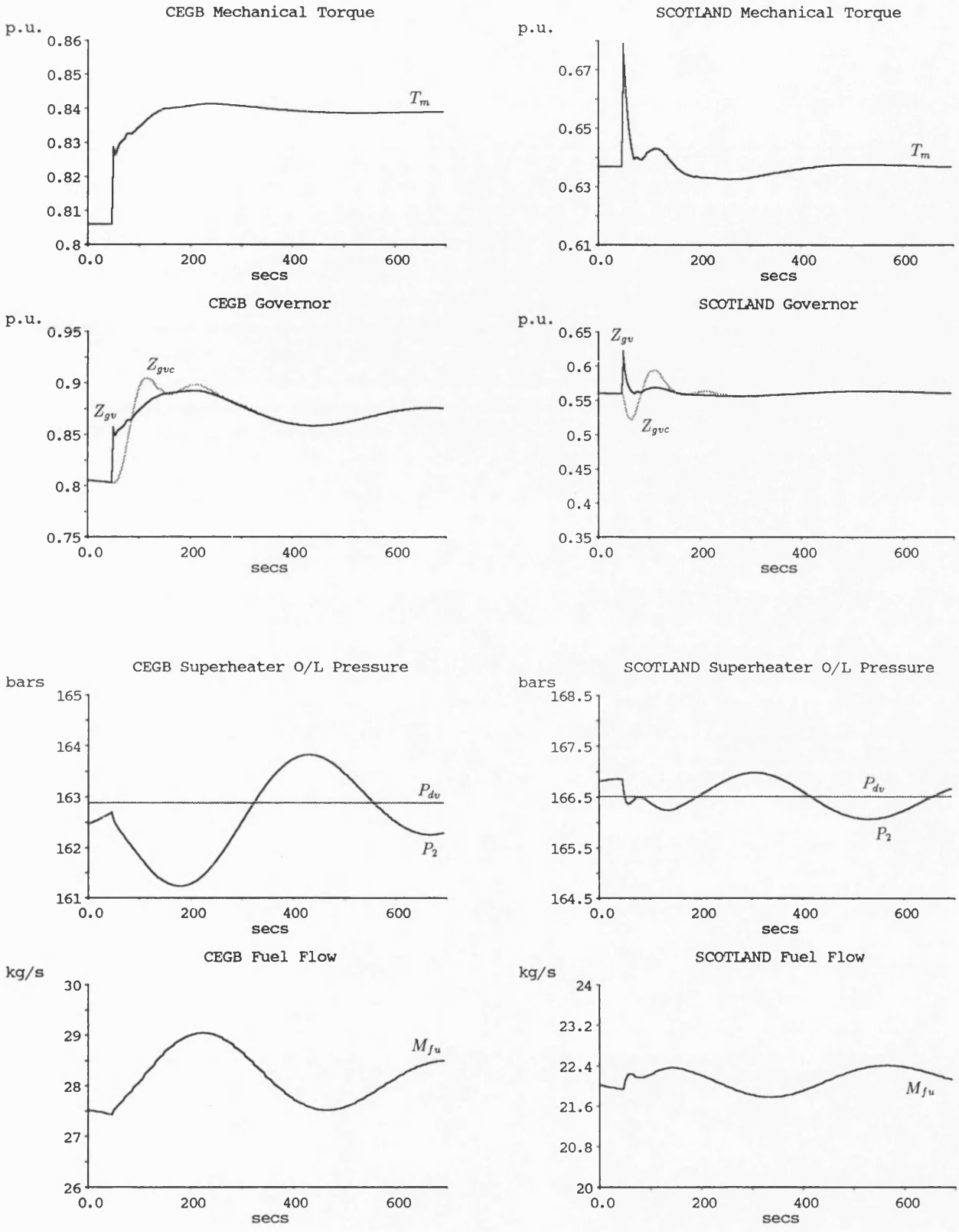

Figure 6.56: (b) 4 m'c Step Load Increase busbar CEGB4 (Run 27b)

Fig 6.56(b)

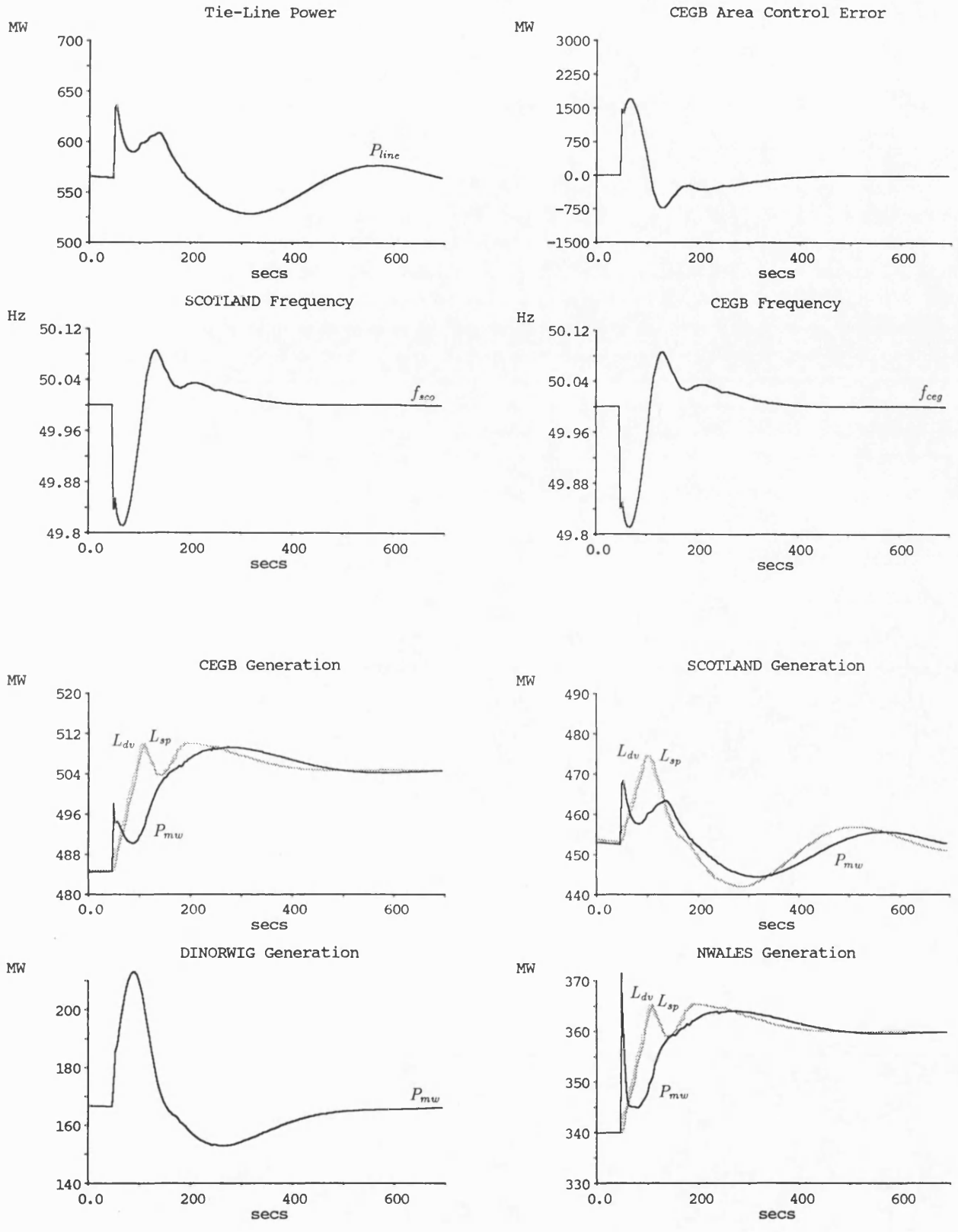

Figure 6.57: (a) 4 m'c Step Load Increase busbar CEGB4 (Run 41)

41 Lg 659(E)

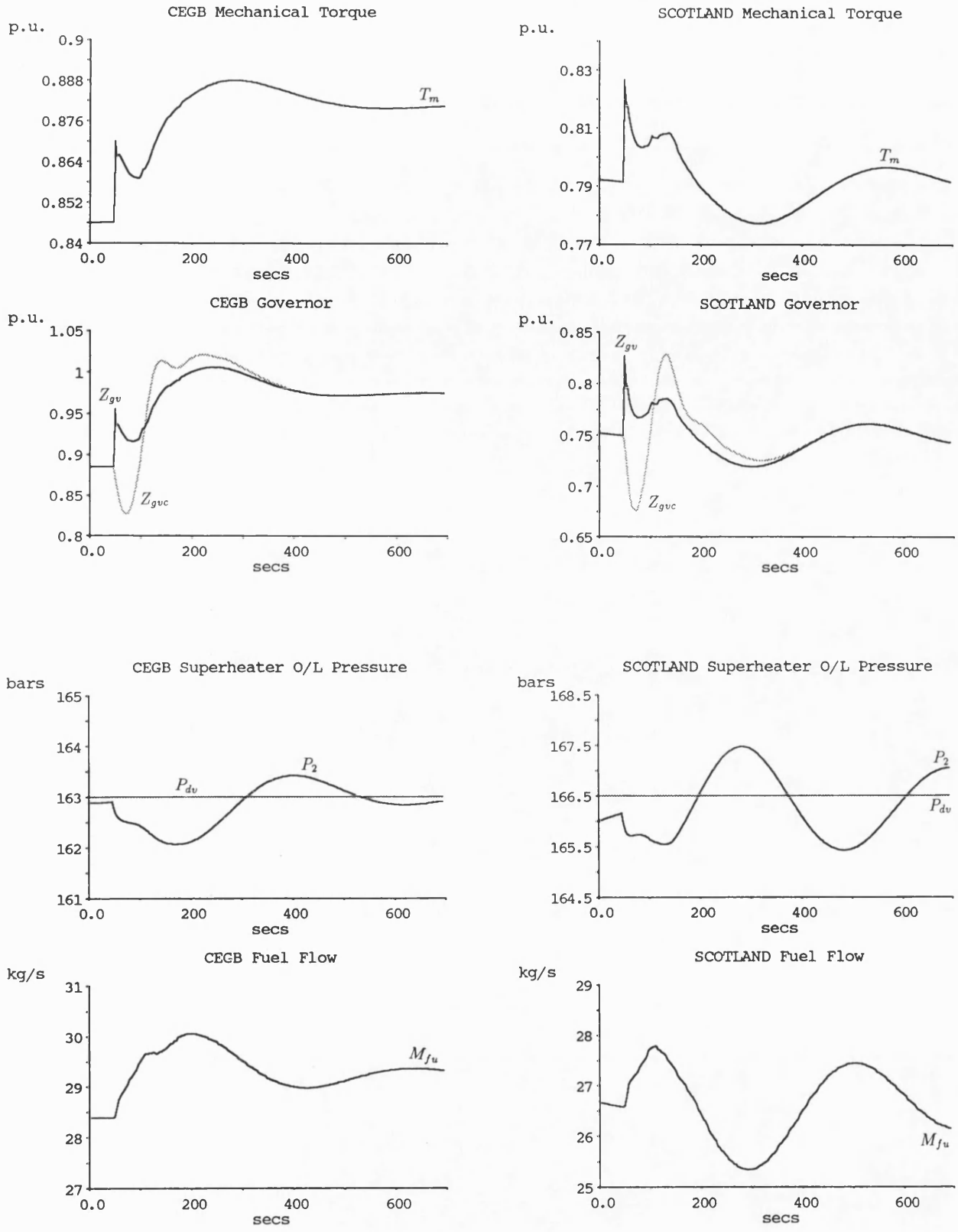

Figure 6.57: (b) 4 m'c Step Load Increase busbar CEGB4 (Run 41)

41 fig 6.59(b)

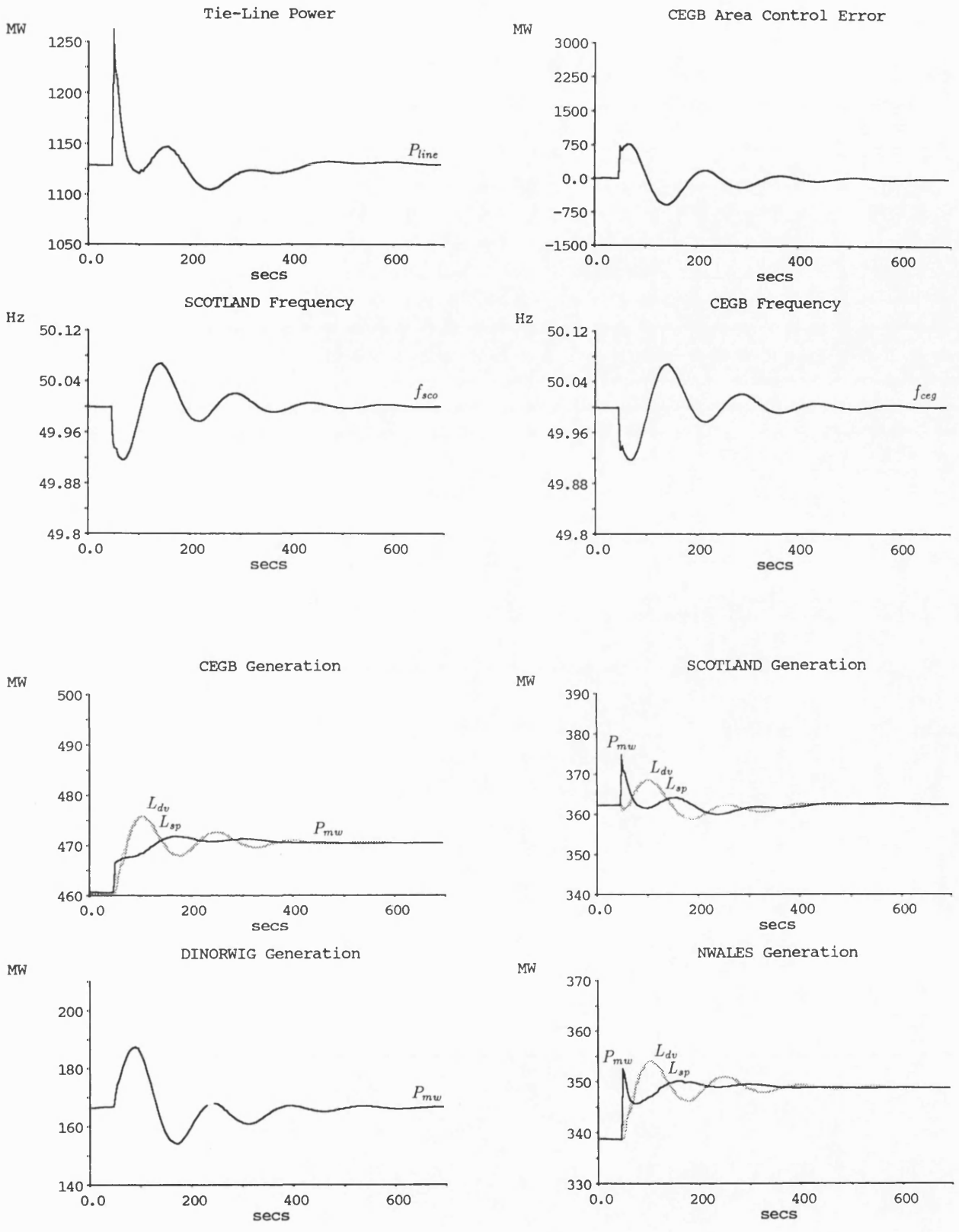

Figure 6.58: (a) 4 m'c Step Load Increase busbar CEGB4 (Run 40)

40 Fig 6.58(b)

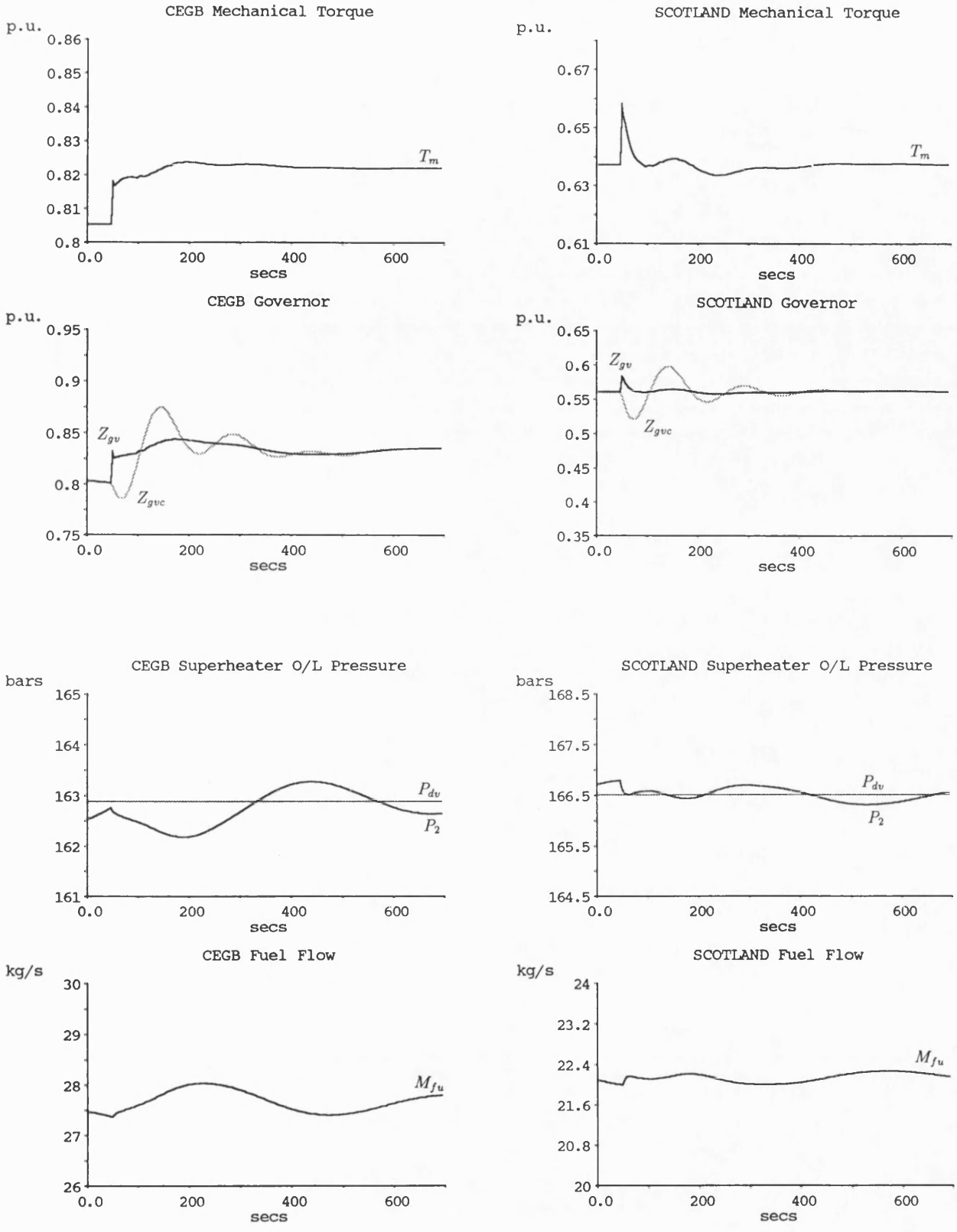

Figure 6.58: (b) 4 m'c Step Load Increase busbar CEGB4 (Run 40)

40 Eg 6.58(b)

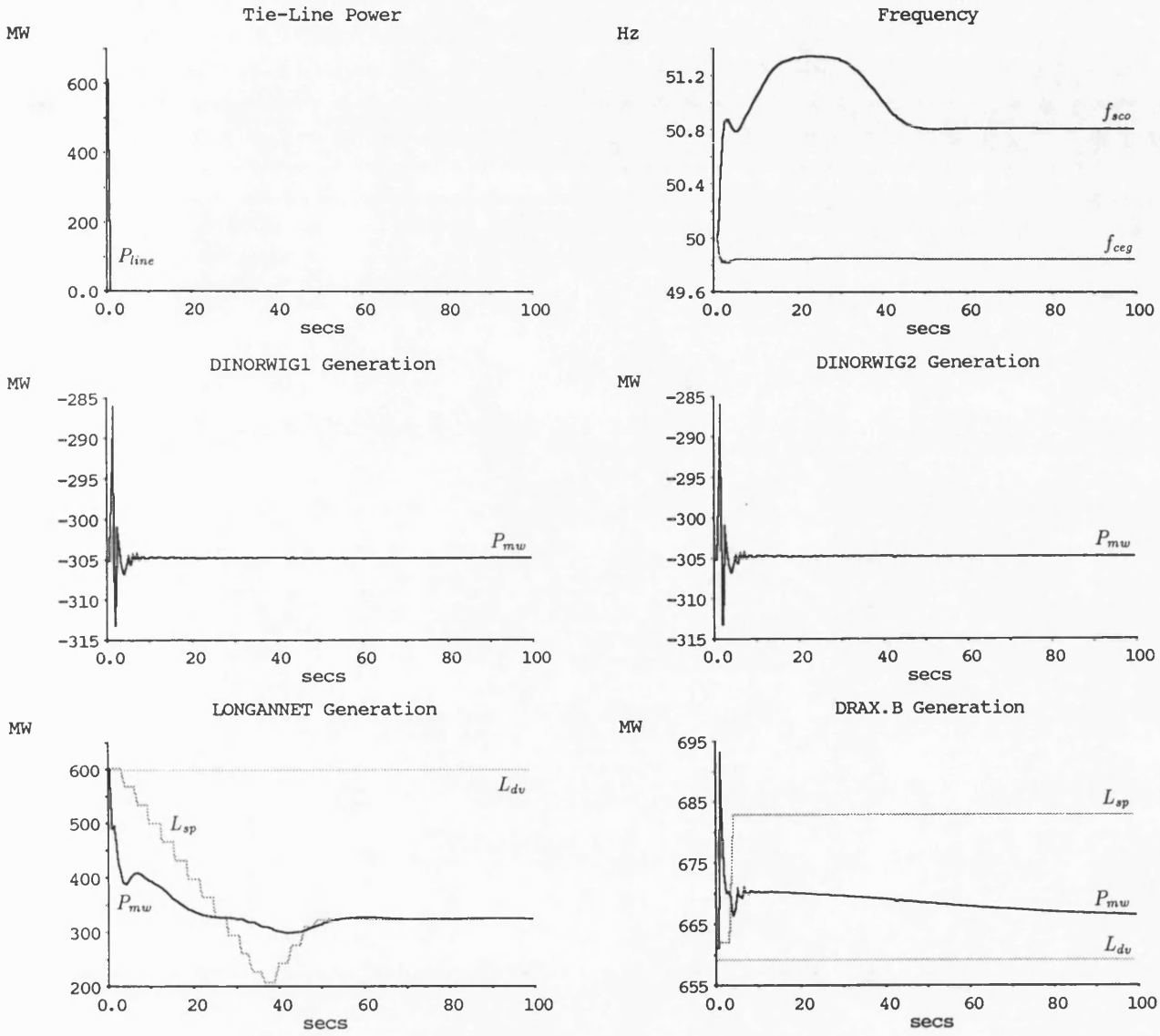

Figure 7.1: (a) 25 m'c Scotland-England Split (Run 1)

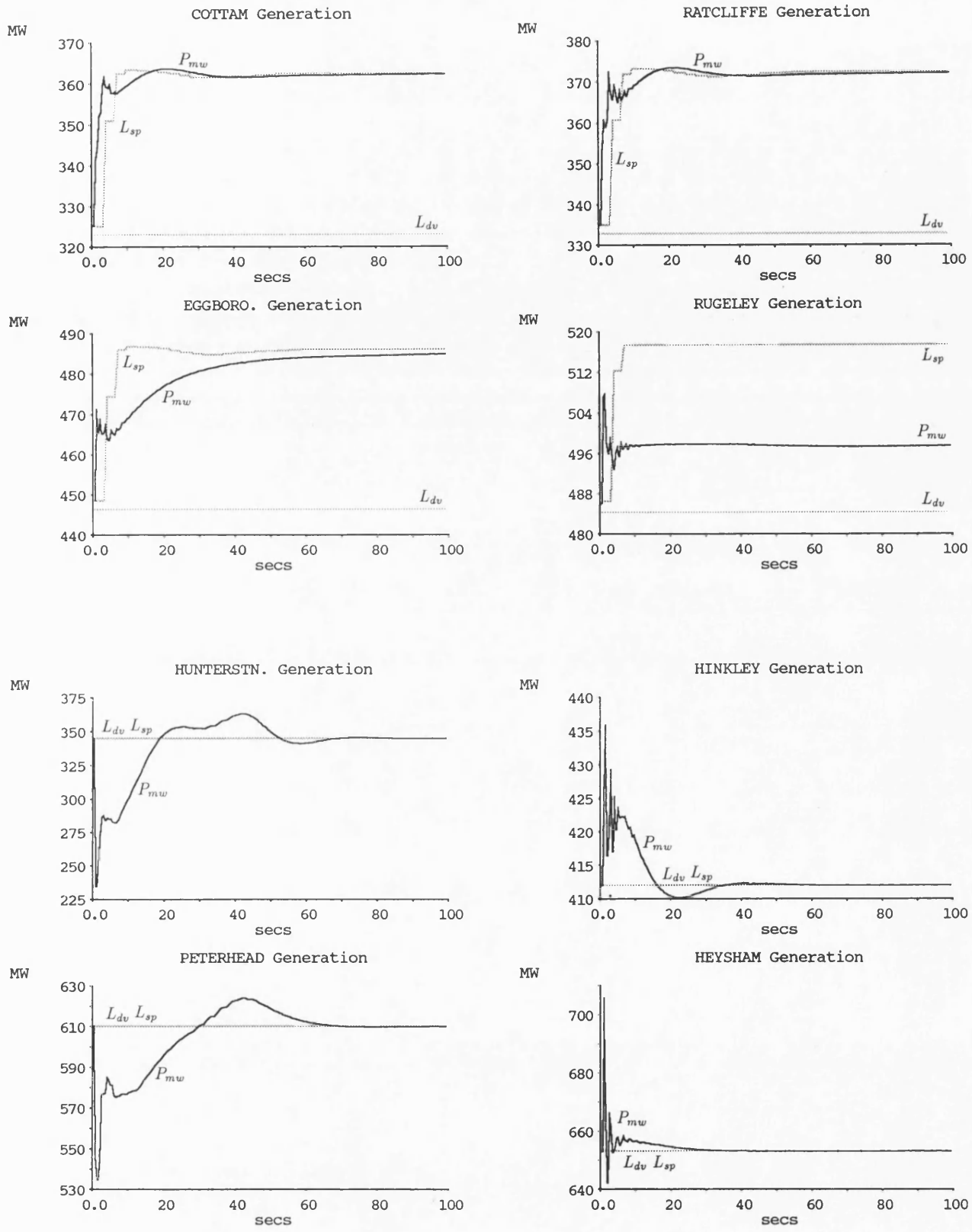

Figure 7.1: (b) 25 m'c Scotland-England Split (Run 1)

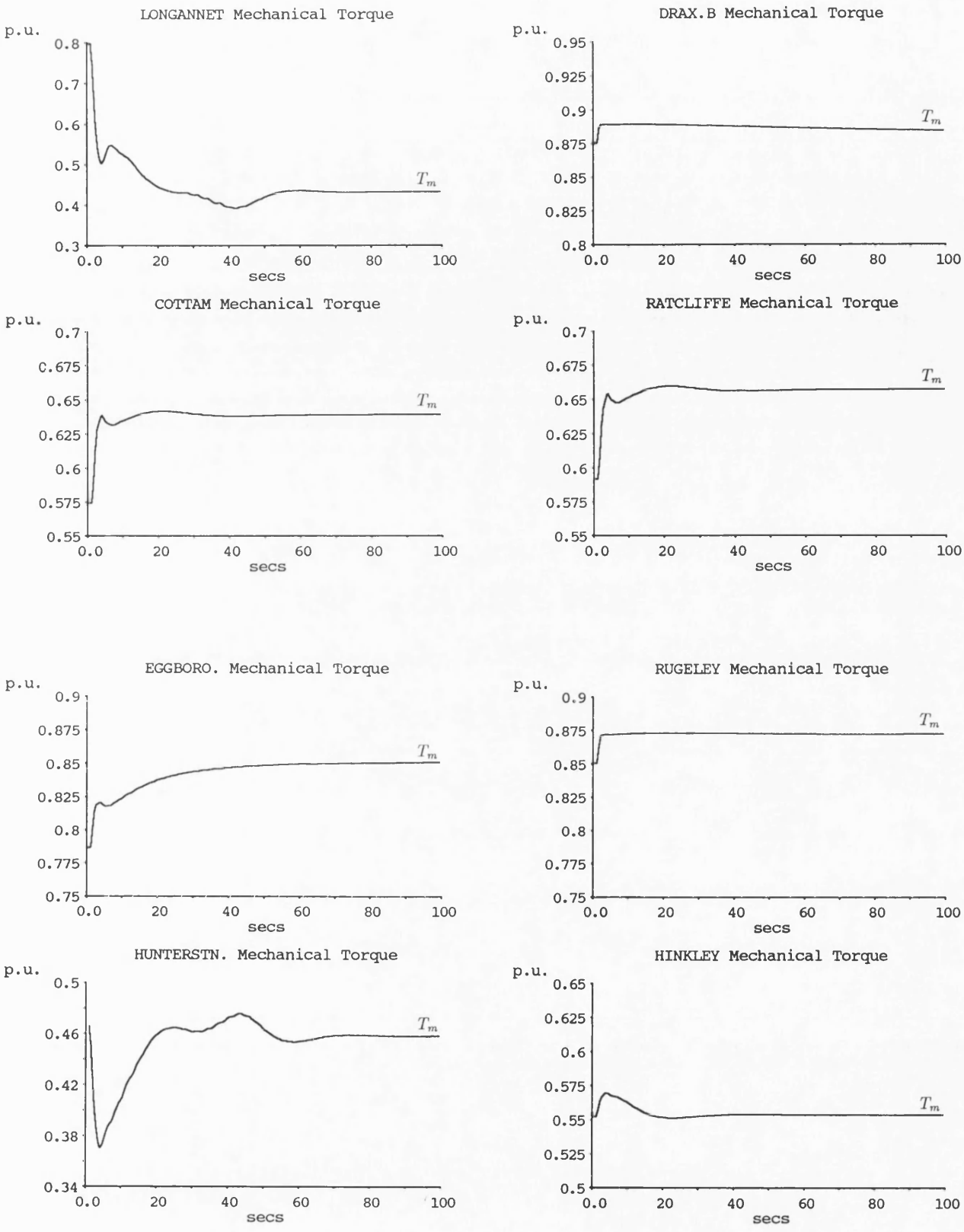

Figure 7.1: (c) 25 m'c Scotland-England Split (Run 1)

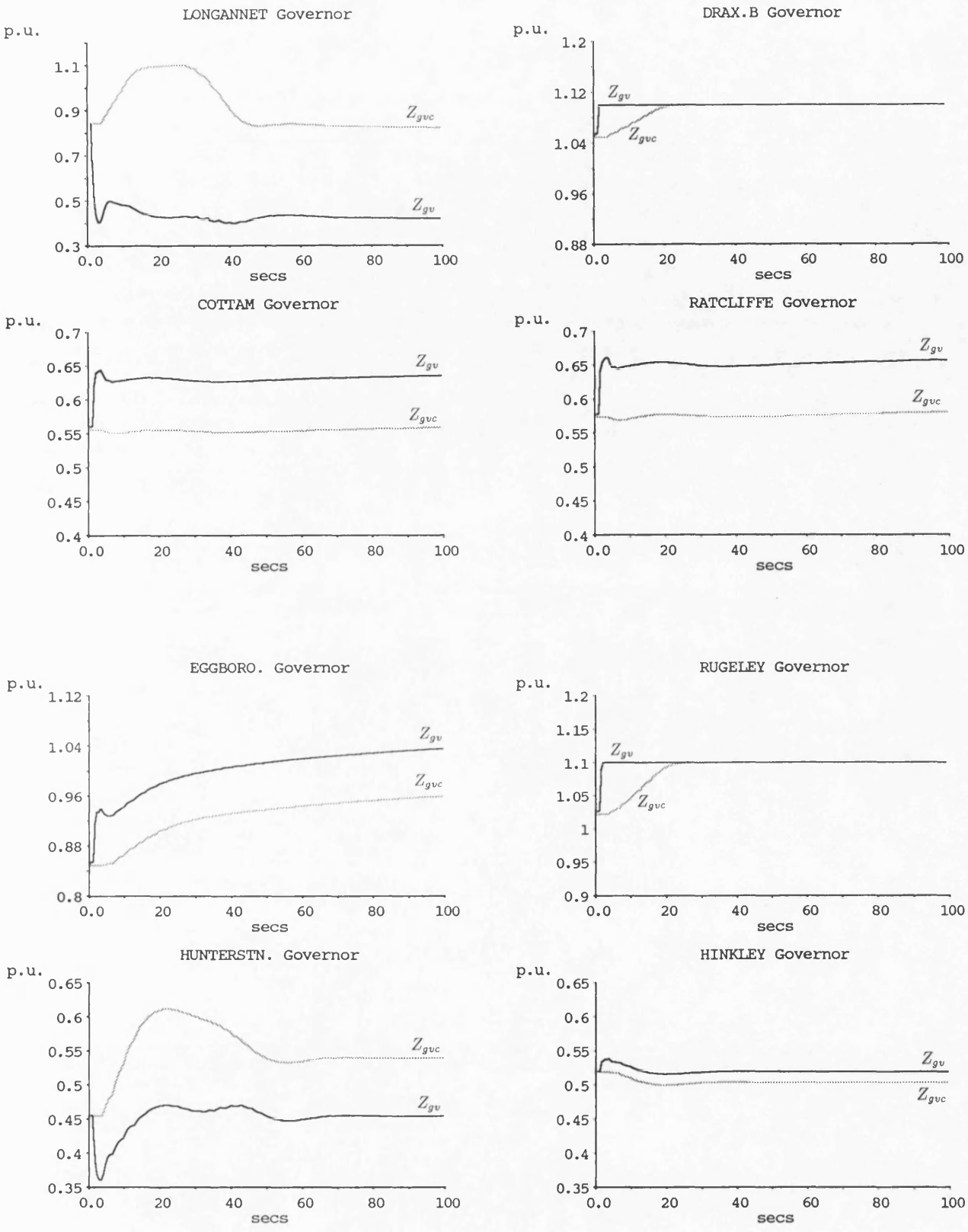

Figure 7.1: (d) 25 m'c Scotland-England Split (Run 1)

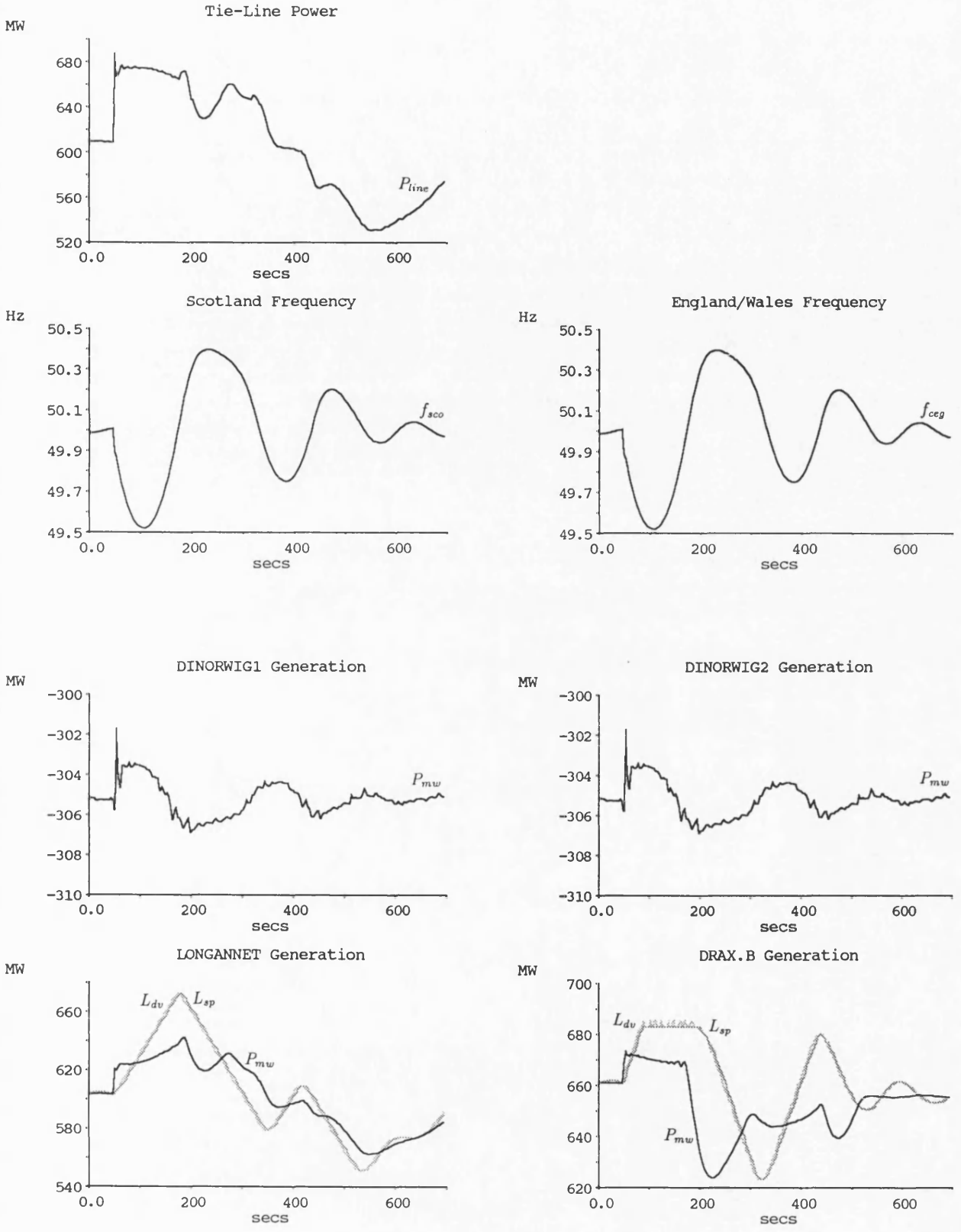

Figure 7.2: (a) 25 m'c Step Load Change (Run 10)

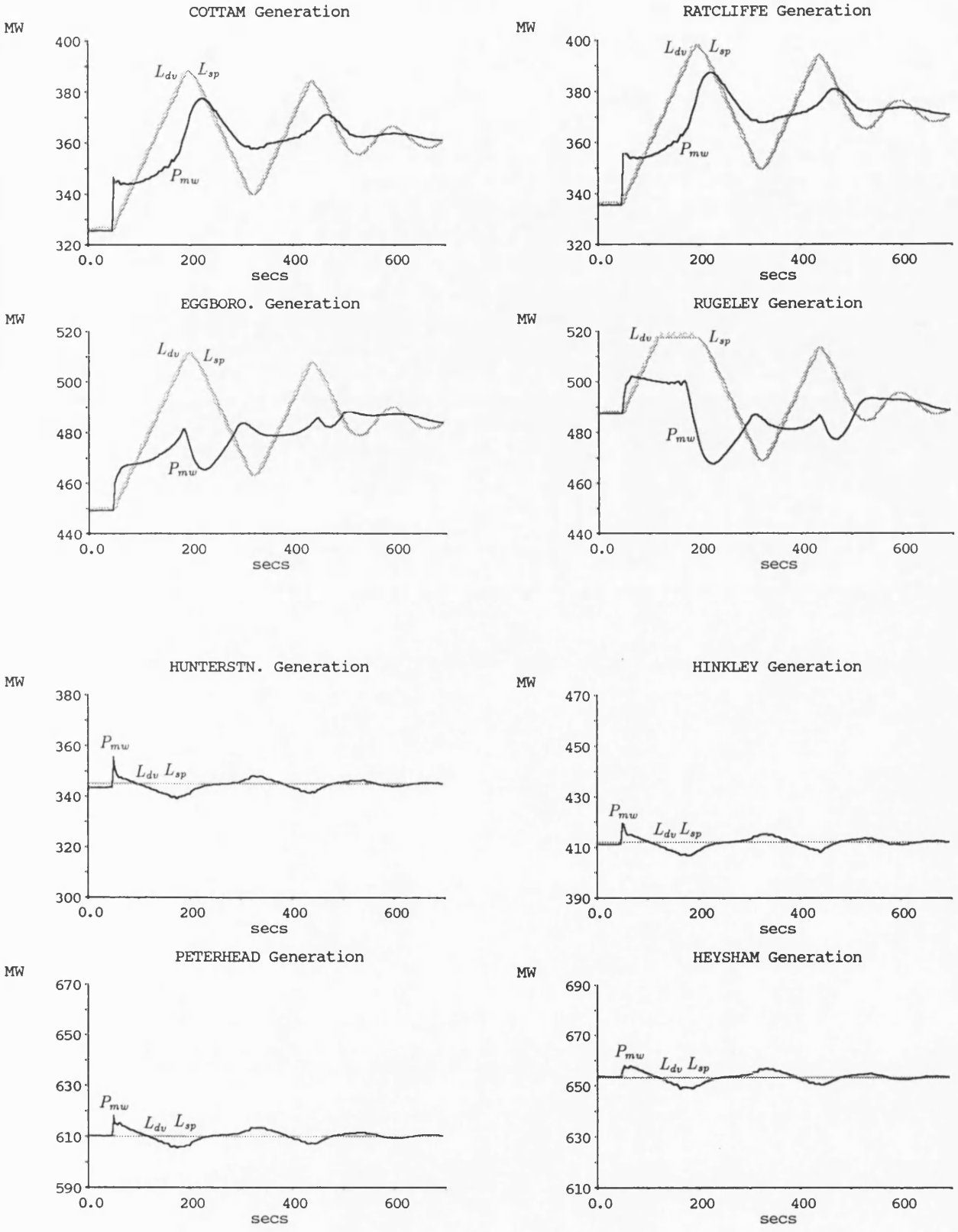

Figure 7.2: (b) 25 m'c Step Load Change (Run 10)

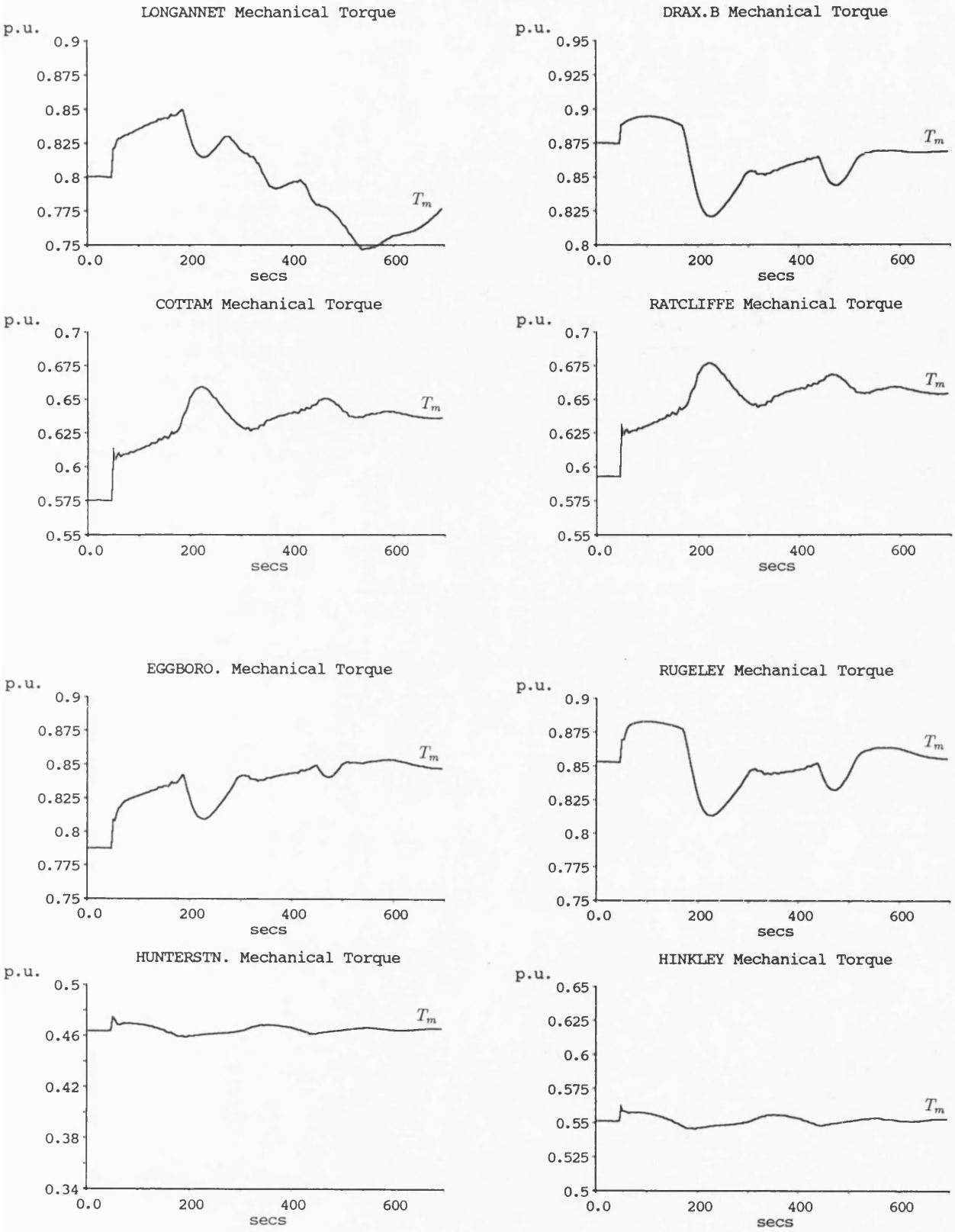

Figure 7.2: (c) 25 m'c Step Load Change (Run 10)

10

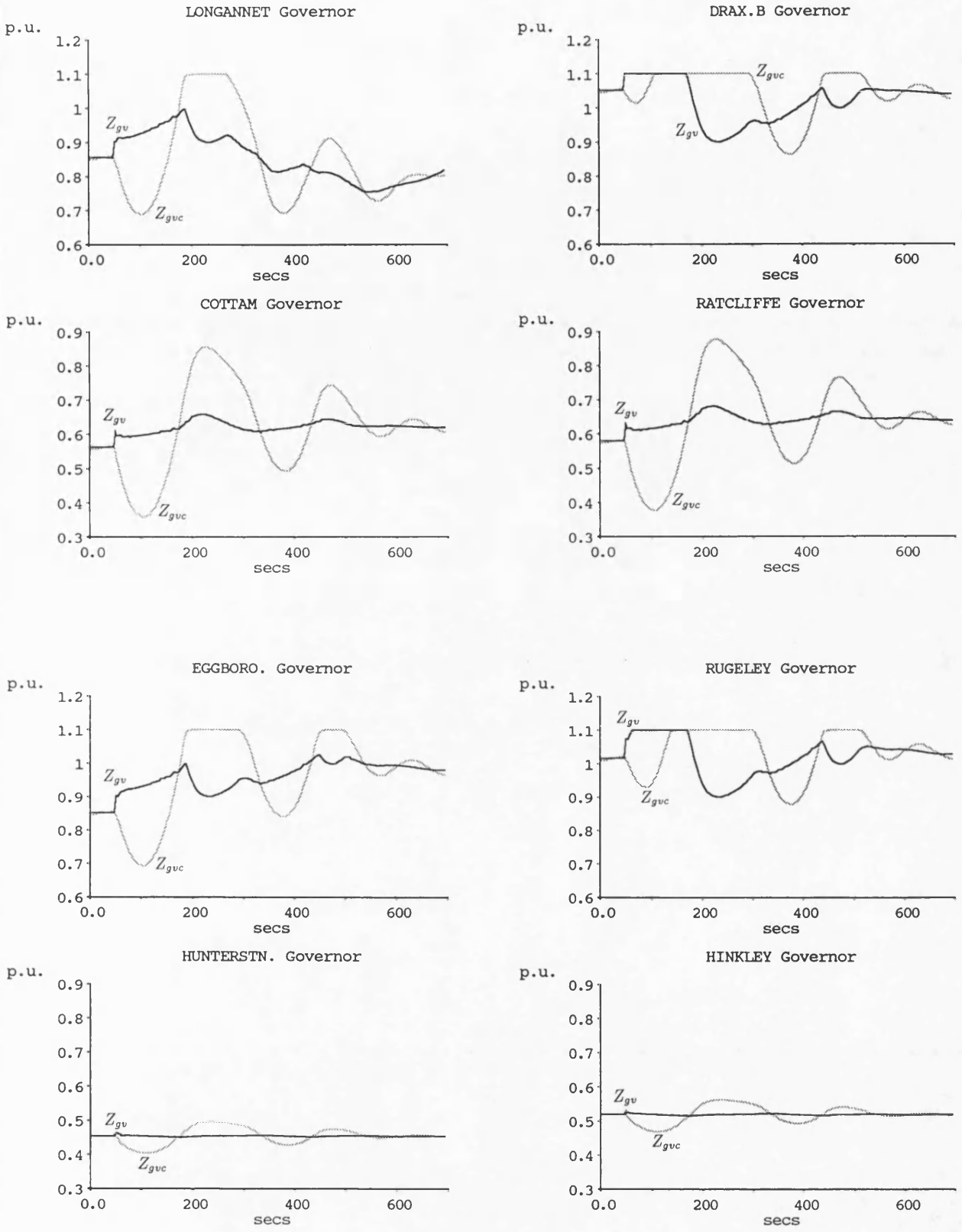

Figure 7.2: (d) 25 m'c Step Load Change (Run 10)

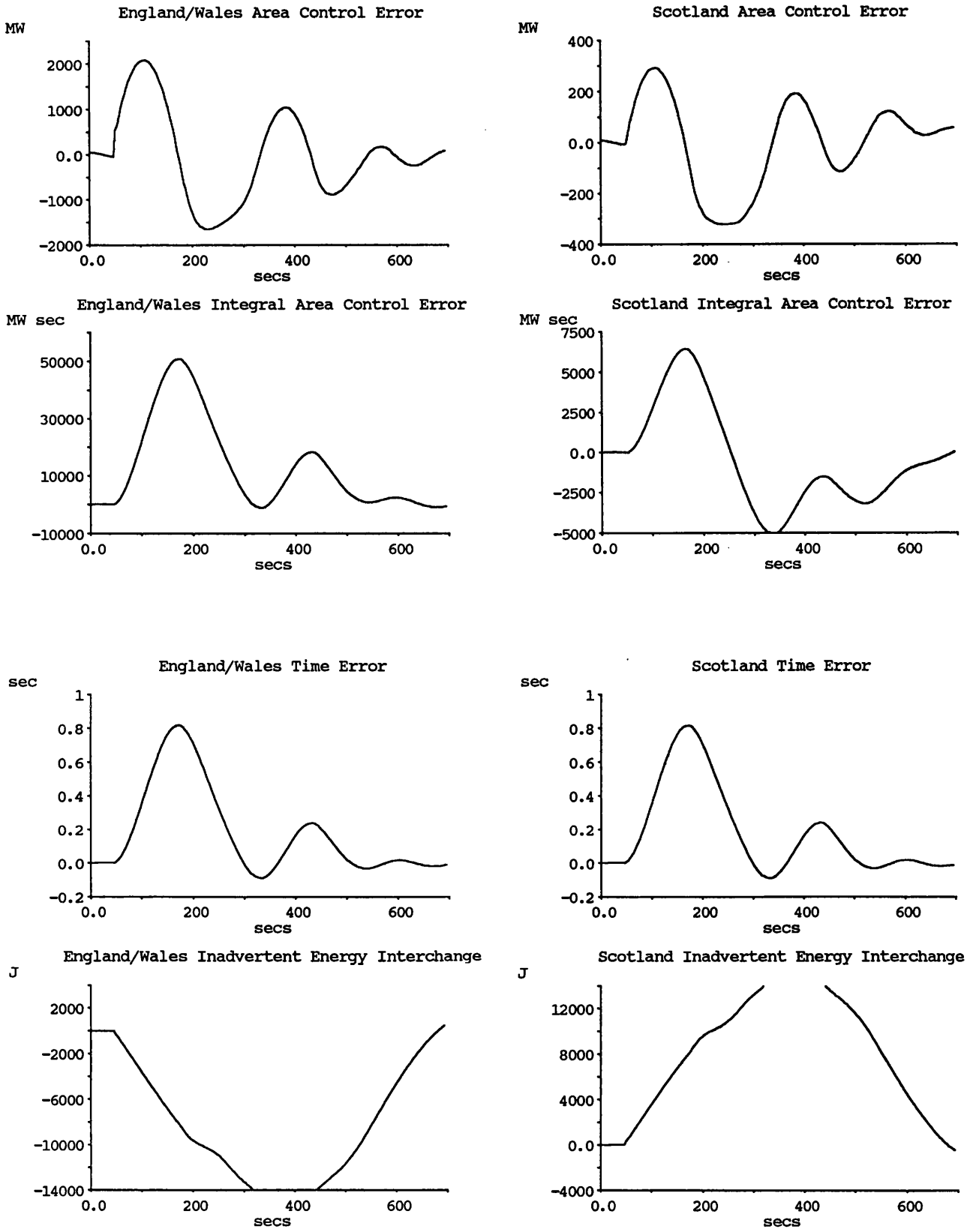

Figure 7.2: (e) 25 m'c Step Load Change (Run 10)

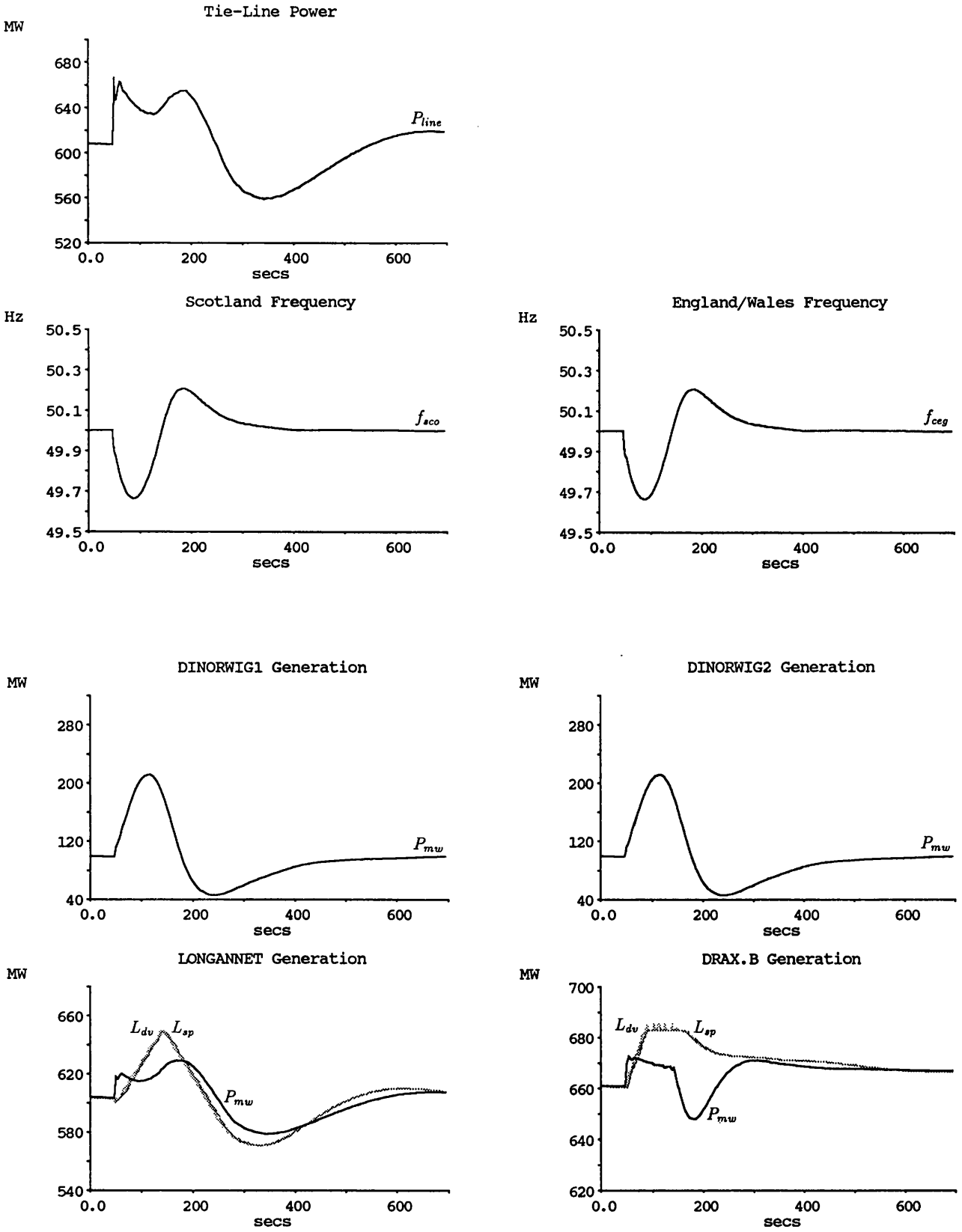

Figure 7.3: (a) 25 m'c Step Load Change (Run 9)

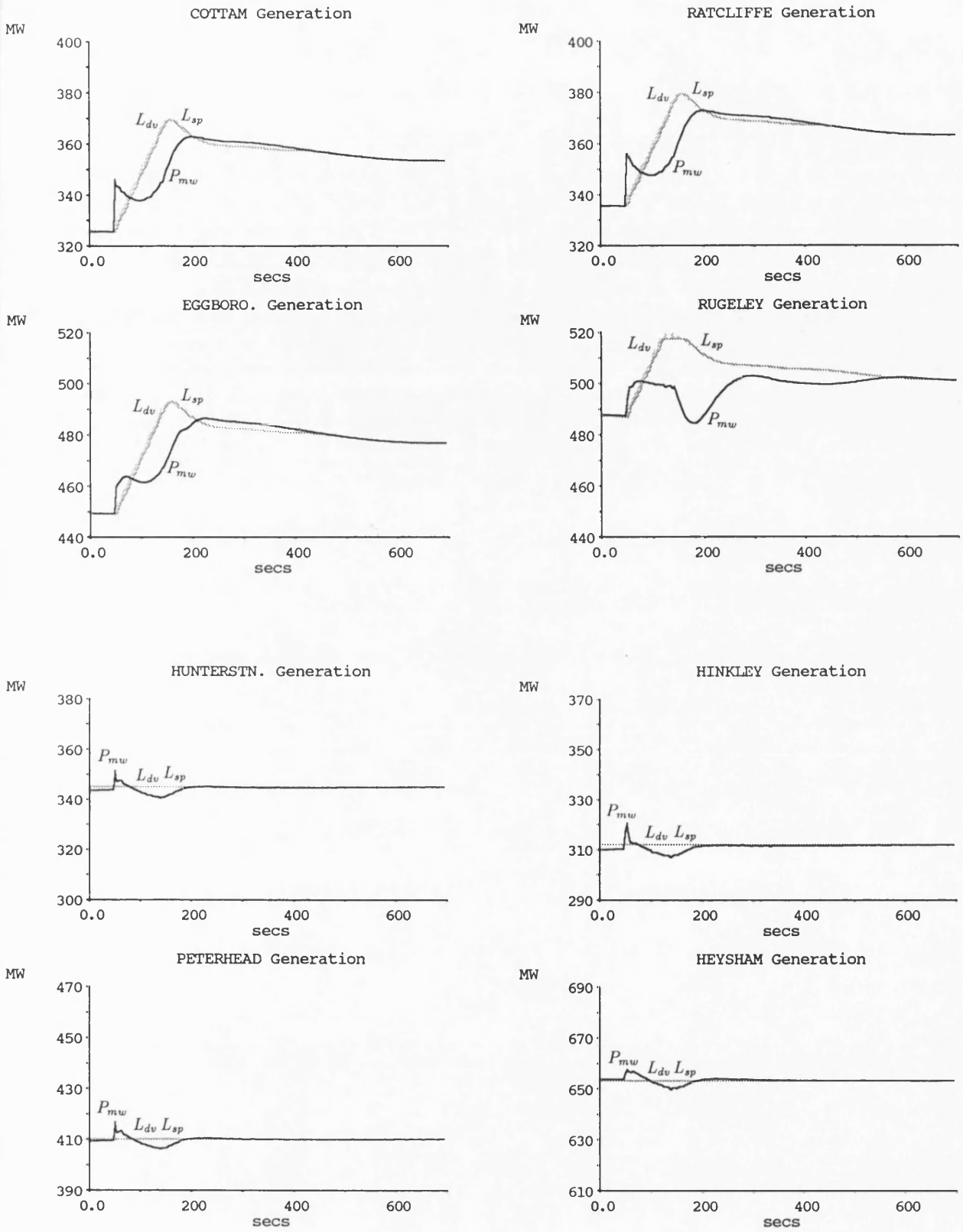

Figure 7.3: (b) 25 m'c Step Load Change (Run 9)

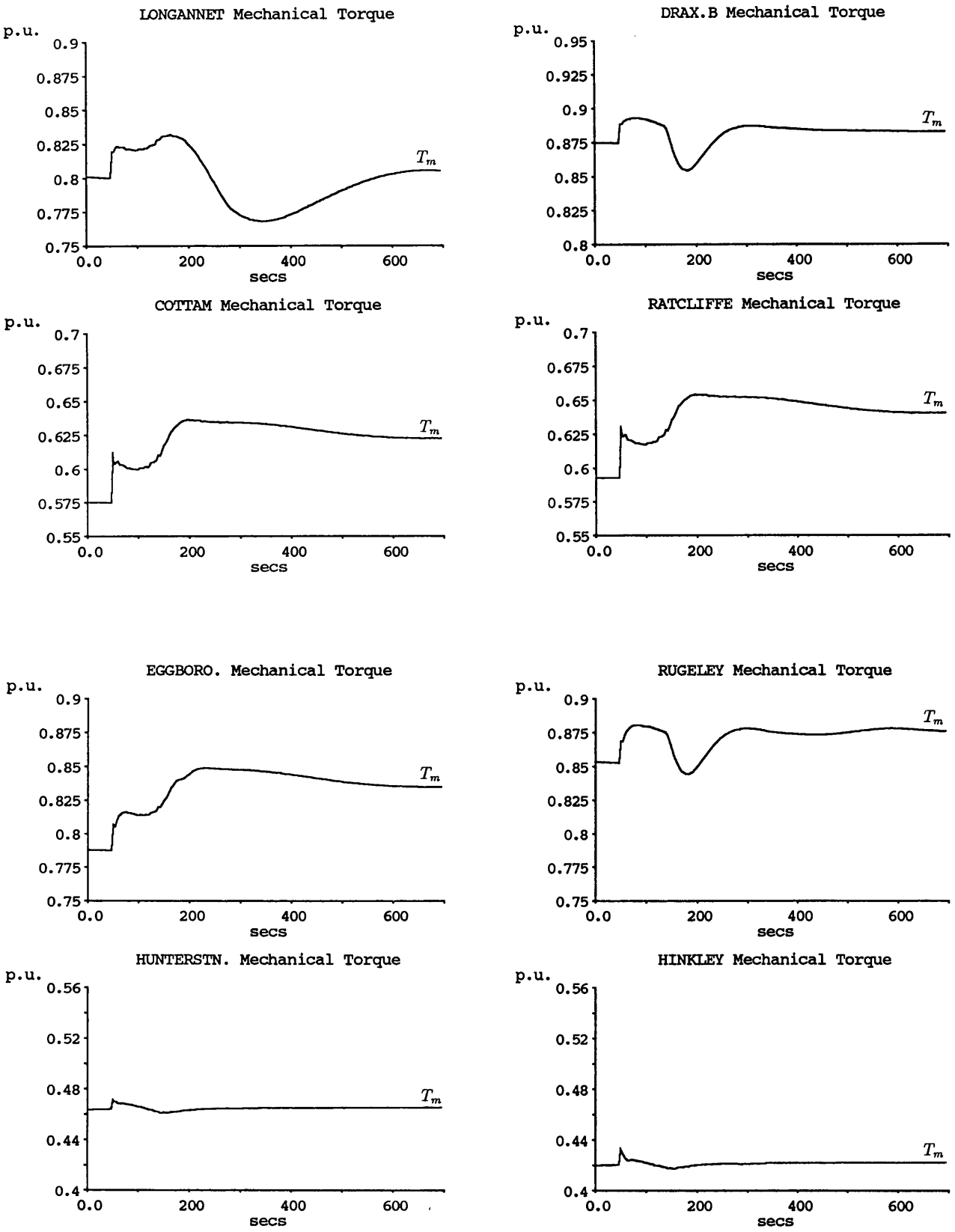

Figure 7.3: (c) 25 m'c Step Load Change (Run 9)

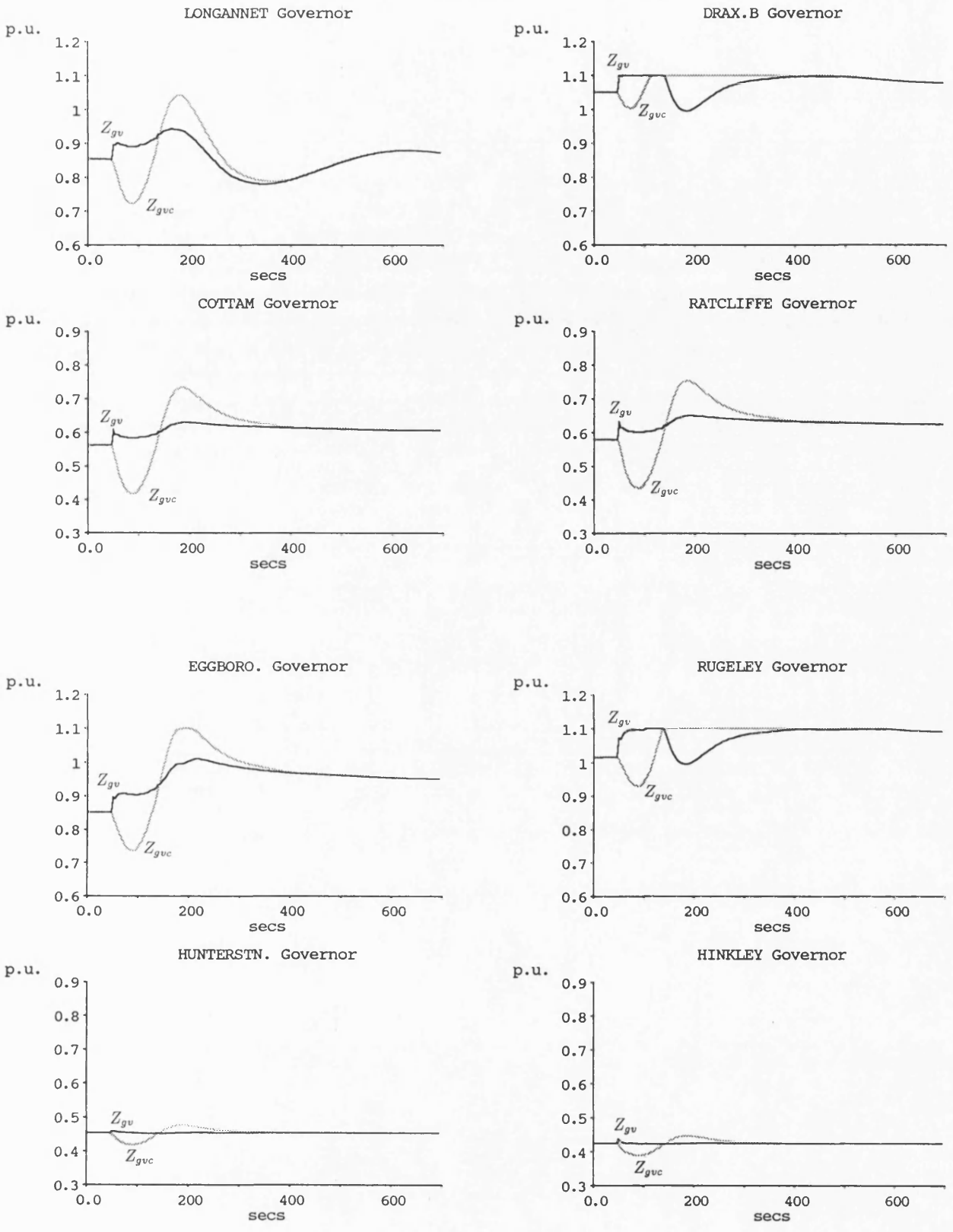

Figure 7.3: (d) 25 m'c Step Load Change (Run 9)

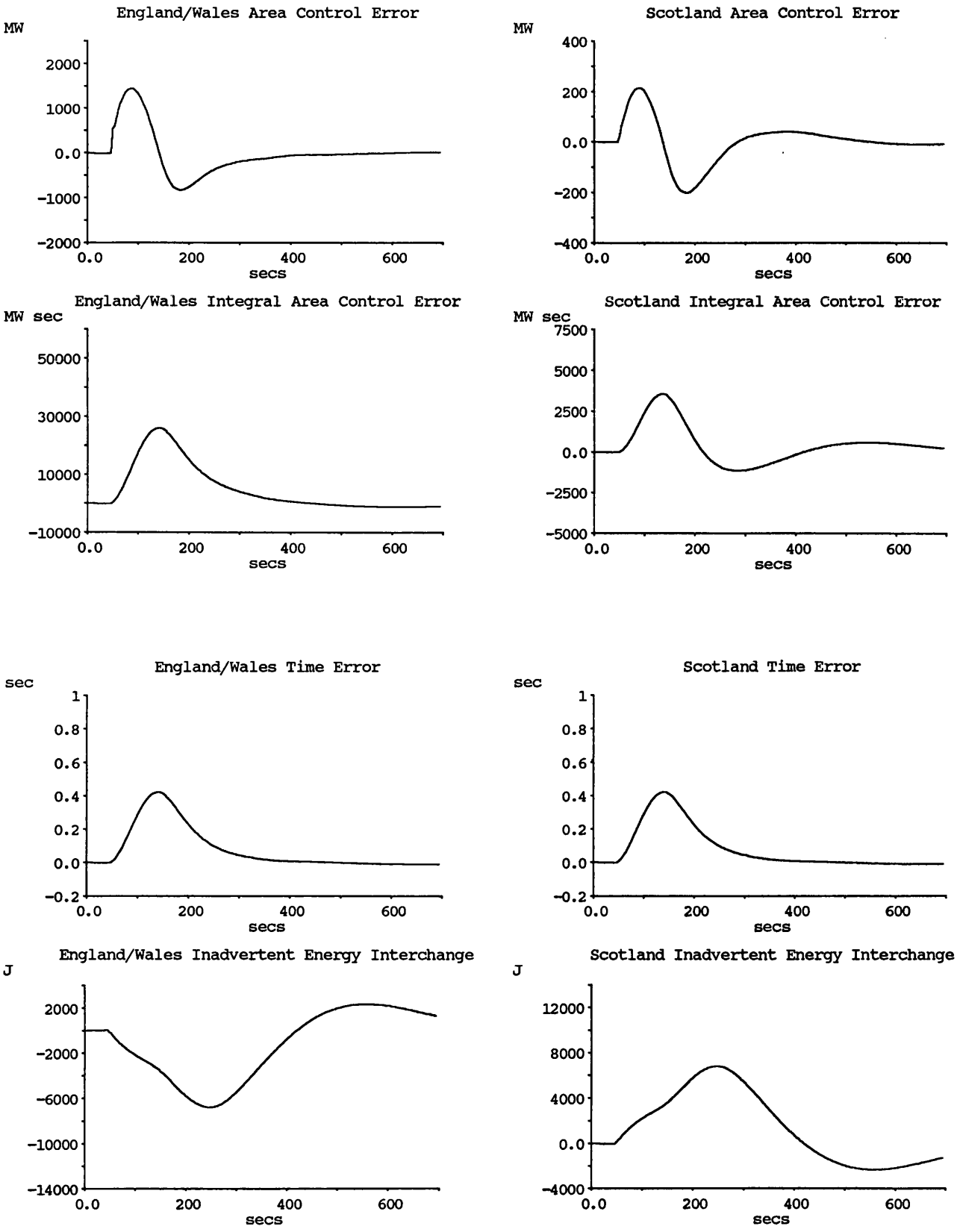

Figure 7.3: (e) 25 m'c Step Load Change (Run 9)

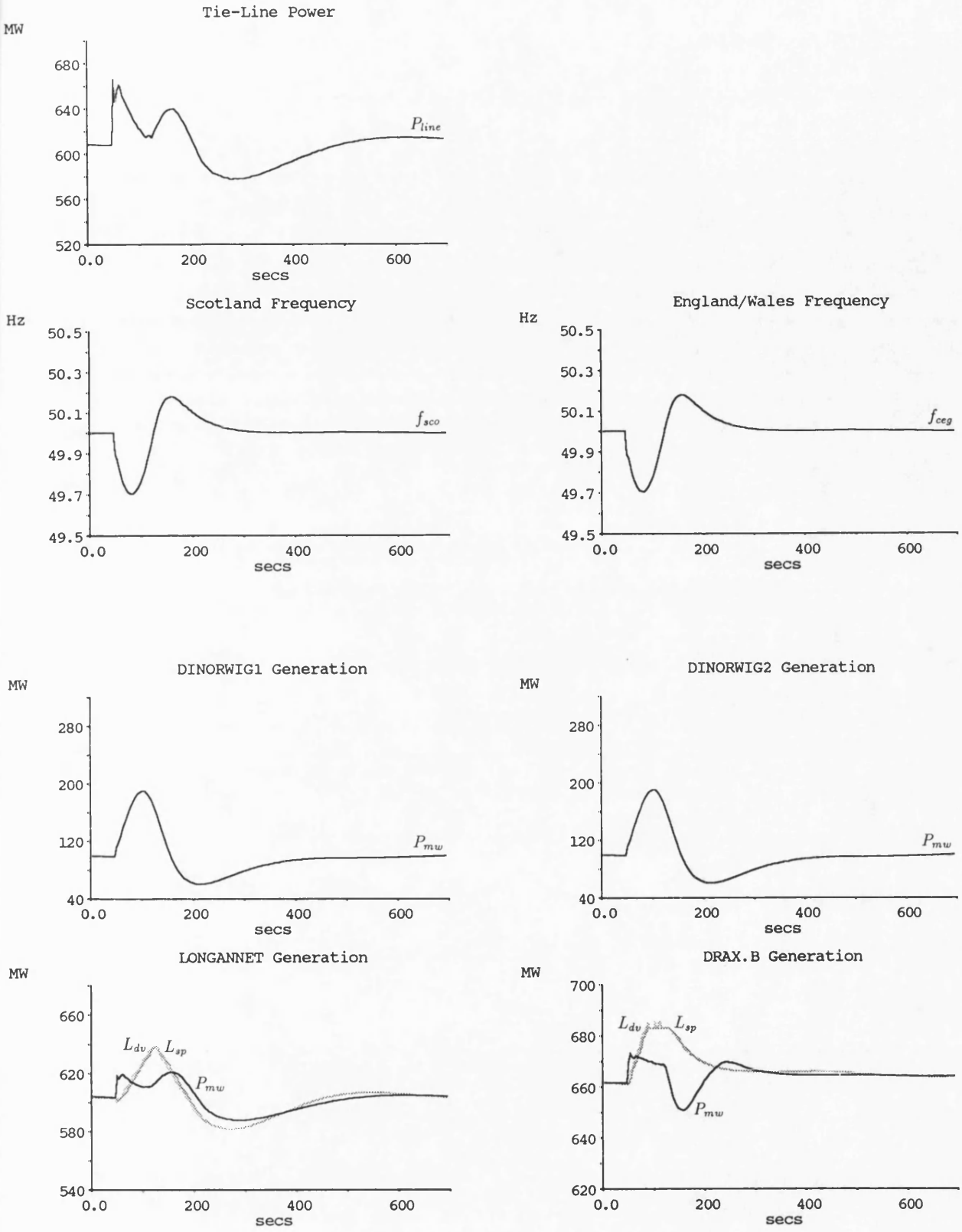

Figure 7.4: (a) 25 m'c Step Load Change (Run 8)

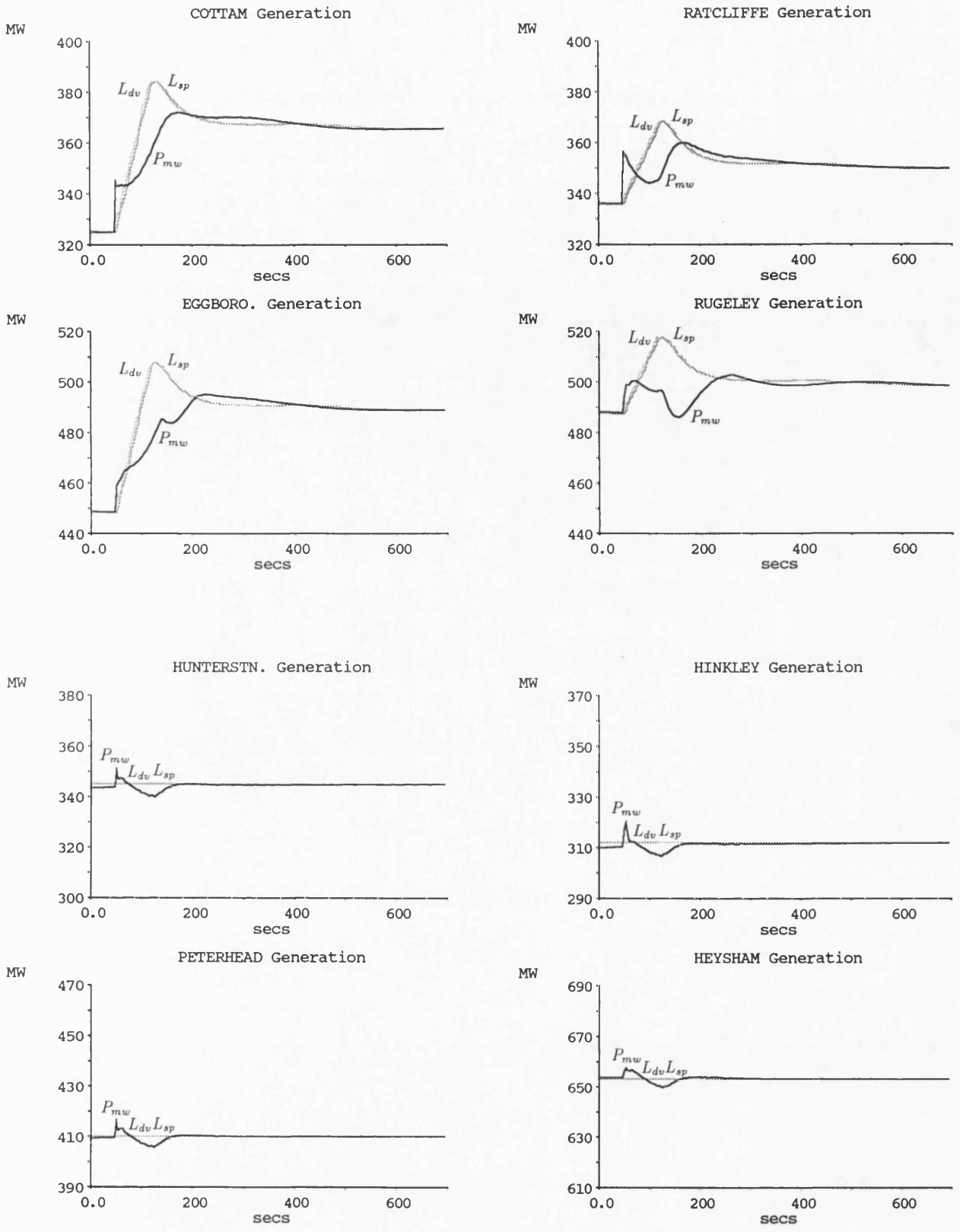

Figure 7.4: (b) 25 m'c Step Load Change (Run 8)

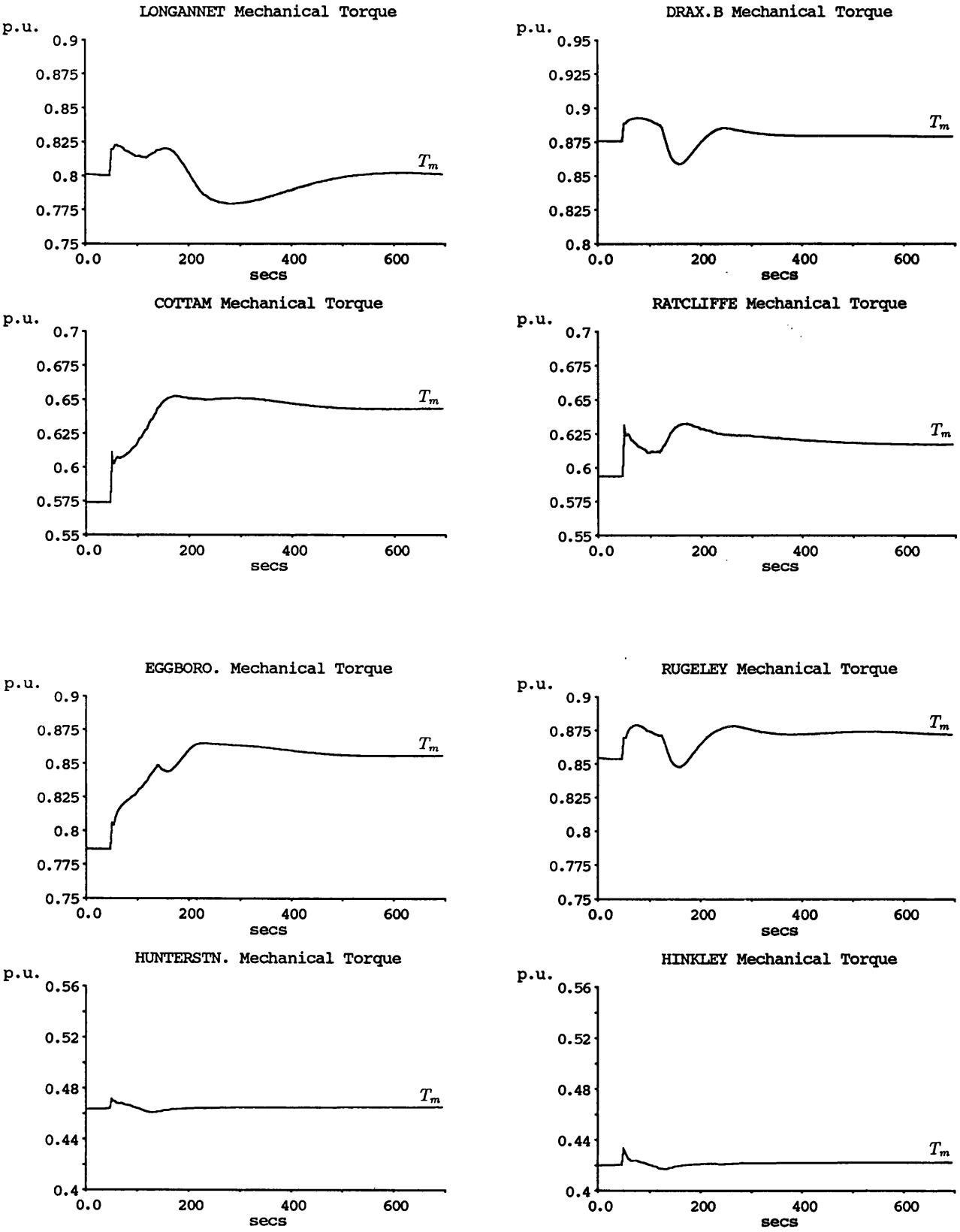

Figure 7.4: (c) 25 m'c Step Load Change (Run 8)

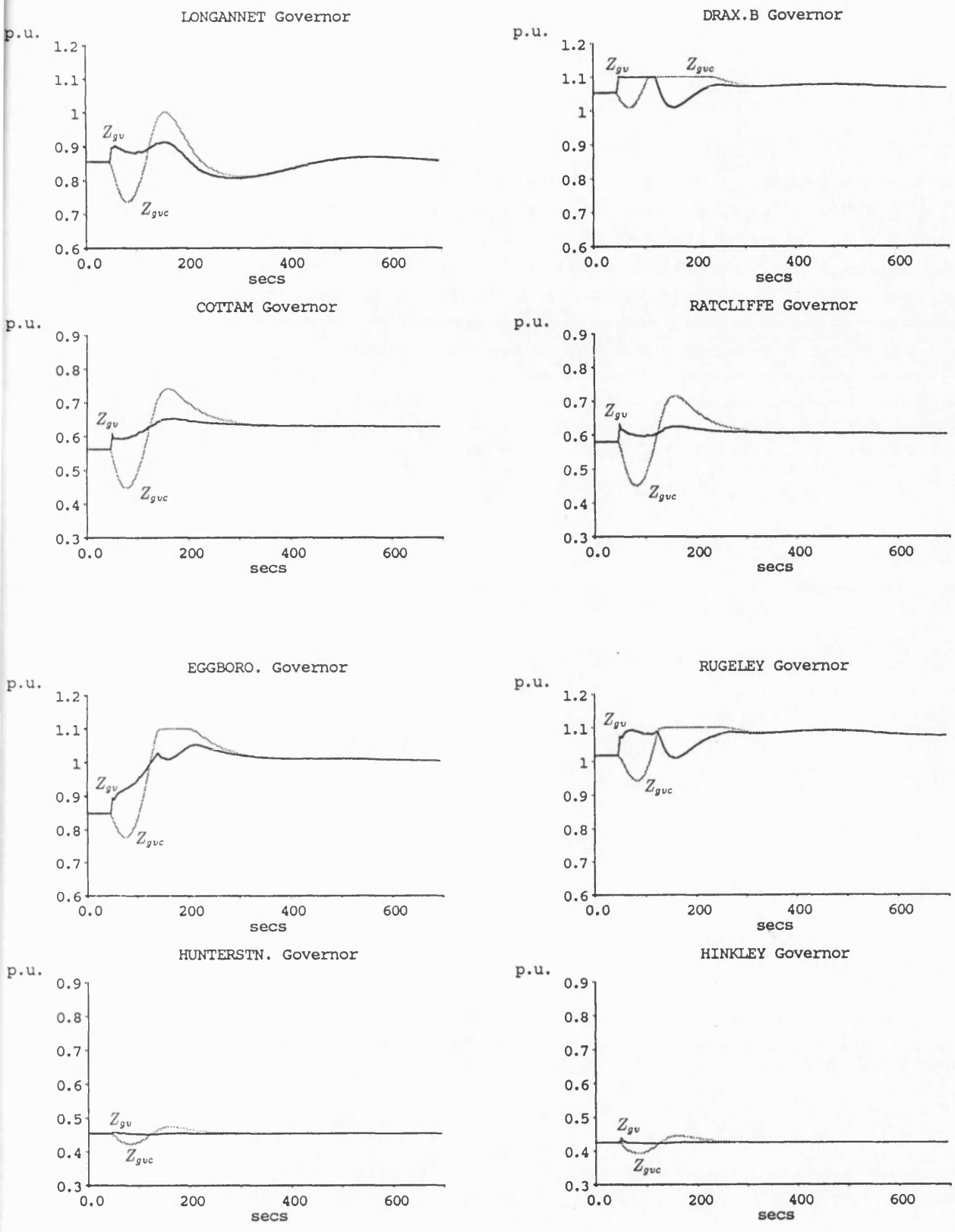

Figure 7.4: (d) 25 m'c Step Load Change (Run 8)

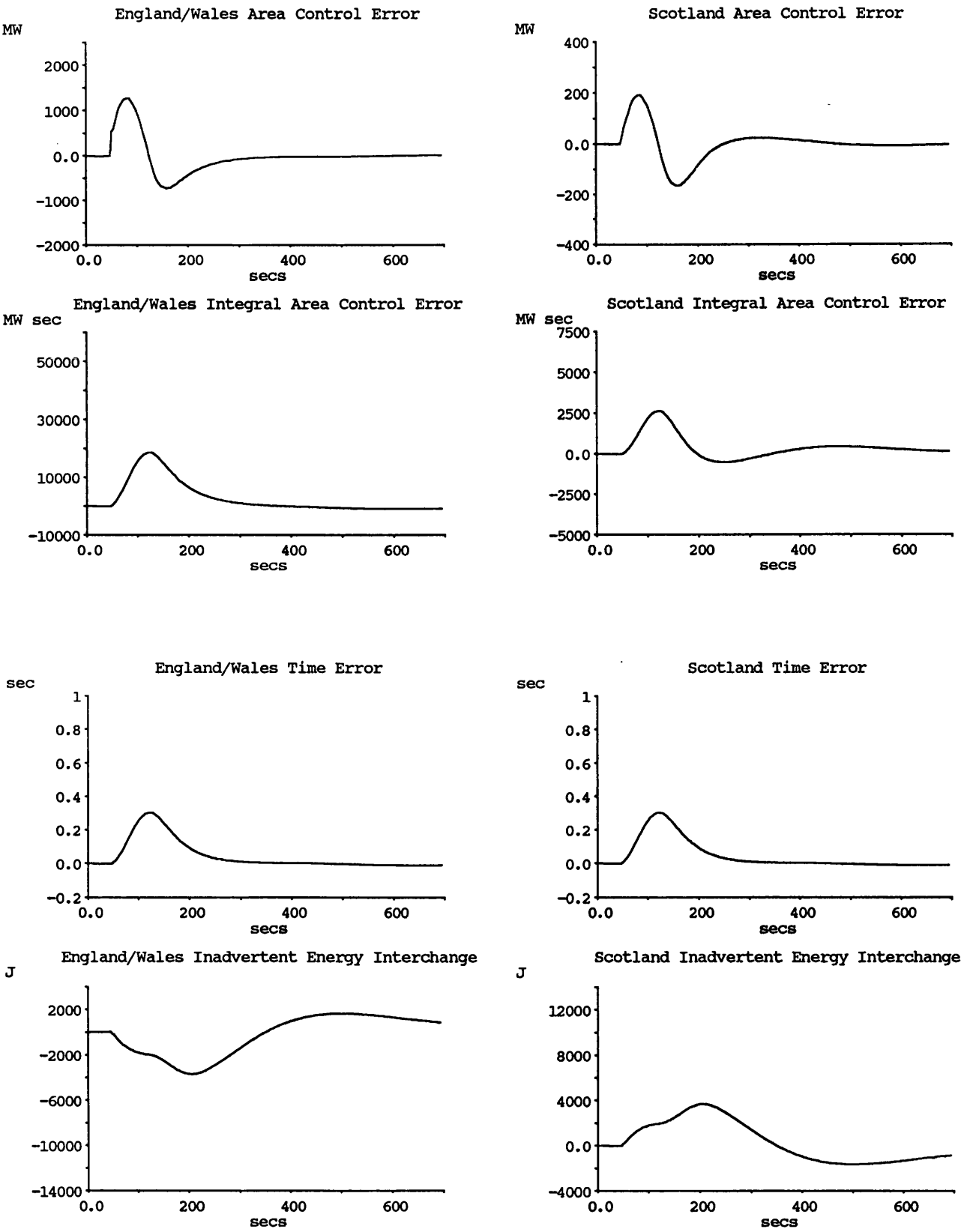

Figure 7.4: (e) 25 m'c Step Load Change (Run 8)

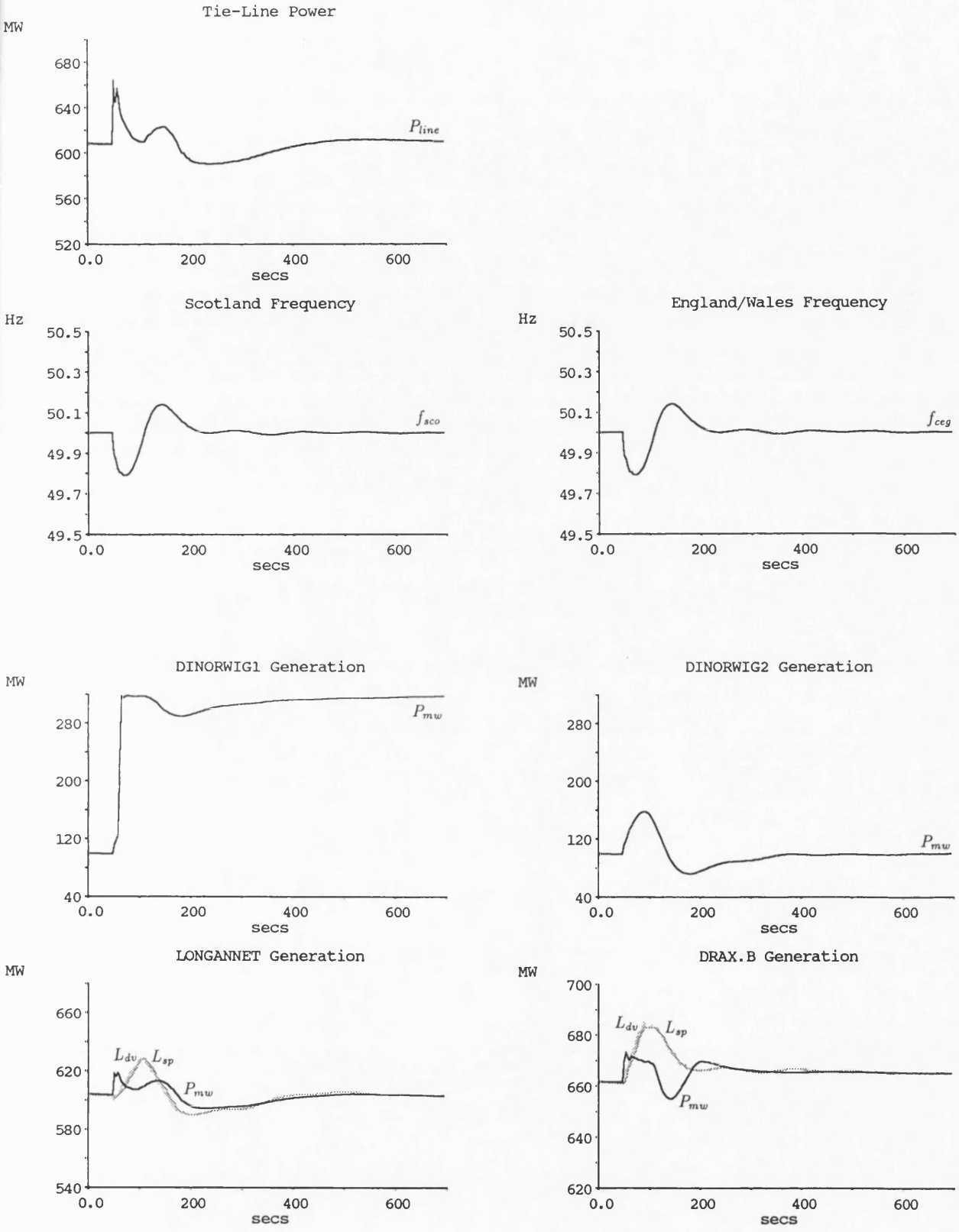

Figure 7.5: (a) 25 m'c Step Load Change (Run 7)

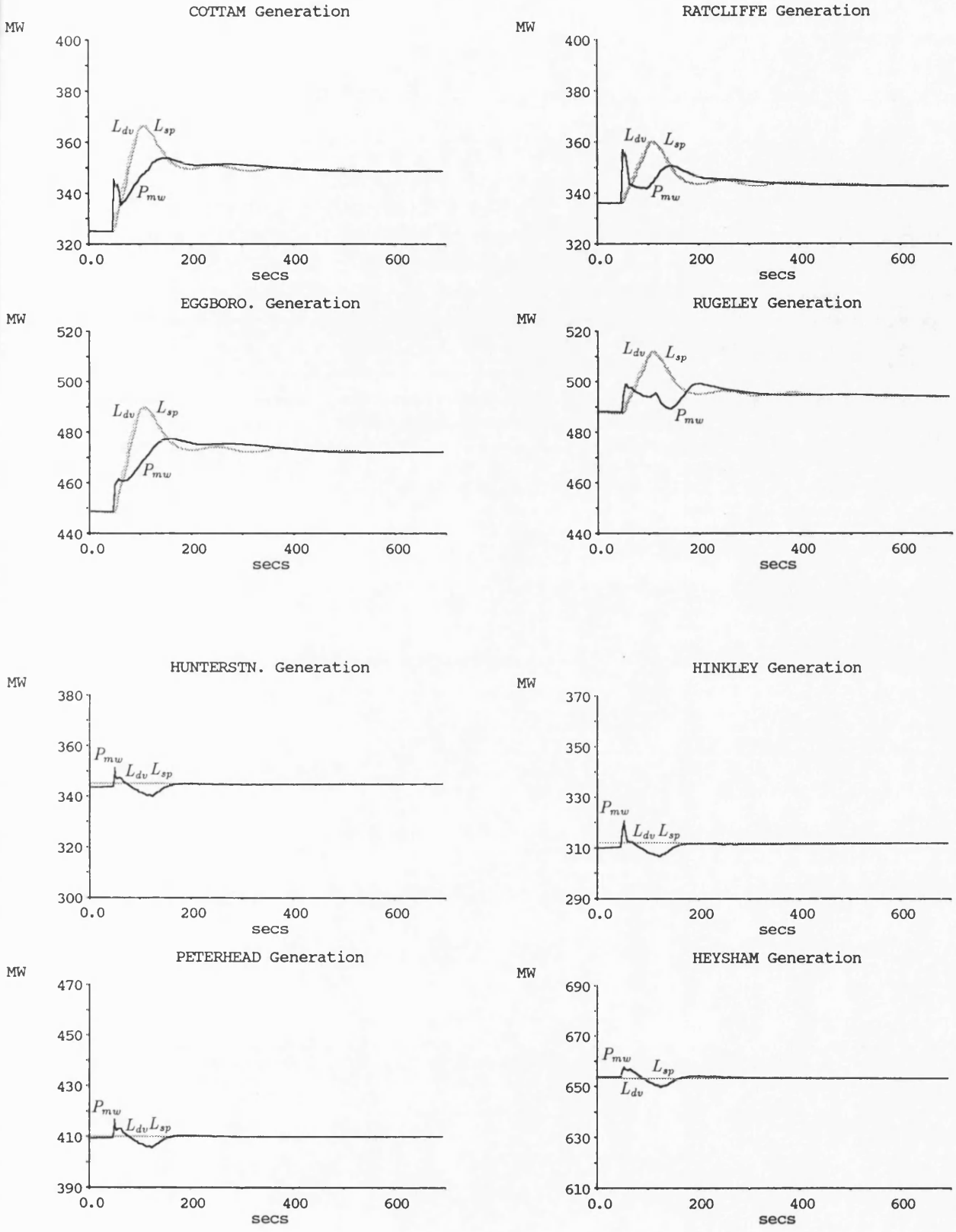

Figure 7.5: (b) 25 m'c Step Load Change (Run 7)

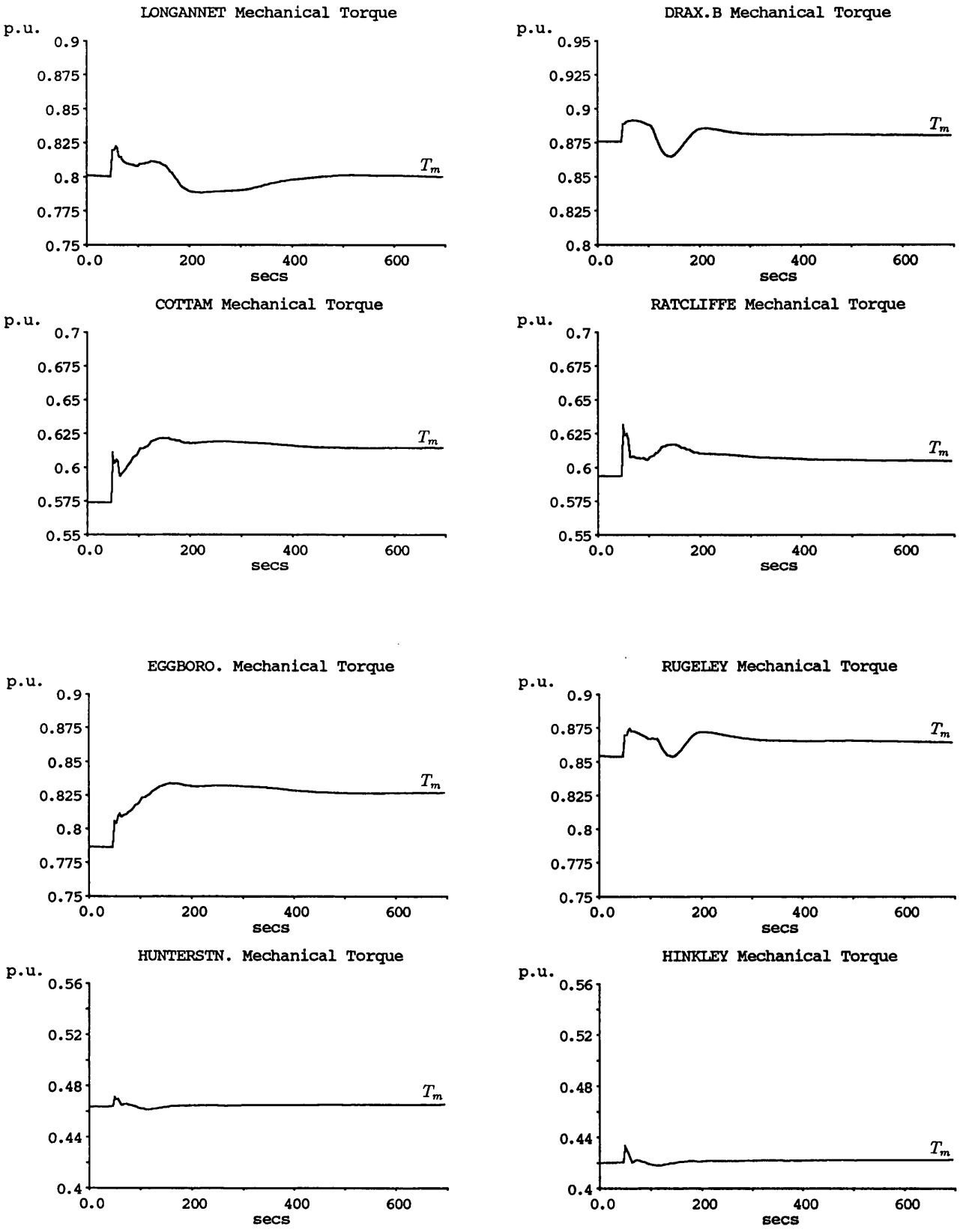

Figure 7.5: (c) 25 m'c Step Load Change (Run 7)

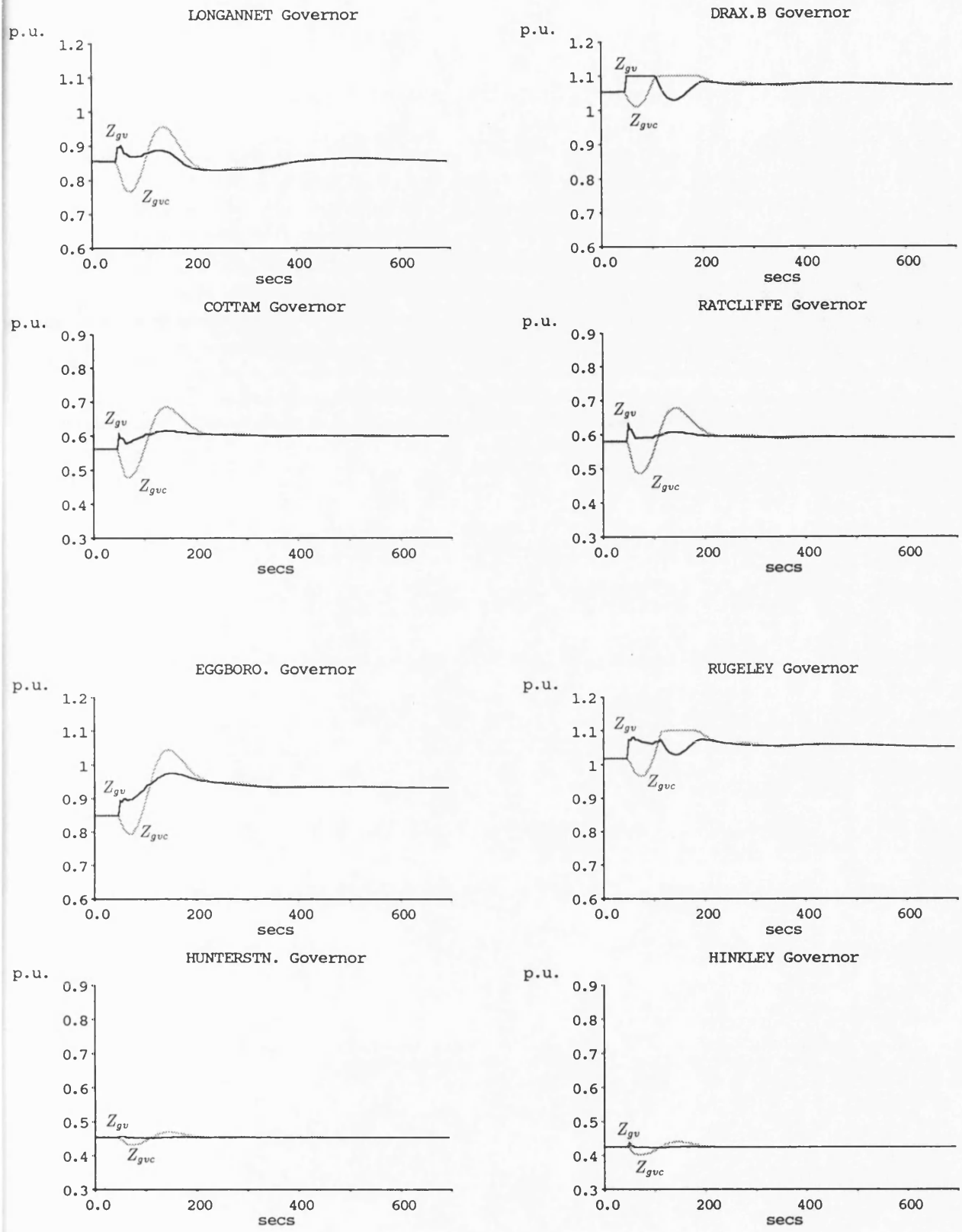

Figure 7.5: (d) 25 m'c Step Load Change (Run 7)

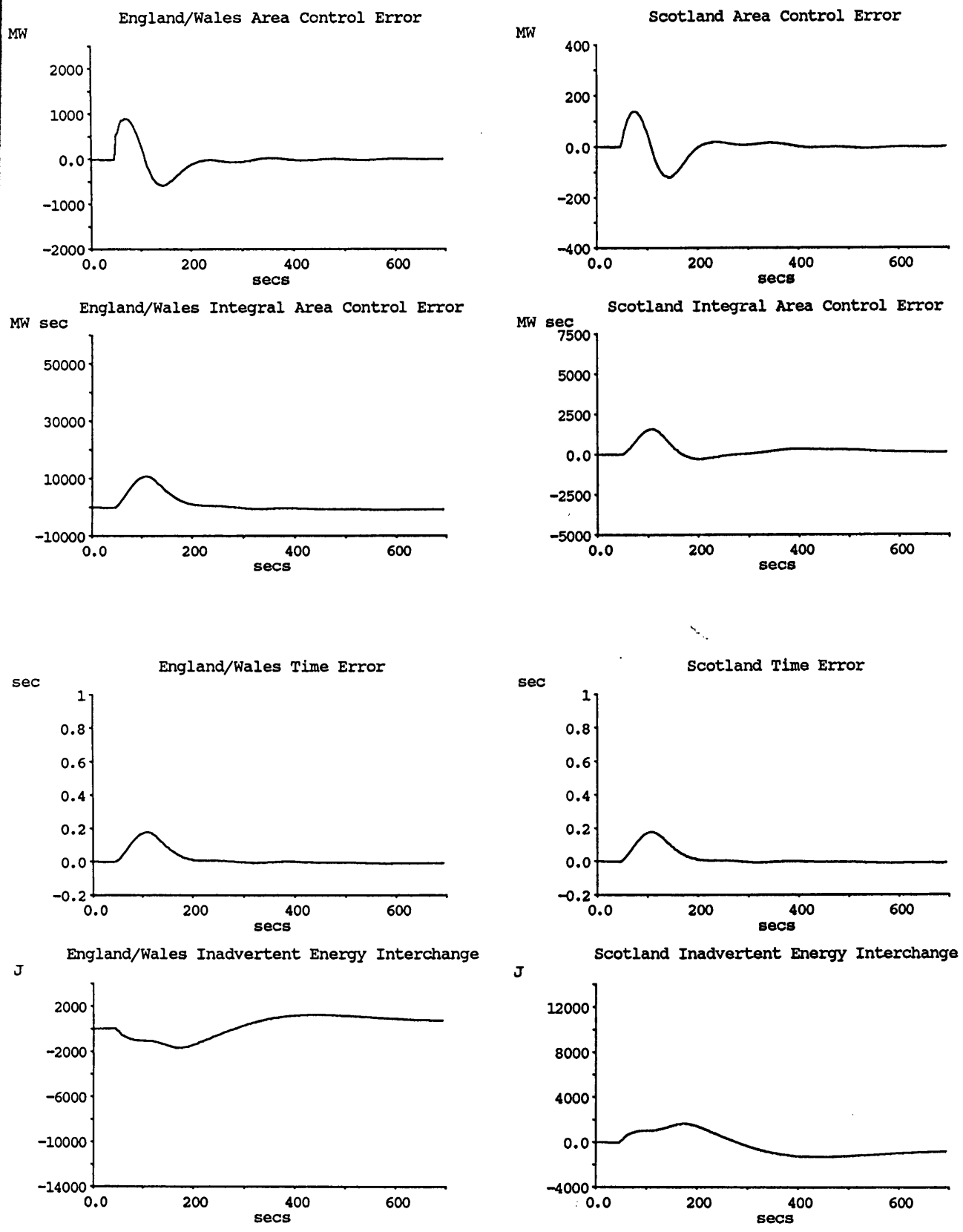

Figure 7.5: (e) 25 m'c Step Load Change (Run 7)

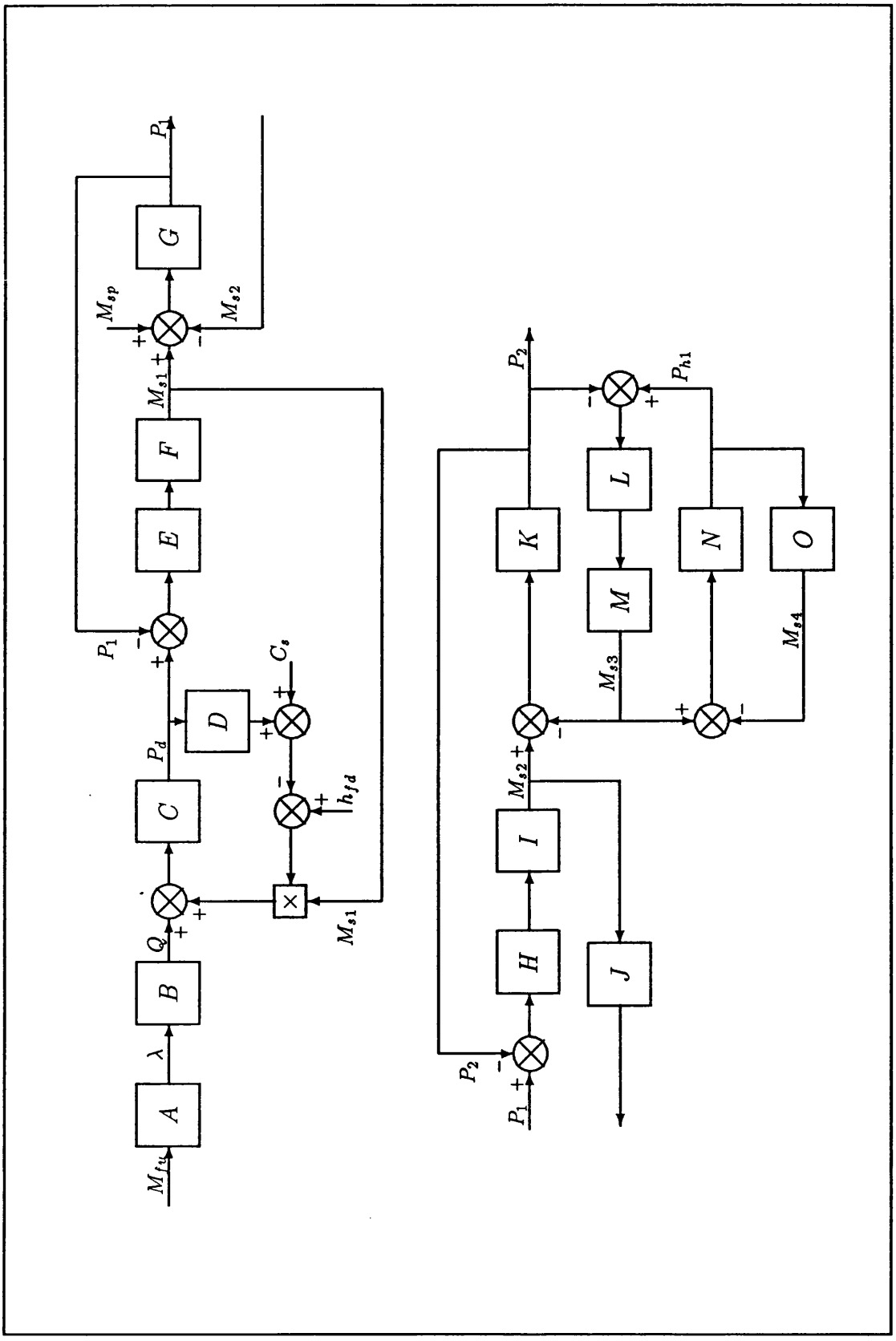

Figure H.1: Block Diagram of Plant in BFT Pressure Loop

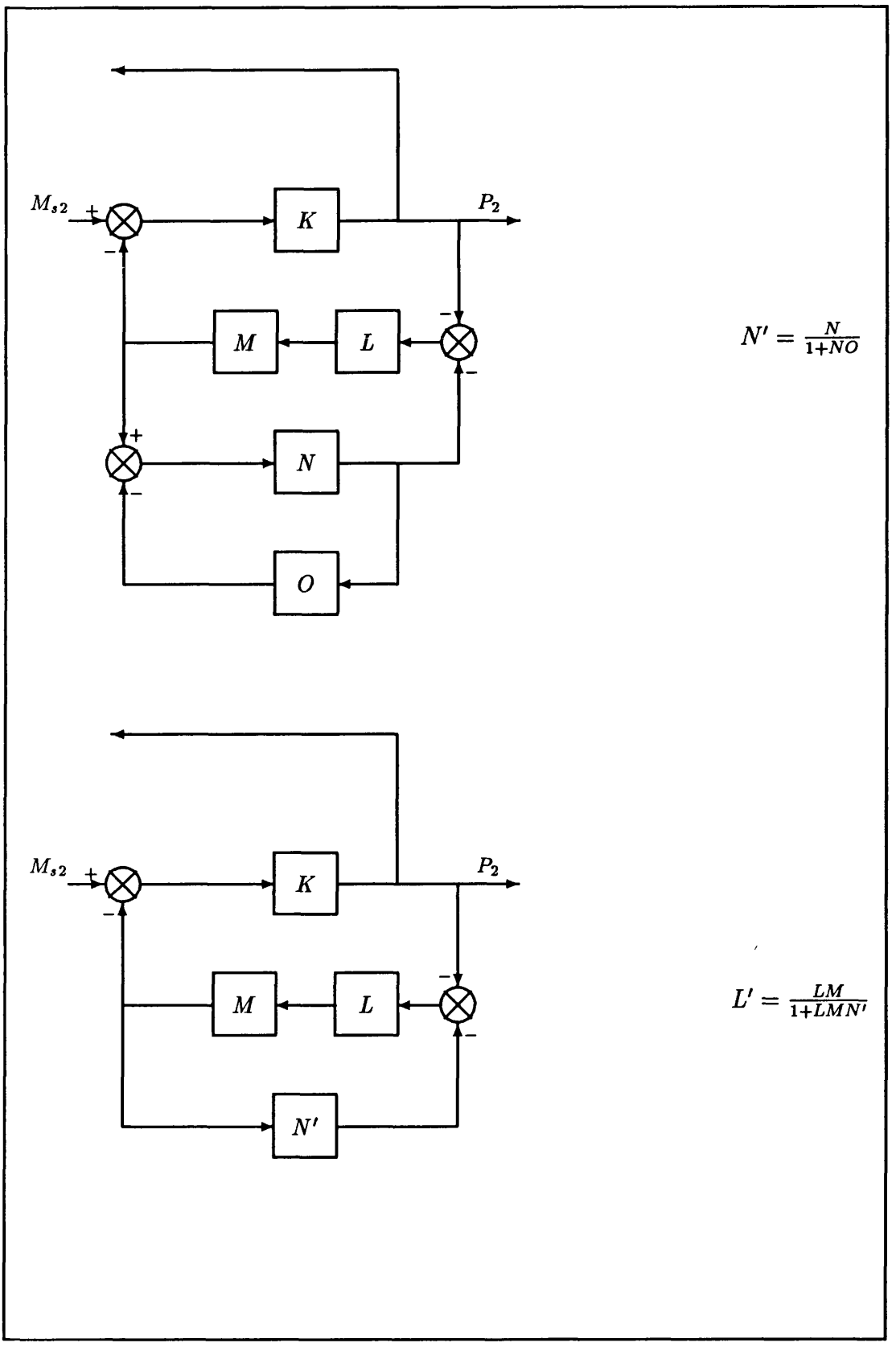

Figure H.2: (a) BFT Pressure Loop Block Diagram Transformation

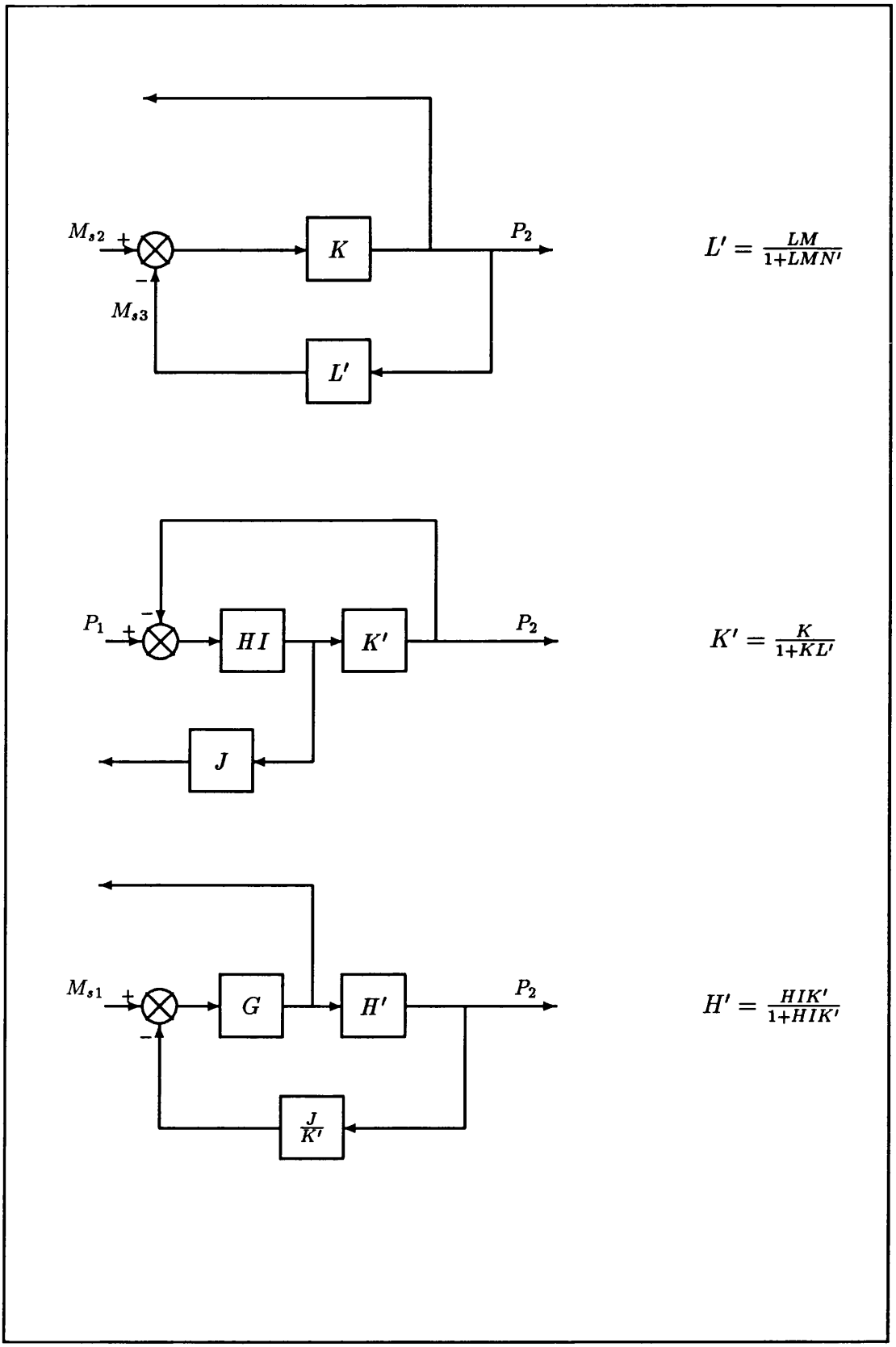

Figure H.2: (b) BFT Pressure Loop Block Diagram Transformation

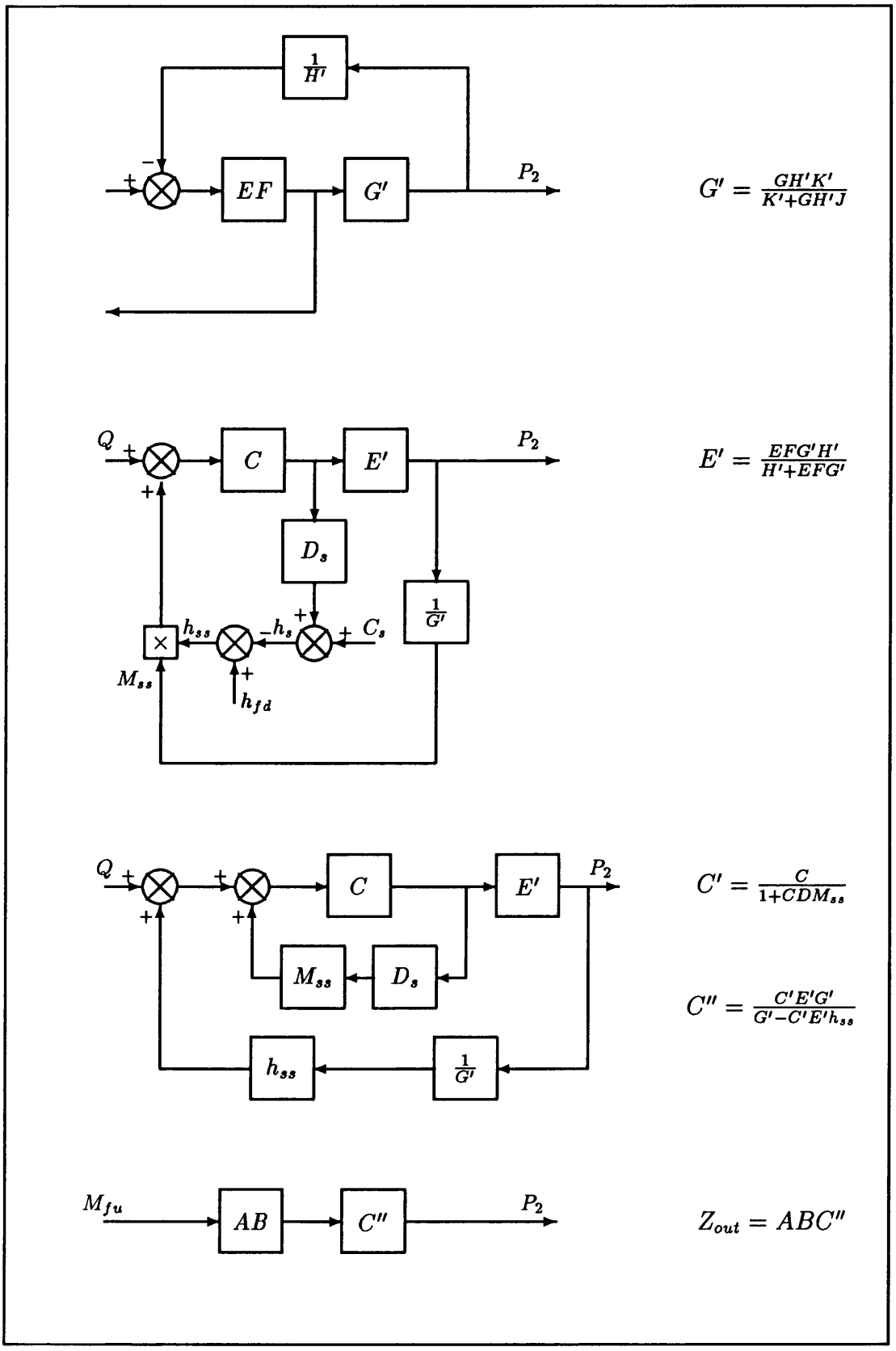

Figure H.2: (c) BFT Pressure Loop Block Diagram Transformation

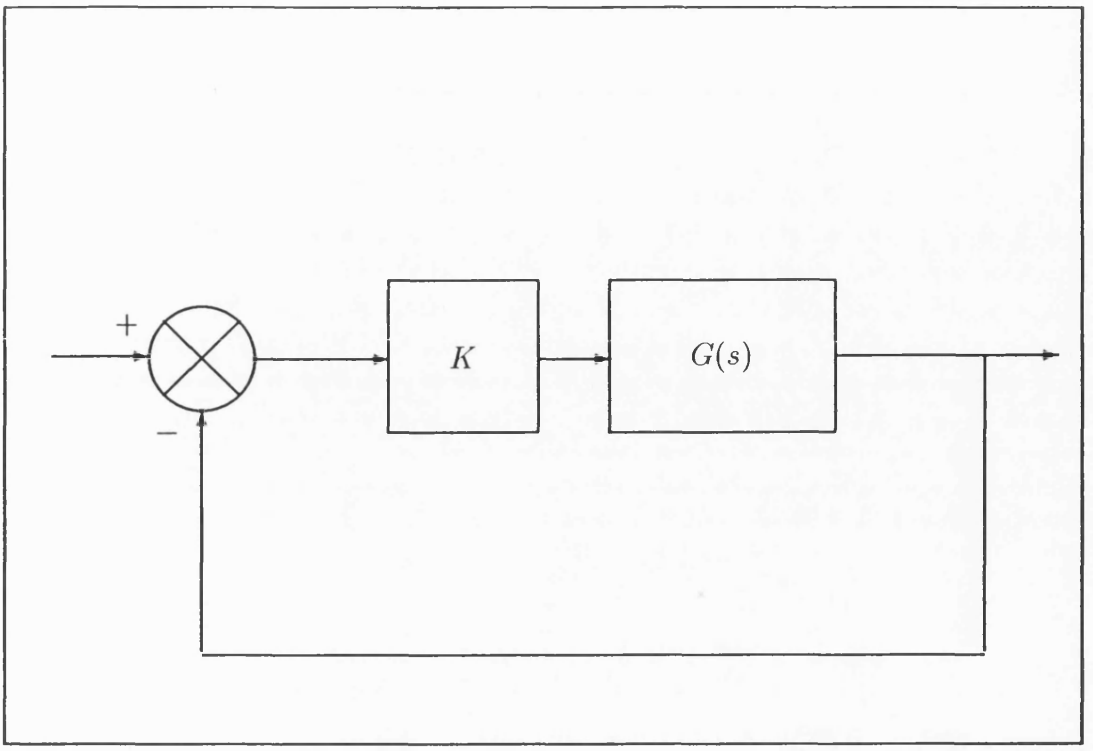

Figure H.3: Block Diagram of Proportional Control

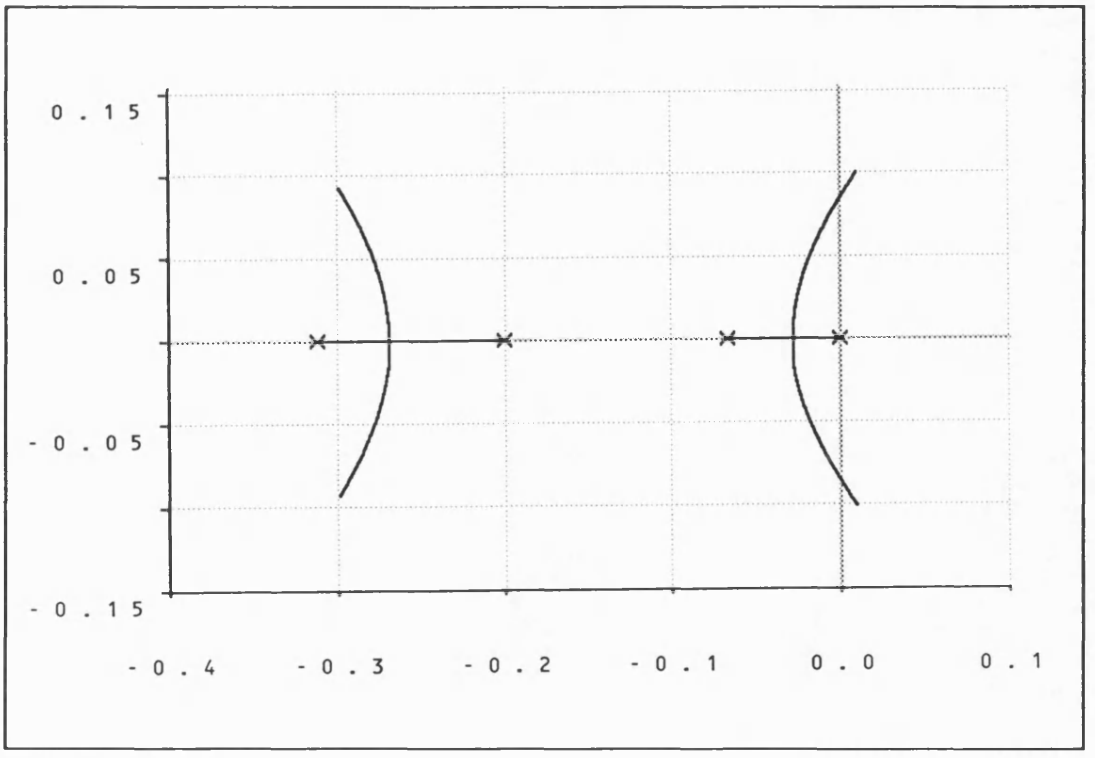

Figure H.4: Pressure Loop Root Locus with Proportional Control

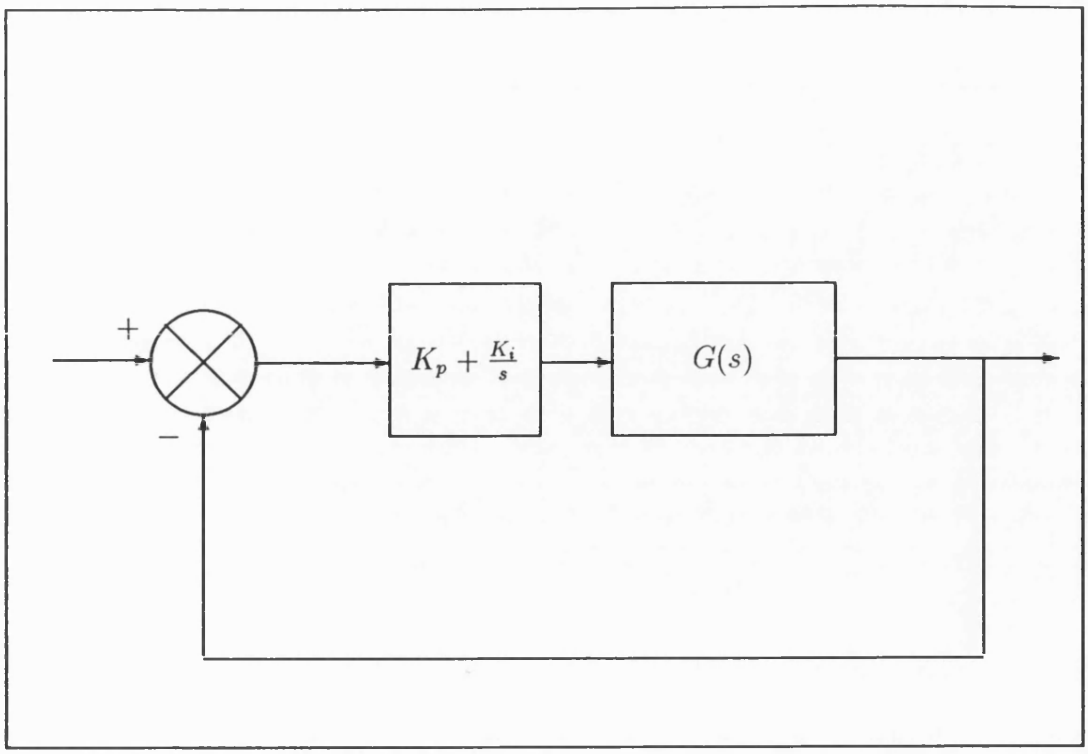

Figure H.5: Block Diagram of Proportional-Integral Control

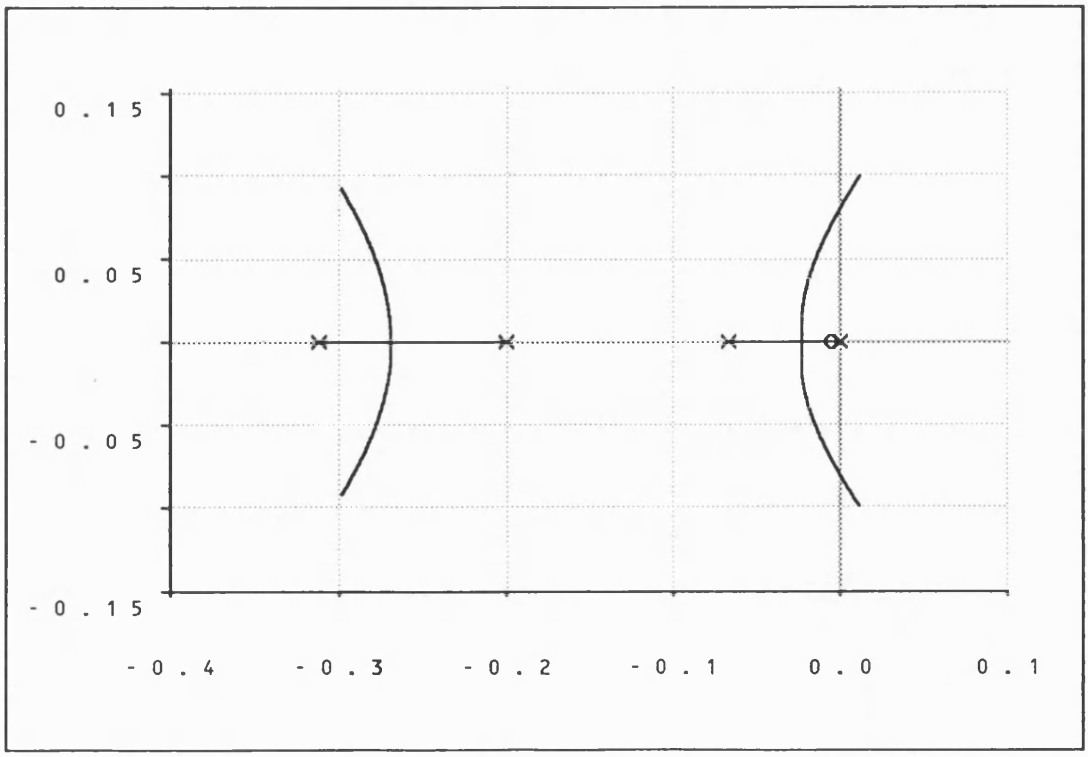

Figure H.6: Root Locus of Pressure Loop with Fast Zero in PI Controller

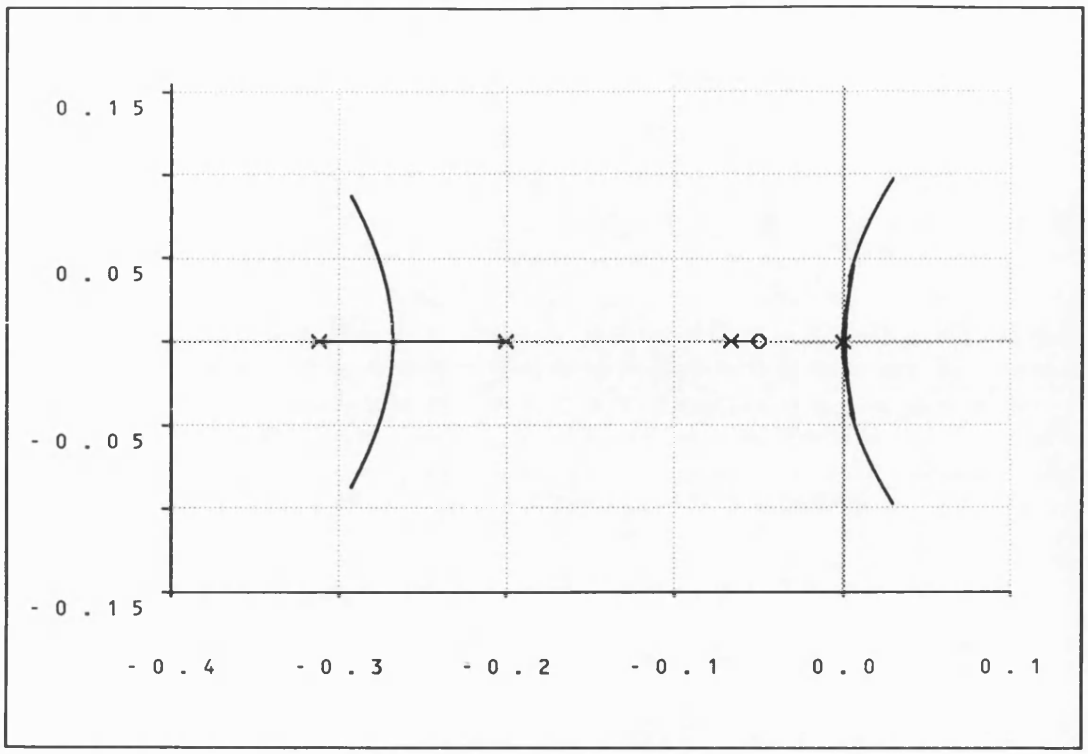

Figure H.7: Root Locus of Pressure Loop with Slow Zero in PI Controller

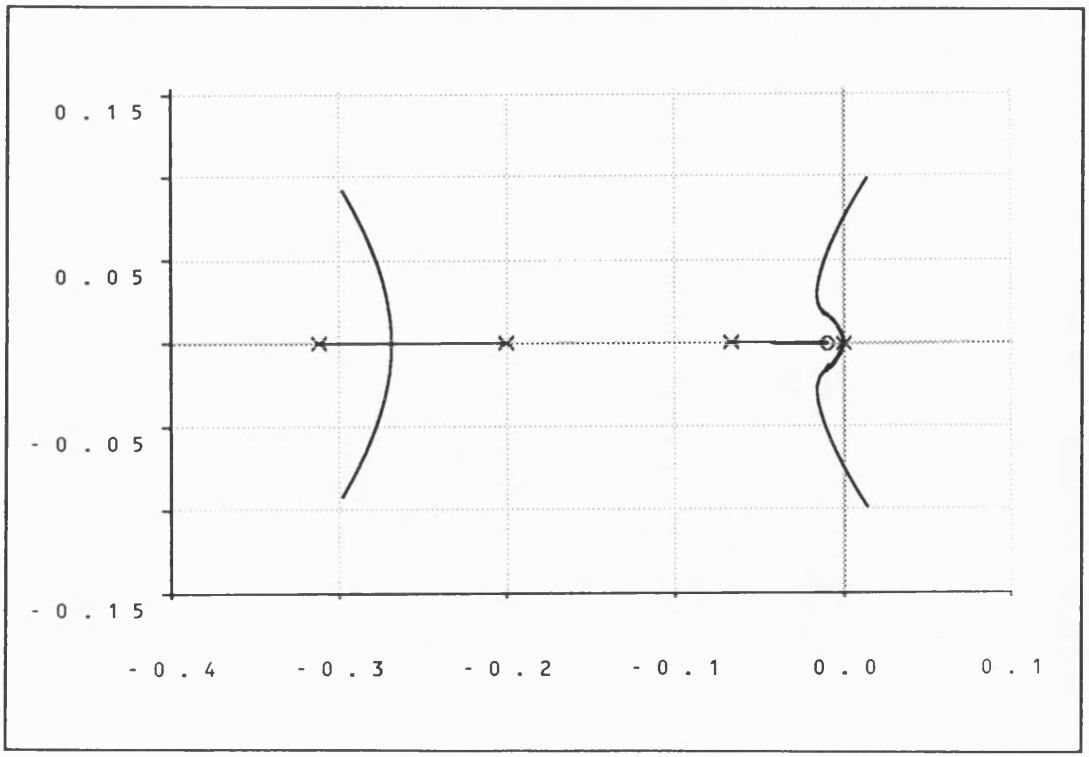

Figure H.8: Root Locus of Pressure Loop with Zero at $s = -0.01$

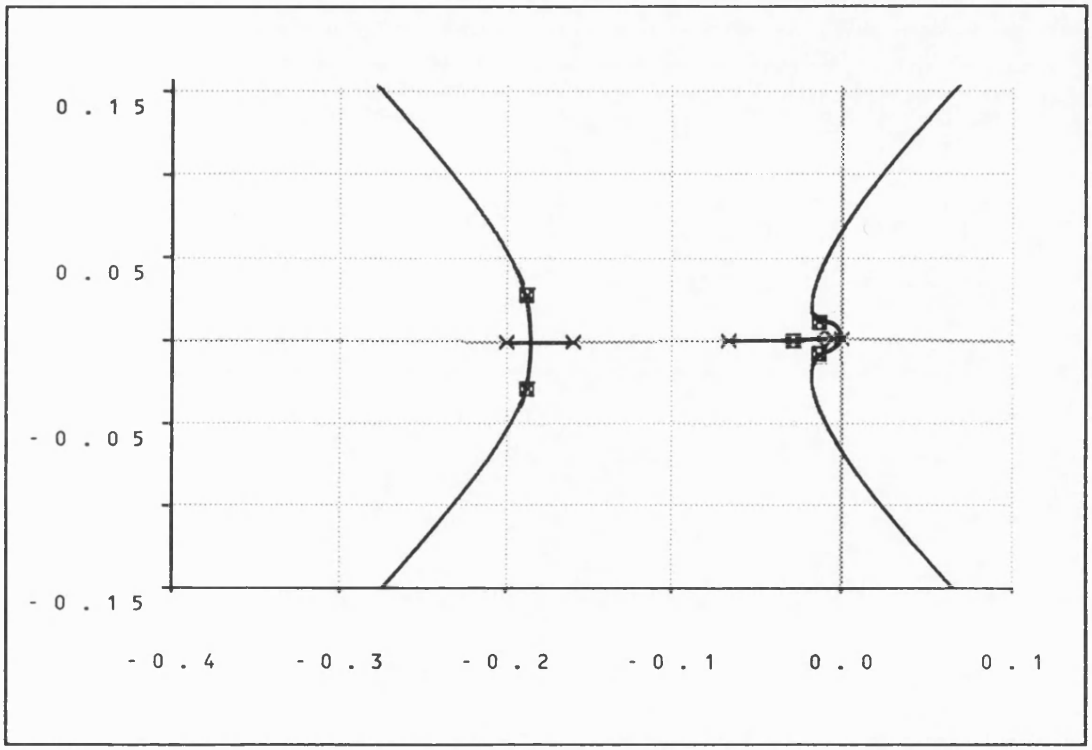

Figure H.9: Root Locus of Pressure Loop at 360 MW with Zero at $s = -0.01$

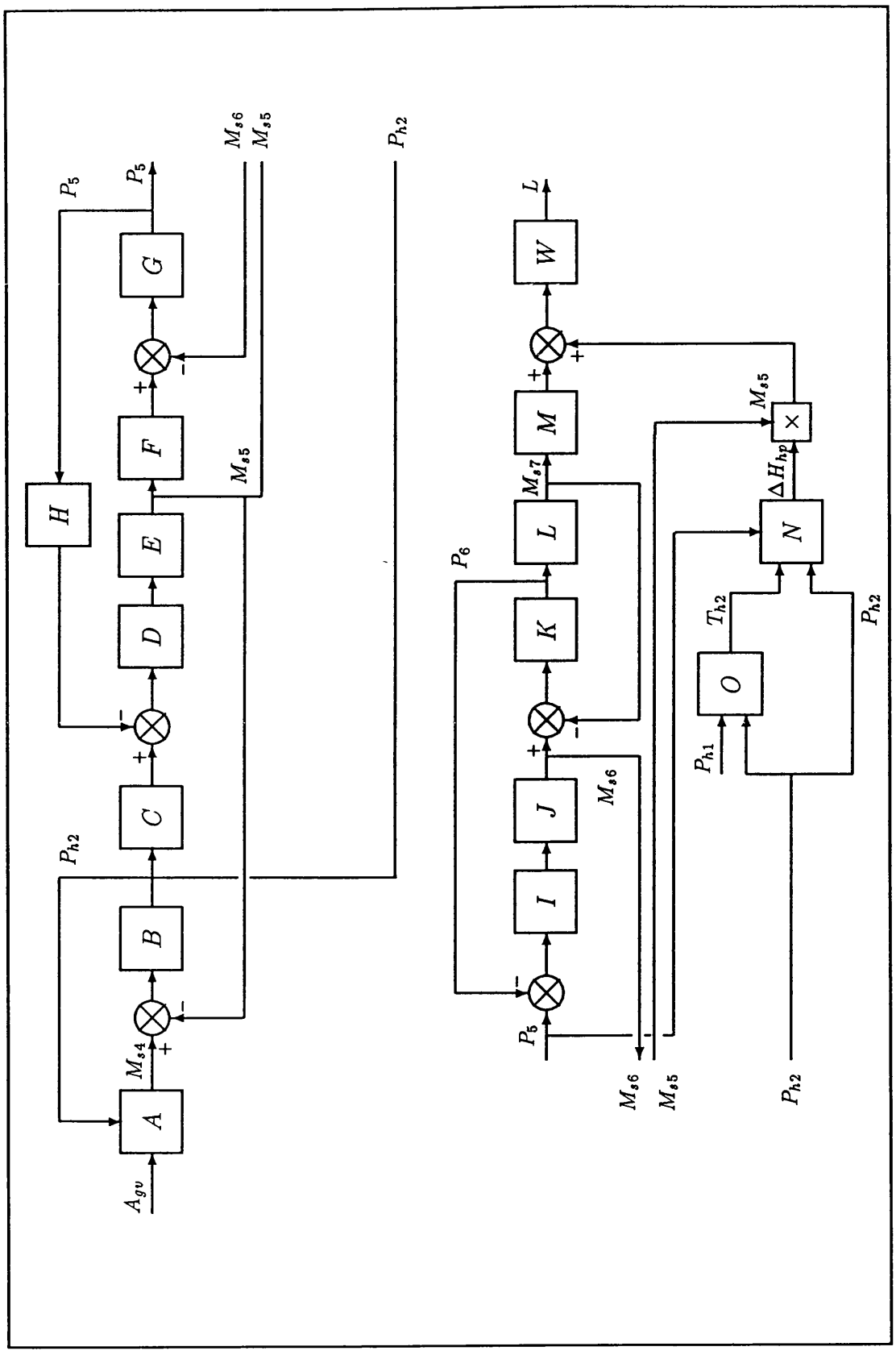

Figure I.1: Block Diagram of Plant in BFT Load Loop

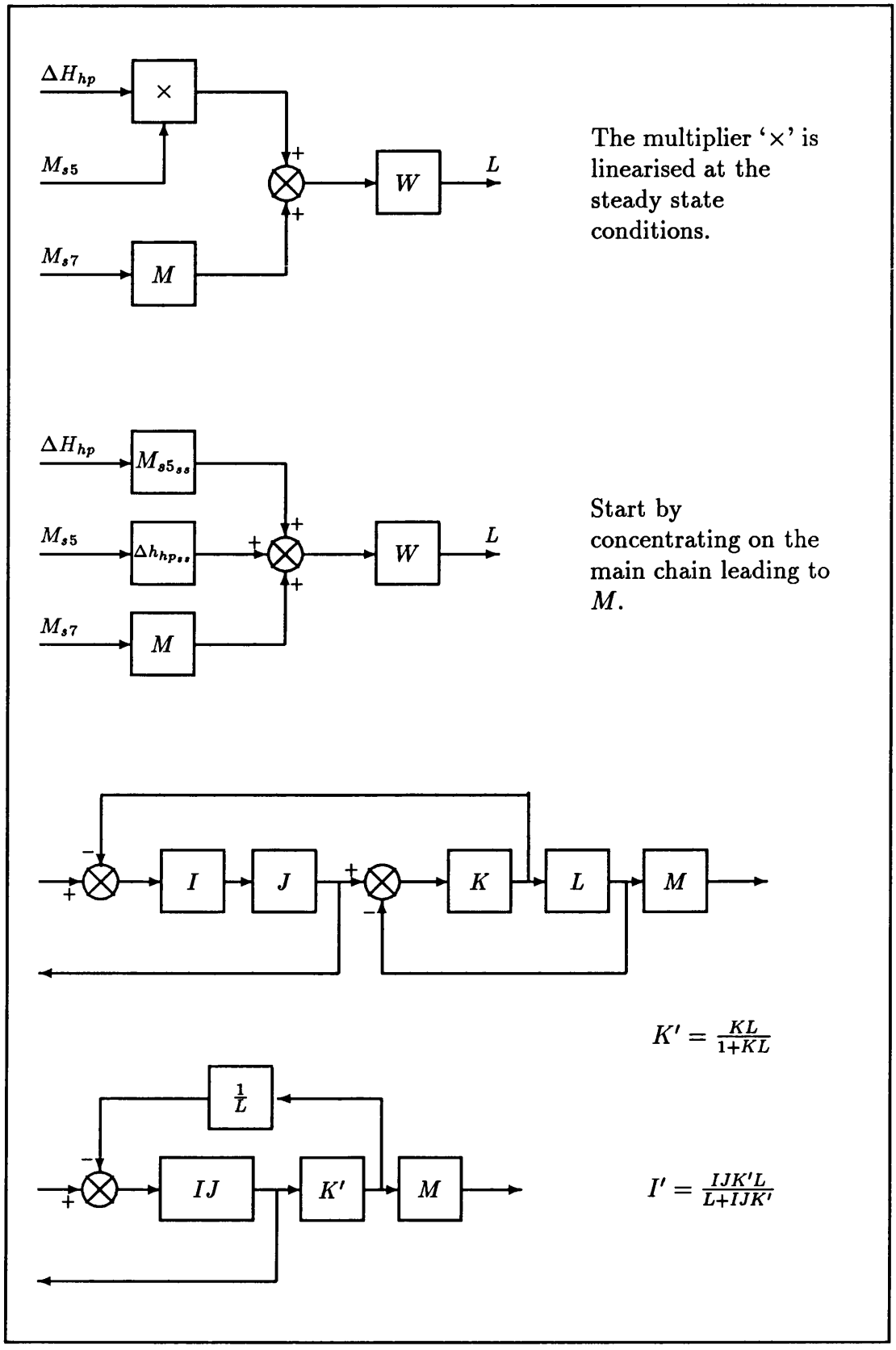

Figure I.2: (a) BFT Load Loop Block Diagram Transformation

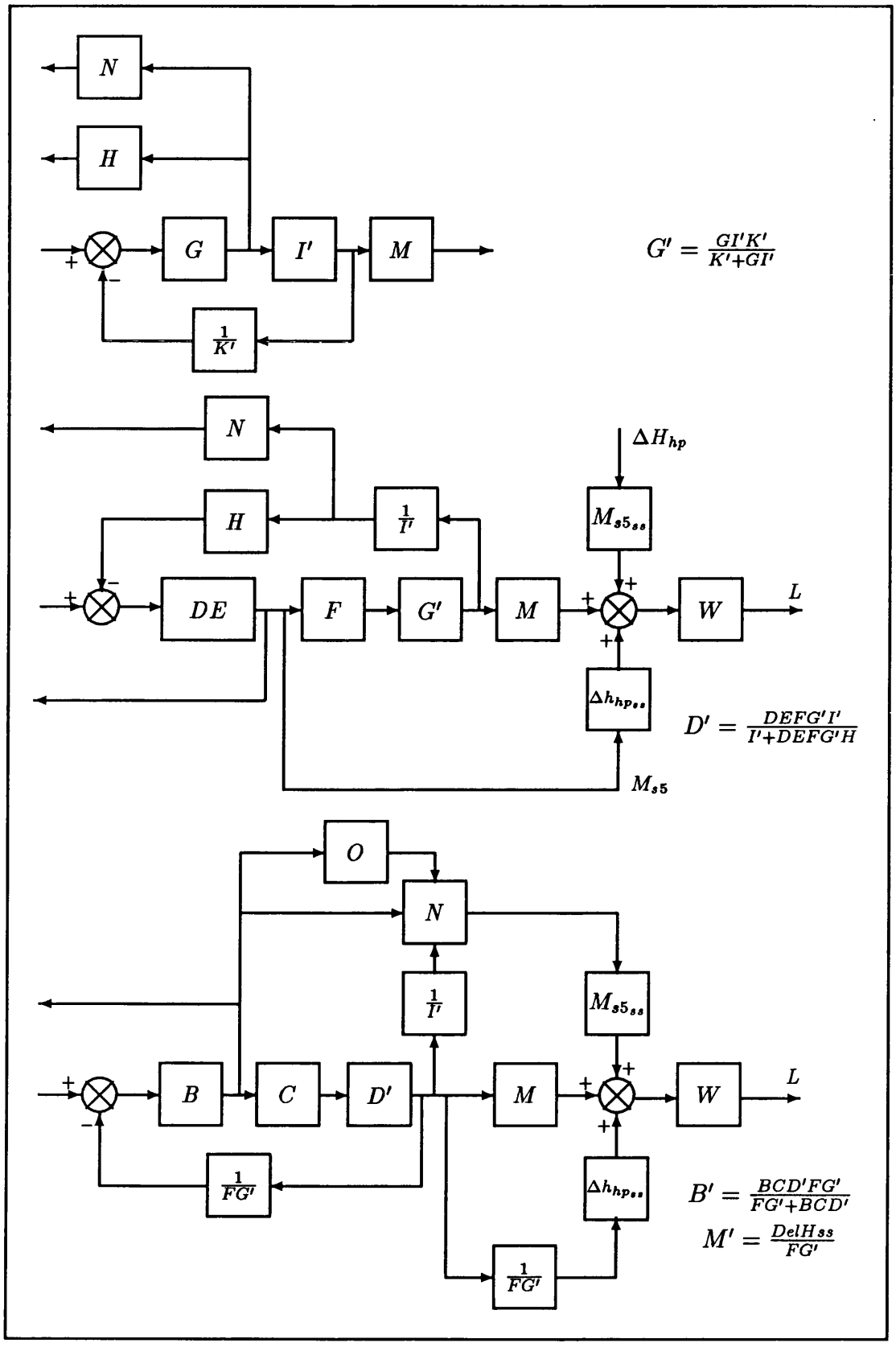

Figure I.2: (b) BFT Load Loop Block Diagram Transformation

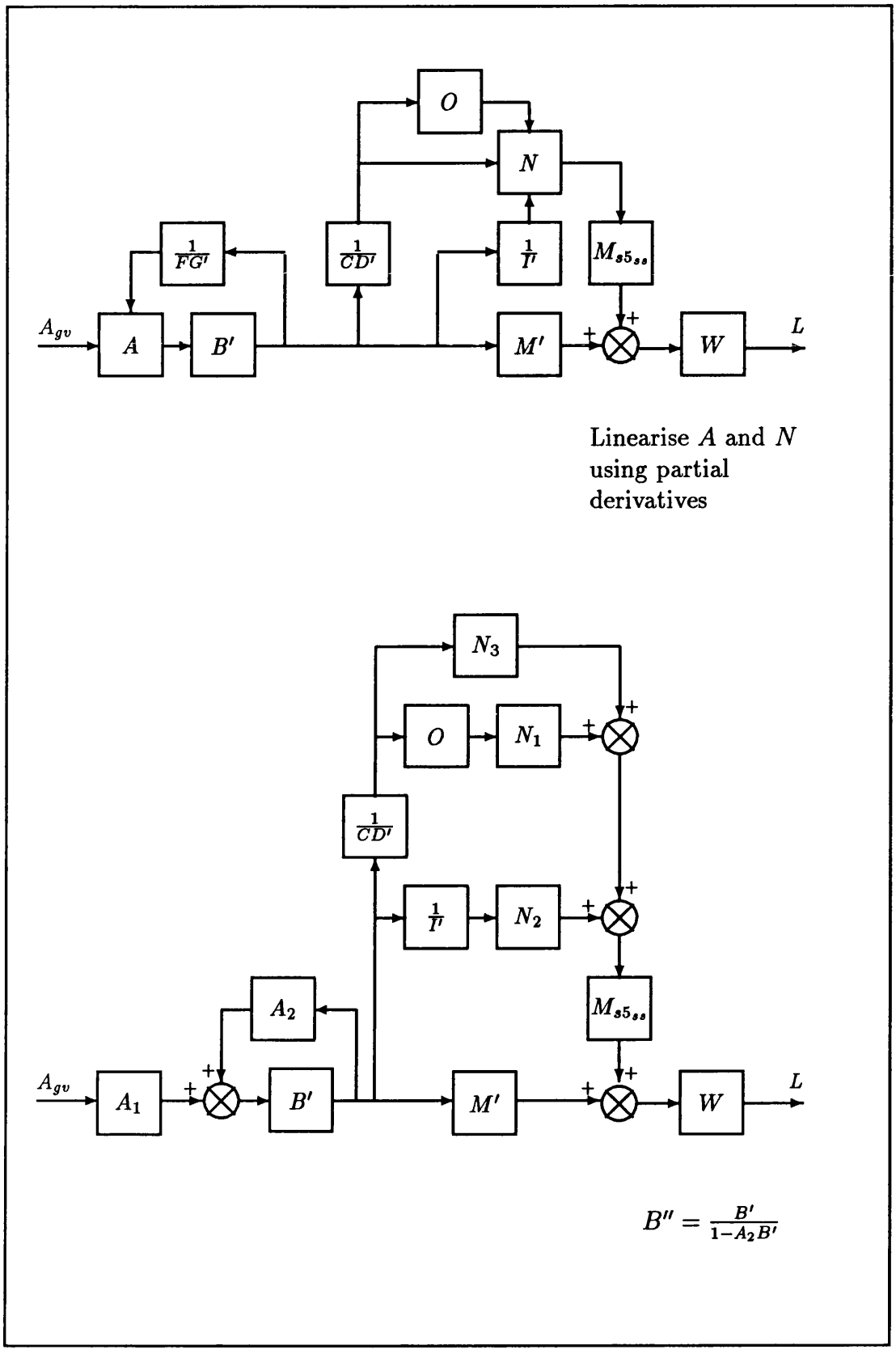

Figure I.2: (c) BFT Load Loop Block Diagram Transformation

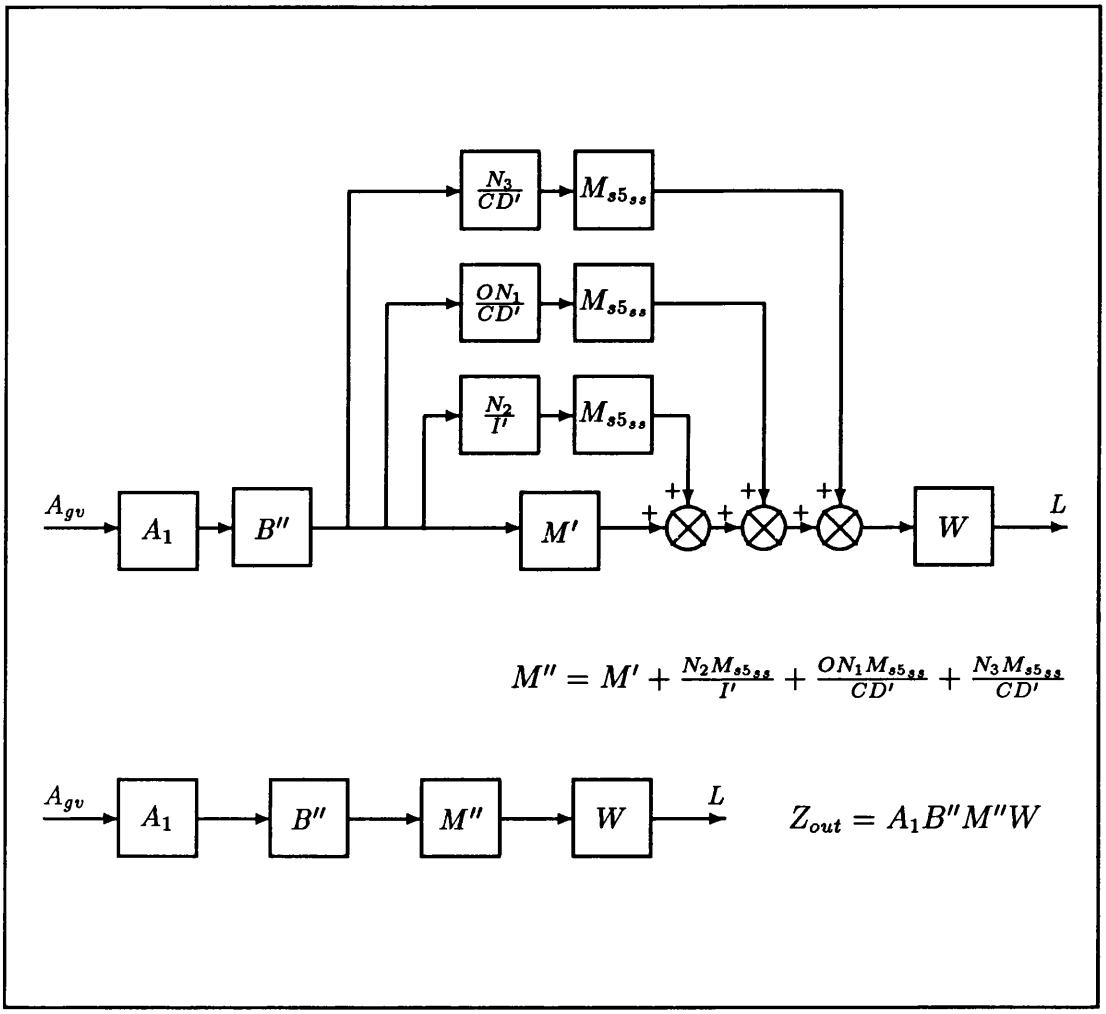

Figure I.2: (d) BFT Load Loop Block Diagram Transformation

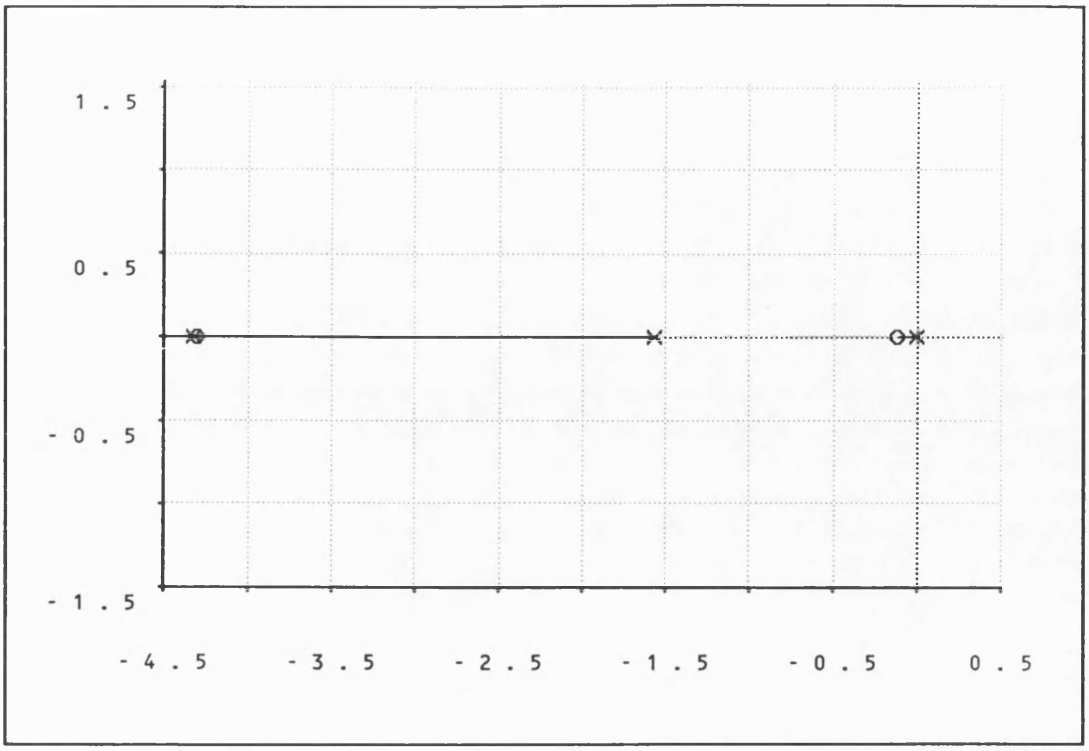

Figure I.3: Root Locus of Load Loop with Proportional Control @ 170 MW

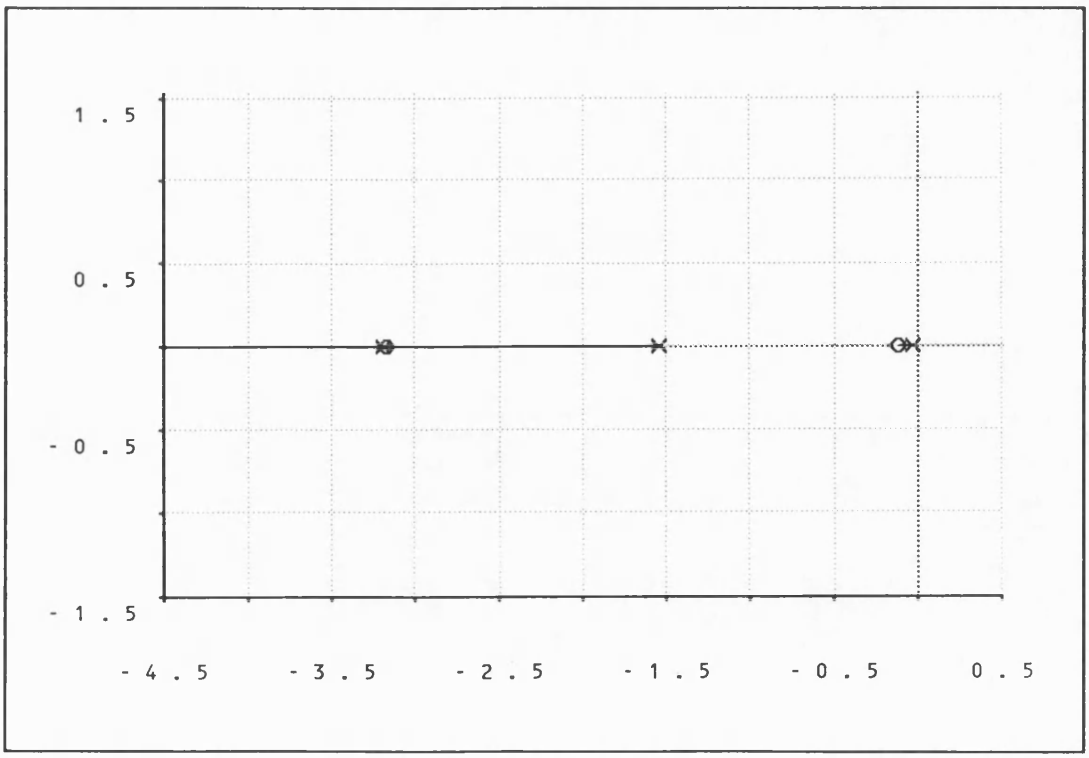

Figure I.4: Root Locus of Load Loop with Proportional Control @ 250 MW

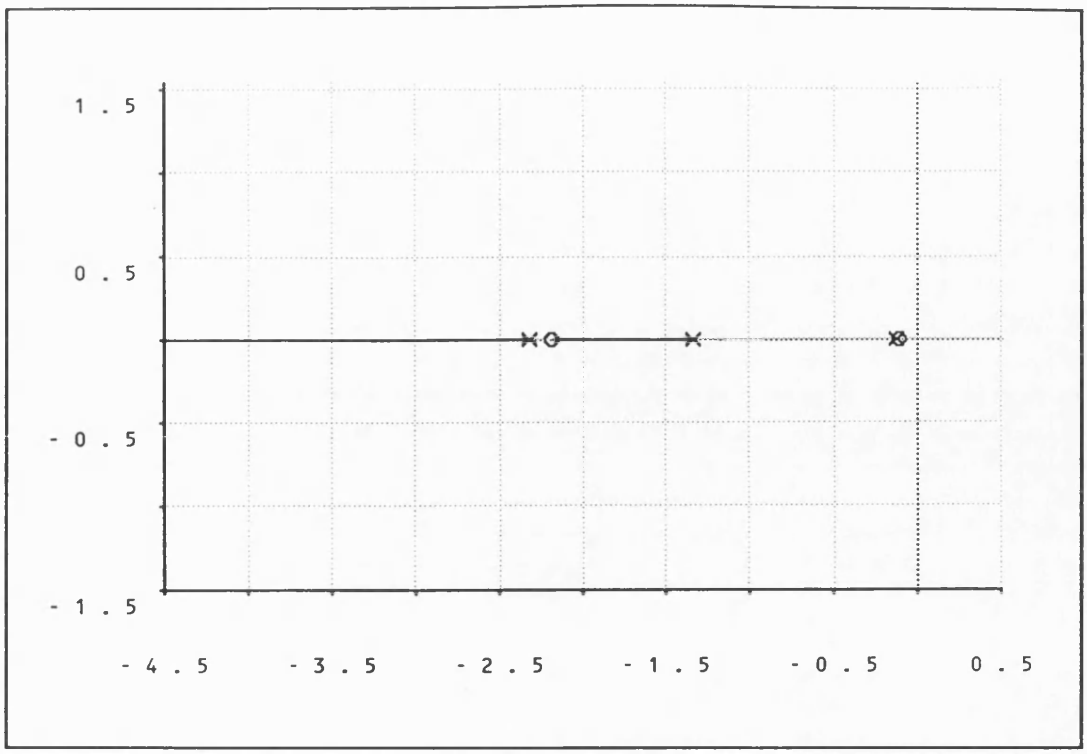

Figure I.5: Root Locus of Load Loop with Proportional Control @ 390 MW

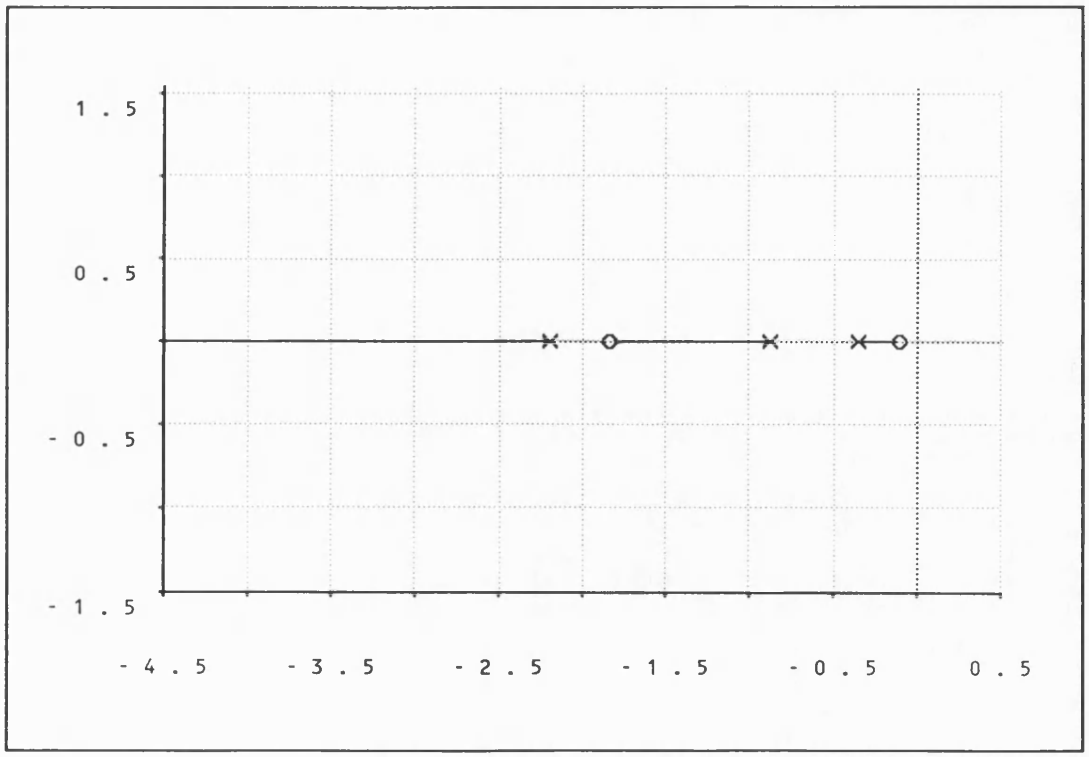

Figure I.6: Root Locus of Load Loop with Proportional Control @ 490 MW

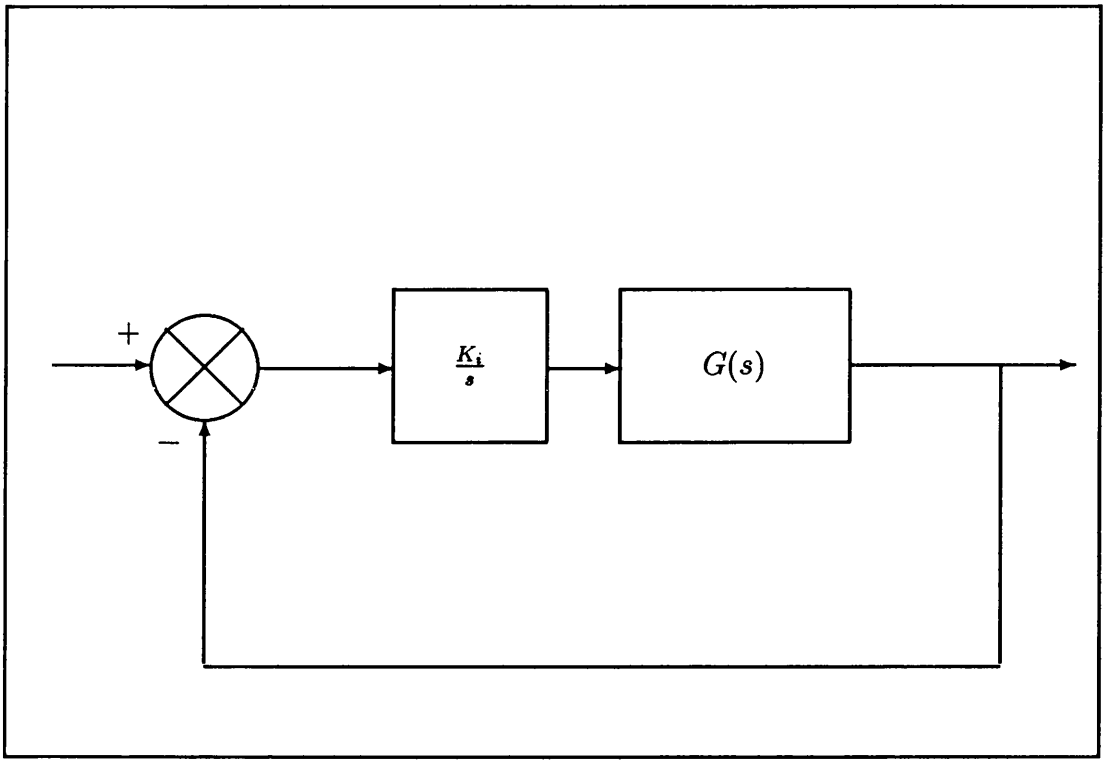

Figure I.7: Block Diagram of Integral Control

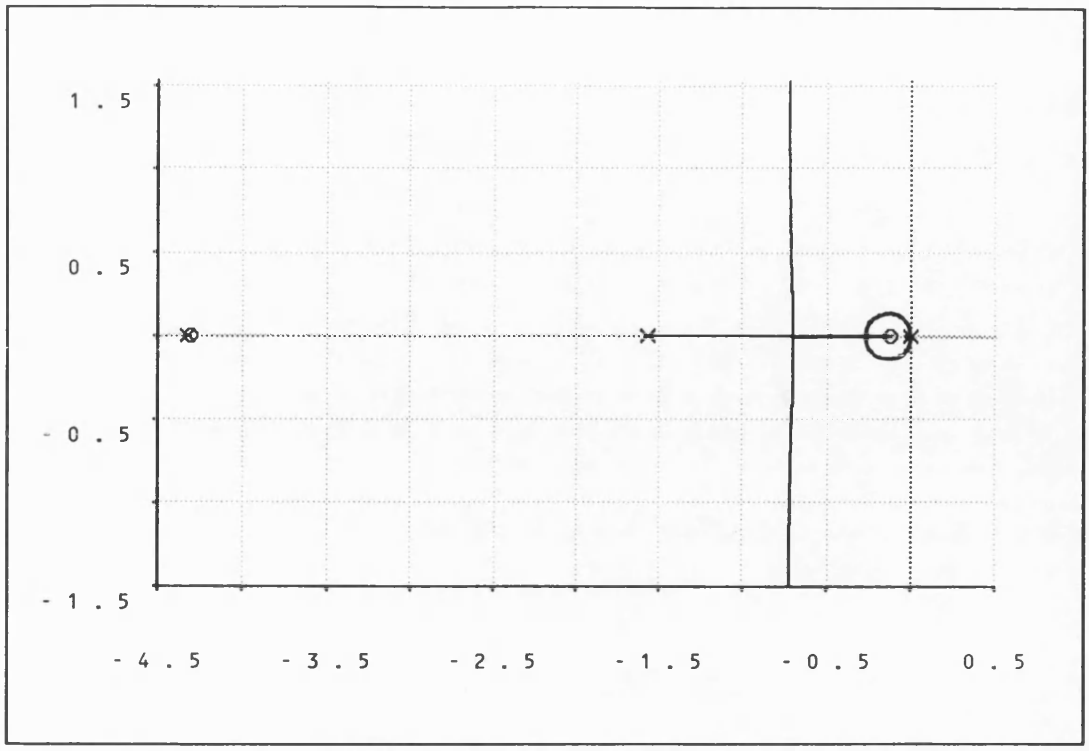

Figure I.8: Root Locus of Load Loop with Integral Control @ 170 MW

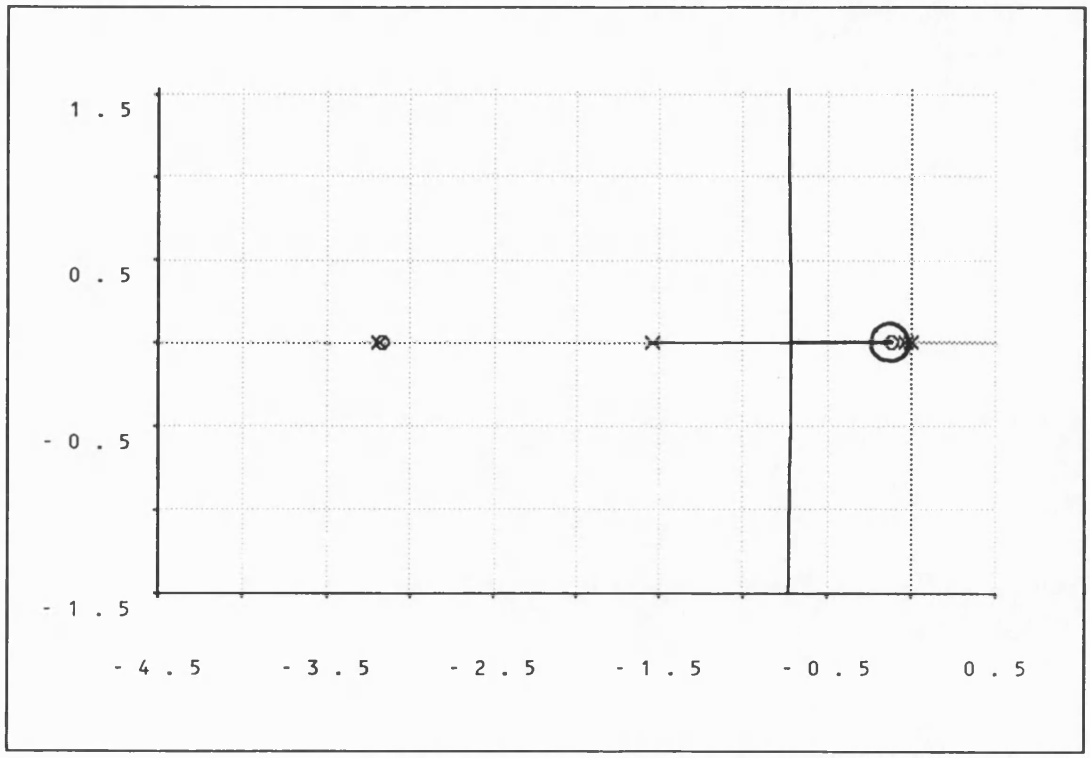

Figure I.9: Root Locus of Load Loop with Integral Control @ 250 MW

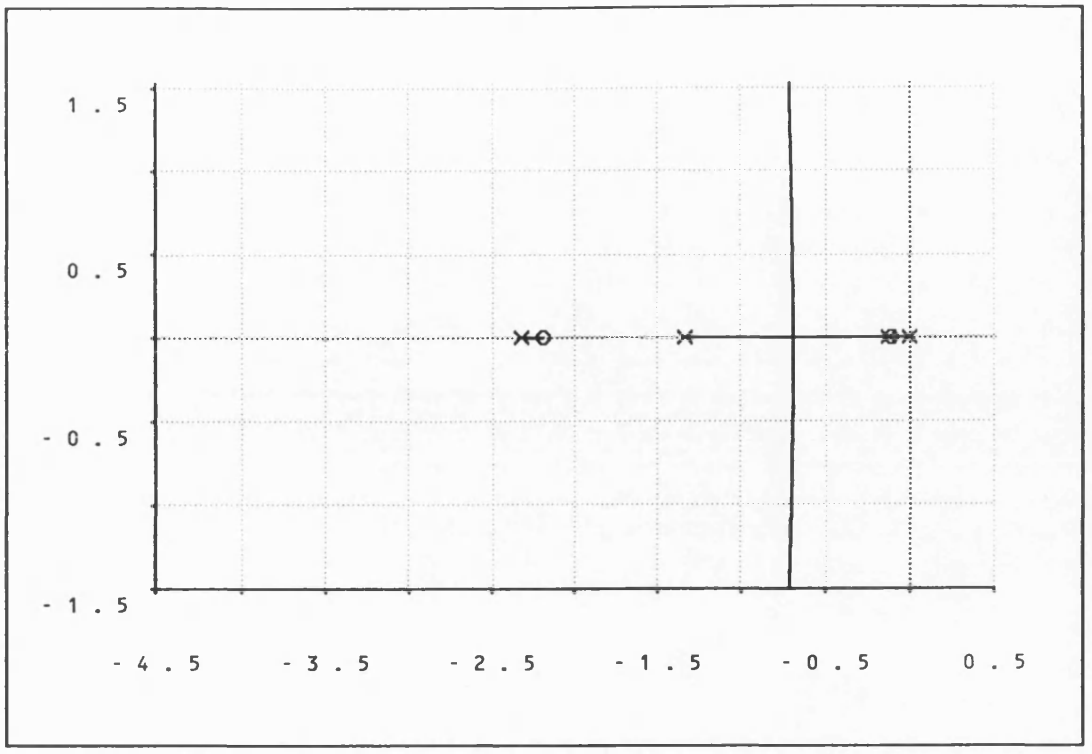

Figure I.10: Root Locus of Load Loop with Integral Control @ 390 MW

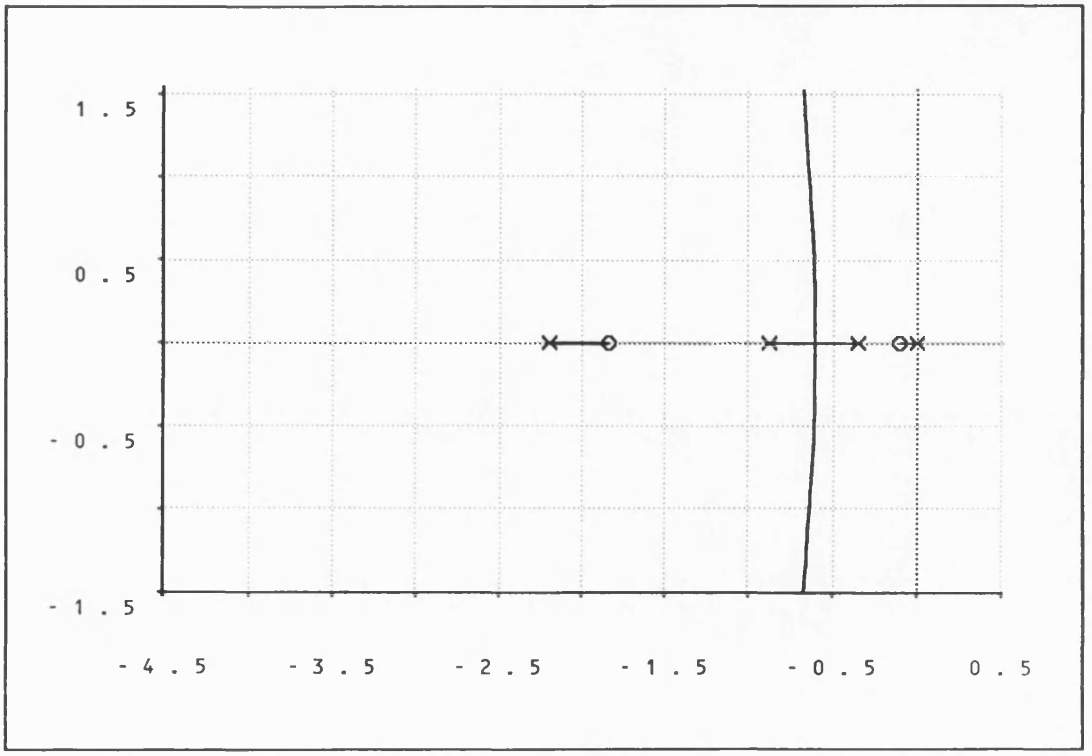

Figure I.11: Root Locus of Load Loop with Integral Control @ 490 MW

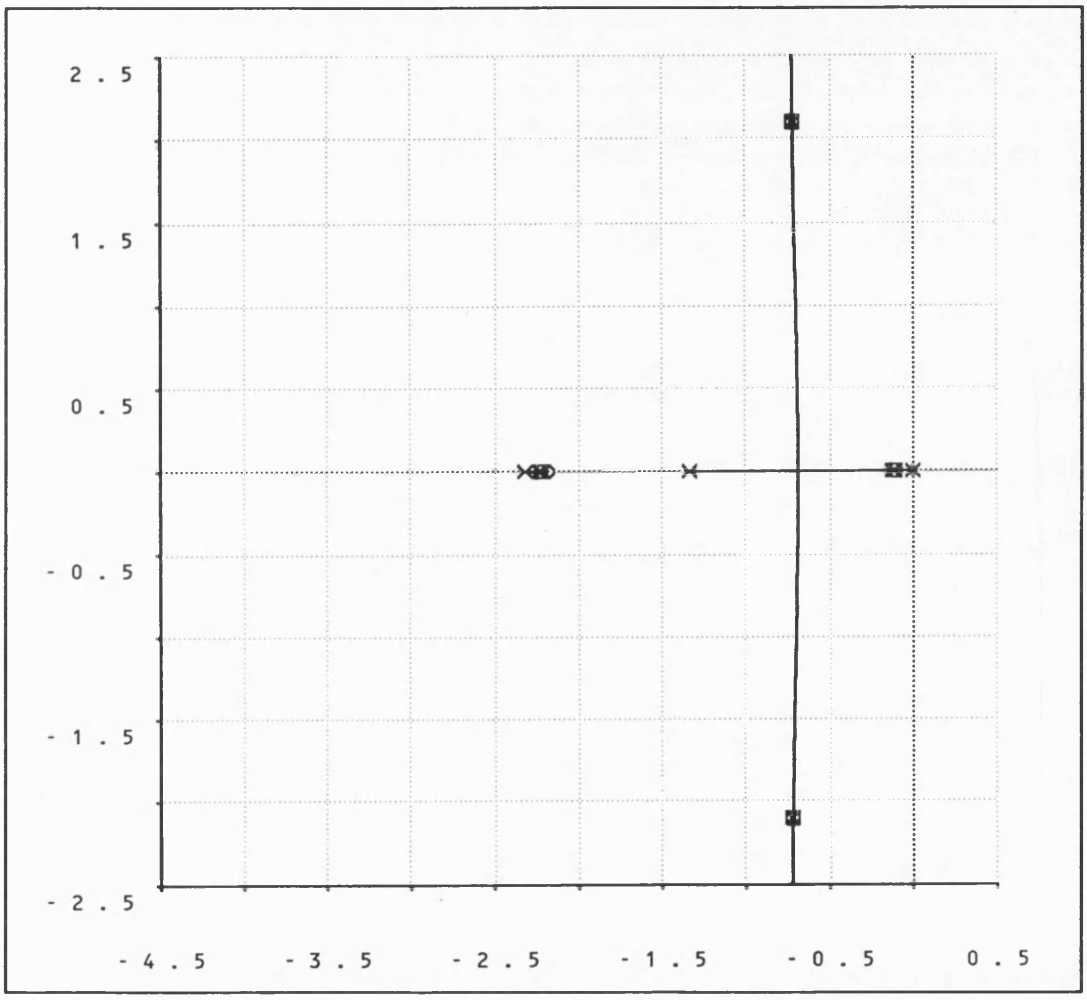

Figure I.12: Root Locus of Load Loop with $K_I = 0.00025$ @ 390 MW

Bibliography

[1] Electricity Council. *History of Electricity in Great Britain, a Chronology*, Dec. 1971. Serial No. RP.3.

[2] Lord Hinton of Bankside. *Heavy Current Electricity in the United Kingdom, History and Development.* Pergamon Press, first edition, 1979. ISBN 0-08-023246-9.

[3] F. D. Boardman. Control and operation of the UK electricity supply system: an account of its development. *IEE Proceedings*, 125(1):61–65, Jan. 1978.

[4] U. G. Knight and F. Moran. The operation and control of the CEGB power system. *Trans. Inst. MC.*, 6(5), Oct. 1984.

[5] H. E. Pulsford. Developments in power system control. *IEE Proceedings*, 114(8):1139–1148, 1967.

[6] J. H. Banks, J. W. Dillow, U. G. Knight, and A. G. Oughton. Paper 2.1.6. In *International Union of Producers and Distributors of Electrical Energy Data Processing Conference*, Lisbon, June 1971.

[7] S. R. Browning, P. H. Plumptre, H. R. W. Lewis, and R. G. Lucas. Development of the generator ordering and loading program (GOAL). In *UPEC-20*, Huddersfield, England, 1985.

[8] P. Brown and A. G. Entwistle. Distributed computer control of a 500MW oil-fired boiler. In *IEE Conf. Distributed Computer Control Systems*, pages 108–113, 1977.

[9] L. R. Johnstone, C. R. Marsland, and S. T. Pringle. A distributed computer control system for a 120MW boiler. In *IEE Conf. Distributed Computer Control Systems*, pages 114–119, 1977.

[10] M. J. Metcalfe, J. Waddington, and R. G. Wilson. Operational experience with fossil-fired generating plant under automatic load control. *IEE Proceedings*, 126(4), Apr. 1979.

[11] J. Waddington. Load-controller design for a regulating coal-fired unit. *IEE Proceedings*, 126(5), May 1979.

[12] J. N. Wallace and R. Clarke. Load control of a 500MW oil-fired boiler-turbine. In *IEE Conf. Control and its Applications*, pages 250–255, 1981.

[13] A. R. Fowkes, G. Wronski, and R. G. Wilson. The management of frequency response of fossil-fired power plant. In *IEE 2nd Int. Conf. Power System Monitoring and Control*, pages 400–405, 1986.

[14] R. Clarke, J. Waddington, and J. N. Wallace. The application of Kalman filtering to the load/pressure control of coal-fired boilers. In *IEE Colloq.*, 1988/89.

[15] Central Electricity Generating Board. Annual report and accounts 1987/88, 1988.

[16] R. M. Dunnett and S. Duckworth. An experimental study of centralised economic dispatch in the CEGB. In *IEE 2nd Int. Conf. Power System Monitoring and Control*, pages 7–12, 1986.

[17] W. D. Laing and C. Brewer. The development of an on-line short-term demand prediction facility. In *IEE 2nd Int. Conf. Power System Monitoring and Control*, pages 1–6, 1986.

[18] H. Glavitsch and J. Stoffel. Automatic generation control. *International Journal of Electrical Power and Energy Systems*, 2(1):21–28, Jan. 1980.

[19] J. Carpentier, A. Gillon, R. Girard, Y. Jegouzo, P. Pruvot, A. Candre, F. Caraman, R. Grimonpont, F. Pellen, and P. Tournebise. Concepts, models and studies for a closed loop secure automatic generation control. In *IASTED Power High Tech 89*, pages 361–366, Valencia, Spain, 1989.

[20] M. Davies, F. Moran, and J. I. Bird. Power/frequency characteristics of the British grid system. *IEE Proceedings*, 106-A:154–162, Nov. 1958.

[21] J. Osanna, H. Graner, and F. Hofmann. Frequenz- und Leistungssteuerung (Netzkennliniensteuerung) von Netzverbänden. German Patent No. 634025, Feb. 1931.

[22] H. Graner. Vorschläge für den Betrieb von Netzverbänden. *Elektrotechn. Z.*, 55:1069, 1934.

[23] G. Darrieus. Frequenz- und Leistungsregulierung in grossen Netzverbänden. *Bull. schweiz. elektrotech.*, 28:525, 1937.

[24] A. de Quervain and W. Frey. Methods of controlling interconnected power systems. *Brown Boveri Review*, 44(11):472–487, Nov. 1957.

[25] G. Quazza. Noninteracting controls of interconnected electric power systems. *IEEE Trans. PAS*, PAS-85(7):727–741, July 1966.

[26] C. W. Ross. Error adaptive control computer for interconnected power systems. *IEEE Trans. PAS*, PAS-85(7):742–749, July 1966.

[27] O. I. Elgerd and C. E. Fosha. Optimum megawatt-frequency control of multiarea electric energy systems. *IEEE Trans. PAS*, PAS-89(4):556–562, Apr. 1970.

[28] C. E. Fosha and O. I. Elgerd. The megawatt-frequency control problem: A new approach via optimal control theory. *IEEE Trans. PAS*, PAS-89(4):563–577, Apr. 1970.

[29] H. Glavitsch and F. D. Galiana. Load-frequency control with particular emphasis on thermal power stations. In E. Handschin, editor, *Real-Time Control of Electric Power Systems*, pages 115–145. Elsevier, 1972.

[30] F. P. deMello, R. J. Mills, and W. F. B'Rells. Automatic generation control. part i - process modeling. *IEEE Trans. PAS*, pages 710–715, Mar/Apr 1973.

[31] F. P. deMello, R. J. Mills, and W. F. B'Rells. Automatic generation control. part ii - digital control techniques. *IEEE Trans. PAS*, pages 716–724, Mar/Apr 1973.

[32] A. J. Connor, F. I. Denny, J. R. Huff, T. Kennedy, C. J. Frank, and M. D. Anderson. Current operating problems associated with automatic generation control. *IEEE Trans. PAS*, PAS-98(1):88–96, Jan/Feb 1979. A report prepared for the System Operations Subcommittee of the Power System Engineering Committee by the Current Operational Problems Working Group (76-1).

[33] M. L. Kothari, P. S. Satsangi, and J. Nanda. Sampled-data automatic generation control of interconnected reheat thermal systems considering generation rate constraints. *IEEE Trans. PAS*, PAS-100(5):2334–2342, May 1981.

[34] A. Kumar and O. P. Malik. Discrete analysis of load-frequency control problem. *IEE Proceedings*, 113-C(4):144–145, July 1984.

[35] S. C. Tripathy, T. S. Bhatti, C. S. Jha, O. P. Malik, and G. S. Hope. Sampled data automatic generation control analysis with reheat steam turbines and governor dead-band effects. *IEEE Trans. PAS*, PAS-103(5):1045–1051, May 1984.

[36] L. Basañez and J. Riera. Load frequency control behaviour with governor dead-band effects. In *IEE 2nd Int. Conf. Power System Monitoring and Control*, pages 23–28, 1986.

[37] E. Davison and N. Tripathi. . *IEEE Trans. AC*, 23:312–325, 1978.

[38] A. Kumar, O. P. Malik, and G. S. Hope. Discrete variable structure controller for load frequency control of multi-area interconnected power systems. *IEE Proceedings*, 134-C(2):116–122, Mar. 1987.

[39] J. Carpentier. Optimal power flows: Uses, methods and developments. In *IFAC Electric Energy Systems*, pages 11–21, Rio de Janeiro, Brazil, 1985.

[40] M. L. Kothari, J. Nanda, D. P. Kothari, and D. Das. Discrete-mode automatic generation control of a two-area reheat thermal system with new area control error. *IEEE Trans. PWRS*, 4(2):730–738, May 1989.

[41] P. D. Henerson, H. Klaiman, J. Ginnetti, T. Snodgrass, N. Cohn, S. Bloor, and L. VansSlyck. Cost aspects of AGC, inadvertent energy and time error. *IEEE Trans. PWRS*, 5(1):111–118, Feb. 1990.

[42] K. Yamashita and H. Miyagi. Multivariable self-tuning regulator for load frequency control system with interaction of voltage on load demand. *IEE Proceedings*, 138-D(2):177–183, Mar. 1991.

[43] M. Aldeen and J. F. Marsh. Decentralised proportional-plus-integral design method for interconnected power systems. *IEE Proceedings*, 138-C(4):263–274, July 1991.

[44] E. Jaggy and A. P. Longley. Implementation of an AGC-algorithm in different power systems and on different control levels. In *IEE 3rd Int. Conf. Power System Monitoring and Control*, pages 162–167, 1991.

[45] K. Kovács, B. Bechtold, and K. Szendy. Adaptive automatic generation control in the Hungarian power system. In *IEE Int. Conf. Power System Monitoring and Control*, pages 143–148, 1980.

[46] I. Vajk, M. Vajta, L. Keviczky, R. Haber, J. Hetthéssy, and K. Kovács. Adaptive load-frequency control of the Hungarian power system. *Automatica*, 21(2):129–137, 1985.

[47] J. Augé, R. Fernandez, A. Merlin, and F. Broussolle. The new real-time computerized control system in the national control center of Electricité de France. In *CIGRE Int. Conf. Large High Voltage Electric Systems, 30th session*, 1984. paper 39–10.

[48] J. Carpentier. The French national control center present state and developments. *IEEE Trans. PWRS*, PWRS-1(4):42–48, Nov. 1986.

[49] J. Carpentier, A. Candre, R. C. Girard, B. A. Heilbronn, L. P. Loevenbruck, and G. J. Nerin. Secure automatic generation control. Principle, simulation models and results. In *IEE 3rd Int. Conf. Power System Monitoring and Control*, pages 156–161, 1991.

[50] V. Garcia-Echave, L. Pradinas, J. M. Ferrer, F. Lasheras, and J. J. Gonzales. Regulating system for the co-ordination of the multiple AGCs of the Spanish peninsular utilities as a unique control area. Description and field experiences. In *CIGRE Int. Conf. Large High Voltage Electric Systems, 30th session*, 1984. Paper 39–11.

[51] J. Biström and K. Lindström. The Finnish power system control centre. *IEEE Trans. PWRS*, PWRS-1(4):49–55, Nov. 1986.

[52] P. Leman and H. Urpinen. Computer aided production planning and control in the Finnish national control centre. In *IEE 2nd Int. Conf. Power System Monitoring and Control*, pages 13–17, 1986.

[53] G. L. Kusic, J. A. Sutterfield, A. R. Caprez, J. L. Haneline, and B. R. Bergman. Automatic generation control for hydro systems. *IEEE Trans. EC*, 3(1):33–39, Mar. 1988.

[54] C. D. Vournas, E. N. Dialynas, N. Hatziargyriou, A. V. Machias, J. L. Souflis, and B. C. Papadias. A flexible AGC algorithm for the Hellenic interconnected system. *IEEE Trans. PWRS*, 4(1):61–68, February 1989.

[55] C. Liang. An overview of the hierarchical dispatch and control system in Taipower. *IEEE Trans. PWRS*, 5(4):1041–1046, Nov. 1990.

[56] K. Matsuzawa, M. Suzuki, Y. Okuhara, Y. Kishidi, Y. Kudo, and T. Yamashita. New energy management system for central dispatching center of Tokyo Electric Power Co., Inc. *IEEE Trans. PWRS*, 5(4):1112–1117, Nov. 1990.

[57] M. Power and G. Schaffer. Upgrading Ireland's national control centre. In *IEE 3rd Int. Conf. Power System Monitoring and Control*, pages 198–203, 1991.

[58] F. Moran. Power system automatic frequency control techniques. *IEE Proceedings*, 106-A:145–153, Nov. 1958.

[59] C. Brewer, G. F. Charles, C. C. M. Parish, J. N. Prewett, D. C. Salthouse, and B. J. Terry. Performance of a predictive automatic load-dispatching system. *IEE Proceedings*, 115(10):1577–1586, Oct. 1968.

[60] C. Brewer, J. Frost, and C. C. M. Parish. Control room in an experimental load-dispatching system for the power supply industry. *IEE Proceedings*, 115(2):318–324, February 1968.

[61] E. D. Farmer. Stability and noise sensitivity of a digital-analogue control system for the automatic loading of a power system. *IEE Proceedings*, 115(3):453–459, Mar. 1968.

[62] E. D. Farmer and M. J. Potton. Development of on-line load-prediction techniques with results from trials in the south-west region of the CEGB. *IEE Proceedings*, 115(10):1549–1558, Oct. 1968.

[63] F. Moran, D. K. S. Bain, and J. S. Sohal. Development of the equipment required for the loading of turbogenerators under automatic power-system control. *IEE Proceedings*, 155(7):1067–1075, July 1968.

[64] F. Moran and D. R. Williams. Automatic control of power-system frequency by machine controllers. *IEE Proceedings*, 115(4):606–614, Apr. 1968.

[65] P. Pettit. Digital-computer programs for an experimental automatic load-dispatching system. *IEE Proceedings*, 115(4):597–605, Apr. 1968.

[66] E. D. Farmer, K. W. James, F. Moran, and P. Pettit. Development of automatic digital control of a power system from the laboratory to a field installation. *IEE Proceedings*, 116(3):436–444, Mar. 1969.

[67] F. Moran and J. N. Prewett. An experiment in the automatic control of power generation. *Automatica*, 6:19–32, 1970.

[68] Casson, Moran, and Taylor. Development and future possibilities of automatic control on the British grid system. In *Proc. 1st IFAC Congress*, pages 78–85, Moscow, 1960.

[69] D. K. S. Bain. Power system model. *IEE Proceedings*, 114(8):1131–1138, 1967.

[70] E. D. Farmer. The economics and dynamics of system loading and regulation. In *IEE Conference Publication 187*, pages 125–131, 1980.

[71] M. Rafian, M. J. H. Sterling, and M. R. Irving. Real-time power system simulation. *IEE Proceedings*, 134-C(3):206–223, May 1987.

[72] M. Rafian, M. J. H. Sterling, and M. R. Irving. Parallel processor algorithm for power system simulation. *IEE Proceedings*, 135-C(4), July 1988.

[73] D. K. Whitlock. RASM05 - Revised transient stability program, version 2.0. Technical Report NS/C/P478, CEGB Computing Services Department, .

[74] L. A. Dale. *Real-Time Modelling of Multi-Machine Power Systems.* PhD thesis, School of Electrical Engineering, University of Bath, UK, 1986.

[75] T. Berry. *Real Time Simulation of Complex Power Systems using Parallel Processors.* PhD thesis, School of Electrical Engineering, University of Bath, UK, 1989.

[76] K. W. Chan. *A Power System Simulator to Model the Transient Mode of Operation of the (UK) National Supergrid in Real-Time.* PhD thesis, School of Electronic and Electrical Engineering, University of Bath, UK, 1992. To be submitted.

[77] V. Kola, A. Bose, and P. M. Anderson. Power plant models for operator training simulators. *IEEE Trans. PWRS*, 4(2), May 1989.

[78] B. W. Empett, R. S. Edgar, and D. R. Battlebury. SYRES01 - System response program. Technical Report MS/C/P129 STB/12/71, Central Electricity Generating Board, July 1971.

[79] P. H. Ashmole, D. R. Battlebury, and R. K. Bowdler. Power system model for large frequency disturbances. *IEE Proceedings*, 121(7):601–608, July 1974.

[80] B. E. Murray. Model specification. Technical Report OD(S)/BEM/, CEGB Systems Operations Department, Aug. 1987. Draft.

[81] D. G. Tanner. *Real Time Simulation of Power Systems.* PhD thesis, School of Electrical Engineering, University of Bath, UK, 1982.

[82] S. K. Williams. *Power System Optimisation and Stability Studies using Real-Time Simulation.* PhD thesis, School of Electrical Engineering, University of Bath, UK, 1986.

[83] T. Berry, A. R. Daniels, R. W. Dunn, and S. Geeves. Real time power system dynamics simulation. In *CIGRE Int. Conf. Large High Voltage Electric Systems*, pages 1–5, 1990. Paper 38–210.

[84] M. Richards and C. Whitby-Strevens. *BCPL, the Language and its Compiler.* Cambridge University Press, 1980. ISBN 0-521-28681-6.

[85] Motorola Inc. *MC68000 16 bit Microprocessor User's Manual*, second edition, 1980.

[86] Motorola Inc. *MC68000 16 bit Microprocessor Programmer's Manual*, 1984.

[87] T. J. King. *Tripos User Guide.* School of Mathematics, University of Bath, 1983.

[88] T. J. King. *Tripos Programming Guide.* School of Mathematics, University of Bath, 1983.

[89] T. J. King. *Tripos Technical Guide.* School of Mathematics, University of Bath, 1983.

[90] Motorola Inc. *MC68020 32 bit Microprocessor User's Manual.* Prentice Hall, 1985.

[91] Motorola Inc. *MC68881 32 bit Coprocessor User's Manual.* Prentice Hall, 1985.

[92] S. P. Harbison and G. L. Steele. *C: A Reference Manual.* Prentice Hall, 1987.

[93] Perihelion Software Ltd. *The Helios Operating System.* Prentice Hall, 1989. ISBN 0-13-386004-3.

[94] Anon. T800 transputer. Technical Report 42 1082 00, Inmos Ltd, Apr. 1987.

[95] W. M. Fu. Real time power system simulation. B.Sc. final year project report, School of Electrical Engineering, University of Bath, 1989.

[96] F. Ng. *A Man Machine Interface for Real Time Power System Simulation.* PhD thesis, School of Electronic and Electrical Engineering, University of Bath, UK, 1992. To be examined.

[97] Microway, Inc., Research Park, Box 79, Kingston, MA 02364, USA. *Number Smasher-860 Owner's Manual*, 1990.

[98] D. A. Briggs. Private communication to the author. National Power Division, CEGB, 1989.

[99] D. A. Briggs. Dinorwic power station. Theoretical study of ASEA governor system dynamics. Technical Report PED/SES/CPK/29, Central Electricity Generating Board, Dec. 1976.

[100] C. F. Gerald and P. O. Wheatley. *Applied Numerical Analysis.* Addison-Wesley, 1984. ISBN 0-201-11579-4.

[101] T. Berry. Private communication to the author. School of Mechanical Engineering, University of Bath, 1991.

[102] J. M. Grzejewski. Private communication to the author. School of Electronic and Electrical Engineering, University of Bath, 1991.

[103] B. M. Weedy. *Electric Power Systems.* John Wiley & Sons Ltd., third edition, Aug. 1983. ISBN 0-471-27584-0.

[104] C. Arkell. Private communication to the author. National Grid Company, 1991.

[105] R. Clarke. Private communication to the author. National Power Division, CEGB, 1989.

[106] The Rand Corporation. *REDUCE 3 Manual*, 1983.

[107] S. Shamail. *Distributed Memory Diesel Engine Simulation Using Transputers.* PhD thesis, School of Electrical Engineering, University of Bath, UK, 1990.

[108] R. W. Dunn, A. R. Daniels, V. Gott, and C. G. Selwyn. A new architecture of high speed performance parallel computer for use in condition monitoring of large diesel engines. In *IEE Int. Conf. on Software Engineering for Real Time Systems*, Sept. 1989.

[109] M. Hafeez. *An Expandable Input/Output and Graphics System for Distributed Memory Parallel Computers.* PhD thesis, School of Electrical Engineering, University of Bath, UK, 1990.

[110] Transtech. *Transtech TMB04 User Manual*, 1989. TMB04MAN0889.

[111] Vision. *BABY 286MB Mini AT-System Board Reference Manual*, 1983.

[112] The British SuperGrid System. From an original supplied by the Central Electricity Generating Board.